Improving the Sustainability of Polymer and Peptide Synthesis

Stefan B. Lawrenson

Doctor of Philosophy

University of York
Chemistry
May 2018

Abstract

This thesis explores methods for improving the sustainability of peptide and polymer chemistry, using alternative solvents and bio-based platform molecules.

Cyclic carbonates were first investigated as replacements for reprotoxic polar aprotic solvents in peptide chemistry. Using the solution-phase approach several tetrapeptides were first synthesised utilising propylene carbonate as the only reaction solvent. Good to excellent yields were observed in all cases for both coupling (65-91%) and deprotection (80-99%) steps. The use of propylene carbonate for solid-phase peptide synthesis was then demonstrated, through the total synthesis of the natural vasodilator bradykinin in an excellent 77% crude purity.

Extending this work, the use of alternative solvents in solid-phase organic synthesis was then explored. The suitability of green solvents for solid-phase organic synthesis was determined by their ability to solvate polymeric supports. In all cases, a solvent was identified that was able to swell a desired resin to >4.0 mL g^{-1}. The outcomes of this investigation were then used to build a computational model of resin swelling using the HSPiP software and verify resin/solvent compatibility through the multicomponent Ugi reaction.

The second half of this thesis then explored the ring-opening metathesis polymerisation of amide derivatives of a novel oxanorbornene-lactone. A number of homo- and random co-polymers were prepared, which were found to possess good molecular weights (M_n = 10,763-28,100) and narrow dispersities (Đ = 1.02-1.11). Thermal analysis also revealed the polymers to be amorphous, possessing high thermal degradation (>300 °C) and glass transition (115-203 °C) temperatures. It was also possible to synthesise a block copolymer, but only when the second monomer was added following 80% conversion of the first monomer. Finally, kinetic data showed that the pendant side chains had a minimal influence on propagation rate (2.3×10^{-3} s^{-1} - 3.1×10^{-4} s^{-1}).

Finally, the synthesis and application of spirocyclic oxanorbornene-imides were investigated. These monomers were found to be unsuitable for ROMP, but LLAMA analysis showed that the hydrogenated variants were highly promising lead-like compounds. The data suggests they lay perfectly within lead-like space (-1 $\leq$ cLog$P$ $\leq$ 3 and M_w = 200-350 Da), are fairly three-dimensional by PMI analysis and had 0% likeness to a random 2% selection of the ZINC database.

Contents

List of Tables

List of Figures

List of Schemes

Acknowledgements

I would first like to thank my supervisor, Prof. Michael North, for the guidance, encouragement and advice he has provided to me throughout my time as a PhD student. I feel incredibly lucky to have had a supervisor that was so actively involved in my research and always had time for me, and my concerns.

I must also express my thanks to the various members of academic and technical staff at the University of York that have played such a vital role in my research. In particular, Dr Anne Routledge and Dr Andy Hunt, for their continued help and their many excellent suggestions.

My sincere thanks must also go to my colleagues within the GCCE. Especially the various members of the North group, and the Cloyster Boys, that made my time in the lab so much more enjoyable.

Last, but by no means least, I would like to thank my parents and my partner, Cressida, for their unwavering support throughout this journey. I know without them I would not be where I am today, and for that, I am eternally grateful.

Declaration

I declare that this thesis is a presentation of original work and I am the sole author. This work has not previously been presented for an award at this, or any other, University. All sources are acknowledged as references. Some of the work in this thesis was carried out by, or in collaboration with, other workers who are fully acknowledged below, all other results were obtained by the author. Part of the work disclosed herein has previously been published in the following articles;

1. Lawrenson, S. B.; North, M.; Peigneguy, F.; Routledge, R. *Green Chem.*, **2017**, 19, 952-962.
2. Lawrenson, S. B.; Arav R.; North, M. *Green Chem.*, **2017**, 19, 1685-1691.
3. Lawrenson, S. B. *Pure Appl. Chem.*, **2018**, 90, 157-165.
4. Lawrenson, S. B.; Hart, S.; Ingram, I. D. V.; North, M.; Parker, R. R.; Whitwood, A. C.; *ACS Sustainable Chem. Eng.*, **2018**, 8, 9744-9752.

The author would like to declare the additional contributions to this thesis from the following workers;

Chapter 2: Cyclic Carbonates as Solvents for Peptide Synthesis

R. Arav - Synthesis of the Phe-Leu-Gly-Ala peptide sequence and associated racemisation study

Chapter 3: Greener Solvents for Solid-Phase Organic Synthesis

F. Peigneguy - Experimental study on the solution- and solid-phase Ugi reaction in green solvents

Chapter 4: Ring-Opening Metathesis Polymerisation of a Novel Bio-based Monomer Framework

I. Ingram - Assistance in the analysis of kinetic data and providing TGA-IR data for the decomposition of the sarcosine homopolymer

A. Whitwood, S. Hart, R. R. Bean - X-ray crystallography data

Chapter 5: Investigation into the Synthesis and Application of an Unusual Spirocyclic Imide Species

A. Whitwood, S. Hart, R. R. Bean - X-ray crystallography data

Chapter 1

General Introduction

Throughout the latter half of the twentieth century the human race has developed at a rather alarming rate. Within the last 100 years alone the global population has multiplied four-fold to 6.4 billion, global economic output has increased more than twenty-fold, and global material consumption has increased eight-fold.[1] This growth has however come at a cost, with anthropogenic activity now widely accepted to have been the root cause of a number of environmental issues, including climate change, global warming, rising sea levels, ozone layer depletion and ocean acidification, to name but a few.[2] Even more worryingly, this growth is not expected to slow down, with the United Nations (UN) predicting that global population will continue to grow, reaching 9.3 billion by 2050 and 10.1 billion by 2100.[3] Furthermore, this growth is expected to be concentrated around the less developed nations of Africa, Asia and Latin America, as they seek to obtain a comparable standard of living to that of more developed regions. Meeting the needs of a more crowded, more consuming human population will therefore result in the greater production of goods and services, which will in turn increase demand for land, energy, materials and resources, placing an ever greater strain on the environment.

In response, in 1972, the UN organised the Stockholm Conference on the Human Environment, the first international meeting to address how human activity was harming the environment and putting lives at risk.[4] In the wake of this meeting a number of reports sought to address the highlighted issues, however, none have been more prominent than *Our Common Future*, a 1987 report from the World Commission on Environment and Development.[5] This report sought to forecast on a global scale, how man-made activities would affect the environment, taking into consideration the industrial, social and economic consequences. This investigation however highlighted a major issue. Whilst it was obvious human activity was having a detrimental effect on the environment, particularly in developed nations, it would be inconceivable for the UN to impose restrictions on developing nations, inhibiting their efforts to enhance their standard of living. Consequently, the report sought to overcome these issues through promoting the concept of "sustainable development" or "meeting the current environmental and human health, economic, and societal needs, without compromising the progress and success of future generations".[5] The concept of sustainable development has appeared in a number of variations since 1987, but has most recently been highlighted by the UN in the form of the Global Goals, 17 sustainable development goals from the 2030 Agenda for Sustainable Development, which are highlighted in Figure 1.1.[6]

Figure 1.1: UN 2030 Agenda for Sustainable Development included with permissions from the United Nations.[6]

1.1 Sustainable Development and the Chemical Industry

If sustainable development is to be realised, widespread change is likely to be necessary. This change is perhaps going to be most impactful within the chemical industry, as it has come to almost define modern society, with the global population relying heavily upon an array of chemical products for their quality of life. These include basic or commodity chemicals (e.g. petrochemicals, petrochemical derivatives); speciality chemicals derived from basic chemicals (e.g. adhesives, sealants, catalysts, coatings); products derived from life science (e.g. pharmaceuticals, pesticides); and consumer care products (e.g. soap, detergents).[7] Being one of the worlds largest industrial sectors it also makes up an important part of the global economy, with recent estimates from The European Chemical Industry Council (CEFIC) valuing turnover within the sector at €3,360 billion, accounting for 7% of global income and 9% of international trade.[8,9] Predictions from the Organisation for Economic Co-operation and Development (OECD) suggest this industry is also expected to grow by approximately 3% annually until 2050.[7] Chemistry is therefore set to play a key role if the societal, economic and environmental objectives set out by sustainable development are to be met.

Unfortunately, public opinion often perceives chemistry as the cause of these problems, rather than the potential solution. This perception is not entirely unwarranted, as the effect of chemicals on human health and the environment is far from benign. It is an industry founded upon petrochemicals, the building block of more than 90% of current organic chemical manufacturing, a resource that is susceptible to widely variable oil prices, and exploitation of which has been directly linked to worsening air pollution and global warming.[10] Moreover, the chemical industry releases more hazardous waste to the environment than any other industrial sector, and more in total than is released by the next nine sectors combined.[9] This is also becoming a growing issue for the industry as the remediation of this waste continues to become more costly, with ever more stringent controls seeking to limit chemical hazards.

There now therefore exist a formidable challenge for chemists, to develop new products, processes and services that meet current and future social and economic needs, but not at the detriment to the environment.[11] This is more commonly referred to as the three pillars of sustainability, which will be key if sustainable development within the chemical industry is to be realised. Consequently, there has been a growing interest in a branch of chemistry that seeks to embed core environmental considerations into everyday practice, an approach that has come to be more commonly known as green chemistry.

1.1.1 Green Chemistry

Green chemistry is defined as the "design of chemical products and processes to reduce or eliminate the use and generation of hazardous substances".[12] It is a concept that was first proposed in a seminal publication from Anastas and Warner in the early 1990s.[12] Fundamentally, green chemistry seeks to achieve sustainability at the molecular level, with the aim of preventing pollution rather than dealing with waste. Anastas and Warner therefore went on to propose the "12 Principles of Green Chemistry", a guiding framework for the design of new chemical products and processes in accordance with sustainability (Table 1.1).[13] Since its inception, green chemistry has grown to receive widespread international interest, in part due to its ability to meet both economic and environmental goals simultaneously.[14]

Table 1.1: The 12 principles of green chemistry.

	Principle	**Explanation**
1.	Prevention	It is better to prevent waste than to treat waste after it is formed
2.	Atom Economy	Synthetic methods should be designed to maximise the incorporation of all materials used in the process into the final product
3.	Less Hazardous Chemical Synthesis	Synthetic methodologies should be designed to use and generate substances that pose little or no toxicity to human health/the environment
4.	Designing Safer Chemicals	Chemical products should be designed to preserve efficacy whilst reducing toxicity
5.	Safer Solvents and Auxiliaries	The use of auxiliary substances should be made unnecessary whenever possible and, when used, innocuous
6.	Design for Energy Efficiency	Energy requirements of chemical processes should be recognised and their environmental and economic impacts minimised
7.	Use of Renewable Feedstocks	A raw material or feedstock should be renewable rather than depleting whenever technically and economically practicable
8.	Reduce Derivatives	Unnecessary derivatisation should be minimised or avoided if possible
9.	Catalysis	Catalytic reagents are superior to stoichiometric reagents
10.	Design for Degradation	Chemical products should be designed so that at the end of their function they break down into innocuous degradation products and do not persist in the environment
11.	Real-Time Analysis for Pollution Prevention	Analytical methodologies need to be further developed to allow for real-time, in-process monitoring and control prior to the formation of hazardous substances
12.	Inherently Safer Chemistry for Accident Prevention	Substances and the form of a substance used in a chemical process should be chosen to minimise the potential for chemical accidents

1.1.2 Thesis Intent

The concepts underpinning green chemistry however are obviously broadly applicable to many sectors of the chemical industry, it is therefore important to narrow the focus of this thesis, setting a general precedent for the proceeding research chapters. The original aim of this project was to investigate the application of cyclic carbonates as alternative solvents. However, as time went on, the focus continued to deviate from this path, such that it is now best discussed in two distinct parts. The first investigating the use of alternative solvents for solid-phase synthesis methodologies, with a particular focus on improving the sustainability of peptide chemistry. The second on improving the sustainability of polymer chemistry, with an investigation into the ring-opening metathesis polymerisation (ROMP) of a novel monomer framework, produced from bio-based platform molecules. The application of green chemistry in the fields of alternative solvents and polymer synthesis will therefore be introduced in more detail, providing relevant background for these topics and highlighting notable developments along the way.

1.2 Green Chemistry and Alternative Solvents

The use of alternative solvents is perhaps one of the most active topics of research within green chemistry.[14] This is in part due to the many roles solvents play within the chemical industry. Solvents are used in chemical processes to aid mass and heat transfer, and to facilitate separation and purification. They are also often the most important components of cleaning agents, adhesives, and coatings, such as paints and varnishes. They often therefore account for the vast majority of waste generated in synthesis and processing. In fact, estimates from GlaxoSmithKline (GSK) have suggested solvent use accounts for between 80-90% of the total waste mass generated in a given batch pharmaceutical or fine-chemical operation.[15] More recently, the American Chemical Society Green Chemistry Institute Pharmaceutical Roundtable (ACS GCIPR) have shown that for a commercial process, the synthesis of 1 kg of active pharmaceutical ingredient (API) will typically generate 46 kg of waste, 56% of which will be due to organic solvents, with a further 32% from aqueous waste.[15] Furthermore, many conventional solvents are toxic, flammable, and/or corrosive. Many are also regarded as volatile organic compounds (VOCs) which present an increased risk of exposure or release to the environment. The environmental impact of a given process is therefore almost always a consequence of the solvent. The biggest gains in terms of reducing environmental impact can therefore be most commonly had through optimisation of the solvent, rather than through changes to the chemistry.[14]

The greenest solvent is of course the use of no solvent at all, as according to the 12 Principles of Green Chemistry the use of auxiliary substances should be made unnecessary whenever possible, this however is impractical in many situations.[14] There has therefore been a great interest in recent years in the utilisation of solvents that present more favourable environmental, health or safety (EHS) considerations. An approach that is particularly prevalent in the pharmaceutical industry is that of solvent selection guides, with companies such as GSK[16], Pfizer[17] and Sanofi[18], along with speciality groups including the ACS GCIPR[19] and Innovative Medicines Initiative (IMI)-CHEM21[20] publishing their own selection guides. In an effort to provide researchers with the ability to make a more informed choice with regards to solvent selection, discouraging the use of harmful or toxic solvents. Alternatively, there has been great interest in the development of neoteric solvents and solvent technologies with more desirable EHS characteristics, such as the use of water, ionic liquids, supercritical carbon dioxide or bio-derived solvents representing some of the most common examples.[21]

1.2.1 Water

Water has long attracted interest as a reaction solvent due to its benign nature and the fact it is the most abundant molecule on the planet. For this reason, water is accepted as the most inexpensive and environmentally friendly solvent available.[14] Hydrophobic effects associated with the use of water have also been shown to enhance reaction rates and improve selectivities, and the poor solubility of oxygen in water has been shown to facilitate air-sensitive transition-metal catalysis in open air.[22] The ability to perform reactions in water therefore presents a number of advantages, particularly for large scale process chemistry. A notable example of the use of water in an industrial synthesis is the revised chemoenzymatic synthesis of pregabalin **1.4** by Pfizer, a blockbuster drug used for the treatment of neuropathic pain. The initial synthesis required 10 steps, producing pregabalin **1.4** in a 33% yield and at a cost that was six times more than the target value.[23] A revised biocatalytic route in water greatly improved process efficiency, by setting the stereogenic centre earlier in the synthesis the undesired enantiomer **1.3** could be efficiently recycled. The remaining chemical steps could also be performed in water, greatly reducing organic solvent waste, resulting in a five-fold reduction in overall E-factor (Scheme 1.1).[23]

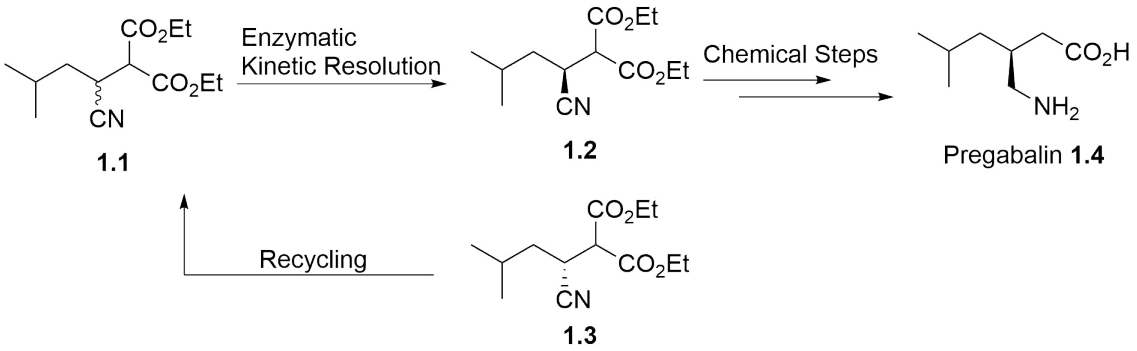

Scheme 1.1: Key chemoenzymatic transformation in the revised manufacturing process for pregabalin **1.4**.

1.2.2 Ionic Liquids

Ionic liquids are ionic salts that are liquid at or below 100 °C, they are a rather more modern neoteric solvent technology that have received a substantial amount of academic interest in the last few decades. This is due to their perceived environmental benefits, as they are typically non-flammable and posses almost non-existent vapour pressures, they are therefore regarded as excellent replacements to conventional VOCs. Additionally, the wide variety of anions and cations that are readily available make ionic liquids highly versatile solvents, that can be tuned to suit a particular purpose. It should be acknowledged however that they are not intrinsically green, due to issues regarding their synthesis and their widely unknown toxicity. Regardless, ionic liquids have come to find use as solvents in a wide variety of laboratory applications to date, including synthesis, catalysis, batteries, and fuel cells.

A rather interesting example, from a green chemistry perspective, of ionic liquid solvents is recent interest in a sub-set of reversible or switchable ionic liquids, pioneered by Jessop and co-workers.[24] These solvents are able to switch between a high polarity or low polarity form, through the use of a CO_2 trigger. Exposure of a guanidine or amidine base to CO_2 in the presence of an alcohol, results in a high polarity ionic liquid. This reaction can then be reversed under a flow of nitrogen (Scheme 1.2). Hart *et al.*, for example, have then utilised this system in the Pd-catalysed Heck reaction, with the intention that the switchable solvent should allow for the sequential separation of product and by-product (Scheme 1.2).[25] The Heck reaction between bromobenzene **1.5** and styrene **1.6** using a 1,8-diazabicyclo[5.4.0]undec-7-ene **1.8** (DBU)/hexanol switchable solvent system under high polarity conditions produced the target product **1.7** in 97% yield, following an extraction with hexane. After switching back to the low polarity solvent mixture the HBr/DBU salt by-product could then be removed using a simple filtration.

The catalyst/solvent system was then found to retain activity in subsequent Heck reactions, provided fresh DBU was added to compensate for losses.[25]

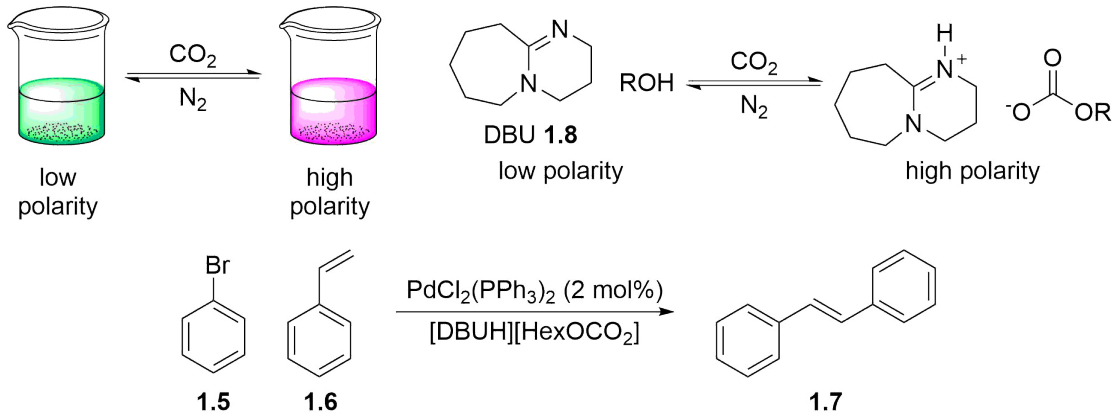

Scheme 1.2: Heck coupling reaction between styrene **1.6** and bromobenzene **1.5** using a DBU/hexanol switchable ionic liquid.

1.2.3 Supercritical Carbon Dioxide

Another neoteric solvent technology that has also received a considerable amount of interest is that of supercritical carbon dioxide ($scCO_2$). Supercritical fluids are fluids that are simultaneously heated and compressed above their critical points, within this region the fluid has properties intermediate between that of a liquid and a gas (Figure 1.2).[14] The use of carbon dioxide as a supercritical fluid is a particularly interesting choice, as it is both plentiful and inexpensive, whilst also requiring fairly mild temperatures and pressures to reach supercritical state (critical temperature 31 °C and critical pressure 74 bar). Additionally, with carbon dioxide being gaseous under ambient conditions, degassing of a reaction vessel will result in the complete removal of the solvent. Consequently, ($scCO_2$) has found a number of industrial applications, the most significant of which being the decaffeination of coffee and the replacement of perchloroethylene in dry cleaning.[14]

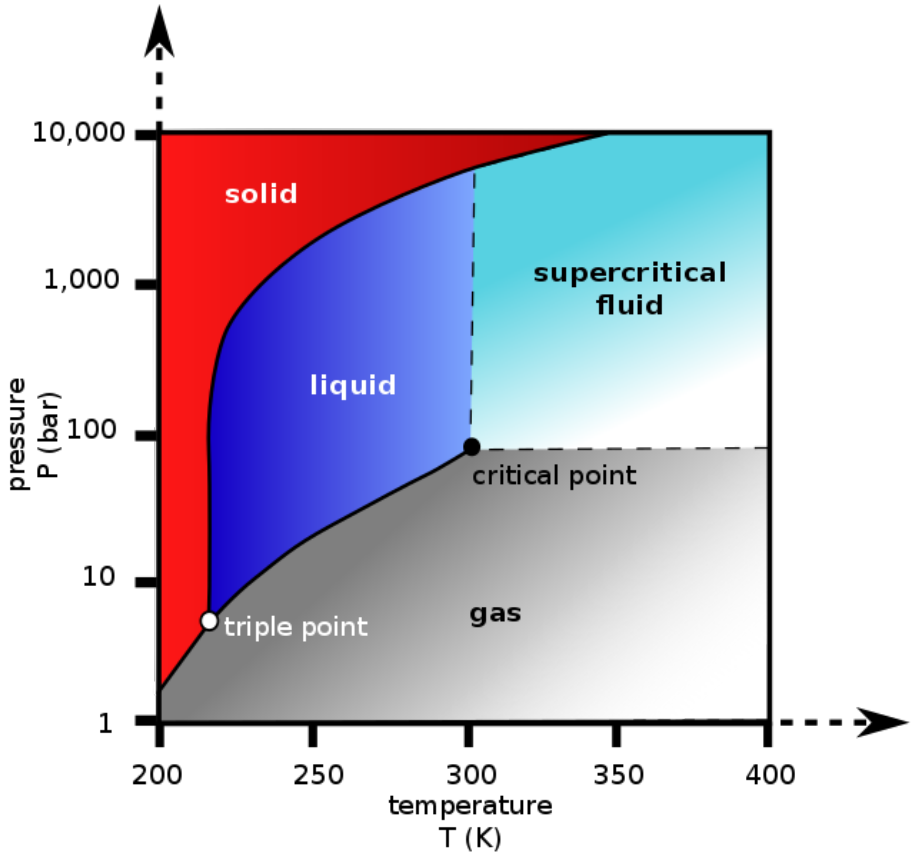

Figure 1.2: Pressure-temperature phase diagram of carbon dioxide highlighting the supercritical region.

1.2.4 Bio-derived Solvents

Finally, there has also been a growing interest in the use of solvents sourced from renewable feedstocks, such as food, forestry and agricultural waste. These are more commonly referred to as bio-based solvents, which are either used as direct replacements to conventional solvents, or functionalised to produce novel molecular structures. Common examples include the bio-based alcohols, such as bio-ethanol or glycerol, moderately polar aprotic solvents, such as 2-MeTHF **1.16** and γ-valerolactone **1.17**, and the apolar aprotic terpene derivatives D-limonene **1.9** and *para*-cymene **1.10** (Scheme 1.3).[26] Despite their advantages, bio-based solvents are not necessarily safer, less toxic or more environmentally benign compared to conventional solvents. Additionally, there is often a distinct lack of data on some of the more novel bio-based solvents, particularly in terms of physical properties, toxicity, performance and cost.[20] For these reasons, the uptake of bio-based solvents for industrial applications has been rather slow to date.[26]

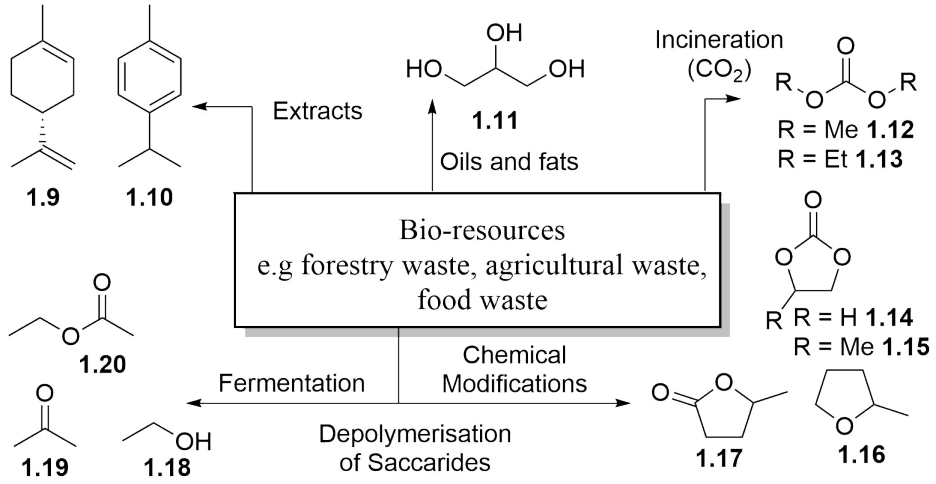

Scheme 1.3: A number of common bio-based solvent structures.

Despite the numerous advances in neoteric solvents and solvent technologies, polar aprotic solvents still present a significant challenge. This is a tremendously valuable class of solvents for chemists, due to their ability to solvate a wide variety of compounds, and promote various chemistries through their high polarities.[27] However, many of the most common polar aprotic solvents, such as dimethylformamide (DMF), dimethylacetamide (DMA) and *N*-methylpyrrolidone (NMP), present human reproductive toxicity and are therefore coming under increasing regulatory constraint. They are also a major environmental concern, as their use is often associated with generating large quantities of mixed aqueous/organic waste. The preferred disposal of which is incineration, this is not only energy intensive but releases nitrogen and sulfur oxides (NO_x and SO_x).[27] Given the utility of these solvents the need for less toxic and environmentally damaging replacements is rather apparent. The first half of this thesis will therefore investigate alternatives to conventional polar aprotic solvents, with a particular focus on improving the sustainability of peptide synthesis.

1.3 Green Chemistry and Polymer Synthesis

The second half of this thesis will then look at improving the sustainability of polymer synthesis. Synthetic polymers have come to be ubiquitous in modern society, finding widespread use in packaging, building materials and consumer products, along with specialist applications including medical devices and electronics. This prominence in such a wide variety of roles has meant that synthetic polymers have come to provide a valuable contribution to our current standard of living. Consequently, there is an ever growing demand for these materials, with synthetic polymers currently produced on a scale of more than 300 million metric tonnes annually.[28] However, this growing demand has also highlighted a number of environmental concerns associated with both the raw materials used to make them and their end-of-life.

Due to their predominantly bulk, low value applications, synthetic polymers are overwhelmingly derived from non-renewable petrochemical feedstocks. In fact, their use accounts for 8% of the global crude oil and gas production, the second largest sector behind fuels.[29] Moreover, the short lifetime of most plastic products results in the generation of large quantities of waste, with current estimates suggesting that of the approximately 8.3 billion metric tonnes of plastic produced between 1905 and 2015, 30% is still in use, 60% has been discarded (landfill or to the environment), and the remaining 10% is either incinerated or recycled.[30] The vast quantity that is discarded is a major concern, as issues surrounding bioaccumulation, particularly in aquatic environments, are only now starting to be realised, presenting physical and chemical hazards that are currently not fully understood.[31]

Whist there appears to be no single solution to this array of environmental problems, one option that has begun to receive considerable attention is the synthesis of more sustainable polymers. This is typically achieved through either replacing petrochemically derived raw materials with renewable ones, such as biomass, or developing alternatives that are more amenable to recycling or biodegradation.[32] In principle, this appears to be a simple idea, but in reality it is a rather complex one. Whilst it is obvious there is a demand for more environmentally benign polymers, these sustainable polymers will need to present more favourable economic or material properties, if they are to be favoured over petrochemically derived polymers. It is probably for this reason that currently only 1.7 million metric tonnes (ca. 0.6%) of polymers produced globally can be regarded as bio-based.[32] Consequently, there has been great interest in recent years, within both academia and industry, in the development of renewable polymers that meet these social, economic, environmental and material needs. This is generally achieved *via* two distinct methods, either the development of sustainable routes to monomers chemically

equivalent to those derived from petrochemical sources, termed bioreplacement, or the synthesis of novel structures from biomass as new sustainable monomer species, termed bioadvantage.[33] Approaches for the synthesis of sustainable polymers from four promising renewable raw materials, carbon dioxide, terpenes, vegetable oils and carbohydrates, will therefore now be highlighted in more detail.

1.3.1 Carbohydrates

Carbohydrates represent the most abundant group of natural polymers on the planet.[34] Each year, more than 150 billion tonnes of these polysaccharides are naturally produced, of which humans currently only consume 1%.[32] This high abundance, combined with their biocompatibility, nontoxicity and biodegradability means they have long been utilised by humans, for uses such as clothing and paper, or modified to produce fibres (rayon) and films (cellophane).[35] The fact that only 1% of naturally produced carbohydrates are currently utilised makes them a highly promising raw material for the future polymers market.

More recent approaches to carbohydrate utilisation in polymer synthesis has focussed on their deconstruction to their constitute monomers, which have been widely utilised as precursors for a number of promising platform molecules. In 2004, the US Department of Energy (DOE) highlighted a number a promising platform molecules, on the grounds of their availability and ability to be transformed into useful products.[36] Some examples include, 2,5-furandicarboxylic acid (FDCA), glycerol and aspartic acid. These molecules have since inspired a great deal of research into their use, or derivatisation, for the synthesis of polymers from renewable raw materials. Perhaps one of the most interesting examples of this is the current contest between the bioadvantage or bioreplacement approach to sustainable soft drink bottles.

Traditionally, soft drink bottles were composed of petrochemically derived polyethylene terephthalate (PET) **1.23**, formed through the polycondensation of ethylene glycol **1.21** and terephthalic acid **1.22** (Scheme 1.4). PET for this purpose, is annually produced on a scale of 15 million metric tonnes, or 5.9% of global plastic production.[37] In 2009, the Coca Cola Company announced that they would switch to using bio-derived ethylene glycol **1.21**, producing PET that was roughly 30% bio-based. The current aim is to eventually be able to produce 100% bio-based PET through the development of a route to bio-derived terephthalic acid **1.22**. Alternatively, Avantium have developed poly(ethylene furanoate) **1.25** (PEF), a 100% biobased alternative to PET, formed through the polycondensation of ethylene glycol **1.21** and 2,5-furandicarboxylic acid **1.24** (FDCA) (Scheme 1.4). PEF **1.25** has been shown to have better gas barrier properties than PET and is currently in development for use in soft drink bottles.[32]

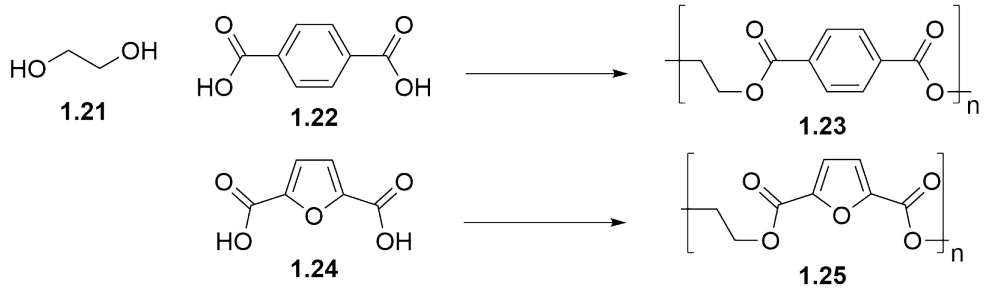

Scheme 1.4: Polycondensation of ethylene glycol **1.21** with terephthalic acid **1.22** or FDCA **1.24** to produce PET **1.23** or PEF **1.25**.

1.3.2 Terpenes

Another very interesting source of renewable platform molecules from biomass are terpenes. Terpenes are a family of unsaturated aliphatic structures **1.9**/**1.26-1.29** linked by a common isoprene unit (Figure 1.3).[38] These structures are predominantly derived from turpentine, the volatile fraction of pine resins, which is currently produced on a 0.3 kilotonnes scale annually. The exception being D-limonene **1.9** which is most commonly extracted from citrus peel waste, on an scale of 0.7 kilotonnes.[32] Whilst current annual production of terpenes is rather modest, they are highly abundant and fairly inexpensive. For this reason, they are currently widely utilised as key components of fragrances, pharmaceuticals, solvents and flavours. They are therefore also rather ideal structures for the synthesis of bio-based polymers. Whilst they have attracted a large amount of interest in recent years, from academia and industry alike, commercialisation of terpene based polymers is fairly limited.[34] The most commonly reported example being the use of thermoplastic polyterpene resins in adhesives and coatings, which has been in commercial production since 1938.[32]

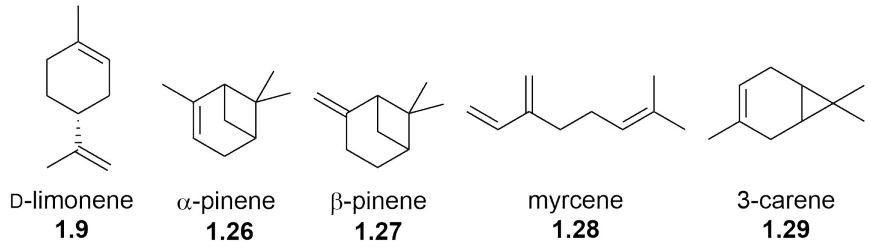

Figure 1.3: Chemical structures of some common terpenes **1.9**/**1.26-1.29**.

1.3.3 Vegetable Oils

Vegetable oils, are also a particularly promising source of monomers for renewable polymers, as they are already produced on a very large scale. In 2012 for example, 156 megatonnes of triglycerides were produced, whilst the majority of this was

used for food or biofuel, 20 megatonnes was used a chemical feedstock.[32] Whilst almost all plants contain triglycerides to some extent, a major issue with their use is the fact that the quantity available is typically rather limited, with even common feedstocks, such as soybeans, containing only 20 wt% of triglycerides.[34] Additionally, the chemical composition of the triglycerides will vary significantly from crop to crop. Despite this, there are currently a number of industrial processes utilising vegetable oils, such as linoleum or the use of epoxidised oils in resins and coatings. Another rather interesting example is the production of 100% bio-based polyamide nylons derived from castor oil. The oil is first hydrolysed to give glycerol **1.31** and ricinoleic acid **1.30** (Scheme 1.5).[39] The ricinoleic acid **1.30** then undergoes pyrolysis and a number of additional chemical steps, to produce 11-aminoundecanoic acid **1.32**. This is then polymerised to produce nylon-11 **1.33**, which has been widely utilised in engineering and automotive applications.[39]

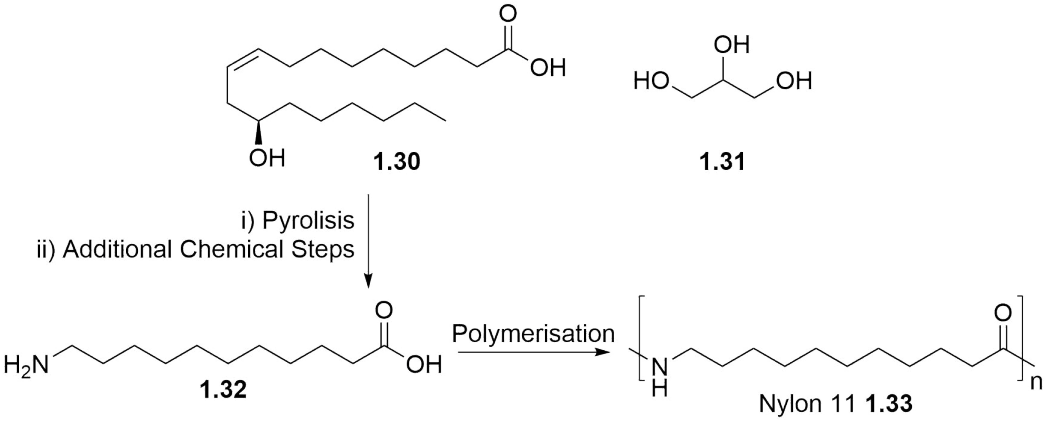

Scheme 1.5: Synthetic route to nylon-11 **1.33** from castor oil derived ricinoleic acid **1.30**.

1.3.4 Carbon Dioxide

The last three categories have all described sustainable feedstocks sourced from biomass. In addition to biomass, carbon dioxide represents a highly promising renewable feedstock for the future bio-economy. This is because carbon dioxide is highly abundant, inexpensive and non flammable, it is also a common by-product of many chemical processes. Additionally, growing concerns over atmospheric carbon dioxide levels have facilitated interest in the use of carbon dioxide within synthetic chemistry. Methods for the valorisation of carbon dioxide as a C_1 building block are rather limited at present, with only the synthesis of urea, salicylic acid and some cyclic carbonates viably produced from CO_2.[40] There is however growing interest in the utilisation of CO_2 for the alternative copolymerisation of epoxides **1.34** and carbon dioxide **1.35**, producing aliphatic polycarbonates **1.36** containing between 30-50 wt% CO_2 (Scheme 1.6).

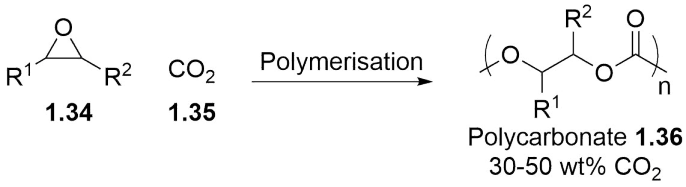

Scheme 1.6: Polycarbonate synthesis through the ring-opening copolymerisation of epoxides **1.34** and carbon dioxide **1.35**.

This process is currently on the verge of commercialisation for a number of applications.[41] The primary one being the production of low molecular weight polycarbonate polyols, which are utilised predominantly in the production of polyurethanes, used to make furniture foams, adhesives and resistant coatings. Alternatively, high molecular weight polycarbonates are already used as binders, and sacrificial materials in fabrication.[41] Early observations are particularly promising, with the use of waste carbon dioxide having been shown to have no detrimental impact on the final product. Life cycle assessment has also shown that polyol synthesis using copolymerisation would lead to a 11-20% reduction in emissions and depletion of fossil resources, compared to the epoxide homopolymerisation.[41]

It is apparent from the aforementioned work that investigations into the use of bio-derived or similarly renewable monomers for sustainable polymer synthesis is a particularly active field of investigation. It is rather surprising then, that despite the current demand for polymeric materials that bio-derived polymers contribute so little (ca. 0.5%). This is most likely due to the need of sustainable polymers to provide both an economic or performance advantage to be preferred over petrochemically derived polymers. This suggests that additional research is necessary. The second half of this thesis will therefore investigate approaches to improving the sustainability of polymer chemistry. This will particularly focus on building upon work investigating the use of itaconic anhydride and furfuryl alcohol, both promising platform molecules, which have been shown to produce a novel monomer structure suitable for ring-opening metathesis polymerisations.

1.4 Thesis Objectives

The core objectives of this thesis are therefore to investigate routes to improving the sustainability of peptide and polymer synthesis, using methods revolving around the use of alternative solvents and bio-based platform molecules. It has made most sense to divide this body of work into four distinct chapters, the first two dealing with the use of alternative solvents in solid-phase synthesis, with a particular focus on peptide chemistry, whilst the last two look at the ring-opening metathesis polymerisation of a novel bio-based molecular framework. Due to the wide variation in topics covered

the relevant background for each chapter will be introduced in more detail in due course. The objectives for each chapter are however as follows:

Firstly, Chapter 2 will explore the use of cyclic carbonates as promising replacements to conventional polar aprotic solvents. This will start with solution-phase peptide synthesis, with the aim of demonstrating the tolerance of cyclic carbonates to the common chemistry associated with this methodology. Following this, the use of cyclic carbonates in solid-phase peptide synthesis methodology will be investigated, with the principal aim of producing a biologically relevant peptide.

Chapter 3 will then look at building on this work, extending the use of green solvents to general solid-phase organic synthesis. It will then attempt to better understand the factors that influence solvent suitability for this chemistry, through the development of a computational model, and experimental verification.

Moving on to the second half of this thesis, Chapter 4 will focus on the use of a novel bio-based molecular framework in ring-opening metathesis polymerisation. Functionalisation of this framework with amines, to produce the corresponding amides, will be attempted. The eventual aim is the production of fully bio-based monomers derived from amino acids or peptides for material or therapeutic applications.

Finally, an unusual spirocyclic species was identified during the previous investigation. Chapter 5 will therefore look to better understand how this species forms, and whether it holds any potential within polymer chemistry or therapeutics.

Chapter 2

Cyclic Carbonates as Solvents for Peptide Synthesis

2.1 Introduction

2.1.1 Peptides and Peptide Synthesis

Peptides, routinely defined as macromolecules consisting of between 2-50 amino acids, are ubiquitous in nature. More than 7000 naturally occurring peptides have been identified, with many playing crucial roles in an array of physiological processes, including as hormones, neurotransmitters, growth factors and anti-infectives, to name but a few.[42] Peptides have been recognised as being highly specific in their binding to *in vivo* targets, resulting in them being highly potent and very selective, whilst having very few negative side effects. However, limitations due to their short plasma half-life and negligible oral bioavailability have previously hampered their application as therapeutics.[43] Recent developments in formulation and novel delivery systems have since revitalised interest in this field.[44] Currently, more than 60 peptide therapeutics have been approved for use in the United States, with 150 currently in clinical development and 260 in human clinical trials.[43] A market that was estimated to be worth US$14.1 billion in 2011 and is expected to grow to around US$25.4 billion by 2018.[42]

Commercial scale manufacture of therapeutic peptides was however initially a very expensive and inefficient process. The breakthrough came with Fuzeon, a treatment for human immunodeficiency virus (HIV) developed by Roche, which demonstrated for the first time that the synthesis of a 36-amino acid peptide on a ton-scale was indeed financially viable.[45] Nowadays, a number of methods exist for the commercial scale production of peptides, which can be divided into two distinct categories, chemical synthesis and biological manufacturing.[46] The choice of which to use is dependent on many factors including, sequence length, degree of modification and scale. Generally, the majority of peptide drugs are produced by chemical methods, this is due to flexibility, as the incorporation of unnatural D- and synthetic-amino acids is not routinely possible with methods based on biotechnology.[45] For this reason, this chapter dealing with improving the sustainability of peptide synthesis will exclusively deal with the chemical approach.

Two distinct methodologies exist for the chemical synthesis of peptides, solution-phase and solid-phase. Others do exist, such as hybrid approaches and chemoselective ligation, but are less explored.[46] Solution-phase synthesis couples suitably protected peptide fragments or single amino acids in solution. Each intermediate is then isolated, allowing for analysis and purification. This method benefits from the relatively cheap building blocks, but is particularly laborious. Consequently, solution-phase peptide synthesis is typically used for small- to medium-length peptides in quantities of hundreds of kilograms to metric ton scale.

The solid-phase approach differs in that one of the amino acids is anchored to an insoluble polymer support, the peptide sequence is then built by coupling protected amino acids to the solid-support. Intermediates are not isolated, and impurities and excess reagents are simply removed by filtration. Once the target sequence has been built it is easily cleaved from the solid support. The simplicity of the solid-phase approach makes it particularly amenable to automation, meaning it is far quicker than the solution-phase approach for the synthesis of long chain peptides.

However, when considered in the context of green chemistry, both solution- and solid-phase peptide synthesis are inherently wasteful processes. The need for a multitude of auxiliary reagents, including protecting groups, solvents and coupling agents, means peptide (or amide) bond formation is characterised by incredibly poor process mass intensity, generating large quantities of waste. In fact, estimates suggest the manufacture of 1 kg of peptide active pharmaceutical ingredient (API) can easily result in 1000 L of waste, although in the majority of cases it is probably significantly more.[44] As previously discussed, solvent use will routinely account for between 80-90% of waste by mass in a typical batch pharmaceutical/fine-chemical operation.[15] Additionally, amide bond forming reactions are typically carried out in highly undesirable solvents, with 86% being performed in either CH_2Cl_2 (36%) or common polar aprotic solvents, such as DMF, NMP or DMA (47%).[47] Although, SPPS is nowadays almost exclusively performed in DMF. This is particularly concerning, due to the number safety issues presented to humans with regards to the use of DMF, which includes, hepatotoxicity, alcohol intolerance, possible embryotoxicity and teratogenicity.[48] Furthermore, there are a number of environmental issues associated with DMF, as its use typically produces large quantities of mixed aqueous/organic waste.[15] This waste is both difficult to separate and costly to dispose of, as high nitrogen content makes discharge to waste water problematic, whilst high water content necessitates the addition of fuel in order to incinerate it, releasing NO_x in the process.[27,49] Finally, both DMF and NMP are highlighted as two of 174 chemicals regarded as substances of very high concern (SVHC), under EU Registration, Evaluation and Authorisation of Chemicals (REACh) legislation, and are therefore likely to face restrictions to their use within the next few years.[50]

It is therefore apparent that the biggest contributor to the environmental impact of peptide synthesis is overwhelmingly from the solvent. The biggest gains in terms of reducing environmental impact will therefore come from optimisation of the solvent, rather than changes to the chemistry. For these reasons, it was felt that the issue of solvent use in peptide synthesis needed to be addressed, in an effort to develop a more sustainable approach to peptide synthesis. It is worth noting that Amgen Inc. and Bachem have recently been awarded the 2017 Green Reaction Conditions

Award by the Environmental Protection Agency (EPA) for their improvements to the synthesis of Etelcalcetide, a peptide therapeutic used for the treatment of secondary hyperparathyroidism.[51] The improved process saw a reduction in solvent waste of 71%, manufacturing operating time of 56% and manufacturing cost of 76%. Ultimately, eliminating 1,440 m^3 of waste, 750 m^3 of which was aqueous waste. Herein, the various literature reports of sustainable peptide synthesis in both solution- and solid-phase, that specifically utilise a green solvent, will be addressed, in an effort to highlight that there is still substantial scope for an investigation into the use of alternative solvents for improving the sustainability of peptide synthesis.

2.1.2 Greener Solvents for Peptide Synthesis

2.1.2.1 Solution-Phase Peptide Synthesis

Water

The use of water represents a highly desirable solvent choice as it is safe, cheap and environmentally benign. Its use has been a long standing challenge in peptide chemistry, as chemists tried to best replicate classical biosynthesis by chemical means. However, poor solubility of common reagents and the susceptibility of the activated intermediates to hydrolysis, means peptide synthesis in water is rather problematic. Since the 1950s a wide variety of approaches have been reported in an effort to overcome these limitations, including the development of water-soluble protecting groups,[52,53] coupling agents[54,55,56,57] and water-compatible dehydrating agents.[58] Many of these however, suffer from limited scope, necessitate the use of organic co-solvents or require extensive derivatisation.

More recent developments have sought to overcome these issues through the development of novel technologies and reagents to enable solution-phase peptide synthesis in water. A rather interesting example from Hojo *et al.* has shown that amino acids with conventional Fmoc- or Boc-protection can be utilised without derivatisation.[59] The protected amino acids were wet milled in water using a planetary ball mill and polyethylene glycol (PEG) as a dispersant, generating dispersed nanoparticles. These nanoparticles were then used in the synthesis of Leu-enkephalin amide (H-Tyr-Gly-Gly-Phe-Leu-NH_2). Coupling was performed using the water-dispersed nanoparticles of the appropriate Boc-amino acid in the presence of 4-(4,6-dimethoxy-1,3,5-triazin-2-yl)-4-methylmorpholinium chloride (DMTMM) in neat water for 12 hours at room temperature. Whilst the deprotection steps were performed using 4.0 M HCl in dioxane, which is undesirable, the target peptide was obtained in 51% total yields over 9 steps. Additionally, minimal purification was required as excess reagents were easily removed through filtration after coupling.

Similarly, Mahindra *et al.* have shown that Boc- and Fmoc-protected amino acids can be used without derivatisation in neat water, when used in conjunction with microwave assisted heating.[60] Coupling was performed using *O*-(benzotriazol-1-yl)-*N*,*N*,*N*',*N*'-tetramethyluronium tetrafluoroborate (TBTU), 1-hydroxybenzotriazole hydrate (HOBt) and *N*,*N*-diisopropylethylamine (DIPEA) with either Boc- or Fmoc-protected amino acids **2.1** (Scheme 2.1). The reagents were poorly soluble at the start of the reaction, but produced a homogeneous solution after heating to 60 °C for 30 mins in a microwave. A range of peptide sequences **2.3** were investigated, typically producing the desired product in good to excellent yield and purity. Finally, the microwave-assisted synthesis of pentagastrin (Boc-HN-Gly-Trp-Met-Asp-Phe-NH_2), a bioactive peptide that stimulates the secretion of gastric acid, was investigated. The developed methodology was able to produce the target sequence in 42% overall yield and excellent purity.

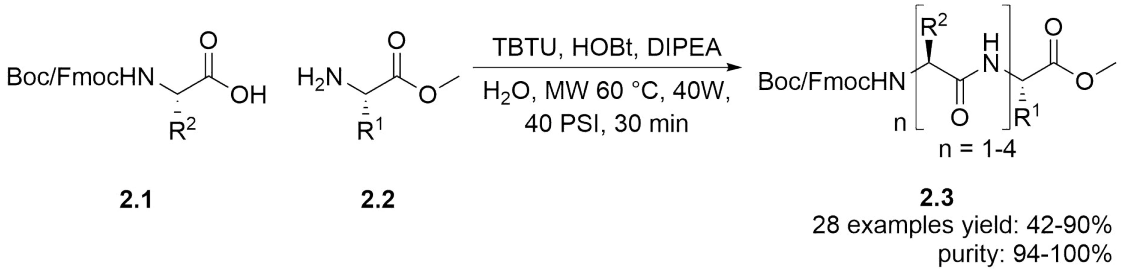

Scheme 2.1: Microwave-assisted solution-phase peptide synthesis in water using Boc- and Fmoc-amino acids.

Finally, Lipshutz and co-workers have reported on a very interesting example utilising micellar "nanoreactor" technology for aqueous solution-phase peptide synthesis.[61] TPGS-750-M **2.7** is a surfactant known to spontaneously assemble into nanomicelles in water. It is these micelles that act as a "nanoreactor", solvating water-insoluble reagents. A range of di- to tetra-peptides **2.6** were prepared using this approach, with a combination of (1-cyano-2-ethoxy-2-oxoethylidenaminooxy)-dimethylaminomorpholino carbenium hexafluorophosphate (COMU) and 2,6-lutidine used for coupling (Scheme 2.2). Using this approach the reactions were found to be complete in 0.5-4.0 hours, with excellent yields obtained for all examples. Lipshutz and co-workers also highlighted that the reaction by-products are very soluble in water, meaning the product can easily be isolated using a small quantity of organic solvent (*i*-PrOAc). Additionally, the aqueous phase can be recycled multiple times using this method, which resulted in incredibly low E-factors of just 2.8 for peptide bond formation.

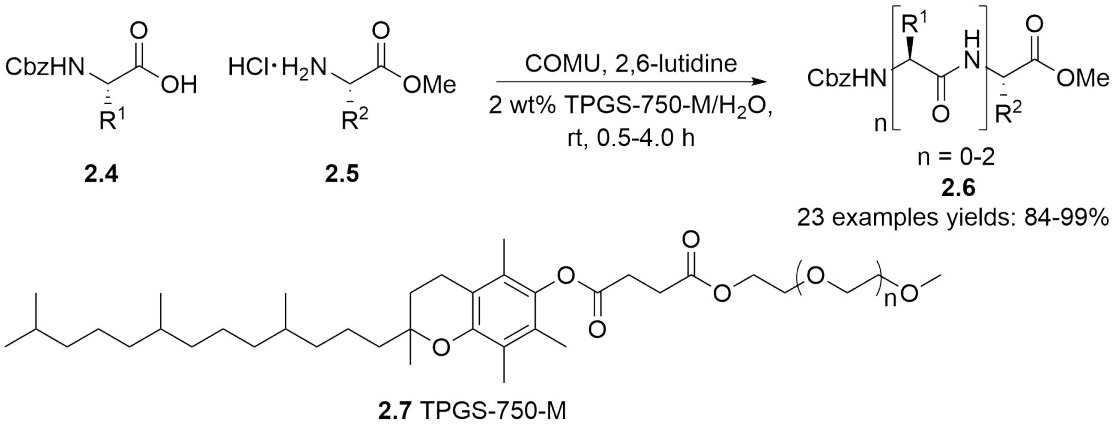

Scheme 2.2: Peptide bond formation in neat water using TPGS-750-M **2.7** under micellar catalysis conditions.

In a subsequent paper, Lipshutz and co-workers have further built upon their micellar "nanoreactor" concept. As previously mentioned, solution-phase peptide synthesis suffers from the laborious isolation and purification of intermediates. Cortes-Clerget *et al.* have therefore looked to enhance the process efficiency by improving the step-economy. The aim was to be able to perform both deprotection and coupling reactions in a one-pot process, using micellar catalysis conditions for both steps (Scheme 2.3).[62] This was done by first performing deprotection of the *N*-terminus **2.8**, by hydrogenation of the Cbz-protecting group. The addition of HCl was necessary to generate the amine salt, as formation of the free amine seemed to inhibit further catalysis through what was believed to be strong chelation. Argon was then bubbled through the reaction mixture to remove any residual HCl, before coupling could be performed using **2.9**, COMU and 2,6-lutidine. A range of peptides **2.10** were prepared in good yield using this method, up to a decapeptide using a convergent strategy. Coupling did however require addition of THF (10%) as a co-solvent, but the methodology does represent a novel and very interesting approach for developing sustainable peptide synthesis in water through enhanced step-economy.

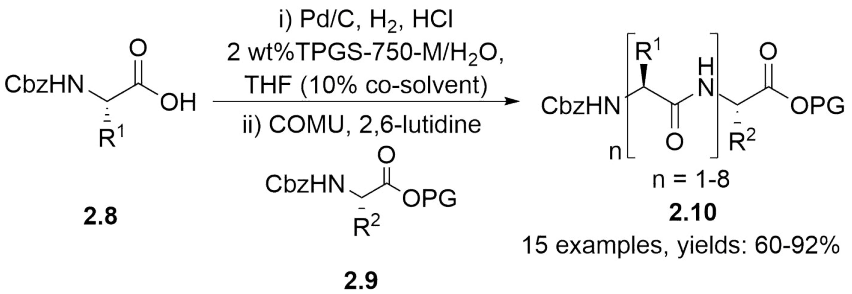

Scheme 2.3: Tri- to deca-peptide synthesis using a tandem deprotection/coupling process under TPGS-750-M **2.7** micellar catalysis conditions.

Chemoenzymatic Peptide Synthesis

Another highly explored method for performing peptide bond formation in water is the chemoenzymatic one. Chemoenzymatic synthesis traverses the line between the chemical and biological approach to peptide synthesis, but is worth mentioning, particularly in the context of sustainability. It is the catalytic formation of peptide bonds using protease enzymes. This approach has been utilised for several decades and has attracted a large amount of interest during this time.[63] This interest is due to the many advantages it holds over the chemical approach. Namely, peptide bond formation occurs in a very stereo- and regio-specific manner, will often tolerate incorporation of non-protected functional groups and occurs under very mild and benign reaction conditions.[64] However, it is not without its limitations, the specificity typically means the synthesis of peptides much longer than a dipeptide is a substantial challenge. Optimisation can also be particularly laborious, due to variations in enzyme activity being strongly influenced by many factors, such as pH, temperature, solvent and additives. Additionally, the equilibrium for amide bond formation using protease enzymes, in water, lies largely towards hydrolysis, rather than aminolysis. A complete review of this field along with adequate explanations for overcoming the hydrolysis equilibrium is much beyond the scope of this report, and these topics have been excellently reviewed elsewhere.[65,66] However, some recent publications have acknowledged that neoteric reaction media can be particularly useful for promoting peptide bond formation using hydrolyse enzymes, which are worth highlighting.

The first example of this was reported by Noritomi *et al.* and their use of supercritical carbon dioxide ($scCO_2$)/acetonitrile (MeCN) solvent mixtures for enzyme catalysed peptide bond formation.[67] *N*-Acetyl-L-tyrosine ethyl ester **2.11** and various amino acid amides **2.12** were coupled using an α-chymotrypsin enzyme, in either MeCN or a mixture of $scCO_2$/MeCN (Scheme 2.4). In all cases, observed yields for the peptides **2.13** were significantly improved when a mixed solvent system was used, rather than MeCN by itself. This is justified on the basis that sedimentation of the enzyme in suspension means catalysis generally becomes a diffusion-controlled process. The use of $scCO_2$ is therefore believed to improve diffusion, significantly enhancing catalysis. This appears to be a rather isolated example, as the use of supercritical carbon dioxide for enzymatic peptide bond formation has not been explored to any great degree since this initial communication.

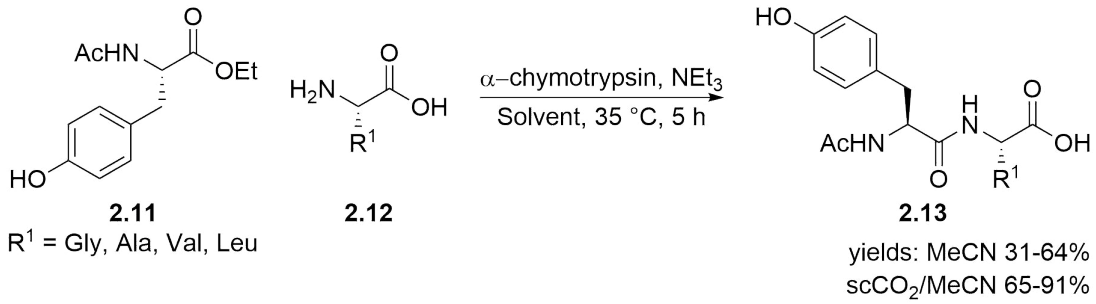

Scheme 2.4: α-Chymotrypsin catalysed peptide bond formation using either MeCN or a mixed $scCO_2$/MeCN solvent system.

More recently, Erbeldinger *et al.* have shown that ionic liquids (ILs) are a suitable reaction media for the chemoenzymatic synthesis of peptides.[68] The natural sweetener derivative Z-aspartame **2.17** was synthesised from carbobenzoxy-L-aspartate **2.14** and L-phenylalanine methyl ester hydrochloride **2.15** through a thermolysin catalysed process, using a 1-butyl-3-methylimidazolium hexafluorophosphate [BIMI][PF_6] **2.16** ionic liquid as the reaction medium (Scheme 2.5). The target peptide was obtained in 95% yield, a result which is comparable to results typically reported for conventional organic solvents. More importantly, due to the significant cost of the solvent used, Erbeldinger *et al.* demonstrated that the IL could be recycled multiple times, with minimal leeching of the target product.

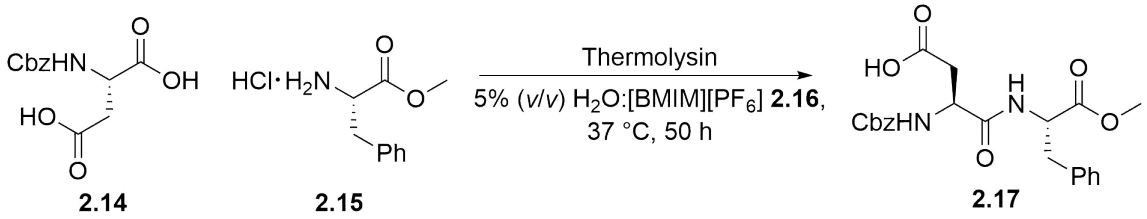

Scheme 2.5: Thermolysin-catalysed synthesis of Z-aspartame **2.17** in [BMIM][PF_6] **2.16** containing 5% (v/v) water.

Following the report by Erbeldinger *et al.* the use of ionic liquids in peptide synthesis has been rather limited, even though they have been highlighted as highly promising solvents on a number of occasions.[69,70] This is most likely due to difficulties in finding a suitable extraction protocol for separating the products from the IL.[71] Additionally, most of the focus has been on the chemical approach to peptide bond formation, rather than the chemoenzymatic one. Most of these reports demonstrate the suitability of various IL cation/anion combinations, which tend to show comparable results to traditional organic solvents. It therefore seems unnecessary to cover this field in considerable detail, particularly since it has been reviewed fairly extensively only recently.[70,71]

Solvent Free Peptide Synthesis

Finally, the use of no solvent would of course be the greenest protocol in terms of minimising solvent waste in solution-phase peptide synthesis. Whilst this is not practical in many cases, Lamaty and co-workers have shown that peptide synthesis in the solid state is possible using ball-milling technology.[72] Amino acids **2.19** were coupled using urethane-protected α-amino acid *N*-carboxyanhydrides (UNCA) **2.20** in the presence of $NaHCO_3$ (Scheme 2.6). The reaction mixture was agitated for 1 hour using steel balls at a frequency of 30 Hz. In this time quantitative conversions were typically obtained, with a diverse range of peptides **2.20** isolated in good to excellent yields following purification. The use of UNCAs is a rather interesting approach, as in this class of mixed anhydride the amino group is protected whilst the carboxylate is simultaneously activated. This means the majority of reagent mass is incorporated into the final peptide, resulting in a very atom economical procedure.

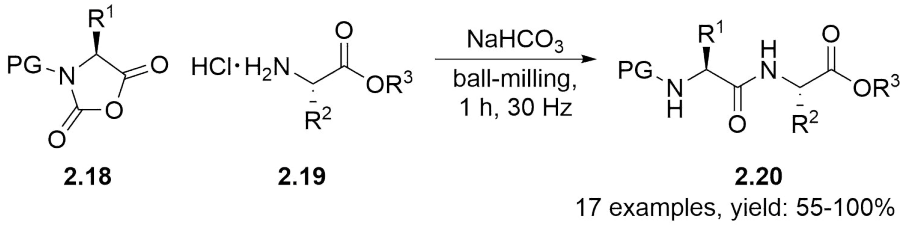

Scheme 2.6: Synthesis of dipeptides under solvent-free ball-milling conditions using urethane-protected α-amino acid *N*-carboxyanhydrides **2.20**.

The original report only demonstrated the synthesis of short di- and tri-peptides, Bonnamour *et al.* have since looked to extend this methodology, to longer sequences and on a larger scale.[73] This however presented an initial problem, as increasing the milling load to 22.5 mg mL^{-1}, from 5.9 mg mL^{-1}, caused serious mass transfer limitations, significantly reducing yields. To remedy this, the addition of small quantities of EtOAc (1.4 μL mg^{-1}) was necessary. The pentapeptide Leu-enkephalin was then synthesised using this liquid-assisted ball-milling approach, with the target peptide obtained in an excellent 46% total yield over the 9 steps.

It is also worth highlighting a recent report from Maurin *et al.*, that directly compares the green credentials of ball-milling, against the more traditional solution- and solid-phase approaches.[74] The VVIA tetrapeptide (H-Val-Val-Ile-Ala-OH) **2.21** was synthesised using all three methods (Table 2.1). Overall, the ball-milling approach produced the target peptide in 59% yield and 88% crude purity. A result that is comparable to the solid-phase approach and significantly better than the solution-phase one. The major advantage of the ball-milling technology is more obvious when the E-factors are considered, with E-factor being defined as the ratio

of the mass of waste per mass of product. Maurin *et al.* showed that the solid-phase approach to peptide synthesis produced 80 times more waste than the ball-milling approach. Maurin *et al.* also noted than the cumulative number of risk phrases for the ball-milling approach was more favourable than both solution- and solid-phase methods. The final conclusion was that, in terms of peptide yield and purity, ball-milling can be considered comparable to that of solid-phase for the synthesis of long peptides, but presents a much more desirable approach for environmental reasons.

Table 2.1: Yield and purity comparison for the synthesis of the VVIA peptide **2.21** by ball-milling-, solution- and solid-phase peptide synthesis.

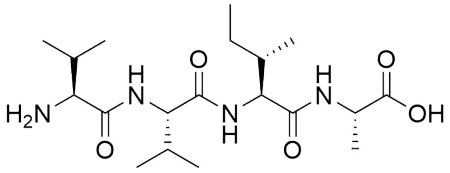

2.21

	Ball-milling		Solution		Solid	
Peptide	Yield[a]	Purity	Yield[a]	Purity	Yield[a]	Purity
Boc-IA-OBn	**89%**	93%	88%	**96%**	-	-
AH·H-IA-OBn	>99%[b]	97%[b]	>99%[c]	99%[c]	-	-
Boc-VIA-OBn	**89%**	**99%**	77%	90%	-	-
AH·H-VIA-OBn	96%[b]	**97%**[b]	**>99%**[c]	92%[c]	-	-
Boc-VVIA-OBn	**78%**	**88%**	64%	85%	-	-
Overall	**59%**	88%	43%	85%	**54%**[d]	**96%**[d]

[a] Isolated yield.[b] HCl.[c] TFA salt.[d] Obtained as TFA·H-VVIA-OH. Result highlighted in bold represents the best result for each peptide sequence.

Building on their work on microwave-assisted peptide synthesis mentioned previously Mahindra *et al.* have also recently reported an example using a solventless approach.[75] Coupling was performed using *N*,*N*'-diisopropylcarbodiimide (DIC) *N*-hydroxy-5-norbornene-2,3-dicarboximide (HONB) and DIPEA 60 °C under microwave irradiation (Scheme 2.7). No solvent was necessary, and coupling was found to be complete in only 15 minutes. Yields and purities were typically found to be excellent, however a slight drop in yield was observed when coupling longer peptide species. Mahindra *et al.* then used the methodology to prepare the therapeutic pentapeptide Thymopentin (H-Arg-Lys-Asp-Val-Tyr-OH) or TP-5. The total synthesis of which was complete in 10 steps, with an overall yield of 53% and a purity of 97%.

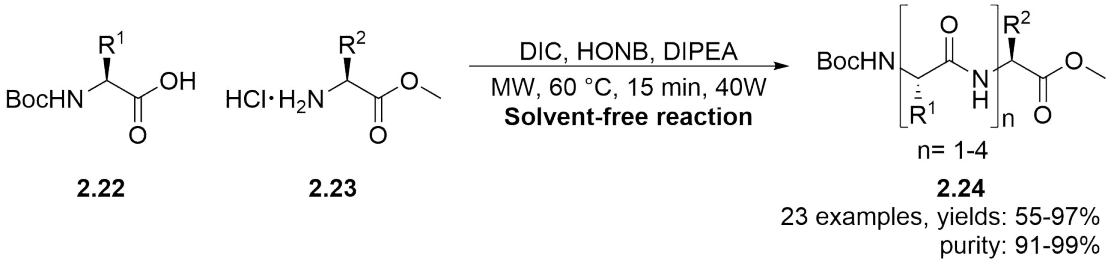

Scheme 2.7: Solvent-free peptide synthesis assisted by microwave irradiation.

Finally, Hernandez *et al.* have combined many aspects of some of the more popular solution-phase methodologies in their mechanoenzymatic approach to sustainable peptide synthesis.[76] Peptide bond formation was catalysed using the cysteine protease papain. The biocatalyst was found to be tolerant to the mechanical stress of ball milling, facilitating peptide bond formation in the absence of a solvent in 2 hours. A diverse range of α,α- **2.27** and α,β-dipeptides **2.28** were generated in moderate to high yields (Scheme 2.8). Whilst yields varied substantially with the substrate this process represents a really interesting approach to sustainable peptide synthesis. Due to the use of a biocatalyst and a mixing method that requires no solvent. It will be interesting to see whether the methodology can be applied to more complicated and longer peptide sequences in the future.

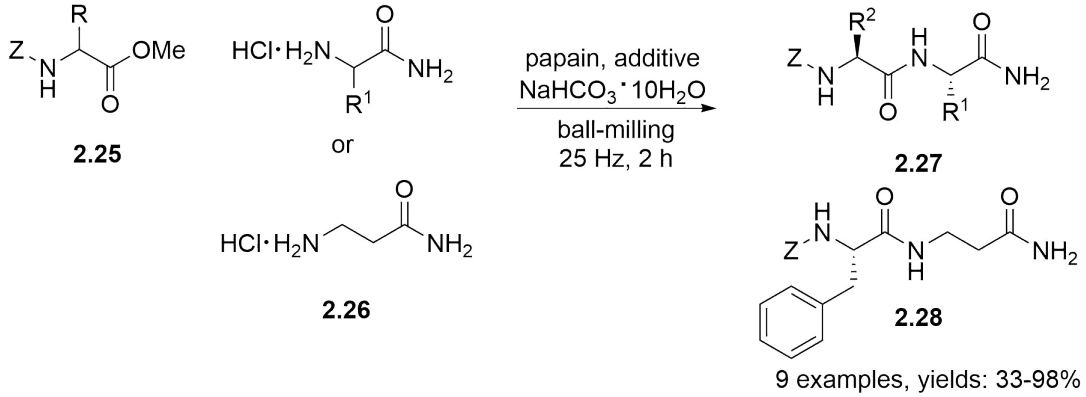

Scheme 2.8: Solvent-free ball milling approach to peptide bond formation catalysed by the cysteine protease papain.

2.1.2.2 Solid-Phase Peptide Synthesis

Nowadays, peptides are more commonly synthesised *via* the solid-phase (SPPS) approach rather than the previously discussed solution-phase method. The use of alternative reaction media for solid-phase peptide synthesis is however rather more challenging. This is because the use of an insoluble solid-support, or resin, places additional considerations on the solvent. Most notably, adequate solvation of the resin, more commonly known as swelling, which is often considered as the most

important prerequisite for SPPS, as inadequate swelling will result in poor active site accessibility and diminished reaction rates. The importance of swelling will be explored in much more detail in a subsequent chapter, for now it is merely important to know that a solvent must be able to solvate the solid-support. This additional complication has meant the use of alternative reaction media for sustainable SPPS is rather limited, with all examples reported within the literature either falling into the category of water or alternative organic solvents.

Water

As was discussed previously, water represents a highly desirable solvent choice for sustainable peptide synthesis. However, its use in SPPS presents an even more substantial challenge than it did for solution-phase peptide synthesis. This is due to the poor solubility of conventional Fmoc-protected amino acids and to the fact that traditionally SPPS was performed on insoluble polystyrene (PS) based resins. Due to the hydrophobic nature of PS, water is unable to adequately solvate the resin, meaning efficient coupling could not be realised. Because of this the use of water in SPPS remained an unexplored challenge for many years.

It was not until the work of Kawasaki and co-workers in 2001 that the entire process of SPPS in water was finally realised.[77,78] This was only made possible however with the advent of PEG-PS hybrid resins, which being amphiphilic in nature are more easily swollen by a wider variety of solvents.[79] However, the issue of classical reagents being poorly soluble and activated intermediates being prone to hydrolysis still remained. Consequently, a range of interesting approaches have been developed to overcome these complications.

One of the most common approaches to overcoming the limitations of SPPS in water, like solution-phase peptide synthesis, has been the development of novel water soluble *N*-protecting groups and coupling agents. The first example of this was reported by Hojo *et al.* with the development of the 2-phenyl(methyl)sulfonio ethoxycarbonyl (Pms) **2.29** protecting group (Figure 2.1). This water soluble *N*-protecting group is easily removed by simply treating the peptide with a 5% sodium bicarbonate solution.[77] Hojo *et al.* then utilised this protecting group in the synthesis of the endogenous opioid peptide Leu-enkephalin amide (H-Tyr-Gly-Gly-Phe-Leu-NH_2). Coupling was performed using water soluble 1-(3-dimethylaminopropyl)-3-ethylcarbodiimide hydrochloride (WSCD) and HONB upon a PEG-grafted Rink amide resin, producing the target peptide in 61% yield. Notably, the addition of 0.2% Triton X, a non-ionic surfactant, was necessary for the coupling and washing procedures to enhance the swelling of the resin. Additionally, the method for

preparing the Pms-amino acids was not initially applicable for Met or Cys, however this was addressed in a subsequent communication.[80]

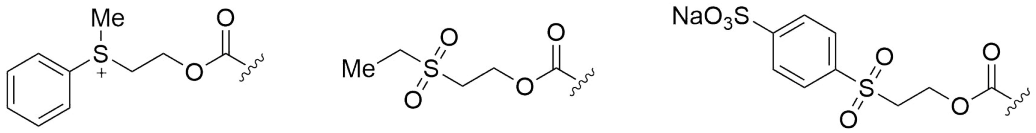

Pms **2.29** Esc **2.30** Sps **2.31**

Figure 2.1: Water soluble protecting groups reported by Kawasaki and co-workers.

The presence of the onium salt in the Pms group meant that unfortunately this protecting group was rather unstable. Kawasaki and co-workers therefore went on to develop a series of additional *N*-protecting groups for SPPS in water (Figure 2.1). The 2-ethanesulfonylethoxycarbonyl (Esc) group **2.30** was found to be moderately base labile and polar, meaning it demonstrated good solubility in both aqueous and organic solutions.[81] The test synthesis of Leu-enkephalin amide was able to produce the target compound in a 71% isolated yield. The lack of aromatic functionality, excluding the aromatic amino acids, made it unsuitable for automated SPPS, as it could not be detected by optical absorbance spectroscopy. Kawasaki and co-workers therefore went on to develop the 2-(4-sulfophenylsulfonyl)ethoxycarbonyl (Sps) **2.31**, which was found to have high base lability and high water solubility, and was used to produce the Leu-enkephalin amide peptide in 61% yield.[82] Whilst these results were highly promising, demonstrating for the first time that SPPS in water was possible, none of the conditions outlined produced Leu-enkephalin amide in an isolated yield greater than control reactions using more conventional methods.

The synthesis of these protecting groups of course comes with additional steps, which is not favourable in the context of green chemistry. Hojo and co-workers have therefore sought an alternative approach that utilises the more conventional, but sparingly soluble, Fmoc- and Boc-protecting groups for SPPS in water. In a similar manner to the approach utilised for solution-phase peptide synthesis Hojo and co-workers have enhanced the solubility of Boc- and Fmoc-amino acids through the preparation of nanoparticle dispersions in aqueous solutions. Fmoc-protected amino acids were milled using zirconium oxide beads and PEG as an aqueous suspension, generating nanoparticles of between 250-500 nm, that were found to be more soluble due to the enhanced surface area.[78,83]

The prepared water-dispersible nanoparticles were then applied to the synthesis of Leu-enkephalin amide, producing the target peptide in 67% yield. Control reactions using the unprocessed amino acids failed to produce the target peptide in any discernible yield. The synthesis of Leu-enkephalin amide was further improved

to 79% through the addition of a non-ionic surfactant (Triton X 0.5%), which is known to enhance the swelling of PEG-PS graft resins in water. It must also be acknowledged that Hojo and co-workers were able to remove excess nanoparticles from the aqueous waste through a simple filtration followed by ultracentrifugation. Subsequent publications from Hojo and co-workers have also gone to demonstrate the application of similar water-dispersed Boc-nanoparticles for SPPS, as well as the use of efficient microwave irradiation for reducing coupling times from 1 h to just 3 min.[84,85]

Galanis *et al.* have also reported an interesting approach to overcoming the limitations of hydrophobic protecting groups in aqueous SPPS.[86] The coupling of Boc-protected amino acids was successfully achieved in water, using water soluble coupling agents WSCD and HONB, under microwave irradiation. The use of the Boc-protecting group is important as they are easily removed under acidic conditions, with Galanis *et al.* using 1N $HCl_{(aq)}$ for the deprotection steps. This represents the first example of SPPS that utilises water for both coupling and deprotection steps. The developed methodology was then applied to the synthesis of Leu-enkephalin (H-Tyr-Gly-Gly-Phe-Leu-OH). Initially, the target peptide was only obtained in a 67% crude purity, but the addition of a non-ionic surfactant (0.5% Trition-X100) resulted in a much improved 81% crude purity.

The chemoenzymatic approach to peptide synthesis in water has also recently been realised for more sustainable SPPS. As previously mentioned, protease enzymes typically favour hydrolysis rather than amide bond formation in water. However, Flitsch and co-workers have shown that by having the amino component affixed to a solid support, in this case a PEGA, a copolymer of PEG and polyacrylamide (PA), the equilibrium can be forced to favour amide bond formation (Scheme 2.9).[87] As is the case with chemoenzymatic amide bond formation, the peptide was formed in a highly enantioselective manner, with only the L,L-diastereomer observed when a racemic acyl donor was used.

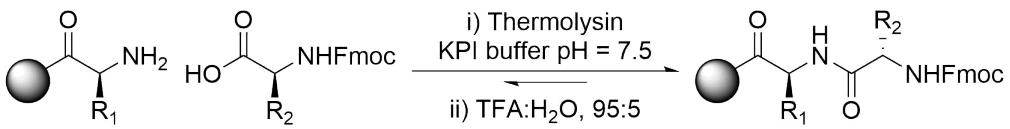

2.32 **2.33** **2.34**

Scheme 2.9: Thermolysin catalysed peptide synthesis upon a solid-support.

Initially, the chemoenzymatic approach for SPPS was restricted to the synthesis of simple dipeptides, with good yields only obtained when hydrophobic amino acids were used.[88] This could be remedied by simply protecting the polar or charged

functionalities with hydrophobic protecting groups. The methodology does present some limitations for the synthesis of longer sequences, as chain growth requires removal of the Fmoc-protecting group using 20% (v/v) piperidine in DMF which is undesirable. Moreover, in the preparation of polyleucine peptides, beyond tetraleucine, the enzymatic hydrolysis of the peptide was observed to compete with amide bond formation, resulting in a mixture of products.

Finally, the use of *N*-carboxyanhydrides (NCAs) **2.35** for SPPS in water has been recently reported by De Marco *et al.* in their synthesis of the opioid tetrapeptide endomorphin-1 **2.36** (H-Tyr-Pro-Trp-Phe-NH_2) (Scheme 2.10).[89] The NCAs were first prepared in quantitative yield from the unprotected amino acid and triphosgene, using a solvent-free microwave assisted process. The synthesis of endomorphin-1 was then performed using the NCAs in a borate buffer (pH=10.4) upon a ChemMatrix-Rammage resin. Washing the resin with citrate buffer (pH=3.0) facilitated the decarboxylation, yielding the free amine for the next coupling. Following assembly of the endomorphin-1 sequence and subsequent cleavage, the peptide was obtained in a 73% crude purity and 52% yield after isolation. Whilst this is a disappointing result, the use of minimal quantities of bulk chemicals, the excellent atom economy and complete removal of all organic solvents represents a highly desirable approach to sustainable SPPS.

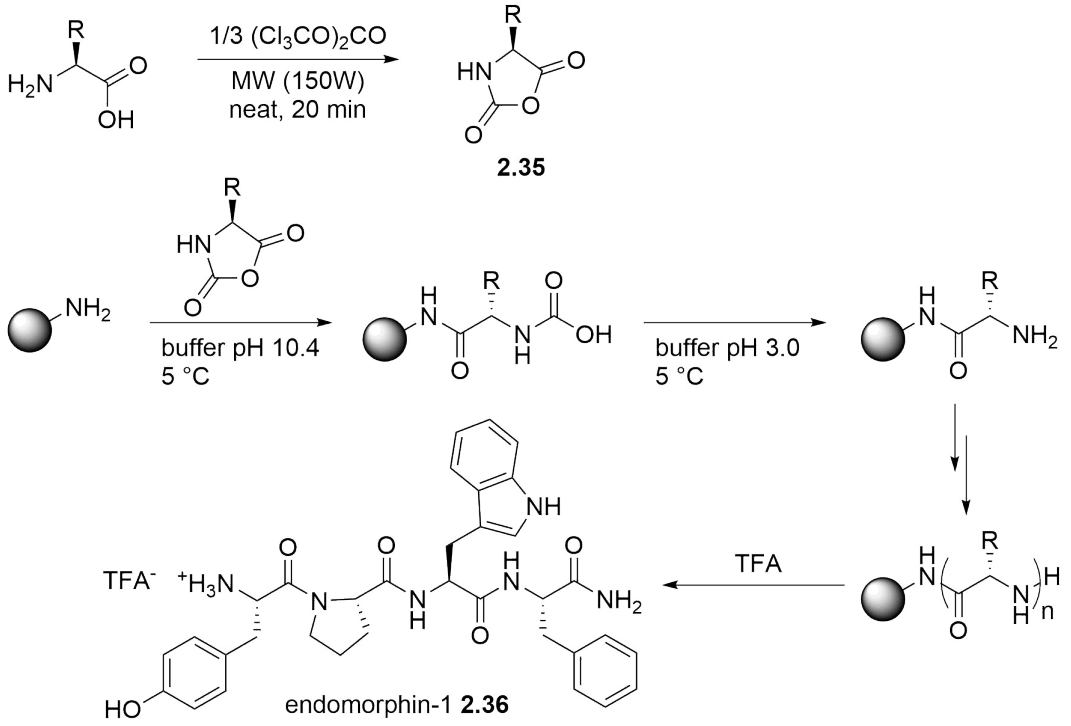

Scheme 2.10: SPPS of endomorphin-1 **2.36** using NCAs **2.35** in an aqueous media.

Alternative Organic Solvents

Whilst water is often cited as the "greenest" solvent, due to the many favourable properties it possesses, its use does not necessarily constitute a benign or "green" process. The contamination of aqueous waste streams with organic compounds or metal catalysts can be a substantial economic and environmental burden, which will vary on a case-by-case basis.[90] More recent approaches to greener solid-phase peptide synthesis have preferred the use of organic solvents that present an advantage in terms of their environmental, health and safety (EHS) characteristics. The use of unconventional solvents, i.e. not DMF, NMP or CH_2Cl_2, for greener SPPS was first explored by Acosta *et al.* in 2009.[91,92] Whilst MeCN is not often considered a green solvent Acosta *et al.* cite that it represents a more desirable and user friendly polar aprotic solvent. This is due to it not being a reproductive toxin and possessing a lower viscosity and boiling point than DMF. The model peptides Leu-enkephalin amide and acyl carrier protein (ACP 65-74) (H-Val-Gln-Ala-Ala-Ile-Asp-Tyr-Ile-Asn-Gly-NH_2) were prepared, using MeCN for both coupling and deprotection reactions upon a Fmoc-Rink-ChemMatrix resin. The use of the ChemMatrix resin was necessary as MeCN was not able to adequately solvate a conventional PS-based resin. Both peptides were obtained in an excellent crude purity of >95%. Subsequently, Albericio and co-workers have investigated a range of more conventional green solvents in SPPS.

A 2015 paper further explored the use of MeCN, along with tetrahydrofuran (THF), in solid- and solution-phase peptide synthesis.[93] Again, THF does not necessarily constitute a green solvent, due to the low boiling point and tendency to form peroxides, but can be considered a usable solvent relative to DMF.[17] Jad *et al.* first studied a series of solution-phase control reactions, using MeCN and THF in combination with DIC and a range of additives **2.37**-**2.40** (Figure 2.2). Overall, both solvents minimised racemisation in the various peptide models, performing better than DMF in the majority of cases. The same solvent and coupling agent combinations were then applied to solid-phase peptide synthesis, with the synthesis of the hindered Aib-enkephalin pentapeptide (H-Tyr-Aib-Aib-Phe-Leu-NH_2) and Aib-ACP decapeptide (H-Val-Gln-Aib-Aib-Ile-Asp-Tyr-Ile-Asn-Gly-NH_2), upon ChemMatrix resin. Misincorporation of one of the Aib residues (des-Aib) is one of the most common side products observed in the synthesis of these peptides. The best results by far were observed when THF was used in conjunction with DIC/OxymaPure **75**, producing Aib-enkephalin pentapeptide in 93.6% yield (des-Aib=6.4%) and the Aib-ACP decapeptide in 69.8% yield (des-Aib=26.8%). Control samples prepared in DMF could only produce the Aib-enkephalin pentapeptide in 53.0% yield (des-Aib=47.0%) and the Aib-ACP

decapeptide in 37.8% yield (des-Aib=34.0%).

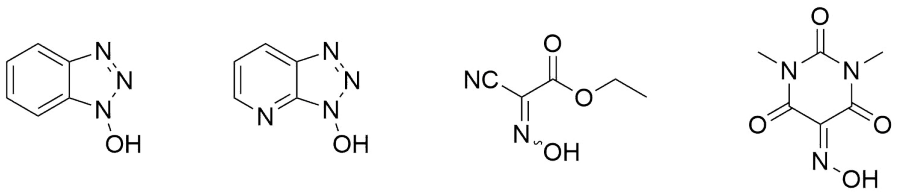

Figure 2.2: Structures of some common coupling additives.

These promising results have since encouraged Albericio and co-workers to report on a diverse range of solvents, the majority of which resemble more classical green solvents. The first example of this looked at the use of 2-MeTHF and cyclopentyl methyl ether (CPME) as more sustainable alternatives to THF.[94] Interestingly, 2-MeTHF and CPME were able to adequately solvate both PS- and PEG-based resins. The synthesis of Aib-enkephalin pentapeptide was therefore investigated in both solvents upon PS and ChemMatrix resins. The use of 2-MeTHF with DIC/OxymaPure **2.39** was found to be optimal, producing the target peptide in 97% yield (des-Aib=3.0%) on the PS resin and 81.9% (des-Aib=18.1%) on the ChemMatrix resin. Whilst Jad *et al.* did still use DMF for the deprotection steps, this work excellently demonstrates that green organic solvents can be viable alternatives to DMF for SPPS.

In an effort to address the use of ungreen solvents in the deprotection steps Jad *et al.*[95] went on to investigate a series of different deprotection and washing protocols, to completely remove the use of ungreen solvents in SPPS. Couplings were performed using the previously optimised conditions of 2-MeTHF/DIC/OxymaPure **2.39**, with washings and deprotection steps then carried out using combinations of 2-MeTHF, IPA and EtOAc. Synthesis of the Aib-enkephalin pentapeptide was optimal when performed upon ChemMatrix resin, using 2-MeTHF for the deprotection and washing between steps with a combination of 2-MeTHF and EtOAc, producing the target peptide in 95% yield. The Aib-ACP decapeptide however proved a much tougher challenge, with identical conditions only producing the target peptide in 37.3% yield, a poor result when compared to the use of DMF which produced the target peptide in 70.0%. Eventually though the use of more forcing conditions, which meant performing both coupling and deprotection at 40 °C, produced the peptide in a much improved 87.1% yield.

Identifying in their preceding communication that Fmoc-removal in green solvents can be particularly troublesome for SPPS Jad *et al.* have further investigated a variety of green solvents for Fmoc-removal.[94] Nine green solvents were investigated,

which included; *N*-formylmorpholine, 2-MeTHF, CPME, dimethyl isosorbide, EtOAc, DMC, GVL, isopropyl alcohol (IPA) and α,α,α-trifluorotoluene. The ability of these solvents to adequately solvate PS- and ChemMatrix-resin was first investigated. Overall, much better results were obtained using ChemMatrix with 7 of 9 solvents giving good swelling, with only 2 of 9 able to solvate PS resins. The success of the Fmoc-deprotection was then determined by first synthesising the Fmoc-Ile-Asp(*t*Bu)-Tyr(*t*Bu)-Ile-Asn(Trt)-Gly-NH-RinkAmide-resin sequence on both ChemMatrix and PS in DMF. Fmoc-deprotection was then performed using 20% (*v*/*v*) solution of piperidine in the chosen solvent. Boc-Gly-OH was then coupled to the peptide sequence. Residual Fmoc-groups were then deprotected using 20% (*v*/*v*) piperidine in DMF and Boc-Leu-OH coupled to the remaining free amino groups. Simultaneous Boc-deprotection and cleavage from the resin was then performed. The ratio of H-Gly-Ile-Asp-Tyr-Ile-Asn-Gly-NH_2 to H-Leu-Ile-Asp-Tyr-Ile-Asn-Gly-NH_2 was then used to determine deprotection success. Overall, the results obtained were fairly poor, with most solvents giving <30% conversion, even with extended deprotection times. GVL however, did adequately remove the Fmoc-protecting group with 95.5% and 100% conversion on PS and ChemMatrix respectively, using only 7 min deprotection times. Efficient removal of the Fmoc-protecting group was also observed for the use of *N*-formylmorpholine, but only when using a ChemMatrix resin, the results for PS were substantially worse, with only 47.9% conversion reported.

Unsurprisingly, Kumar *et al.* have recently evaluated the use of *N*-formylmorpholine and GVL in SPPS.[96] Initially, GVL and *N*-formylmorpholine were only used for the coupling steps. Aib-ACP-decapeptide was produced in 89.7% yield for GVL and 94.4% for *N*-formylmorpholine, with minimal evidence for the des-Aib species. The synthesis of the Aib-ACP-decapeptide was then reattempted but using GVL and *N*-formylmorpholine for all procedures, including washing. Unfortunately, the obtained yields were found to drop significantly to around 50%, a substantial reduction compared to the equivalent synthesis performed exclusively in 2-MeTHF.[95]

In summary, the use of alternative solvents and solvent technologies has been widely explored within the literature, in an effort to develop sustainable routes to peptide synthesis. The vast majority of examples have reported the use of water. However, the poor solubility of classical reagents and susceptibility of activated intermediates to hydrolysis has meant reagents often require significant modification or preprocessing. Additionally, the use of water does not automatically constitute a green or environmentally benign process. This is due to the issues associated with contaminated aqueous waste, which will greatly vary on a case-by-case basis. More recent approaches have demonstrated highly promising results for the use of

alternative organic solvents, in an effort to replace conventional polar aprotic solvents without having to significantly modify existing protocols. However, in many of these reported examples the green credentials of the solvent are often questionable and deprotections still necessitate the use of DMF. It therefore seems as though there is still substantial scope for an investigation into alternative solvents in solution- and solid-phase peptide synthesis for sustainable peptide bond formation.

2.1.3 Cyclic Carbonates as Solvents

Cyclic carbonates, specifically ethylene carbonate (EC) **2.41** and propylene carbonate (PC) **2.42**, have been highlighted as highly promising replacements to conventional polar aprotic solvents.[97] This is due to the many EHS advantages they present as eco-friendly solvents, such as being non-toxic, completely biodegradable and displaying low ecotoxicity. Additionally, incineration also produces no NO_x or SO_x, which has traditionally been a major issue associated with the disposal of other polar aprotic solvents. They also posses many desirable physical properties (Table 2.2). Both EC and PC posses a much wider liquid temperature range, although EC is a solid at ambient temperature. They also have much higher boiling points, resulting in low vapour pressures and higher flash points, meaning cyclic carbonates are also suitable replacements to VOCs. This does however present an issue when it comes to product purification, as distillative removal of cyclic carbonates is known to be rather challenging. Finally, cyclic carbonates also posses very high dielectric constants and dipole moments, which are significantly higher than the other dipolar aprotic solvents listed. This makes cylic carbonates particularly well suited for anhydrous electrochemical applications.

Table 2.2: Physical properties of some common polar aprotic solvents.

Solvent	**MP (°C)**	**BP (°C)**	**FP (°C)**	**Density (g mL^{-1})**	**Dielectric Constant**	**Dipole Moment**
EC **2.41**	36	248	150	1.34	90.0	4.81
PC **2.42**	-49	242	132	1.20	64.0	5.36
DMF **2.43**	-60	153	58	0.94	36.7	3.82
NMP **2.44**	-24	202	96	1.03	32.2	4.09
DMA **2.45**	-20	166	70	0.94	37.8	3.81
DMSO **2.46**	18	189	95	1.10	46.7	3.96
MeCN **2.47**	-44	82	2	0.79	37.5	3.92
CH_2Cl_2 **2.48**	-97	40	-	1.325	8.9	1.60

MP - melting point, BP - boiling point, FP - flash point.

Identification of suitable green alternatives to traditional solvents also requires quantification of the solvation properties before accurate comparisons can be made. Although many different solvent parameters exist for this, Kamlet-Taft solvatochromic parameters are probably the most comprehensive and frequently used measure of solvation properties. The Kamlet-Taft parameters quantify solvation properties according to hydrogen-bond donating ability (acidity α), hydrogen-bond accepting ability (basicity β) and dipolarity/polarizability (π*).[98] Polar aprotic solvents typically have negligible α-values, comparing β and π* is therefore a good indication of relative solvation properties. It can be observed that the common polar aprotic solvents (DMSO **2.46**, DMF **2.43**, DMA **2.45** and NMP **2.44**) all cluster to the top right hand side (red shaded area) of the generated diagram (Figure 2.3). Indicating they all possess high values for both β and π*. In comparison, cyclic carbonates are observed to have essentially equivalent values for π*. The hydrogen-bond basicity β of cyclic carbonates is much lower however, being essentially half of the traditional polar aprotic solvents. This value is essentially equivalent to that of MeCN **2.47**. Suggesting that cyclic carbonates fall into the region of solvatochromic space that could be considered as polar-aprotic. It can therefore be concluded that, on the basis of Kamlet-Taft solvation parameters, cyclic carbonates should present a suitable alternative to traditional polar aprotic solvents.

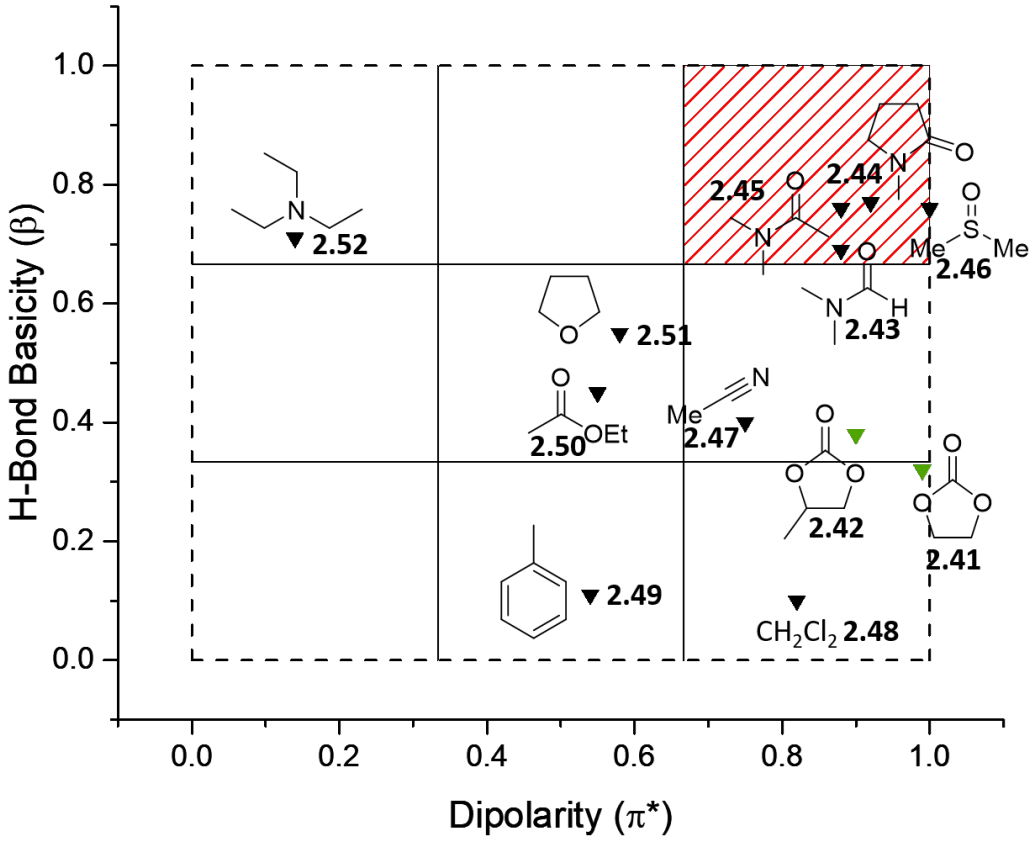

Figure 2.3: Comparison of Kamlet-Taft H-bond basicity (β) and dipolarity (π*) for cyclic carbonates and common polar aprotic solvents.

Finally, cyclic carbonates have been in commercial production since the mid-1950s meaning they are readily available, in large quantities and at low cost.[99] This is an incredibly important consideration for an alternative solvent. Moreover, the synthesis of cyclic carbonates has facilitated a growing interest in their use and application. Cyclic carbonates **2.41**/**2.42** are most commonly produced through the 100% atom economical reaction between epoxides **2.53** and carbon dioxide **2.54** (Scheme 2.11).[100] This transformation is one of the few commercially important reactions which utilises carbon dioxide as a chemical feedstock. Current production of cyclic carbonates is approximately 100 ktonnes per annum, but is expected to grow with increasing demand.[101] The synthesis of cyclic carbonates from epoxides and carbon dioxide has therefore attracted a large amount of interest as a highly promising approach to dealing with rising atmospheric carbon dioxide levels, caused by anthropogenic emissions.[102]

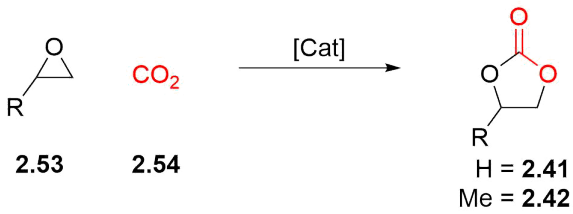

Scheme 2.11: Synthesis of cyclic carbonates from the epoxides and carbon dioxide.

Currently commercial production relies on quaternary ammonium and phosphonium salts as catalysts, which requires the use of high temperatures and pressures. It is envisioned that being able to perform this reaction under conditions closer to ambient would mean cyclic carbonate formation would be a net consumer of carbon dioxide. As a result, there has been great interest in the development of highly active catalysts and catalyst systems, based around privileged metal complexes and organocatalysts, for the synthesis of cyclic carbonates.[103,100]

The many advantageous physical and chemical properties outlined, combined with the fact that they have been in commercial production for over 50 years, has meant cyclic carbonates have found a myriad of uses and applications. This however has predominantly been for electrochemical and extractive processes, the earliest examples of which typically come from the oil processing industry. The FLUOR process, first commercialised in the 1960s and still in use to this day, utilises PC as a solvent for the removal of impurities from natural gas streams.[104] More recently, the Huntsman Corporation have employed PC in combination with carbon dioxide for the recovery of oil from maturing reservoirs.[105] Due to their low toxicity, cyclic carbonates have also proved to be excellent co-solvents for cleaning and cosmetic products. They are approved for use in high concentration for applications that involve contact with human skin.[106] There has also been growing interest in their use as reactive intermediates, whether that is for the synthesis of fine chemicals, or monomers for the production of polycarbonates or polyurethanes.[107] Finally, their high dielectric constants make cyclic carbonates particularly suitable for use as non-aqueous electrolytes in lithium batteries, most commonly found in consumer electronics.[108]

2.1.4 Application of Cyclic Carbonates in Organic Synthesis

In comparison, the use of cyclic carbonates in synthetic chemistry is rather underexplored. Sporadic reports have appeared within the literature over the last 30 years, with examples predominantly demonstrating the suitability of cyclic carbonates in homogeneous catalysis. Reactions that have been reported include hydroformylations,[109] hydrogenations,[110] hydroaminations[111] and some examples of

metal catalysed cross couplings.[112] This work has recently been excellently reviewed by Schaffner *et al.*[97] For this reason, the following literature review will focus on synthetic chemistry utilising cyclic carbonates as the reaction solvent published since 2010. The use of cyclic carbonates for homogeneous metal catalysis is particularly well established. For this reason, homogeneous metal catalysis makes up the majority of the proceeding literature review, followed by limited examples of heterogeneous metal catalysis, organocatalysis and finally anything that falls outside of these three categories.

2.1.4.1 Homogeneous Metal Catalysis

Heck Reaction

The use of PC in the Heck reaction was one of first examples that utilised cyclic carbonates as the reaction solvent in homogeneous catalysis. Reported by Reetz *et al.* electrochemically prepared nanostructured Pd clusters, stabilised by PC, were found to efficiently catalyse the Heck reaction.[113] More recently, Parker *et al.* have investigated the Heck reaction between various aryl halides **2.55** and methyl acrylate **2.56**, to produce the corresponding methyl cinnamate derivatives **2.57** (Scheme 2.12).[114] Yields were generally better in cyclic carbonates than in control reactions using NMP, with quantitative results typically observed for most reactions carried out in EC. Interestingly, Parker *et al.* were also able to correlate the reaction rate to solvent polarity, demonstrating PC was an excellent replacement for NMP in this reaction.

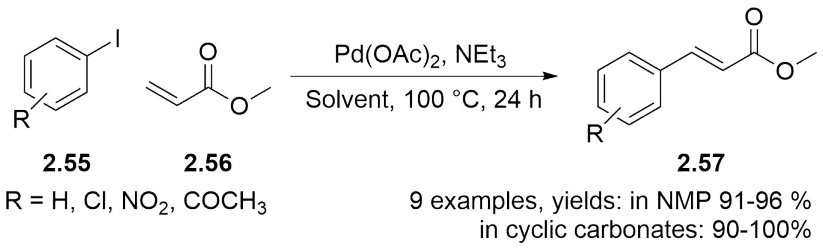

Scheme 2.12: Palladium catalysed Heck reaction of methyl acrylate **2.56** in cyclic carbonates.

Wacker Oxidation

In a similar manner to the work reported by Reetz *et al.*, Wang *et al.* has demonstrated the use of ethylene carbonate for the stabilisation of palladium nanoparticles in the Wacker oxidation.[115] Using molecular oxygen as the sole oxidant, a series of higher alkenes and aryl alkenes **2.58** were converted to the corresponding ketones **2.59**, catalysed by colloidal Pd nanoparticles that were stabilised by EC (Scheme 2.13). Yields were variable, being poor to good depending on the substrate,

but the product was easily separated from the catalyst system, through extraction with *n*-hexane. Unfortunately, the catalyst system could not be reused following the reaction, as agglomerates were observed, reducing the catalyst surface area and severely affecting the overall yields in the second cycle.

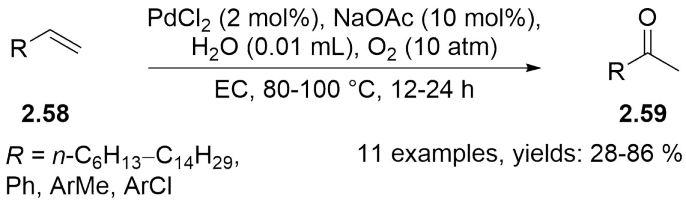

Scheme 2.13: Wacker oxidation reaction catalysed by EC stabilised colloidal Pd-nanoparticles.

Hydroformylation of Piperylene

Hydroformylation in cyclic carbonates had been investigated fairly extensively prior to 2010 by Behr and co-workers.[109,111] More recently though, Neubert *et al.* have reported on the hydroformylation of piperylene **2.60**, using a $Rh(CO)_2$acac/Xantphos **2.63** catalyst system (Scheme 2.14).[116] The catalyst system afforded the desired aldehydes in 82% yield with a liner:branched ratio **2.61**:**2.62** of 1:3.8 in 7 hours, using only 0.3 mol% catalyst loading. This reaction had previously been optimised in toluene, but Neubert *et al.* showed the use of PC was more convenient for recycling the expensive catalyst system. The large difference in boiling point between the products and solvent meant the products could be easily removed by distillation. Catalyst performance was slightly impaired after each reuse, but ligand refreshment after 5 cycles adequately restored performance.

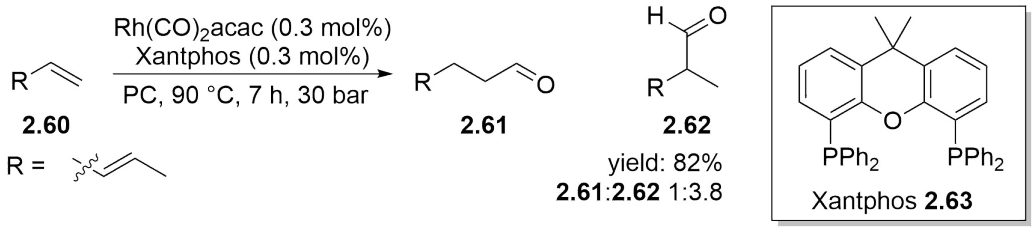

Scheme 2.14: Hydroformylation of piperylene using a recyclable rhodium/Xantphos catalyst system in PC.

Intermolecular Alkyne Hydroacylation

PC has also been found to be an excellent solvent for the hydroacylation of alkynes. Lenden *et al.* first reported this transformation when they found that PC was a suitable replacement for dichloroethane in the rhodium-catalysed intermolecular alkyne hydroacylation. A series of β-*S*-aldehydes **2.64** and alkynes

2.65 were coupled to produce the corresponding enone products **2.66** (Scheme 2.15). Generally, excellent yields were observed in only 1 hour, demonstrating comparable results to control reactions in either acetone or dichloroethane. Unfortunately though, the reaction products had to be purified by flash column chromatography due to the high boiling nature of PC.

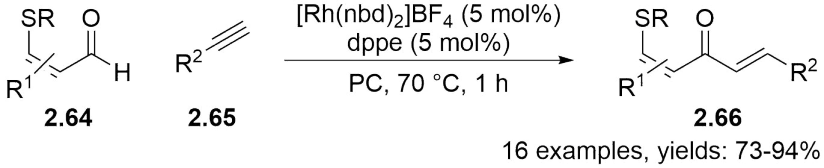

Scheme 2.15: Rhodium-catalysed intermolecular alkyne hydroacylation in PC.

Direct Aerobic Oxidation of 2-Benzylpyridines

The higher boiling points associated with cyclic carbonates may not always be a disadvantage, as recently demonstrated by Pieber *at el.* In their report the direct aerobic oxidation of 2-benzylpyridines **2.67** to the corresponding ketones **2.68** was investigated, using a cheap and abundant $FeCl_3$ catalyst system under continuous flow conditions.[117] Using conventional solvents, such as DMSO or NMP, typically resulted in poor conversions unless very high temperatures were used. However, this often resulted in discolouration of the reaction mixture due to decomposition of the solvent. When PC was used it was found to be much more tolerant to the higher temperatures necessary, resulting in quantitative conversion under otherwise identical conditions to conventional solvents.

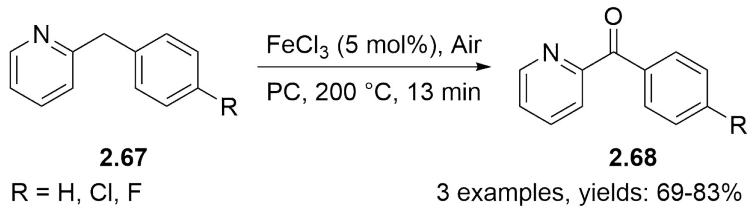

Scheme 2.16: Direct aerobic oxidation of 2-benzylpyridines under continuous flow using propylene carbonate.

Carboxylation of Terminal Alkynes

Finally, Yu *et al.* have utilised EC in the CuI catalysed carboxylation of terminal alkynes (Scheme 2.17).[118] A range of terminal alkynes **2.69** and aryl halides were coupled under mild conditions, to produce the corresponding esters **2.70** in excellent yields. Control reactions demonstrated that EC was superior to DMF for this transformation. This was revealed by DFT calculations to be due to a reduction in the energy barrier for CO_2 insertion.

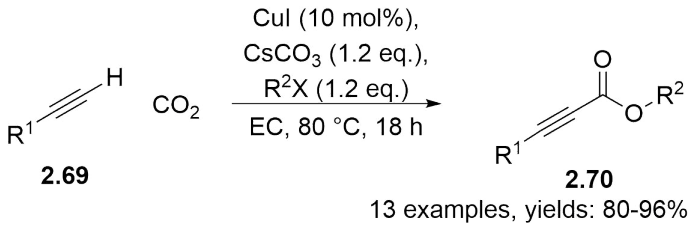

Scheme 2.17: Copper catalysed carboxylation of terminal alkynes in EC.

2.1.4.2 Heterogeneous Metal Catalysis

Phenoxycarbonylation

In comparison to homogeneous metal catalysis, heterogeneous metal catalysis using cyclic carbonates is relatively unexplored. Gautam *et al.* have recently reported on the use of PC in the phenoxycarbonylation of aryl halides **2.71**, using *N*-formylsaccharin **2.73** as a CO surrogate and a heterogeneous Pd/C catalyst (Scheme 2.18).[119] The corresponding phenyl esters **2.74** were obtained under mild conditions in good to moderate yields, in a one-pot process that is free of any co-catalyst, ligand or additive. Gautam *et al.* also demonstrated that the catalyst could be recycled up to four times, and the reaction performed on a gram scale.

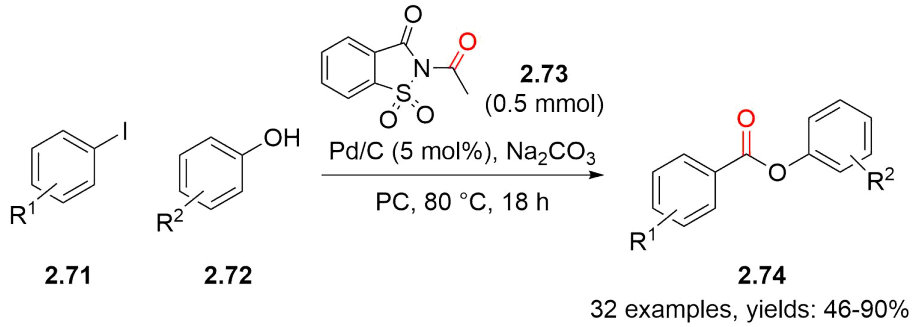

Scheme 2.18: Phenoxycarbonylation of aryl halides **2.71** to phenyl esters **2.74** using a heterogeneous Pd/C catalyst in PC.

Suzuki-Miyaura Cross-Coupling

Using a similar approach to their work on phenoxycarbonylation, Gautam *et al.* have also recently reported on the carbonylative Suzuki-Miyaura cross-coupling reaction.[120] A range of aryl iodides **2.75** and boronic acids **2.76** were coupled using a heterogeneous Pd/C catalyst and *N*-formylsaccharin **2.73** as a CO surrogate, producing a range of aryl ketones **2.77** (Scheme 2.19). Reaction optimisation demonstrated that PC tended to outperform both DMF and 1,4-dioxane in terms of both conversion and selectivity for the aryl ketone **2.77** over a biaryl side-product **2.78**. Additionally, the catalyst could be reused at least 5 times, with minimal losses observed in yield and selectivity.

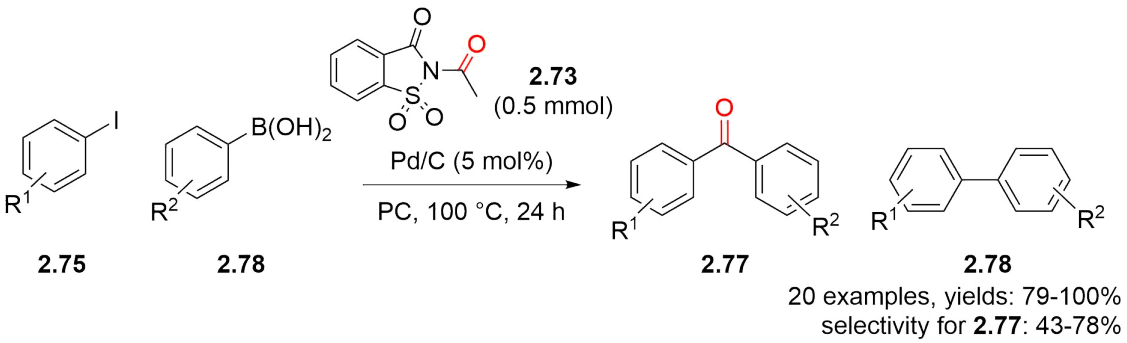

Scheme 2.19: Carbonylative Suzuki-Miyaura reaction for the synthesis of biaryl ketones **2.77** in PC.

2.1.4.3 Organocatalysis

Proline Catalysed Aminations

There are very few reports of organocatalysed reactions being performed in cyclic carbonates. North and co-workers have previously reported on the use of cyclic carbonates as sustainable solvents in asymmetric aldol reactions.[121,122] More recently though, they have extended their methodology to include the proline catalysed α-hydrazinations of aldehydes and ketones by diazodicarboxylates.[123] The reaction of various aldehydes **2.79** with dibenzyl azodicarboxylate **2.80** produced the target alcohol **2.82**, following reduction of the intermediate aldehyde **2.81** with sodium borohydride, in good to excellent yields (Scheme 2.20). However, the reaction had to be performed at a lower temperature and for 24 hours, rather than 2 hours, to obtain enatioselectivities comparable to the control reaction in CH_2Cl_2. The α-hydrazination of ketones was less successful with moderate yields and enatioselectivities observed.

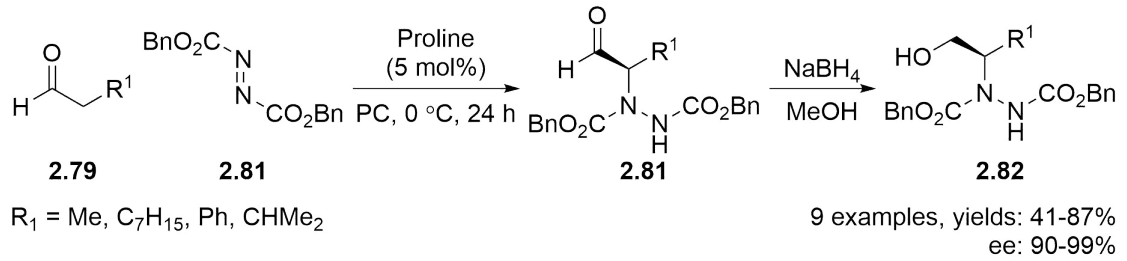

Scheme 2.20: Proline catalysed α-hydrazination of aldehydes in cyclic carbonates.

2.1.4.4 Miscellaneous

Diastereoselective Synthesis of Tetrahydroquinoline Scaffolds

Finally, Forero *et al.* have utilised propylene carbonate as a replacement for common chlorinated solvents in the one-pot imino Diels-Alder cycloaddition reaction, for the

diastereoselective preparation of tetrahydroquinoline scaffolds.[124] Various derivatives of aniline **2.83** and benzaldehyde **2.84** were combined with isoeugenol **2.85** in the presence of a molecular iodine catalyst to produce the tetrahydroquinoline species **2.86** in good to excellent yield and diastereoselectivity, in under 1 hour (Scheme 2.21). Notably, the authors were able to remove PC using a warm aqueous wash, producing pure product without the need for chromatographic purification.

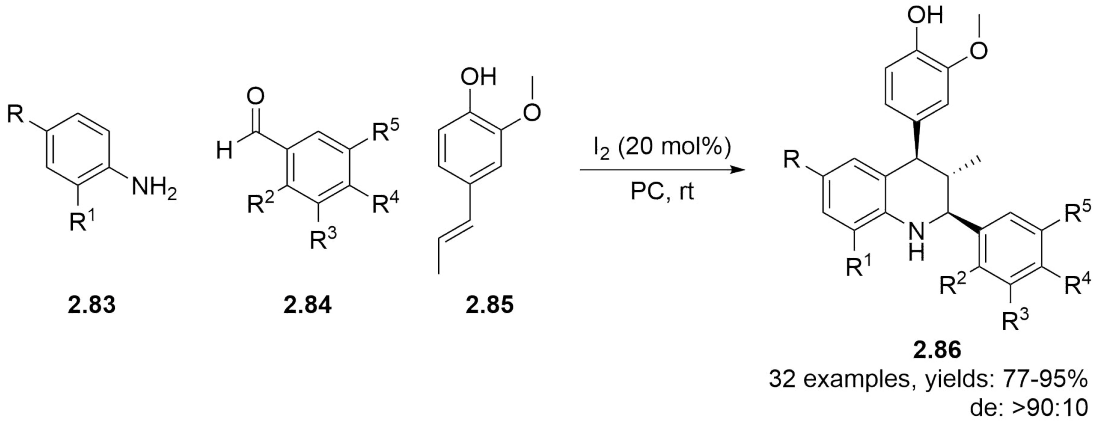

Scheme 2.21: Diastereoselective synthesis of tetrahydroquinoline scaffolds **2.86** in propylene carbonate.

2.1.5 Chapter Aims

It can be concluded from the preceding investigation that cyclic carbonates posses many desirable solvent properties, particularly when considered in the context of green chemistry. However, whilst they have been widely considered for extractive and electrochemical applications, their use in organic synthesis is rather limited. Analysis of the literature indicates that of the few reports of synthetic chemistry utilising cyclic carbonates the majority come from the field of homogeneous metal catalysis. Consequently, the following chapter seeks to expand on the current use of cyclic carbonates as replacements for conventional polar aprotic solvents in synthetic chemistry. Cyclic carbonates would therefore seem particularly well suited as solvents for sustainable peptide synthesis. The preceding literature review identified that more recent approaches to sustainable peptide bond formation have favoured the use of alternative organic solvents, with cyclic carbonates not having been previously investigated. The following chapter will therefore look to analyse the suitability of cyclic carbonates as replacements for DMF, NMP and CH_2Cl_2 in both the solution- and solid-phase synthesis of peptides.

2.2 Results and Discussion

2.2.1 Solution-Phase Peptide Synthesis

Initial investigations sought to determine whether the synthesis of peptides in cyclic carbonates was indeed feasible. Due to the additional complexities associated with using a solid-support in solid-phase peptide synthesis, the use of cyclic carbonates in solution-phase peptide was first investigated. This would make it much easier to identify any compatibility issues between the solvent and the chemistry used. To begin with a simple coupling reaction between unfunctionalised amino acids was investigated. The coupling reaction between phenylalanine benzyl ester **2.88** and Boc-alanine **2.87** to produce the Boc-Ala-Phe-OBn dipeptide **2.89** was therefore chosen, the results of this study are summarised in Table 2.3. This coupling has been previously reported in a conventional solvent system of CH_2Cl_2:DMF (25:75, v/v%) by Nam *et al.* producing the target peptide in an 86% isolated yield (Table 2.3, Entry 1).[125]

Table 2.3: Reaction optimisation for the synthesis of Boc-Ala-Phe-OBn dipeptide **2.89**.

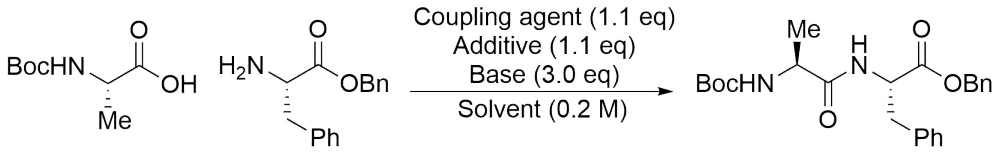

2.87 **2.88** **2.89**

Entry	Coupling Agent	Additive	T (°C)	Base	Solvent	Yield (%)[a]
1	EDC	HOAt	20	$NaHCO_3$	CH_2Cl_2:DMF	86[b]
2	DCC	PFP	20	NEt_3	CH_2Cl_2:DMF	76
3	DCC	PFP	20	NEt_3	PC	83
4	DCC	PFP	40	NEt_3	EC[c]	96
5	EDC	HOBt	20	$NEtiPr_2$	PC	93
6	EDC	HOBt	20	$NEtiPr_2$	CH_2Cl_2:DMF	81
7	EDC	HOBt	20	$NEtiPr_2$	DMF	83
8[d]	EDC	HOBt	70	$NEtiPr_2$	DMF	78
9[d]	EDC	HOBt	70	$NEtiPr_2$	PC	82

[a] isolated yield.[b] literature result.[c] ethylene carbonate melting point is 35-38 °C.[d] performed under microwave irradiation.

Entry 2 demonstrates that when the coupling agent, additive and base are varied, but the solvent system is not, the target dipeptide **2.89** was still obtained in an acceptable 76% yield. Repeating this coupling procedure, but exchanging the solvent for either PC or EC, produced the target dipeptide **2.89** in 83% and 96% yield respectively (Entries 3 and 4). It should however be highlighted that the amino acids were not fully soluble in either EC or PC at the given concentration (0.2 M),

until preactivated, which presents a distinct difference between cyclic carbonates and either DMF or CH_2Cl_2. These promising early results do however demonstrate that it is indeed feasible to use cyclic carbonates as suitable replacements for conventional polar aprotic solvents in solution-phase peptide synthesis. Although, higher temperatures were necessary for couplings performed in ethylene carbonate, in order to maintain a homogeneous reaction mixture, due to the high melting point of ethylene carbonate.

The need for higher temperatures for couplings performed in EC was at the time discouraging, because of concerns over racemisation and the desire to perform the coupling at conditions as close to ambient as possible. It was therefore decided that this coupling reaction would be further optimised for the use of PC. Eventually, optimal yields were obtained when using a combination of EDC, HOBt and DIPEA in PC, producing the target peptide in an excellent 93% yield (Entry 5). The obtained yield being significantly higher than control reactions using the same coupling reagents in either a mixed solvent system of CH_2Cl_2:DMF or pure DMF (Entries 6 and 7).

Finally, whilst it was preferable at the time to carry out coupling reactions under ambient conditions, the use of microwave irradiation for elevated temperature peptide synthesis has become increasingly commonplace in recent years, particularly for challenging sequences.[126] For this reason, the last two entries deal with the synthesis of dipeptide **2.89** at 70 °C in DMF or PC under microwave irradiation (Entries 8 and 9). In both cases the target peptide was obtained in high yield, indicating PC is also suitable for peptide synthesis performed under microwave irradiation.

It is appropriate to highlight at this point that there is literature precedent for the reaction of amines with cyclic carbonates, to produce the corresponding carbamate.[127] No evidence for this was observed in the previously described coupling reactions, but it was felt necessary at the time to investigate this further. A control reaction was therefore performed, phenylalanine benzyl ester **2.88** was first dissolved in PC and NEt*i*Pr_2 (3.0 eq). The mixture was then heated to 70 °C using microwave irradiation and held at this temperature for 3 hours. Even under these conditions, only 1% of the amine was found to react with the solvent, suggesting that even under forcing conditions carbamate formation will not compete with peptide bond formation. The reaction of amines with cyclic carbonates will however be discussed in greater detail in section 2.2.3.1.

2.2.1.1 Racemisation of Activated Amino Acids

A consequence of the strong activation of the carboxy group, necessary to promote amide bond formation, is the increased acidity of the Cα proton, as this proton is easily removed promoting loss of stereochemical integrity. This is one of the most troublesome side reactions in peptide synthesis, as even a small degree of racemisation or epimerisation will lead to a substantial reduction in yield, along with complications in separation, particularly in longer peptide chains. Racemisation is exclusively a base induced process and occurs through two distinct pathways (Scheme 2.22). Firstly, direct enolisation, where the Cα proton is lost during activation. This generates an intermediate enolate **2.91**, that can be reprotonated from either face, generating the corresponding (*R*)- or (*S*)-enantiomer **2.92**/**2.90** (Route A). Alternatively, the activated intermediate can cyclise to generate the oxazolone intermediate **2.93** (Route B). The oxazolone can still be regarded as activated and is therefore still able to form the target peptide bond. This however, is much slower than racemisation through the stabilised anion **2.94**, so any product formed will be derived from a mixture of (*R*)- **2.95** and (*S*)- **2.93** enantiomers.[128]

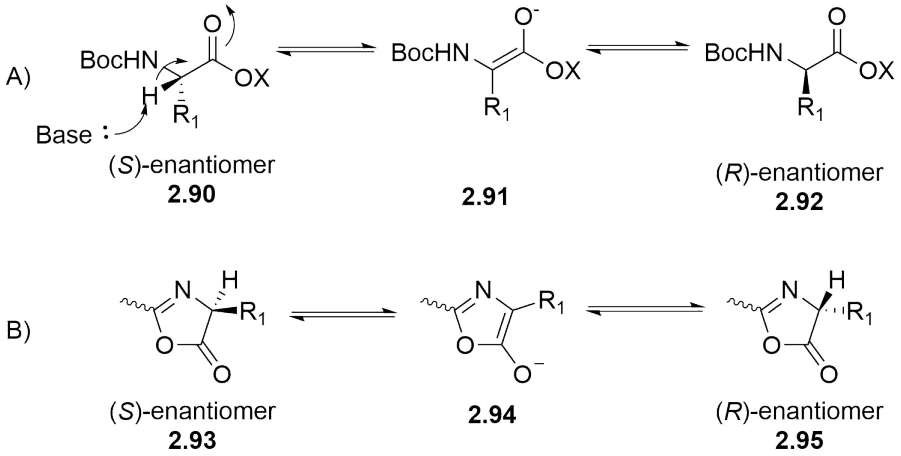

Scheme 2.22: Racemisation mechanisms route A) direct enolisation route B) oxazolone formation.

In order to demonstrate that racemisation is not promoted by the use of PC as a reaction solvent, the diastereomeric dipeptide **2.96** was prepared from Boc-(*R*)-alanine (≥98% e.e.) using the optimised reaction conditions (Table 2.3, Entry 5). Analysis of the (*S*,*S*)-dipeptide **2.89**, (*R*,*S*)-dipeptide **2.96** and a 1:1 mixture of the two by chiral HPLC indicated that the dipeptides were formed with diastereomeric excesses of >98.4% (Figure 2.4). This suggests the use of PC as the reaction solvent in peptide coupling does not actively promote racemisation of the activated intermediates.

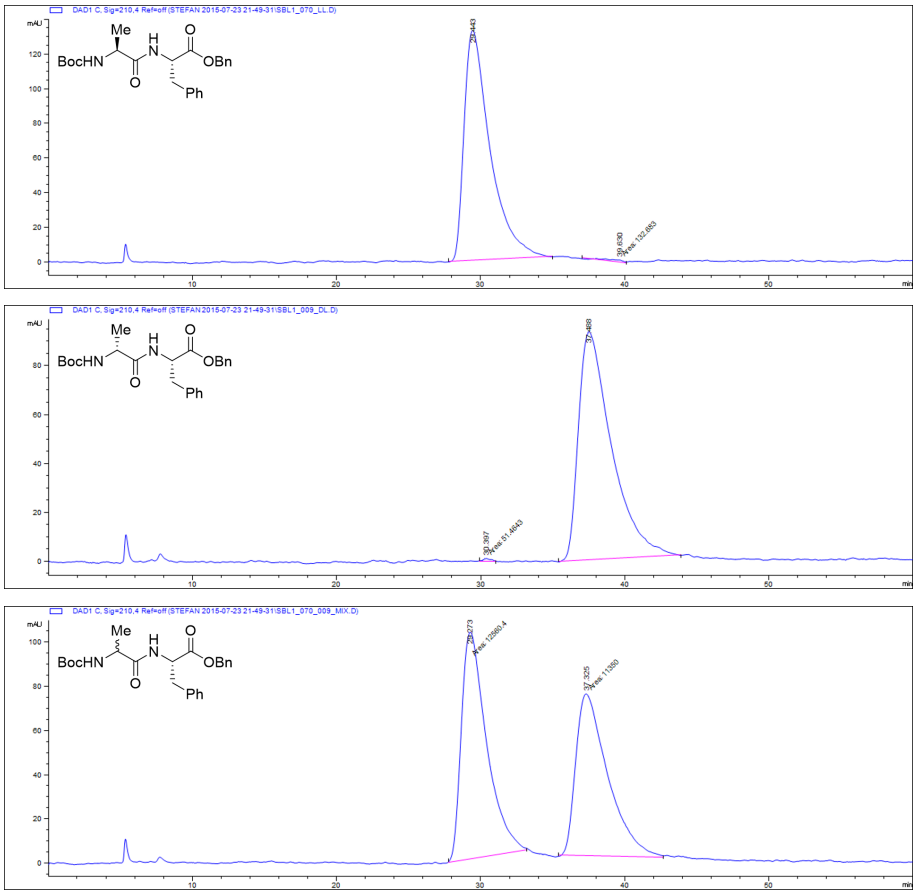

Figure 2.4: Chiral HPLC chromatograms for Boc-Ala-Phe-OBn dipeptide, (*S*,*S*)-top **2.89**, (*R*,*S*)-middle **2.96** and 1:1 mixture-bottom.

To ensure that the observed retention of stereochemistry in the Boc-Ala-Phe-OBn **2.89**/**2.96** dipeptide could be regarded as general, a few additional peptidic systems were investigated, the results of which have been summarised in Table 2.4. The Boc-Leu-Phe-OBn dipeptide was produced in 99.7% and 98.7% diastereomeric excess for the (*S*,*S*) and (*R*,*S*)-dipeptide **2.97**/**2.98** respectively (Entries 3 and 4). A longer peptide system was also investigated, with both the (*R*,*S*,*S*) and (*S*,*S*,*S*) derivatives of the Boc-Leu-Ala-Phe-OBn tripeptide **2.99**/**2.100** obtained in >98.1% purity (Entries 5 and 6). Finally, the synthesis of Boc-Ala-Phe-OBn **2.89** using microwave irradiation in either PC or CH_2Cl_2:DMF was found to produce the target (*S*,*S*)-dipeptide as a single enantiomer in both cases (Entries 7 and 8). This suggests that performing coupling reactions at elevated temperatures may not be as much of an issue as first believed, warranting a further investigation into the use of EC for solution-phase peptide synthesis in the future.

Table 2.4: Summary for the investigation into amino acid racemisation during couplings performed in PC.

Entry	Sequence	T_{R1} (min)	Area	T_{R2} (min)	Area	d.e. %
1	Boc-Ala-Phe-OBn **2.89**	29.44	99.21	39.63	0.79	98.4
2	Boc-(*R*)-Ala-Phe-OBn **2.96**	30.40	0.34	37.49	99.66	99.3
3	Boc-Leu-Phe-OBn **2.97**	17.16	99.84	23.94	0.16	99.7
4	Boc-(*R*)-Leu-Phe-OBn **2.98**	18.01	0.67	22.20	99.33	98.7
5	Boc-Leu-Ala-Phe-OBn **2.99**	28.24	0.97	34.15	99.03	98.1
6	Boc-(*R*)-Leu-Ala-Phe-OBn **2.100**	27.16	99.72	35.22	0.28	99.4
7	Boc-Ala-Phe-OBn[a] **2.89**	27.65	100	-	-	100
8	Boc-Ala-Phe-OBn[b] **2.89**	27.54	100	-	-	100

[a] performed under microwave irradiation in CH_2Cl_2:DMF (25:75, v/v%).[b] performed under microwave irradiation in PC.

To summarise, PC has been found to perform as well as, if not better than, conventional solvents for solution-phase coupling reactions. Isolated yields for the Boc-Ala-Phe-OBn dipeptide **2.89** under identical coupling conditions, were found to be greater for PC than the corresponding reactions in CH_2Cl_2:DMF (25:75) or pure DMF. Couplings were then found to proceed smoothly under microwave irradiation, with PC performing as well as CH_2Cl_2:DMF. Most importantly, the reaction between PC and an amine was found to not compete with peptide bond formation, even under forcing conditions using microwave irradiation. Finally, racemisation of the amino acid chiral centres, due to activation during coupling, was found not to be a concern when couplings were performed in PC, with diastereomeric excesses of >98.1% observed in all cases.

2.2.1.2 *N*-Boc Deprotection in Propylene Carbonate

The other key process in solution-phase peptide synthesis is selective removal of the *N*-Boc protecting group. This is important as it allows the peptide chain to be grown selectively in one direction, from the *C*- to the *N*-terminus. This is typically performed using a strong acid such as hydrochloric acid (HCl) or trifluoroacetic acid (TFA), and has been reported in a variety of solvents, including 1,4-dioxane, CH_2Cl_2, THF, MeCN and DMF. The use of PC for this process has not been previously reported.

The deprotection of the Boc-Ala-Phe-OBn dipeptide **2.89** in various solvents was therefore investigated. Under conventional reaction conditions, 4 M HCl in 1,4-

dioxane, the corresponding hydrochloride salt **2.101** was obtained in an excellent 93% yield in 3 hours (Table 2.5, Entry 1). Performing the equivalent reaction in PC however initially proved challenging, as a solution of hydrochloric acid in PC is not commercially available. It was found that the generation of hydrochloric acid *in situ*, from methanol and acetyl chloride, produced the hydrochloride salt **2.101** in 89% yield (Entry 2). However, in the interest of convenience it was eventually decided that the use of excess trifluoroacetic acid (60 eq.) was optimal, as this furnished the corresponding trifluoroacetate salt **2.102** in a quantitative 99% yield in 3 hours (Entry 3).

Table 2.5: *N*-Boc deprotection of Boc-Ala-Phe-OBn **2.89**.

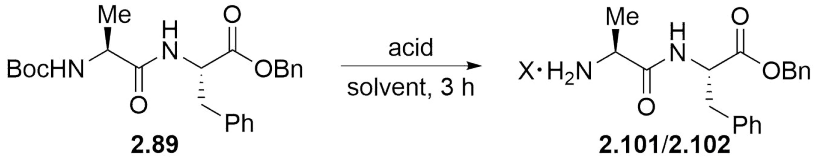

2.89 **2.101/2.102**

Entry	Base	Solvent	X	Yield[a]
1	4 M HCl	1,4-dioxane	HCl **2.101**	93
2	HCl[b]	PC	HCl **2.101**	89
3	CF_3COOH	PC	CF_3COOH **2.102**	99

[a] Isolated yield. [b] generated *in situ*.

Consequently, both coupling and deprotection reactions have been successfully carried out in PC. This demonstrates the solution-phase synthesis of peptides using PC as the only reaction solvent is indeed feasible, indicating that PC appears to be a suitable replacement for DMF, CH_2Cl_2 and 1,4-dioxane. It is apparent from the results obtained that PC does not promote the various side reactions associated with peptide coupling, including racemisation, and appears to tolerate the harsh, acidic conditions associated with *N*-Boc deprotection.

2.2.1.3 Tetrapeptide Synthesis using Solution-Phase Methodology in PC

To illustrate the generality of the developed methodology, a series of five fully protected tetrapeptides **2.107a-e** were then prepared (Scheme 2.23). This was achieved by first coupling *N*-Boc- and *O*-Bn-protected amino acids, according to the optimised conditions developed previously, producing the corresponding dipeptides **2.103a-e**. Selective removal of the *N*-Boc protecting group using TFA in PC then gave the dipeptide salts **2.104a-e**. Repeating the aforementioned coupling/deprotection process furnished the tripeptides **2.105a-e**, followed by the tripeptide salts **2.106a-e**, with a final coupling giving the desired tetrapeptides **2.107a-e**.

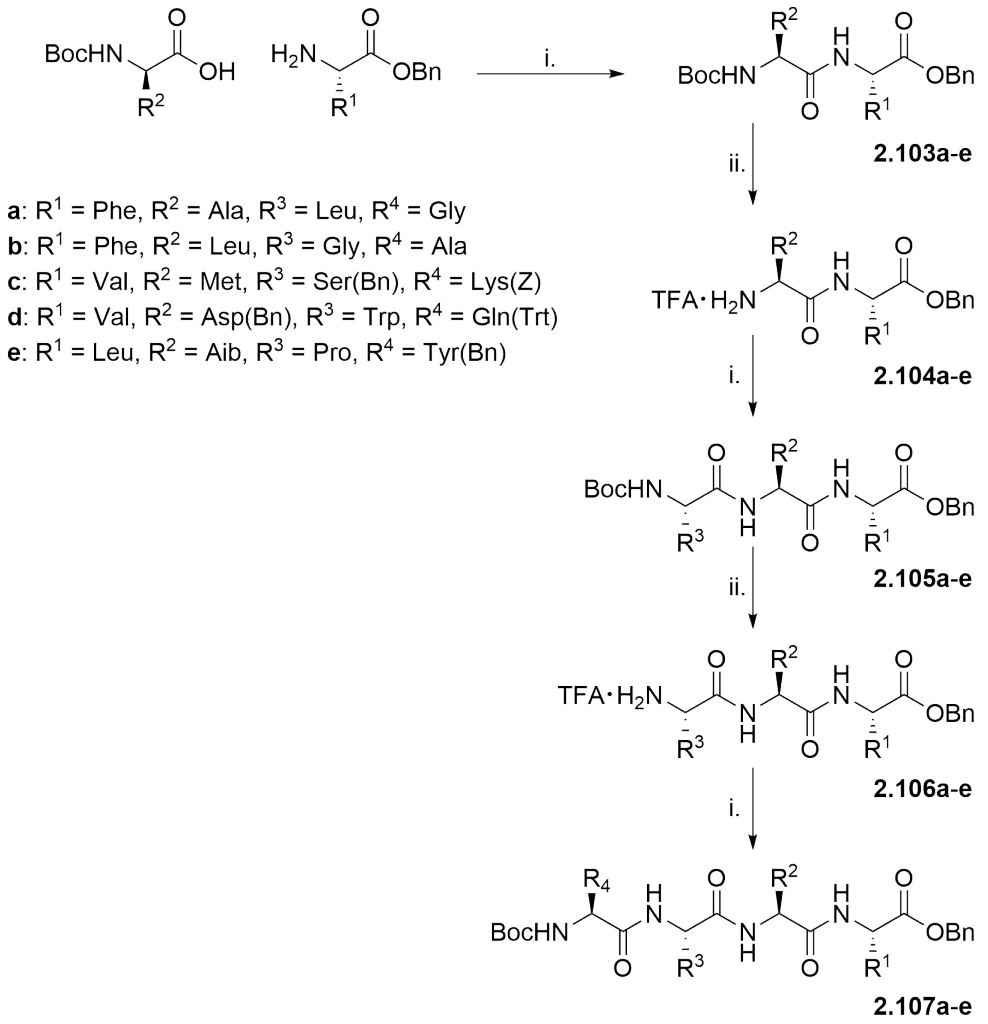

Scheme 2.23: Synthesis of tetrapeptides in propylene carbonate, i) EDC (1.1 eq), HOBt (1.1 eq), DIPEA (3.0 eq), PC (0.2 M solution), 16 h ii) TFA (60 eq), PC, 3 h.

Tetrapeptide sequences **2.107a** and **2.107b** contain only unhindered and unfunctionalised amino acid side chains. This was initially used to demonstrate that it was possible to efficiently build up to the tetrapeptide stage using the optimised conditions for coupling and deprotection described previously. Sequences **2.107c-d** were then chosen to demonstrate the use of functionalised side chains that are protected (Ser(Bn), Lys(Z), Asp(Bn) and Gln(Trt)), functionalised side chains that are not protected (Met and Trp) and unfunctionalised but sterically hindered side chains (Val). This also demonstrates tolerance of the methodology to the key orthogonal protecting groups necessary in solution-phase peptide synthesis (Bn, Z and Trt). Finally, sequence **2.107e** demonstrates incorporation of the only non-proteinogenic amino acid investigated Aib, which is also regarded as very sterically hindered and thus difficult to couple. Along with the only secondary proteinogenic amino acid residue Pro.

Overall, the target sequences were produced with no significant issues, with the products of both coupling (65-93%) and deprotection (80-99%) typically obtained in good to excellent yield, in all cases (Table 2.6). This demonstrates that the methodology developed is tolerant to a wide variety of amino acid residues. Irrespective of whether they contain functionalised (Met, Ser, Lys, Asp, Trp, Gln, Tyr), unfunctionalised (Phe, Ala, Leu, Gly, Pro) or sterically hindered (Aib, Val) side chains.

Table 2.6: Summary of results for the synthesis of tetrapeptides **2.107a-e**.

Entry	**Sequence**	**Step**	**R^1**	**R^2**	**R^3**	**R^4**	**Yield (%)**[a]
1	**a**	**2.103**	Phe	Ala	-	-	93
2	**a**	**2.104**	Phe	Ala	-	-	99
3	**a**	**2.105**	Phe	Ala	Leu	-	75
4	**a**	**2.106**	Phe	Ala	Leu	-	96
5	**a**	**2.107**	Phe	Ala	Leu	Gly	72
6	**b**	**2.103**	Phe	Leu	-	-	80
7	**b**	**2.104**	Phe	Leu	-	-	99
8	**b**	**2.105**	Phe	Leu	Gly	-	78
9	**b**	**2.106**	Phe	Leu	Gly	-	94
10	**b**	**2.107**	Phe	Leu	Gly	Ala	91
11	**c**	**2.103**	Val	Met	-	-	91
12	**c**	**2.104**	Val	Met	-	-	80
13	**c**	**2.105**	Val	Met	Ser(Bn)	-	83
14	**c**	**2.106**	Val	Met	Ser(Bn)	-	84
15	**c**	**2.107**	Val	Met	Ser(Bn)	Lys(Z)	65
16	**d**	**2.103**	Val	Asp(Bn)	-	-	70
17	**d**	**2.104**	Val	Asp(Bn)	-	-	85
18	**d**	**2.105**	Val	Asp(Bn)	Trp	-	68
19	**d**	**2.106**	Val	Asp(Bn)	Trp	-	99
20	**d**	**2.107**	Val	Asp(Bn)	Trp	Gln(Trt)	78
21	**e**	**2.103**	Leu	Aib	-	-	78
22	**e**	**2.104**	Leu	Aib	-	-	97
23	**e**	**2.105**	Leu	Aib	Pro	-	73
24	**e**	**2.106**	Leu	Aib	Pro	-	97
25	**e**	**2.107**	Leu	Aib	Pro	Tyr(Bn)	72

[a] Isolated yield.

2.2.1.4 Global Deprotection of a Tripeptide

Finally, as the terapeptides produced are still protected at the *C*- and *N*-terminus, it was deemed necessary to demonstrate the complete deprotection of a peptide. This was to specifically highlight the ability to perform the hydrogenation reaction, for cleavage of the *O*-Bn protecting group, in PC. The Boc-Leu-Ala-Phe-OBn tripeptide **2.105a** was chosen as a test sequence. The fully deprotected tripeptide **2.110** can be obtained either by first removing the *N*-Boc group, followed by the *O*-Bn group, or vice versa. Both routes were therefore investigated (Scheme 2.24).

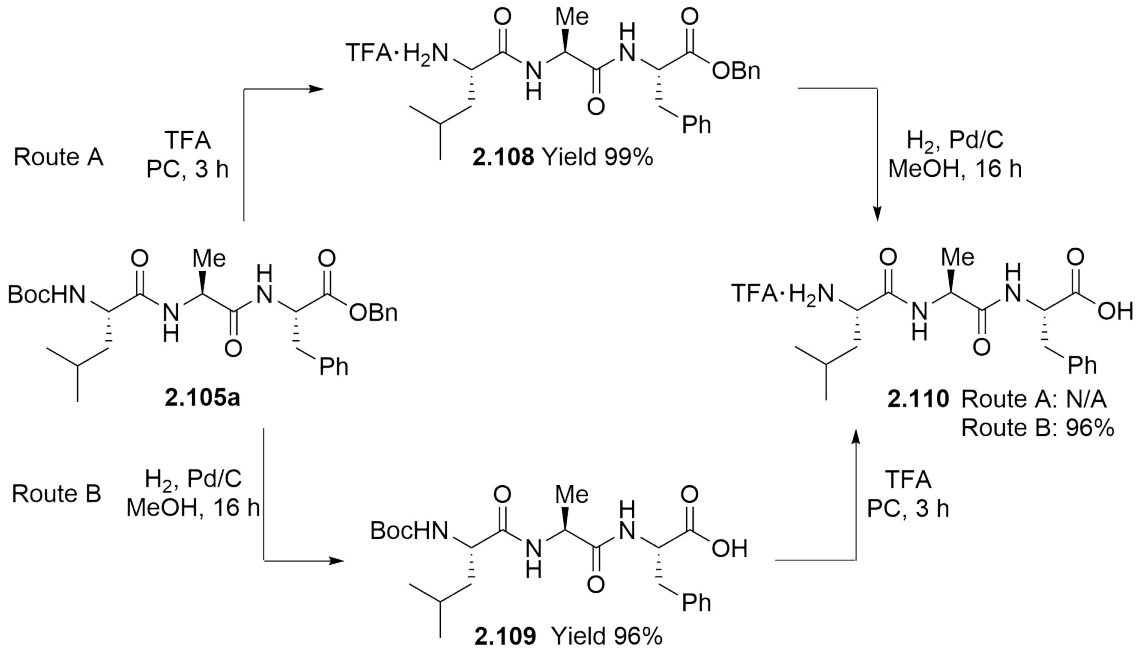

Scheme 2.24: Global deprotection of the Boc-Leu-Ala-Phe-OBn **2.105a** tripeptide.

Firstly, it has previously been shown that the *N*-Boc deprotection can be performed using TFA in PC. The Boc-Leu-Ala-Phe-OBn tripeptide **2.105a** was deprotected to give the intermediate amine salt **2.108** in a quantitative 99% yield (Route A). Problems arose however when trying to perform the subsequent hydrogenation. Efforts to do so in PC failed to produce the target tripeptide **2.110**, even when performed at high pressure (75 bar). This was unexpected as there is significant literature precedent for hydrogenation reactions in PC.[110,129] However, observations suggest the use of PC promotes leeching of the palladium from the solid support, deactivating the catalyst. Even the use of methanol, a more conventional hydrogenation solvent, failed to produce the target peptide **2.110**. This is believed to be due to residual PC from the proceeding step deactivating the catalyst. The obvious solution to this issue is to perform the hydrogenation reaction first (Route B). When the hydrogenation is performed first, under conventional reaction conditions, the target intermediate **2.109** is formed in an excellent 96% yield.

This *N*-Boc protecting group could then be removed producing the target fully deprotected tripeptide **2.110** in a 96% yield, or 92% over the two steps.

It has therefore been shown that cyclic carbonates, specifically PC, represent suitable solvents for the common transformations associated for solution-phase peptide synthesis. Control reactions showed PC was found to produce a target dipeptide in excellent yield, compared to control reactions performed in conventional solvent systems. The use of PC was also found to have little influence on the many side reactions associated with peptide bond formation, particularly racemisation. PC was then shown to tolerate the harsh acidic conditions associated with *N*-Boc deprotection, furnishing the corresponding dipeptide salt in quantitative yield, when exposed to excess TFA. The use of PC for the key reactions for chain elongation in peptide synthesis meant a range of tetrapeptides could be produced, with good to excellent yields observed in all cases for both coupling (65-93%) and deprotection (80-99%) steps. Finally, it was observed in an effort to obtain a fully deprotected tripeptide species that PC was not suitable for the hydrogenation step associated with the removal of the *O*-Bn protecting group. However, performing this reaction under conventional conditions, followed by a *N*-Boc deprotection in PC gave a completely deprotected tripeptide in an excellent 92% yield over the two steps.

2.2.2 Solid-Phase Peptide Synthesis in Cyclic Carbonates

Having demonstrated that PC could be successfully used as a solvent for solution-phase peptide synthesis, its application in solid-phase peptide synthesis was duly investigated. However, there are additional considerations that must be made when performing reactions upon a solid-support, particularly when choosing to do so in an alternative solvent. The most important being the ability of the solvent to adequately solvate the solid-support.[130] As ultimately, poor solvation results in limited accessibility to active sites and diminished reactivity.[131] The ability of a solvent to adequately solvate a solid-support, more commonly referred to as resin swelling, will be discussed in much greater detail in Chapter 3. For now, the ability of cyclic carbonates to swell common solid-phase peptide synthesis resins will be investigated.

2.2.2.1 Resin Swelling in Cyclic Carbonates

For this study nine commercially available resins were chosen. These broadly fall into four distinct categories based on the polymer backbone; polystyrene (PS) (Merrifield, Paramax, JandaJel), polyethylene glycol grafted polystyrene (PEG-PS) (TentaGel, ArgoGel, HypoGel 200, NovaGel), polyethylene glycol (PEG) (ChemMatrix) and polyamide (PA) (SpheriTide). The ability of these resins to swell in EC **2.41**,

PC **2.42**, DMF **2.43** and CH_2Cl_2 **2.48** was then investigated using the method previously reported by Santini *et al* (Figure 2.5).[131] This semi-quantitative approach for determining resin swelling measures the increase in occupied volume of the resin when exposed to a given solvent. Santini *et al.* then defined a solvent in which the resin swells to greater than 4.0 ml g^{-1} as a good solvent, between 4.0-2.0 mL g^{-1} a moderate solvent and less than 2.0 mL g^{-1} a bad solvent.

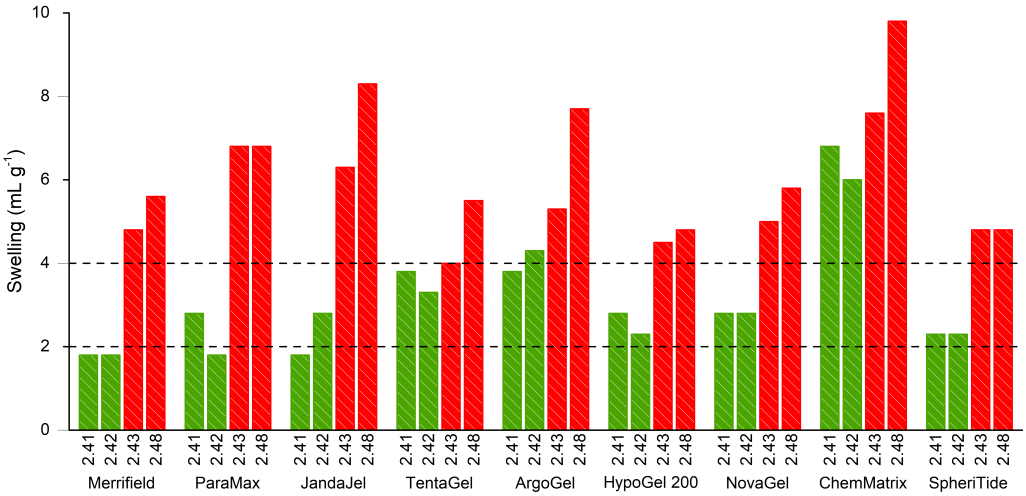

Figure 2.5: Graph of resin swelling for nine commercial solid-phase peptide synthesis resins in EC **2.41**, PC **2.42**, DMF **2.43** and CH_2Cl_2 **2.48**. Green = cyclic carbonates, Red = undesirable solvents.

It is immediately apparent that the undesirable solvents DMF and CH_2Cl_2 swell the commercial resins to a much greater extent than EC or PC. Cyclic carbonates appear to be very poor solvents for the PS based resins, as a value below 2.0 mL g^{-1} is indicative of no swelling. This was initially a rather disappointing result as Merrifield resin, even after 50 years, still remains one of the most commonly used supports for solid-phase peptide synthesis.[132] Only the use of EC with ParaMax and PC with JandaJel produced marginally better swelling for PS resins. Moderately improved swelling was observed with the PEG-PS based resins, with seven of eight results falling within the 2.0-4.0 mL g^{-1} range. Only the use of PC with ArgoGel produced a result that could be regarded as good swelling. ChemMatrix on the other hand, the only 100% PEG based resin, produced good swelling for both cyclic carbonates, with values of 6.8 mL g^{-1} and 6.0 mL g^{-1} obtained for EC and PC respectively. Finally, SpheriTide the only PA based resin, barely produced moderate swelling in both EC and PC. For the above reasoning, the use of ChemMatrix as a suitable resin for solid-phase peptide synthesis in cyclic carbonates was further explored.

2.2.2.2 Synthesis of a Model Tripeptide

The synthesis of tripeptide H-Leu-Ala-Phe-OH **2.110**, which had previously been prepared *via* the solution-phase approach, was chosen as a model substrate. The synthesis of this tripeptide was investigated using a solid-phase approach in both PC and DMF (Scheme 2.25). The synthesis began with the commercially available ChemMatrix resin, preloaded with the acid labile 4-(4-hydroxymethyl-3-methoxyphenoxy)butyric acid (HMPB) linker **2.111** and the phenylalanine amino acid residue as the free amine. Coupling was then performed using three equivalents of the desired *N*-Fmoc protected amino acid, 3-[bis(dimethylamino)methyliumyl]-3*H*-benzotriazole-1-oxide hexafluorophosphate (HBTU), HOBt and DIPEA in the chosen solvent as a 0.2 M solution, preactivated for 3 minutes. Whilst the amino acids examined were soluble in DMF, they were not in PC, they did however become soluble once preactivated. Removal of the *N*-Fmoc protecting group was then achieved using 20% piperidine (*v*/*v*) in either DMF or PC. Once the tripeptide sequence was complete, the peptide was cleaved from the resin using TFA:TIPS:H_2O (95:2.5:2.5), precipitated into cold ether, triturated and isolated to give the target tripeptide H-Leu-Ala-Phe-OH **2.110**.

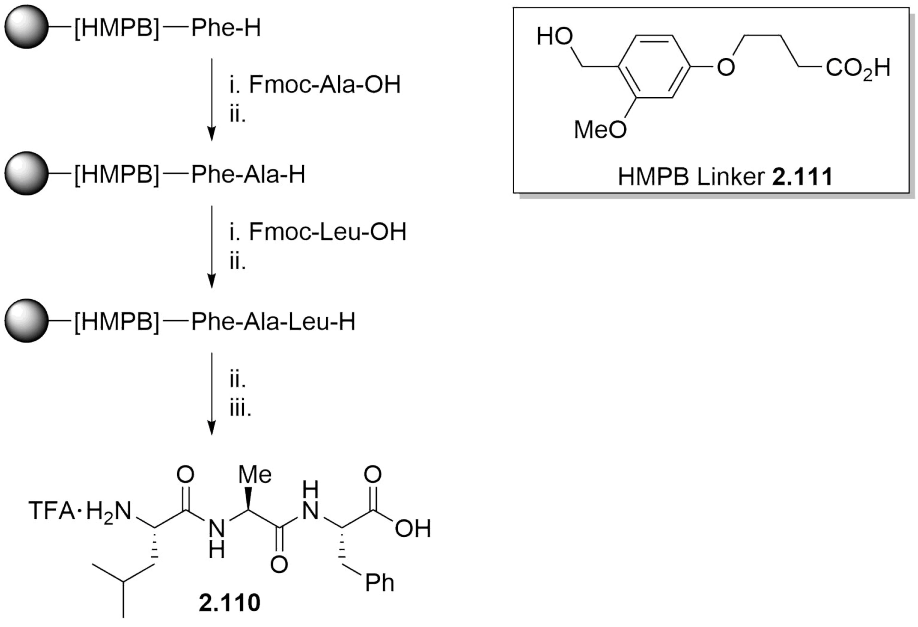

Scheme 2.25: Solid-phase synthesis of H-Leu-Ala-Phe-OH **2.110**, i) Fmoc-Amino Acid (3.0 eq), HBTU (3.0 eq), HOBt (3.0 eq), DIPEA (6.0 eq), 2×1 h, DMF or PC (0.2 M solution), ii) 20% piperidine in DMF or PC, 10 and 20 min, iii) TFA:TIPS:H_2O (95:2.5:2.5) 3 hours.

2.2.2.3 Alternative Washing Procedures

Typically, between synthetic steps the resin is washed with large quantities of solvent to remove any soluble impurities and excess reagents. This is usually done using

solvents such as DMF, CH_2Cl_2 and MeOH. To ensure that the use of non-green solvents was completely avoided, alternative washing procedures were investigated. Initially, just the reaction solvent was used for the washing procedure. However, due to the high boiling points associated with DMF (153 °C) and PC (242 °C), vacuum filtration failed to remove trace impurities of solvent, leading to contamination of the final product. This is apparent in the ^{1}H NMR spectrum of the H-Leu-Ala-Phe-OH tripeptide **2.110** prepared using PC, as residual solvent peaks are clearly visible (Figure 2.6). This was eventually remedied by either washing the resin prior to coupling with a green solvent with appreciable vapour pressure, such as 2-MeTHF, or performing multiple triturations using cold ether.

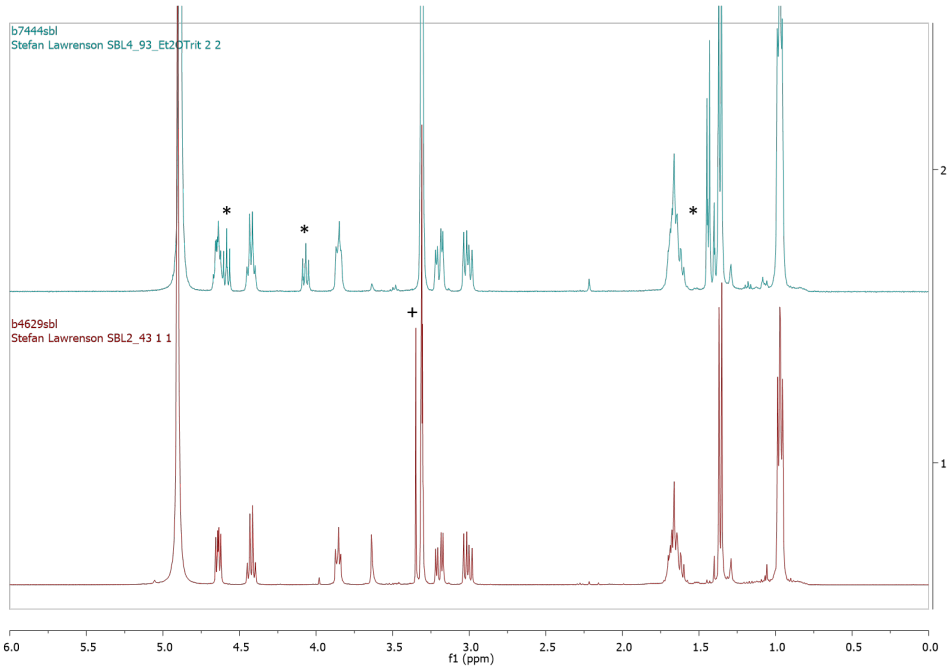

Figure 2.6: NMR spectra for H-Leu-Ala-Phe-OH **141** washed with just PC (top) and washed with 2-MeTHF prior to cleavage (bottom), * PC peaks, $^+$ PEG backbone peak.

Analysis of both samples by ^{1}H NMR spectroscopy indicated that the target peptide produced using PC was obtained in comparable crude purity to that which was prepared in DMF. It has therefore been shown that solid-phase peptide synthesis using PC as the reaction solvent is indeed achievable. Although it was necessary to use a less common solid-support, as ChemMatrix was the only resin found to give appreciable swelling in PC. Finally, it was also found that the use of any undesirable solvents for the washing procedure could be completely removed. This meant a single, green solvent could be used for both reaction and washing procedures, with only a final wash before cleavage necessary to remove any residual PC.

2.2.3 Total Synthesis of Bradykinin in Cyclic Carbonates

Having demonstrated that PC could be used as a solvent for solid-phase peptide synthesis, when used in conjunction with the high swelling ChemMatrix resin, the limitations of the developed methodology was further explored. Therefore, the synthesis of a the naturally occurring nonapeptide bradykinin (H-Arg-Pro-Pro-Gly-Phe-Ser-Pro-Phe-Arg-OH) **2.112**, a biologically relevant peptide was chosen to demonstrate the synthetic usefulness of the developed procedures.

First isolated using the venom of the Brazilian Lancehead snake *Bothrops Jararaca*, bradykinin was identified as being a potent vasodilator, which was in turn found to be particularly important in blood pressure regulation and in inflammatory mediation.[133] In fact, braykinin was found to be one of many pharmacologically active peptides released during the breakdown of kininogen by kallikrein enzymes, more commonly known as the kallikrein-kinin system.[134] Greater understanding of this system led to the development of angiotensin-converting enzyme (ACE) inhibitors, which mitigates bradykinin metabolism, a blockbuster range of drugs used in the treatment of heart failure and hypertension.[135] This is significant as the discovery of bradykinin represents the first time in which the pharmacophore of a protein toxin had been used in the design of peptide-mimetic drugs.[136] Bradykinin was also one of the first physiological peptides synthesised by R. B. Merrifield to demonstrate the utility of solid-phase peptide synthesis.[137,138] Additionally, it was considered that bradykinin was of suitable length and contained a good balance of functionalised and unfunctionalised amino acid residues. For the above reasons, bradykinin represented a suitable target and a reasonable challenge for the developed methodology.

The synthesis of bradykinin was to be carried out starting from ChemMatrix-HMPB preloaded with the Arg(Pbf) amino acid residue (Scheme 2.26). Coupling, deprotection, cleavage and washing steps were to be carried out under the conditions described for the synthesis of the model tripeptide using the solid-phase approach. To allow a direct comparison between the developed methodology and a conventional approach the synthesis of bradykinin was also to be carried out in DMF. This plan immediately hit issues, as repeated attempts to synthesise bradykinin using PC as the reaction solvent failed to produce the target peptide. Meanwhile, the control sample using DMF as the reaction solvent had proven to be successful. The reason for this difference was not immediately obvious, considering the synthesis of a model tripeptide had proceeded without issue. It was not until doubts were raised about the stability of cyclic carbonates, as briefly mentioned earlier, that the underlying issue was finally elucidated.

Scheme 2.26: Solid-phase synthesis of bradykinin **2.112**. i) Fmoc-Amino Acid (3.0 eq), HBTU (3.0 eq), HOBt (3.0 eq), DIPEA (6.0 eq), 2×1 h, DMF or PC (0.2 M solution). ii) 20% piperidine in DMF or PC, 10 and 20 min. iii) TFA:TIPS:H_2O (95:2.5:2.5) 3 hours.

2.2.3.1 Reactivity of Cyclic Carbonates

The use of cyclic carbonates as reactive intermediates first appeared within the literature more than 50 years ago. Consequently, the reaction of cyclic carbonates with aliphatic and aromatic amines, alcohols, thiols and carboxylic acids for the preparation of small molecules and polymers, is well established.[107] Our interest of course lies predominantly in the reaction of cyclic carbonates with amines.

The reaction of cyclic carbonates with aliphatic and aromatic amines is typically known to proceed through two possible reaction mechanisms, depending on amine nucleophilicity (Scheme 2.27). The ring opening of cyclic carbonates **2.114** by alkyl amines is known to proceed under ambient conditions (25-50 °C), generating the corresponding *N*-alkyl carbamates **2.113**. This reaction has been well explored in the context of non-isocyanate polyurethane (NIPU) synthesis.[139] However, of the cyclic carbonates structures widely explored (5-, 6-, 7-, 8-membered or thio-cyclic carbonates), 5-membered cyclic carbonates are known to be the least reactive.[140] The reactivity of 5-membered cyclic carbonates is also known to be very dependent on ring substitution, solvent and temperature.[139] For this reason, aminolysis of 5-membered cyclic carbonates under ambient conditions is typically performed in the presence of a suitable Lewis acid- or organo-catalyst.

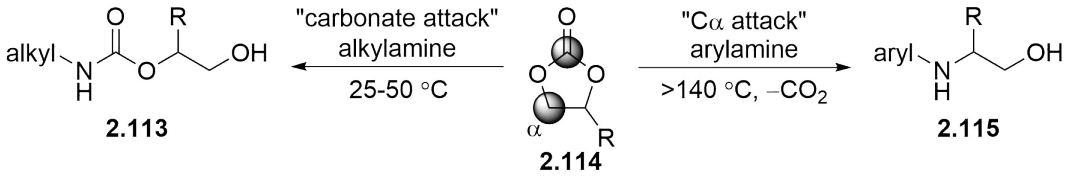

Scheme 2.27: Reaction of cyclic carbonates with alkyl- or aryl-amines.

On the other hand, *N*-aryl amines typically required much harsher conditions due to their low nucleophilicity. However, under these harsh conditions chemoselectivity is compromised, with Cα attack preferred over carbonate attack, generating a range of decarboxylated side-products including *N*-aryl amines **2.115**. More recently, Kleij and co-workers have shown that the poor nucleophilicity can be overcome when a suitable organocatalyst is used, demonstrating the first chemo- and regio-selective synthesis of *N*-aryl carbamates.[141] In a recent communication Kleij and co-workers have extended this methodology to include geminal disubstituted cyclic carbonates and secondary amines.[127] Geminal dimethyl-substituted cyclic carbonate **2.116** were cleanly converted to the corresponding *N*-alykl carbamate **2.118** within 18 hours in the presence 20 mol% triazabicyclodecene (TBD), with >99:1 selectivity for **2.118** over **2.119** (Scheme 2.28).

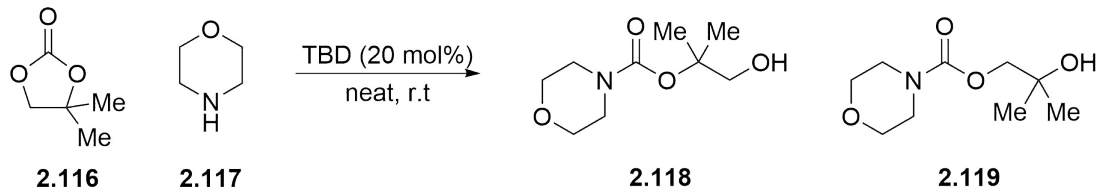

Scheme 2.28: Reaction of geminal dimethyl-substituted cyclic carbonate **2.116** with morpholine **2.117** to generate *N*-alkyl carbamate **2.118**/**2.119**.

More importantly, Kleij and co-workers reported that this transformation occurs but is much slower in the absence of TBD, with 60% conversion observed in 24 hours and a regioselectivity of 63:37 (**2.118**:**2.119**). With this in mind, we had previously investigated the reaction of amino acid amines with cyclic carbonates observing that only 1% conversion was observed within 3 hours under forcing conditions. The reaction of cyclic carbonates with piperidine **2.120**, used in removal of the *N*-Fmoc protecting group, had not been considered. It turns out this reaction has only been explored on two occasions prior to our investigation by Baizer *et al.* and Najer *et al.* more than 50 years ago.[142,143] We therefore decided to carry out the reaction between PC **2.42** and piperidine **2.120**, neat under ambient conditions. As expected the corresponding *N*-alykl carbamate is formed as a 50:50 mixture of regioisomers **2.121**/**2.122** (Scheme 2.29). Monitoring the progress of this reaction by ^{1}H NMR spectroscopy indicates that roughly 80% of the piperidine is consumed within 30 minutes.

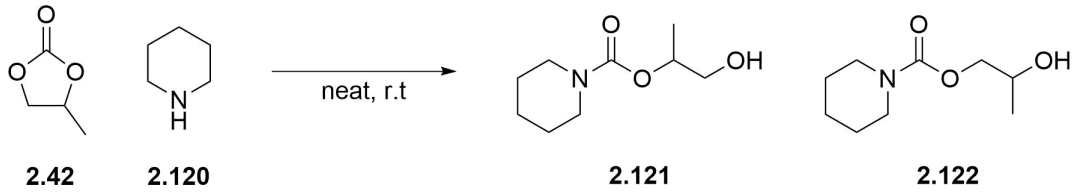

Scheme 2.29: Reaction of PC with piperidine to generate the *N*-alkyl carbamate as a mixture of regioisomers **2.121**/**2.122**.

Returning to the challenge at hand, the total synthesis of bradykinin **2.112**, it was now apparent what the issue had been. Previously, a large quantity of 20% piperidine in PC (v/v) had been prepared beforehand. This of course would rapidly become inactive as the piperidine is quickly consumed. This obviously presents a major issue, however, the half life ($t_{1/2}$) for *N*-Fmoc deprotection is known to be on the scale of 7 seconds. This means 99.99% conversion is obtained within approximately 1.5 minutes.[144] It was therefore hoped that *N*-Fmoc deprotection would occur suitably quickly, relative to the consumption of piperidine, providing the 20% piperidine solution in PC was freshly prepared for each deprotection.

It is also worth acknowledging at this point that prior to attempting the manual synthesis of bradykinin the use of automated SPPS had been investigated. Bradykinin, ACP 65-74 and β-amyloid were identified as suitable targets for the developed methodology using the two days that were available with the instrument. A major issue was initially realised when the amino acids were found to not be soluble at 0.2 M in PC, this could however be overcome using a solvent mixture of 80:20 PC:2-MeTHF, with histidine the only amino acid that appeared to precipitate out of solution upon standing. Unfortunately, following cleavage, no evidence of the target peptides could be identified by high-resolution mass spectroscopy (HRMS). On reflection, this is most likely also due to the fact that the 20% piperidine (v/v) solution in PC was prepared in bulk prior to starting the instrument. Having now realised that the ring-opening of PC by nucleophilic amines is a major side-reaction in this methodology, it may very well be worth revisiting the use of PC in automated SPPS in future.

The total synthesis of bradykinin was therefore reattempted, according to the synthetic procedure outlined previously (Scheme 2.26). Except this time the solution of piperidine in PC (20% v/v) was freshly prepared before each use. Following construction of the desired sequence the crude peptide was precipitated into cold ether, triturated and lyophilised. The presence of bradykinin was then confirmed using HRMS.

Having identified that bradykinin had been successfully synthesised using PC as the reaction and washing solvent, the sample prepared in PC, the control sample prepared in DMF, and a commercial standard were analysed using LCMS. The major peak identified in each case is consistent with bradykinin (Peak 1), with the samples prepared in PC and DMF found to have crude purities of 77% and 79% respectively. Clearly the use of PC as the solvent has no detrimental effect on the overall synthesis when compared to a control sample (Figure 2.7).

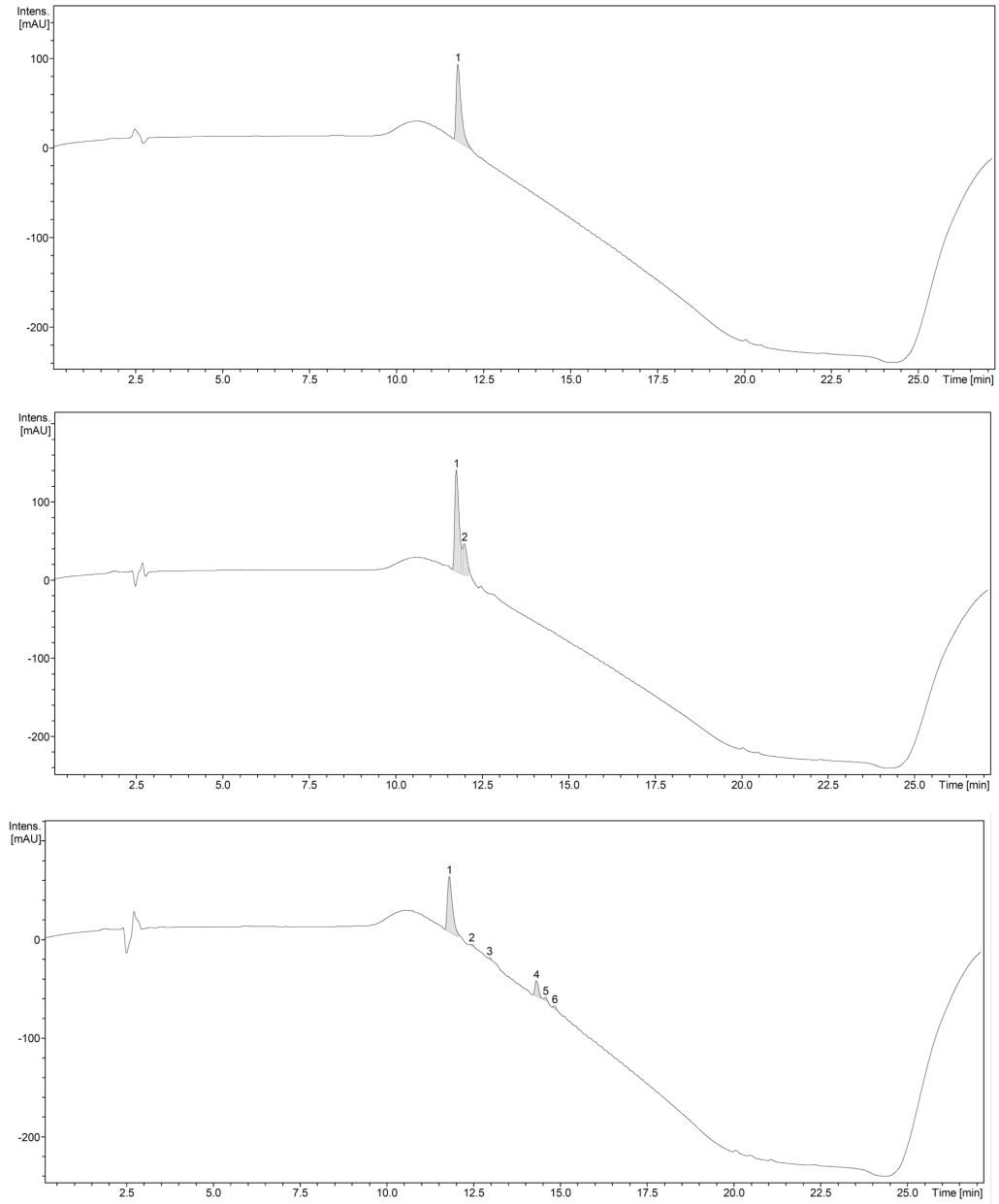

Figure 2.7: HPLC-UV traces of bradykinin **2.113**, commercial standard (top), sample prepared in DMF (middle) and sample prepared in PC (bottom). Peak numbers correlate to the distinct peaks that were identified for HRMS analysis. They do not represent equivalent compounds and have no relation between distinct runs. Identity of these products will be discussed in due course.

2.2.3.2 Identification of Impurities in Bradykinin Total Synthesis

Whilst the use of PC appeared to have no detrimental effect on the synthesis of bradykinin in terms of crude purity. It does appear to have an influence on the impurities generated during the synthesis, as clearly distinct peaks are observed when compared to the control sample (Figure 2.7). Analysis of the control sample spectrum identifies a single impurity on the shoulder of the bradykinin peak. Using the HRMS data generated for this peak, three major impurities can be identified. All of these were found to be deletion sequences, with H-Pro-Phe-Arg-OH **2.123a**, H-Ser-Pro-Phe-Arg-OH **2.123b** and H-Phe-Ser-Phe-Arg-OH **2.123c** detected (Figure 2.8). It should be noted that the presence of deletion sequences of peptidic nature is an issue, as it can often be difficult to remove these impurities using HPLC, due to their similarities relative to the target species.

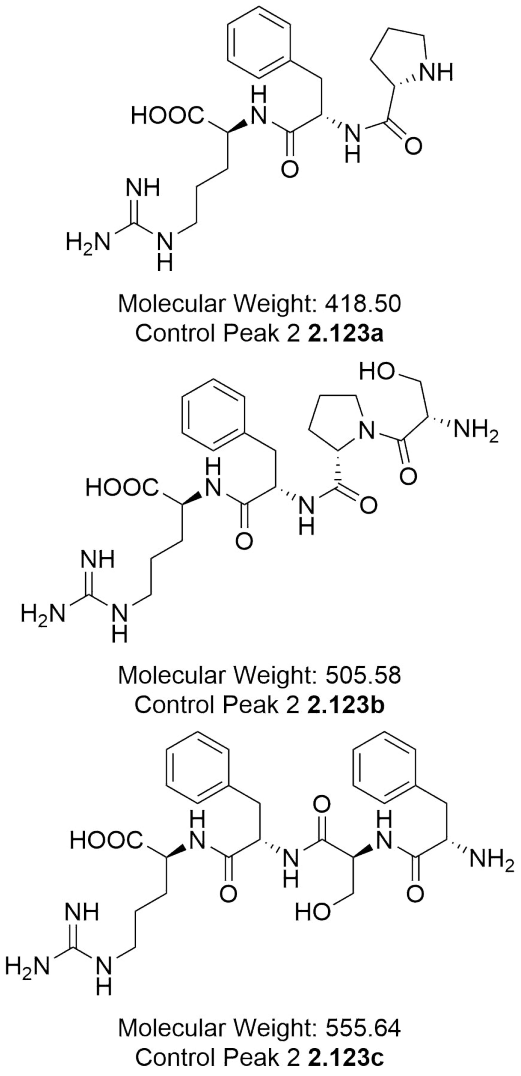

Figure 2.8: Impurities identified in the control sample of bradykinin **2.112** prepared using DMF.

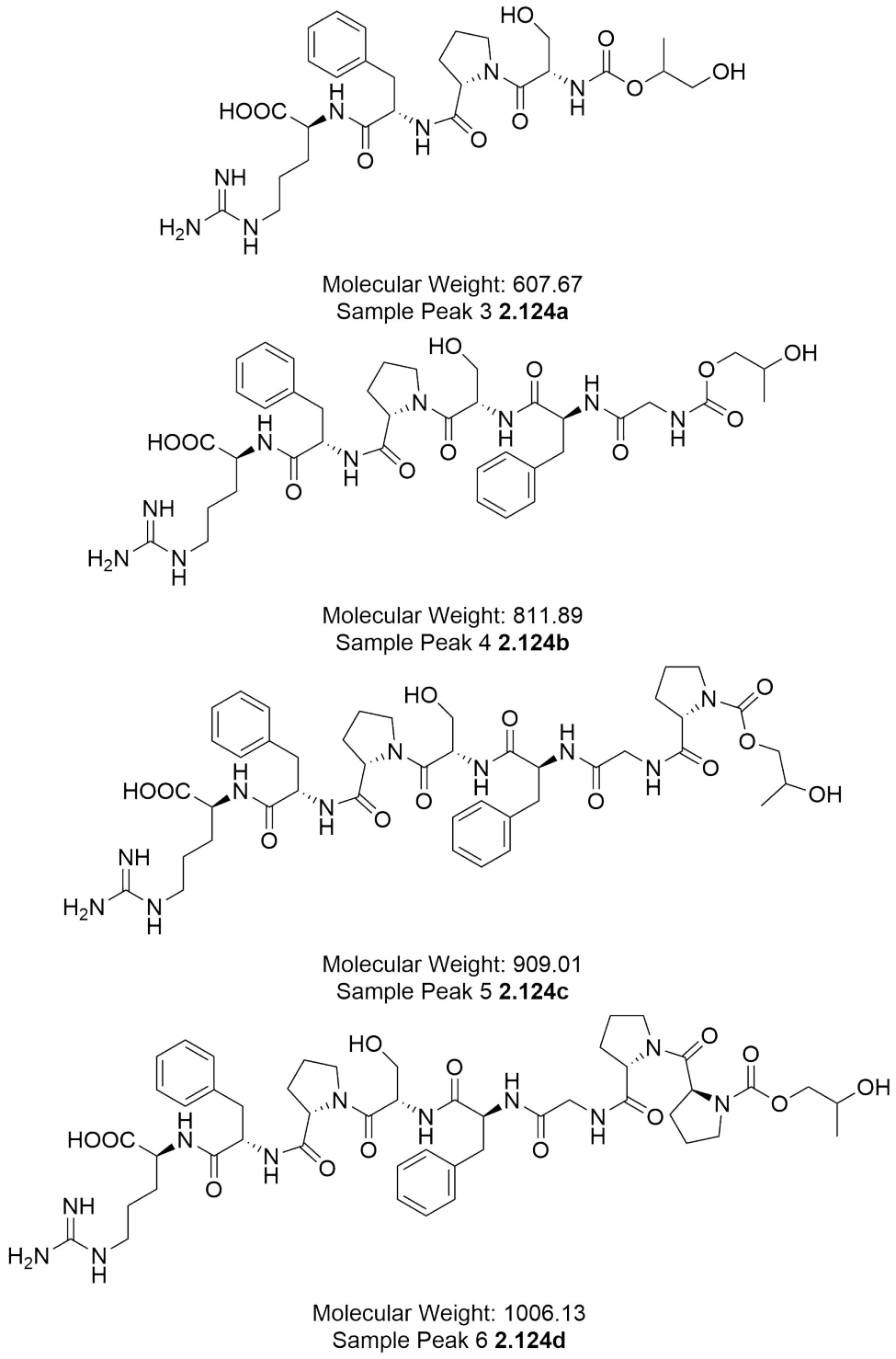

Figure 2.9: Impurities identified in the sample of bradykinin **2.112** prepared using PC.

Analysis of the spectrum obtained for the bradykinin sample prepared using PC identified the presence of five distinct impurities (Figure 2.9). Peak 2, which also appears to be present in the control sample but was not integrated, could not be identified using the HRMS data obtained. The remaining peaks on further analysis appear to be missed couplings, but show very different retention times to those observed in the control sample. This is because each impurity appears to be end-capped with PC, producing the corresponding carbamate, altering the retention time. The four impurities observed have been assigned to the following species; PC-Ser-Pro-Phe-Arg-OH **2.124a**, PC-Gly-Phe-Pro-Ser-Pro-Phe-Arg-OH **2.124b**, PC-Pro-Gly-Phe-Ser-Pro-Phe-Arg-COOH **2.124c** and PC-Pro-Pro-Gly-Phe-Ser-Pro-Phe-Arg-OH **2.124d**. The most abundant (peak 4 **2.124c**) represents 15.2% of the peak area, for the impurities observed. This may be expected as the glycine residue is the least hindered and likely to be the most nucleophilic amino acid in the bradykinin sequence. This is a disappointing observation as it suggests that cyclic carbonates may be more prone to ring-opening than had been first anticipated. On the other hand, the ring-opening of cyclic carbonates by nucleophilic amines does not appear to impair peptide synthesis, as both coupling and deprotection reactions, at first glance, were not affected. The end-capping of the *N*-terminus could also be regarded as advantageous as it makes separation of the target compound from impurities easier, in a similar manner to how long-chain sequences are often acetylated following coupling to make removal of any unreacted sequences easier.

At the time of writing, Olsén *et al.* have reported on the ring-opening of cyclic carbonates using α-amino acids in water.[145] In their investigation Olsen *et al.* found that divinylethylene carbonate **2.125** underwent a ring-opening reaction by glycine **2.126** in the presence of NEt_3 and H_2O, to produce the corresponding carbamate **2.127** (Scheme 2.30). This reaction was found to be fairly general, with a range of carabamates produced in good yield from the corresponding cyclic carbonate, although the reaction could not be performed regioselectively. Variation of the amino acid also showed that more sterically congested side chains generally resulted in lower yields. This report from Olsén *et al.* therefore reaffirms the observation that cyclic carbonates are susceptible to ring-opening by α-amino acids, particularly for unhindered amino acids.

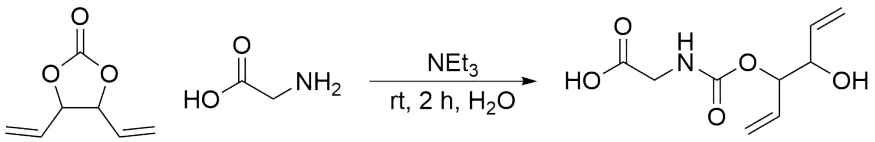

2.125 2.126 2.127

Scheme 2.30: Ring-opening of divinylethylene carbonate **2.125** by glycine **2.126** to produce the corresponding carbamate **2.127**.

2.3 Conclusions

In conclusion, this chapter has identified that the growing interest in therapeutic peptides is likely to be a major issue in the future, due to their inherently ungreen synthesis. The need for numerous auxiliary reagents, including protecting groups, undesirable solvents and coupling agents, means chemical peptide synthesis is commonly associated with poor PMIs and the generation of large quantities of waste. As solvent is often the biggest contributor to waste the largest gains to be had, in terms of reducing environmental impact, will often come with solvent optimisation, rather than changes to the chemistry.

The various approaches within the literature to performing both solution- and solid-phase peptide synthesis have therefore been reviewed. Many of these approaches have sought to utilise water as the principal solvent. These however often require significant changes to the chemistry, in order to overcome the limitations associated with peptide bond formation in water. More recently, the use of alternative organic solvents has attracted much interest, of which cyclic carbonates have not been investigated. Due to the many desirable chemical and physical properties they possess as solvents, cyclic carbonates appear to be ideally suited to the development of a more sustainable approach to peptide synthesis. The use of cyclic carbonates for solution- and solid-phase peptide synthesis has therefore been explored.

Initial investigations into the solution-phase synthesis of a model Boc-Phe-Ala-OBn dipeptide demonstrated PC was able to perform as well, if not better, than conventional DMF or DMF:CH_2Cl_2 solvent mixtures. The model dipeptide was produced in excellent yields, under optimised coupling conditions using EDC, HOBt and DIPEA. This was also shown to occur without racemisation of the chiral centres. Investigation into *N*-Boc deprotection then demonstrated that PC was tolerant to the strongly acidic conditions. The dipeptide salt was typically obtained in quantitative yield, with the use of TFA and PC found to be most convenient. The developed methodology was then applied to the synthesis of a diverse range of tetrapeptides. Good to excellent yields were typically observed for both coupling (65-91%) and deprotection (80-99%) reactions. More importantly, PC was shown to be tolerant to the protecting groups and functionalised side-chains commonly used in

peptide synthesis. Finally, the global deprotection of a tripeptide was investigated. Whilst the *N*-Boc deprotection proceeded smoothly in PC, the *O*-Bn deprotection did not, which is believed to be due to leeching and deactivation of the catalyst by PC. This was eventually remedied by performing the hydrogenation reaction in methanol, with the final H-Leu-Ala-Phe-OH tripeptide obtained in a 92% yield over the two steps.

Extending the use of PC to solid-phase peptide synthesis initially hit a problem, as PC was unable to swell a PS-based resin. This meant that use of the PEG-based ChemMatrix resin was necessary. The model tripeptide H-Leu-Ala-Phe-OH was then successfully synthesised using the HBTU, HOBt and DIPEA in PC, upon a ChemMatrix-HMPB resin. The removal of all undesirable solvents, including those used in the washing procedures, was then attempted. Unfortunately, the use of PC as the only solvent for SPPS resulted in contamination of the final product with the solvent. This was resolved by either washing the resin with a more volatile solvent, such as 2-MeTHF, before cleaving from the resin, or through extended trituration of the final product. The synthesis of bradykinin, a biologically relevant peptide, was then attempted in an effort to test the methodology. Initially, this failed due to what was eventually identified as a side reaction between piperidine and PC. This was easily overcome by freshly preparing the 20% (v/v) solution of piperidine in PC each time, as it was realised that the rate of ring-opening is significantly less than the rate of Fmoc-deprotection. Bradykinin was then synthesised in an excellent 77% crude purity, which is comparable to a control sample produced in DMF. Analysis of the distinctly different impurities generated in the bradykinin synthesis using PC, found that end-capping of the amino acids was occurring via the previously mentioned side-reaction. This however, does not appear to inhibit the synthesis in anyway and actually facilitates separation, due to the vastly different retention times observed within the LC. Cyclic carbonates have therefore been shown to be excellent solvents for a more sustainable approach to both the solution- and solid-phase synthesis of peptides.

Chapter 3

Greener Solvents for Solid-Phase Organic Synthesis

3.1 Introduction

Over the course of the previous investigation (Chapter 2) it became apparent the use of green solvents in SPPS had only seen limited investigation. In comparison, the use of green solvents in the closely related Solid-Phase Organic Synthesis (SPOS) methodology was almost non-existent. SPOS is where an organic transformation is performed upon an insoluble polymer support. This approach has established itself as a powerful tool for the construction of complex biological structures and small organic molecules. This was first reported more than half a century ago by Bruce Merrifield, in his pioneering work on the development of Solid-Phase Peptide Synthesis (SPPS).[146] In his seminal report, Merrifield covalently bound an amino acid to an insoluble polymer, in the form of a resin bead, through the use of a chloromethylated copolymer of styrene and divinylbenzene (DVB). The peptide sequence could then be built upon the resin bead through the stepwise addition of subsequent amino acids. Once the desired sequence was complete, the peptide could simply be cleaved from the solid support and isolated. The advantage of this approach is that when the target product is firmly immobilised to an insoluble support, purification becomes a trivial matter, as excess reagents and soluble by-products can be removed by a simple filtration. Thus, the laborious isolation and purification methods commonly associated with solution-phase peptide synthesis are eliminated. This approach however, was initially met with scepticism by the majority of organic chemists.[147] It took a number of brilliant achievements, such as the total synthesis of a series of biologically active peptides, including bradykinin and the 124-amino acid sequence of ribonuclease A, before the majority could be convinced.[148,137] Merrifield was eventually rewarded for his perseverance with the 1984 Nobel Prize in Chemistry.[147]

Nowadays, advances in the use of synthesis robots has established SPPS as an automated task, resulting in SPPS being the favoured approach for the synthesis of complex biological molecules, such as polypeptides, oligonucleotides and oligosaccharides.[149] Consequently, the speed and efficiency associated with SPPS has led to many synthetic transformations being demonstrated upon solid-supports. This combined with advances in combinatorial techniques has led to a revolution in the drug discovery process, as automated SPOS has allowed for the rapid generation of vast compound libraries, greatly accelerating the search for lead structures and their optimisation, in the preparation of novel pharmaceuticals.

In the context of green chemistry this rapid and efficient synthesis of diverse molecular structures using a variety of synthetic procedures, with minimal steps required for isolation and purification is highly appealing. There are however major issues associated with SPOS, in that the removal of excess reagents and soluble

by-products requires the resin to be washed between procedures, generating large quantities of contaminated solvent waste. Much like SPPS, the most commonly used solvents for SPOS include the reprotoxic polar aprotic solvents, DMF, NMP and DMA. All of which are classified as substances of very high concern under REACh, meaning they are likely to see restriction in their use in the near future.[50] Other common solvents for SPOS also include diethyl ether and CH_2Cl_2, both of which have been highlighted as solvents of concern in recent solvent selection guides.[16] Furthermore, solvent has been typically found to account for as much as 80-90% of the waste mass generated in a given batch pharmaceutical or fine-chemical operation.[15] The overall environmental impact of a process is therefore overwhelmingly a consequence of the solvent, meaning the biggest gains in terms of reducing the environmental impact will come from optimisation of the solvent, rather than changes to the chemistry.

Having previously investigated the use of cyclic carbonates as green solvents for both solution- and solid-phase peptide synthesis (Chapter 2), it made sense to extend this methodology to SPOS. Cyclic carbonates however proved to be poor solvents for the majority of common SPPS/SPOS resins, the focus therefore sought to investigate a wide range of green solvents, in order to find suitable replacements applicable to a number of common SPOS/SPPS resins. Prior to the investigation into SPPS, analysis of the associated literature highlighted that the use of green solvents had been extensively investigated, with water and neoteric organic solvents proving particularly promising. Rather surprisingly, in comparison SPOS has seen relatively little investigation, in fact only two distinct examples could be found within the literature that explicitly utilise a green solvent.

3.1.1 Previous Reports of Greener Solid-Phase Organic Synthesis

The earliest example of this was first reported by Coats *et al.*, in their investigation into the use of a range of unconventional solvents for the solid-phase thionation of amides.[150] The requirement for high temperatures to drive the reactions to completion when performed in parallel, due to less efficient heating and stirring, necessitated the use of a solvent with a high boiling point and low vapour pressure. This is because previous attempts utilising THF or toluene had resulted in various issues, such as solvent evaporation, migration and exposure. In an initial screening benzyl benzoate was identified and found to perform comparably to control reactions in either THF or toluene when the reaction was carried out at 65 °C. Subsequently, the thionation of polystyrene-supported (PS) aryl and alkyl derivatives of phenylalanine **3.1** using Lawesson's reagent **3.3** was investigated under

parallel conditions. When benzyl benzoate was used as the reaction solvent the target thioamides **3.2** were obtained in good to excellent conversions at 100 °C in only 8 hours, an appreciable improvement over the use of THF or toluene (Scheme 3.1).

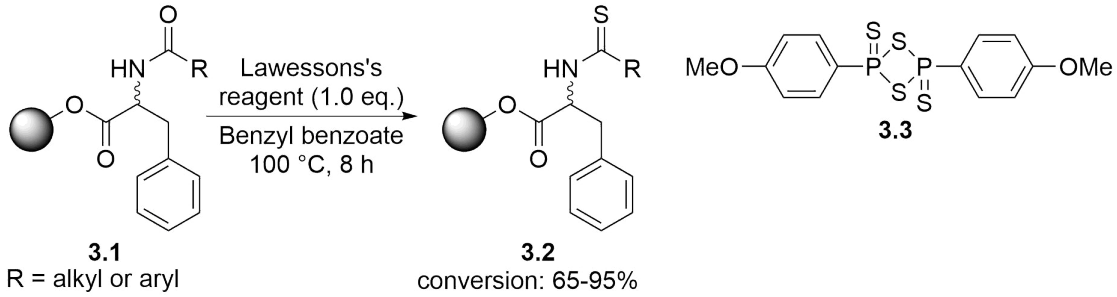

Scheme 3.1: Thionation of PS-supported phenylalanine **3.1** using Lawesson's reagent **3.3** in benzyl benzoate.

More recently, Stobrawe *et al.* have investigated the use of compressed carbon dioxide as a neoteric green reaction medium for SPOS.[151] As previously discussed, solid-supported reactions often suffer from diminished reaction kinetics, due to poor mass transfer between the solid and liquid phase. An issue that is exacerbated in reactions that occur under triphasic conditions (g/l/s). It was hoped that these mass transfer limitations could be overcome with the use of compressed carbon dioxide, as either a supercritical fluid ($scCO_2$) or gas expanded liquid (GXL). Stobrawe *et al.* began their investigation with the rhodium catalysed hydroformylation of 1-hexen-5-ol **3.4** upon a PS resin (Scheme 3.2). Initial attempts using $scCO_2$ were disappointing, resulting in only 10% yield of the target hydroformylation products. It was hypothesised that this was due to inadequate solvation of the PS support in $scCO_2$. This was eventually overcome through the addition of an organic co-solvent, such as 1-hexene, CH_2Cl_2 or toluene, producing the hydroformylation products in a >98% yield, and a 1.2:1 ratio of **3.5**:**3.6**.

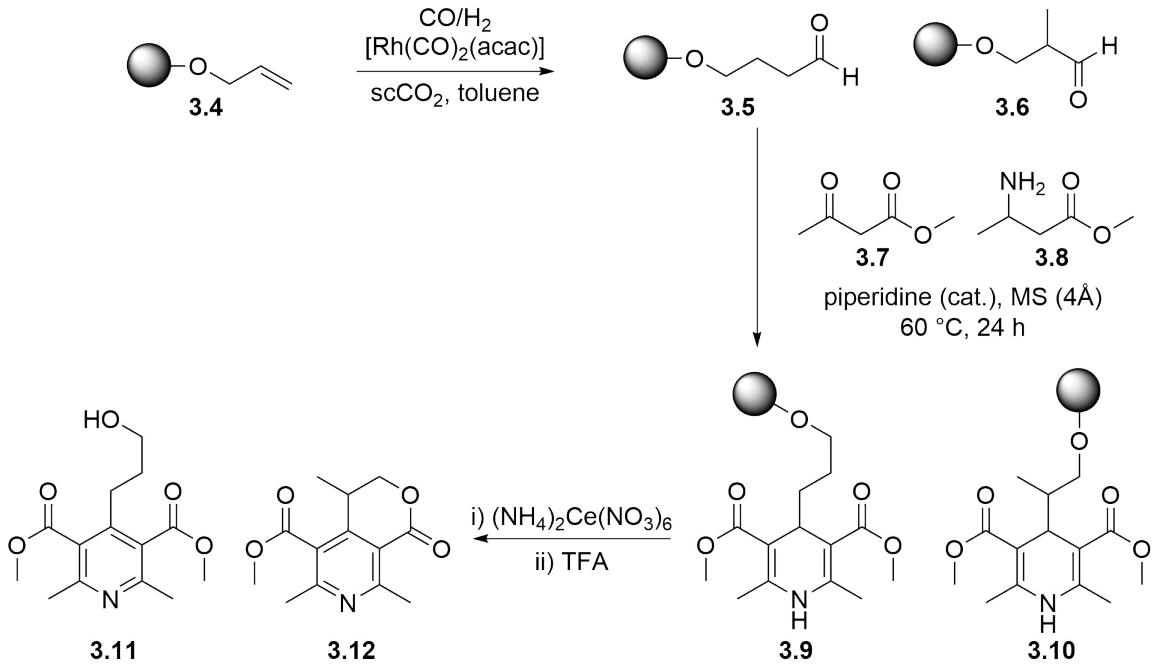

Scheme 3.2: Catalytic hydroformylation upon PS-resin in $scCO_2$ and subsequent Hantzsch pyridine synthesis.

To demonstrate the applicability of the developed methodology to a more complicated product synthesis Stobrawe *et al.* went on to investigate the use of $scCO_2$ in the solid-supported Hantzsch synthesis of pyridines. After formation of the hydroformylation products under the previously described conditions, the solid supported aldehydes **3.5**:**3.6** were utilised in a multi-component coupling with methyl acetoacetonate **3.7** and methyl 3-aminocrotonate **3.8**. Aromatisation of the intermediates **3.9**:**3.10** using ceric ammonium nitrate and subsequent cleavage from the solid support using TFA produced the target isomeric pyridines **3.11**:**3.12** in a 99% yield and a 1.4:1 ratio.

Stobrawe *et al.* then went on to investigate a second benchmark reaction, in the cobalt-catalysed Pauson-Khand reaction (PKR).[151] The PKR between norbornene **3.14a** and 1-pentyn-5-ol **3.13** upon a solid support was first investigated using THF as the reaction solvent, in the presence of a catalytic amount of $[Co_2(CO)_8]$ under CO_2 (20 bar) at 120 °C. After 17 h, cleavage using TFA in CH_2Cl_2 produced the target product **3.15a** in an 80% yield (Scheme 3.3). A significant enhancement was observed when the same reaction was performed in the presence of compressed carbon dioxide. Under GXL conditions quantitative formation of the PKR product **3.15a** was observed. A similar increase in yield was also noted under GXL conditions when using the more challenging norbornadiene **3.14b** as a substrate.

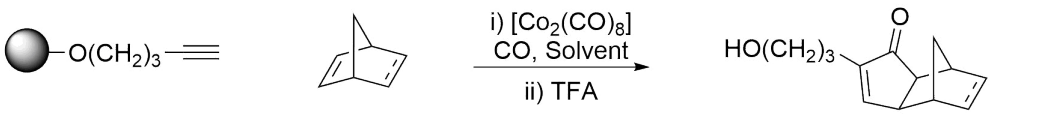

3.13 | **3.14a**: Norbornene, **3.14b**: Norbornadiene | **3.15a**: GXL: 99%, THF: 80%, **3.15b**: GXL: 64%, THF: 42%

Scheme 3.3: Solid-supported Pauson-Khand reaction under conventional and GXL conditions.

3.1.2 Determining the Suitability of Green Solvents for SPOS

The lack of investigation into greener solvents for SPOS could possibly be justified on the basis that solvents such as DMF, NMP, DMA and CH_2Cl_2 are still the most common solvents for SPPS. Since it was identified previously (Chapter 2) that the use of alternative organic solvents in SPPS is something that has only began to receive a significant amount of interest in more recent years.[152] It was therefore reasoned that a systematic investigation into the suitability of various common green solvents for SPOS was indeed necessary, in an effort to aid chemists in their selection of an appropriate green solvent for a given reaction. This however poses a rather substantial challenge, as the use of an insoluble solid support places many additional considerations on the solvent, when compared to traditional solution-phase chemistry. Not only must the polymer resin be insoluble in the desired solvent at a macroscopic level, to facilitate purification by filtration, but the solvent must also be able to adequately solvate or swell the resin. This is something that has been briefly discussed in the previous chapter (Chapter 2), but will now be explored in greater detail.

3.1.2.1 Resin Swelling

Swelling of a cross-linked polymer is essentially equivalent to dissolution of a linear polymer. However, rather than dissolving the polymer, the crosslinker inhibits the excessive motion in the polymer chains necessary to form a solution. Instead the solvent ends up occupying the space between polymer chains, causing an increase in the total volume of the polymer, or causing it to swell. This is often considered to be one of the most important prerequisites for SPOS, as a solvent that does not adequately solvate the solid-support presents little opportunity for reagents to interact with the active sites.[130] This makes sense from a statistical perspective as an even distribution of active sites within a resin sphere results in >99% of active sites residing within the sphere, rather than at the surface.[153] In this regard, the swollen polymer now assumes the role of the solvent, forming an admixture that constitutes the media in which the reaction will occur.

The importance of this phenomenon was actually acknowledged by Merrifield in his initial communication of SPPS.[146] However, early understanding was quickly proved to be inadequate, as a number of failed attempts at the synthesis of difficult peptides, peptides that posses sequences prone to the formation of secondary structures, were attributed to the polymer-supported nature of the reactions.[154] This resulted in Merrifield revising his previous model for resin-swelling. In a subsequent communication by Sarin *et al.* Merrifield addressed two key questions (1) How are the properties of the peptide-resin influenced by each of the components of the system (the peptide, the resin and the solvent)? (2) Is there a fixed maximum volume for a swollen resin bead, which is eventually filled by the growing peptide?[155]

To answer these key questions Sarin *et al.* prepared a range of peptides of up to 6000 molecular weight by SPPS, using the repeating model sequence Leu-Ala-Gly-Val-oxymethylphenylacetic acid upon copoly(styrene-1% divinylbenzene). This produced a series of immobilised peptides ranging from 11-81% peptide (w/w). The diameters of the dry resin beads were then determined by microscopic measurements. These measurements were then repeated for the solvated state, using either CH_2Cl_2 or DMF, to determine the degree of resin swelling. The total swollen volume of the beads against the peptide loading was then plotted for both solvents (Figure 3.1). The volumes for the swollen peptide-resins showed a dramatic increase over the course of the synthesis, and at 80% peptide the volumes per gram of peptide resin were 12 mL in CH_2Cl_2 and 28 mL in DMF.

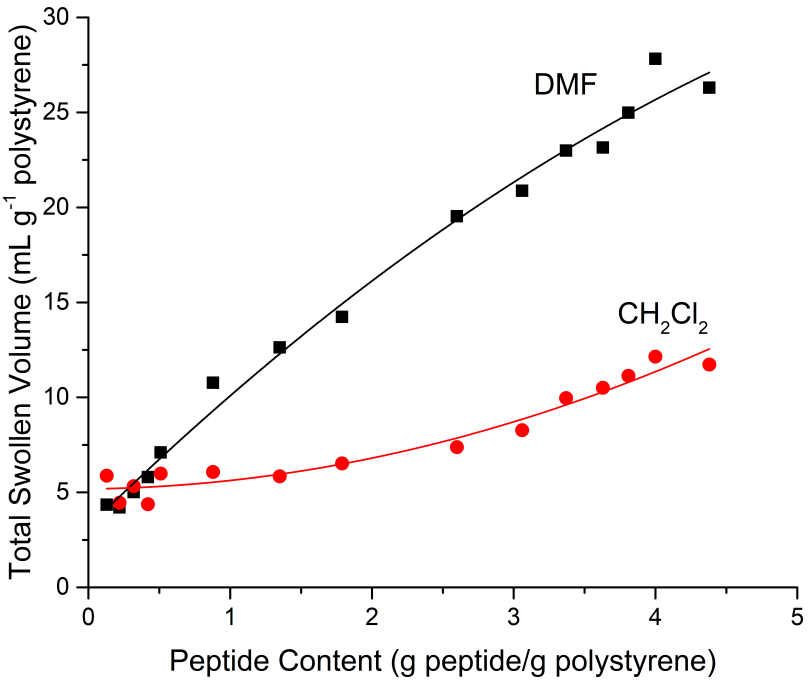

Figure 3.1: Total swollen volumes of peptide-resins of various molecular weights in either CH_2Cl_2 or DMF.[155]

From the results obtained Sarin *et al.* were able to come to the following conclusions. Firstly, it could be explicitly stated that the initial swollen volume of the unsubstituted resin is not the final volume of the highly loaded peptide-resin bead. There was also no evidence for a maximum solvated volume for the range of peptides examined in this study, since the peptide-resin volume increased with the growing peptide chain. Secondly, it is clear that the swelling properties of the resin are influenced by each of the components of the system. Over the course of SPPS solvation of the resin is initially defined by the polymer backbone, but is more strongly influenced by the peptide sequence with increasing peptide content. The polystyrene and protected peptide exert a complimentary solubilising effect on each other, and together they determine the swelling behaviour of the peptide-resin in a given solvent. CH_2Cl_2 is a better swelling solvent than DMF for PS resin, whereas DMF is the better solvating medium for protected peptides.[155]

This report undoubtedly had a marked influence on the SPPS community, as the widespread use of DMF in SPPS is most likely a consequence of Sarin *et al.* identifying that it is an excellent solvent for peptides upon a solid support. It has also generated a major effort to develop a more diverse range of solid supports, specifically ones that have solvation properties similar to those of the peptide product.[155] Consequently, there is now a plethora of solid supports readily available that utilise a variety of resin compositions, cross-linkers and functionalities for optimal SPPS,

a complete review of which would be much beyond this report.[132] Finally, the most important outcome of the report from Sarin *et al.*, with regards to the use of greener solvents for SPOS, is the acknowledgement that solvation of the resin is initially defined by the polymer backbone. Bearing in mind that SPOS is typically used for the construction of small organic molecules, the ability of a solvent to swell a particular resin should be a strong indicator of whether or not it will be a suitable solvent for SPOS. For this reason an investigation into the ability of various green solvents to swell a number of common SPOS resins was planned.

A number of methods for quantifying the degree of swelling have been reported, including, measurements of changes in volume for a single bead, like Sarin *et al.*, or measuring changes in weight after centrifugation.[130] These methods however are rather labour intensive. More recently, Santini *et al.* have reported on a simple and rapid method for determining resin swelling.[131] A sample of dry resin was first weighed into a graduated syringe, equipped with fine polypropylene filter. The appropriate solvent was then added and the plunger inserted. Following agitation for 1 hour the solvent was removed by compressing the syringe barrel. The degree of swelling could then be determined by measuring the increase in volume of the resin. As a rough guideline, Santini *et al.* suggested that a swelling of greater than 4.0 mL g^{-1} was indicative of a good solvent, between 2.0-4.0 mL g^{-1} a moderate solvent, and less than 2.0 mL g^{-1} a bad solvent. This method was then used to record the swelling of four common SPOS resins in thirty nine solvents. Whilst this method is only semi-quantitative, it has proved to be a useful guide for the selection of suitable resin/solvent pairs.[130] For this reason it was deemed that the suitability of a range of green solvents for SPOS would be best demonstrated by determining their ability to solvate SPOS resins according to the method outlined by Santini *et al.* This would allow for a variety of green solvents to be screened against a range of common SPOS resins in a swift and efficient manner.

3.1.3 Resin Swelling and the Physical Properties of Solvents

In an effort to better understand the factors that influence resin swelling, many attempts have been to made to correlate the degree of solvation with various physical properties of the solvent. This has most often been reported in the context of the chemical formulation of polymers, in applications such as coatings, pharmaceuticals and cosmetics.[156] In comparison, linking the swelling of SPOS/SPPS resins to the physical properties of solvents has seen rather little investigation. Whilst Sarin *et al.* had identified that polar solvents were generally better for SPPS with increasing peptide content, a critical evaluation relating solvent properties to resin and peptide-resin solvation was not realised until 1991 and the work of Fields *et al.*[157]

In this investigation, Fields *et al.* sought to rationalise efficient solvation of (aminomethyl)copoly(styrene-1%DVB) with a number of common solvent parameters, including dipole moment (D), Hildebrand solubility parameter (δ), hydrogen-bonding solubility (δ_h), dielectric constant (ϵ) and hydrogen-bonding index (γ_c). Fields *et al.* found that the best correlation between solvent properties and resin solvation is observed for the contour plot where both δ and either δ_h or γ_c are considered (Figure 3.2).[157]

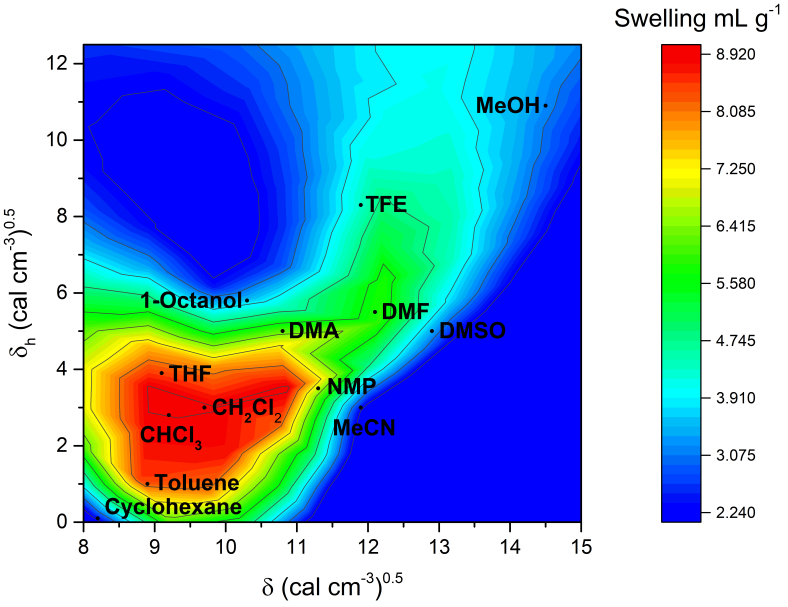

Figure 3.2: Contour solvation plot of (aminomethyl)copoly(styrene-1%DVB) as a function of the Hildebrand solubility parameter (δ) and hydrogen-bonding solubility (δ_h).[157]

The Hildebrand solubility parameter (δ), first described by J. H. Hildebrand in 1936, is a numerical description of solvency behaviour. It is defined as the square root of the cohesive energy density, the heat of vaporisation divided by the molar volume, and has proved to be a good indication of solvent/solute interaction, particularly for non-polar molecules (Equation 3.1). Materials with similar values for δ, will be able to interact, resulting in solvation, miscibility or swelling. It is difficult to directly predict values of δ for polymers as they will most likely degrade before vaporisation occurs.[130] They can however be estimated by various methods, with a δ value of 9.1 (cal cm^{-3})$^{0.5}$ having been previously reported by Suh *et al.* for cross-linked polystyrene, which was determined using turbidimetric titration.[158] It is therefore no surprise that maximum solvation was observed by Fields *et al.* for a range of solvents having solubility parameters similar to those of the polymer. In general, species are considered miscible when the difference in δ values is <1. This is most clearly observed in Figure 3.2, as maximum swelling is seen for solvents possessing

values for δ of 9.0-9.8 (cal cm^{-3})$^{0.5}$, such as THF, CH_2Cl_2 and $CHCl_3$. Contour plots for the other solvent parameters investigated by Fields *et al.* did not appear to give quite such a convincing correlation to resin solvation.

$$\delta = \sqrt{\frac{\Delta H_v - RT}{V_m}} \tag{3.1}$$

Fields *et al.* then extended their study to investigate peptide-resin solvation, with a particular focus on how solvation is influenced by the side-chain protecting group strategy used. The tridecapeptide [Lys_9]-α-conotoxin G1 (Gly-Cys-Cys-Asn-Pro-Ala-Cys-Gly-Lys-His-Tyr-Ser-Cys) was therefore synthesised three times, using either a *tert*-butyl (*t*Bu), benzyl (Bzl) or *para*-methoxybenzyl (mob)/Bzl protecting group strategy. Regardless of the protecting group strategy used, optimal solvation of the peptide-resin was shifted to higher values of δ/δ_h compared to the peptide resin alone. Analysis of the contour plot generated for the Bzl protecting strategy shows that optimal solvation is now found for δ values of 10.8-12.1 (cal cm^{-3})$^{0.5}$ and δ_h values of 3.5-5.5 (cal cm^{-3})$^{0.5}$ (Figure 3.3). A result that is consistent with the observation from Sarin *et al.*, that as the peptide-resin system becomes more peptidic in character, highly polar solvents, such as DMF, NMP and DMA are preferred.[155] This result suggests that there is a good correlation between optimal solvation of SPPS resins, and peptide-resins, with the Hildebrand solubility parameter (δ) and the hydrogen-bonding solubility parameter (δ_h). It is also worth noting that Fields *et al.* were successfully able to optimise mixed solvent systems based on these parameters, by simply combining solubility parameters (δ) according to the relative volume fractions (φ) (Equation 3.2).

$$\delta_{1+2} = \phi_1\delta_1 + \phi_2\delta_2 \tag{3.2}$$

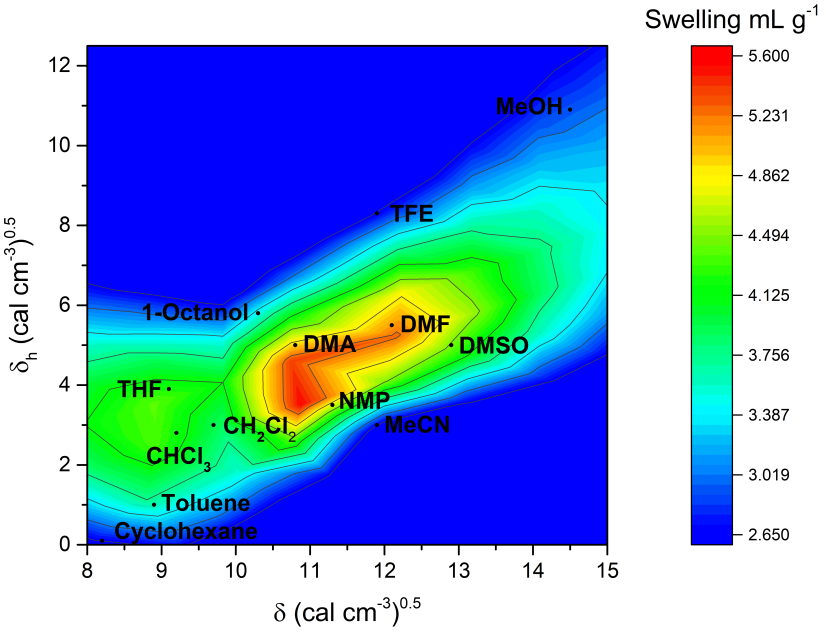

Figure 3.3: Contour solvation plot of Bzl-protected (Lys_9)-α-conotoxin G1 as a function of the Hildebrand solubility parameter (δ) and hydrogen-bonding solubility (δ_h).[157]

More recently, Wilson *et al.* have investigated the influence of mono-, di-, tetra- and hexa-ethylene glycol tethers in cross-linked polystyrene beads, and their influence upon swelling and reagent diffusion.[79] The polystyrene-polyethylene glycol (PS-PEG) copolymers were investigated using a series of solvents possessing a range of Hildebrand solubility parameters. It was found that whilst the 2% PS-PEG copolymers were able to swell to a much greater extent than 2% PS-DVB, the tether link seemed to have little influence on the polymer δ value, as toluene remained the best solvent (Figure 3.4). This was presumed to be due to the low degree of cross-linking relative to the PS-backbone, meaning the tethers would have little synergistic influence on the swelling. When the cross-linking density was increased to around 20% the degree of swelling was found to drop, returning to levels similar to the control sample using 2% PS-DVB. Unfortunately, Wilson *et al.* did not investigate whether the use of a more polar solvent would enhance the swelling of the 20% PS-PEG copolymers, as the Hildebrand solvent parameter (δ) values would be expected to be better matched, based on the previously reported findings of Fields *et al.*

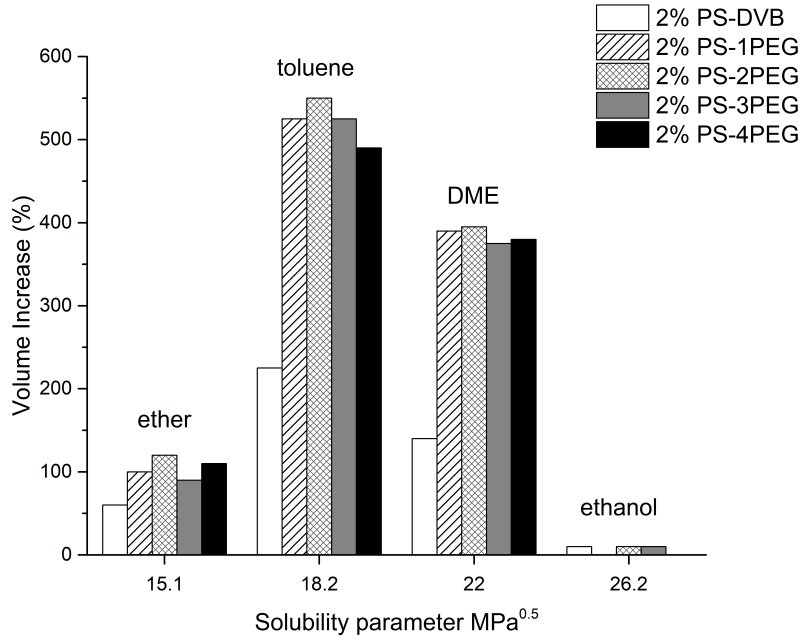

Figure 3.4: Swelling of 2% PS-DVB and 2% PS-PEG beads in various solvents as a function of Hildebrand solubility parameter (δ).[79]

Nakaie and co-workers have also reported a strong link between peptide-resin solvation and the sum of electron acceptor (AN) and electron donor (DN) numbers.[159] These solvent parameters were first proposed by Gutmann, with the intention of describing the solvent effect on a solute molecule simply as an acid-base reaction.[160] Cilli *et al.* therefore believed that the solvation properties of peptide-resins would be influenced by the number of electrophilic (N-H) and nucleophilic (C=O) groups found in the peptide backbone. In order to investigate this, Cilli *et al.* synthesised a model repeating peptide sequence $(Asp\text{-}Ala\text{-}Asp\text{-}Pro)_4$ bearing benzyl protecting groups on the Asp side chains, and bound to a 1.4 mmol g^{-1} benzhydrylamine-resin (BHAR). The swelling was then determined and correlated to a number of solvent parameters, including, ϵ, the Dimroth-Reichard's parameter (ET_{30}), AN, and DN, along with the additive AN+DN parameter in a 1:1 ratio. Cilli *et al.* observed poor relationships between resin solvation and a number of the solvent parameters investigated. However, a fairly convincing correlation was observed for the AN+DN parameters, with maximum solvation appearing for solvents or solvent mixtures with AN+DN number of around 40 (Figure 3.5), with 1-22 representing a number of solvents and solvent mixtures. The two deviations, 21 and 22, which are 50% TFE:DMF and 50% TFE:DMSO respectively, are believed to be due to high AN or DN solvents preferring to self associate, rather than solvate the peptide-resin. Subsequently, Cilli *et al.* went on to investigate the swelling properties of a number of other species, which included the Asp-Ala-Asp-Pro sequence at 0.2

mmol g^{-1} loading, the aggregation prone Ile-Asp-Gly fragment and the 1.4 mmol g^{-1} BHAR resin as a peptide-free resin model. In most cases a very good correlation between observed swelling and solvent AN+DN values was observed.

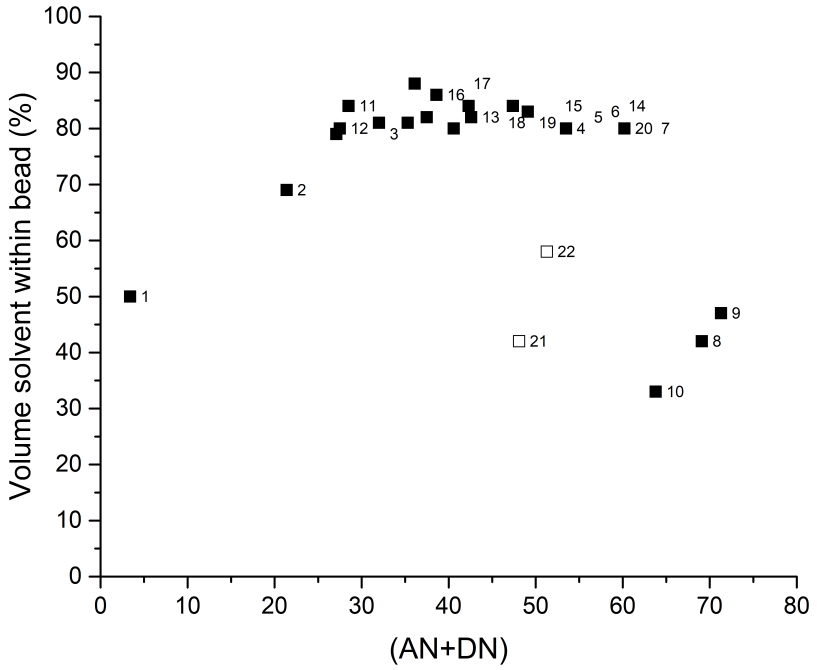

Figure 3.5: Swelling of $(Asp\text{-}Ala\text{-}Asp\text{-}Pro)_4$ resin as a function of (AN+DN) solvent values. The numbers 1-22 represent the solvents and solvent mixtures investigated by Cilli *et al.*[159]

More recently, Malavolta *et al.* have further expanded on the application of the AN+DN solvent parameter for resin swelling.[161] In this study the swelling properties of a much broader range of resin species were investigated, including a highly charged variant of the BHAR resin (BHAR-NH_3^+, 2.4 mmol g^{-1}), an aminoalkyl cross-linked polydimethylacrylamide resin (SPAR-50, 0.6 mmol g^{-1}) and the tetraethylene glycol diacrylate cross-linked polystyrene resin (PS-TTEGDA, 0.7 mmol g^{-1}). Additionally, along with the previously investigated solvent parameters Malavolta *et al.* included the Kamlet-Taft solvent parameters. Kamlet-Taft parameters split the solvent into three distinct parameters quantifying hydrogen-bond accepting ability (α), hydrogen-bond donating ability (β), and polarity/polarisability (π^*). In their investigation Malavolta *et al.* attempted to correlate both (α+β), and (π^*+α+β) to resin solvation. The results obtained however suggest that the best correlation between solvent properties and resin swelling is still given by the combination of AN+DN in a 1:1 ratio.

In summary, a number of investigations have attempted to correlate resin solvation with various physical properties of solvents, in an attempt to better optimise

SPOS/SPPS reactions. Various solvent parameters have been utilised, including dipole moment (D), dielectric constant (ϵ), Hildebrand solubility parameter (δ), hydrogen-bonding solubility parameter (δ_h), hydrogen-bonding index (γ_c), Dimroth-Reichardt's polarity parameter (ET_{30}), acceptor number (AN), donor number (DN) and Kamlet-Taft (α, β and π^*). The most convincing correlation between the degree of resin swelling and these parameters was observed for the use of δ with either δ_h or γ_c, or the use of AN+DN.

Review of the literature has also identified that the degree of resin swelling has not been previously investigated with regards to Hansen Solubility Parameters (HSP). HSP has been proposed as an extension to Hildebrand solubility parameters, and has become an incredibly powerful method for predicting solubility in a wide variety of applications, including pigments, nanoparticles and even DNA.[162] For this reason, it was felt that an investigation into HSP and resin swelling should be incorporated with this investigation into the suitability of green solvents for SPOS.

3.1.4 Hansen Solubility Parameters

A common criticism of the Hildebrand solubility parameter (δ) is that it is a vast oversimplification of solvation theory. The approach had been based of the use of hydrocarbon solvents, meaning no contributions from hydrogen bonding or polarity were incorporated into the calculation. For this reason, the notion that solubility could be based on similarities in δ values soon unravelled, as the use of a single solvent parameter was clearly not powerful enough. In an effort to compensate for these limitations Hansen proposed that the cohesive energy could be regarded in terms of three components, rather than just one. Hansen's approach therefore considered the cohesive energy (E or ΔH_v-RT) as the sum of energies arising from dispersion forces (E_D), polar forces (E_P) and hydrogen bonding forces (E_H) (Equation 3.3).[156]

$$E = E_D + E_P + E_H \tag{3.3}$$

When considered in terms of cohesive energy density, i.e. dividing by molecular volume (V_M), and substituting δ^2 for each energy contribution, where $\delta^2 = E/V_M$, this equation is simplified to the following (Equation 3.4);

$$\delta^2 = \delta D^2 + \delta P^2 + \delta H^2 \tag{3.4}$$

These solvent parameters D, P and H can then be imagined as co-ordinates in a three-dimensional space, commonly referred to as Hansen space. The relative

closeness of molecules within Hansen space can then be used to predict an array of properties such as solvent miscibility or polymer solubility. This relative distance (Ra^2) can be easily calculated based on the difference between the various parameters (Equation 3.5). It is worth acknowledging that the factor of 4 incorporated into the difference in δD values has been highly controversial, but a full explanation for this is far beyond the scope of this report.[162]

$$Ra^2 = 4(\delta D_1 - \delta D_2)^2 + (\delta P_1 - \delta P_2)^2 + (\delta H_1 - \delta H_2)^2 \tag{3.5}$$

A major appeal of the Hansen approach is that Hansen, in collaboration with Abbot and Yamamoto, went on to develop a software package for HSP, known as Hansen Solubility Parameters in Practice (HSPiP).[162] This has meant that HSP can be easily visualised and manipulated in three-dimensional space. This has also made it incredibly easy for users to predict HSP values for a multitude of systems based on experimental data, rather than by measuring enthalpies of vaporisation. For example, the user is able to arbitrarily define whether a solvent is suitable or not for a given process based on whatever determinant they deem most appropriate. The HSPiP software is then able to predict optimal HSP values based on the best fit of the data, using the Hansen fitting algorithm. This is most easily represented as a sphere in Hansen space of radius R_0, more commonly referred to as the interaction radius, which represents the region in which suitable solvents should lie. A relative energy difference (RED) can then be determined to predict likeness, using the relative distance and the interaction radius (Equation 3.6). A RED of <1 means the molecules are alike and will dissolve, RED$=1$ suggest the molecules will partially dissolve, and RED of >1 will not dissolve.

$$RED = \frac{R_a}{R_0} \tag{3.6}$$

The figure below constitutes a typical HSPiP plot for such a system, where the green sphere of radius R_0 represents the predicted optimal region in which the most suitable solvents should reside (Figure 3.6). The smaller central sphere represents the "optimal" solvation parameters as calculated by the HSPiP fitting algorithm. Finally, the blue spheres represent solvents that are regarded by the user as suitable, whilst the red cubes are regarded as unsuitable.

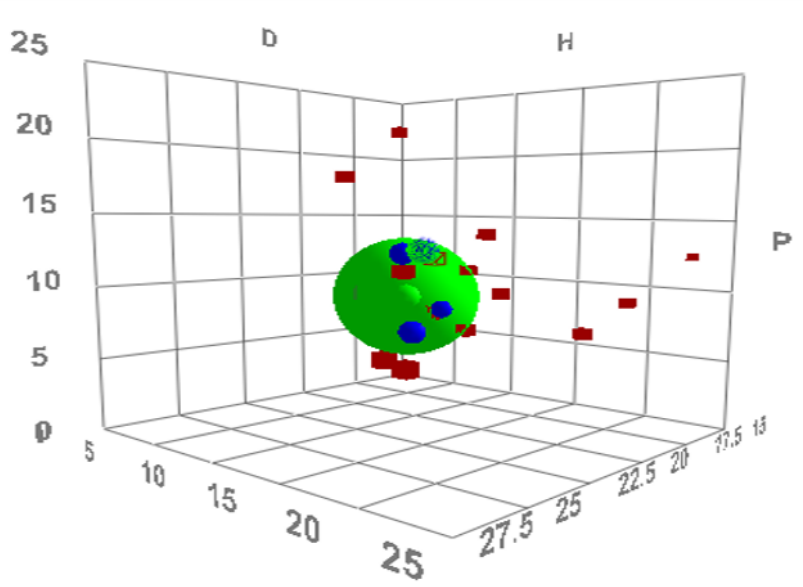

Figure 3.6: An example of an HSPiP plot.

With this in mind, it was hypothesised that the suitability of green solvents for SPOS could be rationalised on the basis of HSP. Santini *et al.* have previously demonstrated how solvent selection for SPOS can be made on the basis of simple resin swelling experiments. This would therefore allow the suitability of a solvent for a particular SPOS resin to be determined in an efficient and quantifiable manner that could be easily input into HSPiP. Optimised solvent parameters could then be predicted for a particular SPOS resin using the HSPiP solvent optimiser algorithm, allowing for the straightforward selection of the most suitable solvent, and also the rapid screening of additional solvents based on relative solvent parameters.

3.1.5 Chapter Aims

It has so far been established that the use of alternative solvents for SPOS has been relatively unexplored, in comparison to the parent methodology SPPS. This is justified on the basis that the use of undesirable solvents is still the most common practice for SPPS, with alternative organic solvents having only recently received notable investigation. This does however present an interesting opportunity to investigate the suitability of green solvents for SPOS. Solvent choice in SPOS is however rather critical to the success of the reaction, as the solvent must be able to adequately solvate, or swell, the solid support. Accordingly, the remainder of this chapter seeks to determine the suitability of a diverse range of green solvents for SPOS, on the basis of their ability to swell various common SPOS resins. A number of attempts within the literature have also attempted to correlate swelling of these supports to physical properties of the solvent, with the Hildebrand solubility

parameter (δ) proving particularly effective. This has however been found to have notable limitations, particularly with regards to polar or hydrogen-bonding solvents. HSP is an extension of Hildebrand's approach that seeks to incorporate these terms, but has not been previously investigated in the context of resin swelling in SPOS. It is therefore believed that a computational model using HSPiP can be built from the outcomes of the resin swelling data, in order to predict and model solvent suitability for SPOS.

3.2 Results and Discussion

3.2.1 Resin Swelling Studies

In order to first determine the suitability of green solvents for solid-phase organic synthesis (SPOS) a number of readily available resins were selected for investigation, the properties of which are summarised in Table 3.1. These resins can generally be grouped into four distinct categories depending on the composition of the polymer backbone. These categories are as follows, polystyrene (PS), grafted polystyrene-polyethylene glycol (PS-PEG), polyethylene glycol (PEG) and polyamide (PA). A number of other resins, consisting of various polymer backbone compositions and functionalities are commercially available, however it is felt that the nine selected represent a broad enough selection for determining the suitability of green solvents for SPOS.[132]

Table 3.1: Physical properties of the commercial solid-phase resins investigated in the solvent swelling study.

Resin	**Polymer Backbone**	**Functionality**	**Bead size (mesh)**	**Capacity (mmol g^{-1})**
Merrifield	PS 1% DVB	Wang ($ArCH_2OH$)	200-400	0.6-1.0
ParaMax	PS 1% DVB	*para*-$ArCH_2OH$	100-200	2.0
JandaJel	PS 2% 1,4-bis (vinyl-phenoxy)-butane	CH_2Cl	100-200	0.8-1.2
TentaGel	PS-PEG Hybrid 50-70% (w/w) PEG	Rink-Fmoc	80-100	0.23
ArgoGel	PS-PEG Hybrid 67-82% (w/w) PEG	Cl	200-400	0.48
HypoGel 200	PS-PEG Hybrid 16% (w/w) PEG	CO_2H	110-150	0.8
NovaGel	PS-PEG Hybrid 48% (w/w) PEG	HMPA ($ArCH_2OH$)	Not stated	0.74
ChemMatrix	PEG 100%	Wang ($ArCH_2OH$)	35-100	0.5-1.2
SpheriTide	PA	Rink-Fmoc	45-140	0.21

Merrifield[146], ParaMax[163] and JandaJel[164] can all be classified as polystyrene (PS) based resins, differing only in their functionality and cross-linkers. Merrifield resin is polystyrene cross-linked with 1% divinylbenzene (DVB). Traditionally Merrifield resin was functionalised with the chloromethyl group, which was first utilised by Merrifield in his seminal report on the synthesis of a tetrapeptide by SPPS.[146] Even after 50 years, this resin remains one of the most commonly employed resins for SPPS/SPOS.[130] The sample in this case is functionalised with a Wang (2-hydroxybenzyl alcohol) linker. Paramax is very similar to Merrifield resin, being a PS based resin containing a 1% DVB cross-linker, except that functionalisation of the resin, using a hydroxymethyl group, occurs exclusively in the *para*-position of the PS backbone. JandaJel has been specially designed to be a high swelling PS-based resin. This has been achieved through the use of a more flexible 1,4-bis(vinylphenoxy)-butane cross-linker, rather than use the more conventional DVB one. JandaJel in this case is obtained as the chloromethyl derivative.

The next category is the grafted PS-PEG resins, consisting of TentaGel[165], ArgoGel[166], HypoGel 200[167] and NovaGel[168]. These structures typically consist of a 1% DVB cross-linked PS core, with a PEG unit of various lengths grafted to the active site. TentaGel contains PEG chains of approximately 2000-3000 Da resulting in a matrix that is 50-70% PEG w/w, and functionalised with a Fmoc-protected Rink linker. Early generations of PS-PEG graft resins, such as TentaGel, typically suffered from low loading and poor stability, due to the use of benzylic or amide-based linkages to the PS-core.[132] ArgoGel was an attempt to overcome these limitations through the use of a branched bifunctional PEG chain. This results in a PS-PEG graft polymer with a very high degree of PEG content (67-82% w/w) and double the loading (0.48 mmol g^{-1}) of the early PS-PEG resins utilising monofunctional linkers. Additionally, the use of chemically inert aliphatic ethers to join the PEG chains to the PS-core resulted in a greatly enhanced stability towards strong acids and nucleophilic reagents. The ArgoGel resin investigated in this case is terminated with a chloro-group. In contrast, HypoGel 200 was developed in an effort to slightly enhance the kinetics of SPOS reactions, but maintain the stability of the PS-core. The use of short 200 Da PEG chains, terminated with carboxylic acid groups, results in a PS-PEG graft polymer containing only a very small quantity of PEG (16% PEG w/w). Finally, NovaGel is a high swelling resin in which the PEG grafts are attached to the PS resin using urethane groups. It is only 48% PEG w/w, resulting in a resin that is intermediate to that of HypoGel 200 and TentaGel/ArgoGel. It was functionalised with (4-hydroxymethylphenyl)acetic acid (HMPA) to provide alcohol functionalities for substrate immobilisation.

More recent approaches to the design of solid supports have tried to completely avoid the use of PS. Instead favouring more amphiphilic polymers, that are able to adequately swell in a much broader array of solvents. For this reason the final two resins chosen contain no PS. ChemMatrix[169] is a solid support that exclusively contains highly cross-linked PEG chains through primary ether bonds. This results in a resin that displays high chemical stability and an ability to swell in a large variety of solvents. The sample chosen in this case is functionalised using a Wang linker. The final resin chosen, which again does not contain any PS in the polymer backbone, was SpheriTide. SpheriTide[170] is an interesting resin choice, as it is a polyamide (PA) matrix made up entirely of cross-linked poly-ε-lysine. Poly-ε-lysine is a naturally occurring short-chain polyamide consisting of 25-35 lysine residues, produced through bacterial fermentation, typically for use as a food preservative. SpheriTide can therefore be regarded as a bio-based SPOS resin, making it rather unique in the context of improving the sustainability of SPOS. SpheriTide is supplied as the low loading Rink-Fmoc derivative.

In order to determine whether or not a green solvent would be suitable for SPOS upon the chosen resins, it was decided that the ability of the chosen solvent to adequately solvate, or swell, the support would be investigated. This is one of the most important considerations for SPOS/SPPS to ensure a complete and rapid transformation, as poor resin swelling results in poor reaction site accessibility and diminished reaction rates.[131] This was discussed extensively within section 3.1, with it established that the semi-quantitative method previously described by Santini *et al.* being the most suitable approach for rapidly quantifying resin swelling.

A broad array of solvents covering a wide range of polarities and hydrogen bond donor/acceptor properties were then selected for screening against the chosen resins, according to the methodology outlined by Santini *et al.* A total of 30 solvents were investigated, 27 of which are known for possessing promising green credentials, along with 3 reference solvents **3.43-3.45** (Figure 3.7). Cyclic carbonates **3.16** and **3.17**, Cyrene **3.18** and *N*-butyl-2-pyrrolidone **3.42** have all been used as green replacements to traditional polar aprotic solvents. As discussed previously, cyclic carbonates can be prepared through the 100% atom economical reaction between epoxides and waste carbon dioxide,[100] whilst Cyrene is prepared in two steps from cellulose.[171] *N*-butyl-2-pyrrolidone is a non-reprotoxic derivative of *N*-methyl-2-pyrrolidone (NMP) **3.43**, although the reprotoxicity is only just below the currently accepted limit.[172]

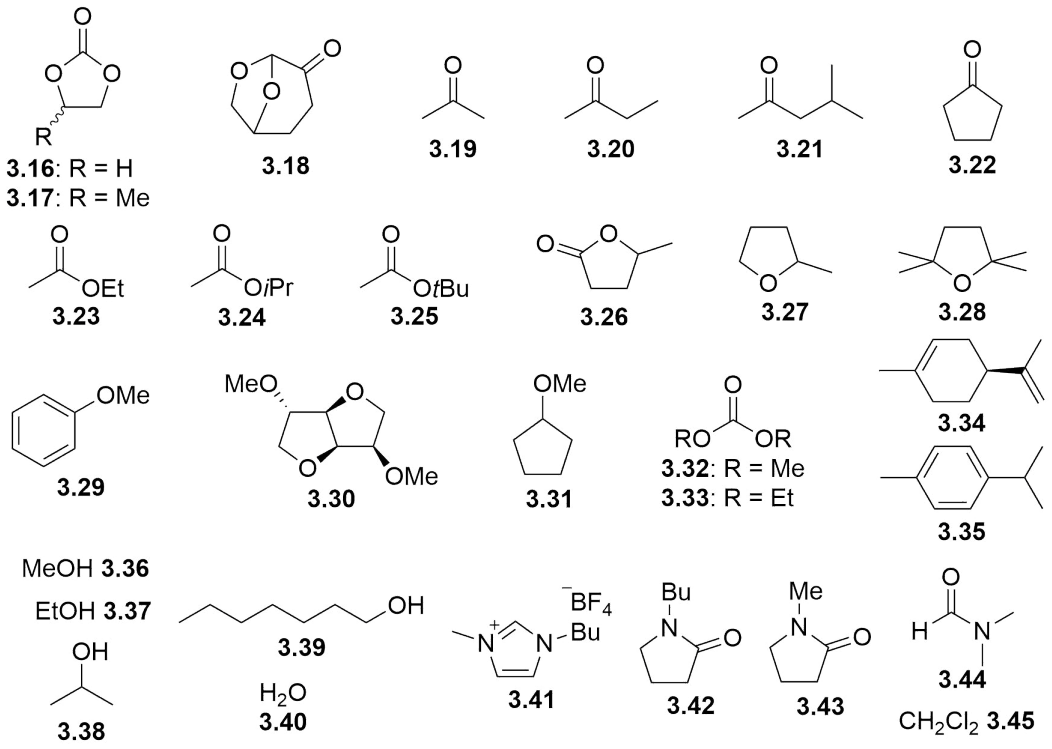

Figure 3.7: Structures of the green solvents (**3.16-3.42**) and undesirable reference solvents (**3.43-3.45**) used in this study.

The majority of ethers, ketones, esters and acyclic carbonates can be considered as moderately polar aprotic solvents. Two well-known conventional solvents, acetone **3.19** and ethyl acetate **3.23**, were included due to their reasonable green credentials. γ-Valerolactone (GVL) **3.26** and 2-methyl tetrahydrofuran (2-MeTHF) **3.27** are both produced from renewable sources of lignocellulosic biomass.[173,174] The acyclic carbonates, dimethyl carbonate **3.32** and diethyl carbonate **3.33**, can be prepared from carbon dioxide and sustainably sourced alcohols.[175] Cyclopentanone **3.22**, isobutyl acetate **3.25** and anisole **3.29** were included as they scored very highly in the most recent iteration of the GSK solvent sustainability guide.[16] Dimethyl isosorbide **3.30**, cyclopentyl methyl ether **3.31**, butan-2-one **3.20**, 4-methyl-pentan-2-one **3.21** and isopropyl acetate **3.24** were identified as promising solvents on the grounds of a computational modelling study using HSPiP, which will be discussed in due course.

2,2,5,5-Tetramethyloxolane (TMO) **3.28** is a non-peroxide forming ether derived from readily available and potentially renewable feedstocks.[176] Whilst it would be expected to be similar to 2-MeTHF in terms of polarity, it is actually a suitable replacement for toluene, making up the apolar aprotic solvents, along with D-limonene **3.34** and *para*-cymene **3.35**. D-Limonene is a natural product, readily available from citrus peels, it is also easily converted to *para*-cymene *via* isomerisation and dehydrogenation.[177] The polar protic solvents selected include

three common alcoholic solvents, methanol **3.36**, ethanol **3.37** and isopropanol **3.38**, all of which can be obtained from sustainable sources. 1-Heptanol **3.39** was also included, due to it scoring very highly in the most recent GSK solvent sustainability guide, along with water **3.40**.[16] The ionic liquid 1-butyl-3-methylimidazolium tetrafluoroborate ([BMIM][BF_6]) **3.41** was also included as an example of a non-conventional solvent. The final three solvents selected NMP **3.43**, DMF **3.44** and CH_2Cl_2 **3.45**, are undesirable solvents commonly associated with SPPS/SPOS. This was done in order to provide a direct comparison against the chosen green solvents and to validate the swelling methodology.

To begin with, the swelling of Merrifield-Wang resin was investigated using the conventional SPOS solvents **3.43**-**3.45**, according to the procedure reported by Santini *et al.* The results obtained indicate an excellent correlation with those previously reported within the literature using this approach.[131,178] To further validate the methodology the swelling of a small subset of 8 solvents (**3.17**, **3.19**, **3.23**, **3.27**, **3.32**, **3.36**, **3.40**, **3.45**) with three of the chosen resins (Merrifield, ArgoGel and ChemMatrix) was investigated. The swelling was determined for all 24 combinations of these resins and solvents. This was then repeated a further 4 times, in order to confirm the reproducibility of the method (Figure 3.8-3.10). The error bars plotted represent the maximum deviation from the mean, indicating that the determination of resin swelling using this method is reproducible to ± 0.5 mL g^{-1}. Having validated the methodology, by demonstrating it is both consistent with literature and reproducible, the ability of all 30 solvents to swell the 9 chosen resins was then investigated, the outcomes of which are summarised in Figures 3.11-3.19.

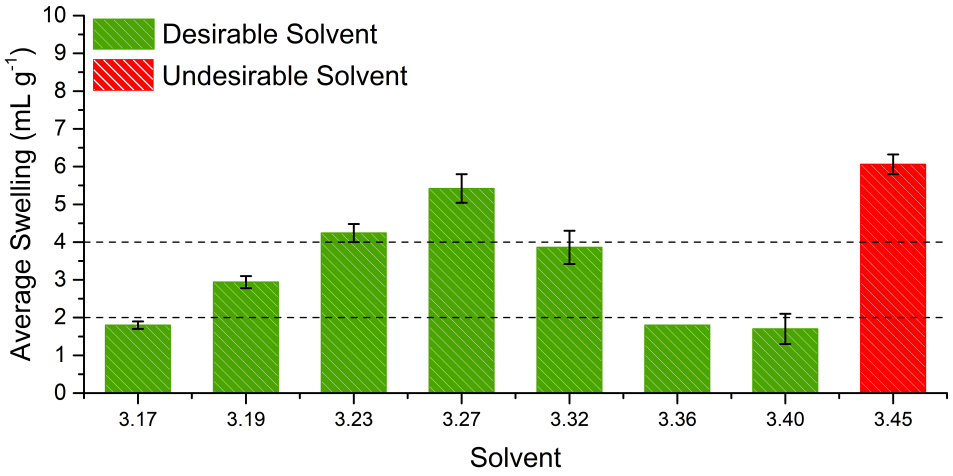

Figure 3.8: Reproducibility of Merrifield resin swelling tests.

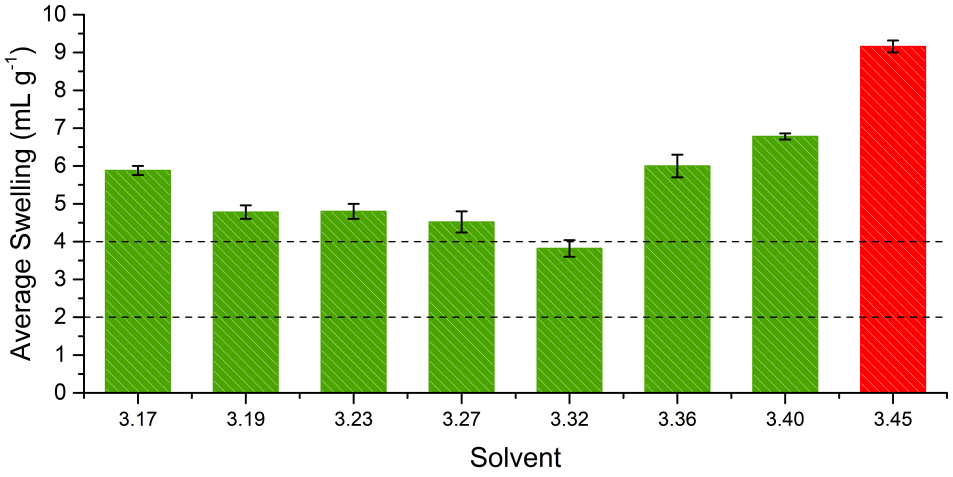

Figure 3.9: Reproducibility of ChemMatrix resin swelling tests.

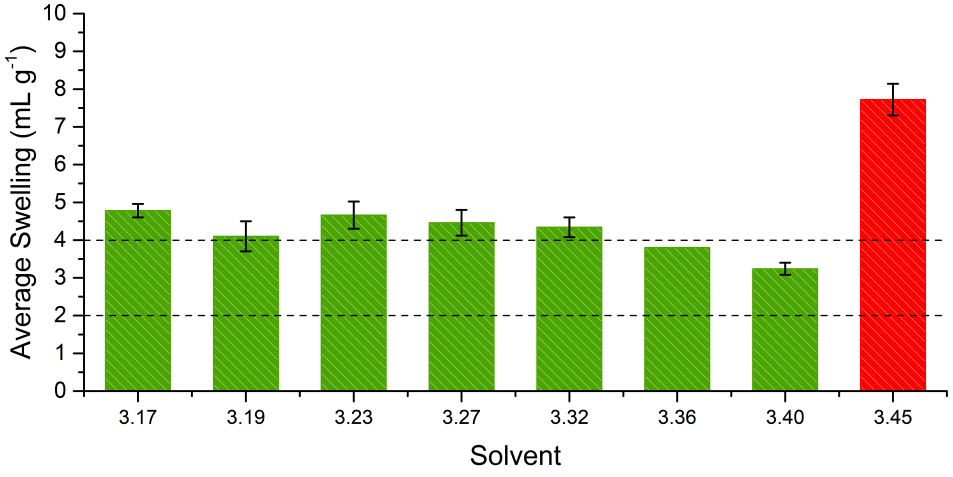

Figure 3.10: Reproducibility of ArgoGel resin swelling tests.

Analysis of the swelling data obtained then allowed for direct comparisons to be made between the various resins, and their associated categories. Comparison of the data in Figures 3.11-3.13 shows differences in the swelling behaviour between the three PS-based resins. The results obtained for Merrifield resin are suggestive of a preference for the moderately polar solvents, as good swelling is observed for solvents **3.20**, **3.22**, **3.27**, **3.29**, **3.30** and **3.31**. The remaining solvents in this category **3.19**, **3.21**, **3.23**, **3.24**, **3.25**, **3.26**, **3.28**, **3.32** and **3.33**, only display moderate swelling, with **3.19** and **3.28** displaying what could be considered as borderline poor swelling. Essentially no swelling is observed for the remaining polar aprotic **3.16-3.18**, apolar aprotic **3.34-3.35** and polar protic **3.36-3.40** solvents, along with the ionic liquid **3.41**. Notably, good swelling is observed for **3.42**, the only nitrogen-containing polar aprotic solvent, which produced results comparable to the conventional reference solvents **3.43-3.45**. This could probably have been predicted, due to the structural similarities between **3.42** and **3.43**.

Rather surprisingly, ParaMax, which only differs to Merrifield in regards to functionalisation being exclusively in the *para*-position, rather than being a mixture of *ortho*/*para*, displays good swelling in a much wider range of solvents. In this case, the moderately polar aprotic solvents **3.19-3.32** all display good swelling for ParaMax resin. However, very little difference is observed for the remaining solvents, with essentially identical results obtained between Merrifield and ParaMax. The exceptions being that moderately better swelling of ParaMax is observed in solvents **3.16**, **3.33** and **3.34** which had been unable to swell Merrifield resin, along with **3.42** which now displays better swelling than the reference solvents **3.43-3.45**.

Finally, JandaJel, which has been designed to be a higher swelling PS resin, through the use of a more flexible 1,4-di(4-vinylphenoxy)butane cross-linker, generally displayed a similar trend to Merrifield resin. Again, the moderately polar aprotic solvents **3.19-3.35** appeared to be most suitable for this resin. Whilst solvents **3.20**, **3.22**, **3.27**, **3.29**, **3.30** and **3.31** all had displayed good swelling for Merrifield resin, a significant enhancement in total swollen volume was now observed. Additionally, solvents **3.21**, **3.23**, **3.24**, **3.25** and **3.26** can now be regarded as good solvents, rather than just moderate ones. It is also worth noting that a similar enhancement was not observed for solvents **3.19** and **3.28**, but solvents **3.34** and **3.35**, which had not previously swollen Merrifield resin, could now be considered good swelling solvents. Ever so slight swelling was also observed for the polar protic solvents **3.36-3.39**, although this is so minimal it is unlikely to be practical.

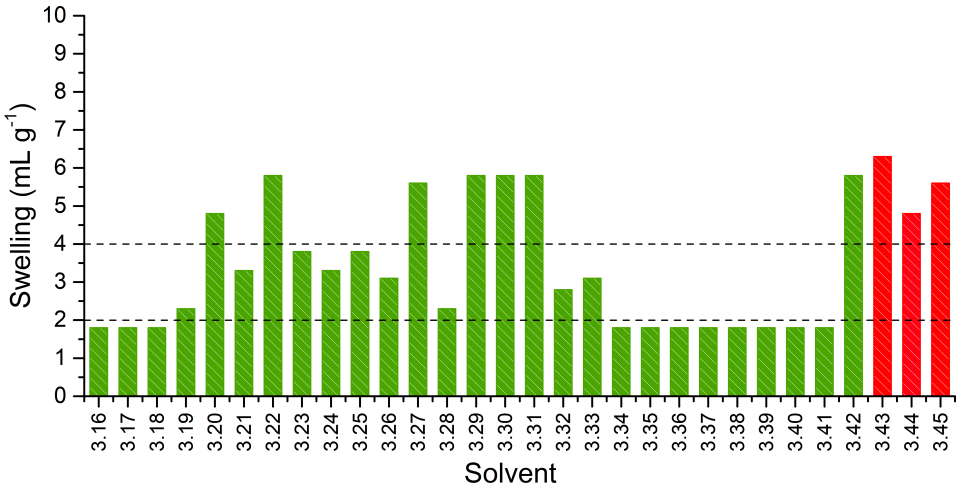

Figure 3.11: Swelling of Merrifield Resin.

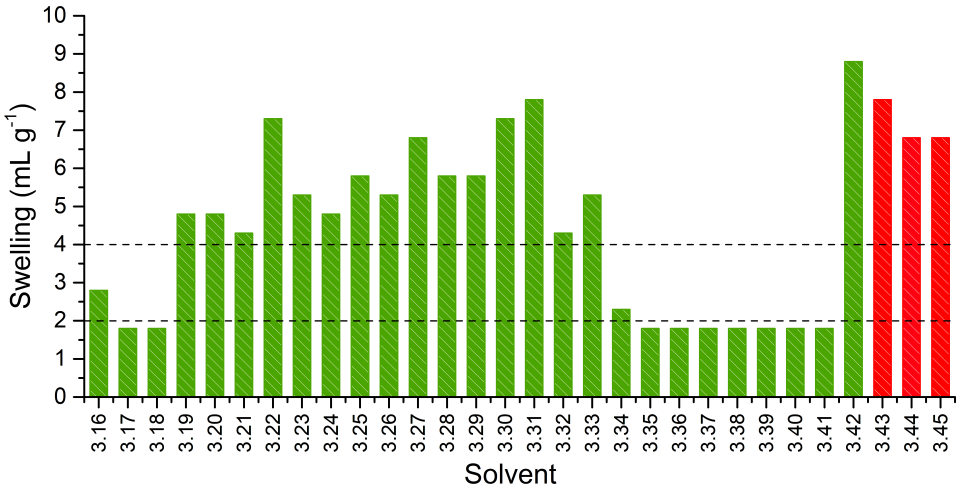

Figure 3.12: Swelling of ParaMax Resin.

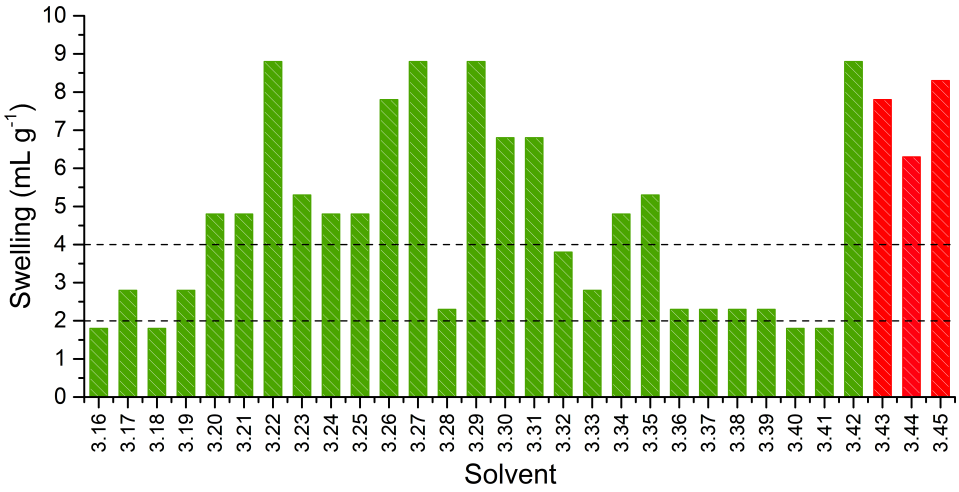

Figure 3.13: Swelling of JandaJel Resin.

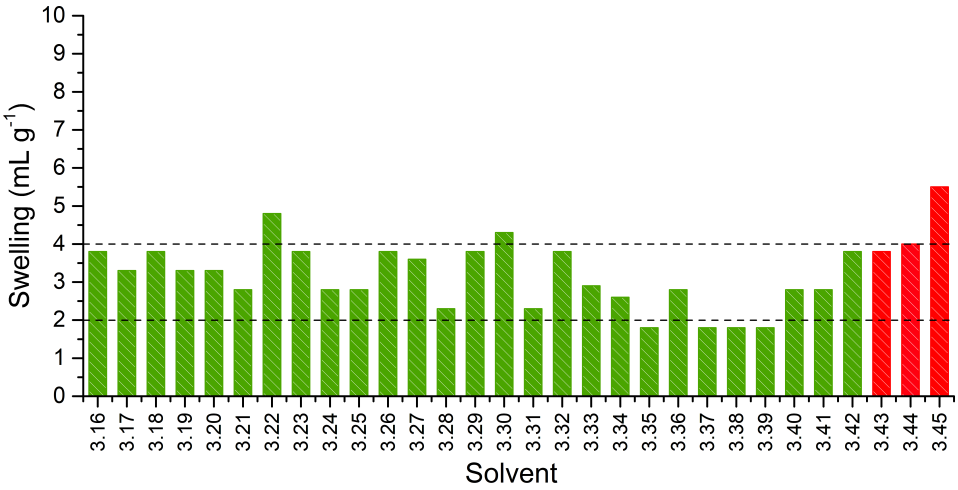

Figure 3.14: Swelling of TentaGel Resin.

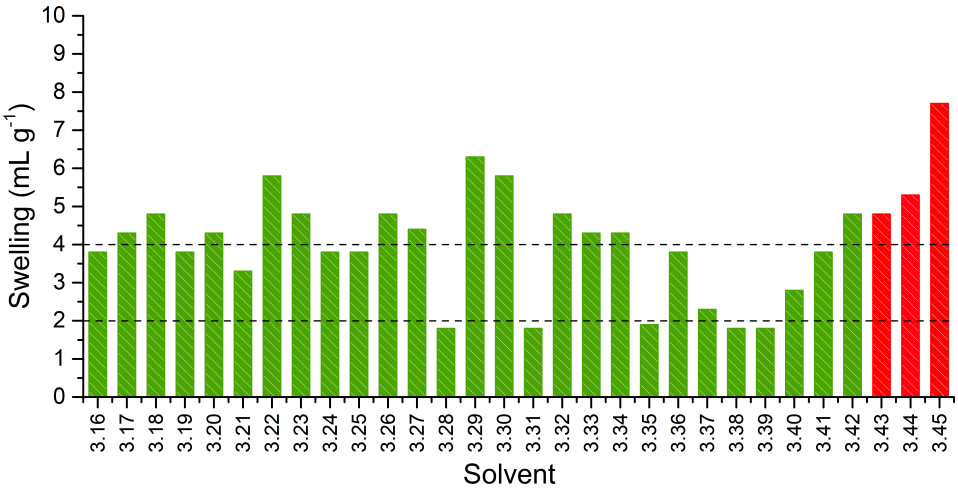

Figure 3.15: Swelling of ArgoGel Resin.

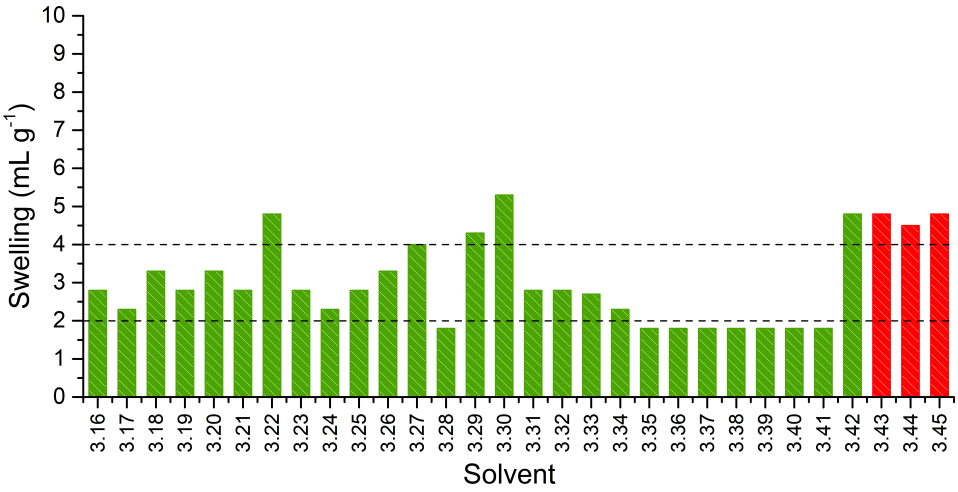

Figure 3.16: Swelling of HypoGel 200 Resin.

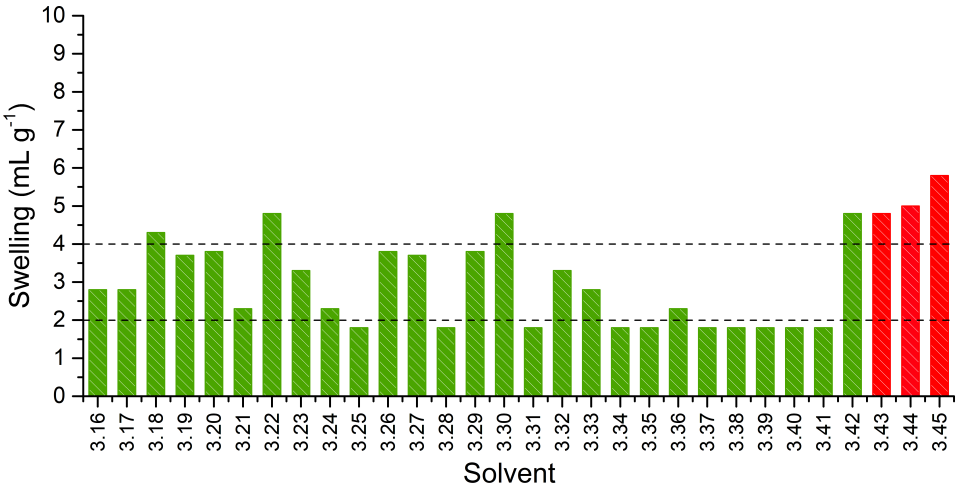

Figure 3.17: Swelling of NovaGel Resin.

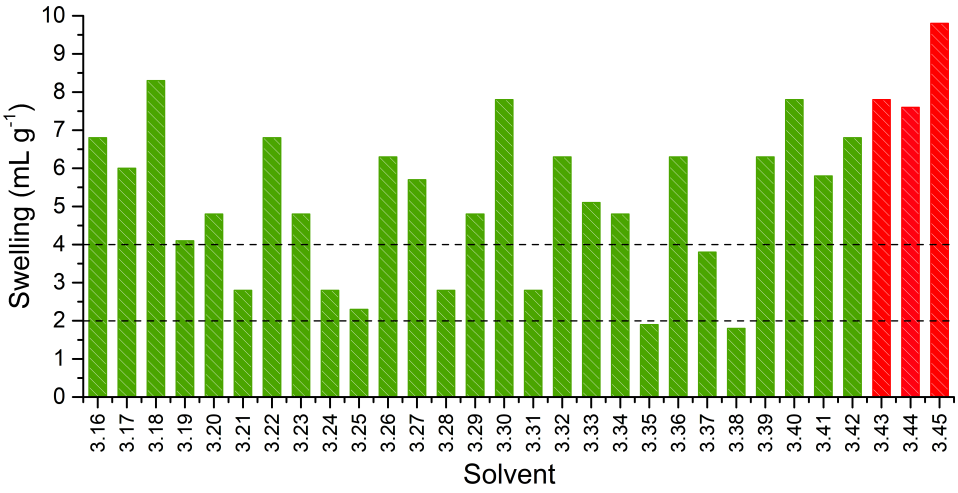

Figure 3.18: Swelling of ChemMatrix Resin.

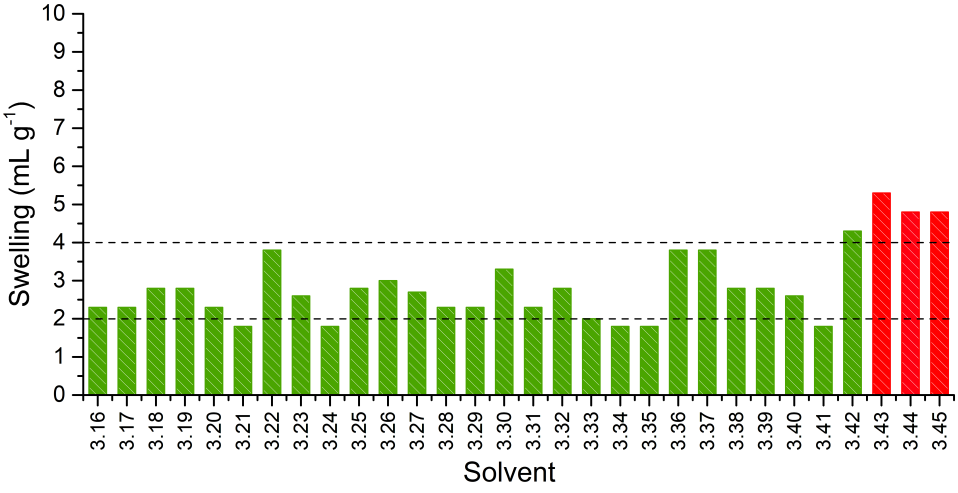

Figure 3.19: Swelling of SpheriTide Resin.

The next series of figures (Figure 3.14-3.17) deal with the PS-PEG grafted resins (TentaGel, ArgoGel, HypoGel 200 and NovaGel), which differ predominantly through the quantity of PEG incorporated into the resin bead. Firstly, TentaGel, which is between 50-70% PEG (w/w) was found to swell in a wide range of solvents, but only to a moderate degree. Swelling of more than 4.0 ml g^{-1} was only observed for solvents **3.22** and **3.30**. The remaining solvents, with the exception of **3.35**, **3.37**, **3.38** and **3.39**, could only swell the resin to between 2.0-4.0 mL g^{-1}. The next PS-PEG grafted resin, ArgoGel (Figure 3.15), was found to perform much better in swelling tests. It displayed an ability to swell in a much broader range of solvents than any of the other PS-PEG resins, with the majority of polar aprotic **3.17**, **3.18**, and **3.42**, moderately polar aprotic solvents **3.20**, **3.22**, **3.23**, **3.26**, **3.27**, **3.29**, **3.30**, **3.32**, **3.33** and *para*-cymene **3.34** all producing good swelling. These results are consistent with ArgoGel possessing the highest quantity of PEG (67-82% w/w) of the PS-PEG resins. Four other oxygenated polar aprotic solvents **3.16**, **3.19**, **3.24** and **3.25** swelled the resin, but only to just below 4.0 mL g^{-1}, as did **3.36** and the ionic liquid **3.41**. The poor solvents were rather similar to those observed with TentaGel with **3.28**, **3.31**, **3.35** and the polar protics **3.38** and **3.39** all producing a swelling value of less then 2.0 mL g^{-1}. HypoGel 200 (Figure 3.16) and NovaGel (Figure 3.17) both gave very similar results to those observed for TentaGel, although **3.27** and **3.29** gave good swelling of HypoGel 200 whilst they only swelled TentaGel to just below 4.0 mL g^{-1}. For NovaGel the polar aprotic solvent Cyrene **3.18** swelled the resin to over 4.0 mL g^{-1}, whilst it swelled TentaGel to just below 4.0 mL g^{-1}. Notably, TentaGel, HypoGel 200 and Novagel were all functionalised in different ways (Fmoc-protected amine, carboxylic acid and benzylic alcohol) yet had very similar swelling properties in the green solvents, which suggests that the observed variation in swelling with solvent is a function of the resin backbone and not of the way in which it is functionalised. This is important for synthetic applications as the nature of the functionality attached to the resin will change during solid-phase synthesis. This also suggests that the grafting of PEG-chains to a PS core only has an appreciable benefit when very high values by weight (w/w) are used, hence ArgoGel displayed the best swelling properties of all the PS-PEG grafted resin.

The final two figures (Figures 3.18 and 3.19) deal with the two resins that contain no PS. ChemMatrix resin (Figure 3.18) was found to swell in a wide range of green solvents. The only solvents that were found not to be suitable for ChemMatrix were **3.21**, **3.24**, **3.25**, **3.28**, **3.31**, **3.35**, **3.37** and **3.38**. The incompatibility of this resin with aromatic solvents is understandable, due to the lack of aromatic functionality within the resin. The lack of swelling in the more non-polar ketones and esters **3.21**, **3.24** and **3.25**, when very similar but more polar ketones **3.19**, **3.20** and ester **3.23**

swell the resin well probably reflects the polar nature of the PEG-based polymer. Curiously, whilst **3.37** and **3.38** were poor solvents for ChemMatrix, good swelling was observed in both the more polar alcohol **3.36** and the less polar one **3.39**.

The SpheriTide resin displayed rather disappointing results for the majority of solvents investigated. Only **3.42** was able to swell the resin to an acceptable degree, though **3.22**, **3.36** and **3.37** did swell it to just below 4.0 mL g^{-1}. The SpheriTide resin was functionalised with an Fmoc-protected linker, which is exactly the same functionality as that present for TentaGel resin. Comparison of both results (Figures 3.14 and 3.19) demonstrate very different behaviour for these two resins across the range of green solvents, again suggesting that interactions between the solvent and polymer backbone overwhelmingly determine the resin swelling, not the nature of the functionalisation.

Comparison of the swelling data obtained (Figure 3.11-3.19) shows that cyclopentanone **3.22** and dimethyl isosorbide **3.30** were able to swell all of the PS, PS-PEG and PEG based resins to more than 4.0 ml g^{-1}. NBP **3.42** was the only solvent that was able to swell the PA based SpheriTide resin. In contrast, ethanol **3.37** and isopropanol **3.38** were not able to swell any of the resins to 4.0 mL g^{-1} and ionic liquid was only suitable for use with ChemMatrix resin. Overall, ChemMatrix and ArgoGel resins appear to have the best overall compatibility with a range of green solvents. Additionally, this swelling study has identified at least one solvent that is able to swell each of the common SPOS resins to over 4.0 ml g^{-1}, making them a promising replacement for the conventional SPOS solvents.

3.2.2 Computational Prediction of Resin Swelling

In an effort to better understand and be able to predict resin swelling in green solvents, a modelling study was undertaken using the HSPiP software. In order to do this a training set of 18 solvents were selected which included **3.16-3.19**, **3.22**, **3.23**, **3.26**, **3.27**, **3.32-3.38** along with the control solvents **3.43-3.45**. The ability of these solvents to swell each resin was quantified in the previous section (Section 3.2.1). HSPiP however requires that this data is input in the form of a series of ranked groups, rather than as raw swelling data. It also requires that two solvents occupy the highest swelling group. For each resin, the solvents were divided into n groups based on their ability to swell the resin. Not knowing the number of groups that would be optimal, values for n = 4-6 were investigated. Thus, the difference between the maximum (S_{max}) and minimum (S_{min}) observed swelling for a given resin with these 18 solvents was divided by n and the solvents allocated to groups based on their ability to swell a particular resin, given by equation 3.7. Where n = 4, 5 or 6 and a = 1 to n. Full data for the grouping allocation can be found in the appendix.

$$\text{Group "a" lower boundary} = S_{max} - a\left(\frac{S_{max} - S_{min}}{n}\right) \tag{3.7}$$

The HSPiP software can then be used to analyse the solvents in terms of their ability to swell the resin. A three-dimensional plot based on the dispersion (D), hydrogen-bonding (H) and dipolar (P) energies ($MPa^{0.5}$) of the solvents is then generated, which predicts optimal solvent parameters based on the best fit of the data, according to the Hansen fitting algorithm. This is represented by a green sphere of radius R_0, which indicates the area in which suitable solvents for resin swelling should exist in Hansen space, as shown in Figure 3.20 for Merrifield resin with n = 5 (plots for all resins with n = 4, 5 and 6 can be found within the appendix). In this plot, the centre of the green sphere represents the optimal HSP values, as predicted by HSPiP, with the blue circles being all the rank 1 (highest swelling) solvents, whilst the red squares are all the other solvents in the training set.

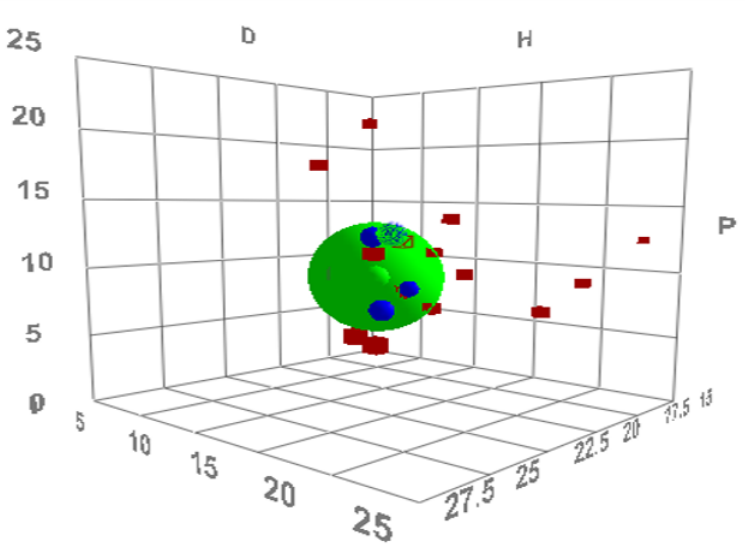

Figure 3.20: HSPiP prediction for Merrifield resin based on $n = 5$ groups.

Table 3.2 summarises the numerical values obtained for all nine resins investigated in the previous swelling experiments, using four, five or six groups ($n = 4$, 5 or 6). As previously mentioned, the HSPiP software requires that there be at least two solvents allocated to the highest swelling group (rank = 1). However, in a number of cases one solvent was able to swell the resin much better than any other, meaning the software is unable to adequately perform the fitting. This was found to be the case with ArgoGel, where CH_2Cl_2 **3.45** produced a much greater swelling than any other solvent. In addition, as the value of n increases, it becomes increasingly likely that there will be only one solvent in the highest swelling group. This was found to be the case for TentaGel, ArgoGel, NovaGel and ChemMatrix where $n = 6$. These issues were overcome by giving equal weighting to solvents found in groups 1 and 2 before allowing the HSPiP software to perform the best fit algorithm.

Table 3.2: HSPiP resin swelling predictions.

	n = 4				n = 5				n = 6			
Resin	D	P	H	R_0	D	P	H	R_0	D	P	H	R_0
Merrifield	17.48	8.51	4.27	3.3	17.47	8.27	4.77	4.9	17.65	11.24	9.43	3.0
ParaMax	17.68	7.87	7.71	4.0	17.68	7.87	7.72	4.0	17.68	7.82	7.75	4.0
JandaJel	17.13	9.34	4.09	3.4	17.30	9.16	4.09	3.4	16.97	10.23	2.48	5.5
TentaGel	17.76	10.88	6.49	1.7	17.72	10.82	6.41	1.7	17.69*	10.78*	6.35*	1.7*
ArgoGel	18.37*	8.44*	8.44*	3.3*	17.68*	10.93*	6.40*	1.7*	17.71*	10.81*	6.40*	1.7*
HypoGel	17.33	11.72	9.05	4.9	17.57	12.02	8.68	3.9	17.78	12.27	9.10	4.9
NovaGel	17.78	11.37	9.57	4.7	17.21	10.87	10.22	3.0	17.90*	12.10*	9.07*	4.9*
ChemMatrix	18.58	9.89	7.04	1.0	18.60	9.82	6.98	1.0	17.80*	11.20*	9.27*	3.2*
SpheriTide	17.45	11.10	9.61	3.0	17.14	11.33	9.35	3.0	17.26	11.24	9.43	3.0

*Value calculated giving equal weighting to solvents in groups 1 and 2

Analysis of the data in Table 3.2, suggests the best predictions are obtained when $n = 5$, in terms of having the lowest values of R_0 (in all cases except Merrifield resin)

and optimal values of D, P and H (DPH) that are comparable to the results for both $n = 4$ and 6. Comparison of the predicted optimal parameters for swelling of PS and PEG based resins were then be compared to the DPH parameters for ethylbenzene (D = 17.8, P = 0.6 and H = 1.4) and ethylene glycol dimethyl ether (D = 15.4, P = 6.3 and H = 6.0) as models for the monomer units. It was observed that for PS resins, the dispersion energies (D) of the model monomer unit and predicted optimal solvents matched quite well (17.1-17.7 to 17.8), but the dipolar (P) and hydrogen-bonding (H) energies were very different. For the PEG based ChemMatrix resin, none of the energy parameters were a particularly good fit. This indicates that it is not possible to assume "like swells like" on the basis of the monomer unit, as the resins are clearly quite distinctly different to the monomer in terms of HSP values.

Having determined the DPH values for an optimal solvent for each resin, the HSPiP software can then be used to predict other suitable solvents from a database of over 1200 compounds. The generated list was then ordered according to the root-mean squared relative distance (Ra), as compounds closest to optimal in three-dimensional space would be most likely to be able to adequately solvate the resin. The solvents, excluding those initially utilised within the training set, were then colour coded green, amber or red, according to the latest version of the GSK green solvents guide.[16] Table 3.3 lists those green or amber solvents that were predicted to swell at least 4 of these resins.

Table 3.3: Resin swelling predictions.[a]

	Solvent						
Resin	**3.20**	**3.21**	**3.24**	**3.30**	**3.31**	**3.46**	**3.47**
Merrifield	3.1	4.9	-	3.0	4.3	-	-
ParaMax	4.4	6.2	6.5	0.8	5.3	4.3	-
JandaJel	2.8	5.0	7.9	4.0	5.0	7.0	-
TentaGel	4.1	7.1	8.7	3.9	7.2	7.3	8.5
ArgoGel	4.1	7.2	8.4	4.0	7.2	7.4	8.5
HypoGel	5.6	-	-	5.1	-	-	6.8
NovaGel	6.0	-	-	4.7	-	6.6	4.7
ChemMatrix	5.6	-	-	3.4	-	-	-
SpheriTide	5.4	-	-	4.7	-	-	5.6

[a] The number given for each solvent is its RMS (Ra) deviation from the DHP parameters for an optimal solvent for the resin.

Glycerol triacetate **3.46** was found to be a very viscous solvent and this prevented experimental determination of its ability to swell resins. Glycerol diacetate **3.47** is only available as a mixture of 1,2- and 1,3-regioisomers, so it was also omitted from experimental studies. The remaining solvents in Table 3.3 (**3.20**, **3.21**, **3.24**, **3.30** and **3.31**) were included in the solvents used in the experimental determination of resin swelling (Figures 3.11-3.19), which allowed the accuracy of the solvent selection

predictions to be tested. The experimental swelling data as compared to the Ra value of each solvent for each resin are shown in Figures 3.21-3.25. The data in these figures is presented as a percentage of the maximum observed swelling for that resin, to compensate for the fact that some resins swell more than others, which allows the data to be compared. The equivalent data comparing the actual swelling values with Ra for each resin can be found within the appendix.

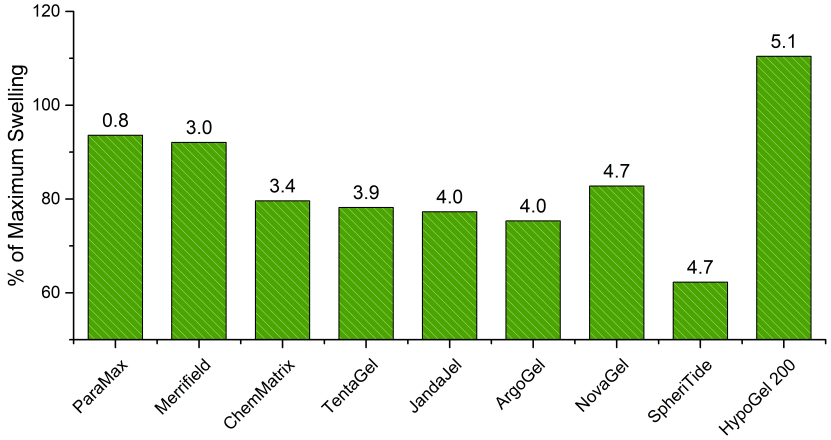

Figure 3.21: Comparison of observed swelling in dimethyl isosorbide **3.30**. Resins are ranked from highest predicted swelling (left) to lowest (right) with the RMS deviation of the solvent parameters for dimethyl isosorbide from those of an ideal solvent given as a number above each bar.

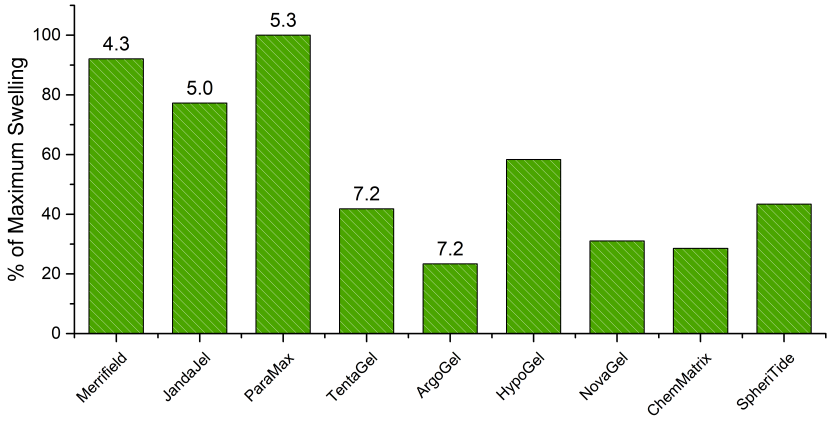

Figure 3.22: Comparison of observed swelling in cyclopentyl methyl ether **3.31**. Resins are ranked from highest predicted swelling (left) to lowest (right) with the RMS deviation of the solvent parameters for cyclopentyl methyl ether from those of an ideal solvent given as a number above each bar.

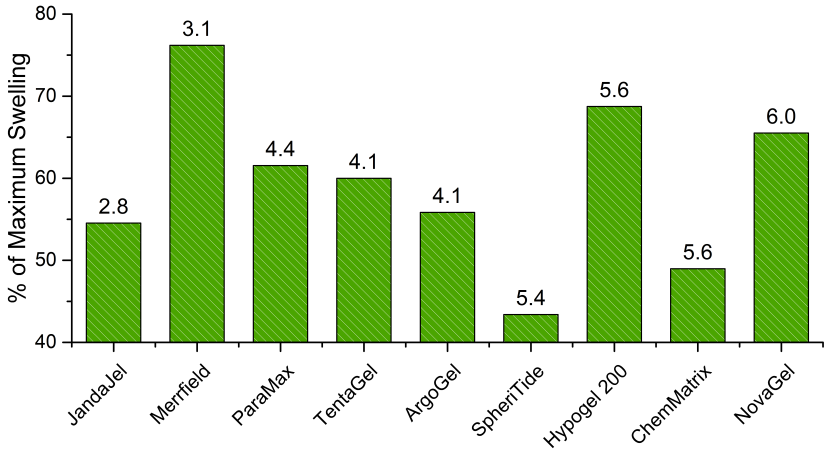

Figure 3.23: Comparison of observed swelling in butan-2-one **3.20**. Resins are ranked from highest predicted swelling (left) to lowest (right) with the RMS deviation of the solvent parameters for butan-2-one from those of an ideal solvent given as a number above each bar.

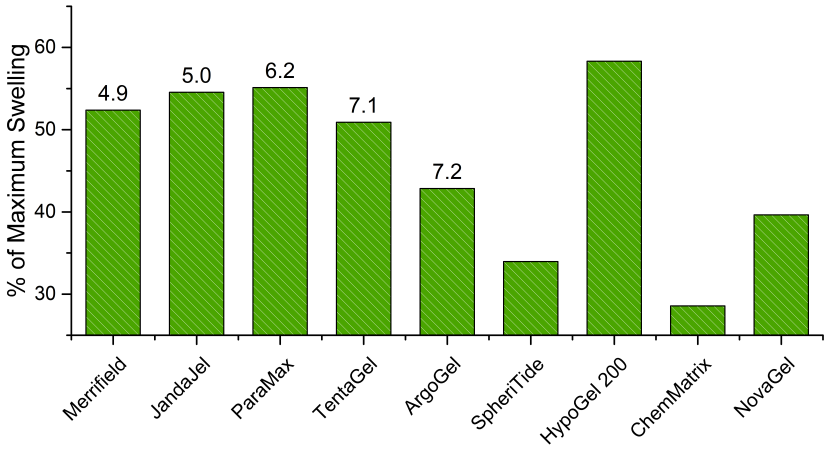

Figure 3.24: Comparison of observed swelling in 4-methylpentan-2-one **3.21**. Resins are ranked from highest predicted swelling (left) to lowest (right) with the RMS deviation of the solvent parameters for 4-methylpentan-2-one from those of an ideal solvent given as a number above each bar.

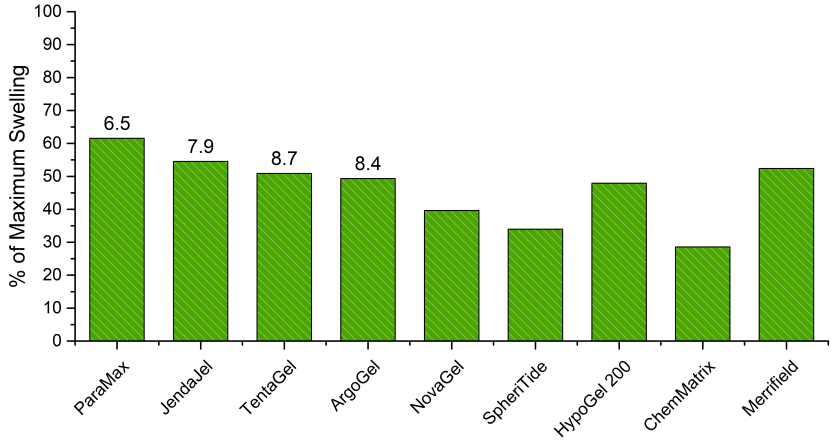

Figure 3.25: Comparison of observed swelling in isopropyl acetate **3.24**. Resins are ranked from highest predicted swelling (left) to lowest (right) with the RMS deviation of the solvent parameters for isopropyl acetate from those of an ideal solvent given as a number above each bar.

It is apparent from Figure 3.21 that there is a good correlation between how close the HSP values for dimethyl isosorbide **3.30** are to the HSP values for the ideal solvent for each resin, and how much the resin was experimentally found to swell in **3.30**. The only exceptions are NovaGel for which the experimental swelling was 10-20% higher than predicted and HypoGel 200. In the latter case dimethyl isosorbide **3.30** was actually found to swell the resin more than any solvent in the training set. This suggests that the swelling of HypoGel 200 is influenced by one or more parameters not adequately covered by the training set. All nine of the resins investigated were predicted to swell in dimethyl isosorbide **3.30** on the basis of the HSPiP model, experimentally all but SpheriTide were found to swell to more than 4.0 mL g^{-1}.

A similar situation is observed for cyclopentyl methyl ether **3.31** (Figure 3.22). In this case **3.31** is found to perform comparatively to NMP **3.43** in the swelling of ParaMax, with the experimental result found to be about 30% higher than would be predicted by the HSPiP study. Otherwise, the experimentally observed swelling of the first five resins would appear to decrease as the Ra distance from the optimal DHP values increases. For this solvent, only the PS based resins, Merrifield, ParaMax and JandaJel were found to swell to more than 4.0 mL g^{-1}.

The data for the resin swelling in butan-2-one **3.20** is more scattered, although a general decrease in the percentage of maximum swelling as the Ra value increases is observed (Figure 3.23). In Figure 3.23, the swelling of JandaJel appears to be very low, and the swelling of HypoGel and NovaGel too high. However, this is largely a feature of the swelling of these resins in other solvents affecting the results obtained, when displayed as a percentage. There was actually very little difference in the

range of swelling observed in **3.20** (2.3-4.8 mL g^{-1}), which is largely responsible for the scatter observed in Figure 3.23. Nevertheless, of the five resins with the lowest Ra deviations for **3.20**, four were found to swell to >4.0 mL g^{-1}.

For 4-methylpentan-2-one **3.21** and isopropyl acetate **3.24** (Figures 3.23 and 3.25) the Ra distances from the optimal DHP parameters in all the solvents were rather large (>4.9). However, a general decrease in maximum swelling is observed with increasing Ra values. This is particularly apparent for isopropyl acetate **3.24**. For both solvents, only two resins were found to swell to >4.0 mL g^{-1}, which were JandaJel and ParaMax.

Overall, the data obtained for resin swelling as predicted by the HSPiP software (Figures 3.21-3.25) shows a good correlation between the degree of swelling and Ra distance from optimal DHP values. This only holds true when differences in swelling between resins is accounted for, by plotting the percentage of maximum swelling. The trends observed suggests that the use of HSPiP can be valuable tool for optimising swelling of SPOS resins on the basis of HSP values. The software has also been shown to be a useful method for suggesting new or unusual green solvents that would be suitable for SPOS.

3.2.2.1 Resin Swelling Prediction for Mixed Solvent Systems

To further investigate the use of HSPiP software in predicting resin swelling in green solvents, its ability to predict mixed solvents systems capable of swelling resins was investigated. The solvent optimisation within HSPiP was edited to contain solvents **3.16-3.41**, except for **3.28** as this data was not available at the time. Optimal solvent mixtures were then predicted for the ideal DPH parameters outlined for n = 5 groups for each resin. This is done using the HSPiP software, which combines solvent HSP values based on relative volume fractions to produce optimal values, in a similar manner to that which was reported by Fields *et al.* in their investigation into Hildebrand solubility parameters. The results of the mixed solvent optimisation and corresponding swelling tests are summarised in Table 3.4.

Table 3.4: Mixed solvent predictions for resin swelling.

Resin	Predicted		Experimental		
	Solvent 1 (%)	Solvent 2 (%)	Solvent 1 (mL g^{-1})	Solvent 2 (mL g^{-1})	Mixture (mL g^{-1})
Merrifield	**3.27** (52)	**3.31** (48)	5.6	5.8	4.8
ParaMax	**3.30** (95)	**3.16** (5)	7.3	2.8	7.8
JandaJel	**3.27** (75)	**3.16** (25)	8.8	1.8	8.3
TentaGel	**3.22** (84)	**3.39** (16)	4.8	1.8	3.8
ArgoGel	**3.22** (84)	**3.39** (16)	5.8	1.8	5.8
HypoGel 200	**3.22** (91)	**3.40** (9)	4.8	1.8	5.3
NovaGel	**3.22** (65)	**3.37** (35)	4.8	1.8	4.3
ChemMatrix	**3.18** (80)	**3.30** (20)	8.3	7.8	8.8
SpheriTide	**3.22** (71)	**3.37** (29)	3.8	3.8	3.8

In five cases (JandaJel, TentaGel, ArgoGel, NovaGel and SpheriTide), the optimal predicted solvent mixture were found to experimentally swell the resin to an amount that was between or the same as the swelling observed for the individual solvents. As would be expected in the absence of any cooperative effects between the two solvents. However, in three cases (ParaMax, HypoGel 200 and ChemMatrix) the predicted solvent mixture was found to swell the resin more than either solvent individually, and in one case (Merrifield) the predicted optimal solvent was found to swell the resin less than either solvent individually. These results could not have been predicted just on the basis of the swelling observed by the solvent components alone and are suggestive of positive or negative effects involving both solvents and their interactions with the resin. The outcome of this investigation is suggestive that HSPiP is able to make reasonable predictions on the swelling ability of mixed solvent systems that are not intuitively obvious.

3.2.3 Solid-Phase Ugi Reaction

In order to experimentally validate the predictions from the resin swelling experiments, the Ugi multicomponent reaction was investigated, in the hope that the reaction would be inhibited when a solvent was used that was deemed unsuitable for the solid support. The Ugi reaction, is a four component condensation between an amine, a carboxylic acid, an isocyanide and either an aldehyde or ketone, to produce an α-acylamino amide.[179] It was selected as a suitable test reaction on the basis that it is pharmaceutically relevant, is known to be tolerant to a wide variety of solvents and both solution- and solid-phase variants have been reported numerous times within the literature.[180]

Two resins, Merrifield and ChemMatrix were chosen, along with two green solvents, methanol **3.36** and 2-MeTHF **3.27**. Methanol **3.36** was chosen over other potentially green alcohols as it is a preferred solvent for solution-phase Ugi reactions. This is due to the poor solubility of the Ugi products in this solvent, but good solubility of the starting reagents.[180] Based on the resin swelling results obtained for this combination of resins and solvents (Figure 3.11 and 3.18), it would be predicted that for a Merrifield resin-supported Ugi reaction, 2-MeTHF **3.27** would be a much better solvent than methanol **3.36**. This is because methanol **3.36** was observed to be an unsuitable solvent for Merrifield resin. As for the ChemMatrix supported reaction, both solvents would be expected to perform similarly, due to both producing what can be regarded as good swelling.

Initially, the solution-phase Ugi reaction was performed in the two solvents, in order to test the suitability of 2-MeTHF and obtain comparable yields in the absence of any resin swelling effects (Scheme 3.4). The Ugi multicomponent coupling was carried out between cyclohexyl isocyanide **3.48**, pentanal **3.49**, benzoic acid **3.51** and benzhydrylamine **3.50**, in either 2-MeTHF **3.27** or MeOH **3.36**. The benzhydrylamine **3.50** was used in an effort to mimic the Rink amide linker that would eventually be used for the solid-phase variant, in order to better compare the solution- and solid-phase reactions. After 1.5 hours at 28 °C the intermediate product **3.52** was obtained in almost identical yields (75-79%) in both solvents, suggesting that when performed in solution the solvent has little influence on the reaction. The benzhydrylamine protecting group was then removed in neat TFA, producing the α-acylamino amide **3.53** in moderate to good yield, resulting in yields of 38% and 50% for MeOH **3.36** and 2-MeTHF **3.27** respectively, over the two steps.

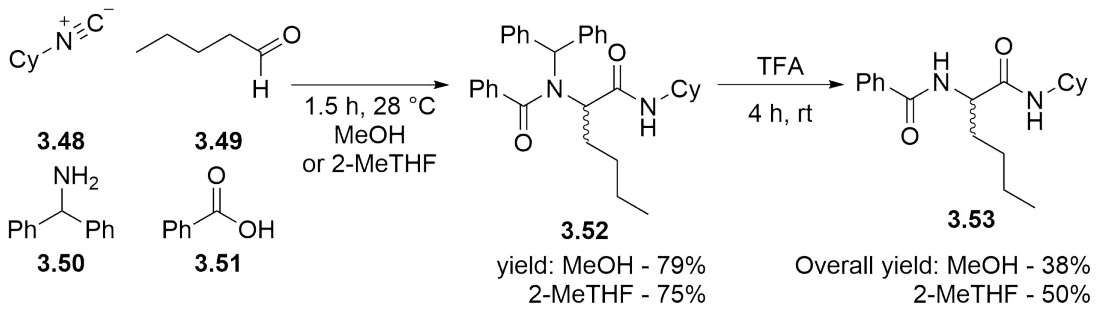

Scheme 3.4: Solution-phase Ugi reaction in MeOH and 2-MeTHF.

In order to then perform the Ugi reaction upon the solid-phase the benzhydrylamine was exchanged for either the Merrifield or ChemMatrix resin, functionalised with a Rink amide linker (Scheme 3.5). Commercial resins supplied as the Fmoc-protected Rink linker were first deprotected using 20% v/v piperidine in DMF. The Ugi reaction was then performed in a similar manner to the solution-phase approach, coupling the resin supported amine **3.54**, benzoic acid **3.51**, pentanal **3.49** and cyclohexyl isocyanide **3.48** for 16 hours at room temperature, to produce the intermediate **3.55**. This reaction was performed in both MeOH **3.36** and 2-MeTHF **3.27** for both Merrifield and ChemMatrix resins. The intermediate **3.55** was then cleaved from the resin using TFA in CH_2Cl_2, to yield the α-acylamino amide **3.56**, following purification by flash column chromatography. DMF and CH_2Cl_2 were used for the initial resin swelling, Fmoc-deprotection and substrate cleavage as they are known to be suitable solvents for both resins. The reason for this was to ensure that the isolated yields for the α-acylamino amide **3.56** were a consequence of the solvent used for the coupling reaction. All solid-supported syntheses were carried out in duplicate to ensure that the results were reproducible, the outcomes of which are summarised in Table 3.5

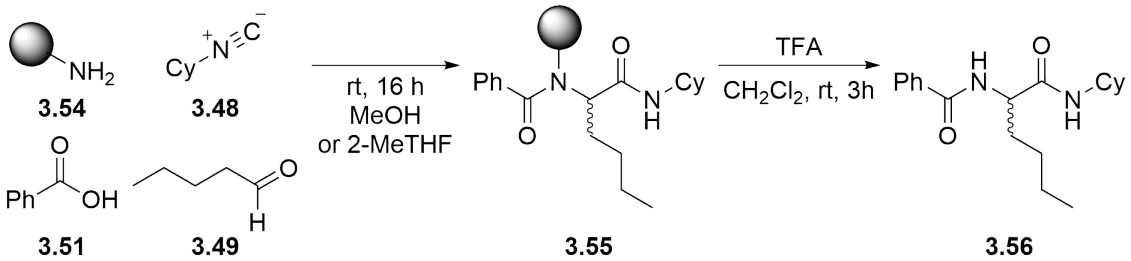

Scheme 3.5: Solid-phase Ugi reaction upon Merrifield and ChemMatrix resins in MeOH and 2-MeTHF.

Table 3.5: Summary of results for the solid-supported Ugi reaction upon PS- and PEG-based resins in MeOH and 2-MeTHF.

Resin name	Capacity[a] (mmol g^{-1})	Solvent	Yield[b] **3.56** (%)
Merrifield	1.0	2-MeTHF	27 and 36
Merrifield	1.0	MeOH	3 and 4
ChemMatrix	0.49	2-MeTHF	52 and 57
ChemMatrix	0.49	MeOH	30 and 32

[a] Obtained from the manufacturer's certificate of analysis and checked by CHN analysis.[b] Isolated yields after purification by column chromatography from two separate reactions.

It is evident from the data summarised in Table 3.5, that when the solid-phase Ugi reaction is performed upon a Merrifield resin the average isolated yield is approximately ten times higher for 2-MeTHF **3.27** than MeOH **3.36**. This is consistent with the hypothesis that the outcome of the reaction would be dependent on the ability of the solvent to adequately solvate the solid support, as 2-MeTHF **3.27** was shown to be a good solvent for Merrifield resin, whilst MeOH **3.36** was shown to be a poor solvent (Figure 3.11). In contrast, for reactions carried out upon a ChemMatrix resin, the average yields are remarkably similar to the results obtained for the solution-phase control reactions (Scheme 3.4). This was to be expected, as both solvents were found to adequately solvate ChemMatrix resin (Figure 3.18). Evidently, the results obtained from the solid-supported Ugi reaction verify that the experimentally determined resin swelling results are indicative of whether a green solvent will (or will not) be suitable for SPOS on a particular resin.

3.3 Conclusions

When analysed from a green perspective SPOS has great potential to simplify reaction work-up and purification. However, solvent will often make up the majority of waste generated from a given synthetic transformation, and with SPOS typically being performed in highly undesirable solvents, if SPOS is to be widely utilised this must be addressed. This chapter has identified that the use of green solvents for SPOS has seen rather little investigation when compared to the parent methodology SPPS, that was investigated in the previous chapter (Chapter 2). In fact, only two examples could be found within the literature that explicitly utilised what could be regarded as a green solvent. For this reason, an investigation into the suitability of a range of green solvents for SPOS was planned.

Solvent choice in SPOS is however rather important, as adequate solvation of the solid support is critical for a successful synthetic transformation. This prerequisite is most often investigated within the literature by quantifying the ability of the solvent to swell the polymeric support. The ability of a range of green solvents to

swell a number of common SPOS resins has therefore been investigated, by simply measuring the increase in volume occupied by the resin following exposure to a particular solvent. This investigation has identified a potentially suitable green solvent for each resin, on the basis of its ability to swell the resin to >4.0 mL g^{-1}.

In an effort to better understand and predict the ability of a green solvent to swell SPOS resins a computational approach to modelling resin swelling was performed, using the HSPiP software. The experimentally determined swelling data was converted to data suitable for HSPiP, through the use of a ranking system, based on the solvents ability to swell a particular resin. This was determined by dividing the swelling range into a number of groups (n), with $n = 5$ being found to be optimal. HSPiP could then be used to determine the best fit of the swelling data, predicting both the region in which suitable solvents would exist within HSP space, along with optimal DPH values.

This data could then be used to predict optimal solvents for a particular resin, on the basis of the calculated DPH values. A number of suitable green solvents that may not have been intuitively obvious choices prior to the investigation were then identified. Overall, HSPiP was found to give fairly good predictions, as a plot of maximum observed swelling for each resin was generally found to decrease as distance from optimal DPH values increased (increasing Ra values). Additionally, HSPiP was shown to be able to predict suitable mixed solvent systems by combining DPH values according to volume ratios.

Finally, this data has been experimentally verified using the solid-supported Ugi reaction. The multi-component coupling was performed upon ChemMatrix and Merrifield resins, in both methanol **3.36** and 2-MeTHF **3.27**. The results obtained indicate that the ability of a solvent to swell a polymer support is paramount to the success of a reaction, as the yields obtained for the α-acylamino amide product were shown to be severely inhibited when an unsuitable solvent/resin combination was used.

A number of suitable green solvents have therefore been identified for a range of SPOS resins on the basis of their ability to swell the resin. The results have been validated using both a computational and experimental approach.

Chapter 4

Ring-Opening Metathesis Polymerisation of a Novel Bio-based Monomer Framework

4.1 Introduction

The remaining chapters will now deal with the second aim of this thesis, on improving the sustainability of polymer synthesis. As was discussed within the introduction (Chapter 1) synthetic polymers have become ubiquitous in modern society, finding widespread application in packaging, building materials and consumer products, to name but a few. Consequently, there is a growing demand for these materials, with synthetic polymers currently produced on a scale of more than 300 million metric tonnes annually, the vast majority of which are derived from non-renewable petrochemical feedstocks.[28] This accounts for approximately 8% of the global crude oil and gas production, the second largest sector behind fuels.[29] However, fluctuating petroleum prices and environmental concerns, pertaining to their depletion and climate change, is driving interest in the production of synthetic polymers from renewable and sustainable resources.

At present, only 1.7 million metric tonnes (ca. 0.57%) of synthetic polymers can be regarded as bio-derived, but market analysis has suggested that as much as 90% of the current global demand for these polymers could be realised with bio-based alternatives.[32,28] Consequently, there has been a rapidly growing interest in the synthesis of bio-derived polymers. This is generally achieved using two distinct approaches, either the synthesis of monomers that are chemically equivalent to those derived from petrochemical sources (bioreplacement), or the development of novel monomers from biomass or platform molecules (bioadvantage).[33] It is the latter that has formed the basis of the work reported herein.

North and co-workers have previously investigated the synthesis of novel functionalised bio-based molecules *via* facile green synthetic routes, with a particular focus the molecules itaconic anhydride **4.1** and furfuryl alcohol **4.2** (Figure 4.1).[181] These structures represent highly promising platform molecules as they are both abundantly available from biomass.[182] Itaconic anhydride **4.1** is readily obtained from citric acid **4.3**, which undergoes a simultaneous decarboxylation and dehydration when distilled.[183] Currently, citric acid **4.3** is produced on over a one million ton scale per annum through the fungal fermentation of glucose-containing sugars, using *Aspergillus niger*.[184,185] Furfuryl alcohol **4.2** is obtained through the hydrogenation of furfural **4.4**, which is currently produced on a scale of over 200,000 tons per annum, through the acid catalysed dehydration of 5-carbon sugars, such as pentoses, which are readily obtained from agricultural waste.[186]

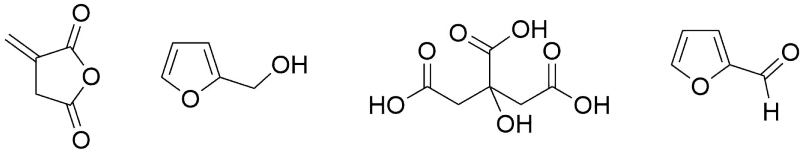

Figure 4.1: Structures of the bio-based platform molecules itaconic anhydride **4.1**, furfuryl alcohol **4.2**, citric acid **4.3** and furfural **4.4**.

In their initial investigation Bai *et al.* were interested in the functionalisation of itaconic anhydride **4.1** with furanic structures, such as furfuryl alcohol **4.2**, to produce bio-based itaconate esters of type **4.5** (Scheme 4.1). This interest was motivated by the fact that the radical polymerisation of itaconic esters is well explored within the literature. However, simple poly(alkyl)itaconates typically possess glass transition temperatures (T_g) below room temperature, significantly limiting their potential applications.[187,188] In contrast, poly(benzyl)itaconates, derived from aromatic itaconic esters, are reported to have much higher T_g values, but are much less easily produced in a sustainable manner and have received little investigation compared to the alkyl equivalents.[189] Therefore, Bai *et al.* sought to investigate the synthesis of poly(benzyl)itaconates from furanic itaconic esters in an effort to produce a fully bio-based polymer possessing practical T_g values.

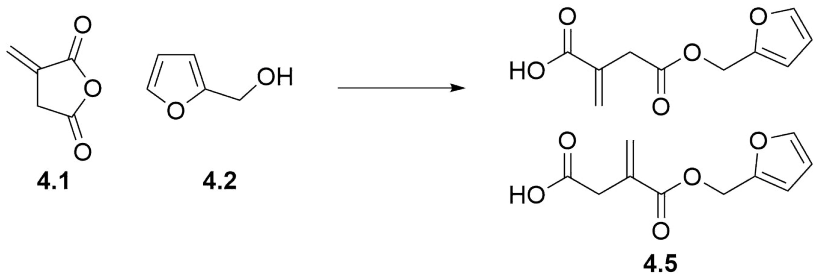

Scheme 4.1: Proposed synthesis of furanic itaconate esters **4.5** from itaconic anhydride **4.1** and furfuryl alcohol **4.2** by Bai *et al.*

The reaction between itaconic anhydride **4.1** and furfuryl alcohol **4.2** did not however produce the target itaconic esters **4.5**, but instead produced the unexpected oxanorbornene-lactone species **4.7** (Scheme 4.2). It was eventually determined that the oxanorbornene-lactone **4.7** is formed *via* a tandem Diels-Alder-lactonisation reaction between itaconic anhydride **4.1** and furfuryl alcohol **4.2**. Rather surprisingly, Bai *et al.* could not find any evidence for this reaction ever having been previously reported, even though Diels-Alder reactions of the analogous maleic anhydride and furans have been extensively explored.[190] Moreover, both furfuryl alcohol **4.2** and itaconic anhydride **4.1** were demonstrated to be suitable dienes and

dienophiles, respectively, in the first two reports of the Diels-Alder reaction from O. Diels and K. Alder almost 90 years ago.[191,192]

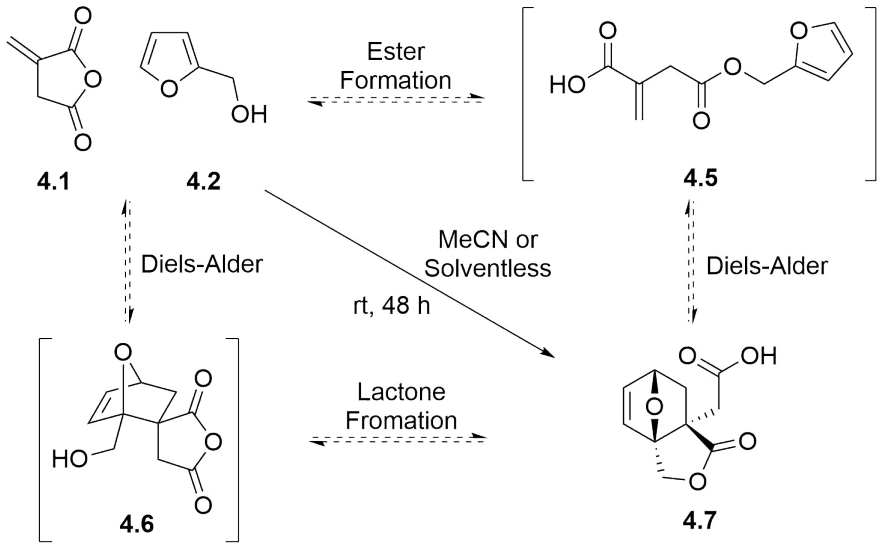

Scheme 4.2: Proposed tandem Diels-Alder-lactonisation for the formation of oxanorbornene-lactone **4.7**.

It was therefore even more remarkable that the same reaction was reported almost simultaneously and independently by Pehere *et al.*[183] In their investigation Pehere *et al.* had been studying the thermodynamics of the Diels-Alder reaction of itaconic anhydride **4.1** with various furans, with an aim to prepare a range of novel reactive monomers for sustainable polymer synthesis. This investigation was planned because the Diels-Alder reactions of furans is typically rather challenging, due to the unfavourable enthalpic change upon product formation. This often results in low equilibrium formation of the target [4+2] adduct, due to loss of heteroaromaticity in the diene and ring strain in the oxanorbornene product.

Much like Bai *et al.*, Pehere *et al.* then stumbled, rather serendipitously, upon the oxanorbornene-lactone **4.7** after monitoring the reaction of itaconic anhydride **4.1** and furfural alcohol **4.2** over an extended period of time. Initially the reaction was heated to 55 °C and only monitored for 10 minutes using ^{1}H NMR spectroscopy. Pehere *et el.* were then able to observe four intermediates, which were subsequently identified as the equilibrium isomeric anhydrides **4.8**-**4.11** resulting from the Diels-Alder step (Scheme 4.3). It was not until the sample was revisited a week later than a unexpected fifth product was observed in approximately 15% yield.

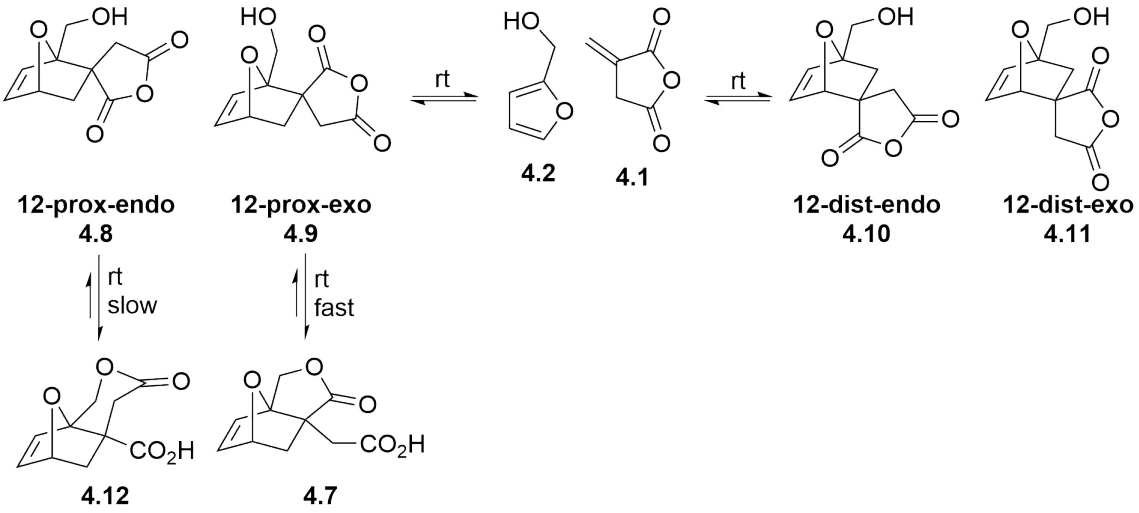

Scheme 4.3: Reaction equilibrium between itaconic anhydride **4.1**, furfuryl alcohol **4.2**, the isomeric anhydrides **4.8**-**4.11** and oxanorbornene-lactone **4.7**.

This fifth product was eventually identified as the oxanorbornene-lactone **4.7**, formed through the ring-opening of the anhydride when in the 12-prox-exo **4.9** configuration. Pehere *et al.* reasoned that formation of the single oxanorbornene-lactone **4.7** was a result of all isomeric anhydrides **4.9**-**4.11** existing in a rapid dynamic equilibrium with itaconic anhydride **4.1** and furfuryl alcohol **4.2**. The driving force for the selective formation of oxanorbornene-lactone **4.7** then results from ring opening of the anhydride being favoured for the 12-prox-exo **4.9** intermediate over the 12-prox-endo **4.8**, and the resulting product crystallising from the reaction solution.[183]

Rather interestingly, whilst reported independently, both Bai *et al.* and Pehere *et al.* acknowledged that oxanorbornene-lactone **4.7** represents a highly promising bio-derived molecular framework amenable to derivatisation for the synthesis of sustainable polymers. This is because the Diels-Alder reaction is 100% atom economical, is performed under ambient conditions, and occurs in the absence of solvents, catalysts or other auxiliaries. The oxanorbornene-lactone **4.7** is also formed exclusively with the *endo* configuration. Hence, in their initial report Bai *et al.* went on to investigate the oxanorbornene-lactone **4.7** in Ring-Opening Metathesis Polymerisation (ROMP). However, as the free acid, oxanorbornene-lactone **4.7** failed to undergo ROMP using any of the commercially available Grubbs catalysts (**G1**, **G2** or **G3**). It was therefore deemed necessary to protect the acid functionality through a Fischer type esterification using methanol, producing the corresponding ester derivative **4.13**, which was isolated in an excellent 77% yield (Scheme 4.4).

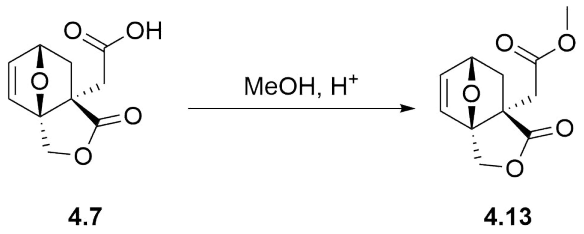

Scheme 4.4: Esterification of oxanorbornene-lactone **4.7** with methanol to produce methyl ester **4.13**.

Methyl ester **4.13** was subsequently investigated for ROMP. Bai *et al.* found that whilst **G1** catalyst was inactive when using **4.13**, both **G2** and Hoveyda-Grubbs **HG2** were able to facilitate ROMP, producing the target homopolymer **4.14** over the course of 72 hours (Scheme 4.5). The authors report that this is the first example of ROMP of a norbornene or oxanorbornene molecule where the bridgehead is substituted. Unfortunately though the resulting polymer was found to be insoluble following reaction work-up through end-capping the polymer with ethyl vinyl ether (EVE), meaning molecular weight data could not be determined using size-exclusion chromatography (SEC).

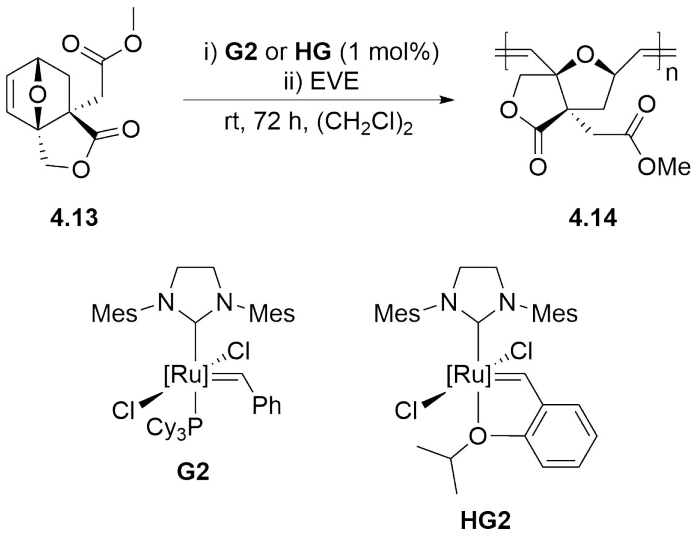

Scheme 4.5: ROMP of methyl ester **4.13** to give homopolymer **4.14**.

In an effort to overcome this Bai *et al.* went on to prepare a range of random copolymers of the methyl ester **4.13** and a commercially available dimethyl *endo*-cis-5-norbornene-2,3-dicarboxylate **4.15** monomer using ROMP (Scheme 4.6). The resultant random copolymers **4.16** were now found to be soluble, provided a minimum of 10% of monomer **4.15** was incorporated. SEC of these polymers showed that they were obtained in good molecular weights (M_n = 9,500-63,200) with narrow dispersities (Đ = 1.11-1.27). Additionally, a linear relationship was observed

for copolymer molecular weight and monomer:catalyst ratio, which is indicative of the polymerisation being a well-controlled chain growth polymerisation. Thermal analysis by thermogravimetric analysis (TGA) and differential scanning calorimetry (DSC) revealed the copolymers possessed high thermal decomposition temperatures ($T_{10\%}$ = 370 °C) and glass transition temperatures (T_g = 158-163 °C).

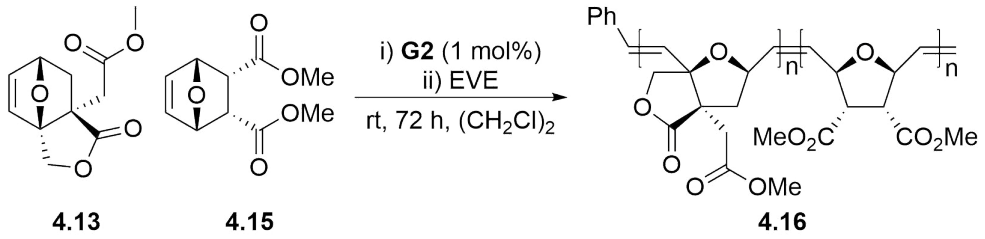

Scheme 4.6: ROMP of methyl ester **4.13** and commercial norbornene **4.15** to give random copolymer **4.16**.

Finally, in their initial report Bai *et al.* went onto investigate the influence of the solvent on ROMP of this copolymer, as this is something that has begun to receive a significant amount of interest in recent years and is particularly important in the context of green chemistry.[193] Previously the polymerisation has been carried out in dichloroethane $(CH_2Cl)_2$, which is a fairly undesirable, due to it being highly hazardous and regarded as a substance of very high concern under REACh.[16] Bai *et al.* therefore repeated the synthesis of copolymer **4.16** in various alternative solvents, the results of which are summarised in Table 4.1. In the majority of cases the results obtained indicated that $(CH_2Cl)_2$ was the most suitable solvent for the synthesis of copolymer **4.16**. The majority of alternative solvents gave rather diminished molecular weights and in the case of THF and DMC poor dispersities also. The results obtained for diethyl carbonate (DEC) were sightly more favourable, but extended reaction times were necessary to obtain acceptable molecular weights.

Table 4.1: SEC data obtained for the preparation of copolymer **4.16** in various solvents.

Solvent	$\mathbf{M_n}$[a]	$\mathbf{M_w}$[a]	**Đ**[b]
Calculated	21,700	-	1
DCE	21,500	23,700	1.11
EtOAc	2,300	2,400	1.08
THF	3,600	5,100	1.40
DMC	4,100	5,600	1.40
DEC	8,600	9,700	1.12
DEC[c]	14,200	15,700	1.11

All polymerisations were carried out using a 50:50:1 molar ratio of monomer:catalyst **4.13**:**4.15**:**G2** at room temperature for 24 hours.[a] molecular weights were obtained by SEC in THF at 23 °C and calibrated relative to polystyrene standards.[b] Đ = M_w/M_n.[c] Reaction time increased to 72 hours.

Bai *et al.* have since gone on to investigate a range of ester derivatives of oxanorbornene-lactone **4.7** in a subsequent publication.[194] This report was particularly interested in the use of bio-based alcohols, in an effort to produce wholly bio-derived ROMP homo- and co-polymers. Firstly, a range of aliphatic ester **4.13a-h** derivatives were prepared in good to excellent yield, these were then subject to homopolymerisation **4.17a-h** under the optimal conditions reported previously (Scheme 4.7). Much like the previous methyl ester, short chain esters were found to be insoluble following polymerisation, it was eventually identified that at least a C_5 alkyl chain was necessary to produce soluble homopolymers. Those that were found to be soluble however were obtained with good molecular weights (M_n = 14,866-34,467) and narrow dispersities (Đ = 1.04-1.16). Additionally, thermal analysis was found to be comparable to the previously reported copolymer **4.16**, with high decomposition ($TD_{10\%}$) (367-371 °C) and glass transition (T_g) (160-196 °C) temperatures observed in most cases. A random copolymer of monomers **4.13a** and **4.13b** was also prepared during this investigation, which was found to be rather similar to the reported homopolymers.

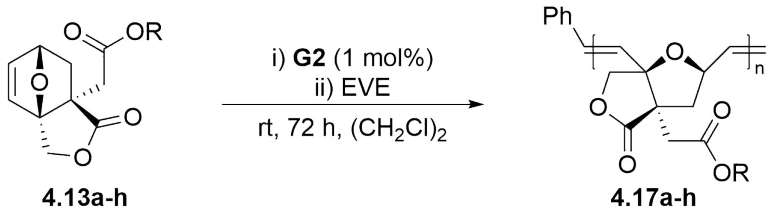

4.13a-h **4.17a-h**

4.13, **4.17**: **a** R=Me; **b** R=$C_{16}H_{33}$; **c** R=C_8H_{17}; **d** R=$CH_2CH_2CHMe_2$; **e** R=C_4H_9; **f** R=CMe_3; **g** R=$CHMe_2$; **h** R=(S)-C(Et)(Me)$(CH_2)_3$CHMe

Scheme 4.7: ROMP homopolymerisation of wholly bio-based ester monomers **4.13a-h**.

The final part of the investigation into the use of wholly bio-derived ester monomers **4.13a-h** sought to synthesise a block copolymer using ROMP. This was however more troublesome than was first anticipated. Long reaction times meant it was difficult to accurately judge the end-point of the first polymerisation, meaning highly bimodal SEC traces were observed following polymerisation of the second monomer **4.13b**. This observation was attributed by the authors to be due to the death of polymer chain ends following polymerisation. To overcome this, Bai *et al.* monitored the polymerisation by ^{1}H NMR spectroscopy. In doing this it was possible to accurately judge the end-point of the first polymerisation, meaning the second monomer **4.13b** could be added slightly prior to **4.13a** being fully consumed. In turn, this produced the target block copolymer **4.19** in good molecular weight (M_n = 10,857) and narrow dispersity (Đ = 1.08) following growth of the second block (Scheme 4.8).

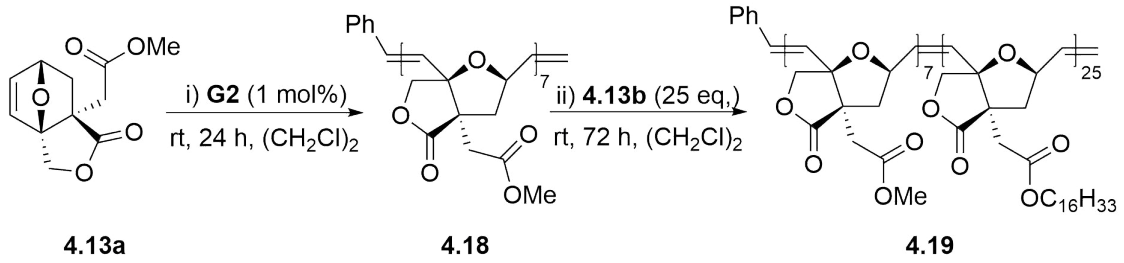

Scheme 4.8: Block copolymerisation of ester monomers **4.13a** and **4.13b**.

In summary, oxanorbornene-lactone **4.7** has been highlighted as a highly promising bio-derived molecular framework for the synthesis of novel, 100% bio-based synthetic polymers. To date, however, only the two reports from Bai *et al.* can be found in the literature that utilise **4.7** within polymer synthesis, both of which focus on derivatisation to the corresponding esters. These esters were then utilised in ROMP producing a range of wholly bio-derived polymers in a well-controlled manner, with SEC data confirming that they were formed with high molecular weights and narrow dispersities. Thermal analysis also showed that in the majority of cases the polymers posses high glass transition (T_g) and decomposition ($T_{10\%}$) temperatures.

The work herein therefore seeks to expand on these existing reports by investigating the synthesis and polymerisation of the analogous amide derivatives. This however presents a dilemma of sorts, as the major appeal of using **4.7** is that it is a molecular framework that is 100% bio-based. It would therefore be counterintuitive to functionalise **4.7** with petrochemically derived molecules, particularly when the focus of this chapter is on improving the sustainability of polymer synthesis. Natural sources of amines are however rather scarce, in fact there are only two main types, chitin and amino acids.[195] Chitin is the second most abundant polymer in the world

after cellulose, commonly found in the shells of crustaceans, it is therefore unlikely to be suitable for this investigation.[195] Amino acids, and the corresponding peptides, could however be a rather promising route to wholly bio-based amide derivatives of **4.7**, as the derivatisation of norbornenes using amino acids or peptides has previously seen some investigation within the literature. Additionally, many of these norbornene derivatives have been explored in the preparation of bioactive, therapeutic and functional materials, which may be a viable and interesting avenue for future investigations.[196,197]

4.1.1 Previous Reports of Amino Acid Derived Norbornenes in ROMP

The use of amino acid derived norbornenes in ROMP was first reported in a series of publications from Gibson, North and co-workers. In their initial report, Coles *et al.* prepared a series of norbornene-imide monomers **4.20**, from the equivalent *exo*- or *endo*-himic anhydrides and either the (*R*)-, (*S*)- or racemic-alanine methyl ester.[198] Homopolymerisation using a molybdenum initiator **4.22** produced the corresponding ROMP polymers **4.21** after 15-24 hours (Scheme 4.9). Analysis of the polymers determined that they were produced with reasonably narrow molecular weights, which were found to be comparable to the expected values. The polymer backbone was also found to predominately consist of *trans* linkages (77-91%). Finally, the polymers derived from optically pure monomers were found to retain optical activity following ROMP, meaning they can be regarded as simple bio-derived peptides in which the amide backbone has been replaced by an all carbon system. In a follow up publication Biagini *et al.* has extended this work, investigating a more diverse range of amino acids as the pendant side chains.[199]

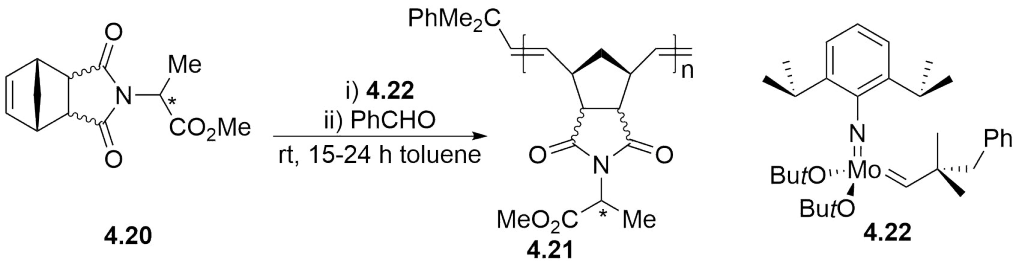

Scheme 4.9: First reported example by Coles *et al.* for the ROMP of amino acid derived norbornene-imides **4.20**.

Subsequently, Biagini *et al.* have gone on to investigate the related peptide derivatives. A series of *exo*- or *endo*-norbornene-imides prefunctionalised with a glycine residue were treated with either an amino acid or dipeptide methyl ester, to produce the corresponding di- or tri-peptide derivatives **4.23** in good

yields.[200] The polymerisation of each species using a range of molybdenum ROMP initiators **4.25a-c** was then investigated (Scheme 4.10). Analysis of the obtained homopolymers **4.24** identified that they were comparable to the previously reported amino acid derivatives. Optical activity was retained during the polymerisation and the polymers were generally obtained with narrow dispersities (Đ = 1.05-1.60), except for the highly hydrophobic species which were found to be insoluble in organic solvents. Rather interestingly, Biagini *et al.* also observed that the *cis*/*trans* ratio in the polymer backbone was directly influenced by the molybdenum initiator **4.25a-c** used, with increasing quantities of *cis* incorporation for increasing fluorination of the ancillary ligands. This also had a direct influence on the reported T_g values, which decreased with increasing *cis* content.

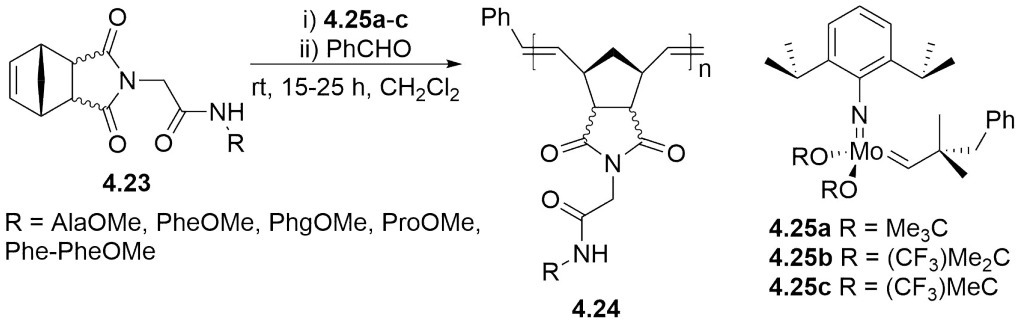

Scheme 4.10: ROMP of peptide methyl ester functionalised norbornene-imides **4.23** using molybdenum initiators **4.25a-c**.

Biagini *et al.* have also reported that the polymerisation can be facilitated using ruthenium based initiators, such as Grubbs 1st generation catalyst **G1** (Scheme 4.11).[201] This catalyst was particularly useful for the synthesis of homopolymers **4.27** when the amino acids were used as the free acids **4.26**, rather than the methyl esters reported previously, as the molybdenum based initiators were not tolerant to the free acid. This was also only possible when the amino acid functionalised norbornene-imide **4.26** had the *exo*-configuration. This is presumably due to the acid lying much closer to the active catalytic species when in the *endo*-orientation, inhibiting the metathesis cycle. Finally, Biagini *et al.* reported that a diverse range of block-, tapered block- and random- copolymers could be prepared using the aforementioned monomer/catalyst combinations.[201,202]

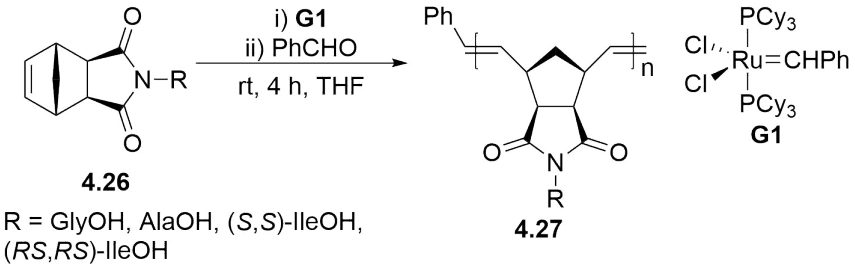

Scheme 4.11: ROMP of amino acid functionalised norbornene-imides **4.26** using Grubbs 1st generation catalyst **G1**.

More recently, Sutthasupa and co-workers have also broadly explored the use of amino acid derived norbornenes in ROMP, differing to the monomers reported by Gibson, North and co-workers in that they incorporate two chiral pendant groups. Sutthasupa *et al.* first synthesised a series of norbornene monomers of type **4.28**, derived from the commercial *cis*-5-norbornene-*endo*-2,3-dicarboxylic anhydride and the corresponding alanine, leucine or phenylalanine methyl esters.[203] The homopolymerisation of these monomers using either **G1** or **G2** catalyst was however not successful. This was reasoned on the grounds that the monomers were derived from an *endo*-anhydride, as these are known to be less active than the equivalent *exo*-monomers on the grounds of steric and electronic factors. Sutthasupa *et al.* were eventually able to incorporate the monomers **4.28** into a copolymer **4.30** with norbornene **4.29** (Scheme 4.12). The results however were rather disappointing, as polymerisation using **G2** catalyst for 2 hours resulted in polymers with broad dispersities (Đ = 2.0-4.7) in poor yield (2-54%).

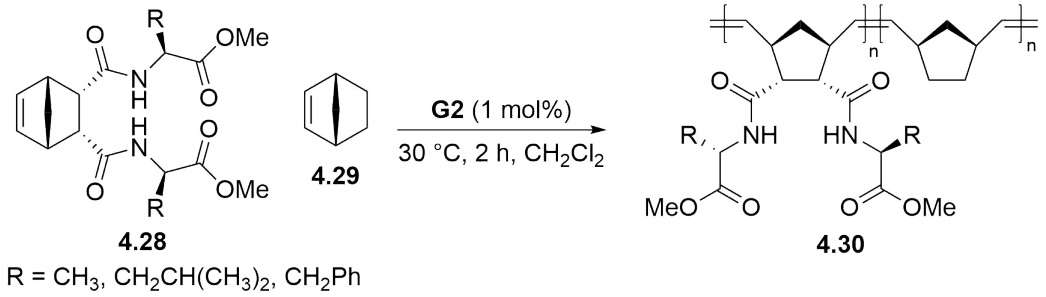

Scheme 4.12: Copolymerisation of *endo*,*endo*-diamino methyl ester norbornene **4.28** and norbornene **4.29** using **G2** catalyst.

Determined to improve on the results obtained for the diamino methyl ester functionalised *endo*,*endo*-norbornene monomers **4.28** Sutthasupa *et al.* went on to investigate the analogous monomers derived from the *exo*,*exo*- and *exo*,*endo*-norbornenes.[204] This time around **G2** catalyst was able to furnish the desired polymers **4.31** in good molecular weights (M_n = 7,300-18,600) and narrow

dispersities (Đ = 1.1-1.4) in only 30 minutes (Scheme 4.13). However, yields after this time were significantly better for the *exo*,*exo*- over *exo*,*endo*-norbornene.

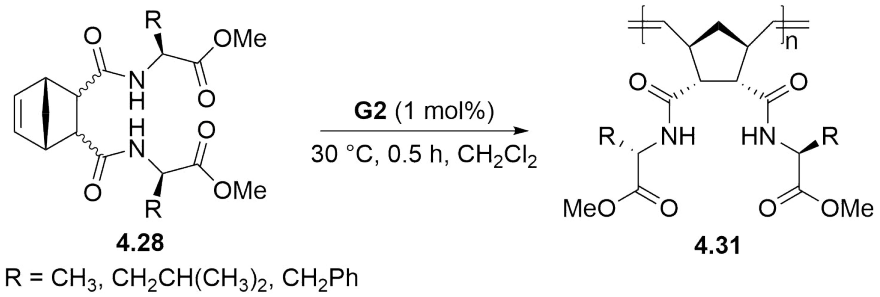

Scheme 4.13: Homopolymerisation of diamino methyl ester derivatives of *exo*,*exo*- and *endo*,*exo*-norbornene using **G2** catalyst.

In a follow up report Sutthasupa *et al.* looked to extend the methodology to the synthesis of self-assembling polymers derived from amino acid functionalised norbornenes. Deprotection of the previously reported diamino methyl ester norbornene **4.28** produced the corresponding diamino acid norbornene **4.32**. This was then found to smoothly undergo ROMP, but only for the monomers derived from the *exo*,*exo*-norbornene, producing polymers in good molecular weight (M_n = 16,000-30,000) and moderate dispersity (Đ = 1.20-1.70). Sutthasupa *et al.* then investigated the synthesis of random- and block-copolymers using the diamino methyl ester **4.28** and diamino acid **4.32** norbornene monomers (Scheme 4.14).[205] The block copolymers are particularly interesting as they were found to form reverse micelles, 100 nm in diameter, in acetone, consisting of a hydrophilic core of poly(**4.28**) and a hydrophobic shell of poly(**4.32**).[205]

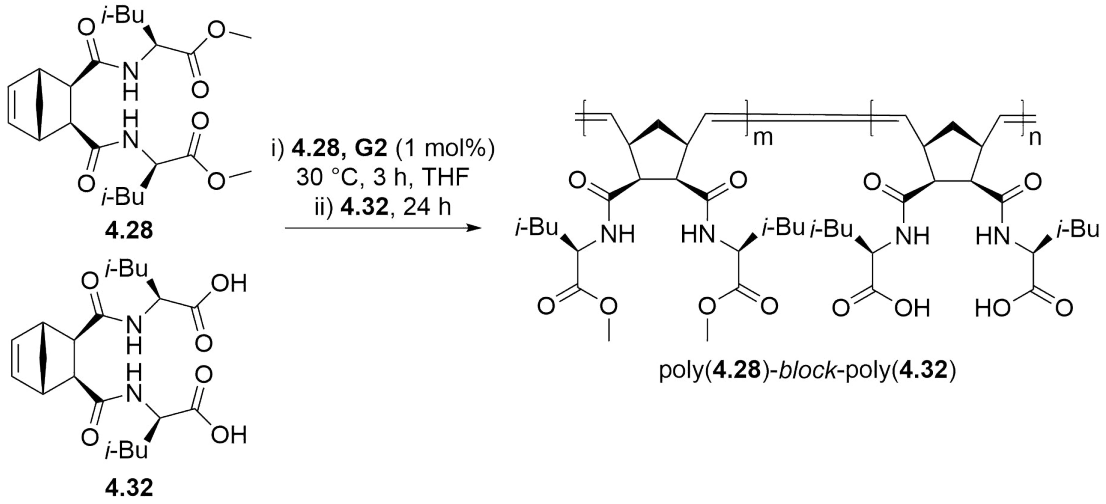

Scheme 4.14: Synthesis of an amphiphilic block copolymer from diamino methyl ester **4.28** and diamino acid **4.32** norbornene monomers.

Following the reports of the aforementioned diamino derived norbornene monomers Sutthasupa *et al.* have gone on to investigate a broader range of norbornene structures incorporating amino acids. The most promising of these has been the various derivatives where the amino acids are tethered to the norbornene *via* an ester linkage to hydroxymethyl groups **4.33a-e** (Figure 4.2). In the initial report of this monomer species, **4.33a** and **4.33b** were found to polymerise using **G2** catalyst incredibly rapidly, with complete consumption of the monomer observed within 4 minutes, regardless of whether the monomer had an *exo*,*exo*- or *endo*,*endo*-orientation.[206] It was hypothesised that this is due to the additional distance from the active site provided by the hydroxymethyl groups and the bulky *t*-Boc protecting groups, meaning the pendant side chains are less able to inhibit polymerisation.

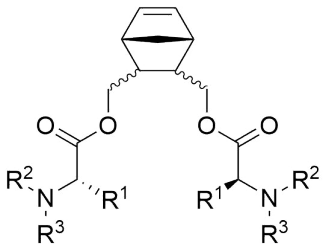

4.33a: R^1 = Me, R^2 = H, R^3 = *t*-Boc
4.33b: R^1 = Me, R^2 = Me, R^3 = *t*-Boc
4.33c: R^1 = Me, R^2 = H, R^3 = H
4.33d: R^1 = Me, R^2 = Me, R^3 = H
4.33e: R^1 = Bzl, R^2 = H, R^3 = Me

Figure 4.2: General structure of the hydroxymethyl functionalised norbornene **4.33a-e**.

Sutthasupa *et al.* then investigated the unprotected variants of these amino acid monomers **4.33c**, by removing the bulky *t*-Boc protecting group. The results obtained for the homopolymerisation of these monomers was rather poor though. The *exo*,*exo*-norbornene produced polymers with moderate molecular weights (M_n = 7,600) and reasonable dispersities (Đ = 1.39) once the quantity of catalyst relative to the monomer was increased, the *endo*,*endo*-norbornene could not be converted however.[207] This is presumably due to catalyst deactivation through co-ordination to the primary amine. Sutthasupa *et al.* therefore introduced a methyl group at this position **4.33d**, which significantly enhanced the results obtained, with the *exo*,*exo*-norbornene now producing a polymer with good molecular weight (M_n = 12,500), dispersity (Đ = 1.29) and in significantly improved yield (81%).

Attempts to then produce random copolymers of these monomers with the previously reported diamino acid monomers **4.32** were found to produce some rather interesting results. Copolymerisation of *N*-methyl-L-phenylalanine derived *exo*,*exo*-disubstituted norbornene monomer **4.33e** and the isoleucine derived *exo*,*exo*-disubstituted norbornene diacid monomer **4.32** was carried out using a 1:1 feed ratio using **G2** catalyst (Scheme 4.15).[208] Analysis of the polymerisation by ^{1}H NMR spectroscopy identified both monomers were consumed at the same rate, a surprising result considering they were previously shown to have significantly

different polymerisation rates. Analysis of the resultant polymer **4.34** confirmed this, showing incorporation of **4.33e**:**4.32** in a 50:50 ratio.

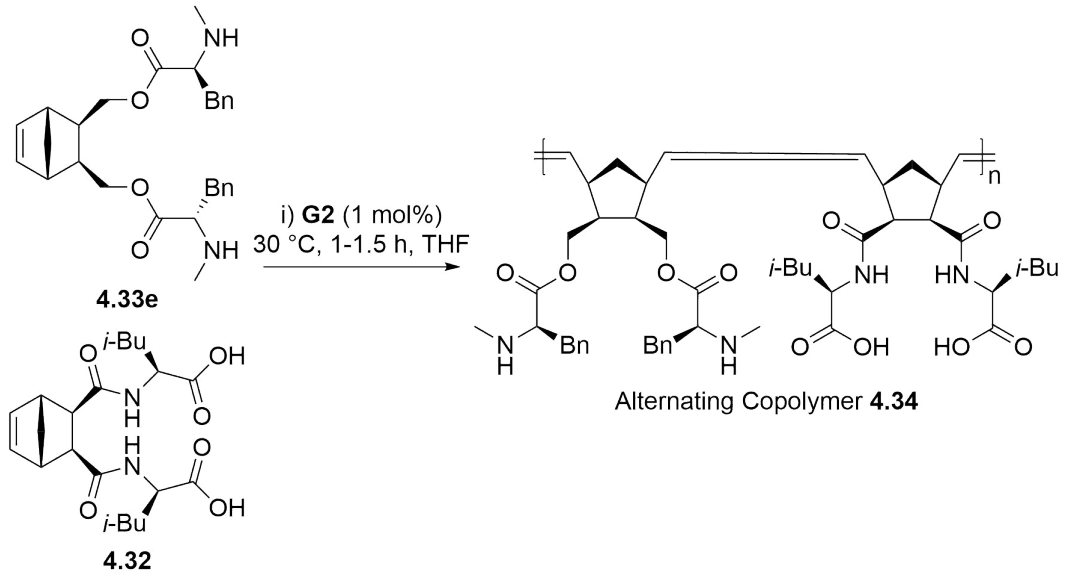

Scheme 4.15: Acid-base assisted alternating copolymerisation of unprotected diamino norbornene monomers **4.32** and **4.33e**.

These observations are indicative of a rather unusual alternating copolymerisation mechanism. This was confirmed using feed ratios of 2:1 and 1:2 of **4.33e**:**4.32**, which again produced polymers containing a 50:50 mixture of both monomers. Sutthasupa *et al.* then determined that this alternating copolymerisation is a consequence of a cooperative acid-base interaction between the two monomers, which is justified on the basis of a control reaction using the corresponding methyl ester **4.28** not producing an alternating copolymer with **4.33e**.

Finally, Sutthasupa *et al.* investigated the synthesis of a number of block copolymers using monomer **4.33e** and the previously reported diamino acid **4.32** and methyl ester **4.28** monomers, in various feed ratios (Scheme 4.16).[209] Amphiphilic block copolymers were then investigated for pH-dependent self assembly, with it being found that micelles of block copolymer poly(**4.32**)-*block*-poly(**4.33e**) form in basic media, consisting of a poly(**4.33e**) core and a poly(**4.32**) shell. These self assembling block copolymers were then shown to be suitable for pH responsive drug delivery, with a poly(**4.33e**)$_{62}$-*block*-poly(**4.28**)$_{38}$ block copolymer shown to release a sample of the nonsteroidal anti-inflammatory indomethacin under acidic conditions. Sutthasupa *et al.* have since gone on to explore a number of derivatives of the aforementioned block copolymers in drug delivery in more recent publications.[210]

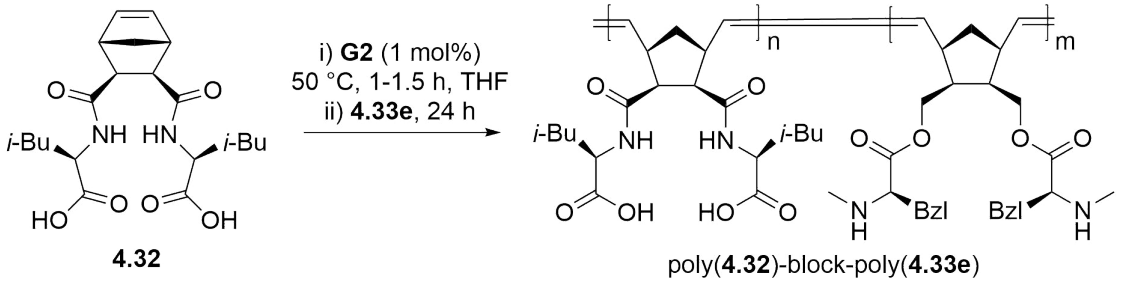

Scheme 4.16: Block copolymer synthesis of unprotected diamino norbornene monomers **4.32**.

Maynard *et al.* have also shown an interest in the use of amino acid functionalised norbornene polymers as therapeutic agents. Many extracellular matrix proteins bind to cell surfaces through the short peptide sequence Arg-Gly-Asp (RGD). Since cell attachment mediated by integrin-protein interactions influences cell survival, differentiation, and migration, the RGD sequence and associated mimics have therefore been investigated as therapeutics for tumour therapy.[211] Maynard *et al.* sought to produce synthetic norbornene polymers substituted with peptides known to be potent cell-binding inhibitors. 5-Norbornene-*exo*-2-carboxylic acid was functionalised with two known inhibitors (GRGDS and PHSRN), and an inactive control peptide (GRGES). These monomers **4.35a-d** were then polymerised using **G1** catalyst producing the target polymers in good molecular weight (M_n = 9,140-12,000) and narrow dispersity (Đ = 1.30-1.37). The peptide protecting groups were then removed from the polymer through treatment with TFA:TIPS:H_2O to produce the corresponding therapeutic peptide polymers **4.36a-d** (Scheme 4.17).

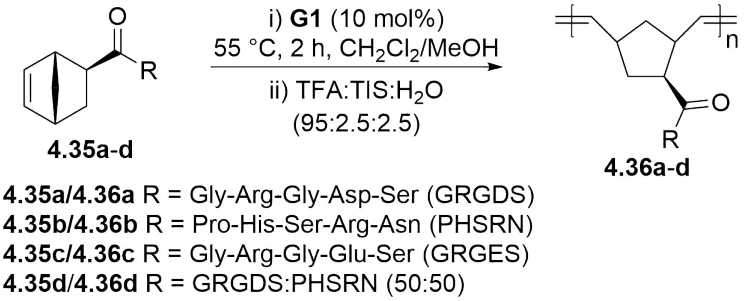

Scheme 4.17: Synthesis of homo- and co-polymers with pendant bioactive oligopeptides by ROMP.

The ability of these peptides to inhibit human foreskin fibroblast cell adhesion to fibronectin coated surfaces was then investigated. The control sequence **4.36c** was found to be completely inactive, along with PHSRN sequence **4.36b** which is known to be inactive unless closely bound to an RGD containing sequence, such as GRGDS. The polymer derived from the known inhibitor **4.36a** was found to be 750% more active than the free GRGDS peptide. Additionally, incorporation

of the synergistic PHSRN to this sequence, as a random copolymer **4.36d**, was found to be 3300% more potent than the GRGDS peptide.[212] The significant enhancement observed further iterates that the synthesis of norbornene derived polymers containing pendant amino acid and peptide side chains is a viable avenue for the development of novel therapeutics.

It is therefore evident that the use of amino acid functionalised norbornene monomers has been widely explored in the context of ROMP. A number of examples have demonstrated that they produce well controlled polymers in good molecular weight and with narrow dispersity, in the presence of either molybdenum or ruthenium catalysts. However, orientation of the pendant side arms of the norbornene has been shown to be an important consideration, as the *endo*-norbornene has been found to be much less active than the *exo*-orientation, particularly when the unprotected amino acid is used. Additionally, the distance of the amino acid from the catalyst active site appears to have a major influence on the polymerisation rate. These may be important considerations for the incorporation of amino acids in the bio-derived framework **4.7** as it is formed exclusively with the *endo*-orientation. Finally, a few interesting reports have investigated the application of deprotected amino acid or peptide functionalised norbornene copolymers as therapeutics and functional materials.

4.1.2 Chapter Aims

The remainder of this chapter will therefore deal with further investigating the novel oxanorbornene-lactone **4.7** reported by Bai *et al.* and Pehere *et al.*, for the synthesis of novel bio-based polymers. Bai *et al.* have previously shown that ester derivatives of **4.13a-h** have produced ROMP polymers in good molecular weight and dispersity. The analogues amide derivatives will therefore be investigated for homopolymerisation using ROMP, and the corresponding polymers characterised by SEC and thermal analysis. Particular attention will be paid to functionalisation of **4.7** with bio-based amines, such as amino acids or peptides, to yield wholly biomass derived polymers. If successful the synthesis of random- and block-copolymers will also be investigated, which may facilitate future investigations into the synthesis of wholly bio-derived polynorbornenes as functional materials or therapeutics.

4.2 Results and Discussion

4.2.1 Monomer Synthesis

To begin this investigation a number of tertiary amide monomers were synthesised in the same manner as the previously reported esters.[194] Acid **4.7** was first converted to the corresponding acid chloride intermediate **4.37** through the use of oxalyl chloride and catalytic quantities of DMF. The acid chloride was then treated with a number of secondary amines **4.38a-k**, to produce the corresponding tertiary amides **4.39a-k**, in good to excellent yields (Scheme 4.18). The structures of **4.39b**, **g** and **h** have also been confirmed by X-ray crystallography (Figure 4.3).

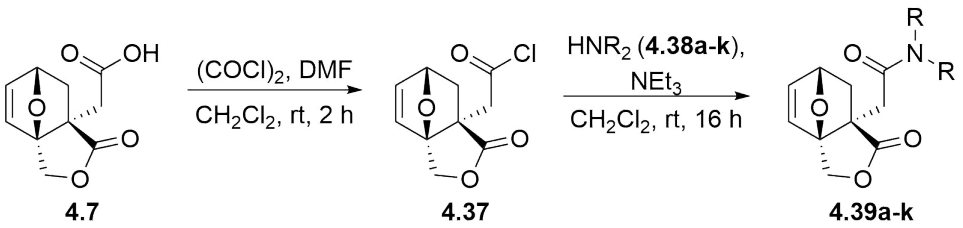

4.38, **4.39**: **a** R = Me; **b** R = Et; **c** R = Pr, **d** R = Bu; **e** R = Oct; **f** R = bis(2-ethylhexyl); **g** R = Bn; **h** R = Pro-OMe; **i** R = Sar-OBn; **j** R = Sar-Gly-OBn; **k** R = Sar-Sar-OBn.

Scheme 4.18: Synthesis of tertiary amide monomers **4.39a-k** from acid framework **4.7**.

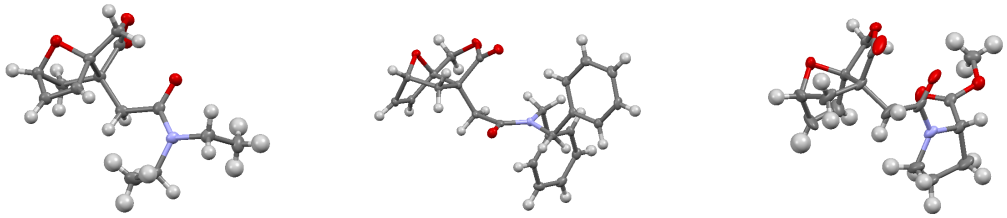

Figure 4.3: Ellipsoid representation of the crystal structures of monomers **4.39b**, **g** and **h**. The tetrahydropyrrole and butyrolactone of **4.39h** were disordered and only the major form of each is shown.

Due to the 100% bio-based nature of the monomer framework **4.7** it would have been preferred that a broad range of bio-based amines could have been utilised. However, as was discussed previously in section 4.1 this is rather difficult, as bio-based amines are typically only readily available from either chitin or amino acids.[195] For this reason, a number of tertiary amide monomers from petrochemically derived amines were first synthesised **4.39a-g**. This was so that the ROMP procedure could be first optimised for simple substrates, before using the potentially more complicated amino acid **4.39h**/**i** and peptide **4.39j**/**k** derived monomers.

It should also be acknowledged at this point as to why all the monomers investigated are derived from secondary amines, producing a range of tertiary amides. This makes little sense if the eventual aim is to utilise amino acids or peptides, because the majority of proteinogenic amino acids are primary, which would yield secondary amides using the procedure described above. The synthesis of secondary amides was actually investigated in parallel with this study, but a rather unexpected result was observed. Exposure of the intermediate acid chloride **4.37** to a primary amine, such as butylamine, actually yielded two products (Figure 4.19). These were eventually identified, using a combination of IR and HMBC spectroscopy experiments, as the secondary amide **4.40** and the spirocyclic species **4.41**. Definitive structural conformation was eventually elucidated using X-ray spectroscopy (Figure 4.4). The rather unusual nature of the spirocyclic species warranted further investigation, which will be explored in much more detail within Chapter 5.

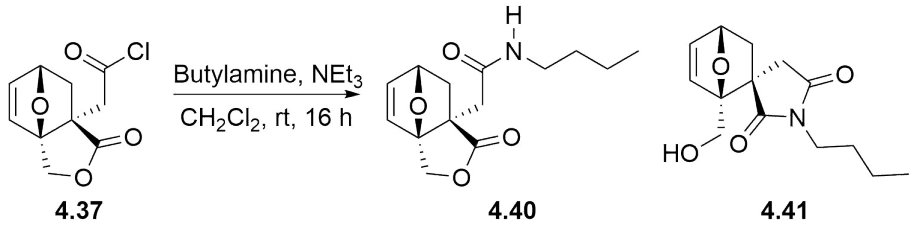

Scheme 4.19: Formation of the secondary amide **4.40** and spirocyclic imide **4.41** species from the acid framework **4.7**.

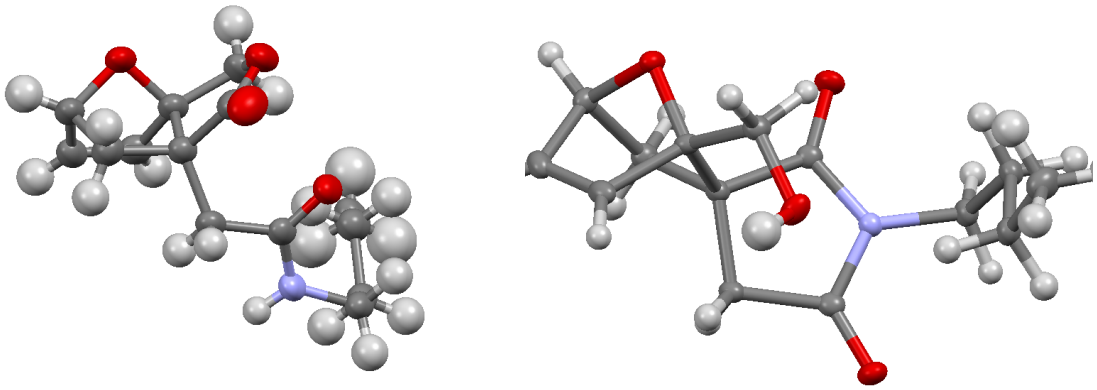

Figure 4.4: Ellipsoid representation of the crystal structures of secondary amide **4.40** and spirocyclic imide **4.41** species.

4.2.2 Polymerisation Optimisation

Having synthesised a range of tertiary amides **4.39a-k** their applicability to ROMP was investigated. The dibenzyl derived tertiary amide **4.39g** was chosen as a suitable model substrate for the initial investigation. Optimisation of the polymerisation process was attempted using 1 mol% of commercial Grubbs catalyst (**G1-G3**), in 1,2-dichloroethane ($(CH_2Cl)_2$) at various temperatures and concentrations. Alternative solvents to $(CH_2Cl)_2$ were omitted from this investigation, as $(CH_2Cl)_2$ had previously been shown to be the most suitable solvent choice for the ester derivatives.[181] After 72 hours a sample was taken and analysed using ^{1}H NMR spectroscopy to determine conversion. The polymerisation was then quenched using ethyl vinyl ether and the resulting polymer analysed by SEC, the results of this optimisation are summarised in Table 4.2.

The polymerisation was first performed using identical conditions to those previously reported for the esters.[194] All three commercial Grubbs catalysts (**G1**, **G2** and **G3**) were investigated, with the polymerisation performed at room temperature using 1 mol% of catalyst at a 0.1 M concentration (Entries 1, 9 and 11). Neither Grubbs 1 or 3 were able to facilitate the polymerisation under these conditions, with 0% conversion to the desired polymer **4.42g** observed. Grubbs 2nd Generation **G2** catalyst however produced the target polymer **4.42g** in a moderate 37% conversion. This was further enhanced by performing the polymerisation at elevated temperatures, with 82% of the monomer **4.39g** converted at 30 °C and 91% of monomer **4.39g** converted at 40 °C (Entries 2 and 3). Diminishing returns were observed when the temperature was elevated much beyond 50 °C, with 93% conversion of monomer observed for both 50 °C and 60 °C (Entries 4 and 5). Conversely, reducing the temperature down to 0 °C completely suppressed polymerisation, with 0% conversion observed (Entry 6). In all cases the molecular weight of the polymer **4.42g** increased with increasing conversion, as would be expected. Additionally, the elevated temperature appears to have no detrimental effect on the dispersities of the polymers obtained (Đ <1.1), which is suggestive of a well-controlled chain growth polymerisation process, where the rate of initiation is fast relative to propagation for all temperatures in this range, and where no significant side reactions exist. The temperature dependence of the polymerisation of monomer **4.42g** is also consistent with the dissociative loss of tricyclohexylphosphine ligand (PCy_3) from **G2**, which is known to be the rate determining step of metathesis initiation for this catalyst. This will be an endothermic process and hence will be facilitated at elevated temperatures.[213]

Table 4.2: Reaction optimisation for the ROMP of dibenzyl amide **4.39g**.[a]

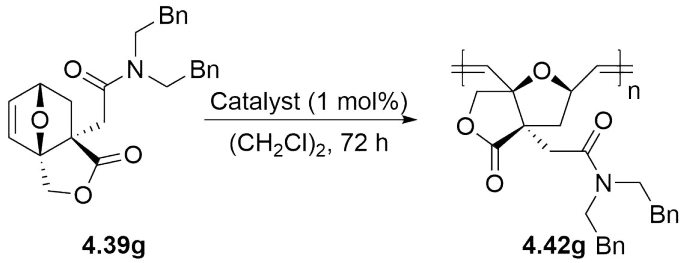

4.39g **4.42g**

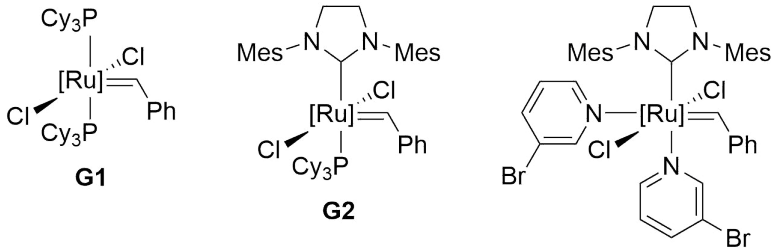

G1 **G2** **G3**

Entry	Catalyst	Temp (°C)	[4.39g] (M)	Conv. (%)[b]	Mn[c]	Mw[c]	Đ[d]
1	G2	rt	0.10	37	16,095	17,019	1.06
2	G2	30	0.10	82	18,513	19,118	1.03
3	G2	40	0.10	91	20,371	21,352	1.05
4	G2	50	0.10	93	23,520	25,083	1.07
5	G2	60	0.10	93	21,962	23,501	1.07
6	G2	0	0.10	0	-	-	-
7	G2	40	0.05	79	17,845	18,993	1.06
8	G2	40	0.20	91	16,934	17,714	1.06
9	G1	rt	0.10	0	-	-	-
10	G1	40	0.10	0	-	-	-
11	G3	rt	0.10	0	-	-	-
12	G3	40	0.10	0	-	-	-

[a] All polymerisations were carried out using a **4.39g**:catalyst ratio of 100:1.[b] Conversion was determined by ^{1}H NMR spectroscopy.[c] Determined by SEC in THF at 23 °C and calibrated relative to polystyrene standards.[d] Đ = M_w/M_n.

The influence of the catalyst concentration was then investigated for polymerisations performed at the optimal temperature of 40 °C. Halving the concentration to 0.05 M resulted in a slight decrease in monomer conversion over 72 hours to 79% (Entry 7), but doubling the concentration to 0.2 M did not appear to increase the conversion (Entry 8). Finally, for completeness, the use of **G1** and **G3** catalyst were revisited at elevated temperatures, which again failed to convert the monomer **4.39g** to the corresponding polymer **4.42g**, with 0% conversion observed in both cases (Entries

10 and 11). Optimal conditions were therefore deemed to be 1 mol% **G2** catalyst at 40 °C in $(CH_2Cl)_2$ at a concentration of 0.1 M, which would be used for the homopolymerisation of monomers **4.39a-k**.

Prior to screening these conditions against the remaining tertiary amide monomers **4.39a-k** the homopolymerisation of dibenzyl amide **4.39g** was repeated under the optimal polymerisation conditions for a range of **4.39g**:**G2** ratios. Values from 20:1 up to 100:1 were investigated, the results of which are summarised in Table 4.3. In each case the polymer **4.42g** was obtained with high molecular weight and narrow dispersity (Figure 4.5). A plot of monomer:catalyst ratio against number averaged molecular weight indicates an excellent linear correlation between the two values (Figure 4.6). This is important as it is indicative of the polymerisation being a well controlled chain-growth polymerisation under the previously optimised conditions.

Table 4.3: Molecular weight data for homopolymers **4.42g** for various **4.39g**:catalyst ratios.

Entry	**4.39g:Catalyst**	**Mn**[a]	**Mw**[a]	**Đ**[b]
1	20:1	8,372	8,885	1.06
2	40:1	14,107	14,882	1.05
3	60:1	18,437	19,634	1.06
4	80:1	23,078	25,092	1.09
5	100:1	26,150	28,887	1.10

[a] Determined by SEC in THF at 23 °C and calibrated relative to polystyrene standards.[b] $Đ = M_w/M_n$.

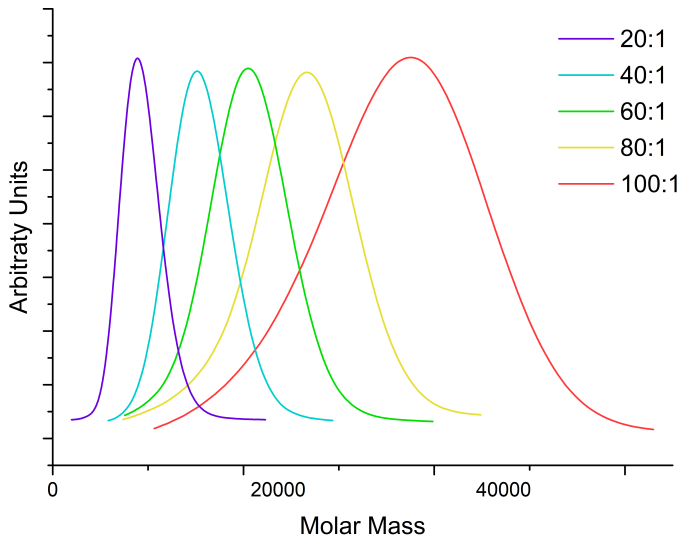

Figure 4.5: SEC of homopolymer **4.42g** prepared using various **4.39g**:**G2** ratios.

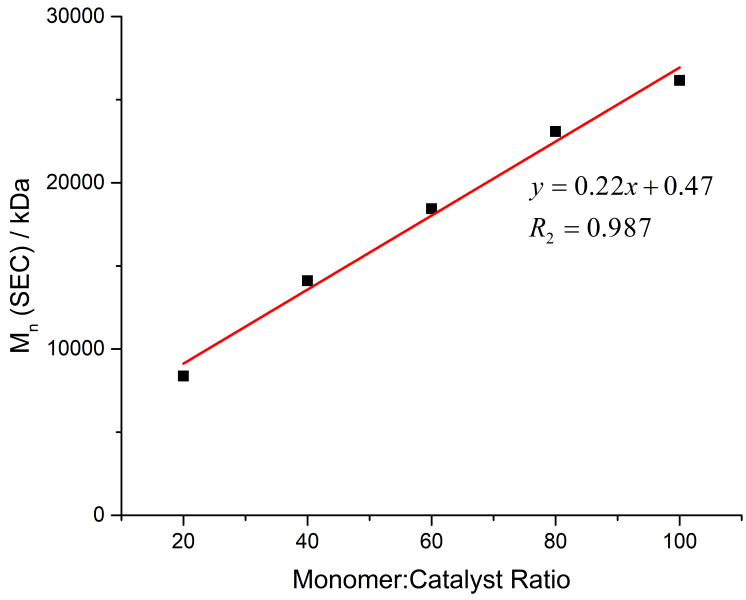

Figure 4.6: Plot of M_n against **4.39g**:**G2** ratio for homopolymer **4.42g**.

4.2.3 Homopolymersation of monomers 4.39a-k

Having demonstrated through the polymerisation of monomer **4.39g** to polymer **4.42g** that this investigation into amide derivatives of acid **4.7** was indeed feasible, and that the polymerisation occurs in well controlled manner, a range of homopolymers **4.42a-k** were then prepared from amides **4.39a-k** (Table 4.4). Generally, the polymers were obtained with good molecular weights and narrow dispersities. Starting with the polymers derived from petrochemical amines **4.39a-g**, polymers **4.42a** and **4.42b** could not be analysed by SEC as they were insoluble in THF (Entries 1 and 2). These polymers are derived from monomers with the shortest alkyl chains, suggesting that a minimum number of carbon atoms are necessary for the polymers to be soluble in organic solvents, an observation that is consistent with the previously reported esters.[194] Soluble polymers with molecular weights close to the expected values and narrow dispersities were obtained for the homopolymers **4.42c** and **4.42d** from the propyl and butyl amides **4.39c** and **4.39d**. In each case conversions over 72 hours were found to be good to excellent with values of between 78-93% observed. However, monomers **4.42e** and **4.42f** which contain much longer alkyl chains appear to inhibit the polymerisation, with conversions found to drop to 52% and 49% respectively (Entries 5 and 6). This produced polymers with molecular weights much lower than would have been predicted, but polymers **4.42e** and **4.42f** were still obtained with narrow dispersities. This effect seems to only be observed for the larger aliphatic monomers, as monomer **4.42g** which contains two large benzyl

groups underwent ROMP without any difficulty (Entry 7).

Having shown symmetrical tertiary amides **4.39a-g** derived from petrochemically sourced secondary amines **4.38a-g** all underwent ROMP, the use of monomers derived from amino acids and peptides were subsequently investigated **4.39h-k**. Initially, this looked at the (*S*)-proline methyl ester, formed through the reaction of acid **4.7** with (*S*)-proline methyl ester hydrochloride, which produced the target amide **4.39h** in a 1:1 mixture of diastereoisomers. This is due to a lack of facial selectivity during the Diels-Alder addition step in the formation of acid framework **4.7**, meaning it is formed as a mixture of enantiomers. Whilst monomer **4.39h** did undergo ROMP to form the corresponding polymer **4.42h**, which was found to be insoluble in THF, it was decided that the remaining monomers **4.39i-k** would be limited to achiral amino acid derivatives to simplify characterisation. The monomer **4.39i** derived from sarcosine (*N*-methylglycine) benzyl ester was therefore prepared. Monomer **4.39i** was then cleanly converted to the corresponding polymer **4.42i**, with 87% conversion observed over 72 hours and the polymer obtained with good molecular weight and narrow dispersity (Entry 9). Thus, it has been shown that the use of amino acid derivatives of acid **4.7** in ROMP is indeed feasible, representing a class of monomers that can be more convincingly regarded as 100% bio-based.

This study was then extended to monomers derived from peptides **4.39j** and **4.39k**, again using achiral amino acids to prevent diastereoisomer formation and simplify monomer characterisation. The two peptidic monomers only differ in either having a hydrogen (**4.39j**) or methyl (**4.39k**) group off the nitrogen of the second amide bond. The reason for this, as will be discussed in greater detail in Chapter 5, is due to the incompatibility of secondary amide derivatives of acid **4.7** in ROMP. In this case, both monomers were found to undergo ROMP, but produced polymers **4.42j** and **4.42k** that were found to be insoluble in THF, so molecular weight and dispersity data could not be determined (Entries 10 and 11). Additionally, in the case of polymer **4.42j** conversion could not be easily determined by ^{1}H NMR spectroscopy as the polymer was found to precipitate from the reaction over the course of 72 hours. These results do however suggest that peptides are indeed tolerated and that the presence of a secondary amide appears to not be a major issue when suitably far from the ROMP active site. This means that the preparation of functional materials or therapeutic agents from the ROMP of peptidic oxanorbornene derivatives could indeed be a viable avenue for future investigation.

Table 4.4: Molecular weight and thermal analysis data for homopolymers **4.42a-k**.[a]

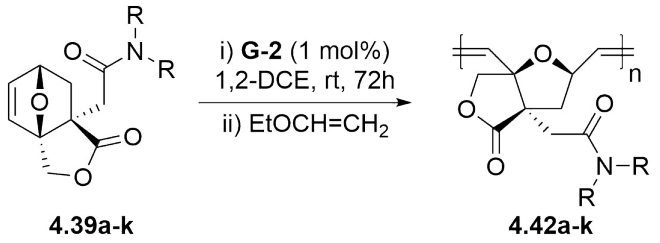

4.39a-k **4.42a-k**

4.39, 4.42: **a** R=Me; **b** R=Et; **c** R=Pr; **d** R=Bu; **e** R=Oct; **f** R=bis(2-ethylhexyl); **g** R=Bn **h** R=(S)-Pro-OMe; **i** R=Sar-OBn; **j** R=Sar-Gly-OBn; **k** Sar-Sar-OBn

Entry	Polymer	Conv. (%)[b]	Mn[c]	Mn[c]	Đ[d]	T_g (°C)	$T_{10\%}$ (°C)
1	4.42a[e]	93	-	-	-	115.0	344.7
2	4.42b[e]	90	-	-	-	145.8	348.5
3	4.42c	78	25,680	28,100	1.09	203.3	350.4
4	4.42d	82	25,030	26,835	1.07	139.0	360.8
5	4.42e	52	23,253	23,662	1.02	136.9	269.2
6	4.42f[e]	49	10,941	12,115	1.11	171.0	321.3
7	4.42g	91	20,127	20,985	1.04	130.1	351.8
8	4.42h[f]	87	-	-	-	149.4	332.4
9	4.42i	87	18,274	19,930	1.09	-	326.9
10	4.42j[f]	-[g]	-	-	-	155.0	305.8
11	4.42k[f]	62	-	-	-	-	314.5

[a] All polymerisations were carried out in 1,2-dichloroethane at 40 °C for 72 hours using catalyst **G2** and a **4.39a-k** ratio of 100:1.[b] Conversion was determined by ^{1}H NMR spectroscopy.[c] Determined by SEC in THF at 23 °C and calibrated relative to polystyrene standards.[d] Đ = M_w/M_n.[e] Amine **4.38f** was used as a mixture of racemic and meso-stereoisomers.[f] polymer was insoluble in THF.[g] Conversion could not be determined as polymer precipitated out of solution over 72 hours.

Having prepared a diverse range of homopolymers **4.42a-k** the thermal properties were duly investigated using TGA and DSC analysis, the results of which are summarised in Table 4.4. The polymers were found to be amorphous, as no melting (T_m) or crystallisation (T_{cryst}) transitions were observed in any case, but showed fairly high glass transition temperatures (T_g) ranging from 115-203 °C. The majority of polymers also displayed very high decomposition temperatures, with temperatures of 10% mass loss ($T_{10\%}$) typically observed between 305-361 °C (Figure 4.7). The only exception was polymer **4.42e** derived from octylamine which had a significantly lower decomposition temperature of 269 °C. Unusual decomposition profiles were also observed for polymers **4.42i** and **4.42j** which produced a step-wise weight loss, losing 10-15% of the sample mass at 100-150 °C, before a second weight loss occurs above 300 °C (Figure 4.7).

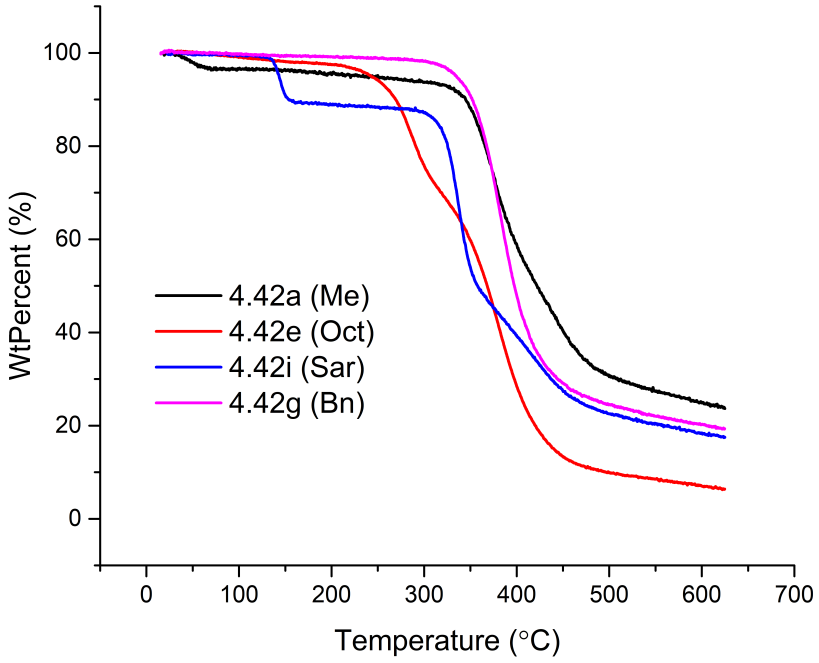

Figure 4.7: TGA traces for homopolymers **4.42a**, **e**, **g** and **i**.

The observed mass loss above 300 °C was assumed to be due to polymer decomposition as this would be consistent with thermal data for the other homopolymers. In order the better understand this unusual decomposition profile the mass loss occurring between 100-150 °C was duly investigated. It was first hypothesised that this could be due to either loss of the benzyl ester or decarboxylation. However, when the a sample was heated to 150 °C for 10 minutes and then analysed by ^{1}H NMR spectroscopy no obvious structural changes were observed. The mass loss was therefore investigated using TGA-FTIR (Figure 4.8). It can clearly be seen that a mass loss of approximately 10% is observed when the sample is heated to just below 150 °C. However, the IR data obtained at this temperature suggests that the mass loss only corresponds to the loss of aliphatic hydrocarbons. This data is consistent with the loss hexane, which was encapsulated during precipitation. This is a rather unusual phenomenon, but it has also previously been reported by Biagini *et al.*, who observed that hexane and other aliphatic hydrocarbons could be bound exclusively by glycine ester functionalised poly(*exo*)-norbornenes.[199]

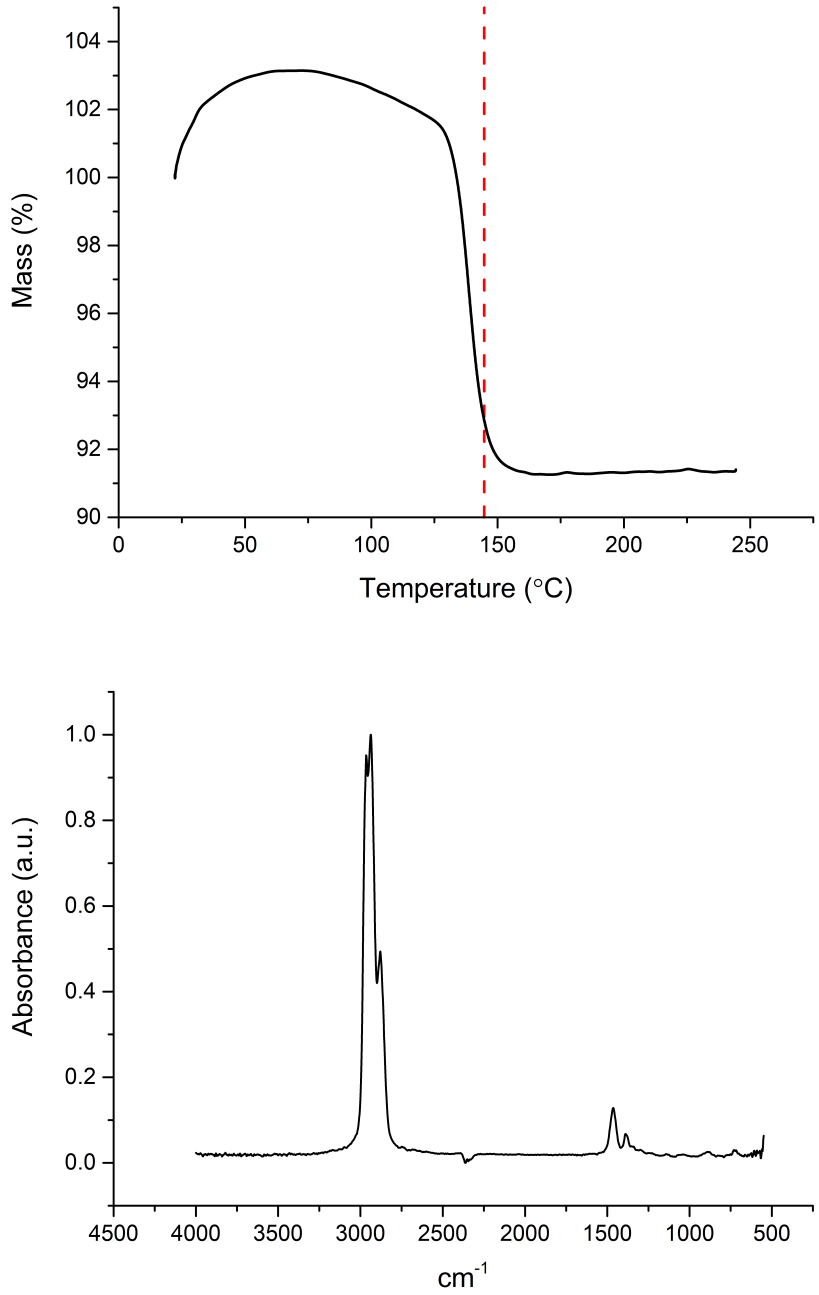

Figure 4.8: TGA analysis (top) of the unexpected mass loss region for the sarcosine homopolymer **4.42i** with FT-IR analysis (bottom) of released gases at the temperature indicated by the dotted line.

Overall, this investigation has so far shown that tertiary amide derivatives of acid **4.7** are amenable to ROMP. They do however require slightly elevated temperatures in comparison to the previously reported ester derivatives, with the use of **G2** catalyst (1 mol%, 0.1 M) at 40 °C in $(CH_2Cl)_2$ found to be optimal.[194] Under these conditions the polymerisation was shown to be a well-controlled chain growth polymerisation for a range of homopolymers, including amino acid and peptide derivatives. Generally, the polymers are obtained with good molecular weights (M_n = 10,941-25,680) and

narrow dispersities (Đ = 1.02-1.09). Thermal analysis has shown the polymers obtained are amorphous and typically display high decomposition temperatures (>300 °C) and glass transition temperatures ranging from 115-203 °C.

4.2.4 Random Copolymers of Monomers 4.39a-k

Having prepared and analysed a range of homopolymers **4.42a-k** from monomers **4.39a-k** a series of random copolymers were investigated. This primarily focused on the monomers **4.39a**, **4.39b** and **4.39h** which had previously produced insoluble homopolymers (Table 4.4). Copolymers **4.43a-d** were all prepared using a 50:50:1 ratio of the two monomers to **G2** catalyst, under the previously determined optimal conditions. The properties of these polymers could then be compared to the homopolymers **4.42a-k** prepared using a 100:1 monomer to catalyst ratio (Table 4.4). Generally, high conversion (>80%) of monomers **4.39** to copolymer **4.43a-d** was observed in all cases over 72 hours (Table 4.5). Polymer **4.43a** was derived from monomers **4.39c** and **4.39i** both of which had given soluble homopolymers previously and not surprisingly gave a soluble copolymer (Entry 1). The other three random copolymers **4.43b-d** were derived from one monomer that produced an insoluble homopolymer and one monomer that had produced a soluble homopolymer. Two of these combinations **4.43b** and **4.43c** were found to give soluble copolymers (Entries 2 and 3), but the third produced a polymer **4.43d** that was insoluble in THF (Entry 4). All the random copolymers that were soluble in THF were found to posses good molecular weights (M_n = 10,763-25,060) and narrow dispersities (Đ = 1.06-1.11) (Figure 4.9).

Thermal analysis of the random copolymers **4.43a-d** also indicated that they possessed very similar properties to the homopolymers **4.42a-k**. T_g values were only determined for polymers **4.43b** and **4.43c**, but were fairly high at 157 and 155 °C respectively (Table 4.5). Thermal decomposition temperatures ($T_{10\%}$) were also found to be fairly similar to the homopolymers **4.42a-k**, in the range 307-355 °C. Additionally, random copolymer **4.43a**, which included the sarcosine benzyl ester monomer **4.43i**, exhibited behaviour consistent with hexane encapsulation previously observed for homopolymers **4.42i** and **4.42j**. The reason for random copolymer **4.43d** not displaying this behaviour is not currently understood.

Table 4.5: Molecular weight and thermal analysis data for random copolymers **4.43a-d**.

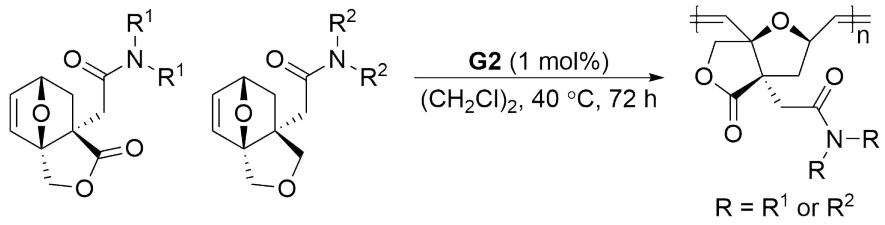

4.39a-d **4.39g-i** **4.43a-d**

Polymer (Monomers)	Conv. (%)[a]	Mn[b]	Mw[b]	Đ[c]	T_g (°C)	T10% (°C)
4.43a (4.39c:4.39i)	80	10,763	11,973	1.11	-	319.2
4.43b (4.39b:4.39g)	89	25,060	27,513	1.10	156.9	354.8
4.43c (4.39d:4.39h)	89	12,166	12,856	1.06	155.3	306.5
4.43d (4.39a:4.39i)[d]	95	-	-	-	-	318.8

Polymerisations were carried out in 1,2-dichloroethane at 40 °C for 72 hours using catalyst **G2** and a monomer:catalyst ratio of (50:50:1).[a] Conversion was determined by ^{1}H NMR spectroscopy.[b] Determined by SEC in THF at 23 °C and calibrated relative to polystyrene standards.[c] Đ = M_w/M_n.[d] Polymer was insoluble in THF.

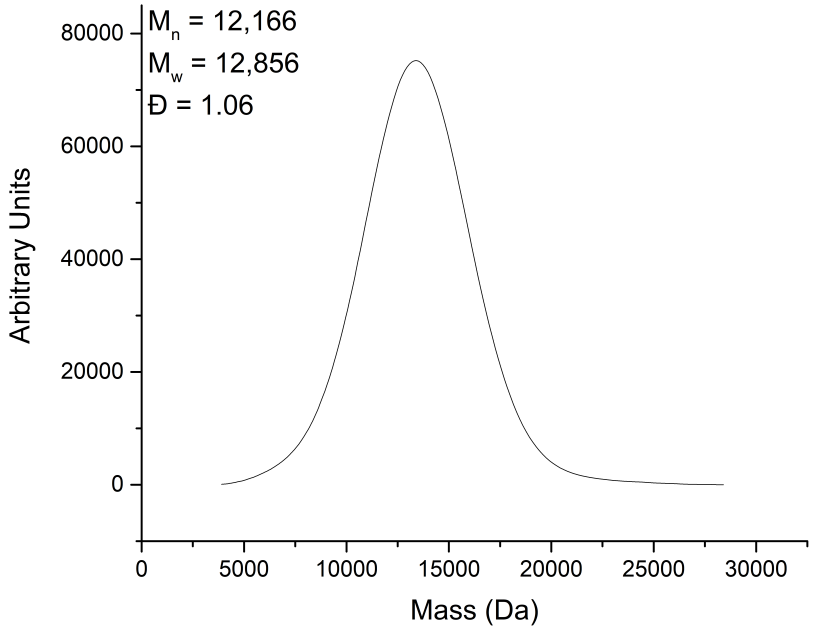

Figure 4.9: SEC trace for the copolymer **4.43c** formed from 50:50:1 mixture of monomers **4.39d** and **4.39h** and **G2** catalyst.

4.2.5 Block Copolymer Synthesis

Having prepared a series of homopolymers **4.42a-k** and random copolymers **4.43a-d** from monomers **4.39a-k** the final challenge was to prepare a block copolymer using tertiary amides. It was therefore decided that the synthesis of a block copolymer from the benzyl **4.39g** and ethyl **4.39b** monomers would be attempted using a

50:50:1 monomer to catalyst ratio, as this had previously produced a soluble random copolymer (Scheme 4.20). This however proved to be more challenging than initially expected. Growth of the first benzyl block **4.44g** proceeded smoothly, with SEC and ^{1}H NMR analysis indicating the polymer was formed with a high molecular weight and narrow dispersity. However, analysis of the resultant polymer 24 hours after the addition of the ethyl monomer **4.39b** produced a bimodal SEC trace. This is suggestive of the death of polymer chain ends prior to the addition of the second monomer, an issue that was also observed for the analogous ester monomers reported previously.[194]

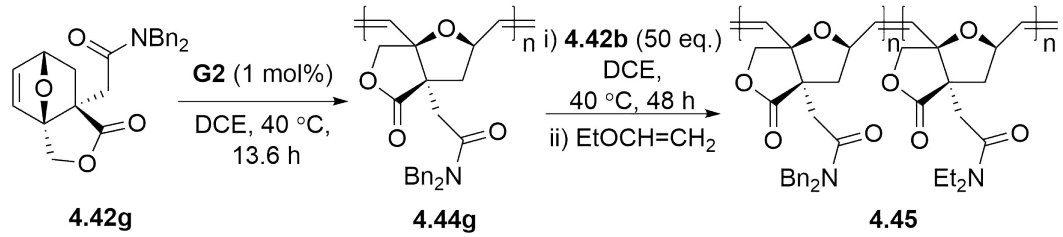

Scheme 4.20: Block copolymerisation of monomers **4.39g** and **4.39b** to produce block copolymer **4.45**.

This issue was previously overcome through judicious addition of the second monomer, which was achieved by monitoring the polymerisation of the first monomer and adding the second monomer slightly prior to complete consumption of the first. The homopolymerisation of monomer **4.39g** was therefore monitored using ^{1}H NMR spectroscopy to allow a more accurate determination of the polymer end-point. Using this data, it was determined that 50 equivalents of monomer **4.39g** were 90% consumed after 19 hours. Addition of the second monomer after 19 hours however again produced a bimodal SEC distribution. Eventually it was determined that a well controlled block copolymer could be grown when the ethyl monomer **4.39b** was added after 80% conversion or 13.6 hours. The SEC traces obtained (Figure 4.10) show that after 24 hours a polymer is obtained with good molecular weight (M_n = 10,020) and narrow dispersity (Đ = 1.06). The second block is then grown in over the next 48 hours after the second monomer is added, with a clear increase in molecular weight (M_n = 15,561) observed and the narrow dispersity (Đ = 1.05) maintained, indicating that there are no issues of dead chain ends provided the second monomer is added after 80% conversion of the first monomer.

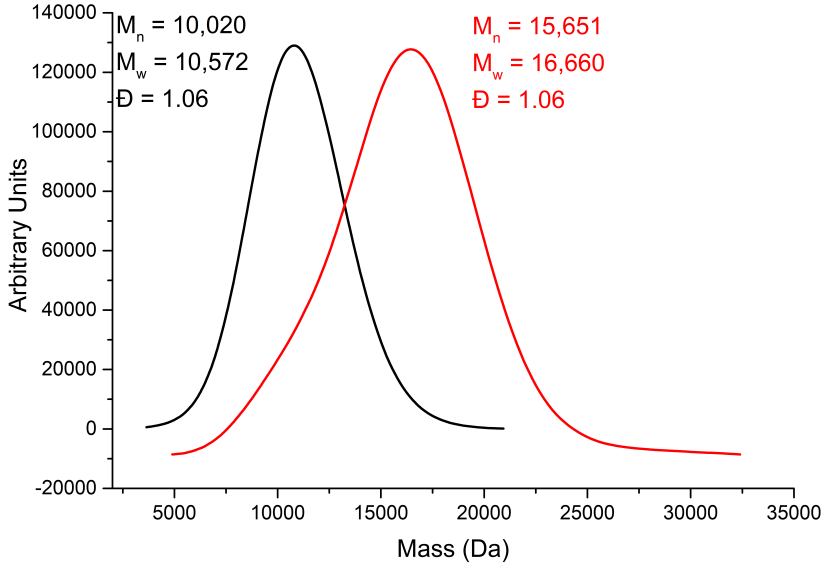

Figure 4.10: SEC trace for the block copolymer **4.45** formed from 50:50:1 **4.39g**:**4.39b**:**G2**. Black: 13.6 hours after addition of monomer **4.39g**. Red: 48 hours after addition of monomer **4.39b**.

4.2.6 Kinetics of Homopolymerisation

Monitoring the reaction profile by ^{1}H NMR spectroscopy for the synthesis of the block copolymer also made it possible to determine kinetic information for the homopolymerisation of tertiary amides. The decrease in concentration of the dibenzyl monomer **4.39g** against time was found to fit first order kinetics at 40 °C in deuterated $(CH_2Cl)_2$. An observed rate constant (K_{obs}) of 2.1×10^{-3} s^{-1} was then determined by plotting the natural logarithm of concentration against time (Figure 4.11). In an effort to understand whether the amide side chain has a significant influence of the reaction kinetics the study was extended to the homopolymerisation of monomers **4.39a**, **d**, **e** and **i**. Monomer **4.39a**, derived from dimethyl amine, was found to have the highest observed rate constant of 2.3×10^{-3} s^{-1}, whilst monomer **4.39e**, derived from dioctylamine, was found to the have the lowest observed rate constant of 3.1×10^{-4} s^{-1}. The relatively small difference in between these rate constants suggests that the amide substituent incorporated onto the acid framework **4.7** does not have a large influence on the observed rate of polymerisation. This relatively small difference in rate would also confirm that the aforementioned random copolymers posses a truly random distribution, rather than producing discrete blocks or tapered blocks within the polymer.

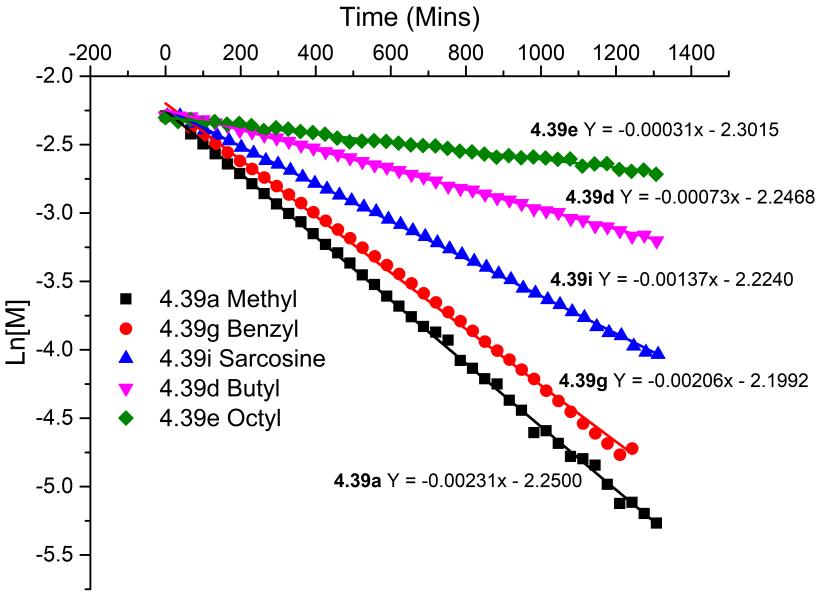

Figure 4.11: First order kinetic plots for the determination of K_{obs} for monomer **4.39a**, **d**, **e**, **g** and **i**.

4.3 Conclusions

In conclusion, the fortuitous discovery of the oxanorbornene-lactone **4.39**, formed *via* the 100% atom economical reaction between itaconic anhydride **4.1** and furfuryl alcohol **4.2**, presents an interesting molecular framework for the synthesis of novel bio-based polymers. Bai *et al.* had previously shown that ROMP of **4.7**, protected as the ester, produced a range of wholly bio-based polymers.[181,194] These polymers were found to form in a well controlled manner, possessing high molecular weights and narrow dispersities, with thermal analysis showing that they generally displayed high glass transition and thermal decomposition temperatures.

The work reported herein has therefore built upon the previous reports from Bai *et al.*, investigating the analogous amide derivatives. ROMP of these amides was shown to proceed in a well-controlled manner, producing a range of homo- and random co-polymers with high molecular weights (M_n = 10,763-28,100) and narrow dispersities (Đ = 1.02-1.11). Thermal analysis showed that the polymers were amorphous with T_g values in the range of 115-203 °C and thermal decomposition temperatures typically above 300 °C. A block copolymer could also be prepared by monitoring the progress of the growth of the first polymer block to ensure that the second monomer was added before death of living chain ends became significant. Monitoring the homopolymerisation also provided kinetic data on the rate of polymerisation of the monomers, showing the pendant side chain had little impact.

Chapter 5

Investigation into the Synthesis and Application of an Unusual Spirocyclic Imide Species

5.1 Introduction

In the previous chapter (Chapter 4), functionalisation of the oxanorbornene-lactone acid framework with primary amines to produce secondary amides was briefly investigated. However, rather unexpectedly, the use of butyl amine resulted in a mixture of products. These were eventually identified, using a combination of ^{1}H NMR and FT-IR spectroscopy, as the secondary amide **5.1** and the spirocyclic oxanorbornene-imide **5.2**. The use of X-ray crystallography also unequivocally confirmed these structures (Figure 5.1). The unusual spirocyclic nature of oxanorbornene-imide **5.2** is what has prompted further investigation into this transformation, which will form the basis of this chapter.

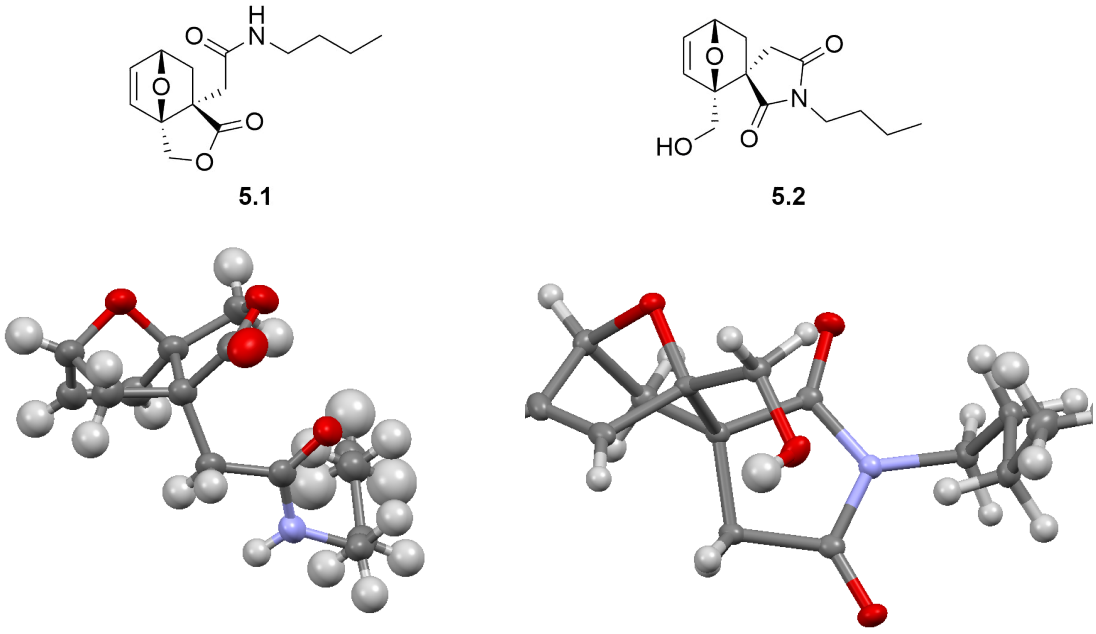

Figure 5.1: Ellipsoid representation of the crystal structures of secondary amide **5.1** and spirocyclic imide **5.2** species.

Spirocyclic compounds are molecules that contain two ring systems fused at a single atom. It is a motif that is widely found in natural products, but has only recently began to attract interest in the development of pharmaceutically relevant molecules. This is in part due to the inherent three-dimensionality of spirocyclic scaffolds and their structural novelty.[214] Furthermore, cyclic imides are known to be an important class of organic compounds, widely utilised in synthetic, medicinal, biological and polymer chemistry.[215] A molecular framework based around a spirocyclic oxanorbornene-imide, such as **5.2**, hence presents a highly novel and potentially valuable structure, that may have a multitude of applications. This chapter will therefore deal with better understanding the conditions under which oxanorbornene-imide **5.2** forms, along with exploring possible applications of

this molecular framework. Since the focus of the previous chapters was on polymer and therapeutic applications, this chapter will once again concentrate on these areas.

5.1.1 Applications of Oxanorbornene-Imides

An investigation into potential applications of oxanorbornene-imides would however prove to be more of a challenge than was first anticipated, as analysis of the literature quickly revealed no evidence for the spirocyclic oxanorbornene-imide **5.2** having ever been reported before. In fact, extending the search to structurally similar compounds produced only a single result, which was that of the isomeric anhydrides **5.5**-**5.8** reported by Pehere *et al.*, in their initial report of the synthesis of oxanorbornene-lactone **5.10** (Figure 5.2).[183] Since these compounds were not isolated, they have not been applied to any relevant applications to date. The lack of reports within the literature for spirocyclic oxanorbornene-imides was rather intriguing, suggesting that these compounds are more unique than initially thought. The search parameters were therefore widened significantly.

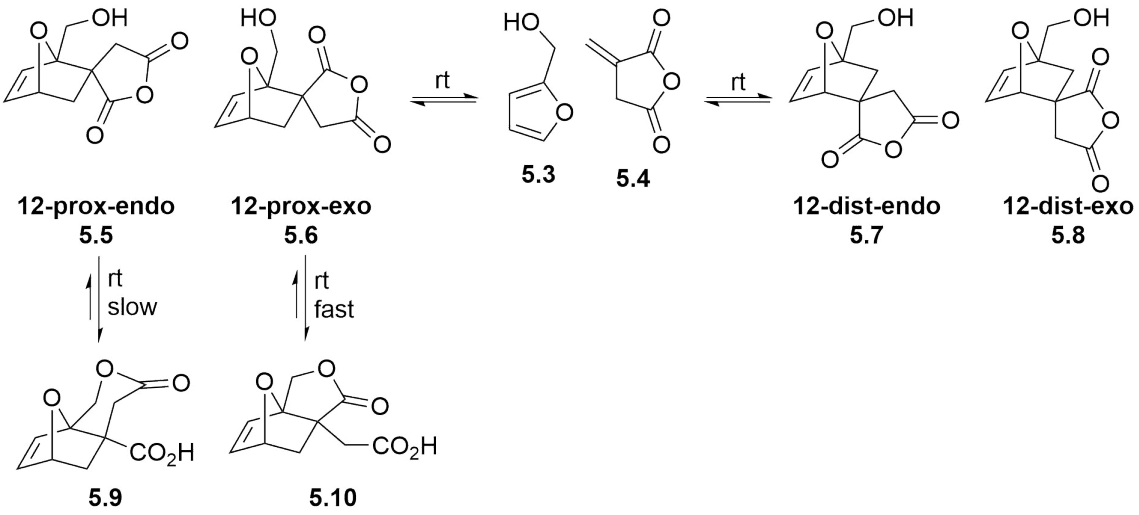

Figure 5.2: Proposed mechanism for the synthesis of oxanorbornene-lactone **5.10** *via* the Diels-Alder-lactonisation of furfuryl alcohol **5.3** and itaconic anhydride **5.4**.

It was eventually realised that spirocyclic oxanorbornene-imide **5.2** was strikingly similar to the norbornene-2,3-dicarboximide framework **5.11** (Figure 5.3). The latter only differs in the cyclic imide being attached at the 2,3-position, rather than only at the 3-position, and the lack of an oxygen atom at the 7-position or norbornene bridgehead. In comparison, this structure and associated derivatives have been widely explored for polymer chemistry, particularly ROMP. This was previously discussed in detail within Chapter 4, in the various reports by Gibson, North and co-workers on the ROMP of *N*-amino acid and peptide functionalised norbornene-2,3-dicarboximides.[198] Additionally, numerous reports exist reviewing the use of

simpler norbornene-2,3-dicarboximide derivatives for ROMP, this will therefore not be covered in in any further detail.[216,217] Instead, the remainder of this literature review will cover the use of similar structures to spirocyclic oxanorbornene-imide **5.2** in therapeutic applications.

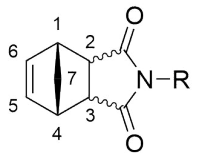

5.11

Figure 5.3: General structure of norbornene-2,3-dicarboximide framework **5.11**.

In terms of therapeutic activity, the presence of a cyclic imide within spirocyclic oxanorbornene-imide **5.2** is particularly promising, as this motif has been reported numerous times within biologically active compounds and natural products **5.12**-**5.17**, a number of which are highlighted within Figure 5.4.[215] What is particularly striking is the structural similarities between the spirocyclic oxanorbornene-imide **5.2** and norcantharimide **5.17**. Both species contain a cyclic imide, attached to either a 7-oxanorbornene or 7-oxanorbornane scaffold, with the major difference being the attachment of the imide occurring at the 2,3-position in norcantharimide **5.17**, rather than exclusively at the 3-position. Norcantharimide **5.17** could therefore be considered as a reasonable comparison for rationalising the therapeutic activity of spirocyclic oxanorbornene-imide **5.2**.

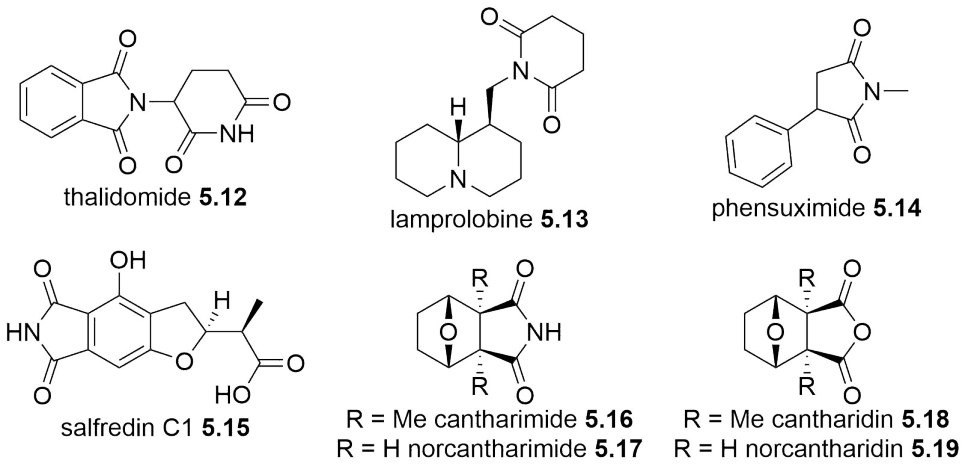

Figure 5.4: Examples of bioactive compounds containing cyclic imides.

Cantharimide **5.16** and norcantharimide **5.17** are natural products first isolated from the Meloidae and Oedemeridae families of the Chinese blister beetle.[218] The dried bodies of these beetles have been utilised within Chinese medicine for over 2000 years, as a natural remedy for a number of ailments including rabies, impotence

and fever.[219] More recently, the closely related anhydride analogue of cantharimide **5.16**, cantharidin **5.18**, was shown to be a potent anti-proliferative against a number of human cancer cell lines.[220] Synthetic analogues of cantharimide **5.16** and norcantharimide **5.17** have therefore begun to attract significant interest from chemists and pharmacologists for potential therapeutic applications.

The earliest example investigating cantharidin derivatives in such applications was reported by McCluskey *et al.* In previous reports, McClusky *et al.* had shown that cantharidin **5.18** and norcantharidin **5.19** are potent inhibitors of PP1 and PP2A, enzymes responsible for regulating cellular processes by controlling phosphorylated protein levels.[221] They therefore extended their investigation to a number of norcantharimide analogues. The study began by first producing a range of derivatives of norcantharimide **5.20**, through the dehydrative condensation of norcantharidin **5.19** with various D- or L-amino acids (Scheme 5.1).

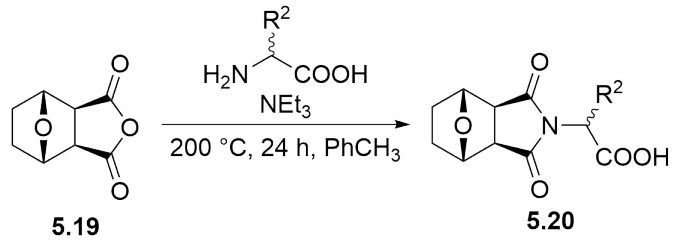

5.19 **5.20**

R^2 = D or L-Ala, Phe, Leu, Ile, Tyr, His, Trp, Glu or Met

Scheme 5.1: Synthesis of norcantharimide derivatives **5.20** through the dehydrative condensation of norcantharidin **5.19**.

These derivatives **5.20** were then screened for their ability to inhibit PP1 and PP2A. Rather interestingly, only the analogues possessing basic amino acid side chains were found to inhibit PP1 or PP2A. This was reasoned on the grounds of a modelling study which suggested there was an "acidic groove" within the vicinity of the active site, enhancing the binding of analogues possessing basic side chains.[221] This was found to be best when a histidine side-chain was present, which was shown to be equipotent to cantharidin **5.18** and superior to norcantharidin **5.19** for the inhibition of PP1 or PP2A.[222]

Further investigations from McCluskey and co-workers have subsequently shown that the ability of these analogues to inhibit PP1 or PP2A has generally correlated well with their cytotoxicity against various cancer cell lines.[223] Consequently, McCluskey and co-workers have extended their investigation to study the anti-cancer activities of a much broader range of norcantharimide analogues. Following on from their previous report, McCluskey *et al.* have synthesised a range of alkyl, allyl and

aryl derivatives of norcantharimide, again through the dehydrative cyclisation of norcantharidin **5.19**.[224] The allyl derivatives **5.21** are particularly interesting as McCluskey and co-workers demonstrated that they are amenable to further derivatisation, such as osmylation to the 1,2-diol **5.23** or epoxidation/methanolysis to the methoxy alcohol **5.22** (Scheme 5.2).

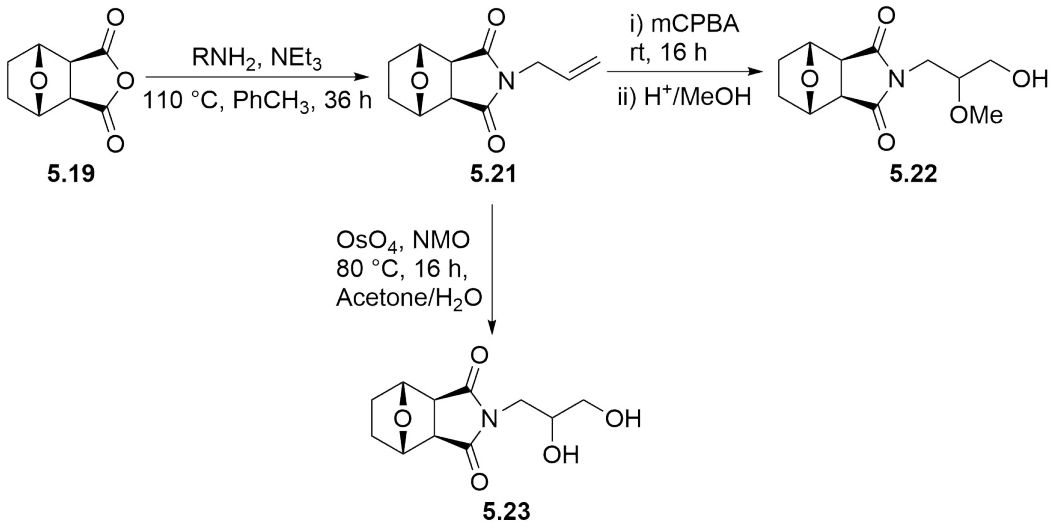

Scheme 5.2: Synthesis of allyl norcantharimide **5.21** and corresponding routes to the 1,2-diol **5.23** and methoxy alcohol **5.22** derivatives.

These norcantharimide analogues were then investigated for their cytotoxicity against nine human cancer cell lines. In general, the majority of the 32 analogues investigated were found to possess moderate to good cytotoxicity against the majority of cancer cells, with the most potent analogues found to contain either a C_{10}, C_{12} or C_{14} alkyl chain, or a 1,2-diol moiety. These results are also shown to be a marked improvement on those obtained for a control sample of norcantharidin **5.19**.[224]

In their most recent study, McCluskey and co-workers have further extended their study to norcantharimide analogues possessing terminal phosphate esters.[225] Norcantharidin **5.19** was first functionalised with a series of terminal alcohols through dehydrative cyclisation to yield the *N*-alcohol analogues **5.24** (Scheme 5.3). Rather surprisingly, the *N*-alcohol derivatives demonstrated no cytotoxicity to any of the cancer cell lines investigated, even though the previously reported 1,2-diols **5.23** had produced rather promising results.[224] Robertson *et al.* therefore decided to further derivatise these species to the corresponding phosphate esters **5.25**.[225]

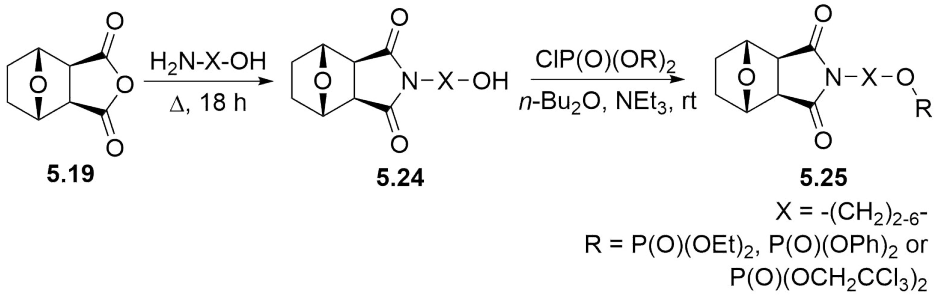

Scheme 5.3: Synthetic route to terminal phosphate ester analogues **5.25** of norcantharimide from norcantharidin **5.19**.

Biological screening of these analogues against a number of cancer cell lines revealed that the norcantharimide phosphate esters **5.25** presented a new series of functionalised norcantharimides with enhanced broad spectrum anti-proliferative activity.[225] A number of the analogues were found to be at least equipotent to norcantharidin **5.19**, whilst many others were found to be five times more potent, with the best results obtained for the diphenyl and bis-trichloroethyl phosphate esters. Robertson *et al.* suggested that the observed cytotoxicity was generally a consequence of how easily the phosphate ester was able to undergo hydrolysis. Additionally, the synthesis of a pthalimido analogue of the diphenyl ester was found to be completely void of anti-proliferative activity, demonstrating that the cytotoxicity is highly dependent on the norcantharidin framework.[225]

Building upon this observation, McCluskey and co-workers have also reported a number of investigations into the influence of the various functional groups around the norcantharidin framework on cytotoxicity (Scheme 5.4).[226] The amide acid derivative **5.26**, formed through the ring opening of norcantharidin with an amine, were found to be poor growth inhibitors for the majority of cancer cell lines investigated.[223] This was also observed when McCluskey and co-workers removed the 5,6-ethyl bridge **5.27** or further functionalised the anhydride to the hydroxy ethyl ester **5.28**.[227,228] This work therefore suggests that the 7-oxanorbornane scaffold and cyclic imide are paramount for synthetic norcantharimides to display significant cytotoxicity.

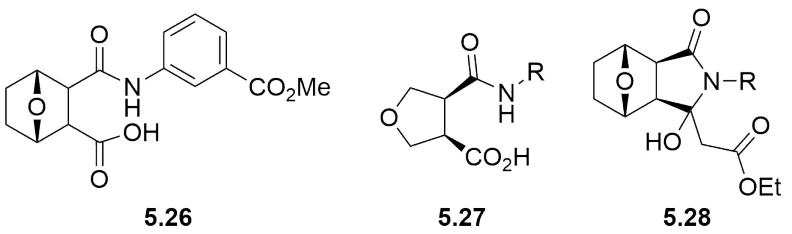

Scheme 5.4: Structural variations of the norcantharimide framework reported by McCluskey and co-workers.

An interest in the cytotoxicity of the cantharimide/norcantharimide **5.16**/**5.17** framework has also been reported by Kok *et al.*[220] In their investigation, Kok *et al.* functionalised cantharidin **5.18** with a range of 2-aminobenzothiazole derivatives **5.29** to produce the corresponding cantharimide analogues **5.30** (Scheme 5.5). 2-Aminobenzothiazole **5.29** was chosen as it has long been recognised as a therapeutically active framework for a number of applications, including antitumour agents, neurotransmission blockers and neuroprotective agents.[220] These analogues were then screened against the hepatocellular carcinoma cell line, producing a significant cytotoxic response, one that was found to be comparable to that of a cantharidin **5.18** control sample.

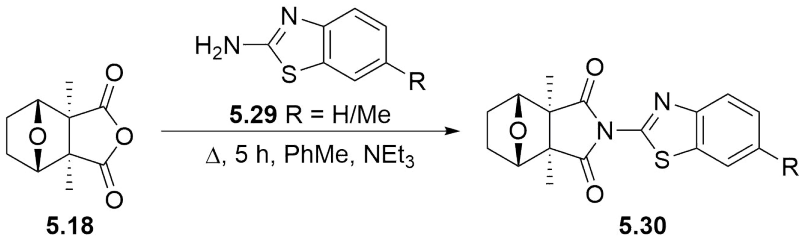

Scheme 5.5: Dehydrative condensation of cantharidin **5.18** to produce the 2-aminobenzothiazole cantharimide derivatives **5.30**.

A major issue associated with the use of cantharidin **5.18**-based therapies for cancer treatment is their lack of selectivity, which results in a number of known side-effects, including bone-marrow suppression, as well as gastrointestinal and urinary tract toxicity.[220] Kok *et al.* therefore chose to investigate the cytotoxicity of analogues **5.30** towards non-malignant bone marrow cell lines.[220] The results obtained indicate that the cantharimide derivatives **5.30** are 2- to 4- fold less active towards the benign cells than cantharidin **5.18**.[220] These analogues therefore represent a highly potent and selective anti-proliferative against hepatocellular carcinoma cell lines.

More recently, Galkin *et al.* have reported on a rather interesting route to norcantharimide derivatives from bio-derived starting materials, which is particularly interesting in the context of green chemistry and the focus of the current chapter.[229] In their report, Galkin *et al.* began by first investigating the reductive amination of 2,5-diformylfuran (DFF) **3.31**, a promising platform molecule readily obtained through the oxidation of 5-hydroxymethylfurfural (HMF), which can be directly obtained from fructose. The resulting products **5.32** then underwent a modified one-pot Diels-Alder hydrogenation reaction to yield the corresponding norcantharimide derivatives **5.33** (Scheme 5.6).[229]

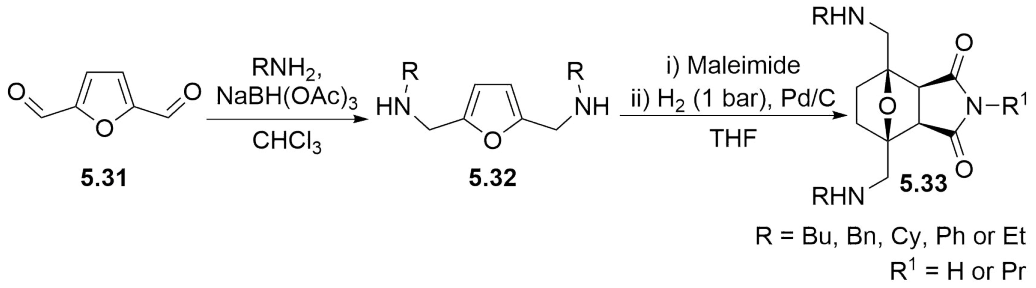

Scheme 5.6: Reductive amination of DFF **5.31** and subsequent one-pot Diels-Alder hydrogenation to yield norcantharimide analogues **5.33**.

Galkin *et al.* then went on to investigate the norcantharimide **5.33** analogues for biological activity. A cytotoxicity study of **5.33** against the human colorectal adenocarcinoma cell line was therefore carried out. Overall, norcantharimide derivatives **5.33** were found to be fairly poor, except for when a phenylaminomethyl moiety was incorporated into the bicyclic core. The cytotoxicity of this species was found to be significantly higher than that of norcantharimide **5.17**, but lower than that of norcantharidin **5.19**.[229] Therefore, this demonstrates that the Diels-Alder addition of bio-based platform molecules is a viable route to cytotoxic norcantharimide derivatives.

Finally, Spare *et al.* have reported on a series of cantharimide derivatives based around a tricyclic lactam core.[226] These are particularly worth mentioning due to their striking resemblance to the oxanorbornene-lactone scaffold **5.10**, which has formed the basis of this chapter as well as the previous one (Chapter 4). Spare *et al.* were able to synthesise highly decorated scaffolds **5.35** in good yields, with a 1:1.2 ratio of *cis*- and *trans*-diastereoisomers using a two step Ugi intramolecular Diels-Alder addition (Scheme 5.7).[226]

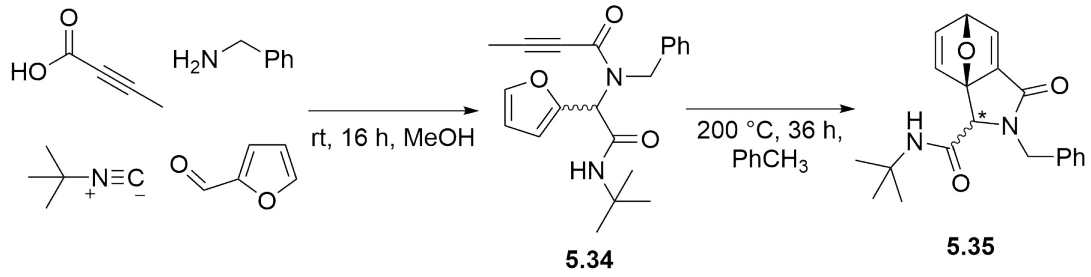

Scheme 5.7: Two step Ugi intramolecular Diels-Alder route to the tetrahydroepoxyisoindole carboxamide scaffold **5.35**.

The cytotoxicity of this framework was then investigated against a number of cancer cell lines and compared to norcantharidin **5.19** and the widely used chemotherapeutics, cisplatin and oxaliplatin. A number of the synthesised analogues

were found to possess whole-cell cytotoxicity comparable to those of the control samples.[226] More importantly, this report contradicts some of the previous work from McCluskey *et al.*, which suggested molecules possessing significant alterations of the central scaffold are devoid of cytotoxicity.[227] The report from Spare *et al.* suggested that the molecule is likely to present a degree of cytotoxicity provided the bridgehead oxygen is intact and the molecules possess a cyclic imide or lactam functionality, seemingly regardless of position.[226] This is a really promising outcome with regards to an interest in the application of spirocyclic oxanorbornene-imide **5.2** in therapeutic applications.

In summary, spirocyclic oxanorbornene-imides **5.2** represent a highly promising molecular framework for a number of potential applications. Whilst analysis of the literature highlighted that **5.2** has not previously been reported, the analogous norbornene-2,3-dicarboximides **5.11** and norcantharimide derivatives have been widely explored within polymer and medicinal chemistry respectively. The previous chapter (Chapter 4) had extensively reviewed the use of amino acid and peptide derived norbornene-2,3-dicarboximides **5.11** within ROMP and for this reason it was not expanded upon further. This chapter has therefore predominantly focussed so far on the potential of norcantharimide derivatives as therapeutics, highlighting a number of investigations regarding the use of a range of diverse norcantharimide analogues, and their associated cytotoxicity against a series of cancer cell lines. These results suggest that oxanorbornene-imide **5.2** is rather likely to possess some form of cytotoxicity, due to the presence of the oxygen bridgehead and the cyclic imide.

5.1.2 Chapter Aims

This chapter will therefore aim to produce a number of derivatives of the oxanorbornene imide **5.2** and isomeric secondary amide **5.1**. These compounds will then be investigated for use within polymer and medicinal chemistry. Firstly, this investigation will look to build on the work reported in the previous chapter (Chapter 4) looking at the use of both structures within ROMP. It will then look at the suitability of the spirocyclic oxanorbornene-imides **5.2** as potential therapeutics, with an eventual aim to investigate their cytotoxicity against a number of cancer cell lines.

5.2 Results and Discussion

It was immediately apparent that in order for an investigation into the applications of *N*-substituted secondary amides and spirocyclic oxanorbornene-imides, such as **5.1** and **5.2**, to be viable it would first be necessary to better understand the circumstances under which they form. It was hypothesised that formation of the secondary amide **5.1** occurs first, which then most likely undergoes an intramolecular rearrangement where the secondary amide ring-opens the lactone, producing the isomeric oxanorbornene-imide **5.2** (Scheme 5.8). Conventionally, cyclic imides are most commonly formed by methods such as dehydrative condensation of an anhydride with an amine at high temperatures or with the help of a Lewis acid, or the cyclisation of a carboxylic acid amide in the presence of acidic reagents.[215] The above proposal therefore presents an interesting atom-economical route to cyclic imides, which appears to have not been reported within the literature to date, although a similar intramolecular elimination has previously been reported for the analogous esters.[230]

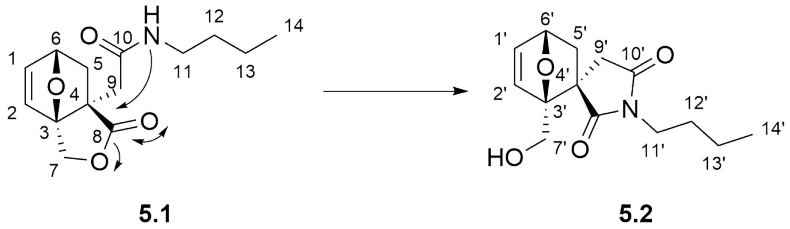

Scheme 5.8: Proposed mechanism for the conversion of butyl secondary amide **5.1** to spirocyclic butyl oxanorbornene-imide **5.2**.

If the proposed mechanism was indeed the case then the formation of imide **5.2** would be dependent on the nucleophilicity of the amide. Since amides are known to be fairly poor nucleophiles, due to conjugation of the nitrogen lone pair with the carbonyl, nucleophilicity will be dependent on a number of factors such as substituents and basicity of the reaction solution.[215] The synthesis of either **5.1** or **5.2** from oxanorbornene-lactone **5.10** was therefore revisited, using varying quantities of butylamine to see whether this would have any influence on the preference towards either **5.1** or **5.2** under otherwise identical reaction conditions (Scheme 5.9). The observed trend suggests that the imide **5.2** is formed in greater quantities as the equivalents of butyl amine are increased, with imide **5.2** not observed at all until at least 2.5 equivalents are used. This is most easily seen in the ^{1}H NMR spectrum when the protons at the 7/7' and 9/9' carbons are monitored. This is in agreement with the previous claim of a basic solution being necessary for **5.2** to form, as a minimum of 2.0 equivalents are needed to neutralise the reaction mixture, due to

1.0 equivalent acting as the nucleophile in this system, whilst another 1.0 equivalent being necessary to neutralise the HCl generated from the acyl chloride.

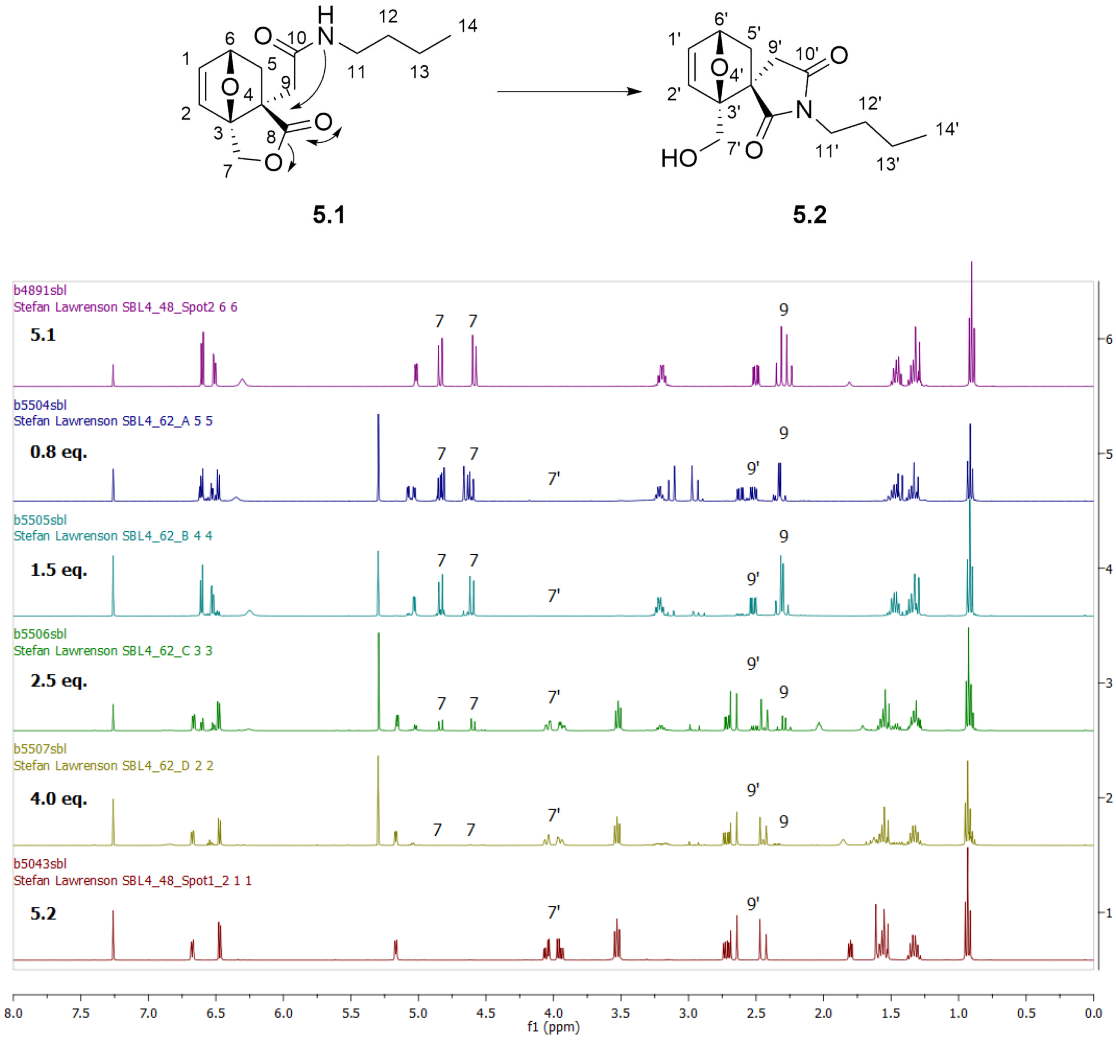

Scheme 5.9: ^{1}H NMR spectroscopy of **5.1** (Top), **5.2** (Bottom) and the crude reaction mixture for varying quantities of butylamine.

Using this information, a number of bases were screened for the formation of the amide to see if a link between basicity and preference for either **5.1** or **5.2** could be discerned. The results of this investigation did not suggest an obvious trend, but it was determined that the secondary amide could be selectivity produced through the use of a weaker base than NEt_3, such as pyridine. Again this provides even more evidence to show that formation of the imide **5.2** is reliant on strongly basic conditions. As such, a series of secondary amides could be produced by exposing the intermediate acid chloride to one equivalent of the desired amine and one equivalent of pyridine (Scheme 5.10). In this way a number of alkyl, benzyl and even amino acid containing secondary amides were produced in moderate to good (31-69%) yields.

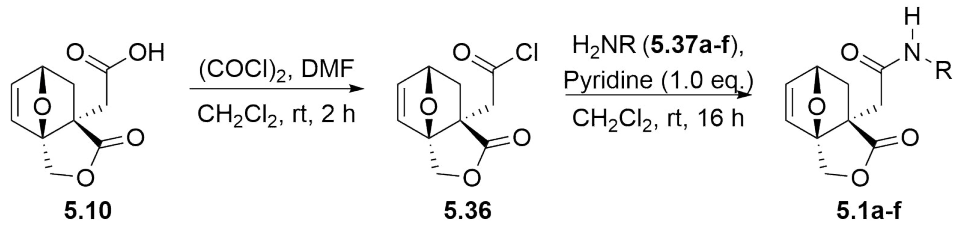

5.1, 5.37: a R = *i*Pr; **b** R = Bu; **c** R = Hex, **d** R = Oct; **e** R = Bn; **f** R = GlyOBn.

Scheme 5.10: Synthesis of a series of secondary amide monomers **5.1a-f** from oxanorbornene-lactone **5.10**.

Now that it was possible to selectively produce a number of secondary amide species **5.1a-f** in reasonable quantities, the consequence of exposing **5.1b** to an excess of NEt_3 was investigated. Monitoring the reaction mixture using ^1H NMR spectroscopy would also give an idea of whether, and how, the imide **5.2** forms over time following exposure to a stronger base (pKb: pyridine 5.21, NEt_3 11.01, *n*-butylamine 10.78) (Scheme 5.11). It was observed that following the addition of 2.0 equivalents of NEt_3, the secondary amide **5.1b** was slowly converted to the desired imide **5.2** over the course of a few hours. The relative concentration of **5.2** was then found to peak after about 8-10 hours. However, monitoring the reaction mixture over an extended period of time revealed that a third species formed in reasonable quantities. It was eventually identified that this was in fact two species, furfuryl alcohol **5.3** and 1-butyl-3-methylene-pyrrolidine-2,5-dione **5.38**, formed as a result of a retro-Diels-Alder reaction of imide **5.2**. This unfortunately suggests that imide **5.2** is not as stable as originally hoped when the alkene is still present within the norbornene and the lactone is broken. Additionally, the approach of exposing the secondary amide to a strong base like NEt_3 to form the corresponding imide was subsequently found not to be generally applicable, as the other secondary amides investigated **5.1a-f** often produced complicated mixtures of products after 8-10 hours. It was therefore decided that the application of norbornene **5.1b** and imide **5.2** would be investigated in ROMP before committing more time to investigating the factors that influence the conversion of secondary amides **5.1a-f** to imides.

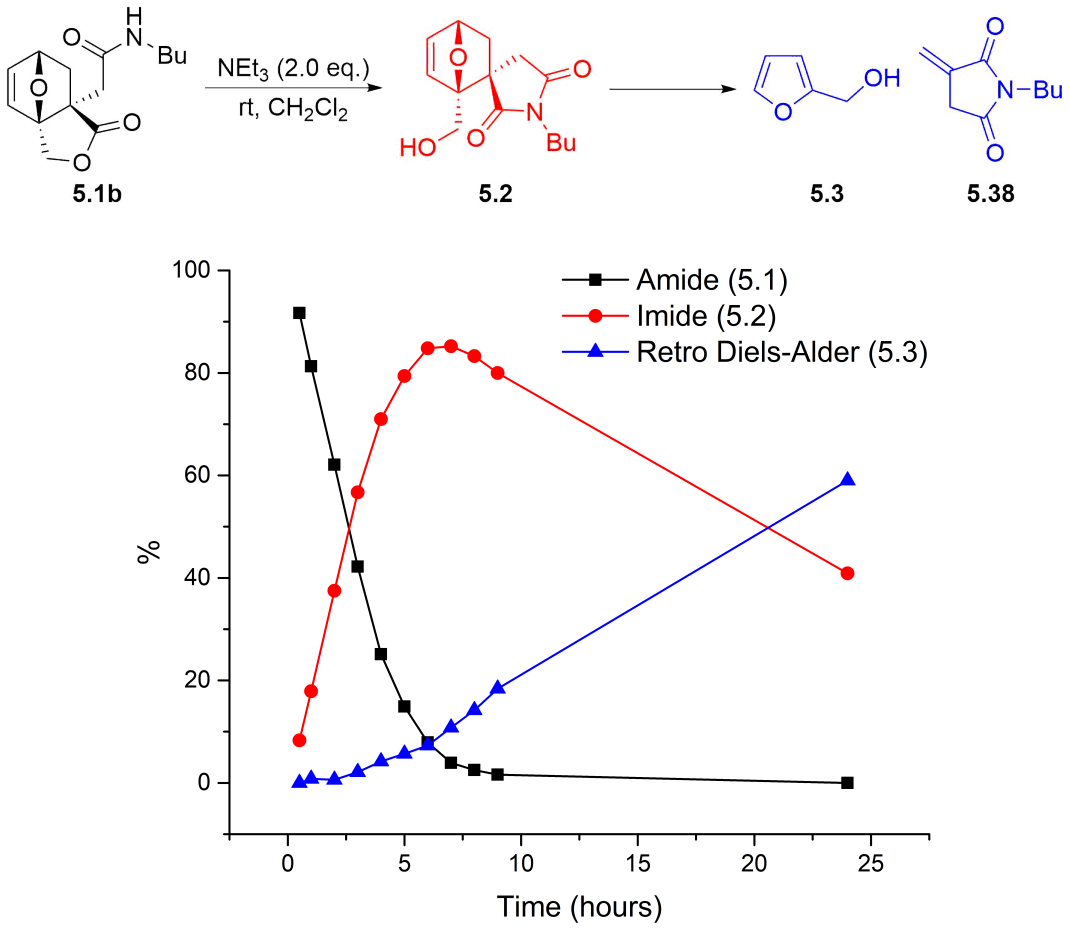

Scheme 5.11: Interconversion of butyl amide **5.1b** to butyl imide **5.2** over time and subsequent retro-Diels-Alder to furfuryl alcohol **5.3** and 1-butyl-3-methylene-pyrrolidine-2,5-dione **5.38**. Reaction was monitored using ^{1}H NMR spectroscopy.

5.2.1 Ring-Opening Metathesis Polymerisation of Secondary Amides and Spirocyclic Oxanorbornene-Imides

To begin with, the butyl secondary amide **5.1b** was screened against a range of commercial metathesis catalysts **G1**-**G3**, under similar conditions to those that were deemed optimal for the previous investigation (Chapter 4). The use of **G1** catalyst proved unsuccessful, with reactions at room and elevated temperature both failing to produce the target polymer **5.39b** (Table 5.1, Entries 1 and 2). The use of **G2** however produced a cloudy suspension when ROMP was performed at 40 °C, which is most likely due to the oligomeric material precipitating out of the reaction mixture (Entry 4). The use of alternative solvents to $(CH_2Cl)_2$ had previously yielded poor results, an alternative secondary amide monomer was therefore investigated.[181]

Table 5.1: Screening of reaction conditions for the polymerisation of secondary amides.

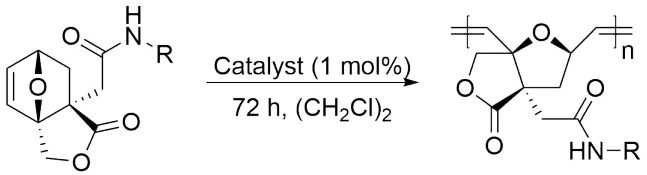

5.1a-f **5.39a-f**

Entry	R Group	Catalyst	Temp (°C)	Conv. (%)[a]	Mn	Mw	Đ[b]
1	Bu **5.1b**	G1	rt	-	-	-	-
2	Bu **5.1b**	G1	40	-	-	-	-
3	Bu **5.1b**	G2	rt	-	-	-	-
4[c]	Bu **5.1b**	G2	40	-	-	-	-
5	Oct **5.1d**	G1	rt	-	-	-	-
6	Oct **5.1d**	G1	40	-	-	-	-
7	Oct **5.1d**	G2	rt	-	-	-	-
8	Oct **5.1d**	G2	40	-	-	-	-
9	Oct **5.1d**	G3	rt	-	-	-	-
10	Oct **5.1d**	G3	40	-	-	-	-
11	Gly-OBn **5.1f**	G1	rt	-	-	-	-
12	Gly-OBn **5.1f**	G1	40	-	-	-	-
13	Gly-OBn **5.1f**	G2	rt	-	-	-	-
14	Gly-OBn **5.1f**	G2	40	-	-	-	-
15	Gly-OBn **5.1f**	G3	rt	-	-	-	-
16	Gly-OBn **5.1f**	G3	40	-	-	-	-
17[d]	Gly-OBn **5.1f**	G2	40	-	-	-	-
18[e]	Gly-OBn **5.1f**	G2	40	-	-	-	-

All polymerisations were carried out using a monomer:catalyst ratio of 100:1.[a] Conversion was determined using ^{1}H NMR spectroscopy.[b] Đ = M_w/M_n.[c] formed a gel after a short period of time.[d] 10 eq. of a 0.4 M solution of LiCl in DMF was added.[e] 10 eq. of Ti(O*i*Pr)$_4$ was added.

Subsequently, a similar catalyst screen was investigated for the octyl derivative **5.1d** (Entries 5-10). Polymerisation was attempted using each of the commercial ROMP catalysts (**G1**, **G2** and **G3**) at either room or elevated temperature. However, in all cases no evidence for the target polymer **5.39d** was observed. In the interest of completeness, the same conditions were also investigated for the glycine benzyl ester monomer **5.1f**. Again, polymerisation using the commercial ROMP catalysts at room or elevated temperature failed to produce the target polymer **5.39f** (Entries 11-16). Even attempts using the most promising conditions (**G2** at 40 °C) with

additives that are known to disrupt aggregates and promote ROMP, such as lithium chloride (LiCl) and titanium isopropoxide ($Ti(O\textit{i}Pr)_4$), failed to produce the target polymer **5.39f** (Entries 17 and 18).[231]

This failure is most likely due to the nature of the secondary amides **5.1a-f**, as any pendant side chains will lie in the *endo* orientation. This was previously shown to be much less reactive than the *exo*-counterparts in Chapter 4. Additionally, as the amide is secondary it could be imagined that the amide bond is able to coordinate to the active catalyst through the N-H bond, inhibiting catalysis, an issue that was observed for deprotected amino acids in the *endo*-orientation by Sutthasupa *et al.*[203] This is also reinforced by the observation that glycine secondary amide **5.1f** does not polymerise, but the *N*-methyl glycine derivative (Sarcosine) **4.42i** was found to polymerise in the previous chapter (Chapter 4). Based on these observations and the results presented in Table 5.1, it was deemed that the secondary amides **5.1a-f** would not likely undergo ROMP. Efforts therefore turned to the spirocyclic oxanorbornene-imide **5.2**.

Attempts to polymerise the butyl-imide **5.2** using the previously investigated catalysts at various temperatures again failed to produce the target polymer (Table 5.2, Entries 1-6). This monomer no longer contains the secondary amide functionality, but the hydroxymethyl group now off the bridgehead was anticipated to be an issue for catalyst deactivation. The standard condition screening was therefore reattempted using the acetylated derivative **5.40** (Entries 7-12). Unfortunately, again this failed to produce the target polymer **5.41**. Closer investigation of the polymerisation of either **5.2** or **5.39** revealed that both monomers would actually rather undergo a retro-Diels-Alder reaction back to furfuryl alcohol **5.3**, or the acetylated derivative and 1-butyl-3-methylene-pyrrolidine-2,5-dione **5.38** rather than polymerise. It therefore seems very unlikely that either secondary amide **5.1b** or spirocyclic oxanorbornene-imide **5.2** will undergo ROMP.

Table 5.2: Screening of reaction conditions for the polymerisation of norbornene-imide **5.2**.

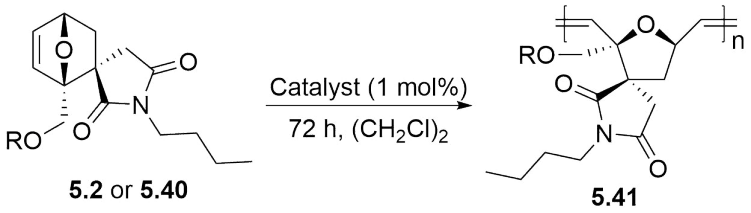

5.2 or **5.40** → **5.41**

Entry	R Group	Catalyst	Temp (°C)	Conv. (%)[a]	Mn	Mw	Đ[b]
1	H **5.2**	G1	rt	-	-	-	-
2	H **5.2**	G1	40	-	-	-	-
3	H **5.2**	G2	rt	-	-	-	-
4	H **5.2**	G2	40	-	-	-	-
5	H **5.2**	G3	rt	-	-	-	-
6	H **5.2**	G3	40	-	-	-	-
7	Ac **5.40**	G1	rt	-	-	-	-
8	Ac **5.40**	G1	40	-	-	-	-
9	Ac **5.40**	G2	rt	-	-	-	-
10	Ac **5.40**	G2	40	-	-	-	-
11	Ac **5.40**	G3	rt	-	-	-	-
12	Ac **5.40**	G3	40	-	-	-	-

All polymerisations were carried out using a monomer:catalyst ratio of 100:1.[a] Conversion was determined using ^{1}H NMR spectroscopy.[b] Đ = M_w/M_n.

5.2.2 DEMETA Catalysts

In a final last ditch effort to polymerise the secondary amides, as they were at least stable to the polymerisation conditions, a range of catalysts supplied by DEMETA S. A. S were investigated. These catalysts have been widely explored for ring-closing metathesis (RCM), but have not previously been investigated for ROMP.[232,233] Before investigating the secondary amides **5.1a-f**, a model norbornene substrate was investigated for ROMP using these catalysts, the results of which can be found within the appendix. Structures M831 SiPr **5.42** and M73 SiPr **5.43** were then selected for further investigation (Figure 5.5).

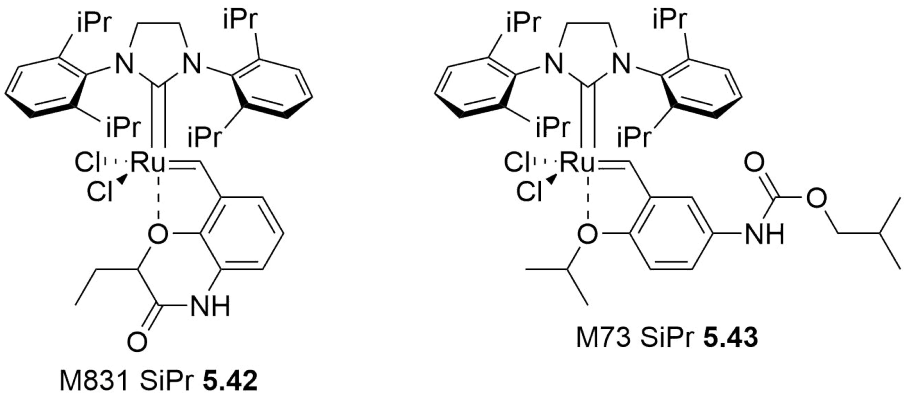

Figure 5.5: Structures of the M831 SiPr **5.42** and M73 SiPr **5.43** catalysts supplied by DEMETA S.A.S.

These catalyst were first screened against the octyl monomer **5.1d** at room temperature and at 40 °C (Table 5.3, Entries 1-4). No evidence for the target polymer **5.39** was observed in any case. The same combinations were then tested with the glycine benzyl ester **5.1f**. Again, no polymer was observed for any of the conditions investigated (Entires 5-8). It was therefore concluded that the secondary amide monomers **5.1a-f** are unsuitable for ROMP on the grounds of the *endo*-pendent side chains not being suitably hindered to prevent catalyst deactivation.

Table 5.3: Demeta catalyst screening for the octyl **5.1d** and glycine benzyl ester **5.1f** secondary amide monomers.

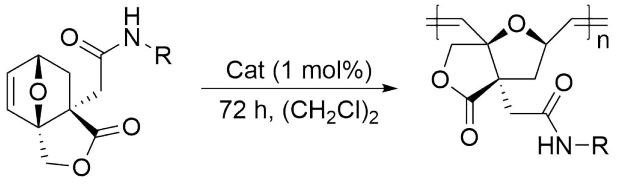

5.1d/f **5.39d/f**

Entry	R Group	Catalyst	Temp (°C)	Conc. (M)	Conv. (%)	Mn	Mw	Đ
1	Oct **5.1d**	M831 SiPr	rt	0.10	-	-	-	-
2	Oct **5.1d**	M831 SiPr	40	0.10	-	-	-	-
3	Oct **5.1d**	M73 SiPr	rt	0.10	-	-	-	-
4	Oct **5.1d**	M73 SiPr	40	0.10	-	-	-	-
5	Gly-OBn **5.1f**	M831 SiPr	rt	0.10	-	-	-	-
6	Gly-OBn **5.1f**	M831 SiPr	40	0.10	-	-	-	-
7	Gly-OBn **5.1f**	M73 SiPr	rt	0.10	-	-	-	-
8	Gly-OBn **5.1f**	M73 SiPr	40	0.10	-	-	-	-

.

5.2.3 Spirocyclic Oxanorbornene-Imides as Therapeutics

Having shown in the previous sections (Sections 5.2.1 and 5.2.2) that the ROMP of secondary amides **5.1a-f** and the spirocyclic oxanorbornene-lactone **5.2** was not viable for a multitude of reasons, attention then turned to an investigation into derivatives of **5.2** as potential therapeutics. It was hypothesised that since it was possible to selectively isolate the secondary amides **5.1a-f**, hydrogenation prior to converting to the spirocyclic-imide would then remove the possibility of the retro-Diels-Alder reaction from occurring (Scheme 5.12). It would then hopefully be possible to isolate stable spirocyclic 7-oxabicyclo[2.2.1]heptane-imide derivatives **5.45a-f** that could potentially be investigated for therapeutic applications.

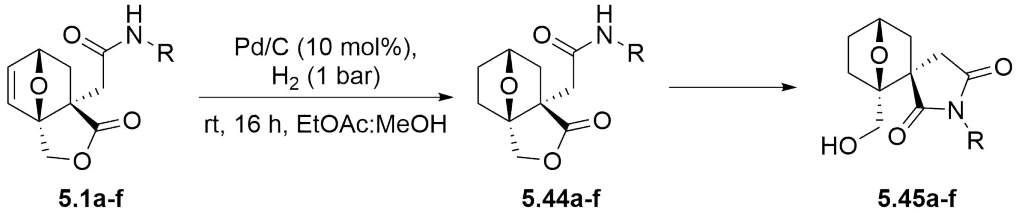

Scheme 5.12: Proposed synthetic route to derivatives of spirocyclic 7-oxabicyclo[2.2.1]heptane-imide **5.45a-f**.

This investigation therefore started by first hydrogenating the butyl secondary amide **5.2b** as a model substrate (Scheme 5.13). A single species was isolated in good yield, but characterisation of this product proved to be rather troublesome and ended up producing a particularly unexpected result. Whilst the majority of the data agreed with the formation of secondary amide **5.44b**, the IR spectroscopy data obtained was particularly peculiar. On the basis of this result, it was reasoned that it would be perfectly plausible for the isomeric spirocyclic species **5.45b** to form directly following hydrogenation. It was eventually determined that this was in fact the case, as 2D ^{1}H and ^{13}C heteronuclear multiple bond correlation (HMBC) NMR spectroscopy indicated that a correlation was present between the protons at the 11 position and both carbonyl groups, a correlation that would only be possible in the imide **5.45b** configuration rather than as the amide **5.44b** (Figure 5.6).

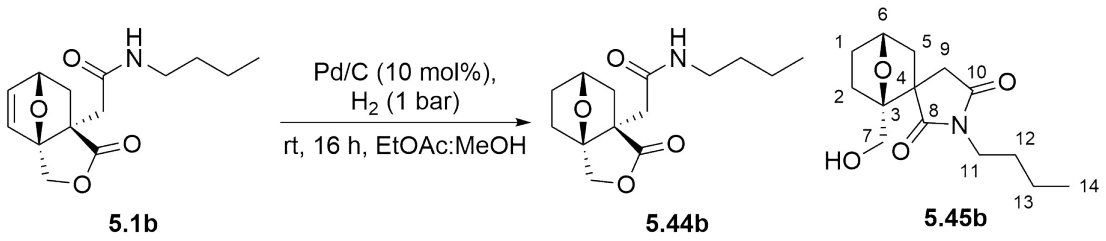

Scheme 5.13: Hydrogenation of the butyl secondary amide **5.1b** and the two possible products **5.44b** and **5.45b**.

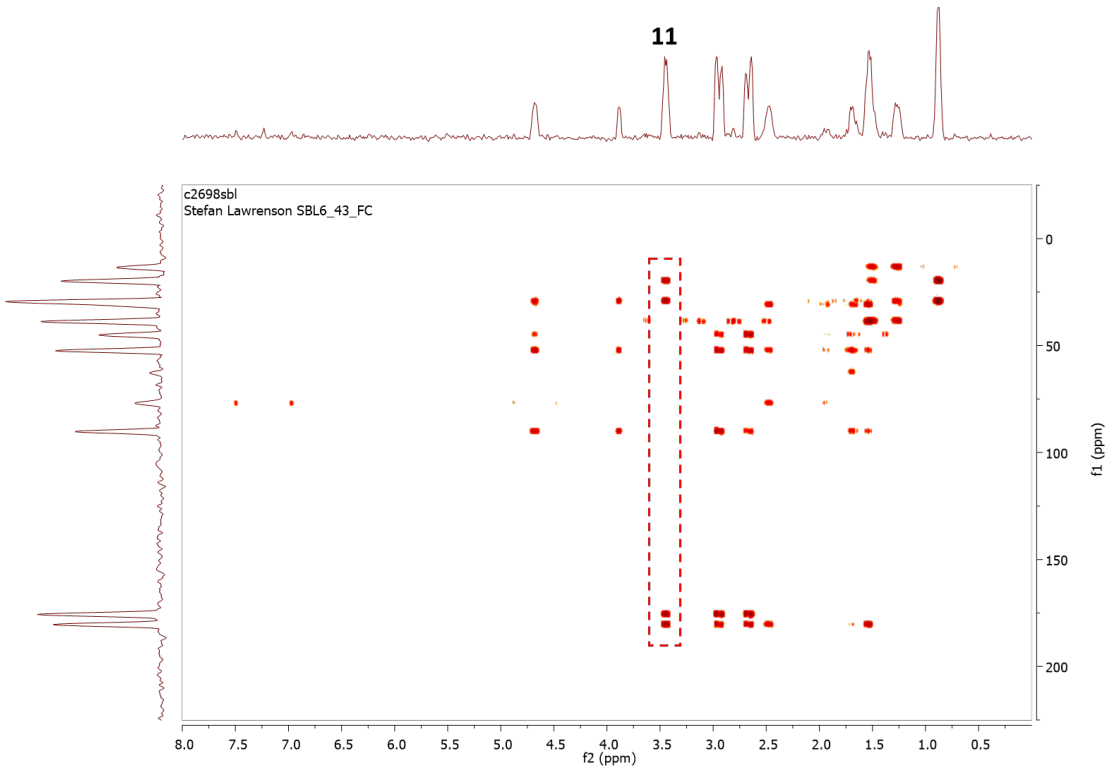

Figure 5.6: HMBC plot of species **5.45b**.

The remaining amide monomers **5.1a-f** were therefore hydrogenated and analysed by IR and 2D ^{1}H and ^{13}C HMBC NMR spectroscopy, where applicable, to see if this observation was general to this class of secondary amides (Table 5.4). It was observed that in the case of long alkyl and benzyl derived amides, the spirocyclic imides **5.45b-e** are formed exclusively, which were all isolated in excellent yields (>90%) (Entries 2-5). Issues however arose when using more hindered alkyl or amino acid functionalised amides, which formed a mixture of both the hydrogenated secondary amide **5.44a**/**f** and the spirocyclic imide **5.45a**/**f** (Entries 1 and 6). This is most likely a consequence of reduced nucleophilicity as a result of steric or electronic factors. It should also be acknowledged that the hydrogenation conditions will remove the benzyl ester protecting group present in **5.1f**, meaning the crude material was actually a mixture of **5.44f** and **5.45f** as the free amino acid. Finally, unequivocal structural conformation was obtained for the formation of spirocyclic 7-oxabicyclo[2.2.1]heptane-imides when a crystal of **5.45e** was successfully grown (Figure 5.7).

Table 5.4: Hydrogenation of secondary amides **5.1a-f** to yield either the secondary amides **5.44a-f** or spirocyclic imide **5.45a-f**.

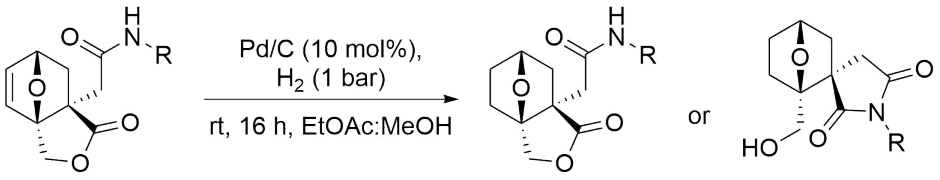

5.1a-f **5.44a-f** **5.45a-f**

5.1/5.44/5.45: a R = *i*Pr; **b** R = Bu; **c** R = Hex, **d** R = Oct; **e** R = Bn; **f** R = GlyOBn.

Entry	R Group	Selectivity[a] 5.44:5.45	Isolated Yield (%)
1	*i*Pr **5.1a**	50:50	-[b]
2	Bu **5.1b**	0:100	90
3	Hex **5.1c**	0:100	94
4	Oct **5.1d**	0:100	98
5	Bn **5.1e**	0:100	95
6	GlyOBn **5.1f**	32:68	-[b]

[a] Determined by ^{1}H NMR spectroscopy.[b] Not isolated due to forming a mixture of products.

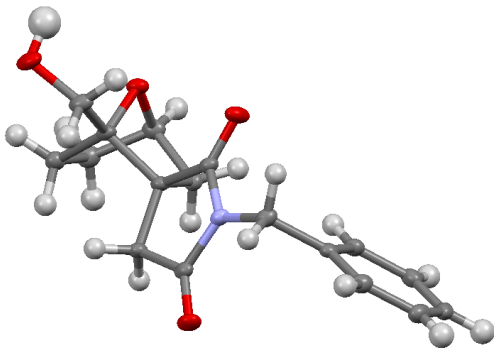

Figure 5.7: Ellipsoid representation of the crystal structure of hydrogenated spirocyclic benzyl oxanorbornene-imide **5.45e**.

5.2.4 LLAMA Analysis

Unfortunately, time constraints have prevented any further investigation into the synthesis of hydrogenated spirocyclic imides similar to **5.45a-f**. This also meant it was not possible to better understand the factors that influence formation of the spirocyclic imide over the secondary amide, or investigate their properties as potential therapeutic agents. It has however been possible to predict their suitability as drug molecules and where they lie in drug-relevant chemical space using a computational model. Lead-Likeness and Molecular Analysis (LLAMA) is an open

access, web based tool for decorating and analysing molecular scaffolds. The software is able to decorate structures using a number of common and pharmaceutically relevant synthetic transformations to generate a library of chemical structures. This library can then be analysed using a number of useful tools to rapidly assess the novelty and lead-likeness of new molecular structures.[234]

Nadin *et al.* have previously described a number of physiologically important properties of molecules, such that similar compounds will have greater flexibility and potential for development into promising clinical candidates.[235] Molecules within this chemical space typically have a defined lipophilicity (-1 $\leq$ cLog$P$ $\leq$ 3) and molecular weight (M_w = 200-350 Da). Nadin *et al.* also suggested that promising candidates should not contain chemically reactive, electrophilic or redox active functionalities, and would be more 3D in structure, possessing a low degree of aromatic character. It is the combination of these factors that form the basis of LLAMA analysis, as the closer molecules lie to the chemical space described by Nadin *et al.* the more lead-like they are deemed to be.

The spirocyclic imides **5.45a-f** were therefore assessed using LLAMA. Each structure was uploaded to create a new database, however derivatisation was turned off, meaning only the structures **5.45a-f** were assessed. Following assessment LLAMA first plots the molecules in 2D space on the basis of their molecular weights and predicted lipophilicity. The software then applies a lead-likeness penalty based on heavy atom count, lipophilicity, number of aromatic rings and the presence of reactive functional groups, the higher this penalty the less lead-like the structures are. Analysis of compounds **5.45a-f** showed that they were found to be very promising candidates as potential therapeutics, with all compounds found to lie perfectly within lead-like chemical space, based on their predicted lipophilicity and molecular weight (Figure 5.8). Additionally, LLAMA applied no lead-likeness penalty to **5.45a-f**, except for **5.45e** due to the presence of the benzylic functional group.

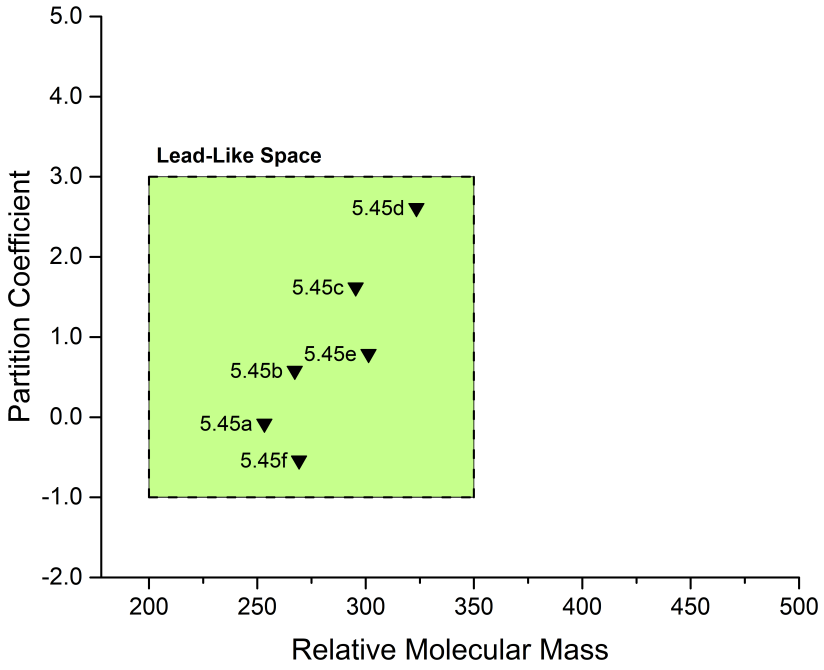

Figure 5.8: Plot of relative molecular mass against lipophilicity for **5.45a-f** highlighting lead-like chemical space.

LLAMA then analyses the structures to determine their 3-dimensionality using principal moment of inertia (PMI) analysis. To generate the PMI coordinates for each molecule, the system randomly generates a number of 3D conformers, minimises their energy and selects the lowest-energy conformer. The system then calculates the moments of inertia in the x, y and z axes. The PMI plot I1 coordinates are calculated by dividing inertia(x) by inertia(z). The PMI I2 coordinates are calculated by dividing inertia(y) by inertia(z).[234] The reason for doing this is due to current trends in medicinal chemistry to move into the relatively unexplored 3D space, as the region lying between rod-like and disc-like has been extensively explored to date. For example, analysis of 1439 FDA approved small molecule drugs has shown only 23% lie within 3D space.[236] In this case, 3D chemical space is defined as the region where (PMI X + PMI Y) > 1.2. PMI analysis of **5.45a-f** showed that **5.45a**, **b** and **f** all lay within the 3D region of chemical space, whilst the structures containing long alkyl or bulky benzyl units **5.45c**, **d** and **e** were more rod-like in structure (Figure 5.9).

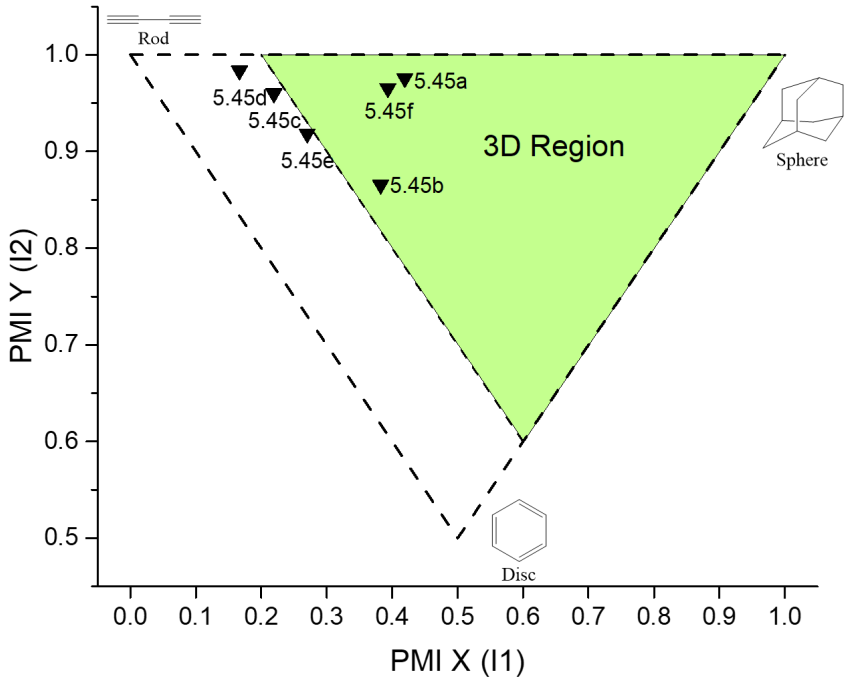

Figure 5.9: PMI analysis of structures **5.45a-f**.

Finally, the structures are assessed by LLAMA for novelty. The molecules are first stripped of any side chains to reduce them down to the ring systems and any linkers between them, this is referred to as the Murcko framework.[237] The Murcko framework is then compared to a random 2% of molecules residing in the ZINC database, a commercial database of over twenty million compounds from Irwin *et al.*[238] The Murcko frameworks of molecules **5.45a-f** were found to possess a 0% likeness to a random 2% of molecules within the ZINC framework, even when analysed as a substructure. This suggests compounds **5.45a-f** are novel molecular frameworks that have not previously been investigated within medicinal chemistry. The secondary amides were also analysed using LLAMA but have not been reported, this is due to the heavy lead-likness penalty they suffer from, due to the presence of undesirable functional groups. The lead-likeness and PMI plot for these compounds can however be found within the appendix.

Overall, analysis of spirocyclic imides **5.45a-f** using LLAMA has suggested they represent very promising molecules for future investigations into their application as potential therapeutics. They have been found to lie directly within lead-like chemical space according to the criteria outlined by Nadin *et al.*, with all molecules also scoring very well for potential lead-likeness penalties. PMI analysis then found that when the spirocyclic imides were functionalised with short alkyl or amino acid side chains, they could be regarded as 3-dimensional in structure. Finally, stripping

the molecules back to their Murcko framework suggested that they represented a very novel cyclic structure, displaying a 0% similarity to a database of over twenty million compounds.

5.3 Conclusions

In conclusion, the unusual oxanorbornene-imide and associated secondary amide, resulting from the treatment of the acid chloride derivatives of **5.10** with butyl amine, has been investigated. Initial analysis of the literature associated with this compound revealed this structure represented a highly novel and functional molecular framework. It was eventually realised that it possessed a number of similarities to the norbornene-2,3-dicarboximides **5.11** and norcantharimide **5.17** frameworks, which have been widely utilised in ROMP and as chemotherapeutics respectively. This chapter has therefore predominantly focussed on understanding the factors that influence how the oxanorbornene-imide and secondary amide form, along with their application in ROMP and as potential therapeutics.

Initial investigations found that the secondary amide **5.1b** slowly converts to the imide **5.2** under very basic conditions, by what is believed to be an intramolecular rearrangement. However, extended reaction times result in the imide undergoing a retro Diels-Alder to furfuryl alcohol **5.3** and the 1-butyl-3-methylene-pyrrolidine-2,5-dione **5.38** species. It was eventually realised that a range of secondary amides **5.1a-f** could be selectively synthesised using exact quantities of the nucleophile and a weaker base than NEt_3, such as pyridine. However, selective formation of a range of the imides was unfortunately not possible.

To avoid losing too much time to this study, the use of secondary amides and spirocyclic oxanorbornene-imides in ROMP was investigated. Unfortunately, neither species produced the target polymer using a range of monomer derivatives, catalysts and reaction temperatures. This is reasoned for the secondary amides on the grounds of the pendant side chain lying in the *endo*-orientation, and not being suitably hindered to inhibit catalyst deactivation through coordination. The spirocyclic oxanorbornene-imides on the other hand appear to prefer the retro Diels-Alder reaction over polymerisation.

Finally, the secondary amides were hydrogenated, with the intention of converting the amide to the corresponding spirocyclic imide. It was however found that the use of unhindered alkyl or benzyl amides produced the spirocyclic imides directly following hydrogenation. These were subsequently investigated for potential as therapeutics. LLAMA analysis suggests this framework falls perfectly within lead-like space, is particularly three-dimensional with amino acid or short alkyl side

chains, and represents a highly novel cyclic system. Unfortunately, time constraints have limited any further investigation into the potential cytotoxicity of these compounds. Nonetheless, initial analysis using LLAMA shows great promise for investigating and potentially using these molecules as therapeutic agents.

Chapter 6

Concluding Remarks and Future Work

This thesis sought to investigate methods utilising green chemistry principles in various approaches towards improving the sustainability of peptide and polymer chemistry. The key findings from each chapter will therefore now be summarised and possible avenues for future work discussed.

Chapter 2: Cyclic Carbonates as Solvents for Peptide Synthesis

The first two research chapters focussed on the use of green solvents in solid-phase synthesis, with Chapter 2 investigating the use of cyclic carbonates as replacements for conventional polar aprotic solvents in peptide synthesis. This began by investigating the synthesis of a model Boc-Phe-Ala-OBn dipeptide using the solution-phase approach, with cyclic carbonates found to produce the target dipeptide in a greater yield than control reactions using DMF or a DMF:CH_2Cl_2 solvent mixture. Optimal coupling conditions were then found to use a combination of PC, EDC, HOBt and DIPEA, producing the target dipeptide in an excellent 93% yield. Coupling was also found to occur with no evidence for racemisation of the amino acids (d.e. >98.4%). PC was then shown to tolerate the harshly acidic conditions associated with Boc-deprotections, with a combination of PC and TFA found to conveniently produce the dipeptide salt product in a quantitative yield. Using the developed methodology a number of tetrapeptides were prepared using PC as the only reaction solvent. These were typically obtained with good to excellent yields observed for all coupling (65-91%) and deprotection (80-99%) reactions, demonstrating PC is tolerant to a range of structurally diverse amino acids and protecting groups commonly associated with peptide synthesis. The only issues arose when attempting to obtain a fully deprotected tripeptide, with PC found to inhibit hydrogenation of the Bn-protecting group. This was eventually overcome using MeOH, a more conventional solvent for hydrogenation reactions.

Having demonstrated the suitability of PC for solution-phase peptide synthesis the associated solid-phase approach was investigated. This immediately hit an issue, as one of the most important considerations for SPPS is the ability of the solvent to adequately solvate, or swell, the solid support. Whilst PC was unable to adequately swell polystyrene-based Merrifield resin, it was found to swell polyethylene glycol based ChemMatrix resin. A model H-Leu-Ala-Phe-OH tripeptide was then synthesised using HBTU, HOBT and DIPEA upon a ChemMatrix resin, using PC as the only reaction solvent. In an effort to really demonstrate the utility of this methodology the synthesis of the biologically relevant peptide bradykinin was attempted. Multiple attempts however failed to produce the target peptide, which was eventually determined to be due to a side-reaction between piperidine and PC, inhibiting the deprotection step. This was overcome

by simply freshly preparing the deprotection cocktail each time. Bradykinin was eventually obtained in a 77% crude purity, an excellent result when compared to a control sample which was obtained in 79% crude purity. Chapter 2 has therefore successfully shown that cyclic carbonates are suitable solvents for both solution- and solid-phase peptide synthesis.

Whilst solvents often present the biggest source of waste, there are still many issues associated with peptide synthesis in the context of green chemistry, such as poor coupling efficiency and the need for toxic reagents. Addressing these issues therefore presents substantial scope for future work investigating methods for improving the sustainability of peptide synthesis. GSK have for example, recently published both an amide bond forming and acid/base reagent guide for embedding sustainability into reagent selection.[239,240] The use of HOBt and HBTU is something that presents a major concern, due to the formation of a urea by-product that is cytotoxic. The use of more desirable coupling agents, such as 1,1'-carbonyldiimidazole (CDI) or COMU in PC, would therefore be a valuable investigation. A number of the bases associated with peptide synthesis are also highlighted as being problematic, due to their flammability and piperidine being a restricted drug precursor, an investigation into suitable alternatives would therefore be worthwhile. This would be particularly beneficial for the use of PC, as it may identify a base that is suitable for Fmoc-deprotections but less prone to ring-opening PC.

Chapter 3: Greener Solvents for Solid-Phase Organic Synthesis

The investigation into the ability of PC to swell common SPOS resins in the previous chapter highlighted that a systematic study into the ability of green solvents to swell SPOS resins had not been previously reported. Chapter 3 therefore investigated the ability of a wide variety of green solvents to swell common SPOS resins. Santini *et al.* had previously reported a method for measuring resin swelling that defined good swelling as >4.0 mL g^{-1}.[131] The swelling of nine common SPOS resins in thirty solvents was then determined according to the method outlined by Santini *et al.* In all cases at least one green solvent was identified to swell each SPOS resin to >4.0 mL g^{-1}.

Having studied resin swelling in green solvents the results were further examined using both a computational and experimental approach. To begin with, a computational model of resin swelling was constructed using the HSPiP software. Using this approach, a training set of solvents was grouped and ranked according to their ability to swell a particular resin, with it found that $n = 5$ groups was best. The HSPiP fitting algorithm was then able to predict optimal Hansen solubility parameters for each resin. The solvent optimiser within HSPiP is then

able to predict other suitable solvents based on these solubility parameters. Plotting the percentage of maximum observed swelling for each resin for a specific solvent generally demonstrated an excellent correlation between swelling and the distance (Ra) from optimal HSP values.

The swelling data was then verified experimentally using the multicomponent Ugi reaction. Solution-phase control reactions found that yields of the α-acylamino amide product in either MeOH or 2-MeTHF were essentially equivalent. The same coupling reaction was then performed upon either a Merrifield or ChemMatrix solid-support, in both 2-MeTHF and MeOH. When a solvent was used that was found to swell both resins the isolated yields of the α-acylamino amide product were found to be comparable. However, when a poor solvent/resin combination was used, yields were found to be substantially reduced, confirming that adequate solvation (>4.0 mL g^{-1}) by a green solvent is a necessary prerequisite.

These results do of course present numerous avenues for future work, since it was identified that SPOS using green solvents had only been reported twice previously. There therefore exists numerous organic transformations that could be performed in green solvents upon solid-supports. Particularly appealing options would be synthetic reactions that already have green credentials, such as organocatalysed reactions or further multicomponent reactions (Passerini, Biginelli etc.). Further computational modelling of resin swelling using HSPiP could also be an interesting avenue for future work. For example, Fields *et al.* had previously suggested that peptide-resin swelling should be considered in two parts, the peptide and the resin.[157] New capabilities in HSPiP allow for the modelling of two distinct regions through the use of a dual sphere model. Using this approach it may be possible to optimise the swelling of both components of the peptide-resin model, facilitating accurate solvent selection for difficult peptide sequences.

Chapter 4: Ring-Opening Metathesis Polymerisation of a Novel Bio-based Monomer Framework

The second half of this thesis then investigated a method for improving the sustainability of polymer synthesis, with Chapter 4 specifically looking at the ROMP of tertiary amide derivatives of a novel bio-based molecular framework. To begin, a number of amide derivatives containing a variety of pendant side chains were synthesised in good to excellent yields. This even included amino acid and peptide derived monomers, in an effort to produce amide derivatives that could be more easily conceived as 100% bio-based. Homopolymerisation of these substrates by ROMP was then investigated. Using a simple dibenzyl species as a model substrate, optimal conditions were found to be 1 mol% **G2** catalyst at 40 °C and 0.1 M in

$(CH_2Cl)_2$. A broad range of homo- and random co-polymers were then produced with good molecular weights (M_n = 10,763-28,100) and excellent dispersities (Đ = 1.02-1.11). Thermal analysis also revealed that the polymers were amorphous, with T_g values in the range of 115-203 °C and thermal decomposition temperatures typically above 300 °C. Finally, it was shown to be possible to synthesise a block copolymer under these reaction conditions. This was only made possible however after monitoring polymerisation of the first monomer by ^{1}H NMR spectroscopy, to ensure accurate addition of the second monomer following 80% consumption. This information also provided some kinetic data, with additional investigations finding that the pendant side chains appeared to have little influence on the observed rate constants (K_{obs} = 2.3×10^{-3} s^{-1} - 3.1×10^{-4} s^{-1}).

These results certainly present promising avenues for future investigations into the use of amino acid or peptide derived ROMP polymers for therapeutic or functional material applications. However, two issues should probably be addressed beforehand. Firstly, functionalisation of a racemic monomer framework with enantiopure substrates creates many issues with regards to characterisation, due to the presence of diastereoisomers and rotamers. Methods for the isolation of an enantiopure monomer framework, whether through stereoselective synthesis or chiral resolution, would certainly prove to be very valuable. Secondly, the *endo*-orientation of the molecular framework has been attributed to the slow propagation rates observed for these monomers and the associated esters. Additionally, this has prevented the use of primary amino acids in this investigation, as secondary amide monomers appear to not be amenable to ROMP, due to deactivation of the active catalyst. Further investigations into the Diels-Alder reactions of other bio-based anhydrides with furfuryl derivatives could therefore be a valuable study, particularly if *exo*-monomers are obtained.

Chapter 5: Investigation into the Synthesis and Application of Unusual Spirocyclic Imide Species

Finally, the previous chapter had identified that when a primary amine was used to functionalise the oxanorbornene-lactone framework a mixture of products was formed. These were determined to be the expected secondary amide and a rather unusual spirocyclic oxanorbornene structure. Chapter 5 therefore focussed on better understanding how these two species form and whether they had potential in polymer or therapeutic applications. It was identified rather quickly that formation of either species generally coincided with the basicity of the reaction solution during amide formation. Further investigations found that the secondary amide could be selectively formed through use of exact quantities of a weak base, like pyridine.

Exposure of the secondary amide to a base such of NEt_3 was then shown to form the spirocyclic oxanorbornene-imide over time, with the retro-Diels-Alder products observed after several hours. Further investigation into this transformation was put on hold, until the application of these species in ROMP had been investigated. Unfortunately, extensive investigation found that neither substrate would undergo ROMP. In the case of the secondary amide this was believed to be due to *endo*-nature of the substituent side chain facilitating catalyst deactivation, whilst the spirocyclic oxanorbornene-imide appeared to prefer the retro-Diels-Alder pathway over polymerisation.

The use of the spirocyclic oxanorbornene-imides as a potential therapeutic agent was therefore duly investigated. This was inspired by the structural similarities between this species and the norcantharimide family of natural products. The secondary amides were first hydrogenated to remove the possibility of the oxanorbornene-imide undergoing a retro-Diels-Alder. However, it was identified that in a number of cases the oxanorbornene-imide formed directly following hydrogenation. It is not currently fully understood why this occurs, but it is hypothesised to be due to the nucleophilicity of the associated amide, with sterically hindered and electron deficient amides typically producing a mixture of products. To determine whether these substrates had potential as therapeutics they were analysed using LLAMA analysis. This determined that the spirocyclic oxanorbornene-imides fall perfectly within lead-like space (-1 $\leq$ cLog$P$ $\leq$ 3 and M_w = 200-350 Da), are rather three-dimensional by PMI analysis and have a 0% similarity to a database of twenty million compounds on the basis of their Murcko framework.

Unfortunately, time constraints have limited further investigation into these spirocyclic oxanorbornene-imides. However the results obtained certainly present a promising case for future work. The most pressing would be a better understanding of the factors that influence formation of spirocyclic species following hydrogenation of the secondary amide. It would also be worth investigating whether the species that formed mixtures of the oxanorbornene-imide and secondary amide could be encouraged to favour formation of the imide. Finally, LLAMA has highlighted the spirocyclic oxanorbornene-imides as highly promising therapeutics. It would therefore be worthwhile investigating their efficacy in cancer cell growth inhibition assays, to check for any cytotoxicity.

This thesis has therefore highlighted a number of novel approaches for improving the sustainability of peptide and polymer chemistry. The first research chapter demonstrated the suitability of cyclic carbonates, highly promising green solvents to replace reprotoxic polar aprotic solvents, in both solution- and solid-phase peptide synthesis. This work was then extended to solid-phase organic synthesis.

Identifying suitable green solvents for a number of common SPOS resins through swelling experiments, which were then validated through a computational and experimental approach. The second half of this thesis then addressed polymer chemistry, investigating a novel bio-based molecular framework. A number of novel polymers derived from tertiary amides were successfully synthesised, including amino acid and peptidic side chains, which could be more convincingly regarded as fully bio-based. Finally, an unusual spirocyclic oxanorbornene-species derived from the bio-based molecular framework was studied in more detail. Whilst it did not undergo ROMP, it does have promising potential within therapeutics. At the time of writing, the majority of this work is either published, or is currently under consideration for publication in academic journals. It can therefore be unequivocally concluded that the work reported herein presents a valuable contribution to improving the sustainability of polymer and peptide chemistry.

Chapter 7

Experimental

7.1 General Information

All air- and water-sensitive reactions were carried out in oven-dried glassware under either a nitrogen or argon atmosphere. Analytical TLC was performed on aluminium backed plates pre-coated (0.25 mm) with Merck KGaA silica gel 60 F_{254}. Compounds were visualised by exposure to UV-light (254 nm) and stained using $KMnO_4$ or phosphomolybdic acid (PMA) followed by heating. Flash column chromatography was performed using Fluorochem silica gel LC60A (40-60 μM). Brine refers to a saturated solution of aqueous sodium chloride. All mixed solvent eluents are reported as v/v solutions. All amino acid derivatives have *S*-configuration unless otherwise stated.

^{1}H- and ^{13}C-Nuclear Magnetic Resonance (NMR) spectra were acquired at various field strength as indicated using a JEOL ECS 400 MHz spectrometer. ^{1}H spectra were referenced internally to the residual protic solvent resonance ($CDCl_3$ = 7.27 ppm, CD_3OD = 3.31 ppm, DMSO-d_6 = 2.50 ppm, $(CH_2Cl)_2$ = 3.72 (br.), CF_3COOD = 11.50). ^{13}C-spectra were referenced internally to the solvent resonance ($CDCl_3$ = 77.16 ppm, CD_3OD = 49.00 ppm, DMSO-d_6 = 39.52 ppm). ^{1}H- and ^{13}C-NMR coupling constants are reported in Hertz (Hz). Coupling constants are reported using the following notation, or combination of; s = singlet, br. = broad, d = doublet, t = triplet, q = quartet, quin = quintet, sex = sextet, sept = septet, oct = octet, non = nonet, m = multiplet. Assignment of signals in ^{1}H- and ^{13}C-spectra was performed using ^{1}H-^{1}H COSY, DEPT-135, ^{1}H-^{13}C HMQC and HMBC experiments where appropriate.

High resolution mass spectra were recorded using Electrospray Ionisation (ESI), on a Bruker micrOTOF mass spectrometer in tandem with an Agilent series 1200 Liquid Chromatography (LC) system. All Infra-Red (IR) data was obtained using a Perkin-Elmer Spectrum Two or Spectrum 400 FT-IR spectrometer. Absorbances are reported using the following notation; w = weak, m = medium, s = strong. Optical rotations were obtained on a Jasco DIB370 polarimeter, with concentrations given in g 100 mL^{-1}. Melting points were determined using either a Stuart SMP3 or SMP20 hot stage apparatus and were not corrected.

Chiral normal phase HPLC was performed using Daicel Chiralpak OD or OD-H columns (4.6 mm × 250 mm × 5 μm) fitted with the respective guard column and monitored by Diode Array Detector (DAD) on an Agilent Infinity 1220 LC system equipped with Agilent OpenLab software. Flow rate: 0.7 mL min^{-1}, 97:3 Hexane: *i*-PrOH, detection at 210 and 254 nm

Bradykinin samples were analysed on a Bruker microTOF mass spectrometer in tandem with an Agilent series 1200 LC system with an additional diode array

detector. Chromatography was carried out at 40 °C on a Waters Sunfire C_{18} column (3.5 μm packing, 2.1 mm × 100 mm) with a solvent flow rate of 0.2 mL min^{-1} and UV detection at 214 nm. A dual solvent system was employed:
Solvent A: MeCN + 0.1% (*v*/*v*) formic acid
Solvent B: Water + 0.1% (*v*/*v*) formic acid
The solvent system was varied following the sequence: 10% A / 90% B for 5 min, then ramp to 50% A / 50% B over the next 10 min, hold at 50% A / 50% B for 5 min then ramp back to 10% A / 90% B.

Microwave reactions were carried out in a G10 microwave vial equipped with a rare Earth stirrer bar, using an Anton Paar Monowave 300 microwave reactor. The temperature was held at 70 °C (monitored using a ruby thermometer) for the duration of the reaction.

Size-exclusion chromatography was carried out using a set of PSS SDV High analytical columns (300 mm × 8 mm × 5 μm) of 1000, 10^5 and 10^6 Å pore sizes, with corresponding guard columns, supplied by Polymer Standards Service GmbH (PSS) and installed on a PSS SECcurity SEC system. Elution was with THF stabilised by 0.025% butylated hydroxytoluene, at a flow rate of 1.0 mL^{-1}, a column temperature of 23 °C and detection by refractive index. 20 μL of a 1 mg mL^{-1} sample in THF, containing one drop of toluene as an internal reference, was injected for each measurement and eluted for 40 min. Calibration was carried out in the molecular weight range 400-2×10^6 Da using ReadyCal polystyrene standards supplied by Sigma Aldrich.

Modulated differential scanning calorimetry (MDSC) experiments were carried out on a DSC TA Q2000, under nitrogen atmosphere, at a heating rate of 10 °C min^{-1} up to a temperature of either 100, 200 or 300 °C, and using a sample mass of approximately 10 mg. Thermogravimetric analysis (TGA) was carried out using a PL Thermal Sciences STA 625 instrument from ambient (22 °C) to 625 °C at a ramp rate of 10 °C min^{-1} in an open aluminium sample pan under N_2. TG-IR spectroscopy data was collected using a Netzsch STA 409 instrument at a ramp rate of 10 °C min^{-1} under a 100 mL min^{-1} flow of nitrogen. This instrument was connected with a heated gas transfer line to a Bruker Equinox 55 FT-IR spectrometer equipped with a gas cell and an MCT detector.

Diffraction data were collected at 110 K on an Oxford Diffraction SuperNova diffractometer with Cu-Kα radiation (λ = 1.54184 Å) using an EOS CCD camera. The crystal was cooled with an Oxford Instruments Cryojet. Diffractometer control, data collection, initial unit cell determination, frame integration and unit-cell refinement was carried out with "Crysalis". Face-indexed absorption corrections

were applied using spherical harmonics, implemented in SCALE3 ABSPACK scaling algorithm. OLEX2 was used for overall structure solution, refinement and preparation of computer graphics and publication data. Within OLEX2, the algorithm used for structure solution was ShelXT, charge-flipping. Refinement by full-matrix least-squares used the SHELXL algorithm within OLEX2. Hydrogen atoms were placed using a ”riding-mode“ and included in the refinement at calculated positions.

7.2 Cyclic Carbonates as Solvents for Peptide Synthesis

7.2.1 Solution-Phase Peptide Synthesis

7.2.1.1 General Procedure for Peptide Coupling Reactions in PC

To a suspension of an *N*-Boc-amino acid (1.0 eq.) and an amino acid or peptide benzyl ester (1.0 eq.) in PC (5 mL $mmol^{-1}$), at 0 °C, was added a solution of HOBt (1.1 eq.) and *i*-Pr_2EtN (3.0 eq.) in a minimal quantity of PC. EDC (1.1 eq.) was added dropwise and the reaction mixture was allowed to stir at room temperature for 16 h. The reaction mixture was then diluted using EtOAc (50 mL) and washed with 1 M HCl_{aq} (3 × 25 mL), saturated Na_2CO_3 (3 × 25 mL) and H_2O (3 × 25 mL). The organic layer was dried ($MgSO_4$), filtered and concentrated *in vacuo*. Any residual PC was removed *via* short path distillation.

7.2.1.2 Synthesis of Boc-Ala-Phe-OBn 2.89 in a Microwave Reactor

N-Boc-alanine (189 mg, 1.0 mmol, 1.0 eq.), phenylalanine benzyl ester (292 mg, 1.0 mmol, 1.0 eq.) and HOBt (149 mg, 1.0 mmol, 1.1 eq.) were combined in a G10 microwave vial. PC (2 mL) and *i*-Pr_2EtN (523 μL, 3.0 mmol, 6.0 eq.) were then added. The vial was cooled to 0 °C and EDC (195 μL, 1.1 mmol, 1.1 eq.) was added dropwise. The reaction mixture was then heated at 70 °C for 3 h using an Anton Parr Monowave 300 microwave reactor. The reaction was then diluted with EtOAc (50 mL) and washed with 1 M HCl_{aq} (50 mL), saturated Na_2CO_3 (50 mL) and brine (50 mL). The organic fraction was dried ($MgSO_4$), filtered and concentrated *in vauco*. Residual PC was removed *via* short path distillation. The residue was purified using flash column chromatography (40:60, EtOAc:PE) to give Boc-Ala-Phe-OBn **2.89** as a white solid (352 mg, 82%).

7.2.1.3 General Procedure for Boc Deprotections in PC

An *N*-Boc-peptide benzyl ester (1.0 eq.) was dissolved in a minimum amount of PC and trifluoroacetic acid (60 eq.) was added. The reaction mixture was allowed to stir for 3 h at room temperature before being concentrated *in vacuo*. Any residual PC was removed *via* short path distillation.

7.2.1.4 Procedure for Boc Deprotection of Dipeptide 2.89 using HCl in PC

Boc-Ala-Phe-OBn **2.89** (50 mg, 0.117 mmol) was dissolved in PC (2.34 mL). MeOH (0.40 mL, 9.8 mmol) was added and the solution cooled to 0 °C. Acetyl chloride (0.67 mL, 9.36 mmol) was added dropwise and the solution allowed to stir at room

temperature for 2 h. Residual PC was removed *via* short path distillation. The residue was suspended in cold Et_2O and triturated to give HCl·H-Ala-Phe-OBn **2.101** as a white solid (46 mg, 86%).

Boc-Ala-Phe-OBn (2.103a)

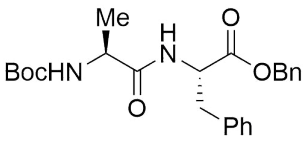

Boc-Ala-OH (324 mg, 1.71 mmol) and HCl·H-Phe-OBn (500 mg, 1.71 mmol) were coupled according to the general coupling procedure. The residue was purified using flash column chromatography (35:65, EtOAc:PE) to give Boc-Ala-Phe-OBn **2.103a** as a white crystalline solid (682 mg, 93%).[125,241] $\boldsymbol{R_F}$ = 0.34, (40:60, EtOAc:PE); **m.p.** 95-96 °C; $\boldsymbol{[\alpha]^{23}_D}$ = − 27.7 (*c* 1.0 in MeOH) [lit.[125] − 35 (c 0.35 in MeOH)]; **IR (Neat)** ν_{max} 3347 (m), 3063 (w), 3029 (w), 2928 (m), 2852 (w), 1735 (w), 1684 (w) 1666 (w) and 1521 (s) cm^{-1}; **^{1}H NMR** (400 MHz, $CDCl_3$): δ = 7.36-7.31 (m, 3H, ArH), 7.29-7.24 (m, 2H, ArH), 7.26-7.21 (m, 3H, ArH), 7.04-6.97 (m, 2H, ArH), 6.72 (d *J* 7.7 Hz, 1H, Phe-NH), 5.16-5.10 (m, 1H, Ala-NH), 5.13 (d *J* 12.1 Hz, 1H, OCH_2Ph), 5.07 (d *J* 12.1 Hz, 1H, OCH_2Ph), 4.88 (dt *J* 7.7, 5.9 Hz, 1H, Phe-NCH), 4.11 (br, 1H, Ala-NCH), 3.13 (dd *J* 13.9, 6.1 Hz, 1H, CH_2Ph), 3.08 (dd *J* 13.9, 6.1 Hz, 1H, CH_2Ph), 1.41 (s, 9H, $C(CH_3)_3$), 1.29 (d *J* 6.6 Hz, 3H, CH_3); **^{13}C NMR** (100 MHz, $CDCl_3$): δ = 172.3 (C=O), 171.2 (C=O), 155.6 (NC=O), 135.7 (ArC), 135.1 (ArC), 129.5 (ArCH), 128.7 (ArCH), 128.6 (ArCH), 127.2 (ArCH), 80.2 (CMe_3), 67.4 (OCH_2Ph), 53.3 (Phe-NCH), 50.3 (Ala-NCH), 38.0 (CH_2Ph), 28.4 ($C(CH_3)_3$), 18.5 (CH_3); **HRMS (ESI)** *m/z* calculated for $C_{24}H_{30}N_2NaO_5$ 449.2048 $(M+Na)^+$, found 449.2047, 0.6 ppm error.

Boc-(*R*)-Ala-Phe-OBn 2.96

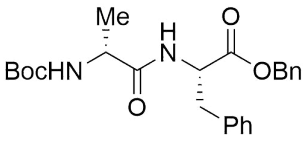

Boc-(*R*)-Ala-OH (164 mg, 0.87 mmol) and HCl·H-Phe-OBn (250 mg, 0.87 mmol) were coupled according to the general coupling procedure. The residue was purified using flash column chromatography (40:60, EtOAc:PE) to give Boc-(*R*)-Ala-Phe-OBn **2.96** as an off-white solid (323 mg, 87%). $\boldsymbol{R_F}$ = 0.38, (40:60, EtOAc:PE); **m.p.** 75-76 °C; $\boldsymbol{[\alpha]^{23}_D}$ = 6.5 (*c* 1.0 in MeOH); **IR (Neat)** ν_{max} 3294 (m), 3066 (w), 3030 (w), 2977 (m), 2930 (m), 1717 (m), 1687 (m) and 1648 (s) cm^{-1}; **^{1}H NMR**

(400 MHz, $CDCl_3$): δ = 7.39-7.32 (m, 3H, ArH), 7.32-7.27 (m, 2H, ArH), 7.25-7.16 (m, 3H, ArH), 7.06-6.98 (m, 2H, ArH), 6.80 (br, 1H, Phe-NH), 5.15 (d *J* 12.4 Hz, 1H, OCH_2Ph), 5.11 (br, 1H, Ala-NH), 5.08 (d *J* 12.4 Hz, 1H, OCH_2Ph), 4.90 (dt *J* 7.7, 6.2 Hz, 1H, Phe-NCH), 4.20 (br, 1H, Ala-NCH), 3.13 (dd *J* 13.9, 6.0 Hz, 1H, CH_2Ph), 3.07 (dd *J* 13.9, 6.0 Hz, 1H, CH_2Ph), 1.42 (s, 9H, $C(CH_3)_3$), 1.27 (d *J* 7.1 Hz, 3H, CH_3); **^{13}C NMR** (100 MHz, $CDCl_3$): δ = 172.3 (C=O), 171.3 (C=O), 155.6 (NC=O), 135.7 (ArC), 135.2 (ArC), 129.4 (ArCH), 128.8 (ArCH), 128.7 (ArCH), 128.6 (ArCH), 127.2 (ArCH), 80.3 (CMe_3), 67.4 (OCH_2Ph), 53.2 (Phe-NCH), 50.1 (Ala-NCH), 38.0 (CH_2Ph), 28.4 ($C(CH_3)_3$), 18.5 (CH_3); **HRMS (ESI)** *m/z* calculated for $C_{24}H_{31}N_2O_5$ 427.2155 $(M+H)^+$, found 427.2227, − 0.3 ppm error.

Boc-Leu-Phe-OBn 2.103b

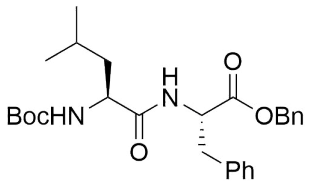

Boc-Leu-OH (100 mg, 0.43 mmol) and HCl·H-Phe-OBn (110 mg, 0.43 mmol) were coupled according to the general coupling procedure. The residue was purified using flash column chromatography (40:60, EtOAc:PE) to give Boc-Leu-Phe-OBn **2.103b** as a white powder (162 mg, 80%).[242] $\boldsymbol{R_F}$ = 0.42, (30:70, EtOAc:PE); **m.p.** 100-102 °C (lit. 103-105 °C); $\boldsymbol{[\alpha]^{23}_D}$ = − 27.4 (*c* 1.0 in MeOH) [lit. − 33.8 (*c* 1.0 in MeOH)]; **IR (Neat)** ν_{max} 3339 (m), 3064 (w), 3034 (w), 2956 (w), 2935 (w), 2879 (w), 1731 (s), 1679 (m), 1665 (s) and 1518 (s) cm^{-1}; **^{1}H NMR** (400 MHz, $CDCl_3$): δ = 7.39-7.34 (m, 3H, ArH), 7.29-7.26 (m, 2H, ArH), 7.22-7.19 (m, 3H, ArH), 7.03-7.01 (m, 2H, ArH), 6.53 (d *J* 7.6 Hz, 1H, Phe-NH), 5.15 (d *J* 12.0 Hz, 1H, OCH_2Ph), 5.10 (d *J* 12.0 Hz, 1H, OCH_2Ph), 4.88 (dt *J* 7.7, 6.0 Hz, 1H, Phe-NCH), 4.86 (br, 1H, Leu-NH), 4.08 (br, 1H, Leu-NCH), 3.14 (dd *J* 14.0, 6.4 Hz, 1H, CH_2Ph), 3.09 (dd *J* 14.0, 6.4 Hz, 1H, CH_2Ph), 1.68-1.58 (m, 2H, CH_2CHMe_2), 1.43 (s, 9H, $C(CH_3)_3$), 1.45-1.35 (m, 1H, $CH(Me)_2$), 0.90 (d *J* 6.4 Hz, 3H, $CH(CH_3)_2$), 0.89 (d *J* 6.4 Hz, 3H, $CH(CH_3)_2$); **^{13}C NMR** (100 MHz, $CDCl_3$): δ = 172.3 (C=O), 171.2 (C=O), 155.6 (NC=O), 135.7 (ArC), 135.1 (ArC), 129.5 (ArCH), 128.7 (ArCH), 128.6 (ArCH), 127.2 (ArCH), 80.1 (CMe_3), 67.4 (OCH_2Ph), 53.3 (Phe-NCH), 53.2 (Leu-NCH), 41.4 (CH_2CHMe_2), 38.0 (CH_2Ph), 28.4 ($C(CH_3)_3$), 24.8 ($CHMe_2$), 23.0 ($CH(CH_3)_2$), 22.0 ($CH(CH_3)_2$); **HRMS (ESI)** *m/z* calculated for $C_{27}H_{37}N_2O_5$ 469.2697 $(M+H)^+$, found 469.2691, 1.2 ppm error.

Boc-(*R*)-Leu-Phe-OBn 2.98

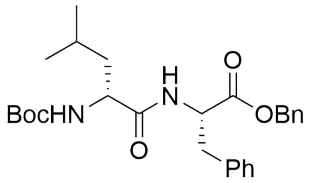

Boc-(*R*)-Leu-OH (100 mg, 0.43 mmol) and HCl·H-Phe-OBn (110 mg, 0.43 mmol) and were coupled according to the general coupling procedure. The residue was purified using flash column chromatography (20:80-30:70, EtOAc:PE) to give Boc-(*R*)-Leu-Phe-OBn **2.98** as a white powder (187 mg, 92%).[243] $\boldsymbol{R_F}$ = 0.48, (30:70, EtOAc:PE); **m.p.** 96-97 °C (lit. 97 °C); $\boldsymbol{[\alpha]^{23}_D}$ = +4.8 (*c* 1.0 in MeOH); **IR (Neat)** ν_{max} 3334 (m), 3064 (w), 3031 (w), 2961 (w), 1739 (m), 1726 (m), 1686 (m), 1652 (s) and 1519 (s) cm^{-1}; **^{1}H NMR** (400 MHz, $CDCl_3$): δ = 7.39-7.34 (m, 3H, ArH), 7.31-7.28 (m, 2H, ArH), 7.22-7.19 (m, 3H, ArH), 7.04-7.00 (m, 2H, ArH), 6.61 (d *J* 6.4 Hz, 1H, Phe-NH), 5.17 (d *J* 12.0 Hz, 1H, OCH_2Ph), 5.10 (d *J* 12.4 Hz, 1H, OCH_2Ph), 4.89 (dt *J* 7.9, 6.0 Hz, 1H, Phe-NCH), 4.78 (d *J* 6.8 Hz, 1H, Leu-NH), 4.17-4.05 (m, 1H, Leu-NCH), 3.13 (dd *J* 14.0, 6.0 Hz, 1H, CH_2Ph), 3.08 (dd *J* 14.0, 6.4 Hz, 1H, CH_2Ph), 1.65-1.50 (m, 2H, CH_2CHMe_2), 1.42 (s, 9H, $C(CH_3)_3$), 1.41-1.30 (m, 1H, $CH_2CH(CH_3)_2$), 0.88 (d *J* 6.0 Hz, 6H, $CH(CH_3)_2$); **^{13}C NMR** (100 MHz, $CDCl_3$): δ = 172.3 (C=O), 171.3 (C=O), 155.7 (NC=O), 135.7 (ArC), 135.1 (ArC), 129.4 (ArCH), 128.8 (ArCH), 128.7 (ArCH), 128.6 (ArCH), 127.2 (ArCH), 80.2 ($OCMe_3$), 67.4 (OCH_2Ph), 53.2 (Phe-NCH), 53.1 (Leu-NCH), 41.3 (CH_2CHMe_2), 38.0 (CH_2Ph), 28.4 ($C(CH_3)_3$), 24.8 ($CHMe_2$), 23.0 ($CH(CH_3)_2$), 21.9 ($CH(CH_3)_2$); **HRMS (ESI)** *m/z* calculated for $C_{27}H_{37}N_2O_5$ 469.2697 $(M+H)^+$, found 469.2694, 0.2 ppm error.

Boc-Met-Val-OBn 2.103c

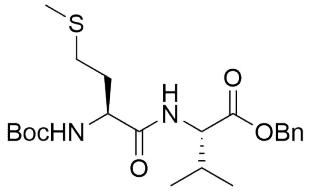

Boc-Met-OH (374 mg, 1.5 mmol) and H-Val-OBn (569 mg, 1.5 mmol) were coupled according to the general coupling procedure. The residue was purified using flash column chromatography (30:70, EtOAc:PE) to give Boc-Met-Val-OBn **2.103c** as a clear oil (603 mg, 91%).[244] $\boldsymbol{R_F}$ = 0.33, (30:70, EtOAc:PE); $\boldsymbol{[\alpha]^{23}_D}$ = − 25.1 (*c* 1.0 in MeOH); **IR (Neat)** ν_{max} 3314 (w), 2968 (w), 2932 (w), 1739 (m), 1658 (s) and 1521 (m) cm^{-1}; **^{1}H NMR** (400 MHz, $CDCl_3$): δ = 7.39-7.29 (m, 5H, ArH), 6.72 (d

J 8.2 Hz, 1H, Val-NH), 5.23 (br, 1H, Met-NH), 5.19 (d *J* 12.4 Hz, 1H, OCH_2Ph), 5.12 (d *J* 12.4 Hz, 1H, OCH_2Ph), 4.56 (dd *J* 8.8, 4.7 Hz, 1H, Val-NCH), 4.31 (dt *J* 7.3, 7.1 Hz, 1H, Met-NCH), 2.58 (t *J* 7.2 Hz, 2H, CH_2CH_2SMe), 2.21 (dsept *J* 7.0, 4.7 Hz, 1H, $CHMe_2$), 2.09 (s, 3H, SCH_3), 2.03 (dt *J* 14.0, 7.1 Hz, 1H, CH_2CH_2SMe), 1.95 (dt *J* 14.0, 7.1 Hz, 1H, CH_2CH_2SMe), 1.43 (s, 9H, $C(CH_3)_3$), 0.91 (d *J* 7.0 Hz, 3H, $CH(CH_3)_2$), 0.86 (d *J* 7.0 Hz, 3H, $CH(CH_3)_2$); **^{13}C NMR** (100 MHz, $CDCl_3$): δ = 171.6 (C=O), 171.5 (C=O), 155.6 (NC=O), 135.4 (ArC), 128.7 (ArCH), 128.6 (ArCH), 128.5 (ArCH), 80.2 (CMe_3), 67.2 (OCH_2Ph), 57.3 (Val-NCH), 53.3 (Met-NCH), 31.3 (CH_2SMe), 31.2 ($CHMe_2$), 30.2 (CH_2CH_2SMe), 28.4 ($C(CH_3)_3$), 19.1 ($CH(CH_3)_2$), 17.6 ($CH(CH_3)_2$), 15.2 (CH_2SCH_3); **HRMS (ESI)** *m/z* calculated for $C_{22}H_{34}N_2NaO_5$ 461.2086 $(M+Na)^+$, found 461.2081, − 2.2 ppm error.

Boc-Asp(OBn)-Val-OBn 2.103d

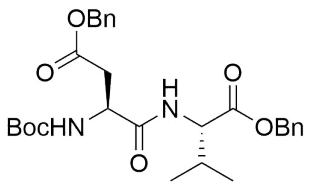

Boc-Asp(OBn)-OH (808 mg, 2.5 mmol) and H-Val-OBn *para*-toluenesulfonate (949 mg, 25 mmol) were coupled according to the general coupling procedure. The residue was purified using flash column chromatography (25:75, EtOAc:PE) to give Boc-Asp(OBn)-Val-OBn **2.103d** as a pale yellow oil (897 mg, 70%).[245] $\boldsymbol{R_F}$ = 0.29, (25:75, EtOAc:PE); $\boldsymbol{[\alpha]^{23}_D}$ = − 28.4 (*c* 1.0 in MeOH) [lit. − 33.3 (*c* 1.07 in MeOH)]; **IR (Neat)** ν_{max} 3332 (w), 3033 (w), 2967 (w), 2934 (w), 1734 (s), 1679 (s) and 1517 (m) cm^{-1}; **^{1}H NMR** (400 MHz, $CDCl_3$): δ = 7.40-7.29 (m, 10H, ArH), 7.07 (d *J* 8.9 Hz, 1H, NH), 5.75 (d *J* 8.2 Hz, 1H, NH), 5.19 (d *J* 12.0 Hz, 1H, OCH_2Ph), 5.17-5.08 (m, 3H, 3×OCH_2Ph) 4.61-4.50 (m, 2H, 2×NCH), 3.03 (dd *J* 17.2, 4.7 Hz, 1H, CH_2CO_2) 2.71 (dd *J* 17.2, 4.7 Hz, 1H, CH_2CO_2), 2.26-2.12 (m, 1H, $CHMe_2$), 1.45 (s, 9H, $C(CH_3)_3$), 0.91 (d *J* 6.9 Hz, 1H, $CH(CH_3)_2$), 0.86 (d *J* 6.9 Hz, 1H, $CH(CH_3)_2$); **^{13}C NMR** (100 MHz, $CDCl_3$): δ = 172.1 (C=O), 171.4 (C=O), 170.8 (C=O), 155.8 (NC=O), 135.6 (CAr), 135.4 (CAr), 128.7 (ArCH), 128.6 (ArCH), 128.5 (ArCH), 128.4 (ArCH), 128.3 (ArCH), 80.6 (CMe_3), 67.1 (OCH_2Ph), 67.0 (OCH_2Ph), 57.5 (Val-NCH), 50.7 (Asp(OBn)-NCH), 36.0 (CH_2CO_2), 31.3 ($CHMe_2$), 28.4 ($C(CH_3)_3$), 19.1 ($CH(CH_3)_2$), 17.6 ($CH(CH_3)_2$); **HRMS (ESI)** *m/z* calculated for $C_{28}H_{36}N_2NaO_7$ 535.2429 $(M+Na)^+$, found 535.2417, − 0.1 ppm error.

Boc-Aib-Leu-OBn 2.103e

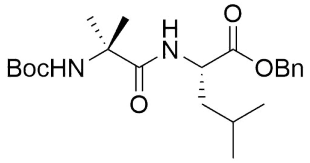

Boc-Aib-OH (508 mg, 2.5 mmol) and H-Leu-OBn *para*-toluenesulfonate (934 mg, 2.5 mmol) were coupled according to the general coupling procedure. The residue was purified using flash column chromatography (30:70, EtOAc:PE) to give Boc-Aib-Leu-OBn **2.103e** as a white powder (794 mg, 78%).[246] $\boldsymbol{R_F}$ = 0.25, (25:75, EtOAc:PE); **m.p.** 93-95 °C; $\boldsymbol{[\alpha]^{23}_D}$ = − 16.3 (*c* 0.5 in MeOH); **IR (Neat)** ν_{max} 3308 (m), 2953 (m), 2869 (w), 1720 (m), 1685 (s), 1659 (s), 1534 (m) and 1507 (s) cm^{-1}; **^{1}H NMR** (400 MHz, $CDCl_3$): δ = 7.39-7.29 (m, 5H, ArH), 6.88 (br, 1H, NH), 5.16 (d *J* 12.4 Hz, 1H, OCH_2Ph), 5.11 (d *J* 12.4 Hz, 1H, OCH_2Ph), 4.89 (br, 1H, NH), 4.66-4.60 (m, 1H, NCH), 1.72-1.56 (m, 3H, CH_2CHMe_2), 1.49 (s, 3H, $C(CH_3)_2$), 1.45 (s, 3H, $C(CH_3)_2$), 1.42 (s, 9H, $C(CH_3)_3$), 0.91 (d *J* 6.6 Hz, 3H, $CH(CH_3)_2$), 0.89 (d *J* 6.6 Hz, 3H, $CH(CH_3)_2$); **^{13}C NMR** (100 MHz, $CDCl_3$): δ = 174.5 (C=O), 173.0 (C=O), 154.7 (NC=O), 135.6 (ArC), 128.7 (ArCH), 128.5 (ArCH), 128.3 (ArCH), 77.4 ($OCMe_3$), 67.1 (OCH_2Ph), 56.9 ($NCMe_2$), 50.9 (NCH), 41.7 (CH_2CHMe_2), 28.4 ($C(CH_3)_3$), 26.3 (CH_2CHMe_2), 24.8 ($C(CH_3)_2$), 23.0 ($CH(CH_3)_2$), 21.9 ($CH(CH_3)_2$); **HRMS (ESI)** *m/z* calculated for $C_{22}H_{34}N_2NaO_5$ 429.2365 $(M+Na)^+$, found 429.2373, − 2.7 ppm error.

TFA·H-Ala-Phe-OBn 2.104a

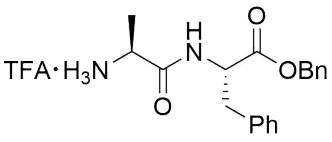

Boc-Ala-Phe-OBn **2.103a** (340 mg, 0.8 mmol) was deprotected according to the general procedure for Boc deprotections to give TFA·H-Ala-Phe-OBn **2.104a** as an off white solid (351 mg, 99%).[247] **m.p.** 180-181 °C; $\boldsymbol{[\alpha]^{23}_D}$ = − 8.1 (*c* 0.5 in MeOH); **IR (Neat)** ν_{max} 3333 (m), 3165 (w), 3031 (w), 2938 (w), 1725 (s), 1660 (s), 1547 (m) and 1523 (m) cm^{-1}; **^{1}H NMR** (400 MHz, CD_3OD): δ = 7.40-7.15 (m, 10H, ArH), 5.16 (d *J* 12.1 Hz, 1H, OCH_2Ph), 5.11 (d *J* 12.1 Hz, 1H, OCH_2Ph), 4.76 (dd *J* 8.9, 5.8 Hz, 1H, Phe-NCH), 3.86 (q *J* 6.8 Hz, 1H, Ala-NCH), 3.20 (dd *J* 14.1, 5.9 Hz, 1H, CH_2Ph), 2.98 (dd *J* 14.1, 5.9 Hz, 1H, CH_2Ph), 1.42 (d *J* 6.9 Hz, 3H, CH_3); **^{13}C NMR** (100 MHz, CD_3OD): δ = 172.4 (C=O), 171.1 (C=O), 137.9 (ArC), 136.9 (ArC), 130.2 (ArCH), 129.6 (ArCH), 129.6 (ArCH), 129.6 (ArCH),

129.5 (ArCH), 128.0 (ArCH), 68.2 (OCH_2Ph), 55.6 (Phe-NCH), 50.0 (Ala-NCH), 38.1 (CH_2Ph), 17.6 (CH_3); **HRMS (ESI)** m/z calculated for $C_{19}H_{23}N_2O_3$ 327.1709 $(M\text{-}CF_3CO_2^-)^+$, found 327.1695, 2.3 ppm error.

TFA·H-Leu-Phe-OBn 2.104b

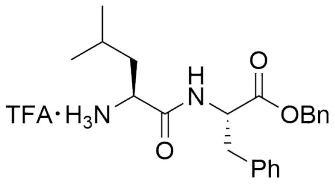

Boc-Leu-Phe-OBn **2.103b** (600 mg, 1.28 mmol) was deprotected according to the general procedure for Boc deprotections to give TFA·H-Leu-Phe-OBn **2.104b** as an off white solid (1.33 g, 99%).[248] **m.p.** 172-174 °C; **IR (Neat)** ν_{max} 2960 (w), 2485 (w), 1731 (s), 1723 (s), 1679 (m), 1674 (s), 1665 (s) and 1518 (s) cm^{-1}; **^{1}H NMR** (400 MHz, CD_3OD): δ = 7.35-7.30 (m, 3H, ArH), 7.29-7.23 (m, 4H, ArH), 7.22-7.16 (m, 3H, ArH), 5.12 (d *J* 12.0 Hz, 1H, OCH_2Ph), 5.08 (d *J* 12.0 Hz, 1H, OCH_2Ph), 4.74 (dd *J* 8.8, 6.0 Hz, 1H, Phe-NCH), 4.59 (br, 1H, NH), 3.77 (dd *J* 8.8, 6.0 Hz, 1H, Leu-NCH), 3.18 (dd *J* 14.0, 6.4 Hz, 1H, CH_2Ph), 3.01 (dd *J* 14.0, 8.8 Hz, 1H, CH_2Ph), 1.73-1.53 (m, 2H, CH_2CHMe_2), 0.91 (d *J* 6.4 Hz, 3H, $CH(CH_3)_2$), 0.90 (d *J* 6.4 Hz, 3H, $CH(CH_3)_3$); **^{13}C NMR** (100 MHz, CD_3OD): δ = 172.3 (C=O), 170.9 (C=O), 137.9 (ArC), 136.9 (ArC), 130.2 (ArCH), 129.6 (ArCH), 129.6 (ArCH), 129.6 (ArCH), 129.5 (ArCH), 128.0 (ArCH), 68.2 (OCH_2Ph), 55.7 (Phe-NCH), 52.7 (Leu-NCH), 41.7 (CH_2CHMe_2), 38.0 (CH_2Ph), 25.2 ($CH(Me)_2$), 23.2 ($CH(CH_3)_2$), 21.8 ($CH(CH_3)_2$); **HRMS (ESI)** m/z calculated for $C_{22}H_{29}N_2O_3$ 369.2173 $(M\text{-}CF_3CO_2^-)^+$, found 369.2173, 0.3 ppm error.

TFA·H-Met-Val-OBn 2.104c

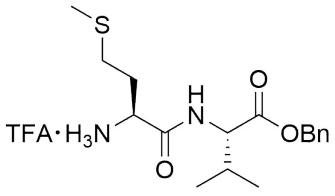

Boc-Met-Val-OBn **2.103c** (603 mg, 1.37 mmol) was deprotected according to the general procedure for Boc deprotections to give TFA·H-Met-Val-OBn **2.104c** as a white solid (474 mg, 80%). **m.p.** 169-170 °C; **$[\alpha]^{23}_D$** = − 10.0 (*c* 1.0 in MeOH); **IR (Neat)** ν_{max} 3344 (w), 2975 (w), 1693 (s), 1663 (s), 1544 (m) and 1518 (m) cm^{-1}; **^{1}H NMR** (400 MHz, DMSO-d_6): δ = 8.74 (d *J* 7.9 Hz, 1H, NH), 8.20 (br, 3H, NH_3^+), 7.41-7.32 (m, 5H, ArH), 5.16 (d *J* 12.0 Hz, 1H, OCH_2Ph), 5.13 (d *J* 12.0 Hz, 1H,

OCH_2Ph), 4.26 (dd *J* 7.5, 6.1 Hz, 1H, Val-NCH), 3.97 (t *J* 6.2 Hz, 1H, Met-NCH), 2.50-2.44 (m, 2H, CH_2SMe), 2.19-2.06 (m, 1H, $CHMe_2$), 2.01 (s, 3H, SCH_3), 2.02-1.89 (m, 2H, CH_2CH_2SMe), 0.91 (d *J* 6.8 Hz, 3H, $CH(CH_3)_2$), 0.90 (d *J* 6.8 Hz, 3H, $CH(CH_3)_2$); **^{13}C NMR** (100 MHz, DMSO-d_6): δ = 170.9 (C=O), 168.9 (C=O), 135.7 (ArC), 128.5 (ArCH), 128.2 (ArCH), 128.1 (ArCH), 66.2 (OCH_2Ph), 57.8 (Val-NCH), 51.4 (Met-NCH), 31.2 (CH_2CH_2SMe), 29.7 ($CHMe_2$), 28.0 (CH_2SMe), 18.9 ($CH(CH_3)_2$), 18.0 ($CH(CH_3)_2$), 14.5 (SCH_3); **HRMS (ESI)** *m/z* calculated for $C_{17}H_{27}N_2O_3S$ 339.1742 $(M\text{-}CF_3CO_2^-)^+$, found 339.1737, 2.9 ppm error.

TFA·H-Asp(OBn)-Val-OBn 2.104d

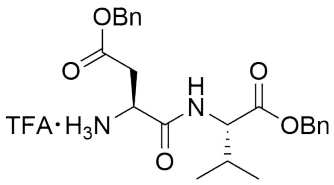

Boc-Asp(OBn)-Val-OBn **2.103d** (747 mg, 1.46 mmol) was deprotected according to the general procedure for Boc deprotections to give TFA·H-Asp(OBn)-Val-OBn **2.104d** as an off-white solid (650 mg, 85%). **m.p.** 147-148 °C; **$[\alpha]^{23}_D$** = − 16.0 (*c* 1.0 in MeOH); **IR (Neat)** ν_{max} 3328 (m), 3032 (w), 2976 (w), 2884 (w), 2586 (w), 1734 (m), 1705 (s), 1661 (s), 1558 (m) and 1519 (w) cm^{-1}; **^{1}H NMR** (400 MHz, DMSO-d_6): δ = 8.77 (d *J* 8.2 Hz, 1H, NH), 8.34 (br, 3H, NH_3^+), 7.46-7.27 (m, 10H, ArH), 5.20-5.07 (m, 4H, 2×OCH_2Ph), 4.33-4.24 (m, 2H, 2×NCH), 2.88 (dd *J* 17.6, 3.9 Hz, 1H, CH_2CO_2Bn), 2.78 (dd *J* 17.6, 8.9 Hz, 1H, CH_2CO_2Bn) 2.11 (oct *J* 6.7 Hz, 1H, $CHMe_2$), 0.89 (d *J* 7.3 Hz, 3H, $CH(CH_3)_2$), 0.87 (d *J* 7.3 Hz, 3H, $CH(CH_3)_2$); **^{13}C NMR** (100 MHz, DMSO-d_6): δ = 170.7 (C=O), 169.1 (C=O), 168.9 (C=O), 135.7 (ArC), 135.6 (ArC), 128.5 (ArCH), 128.5 (ArCH), 128.3 (ArCH), 128.3 (ArCH), 128.2 (ArCH), 66.4 (OCH_2Ph), 66.3 (OCH_2Ph), 57.8 (Val-NCH), 48.6 (Asp-NCH), 35.5 (CH_2CO_2Bn), 29.8 ($CHMe_2$), 18.9 ($CH(CH_3)_2$), 17.9 ($CH(CH_3)_2$); **HRMS (ESI)** *m/z* calculated for $C_{23}H_{29}N_2O_5$ 413.2076 $(M\text{-}CF_3CO_2^-)^+$, found 413.2060, 3.5 ppm error.

TFA·H-Aib-Leu-OBn 2.104e

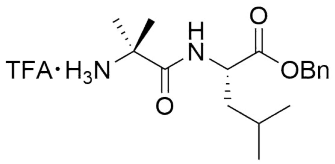

Boc-Aib-Leu-OBn **2.103e** (100 mg, 0.25 mmol) was deprotected according to the general procedure for Boc deprotections to give TFA·H-Aib-Leu-OBn **2.104e** as a yellow oil (102 mg, 97%). **IR (Neat)** ν_{max} 2960 (w), 1728 (m), 1661 (s) and 1530 (m) cm^{-1}; **^{1}H NMR** (400 MHz, DMSO-d_6): δ = 8.59 (d *J* 8.3 Hz, 1H, NH), 8.23 (s, 3H, NH_3^+), 7.42-7.31 (m, 5H, ArH), 5.13 (d *J* 12.9 Hz, 1H, OCH_2Ph), 5.10 (d *J* 12.9 Hz, 1H, OCH_2Ph), 4.44-4.37 (m, 1H, Leu-NCH), 1.77-1.52 (m, 3H, CH_2CHMe_2), 1.48 (s, 3H, $C(CH_3)_2$), 1.45 (s, 3H, $C(CH_3)_2$), 0.90 (d *J* 6.1 Hz, 3H, $CH(CH_3)_2$), 0.83 (d *J* 6.1 Hz, 3H, $CH(CH_3)_2$); **^{13}C NMR** (100 MHz, DMSO-d_6): δ = 172.0 (C=O), 171.9 (C=O), 135.8 (ArC), 128.5 (ArCH), 128.2 (ArCH), 127.9 (ArCH), 66.2 (OCH_2Ph), 56.4 (Aib-NC), 50.8 (Leu-NCH), 39.3 (CH_2CHMe_2), 24.4 ($CHMe_2$), 23.4 ($C(CH_3)_2$), 23.3 ($C(CH_3)_2$), 22.8 ($CH(CH_3)_2$), 20.9 ($CH(CH_3)_2$); **HRMS (ESI)** *m/z* calculated for $C_{17}H_{27}N_2O_3$ 307.2022 $(M\text{-}CF_3CO_2^-)^+$, found 307.2008, 2.0 ppm error.

Boc-Leu-Ala-Phe-OBn 2.105a

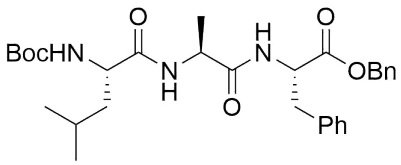

Boc-Leu-OH (185 mg, 0.8 mmol) and TFA·H-Ala-Phe-OBn **2.104a** (352 mg, 0.8 mmol) were coupled according to the general coupling procedure. The residue was purified using flash column chromatography (35:65-60:40, EtOAc:PE) to give Boc-Leu-Ala-Phe-OBn **2.105a** as a white solid (325 mg, 75%). $\boldsymbol{R_F}$ = 0.35, (60:40, EtOAc:PE); **m.p.** 143-145 °C; $\boldsymbol{[\alpha]^{23}_D}$ = − 37.4 (*c* 1.0 in MeOH); **IR (Neat)** ν_{max} 3326 (m), 2955 (w), 1983 (w), 1730 (m), 1688 (m), 1639 (s) and 1523 (m) cm^{-1}; **^{1}H NMR** (400 MHz, $CDCl_3$): δ = 7.38-7.29 (m, 3H, ArH), 7.29-7.22 (m, 2H, ArH), 7.21-7.13 (m, 3H, ArH), 7.04-6.91 (m, 2H, ArH), 6.65 (d *J* 7.1 Hz, Ala-NH), 6.59 (d *J* 7.0 Hz, Phe-NH), 5.14 (d *J* 12.0 Hz, 1H, OCH_2Ph), 5.06 (d *J* 12.0 Hz, 1H, OCH_2Ph), 4.90 (br, 1H, Leu-NH), 4.87 (dt *J* 7.5, 6.9 Hz, 1H, Phe-NCH), 4.46 (q *J* 7.2 Hz, 1H, Ala-NCH), 4.09 (br, 1H, Leu-NCH), 3.10 (dd *J* 14.2, 6.6 Hz, CH_2Ph), 3.05 (dd *J* 14.2, 6.6 Hz, CH_2Ph), 1.70-1.58 (m, 1H, $CHMe_2$), 1.59-1.51 (m, 2H, CH_2CHMe_2), 1.42 (s, 9H, $OC(CH_3)_3$), 1.29 (d, *J* 7.2 Hz, 3H, $NCHCH_3$), 0.90 (d *J* 6.6 Hz, 6H, $CH(CH_3)_2$); **^{13}C NMR** (100 MHz, $CDCl_3$): δ = 172.6 (C=O), 171.8 (C=O), 171.2

(C=O), 155.8 (NC=O), 135.7 (ArC), 135.1 (ArC), 129.3 (ArCH), 128.7 (ArCH), 128.6 (ArCH), 127.2 (ArCH), 80.2 ($OCMe_3$), 67.4 (OCH_2Ph), 53.5 (Phe-NCH), 53.0 (Leu-NCH), 48.9 (Ala-NCH), 41.2 (CH_2CHMe_2), 37.9 (CH_2Ph), 28.4 ($OC(CH_3)_3$), 24.8 ($CH(CH_3)_2$), 23.2 ($CH(CH_3)_2$), 21.9 ($CHMe_2$), 18.3 ($NCHCH_3$); **HRMS (ESI)** m/z calculated for $C_{30}H_{41}N_3NaO_6$ 562.3074 $(M+Na)^+$, found 562.2888, − 1.3 ppm error.

Boc-(*R*)-Leu-Ala-Phe-OBn 2.101

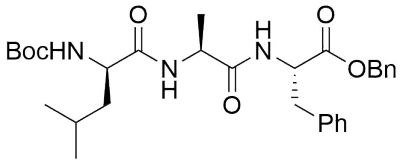

Boc-(*R*)-Leu-OH (69 mg, 0.3 mmol) and TFA·H-Ala-Phe-OBn **2.104a** (164 mg, 0.3 mmol) were coupled according to the general coupling procedure. The residue was purified using flash column chromatography (30:20:50-40:20:40, EtOAc:CH_2Cl_2:PE) to give Boc-(*R*)-Leu-Ala-Phe-OBn **2.101** as a white solid (132 mg, 82%). $\boldsymbol{R_F} = 0.18$, (30:20:50, EtOAc:CH_2Cl_2:PE); **m.p.** 131-133 °C; $\boldsymbol{[\alpha]^{23}_D} = 9.3$ (c 1.0 in MeOH); **IR (Neat)** ν_{max} 3319 (m), 3277 (m), 2930 (w), 1730 (m), 1686 (m), 1638 (s) and 1528 (s) cm^{-1}; **^{1}H NMR** (400 MHz, $CDCl_3$): δ = 7.37-7.32 (m, 3H, ArH), 7.29-7.24 (m, 2H, ArH), 7.23-7.18 (m, 3H, ArH), 7.05-7.00 (m, 2H, ArH), 6.67 (br, 1H, Phe-NH), 6.60 (d J 7.6 Hz, 1H, Ala-NH), 5.14 (d J 12.3 Hz, 1H, OCH_2Ph), 5.08 (d J 12.3 Hz, 1H, OCH_2Ph), 4.88-4.78 (m, 2H, Leu-NH + Phe-NCH), 4.50 (q J 7.3 Hz, 1H, Ala-NCH), 4.06 (br, 1H, Leu-NCH), 3.12 (dd J 14.0, 5.1 Hz, 1H, CH_2Ph), 3.05 (dd J 14.0, 5.1 Hz, 1H, CH_2Ph), 1.69-1.55 (m, 3H, CH_2CHMe_2), 1.43 (s, 9H, $C(CH_3)_3$), 1.29 (d J 6.3 Hz, 3H, $NCHCH_3$), 0.92 (d J 6.2 Hz, 3H, $CH(CH_3)_2$), 0.91 (d J 6.2 Hz, 3H, $CH(CH_3)_2$); **^{13}C NMR** (100 MHz, $CDCl_3$): δ = 172.5 (C=O), 171.8 (C=O), 171.2 (C=O), 155.8 (NC=O), 135.2 (ArC), 129.4 (ArC), 128.7 (ArCH), 128.7 (ArCH), 127.2 (ArCH), 80.3 ($OCMe_3$), 67.4 (OCH_2Ph), 53.5 (Phe-NCH), 53.3 (Leu-NCH), 48.8 (Ala-NCH), 41.3 (Leu-CH_2CHMe_2), 34.7 (CH_2Ph), 28.4 ($C(CH_3)_3$), 24.9 ($CH(CH_3)_2$), 23.1 ($CH(CH_3)_2$), 22.0 ($CHMe_2$), 18.1 ($NCHCH_3$); **HRMS (ESI)** m/z calculated for $C_{30}H_{41}N_3NaO_6$ 562.2893 $(M+Na)^+$, found 562.2876, 1.9 ppm error.

Boc-Gly-Leu-Phe-OBn 2.105b

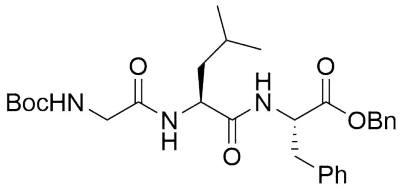

Boc-Gly-OH (145 mg, 0.83 mmol) and TFA·H-Leu-Phe-OBn **2.104b** (400 mg, 0.83 mmol) were coupled according to the general coupling procedure. The residue was purified using flash column chromatography (50:50-60:40, EtOAc:PE) to give Boc-Gly-Leu-Phe-OBn **2.105b** as a white powder (371 mg, 78%).[249] $\boldsymbol{R_F}$ = 0.46, (50:50, EtOAc:PE); **m.p.** 86-87 °C; $\boldsymbol{[\alpha]^{23}_D}$ = − 23.4 (*c* 1.0 in MeOH); **IR (Neat)** ν_{max} 3295 (w), 2958 (w), 1714 (s), 1640 (s) and 1546 (m) cm^{-1}; **^{1}H NMR** (400 MHz, $CDCl_3$): δ = 7.38-7.34 (m, 3H, ArH), 7.30-7.27 (m, 2H, ArH), 7.24-7.20 (m, 3H, ArH), 7.04-7.02 (m, 2H, ArH), 6.57 (d *J* 7.6 Hz, 1H, Phe-NH), 6.46 (d *J* 8.4 Hz, 1H, Leu-NH), 5.26 (t *J* 5.7 Hz, 1H, Gly-NH), 5.16 (d *J* 12.4 Hz, 1H, OCH_2Ph), 5.10 (d *J* 12.4 Hz, 1H, OCH_2Ph), 4.87 (dt *J* 8.0, 6.4 Hz, 1H, Phe-NCH), 4.50-4.40 (m, 1H, Leu-NCH), 3.76 (dd *J* 16.8, 5.6 Hz, 1H, Gly-NCH_2), 3.67 (dd *J* 16.8, 5.2 Hz, 1H, Gly-NCH_2), 3.14 (dd *J* 14, 6.0 Hz, 1H, CH_2Ph), 3.06 (dd *J* 14.0, 6.4 Hz, 1H, CH_2Ph), 1.65-1.54 (m, 2H, CH_2CHMe_2), 1.53-1.46 (m, 1H, CHMe_2), 1.45 (s, 9H, OC(CH_3)$_3$), 0.87 (d *J* 6.0 Hz, 3H, CH(CH_3)$_2$), 0.86 (d *J* 6.0 Hz, 3H, CH(CH_3)$_2$); **^{13}C NMR** (100 MHz, $CDCl_3$): δ = 171.6 (C=O), 171.2 (C=O), 169.6 (C=O), 156.1 (NC=O), 135.8 (ArC), 135.1 (ArC), 129.4 (ArCH), 128.7 (ArCH), 128.6 (ArCH), 128.6 (ArCH), 127.1 (ArCH), 77.4 (OC(CH$_3$)$_3$), 67.4 (OCH_2Ph), 53.3 (Phe-NCH), 51.6 (Leu-NCH), 44.3 (Gly-NCH_2), 40.1 (CH$_2$CHMe_2), 37.9 (CH$_2$Ph), 28.4 (OC(CH$_3$)$_3$), 24.7 (CH$_2$$CHMe_2$), 22.9 (CH($CH_3$)$_2$), 22.1 (CH($CH_3$)$_2$); **HRMS (ESI)** *m*/*z* calculated for $C_{29}H_{39}N_3NaO_6$ 548.2731 $(M+Na)^+$, found 548.2719, 2.4 ppm error.

Boc-Ser(OBn)-Met-Val-OBn 2.105c

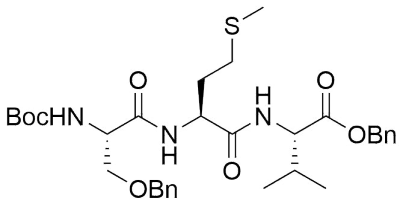

Boc-Ser(OBn)-OH (313 mg, 1.1 mmol) and TFA·H-Met-Val-OBn **2.104c** (478 mg, 1.1 mmol) were coupled according to the general coupling procedure. The residue was then purified using flash column chromatography (47.5:52.5, EtOAc:PE) to give Boc-Ser(OBn)-Met-Val-OBn **2.105c** as a colourless oil (537 mg, 83%). $\boldsymbol{R_F}$ =

0.46, (47.5:52.5, EtOAc:PE); **[α]$^{23}_{D}$** = − 26.8 (*c* 1.0 in MeOH); **IR (Neat)** ν_{max} 3299 (w), 2967 (w), 2930 (w), 1738 (m), 1714 (m) and 1644 (s) cm^{-1}; **^{1}H NMR** (400 MHz, $CDCl_3$): δ = 7.40-7.26 (m, 10H, ArH), 7.22 (d *J* 6.9 Hz, 1H, Met-NH), 6.79 (d *J* 8.4 Hz, 1H, Val-NH), 5.38 (d *J* 6.0 Hz, 1H, Ser-NH), 5.19 (d *J* 12.4 Hz, 1H, CO_2CH_2Ph), 5.12 (d *J* 12.4 Hz, 1H, CO_2CH_2Ph) 4.63 (dt *J* 7.6, 6.8 Hz, 1H, Met-NCH), 4.56 (d *J* 11.8 Hz, 1H, CH_2OCH_2Ph), 4.51 (d *J* 11.8 Hz, 1H, CH_2OCH_2Ph), 4.56-4.51 (m, 1H, Val-NCH), 4.29 (br, 1H, Ser-NCH), 3.91 (dd *J* 9.4, 3.7 Hz, 1H, CH_2OBn), 3.57 (dd *J* 9.4, 6.0 Hz, 1H, CH_2OBn) 2.54 (t *J* 7.1 Hz, 2H, CH_2SMe), 2.24-2.13 (m, 1H, Val-$CHMe_2$), 2.06 (s, 3H, SCH_3), 2.06-1.95 (m, 2H, CH_2CH_2SMe), 1.44 (s, 9H, $OC(CH_3)_3$), 0.89 (d *J* 7.0 Hz, 3H, $CH(CH_3)_2$), 0.85 (d *J* 7.0 Hz, 3H, $CH(CH_3)_2$); **^{13}C NMR** (100 MHz, $CDCl_3$): δ = 171.5 (C=O), 170.7 (C=O), 170.5 (C=O), 155.7 (NC=O), 137.4 (ArC), 135.4 (ArC), 128.7 (ArCH), 128.6 (ArCH), 128.6 (ArCH), 128.1 (ArCH), 127.9 (ArCH), 73.6 (OCH_2Ph), 69.9 (CH_2OBn), 67.2 (OCH_2Ph), 57.5 (Val-NCH), 54.3 (Ser-NCH) 52.4 (Met-NCH), 31.1 ($CHMe_2$), 30.8 (CH_2CH_2SMe), 30.0 (CH_2SMe), 28.4 ($OC(CH_3)_2$), 19.2 ($CH(CH_3)_2$), 17.7 ($CH(CH_3)_2$), 15.0 (SCH_3); **HRMS (ESI)** *m*/*z* calculated for $C_{32}H_{45}N_3NaO_7S$ 638.2876 $(M+Na)^+$, found 638.2870, 4.2 ppm error.

Boc-Trp-Asp(OBn)-Val-OBn 2.105d

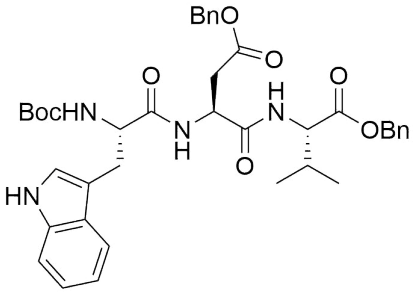

Boc-Trp-OH (231 mg, 0.76 mmol) and TFA·H-Asp(OBn)-Val-OBn **2.104d** (400 mg, 0.76 mmol) were coupled according to the general coupling procedure. The residue was purified using flash column chromatography (50:50, EtOAc:PE) to give Boc-Trp-Asp(OBn)-Val-OBn **2.105d** as a pale yellow solid (363 mg, 68%). $\boldsymbol{R_F}$ = 0.32, (50:50, EtOAc:PE); **m.p.** 57-59 °C; **[α]$^{23}_{D}$** = − 36.2 (*c* 0.5 in MeOH); **IR (Neat)** ν_{max} 3320 (m), 3062 (w), 2967 (w), 2932 (w), 1729 (s) and 1646 (s) cm^{-1}; **^{1}H NMR** (400 MHz, $CDCl_3$): δ = 8.17 (s, 1H, ArNH), 7.62 (d *J* 7.5 Hz, 1H, ArH), 7.40-7.27 (m, 11H, ArH), 7.19-7.09 (m, 3H, ArH), 7.03 (d *J* 2.1 Hz, 1H, Asp-NH), 7.01 (d *J* 8.8 Hz, 1H, Val-NH), 5.18 (d *J* 11.8 Hz, 1H, OCH_2Ph), 5.10 (d *J* 11.8 Hz, 1H, OCH_2Ph), 5.06-5.01 (m, 3H, OCH_2Ph + Trp-NH), 4.80-4.72 (m, 1H, Asp-NCH), 4.46-4.39 (m, 2H, Val-NCH + Trp-NCH), 3.33 (dd *J* 14.4, 5.2 Hz, 1H, Trp-CH_2), 3.18 (dd *J* 14.7, 6.6 Hz, 1H, Trp-CH_2), 2.91 (d *J* 16.2 Hz, 1H, CH_2CO_2Bn), 2.36 (dd *J* 17.2, 6.6 Hz, 1H, CH_2CO_2Bn), 2.11 (oct *J* 6.8 Hz, 1H, $CHMe_2$), 1.41 (s, 9H,

$OC(CH_3)_3$), 0.87 (d J 6.7 Hz, 3H, $CH(CH_3)_2$), 0.78 (d J 6.7 Hz, 3H, $CH(CH_3)_2$); **^{13}C NMR** (100 MHz, $CDCl_3$): δ = 172.2 (C=O), 172.0 (C=O), 171.4 (C=O), 170.1 (C=O), 155.6 (NC=O), 136.3 (ArC), 13.6 (ArC), 135.5 (ArC), 128.7 (ArCH), 128.6 (ArCH), 128.5 (ArCH), 128.5 (ArCH), 128.4 (ArCH), 128.4 (ArCH), 127.4 (ArC), 123.2 (ArCH), 122.5 (ArCH), 119.9 (ArCH), 118.9 (ArCH), 111.4 (ArCH), 110.3 (ArC), 80.5 ($OCMe_3$) 67.1 (OCH_2Ph), 66.9 (OCH_2Ph), 57.7 (Val-NCH), 55.4 (Asp-NCH), 49.3 (Trp-NCH), 35.5 (Trp-CH_2), 31.0 ($CHMe_2$), 28.4 ($C(CH_3)_3$), 19.1 ($CH(CH_3)_2$), 17.7 ($CH(CH_3)_2$); **HRMS (ESI)** m/z calculated for $C_{39}H_{46}N_4NaO_8$ 721.3213 $(M+Na)^+$, found 721.3208, 1.8 ppm error.

Boc-Pro-Aib-Leu-OBn 2.105e

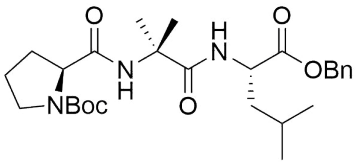

Boc-Pro-OH (357 mg, 1.66 mmol) and TFA·H-Aib-Leu-OBn **2.104e** (700 mg, 1.66 mmol) were coupled according to the general coupling procedure. The residue was purified using flash column chromatography (2:98-5:95, MeOH:CH_2Cl_2) to give Boc-Pro-Aib-Leu-OBn **2.105e** as a white powder (618 mg, 73%). $\boldsymbol{R_F}$ = 0.18, (2:98, MeOH:CH_2Cl_2); **m.p.** 157-158 °C; **$[\alpha]^{23}_D$** = − 51.9 (c 0.5 in MeOH); **IR (Neat)** ν_{max} 3382 (w), 3274 (w), 3060 (w), 2974 (w), 2871 (w), 1735 (m), 1681 (s), 1643 (s), 1549 (m) and 1522 (m) cm^{-1}; **^{1}H NMR** (400 MHz, CD_3OD): δ = 7.40-7.22 (m, 5H, ArH), 5.17 (d J 12.6 Hz, 1H, CH_2Ph), 5.11 (d J 12.6 Hz, 1H, CH_2Ph), 4.57-4.44 (m, 1H, Leu-NCH), 4.18-4.07 (m, 1H, Pro-NCH), 3.54-3.33 (m, 2H, CH_2N), 2.26-2.09 (m, 1H, $CH_2CH_2CH_2N$), 2.09-1.75 (m, 3H, $CH_2CH_2CH_2N$), 1.73-1.57 (m, 3H, CH_2CHMe_2), 1.45 (s, 9H, $OC(CH_3)_3$), 1.43 (s, 3H, $C(CH_3)_2$), 1.41 (s, 3H, $C(CH_3)_2$), 0.91 (d J 5.7 Hz, 3H, $CH(CH_3)_2$), 0.89 (d J 4.8 Hz, 3H, $CH(CH_3)_2$); **^{13}C NMR** (100 MHz, CD_3OD, major rotomer): δ = 176.8 (C=O), 174.5 (C=O), 173.8 (C=O), 156.4 (NC=O), 137.3 (ArC), 129.5 (ArCH), 129.4 (ArCH), 129.3 (ArCH), 81.3 ($OCMe_3$), 67.7 (OCH_2Ph), 61.5 (Pro-NCH), 57.8 (Aib-NC), 52.5 (Leu-NCH), 47.9 (CH_2N), 41.5 ($CH_2CH_2CH_2N$), 31.3 (CH_2CH_2N), 28.9 ($OC(CH_3)_3$), 26.5 ($CHMe_2$), 25.7 (CH_2CHMe_2), 25.4 ($C(CH_3)_2$), 24.5 ($C(CH_3)_2$), 23.2 ($CH(CH_3)_2$), 22.2 ($CH(CH_3)_2$); **HRMS (ESI)** m/z calculated for $C_{27}H_{41}N_3NaO_6$ 526.2893 $(M+Na)^+$, found 526.2893, − 0.9 ppm error.

TFA·H-Leu-Ala-Phe-OBn 2.106a

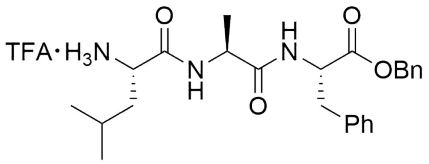

Boc-Leu-Ala-Phe-OBn **2.105a** (260 mg, 0.48 mmol) was deprotected according to the general procedure for Boc deprotections, giving TFA·H-Leu-Ala-Phe-OBn **2.106a** as an off white solid (257 mg, 96%).[250] **m.p.** 196-197 °C; **[α]$^{23}_{D}$** = − 15.2 (*c* 1.0 in MeOH); **IR (Neat)** ν_{max} 3394 (w), 3262 (w), 2957 (m), 1732 (w), 1648 (s) and 1516 (m) cm^{-1}; **^{1}H NMR** (400 MHz, CD_3OD): δ = 7.32-7.12 (m, 10H, ArH), 5.10 (d *J* 12.4 Hz, 1H, OCH_2Ph), 5.06 (d *J* 12.4 Hz, 1H, OCH_2Ph), 4.65 (dd *J* 7.8, 6.2 Hz, 1H, Phe-NCH), 4.39 (q *J* 7.2 Hz, 1H, Ala-NCH), 3.86-3.78 (m, 1H, Leu-NCH), 3.10 (dd *J* 13.8, 6.1 Hz, 1H, CH_2Ph), 2.99 (dd *J* 13.8, 6.1 Hz, 1H, CH_2Ph), 1.71-1.55 (m, 3H, Leu-CH_2CHMe$_2$), 1.29 (d *J* 7.2 Hz, 3H, NCHCH_3), 0.95 (d *J* 6.0 Hz, 3H, CH(CH_3)$_2$), 0.93 (d *J* 6.0 Hz, 3H, CH(CH_3)$_2$); **^{13}C NMR** (100 MHz, CD_3OD): δ = 174.3 (C=O), 172.6 (C=O), 172.5 (C=O), 137.8 (ArC), 136.9 (ArC), 130.3 (ArCH), 129.5 (ArCH), 129.5 (ArCH), 129.4 (ArCH), 127.9 (ArCH), 68.1 (OCH_2Ph), 55.4 (Phe-NCH), 52.8 (Ala-NCH), 50.0 (Leu-NCH), 41.7 (*C*H$_2$CHMe$_2$), 38.3 (CH_2Ph), 25.3 (*C*HMe$_2$), 23.1 (CH(*C*H$_3$)$_2$), 22.0 (CH(*C*H$_3$)$_2$), 18.3 (NCH*C*H$_3$); **HRMS (ESI)** *m*/*z* calculated for $C_{25}H_{33}N_3NaO_4$ 462.2369 (M-CF_3COO^-+Na)$^+$, found 462.2363, 3.2 ppm error.

TFA·H-Gly-Leu-Phe-OBn 2.106b

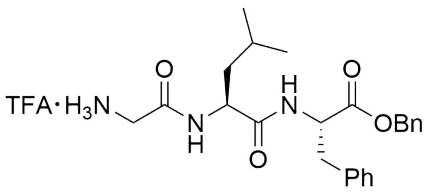

Boc-Gly-Leu-Phe-OBn **2.105b** (200 mg, 0.38 mmol) was deprotected according to the general procedure for Boc deprotections to give TFA·H-Gly-Leu-Phe-OBn **2.106b** as an off white solid (192 mg, 94%).[249] **m.p.** 185-186 °C; **[α]$^{23}_{D}$** = − 28.4 (*c* 0.5 in MeOH); **IR (Neat)** ν_{max} 3405 (w), 3277 (w), 2955 (w), 1721 (m), 1693 (m), 1641 (s) and 1528 (m) cm^{-1}; **^{1}H NMR** (400 MHz, DMSO-d_6): δ = 7.34-7.29 (m, 3H, ArH), 7.27-7.23 (m, 2H, ArH), 7.22-7.18 (m, 2H, ArH), 7.17-7.13 (m, 3H, ArH), 5.10 (d *J* 12.0 Hz, 1H, OCH_2Ph), 5.06 (d *J* 12.0 Hz, 1H, OCH_2Ph), 4.65 (dd *J* 8.0, 6.4 Hz, 1H, Phe-NCH), 4.42 (dd *J* 8.0, 6.8 Hz, 1H, Leu-NCH), 3.68 (d, *J* 16.0 Hz, 1H, Gly-NCH_2), 3.62 (d, *J* 16.0 Hz, 1H, Gly-NCH_2), 3.12 (dd *J* 14.0, 6.0 Hz, 1H,

CH_2Ph), 2.99 (dd *J* 14.0, 8.4 Hz, 1H, CH_2Ph), 1.62 (non *J* 6.8 Hz , 1H, $CHMe_2$), 1.53-1.42 (m, 2H, CH_2CHMe_2), 0.87 (d *J* 8.8, 6.4 Hz, 3H, $CH(CH_3)_2$), 0.85 (d *J* 8.8, 6.4 Hz, 3H, $CH(CH_3)_2$); **^{13}C NMR** (100 MHz, DMSO-d_6): δ = 174.5 (C=O), 172.6 (C=O), 167.0 (C=O), 138.0 (ArC), 136.9 (ArC), 130.3 (ArCH), 129.6 (ArCH), 129.5 (ArCH), 129.4 (ArCH), 127.9 (ArCH), 68.1 (CH_2Ph), 55.5 (Phe-NCH), 53.0 (Leu-NCH), 42.2 (CH_2CHMe_2), 41.4 (Gly-NCH_2), 38.2 (CH_2Ph), 25.8 ($CHMe_2$), 23.4 ($CH(CH_3)_2$), 21.9 ($CH(CH_3)_2$); **HRMS (ESI)** *m/z* calculated for $C_{24}H_{32}N_3O_4$ 426.2387 $(M\text{-}CF_3COO^-)^+$, found 426.2374, 2.6 ppm error.

TFA·H-Ser(OBn)-Met-Val 2.106c

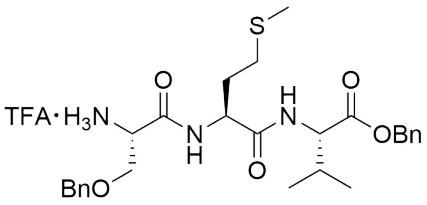

Boc-Ser(OBn)-Met-Val-OBn **2.105c** (300 mg, 0.49 mmol) was deprotected according to the general procedure for Boc deprotections to give TFA·H-Ser(OBn)-Met-Val-OBn **2.106c** as an off-white solid (257 mg, 84%). **m.p.** 137-138 °C; **IR (Neat)** ν_{max} 3274 (w), 3035 (w), 2922 (w), 2964 (w), 1728 (m), 1671 (s), 1644 (s) and 1553 (s) cm^{-1}; **^{1}H NMR** (400 MHz, DMSO-d_6): δ = 8.69 (d, *J* 8.1 Hz, 1H, Met-NH), 8.38 (d *J* 7.7 Hz, 1H, Val-NH), 8.18 (br, 3H, NH_3^+), 7.43-7.24 (m, 10H, ArH), 5.15 (d *J* 12.4 Hz, 1H, CO_2CH_2Ph), 5.10 (d *J* 12.4 Hz, 1H, CO_2CH_2Ph) 4.66-4.53 (m, 1H, Met-NCH), 4.53 (d *J* 7.7 Hz, 1H, OCH_2Ph), 4.49 (d *J* 7.7 Hz, 1H, OCH_2Ph), 4.20 (dd *J* 7.9, 6.1 Hz, Val-NCH), 4.09 (dd *J* 6.3, 3.9 Hz, 1H, Ser-NCH), 3.75 (dd *J* 10.7, 4.1 Hz, 1H, CH_2OBn), 3.67 (dd *J* 10.7, 4.1 Hz, 1H, CH_2OBn), 2.49-2.36 (m, 2H, CH_2SMe), 2.12-2.02 (m, 1H, $CHMe_2$), 2.01 (s, 3H, SCH_3), 1.97-1.72 (m, 2H, CH_2CH_2SMe), 0.86 (d *J* 6.8 Hz, 3H, $CH(CH_3)_2$), 0.85 (d *J* 6.8 Hz, 3H, $CH(CH_3)_2$); **^{13}C NMR** (100 MHz, DMSO-d_6): δ = 171.2 (C=O), 170.9 (C=O), 166.4 (C=O), 137.6 (ArC), 135.9 (ArC), 128.5 (ArCH), 128.3 (ArCH), 128.2 (ArCH), 128.1 (ArCH), 127.8 (ArCH), 72.5 (CH_2OCH_2Ph), 68.5 (CH_2OBn), 66.0 (CO_2CH_2Ph), 57.6 (Val-NCH), 52.4 (Ser-NCH), 51.9 (Met-NCH), 32.4 (CH_2CH_2SMe), 29.7 ($CHMe_2$), 29.3 (CH_2SMe), 18.9 ($CH(CH_3)_2$), 18.1 ($CH(CH_3)_2$), 14.6 (SCH_3); **HRMS (ESI)** *m/z* calculated for $C_{27}H_{38}N_3O_5S$ 516.2532 $(M\text{-}CF_3COO^-)^+$, found 516.2527, 1.8 ppm error.

TFA·H-Trp-Asp(OBn)-Val-OBn 2.106d

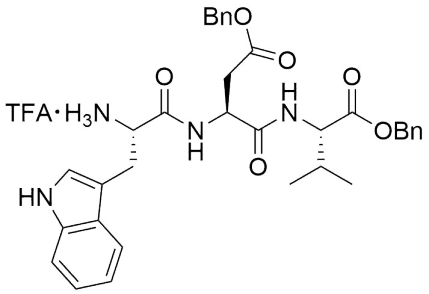

Boc-Trp-Asp(OBn)-Val-OBn **2.105d** (100 mg, 0.14 mmol) was deprotected according to the general procedure for Boc deprotections to give TFA·H-Trp-Asp(OBn)-Val-OBn **2.106d** as a yellow solid (102 mg, 99%). **m.p.** 78-79 °C; **[α]$^{23}_{D}$** = − 27.0 (*c* 0.5 in MeOH); **IR (Neat)** ν_{max} 3313 (m), 3032 (w), 2938 (w), 1693 (s), 1655 (s) and 1514 (s) cm^{-1}; **^{1}H NMR** (400 MHz, CD_3OD): δ = 7.67 (d *J* 7.9 Hz, 1H, ArH), 7.42-7.20 (m, 12H, ArH), 7.17-7.11 (m, 1H, ArH), 7.09-7.03 (m, 1H, ArH), 5.17 (d *J* 12.1 Hz, 1H, OCH_2Ph), 5.12 (s, 2H, OCH_2Ph), 5.09 (d *J* 12.1 Hz, 1H, OCH_2Ph), 4.91-4.86 (m, 1H, Asp-NCH), 4.34 (d *J* 5.5 Hz, 1H, Val-NCH), 4.19-4.12 (m, 1H, Trp-NCH), 3.44 (dd *J* 15.1, 5.3 Hz, 1H, Trp-CH_2), 3.18 (dd *J* 15.1, 8.7 Hz, 1H, Trp-CH_2), 2.87 (dd *J* 16.7, 5.7 Hz, 1H, CH_2CO_2), 2.76 (dd *J* 16.7, 7.9 Hz, 1H, CH_2CO_2), 2.14 (oct *J* 6.8 Hz, 1H, $CHMe_2$), 0.93 (d *J* 6.6 Hz, 3H, $CH(CH_3)_2$), 0.91 (d, *J* 6.6 Hz, 3H, $CH(CH_3)_2$); **^{13}C NMR** (100 MHz, CD_3OD): δ = 172.5 (C=O), 172.4 (C=O), 171.6 (C=O), 170.2 (C=O), 138.3 (ArC), 137.2 (ArC), 137.1 (ArC), 129.6 (ArCH), 129.6 (ArCH), 129.5 (ArCH), 129.4 (ArCH), 129.3 (ArCH), 128.2 (ArC), 125.7 (ArCH), 122.9 (ArCH), 120.3 (ArCH), 119.1 (ArCH), 112.6 (ArCH), 107.7 (ArC), 68.0 (OCH_2Ph), 67.8 (OCH_2Ph), 59.5 (Val-NCH), 54.7 (Trp-NCH), 51.3 (Asp-NCH), 37.1 (CH_2CO_2), 31.7 ($CHMe_2$), 28.9 (Trp-CH_2), 19.5 ($CH(CH_3)_2$), 18.5 ($CH(CH_3)_2$); **HRMS (ESI)** *m*/*z* calculated for $C_{34}H_{38}N_4NaO_6$ 621.2689 (M-CF_3COO^-+Na)$^+$, found 621.2684, − 4.0 ppm error.

TFA·H-Pro-Aib-Leu-OBn 2.106e

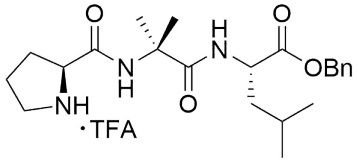

Boc-Pro-Aib-Leu-OBn **2.105e** (200 mg, 0.39 mmol) was deprotected according to the general procedure for Boc deprotections to give TFA·H-Pro-Aib-Leu-OBn **2.106e** as a yellow solid (200 mg, 97%). **m.p.** 105-106 °C; **[α]$^{23}_{D}$** = − 52.7 (*c* 0.5 in MeOH); **IR (Neat)** ν_{max} 3034 (w), 2957 (w), 1735 (m), 1670 (s) and 1645

(m) cm^{-1}; **^{1}H NMR** (400 MHz, DMSO-d_6): δ = 9.50 (br, 1H, NH_2^+), 8.54 (s, 1H, $NHCMe_2$), 8.50 (br, 1H, NH_2^+), 7.90 (d *J* 7.9 Hz, 1H, N*H*CH), 7.41-7.29 (m, 5H, ArH), 5.11 (d *J* 12.5 Hz, 1H, OCH_2Ph), 5.07 (d *J* 12.5 Hz, 1H, OCH_2Ph), 4.37-4.30 (m, 1H, Leu-NCH), 4.18 (dd *J* 8.2, 6.4 Hz, 1H, Pro-NCH), 3.25-3.13 (m, 2H, CH_2N), 2.31-2.20 (m, 1H, 1×Pro-CH_2), 1.99-1.75 (m, 3H, 3×Pro-CH_2), 1.73-1.45 (m, 3H, Leu-CH_2CHMe_2), 1.40 (s, 3H, $C(CH_3)_2$), 1.37 (s, 3H, $C(CH_3)_2$), 0.86 (d *J* 6.4 Hz, 3H, $CH(CH_3)_2$), 0.81 (d *J* 6.4 Hz, 3H, $CH(CH_3)_2$); **^{13}C NMR** (100 MHz, DMSO-d_6): δ = 173.3 (C=O), 172.4 (C=O), 167.6 (C=O), 135.9 (ArC), 128.4 (ArCH), 128.1 (ArCH), 127.9 (ArCH), 65.9 (CH_2Ph), 59.1 (Pro-NCH), 54.5 (Aib-NC), 50.6 (Leu-NCH), 45.9 (CH_2N), 39.8 (CH_2CHMe_2), 29.5 ($CH_2CH_2CH_2N$), 25.0 ($C(CH_3)_2$), 24.5 ($C(CH_3)_2$), 24.1 ($CHMe_2$), 23.5 (CH_2CH_2N), 22.9 ($CH(CH_3)_2$), 21.2 ($CH(CH_3)_2$); **HRMS (ESI)** *m/z* calculated for $C_{22}H_{34}N_3O_4$ 404.2549 $(M\text{-}CF_3COO^-)^+$, found 404.2379, 3.1 ppm error.

Boc-Gly-Leu-Ala-Phe-OBn 2.107a

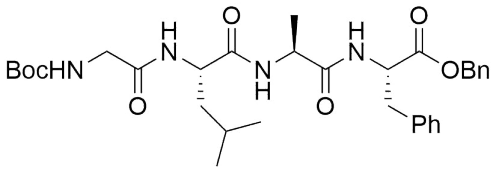

Boc-Gly-OH (44 mg, 0.25 mmol) and TFA·H-Leu-Ala-Phe-OBn **2.106a** (140 mg, 0.25 mmol) were coupled according to the general coupling procedure. The residue was purified using flash column chromatography (95:5, EtOAc:PE) to give Boc-Gly-Leu-Ala-Phe-OBn **2.107a** as a white solid (109 mg, 72%). $\boldsymbol{R_F}$ = 0.31, (95:5, EtOAc:PE); **m.p.** 77-78 °C; $\boldsymbol{[\alpha]^{23}_D}$ = − 22.5 (*c* 1.0 in MeOH); **IR (Neat)** ν_{max} 3278 (m), 3066 (w), 2957 (m), 1742 (m), 1711 (m) and 1634 (s) cm^{-1}; **^{1}H NMR** (400 MHz, $CDCl_3$): δ = 7.40-7.30 (m, 5H, 3×ArCH + Phe-NH + Leu-NH), 7.28-7.23 (m, 2H, ArCH), 7.21-7.14 (m, 4H, 3×ArCH + Ala-NH), 7.07-7.00 (m, 2H, ArCH), 5.46 (br t, 1H, Gly-NH), 5.15 (d *J* 12.4 Hz, 1H, OCH_2Ph), 5.07 (d *J* 12.4 Hz, 1H, OCH_2Ph), 4.96-4.87 (m, 1H, Phe-NCH), 4.75-4.63 (m, 1H, Ala-NCH), 4.63-4.52 (m, 1H, Leu-NCH), 3.89-3.72 (m, 2H, Gly-NCH_2), 3.13 (dd *J* 13.9, 6.0 Hz, 1H, CH_2Ph), 3.04 (dd *J* 13.9, 6.0 Hz, 1H, CH_2Ph), 1.66-1.56 (m, 1H, C*H*Me_2), 1.58-1.49 (m, 2H, CH_2CHMe_2), 1.43 (s, 9H, $OC(CH_3)_3$), 1.32 (d *J* 7.0 Hz, 3H, NCHCH_3), 0.91 (d *J* 6.0 Hz, 3H, $CH(CH_3)_2$), 0.90 (d *J* 6.0 Hz, 3H, $CH(CH_3)_2$); **^{13}C NMR** (100 MHz, $CDCl_3$): δ = 172.2 (C=O), 171.9 (C=O), 171.3 (C=O), 169.4 (C=O), 156.2 (NC=O), 136.0 (ArC), 135.2 (ArC), 129.4 (ArCH), 128.7 (ArCH), 128.6 (ArCH), 128.6 (ArCH), 127.1 (ArCH), 80.3 (O*C*Me_3), 67.3 (OCH_2Ph), 53.5 (Phe-NCH), 51.0 (Leu-NCH), 48.9 (Ala-NCH), 44.3 (Gly-NCH_2), 41.9 (CH_2CHMe_2), 37.9 (CH_2Ph), 28.4 ($C(CH_3)_3$), 23.1 ($CH(CH_3)_2$), 22.2 ($CH(CH_3)_2$), 18.6 (NCHCH_3); **HRMS**

(ESI) m/z calculated for $C_{22}H_{44}N_4NaO_7$ 619.3108 $(M+Na)^+$, found 619.3088, 2.7 ppm error.

Boc-Ala-Gly-Leu-Phe-OBn 2.107b

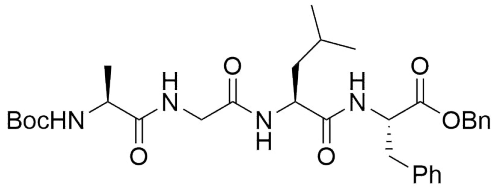

Boc-Ala-OH (35 mg, 0.19 mmol) and TFA·H-Gly-Leu-Phe-OBn **2.106b** (100 mg, 0.19 mmol) were coupled according to the general coupling procedure. The residue was purified using flash column chromatography (80:20, EtOAc:PE) to give Boc-Ala-Gly-Leu-Phe-OBn **2.107b** as a white powder (101 mg, 91%). $\boldsymbol{R_F}$ = 0.49, (80:20, EtOAc:PE); **m.p.** 119-121 °C; $\boldsymbol{[\alpha]^{23}_D}$ = − 21.8 (c 1.0 in MeOH); **IR (Neat)** ν_{max} 3287 (m), 2961 (w), 1718 (m), 1643 (s), 1564 (m) and 1510 (s) cm^{-1}; **^{1}H NMR** (400 MHz, $CDCl_3$): δ = 7.37-7.34 (m, 3H, ArH), 7.30-7.27 (m, 2H, ArH), 7.24-7.20 (m, 3H, ArH), 7.06-7.04 (m, 2H, ArH), 6.79 (t J 6.2 Hz, 1H, Gly-NH), 6.76 (br d, 1H, Phe-NH), 6.70 (d J 6.3 Hz, Leu-NH), 5.16 (d J 12.0 Hz, 1H, OCH_2Ph), 5.09 (d J 12.0 Hz, 1H, OCH_2Ph), 5.08 (br, 1H, Ala-NH), 4.87 (dd J 14.0, 6.4 Hz, 1H, Phe-NCH), 4.43 (dt J 14.0, 8.8 Hz, 1H, Leu-NCH), 4.07 (quin J 6.9 Hz, 1H, Ala-NCH), 3.99 (dd J 14.0, 6.4 Hz, 1H, Gly-NCH_2), 3.79 (dd J 16.8, 5.2 Hz, 1H, Gly-NCH_2), 3.15 (dd J 14.0, 6.0 Hz, 1H, CH_2Ph), 3.06 (dd J 14.0, 6.8 Hz, 1H, CH_2Ph), 1.69-1.52 (m, 2H, CH_2CHMe_2), 1.50-1.37 (m, 1H, CHMe_2), 1.44 (s, 9H, OC$(CH_3)_3$), 1.32 (d J 6.8 Hz, 3H, NCHCH_3), 0.87 (d J 6.8 Hz, 3H, CH(CH_3)$_2$), 0.85 (d J 6.8 Hz, 3H, CH(CH_3)$_2$); **^{13}C NMR** (100 MHz, $CDCl_3$): δ = 173.7 (C=O), 171.8 (C=O), 171.5 (C=O), 169.0 (C=O), 155.8 (NC=O), 136.0 (ArC), 135.2 (ArC), 129.5 (ArCH), 128.7 (ArCH), 128.6 (ArCH), 128.5 (ArCH), 127.0 (ArCH), 77.4 (OCMe_3), 67.4 (OCH_2Ph), 53.4 (Phe-NCH), 52.0 (Leu-NCH), 50.7 (Ala-NCH), 43.3 (Gly-NCH_2), 40.1 (CH$_2$CHMe_2), 37.9 (CH_2Ph), 28.5 (OC(CH$_3$)$_3$), 24.8 (CHMe_2), 22.9 (CH(CH$_3$)$_2$), 22.1 (CH(CH$_3$)$_2$), 18.3 (NCHCH$_3$); **HRMS (ESI)** m/z calculated for $C_{32}H_{44}N_4NaO_7$ 619.3108 $(M+Na)^+$, found 619.3098, 1.0 ppm error.

Boc-Lys(Z)-Ser(OBn)-Met-Val-OBn 2.107c

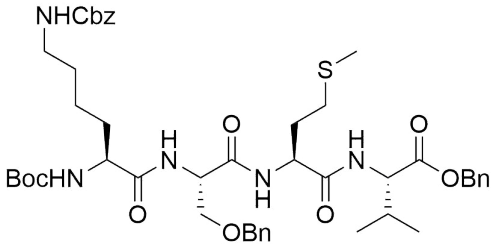

Boc-Lys(Z)-OH (61 mg, 0.16 mmol) and TFA·H-Ser(OBn)-Met-Val-OBn **2.106c** (100 mg, 0.16 mmol) were coupled according to the general coupling procedure. The residue was then purified using flash column chromatography (60:40-70:30, EtOAc:PE) to give Boc-Lys(Z)-Ser(OBn)-Met-Val-OBn **2.107c** as a white solid (91 mg, 65%). $\boldsymbol{R_F}$ = 0.44, (70:30, EtOAc:PE); **m.p.** 75-76 °C; $\boldsymbol{[\alpha]^{23}_D}$ = 23.77 (*c* 1.0 in MeOH); **IR (Neat)** ν_{max} 3282 (w), 2930 (w), 1689 (m), 1635 (s) and 1519 (s) cm^{-1}; **^{1}H NMR** (400 MHz, $CDCl_3$): δ = 7.46 (d *J* 8.3 Hz, 1H, Met-NH), 7.40-7.21 (m, 15H, ArH), 7.06-6.93 (m, 2H, Ser-NH + Val-NH), 5.64 (d *J* 3.2 Hz, 1H, Lys-NH), 5.18 (d *J* 11.8 Hz, 1H, CO_2CH_2Ph), 5.15-5.04 (m, 4H, Lys-ε-NH + 3×CO_2CH_2Ph), 4.69 (dt *J* 8.6, 5.1 Hz, 1H, Met-NCH), 4.54 (d *J* 11.7 Hz, 1H, OCH_2Ph), 4.51 (d *J* 11.7 Hz, 1H, OCH_2Ph), 4.51-4.42 (m, 2H, Val-NCH, Ser-NCH), 4.07-3.99 (m, 1H, CH_2OBn), 3.96-3.88 (m, 1H, Lys-NCH), 3.59 (dd, *J* 9.5, 4.6 Hz, 1H, CH_2OBn), 3.30-3.09 (m, 2H, CH_2NH), 2.51 (t *J* 7.5 Hz, 2H, CH_2SMe), 2.37-2.23 (m, 1H, CH_2CH_2SMe), 2.20-2.10 (m, 1H, $CHMe_2$), 2.04 (s, 3H, SCH_3), 1.97-1.79 (m, 2H, CH_2CH_2SMe + $(CH_2)_3$), 1.74-1.61 (m, 1H, $(CH_2)_3$), 1.56-1.36 (m, 4H, $(CH_2)_3$), 1.35 (s, 9H, $OC(CH_3)_3$), 0.90 (d *J* 6.9 Hz, $CH(CH_3)_2$), 0.89 (d *J* 6.6 Hz, $CH(CH_3)_2$); **^{13}C NMR** (100 MHz, $CDCl_3$): δ = 172.6 (C=O), 171.4 (C=O), 171.1 (C=O), 170.0 (C=O), 157.3 (C=O), 156.8 (NC=O), 137.3 (ArC), 136.5 (ArC), 135.7 (ArC), 128.7 (ArCH), 128.6 (ArCH), 128.4 (ArCH), 128.3 (ArCH), 128.2 (ArCH), 128.1 (ArCH), 128.0 (ArCH), 80.9 ($OCMe_3$), 73.6 (OCH_2Ph), 69.0 (CH_2OBn), 66.9 (2×CO_2CH_2Ph), 57.7 (Val-NCH), 55.9 (Lys-NCH), 54.0 (Ser-NCH), 52.7 (Met-NCH), 39.0 ($(CH_2)_4$), 31.1 ($(CH_2)_4$), 31.0 ($CHMe_2$), 30.5 ($(CH_2)_4$), 30.5 (CH_2SMe), 29.7 (CH_2CH_2SMe), 28.3 ($OC(CH_3)_3$), 22.4 ($(CH_2)_4$), 19.1 ($CH(CH_3)_2$), 18.1 ($CH(CH_3)_2$), 15.2 (SCH_3); **HRMS (ESI)** *m/z* calculated for $C_{46}H_{63}N_5NaO_{10}S$ 900.4193 $(M+Na)^+$, found 900.4188, 0.1 ppm error.

Boc-Gln(Trt)-Trp-Asp(OBn)-Val-OBn 2.107d

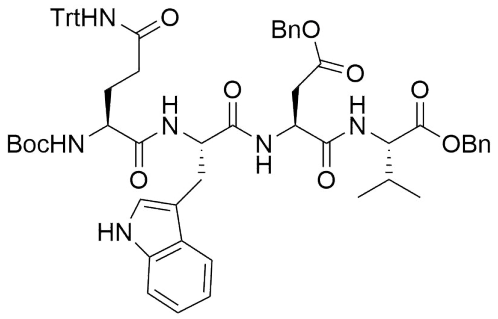

Boc-Gln(Trt)-OH (137 mg, 0.28 mmol) and TFA·H-Trp-Asp(OBn)-Val-OBn **2.106d** (200 mg, 0.28 mmol) were coupled according to the general coupling procedure. The residue was purified using flash column chromatography (50:50, EtOAc:PE) to give Boc-Gln(Trt)-Trp-Asp(OBn)-Val-OBn **2.1067d** as an off white solid (166 mg, 78%). $\boldsymbol{R_F}$ = 0.23, (45:55, EtOAc:PE); **m.p.** 78-79 °C; $\boldsymbol{[\alpha]^{23}_D}$ = − 27.4 (*c* 0.5 in MeOH); **IR (Neat)** ν_{max} 3301 (m), 2967 (w), 1666 (s) and 1513 (s) cm^{-1}; **^{1}H NMR** (400 MHz, $CDCl_3$): δ = 7.82 (s, 1H, NH), 7.54 (d *J* 8.0 Hz, 1H, ArH), 7.38-6.97 (m, 31H, 29×ArH + NH + Asp-NH), 6.93 (d *J* 7.1 Hz, 1H, Val-NH), 6.86 (d *J* 2.4 Hz, 1H, Trp-NH), 5.60 (d *J* 4.9 Hz, 1H, Gln-NH), 5.18 (d *J* 12.2 Hz, 1H, OCH_2Ph), 5.10 (d *J* 12.2 Hz, 1H, OCH_2Ph), 4.98 (s, 2H, OCH_2Ph), 4.79-4.75 (m, 1H, Asp-NCH), 4.56 (dt *J* 6.3, 6.0 Hz, 1H, Trp-NCH), 4.42 (dd *J* 8.7, 4.5 Hz, 1H, Val-NCH), 3.91 (dd *J* 6.2, 6.0 Hz, 1H, Gln-NCH), 3.30 (dd *J* 15.1, 6.2 Hz, 1H, Trp-CH_2), 3.09 (dd *J* 14.5, 6.2 Hz, 1H, Trp-CH_2), 2.49 (dd *J* 16.7, 4.5 Hz, 1H, Gln-CH_2CO), 2.41-2.20 (m, 3H, 1×Gln-CH_2CO + 2×CH_2CO_2Bn), 2.12 (oct *J* 6.7 Hz, 1H, $CHMe_2$), 2.05-1.83 (m, 2H, Gln-CH_2CH_2CO), 1.34 (s, 9H, $OC(CH_3)_3$), 0.85 (d *J* 6.8 Hz, 3H, $CH(CH_3)_2$), 0.82 (d *J* 6.8 Hz, 3H, $CH(CH_3)_2$); **^{13}C NMR** (100 MHz, $CDCl_3$): δ = 172.1 (C=O), 171.6 (C=O), 171.5 (C=O), 171.3 (C=O), 170.3 (C=O), 156.1 (NC=O), 144.6 (ArC), 136.2, (ArC), 136.2 (ArC), 135.7 (ArC), 128.8 (ArCH), 128.7 (ArC), 128.6 (ArCH), 128.4 (ArCH), 128.4 (ArCH), 128.1 (ArCH), 127.3 (ArCH), 127.3 (ArCH), 123.8 (ArCH), 122.3 (ArCH), 119.8 (ArCH), 118.9 (ArCH), 111.3 (ArCH), 109.6 (ArC), 80.2 ($OCMe_3$), 70.9 (CPh_3), 66.9 (OCH_2Ph), 66.7 (OCH_2Ph), 57.8 (Val-NCH), 54.6 (Gln-NCH), 54.2 (Asp-NCH), 49.4 (Trp-NCH), 35.2 (Trp-CH_2), 33.4 (CH_2CH_2CO), 31.0 ($CHMe_2$), 28.5 (CH_2CH_2CO); 28.4 ($C(CH_3)_3$), 27.1 (CH_2CO_2Bn), 19.1 ($CH(CH_3)_2$), 17.8 ($CH(CH_3)_2$); **HRMS (ESI)** *m*/*z* calculated for $C_{63}H_{68}N_6NaO_{10}$ 1091.4895 $(M+Na)^+$, found 1091.4889, − 0.7 ppm error.

Boc-Tyr(OBn)-Pro-Aib-Leu-OBn 2.107e

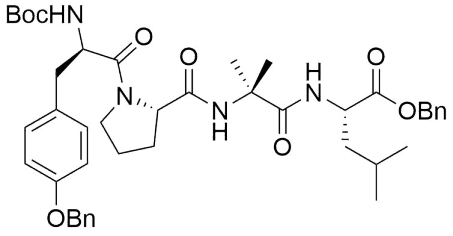

Boc-Tyr(OBn)-OH (71 mg, 0.19 mmol) and TFA·H-Pro-Aib-Leu-OBn **2.106e** (100 mg, 0.19 mmol) were coupled according to the general coupling procedure. The residue was purified using flash column chromatography (5:95, MeOH:CH_2Cl_2) to give Boc-Tyr(OBn)-Pro-Aib-Leu-OBn **2.107e** as a white powder (105 mg, 72%). $\boldsymbol{R_F}$ = 0.21, (4:96, MeOH:CH_2Cl_2); **m.p.** 117-118 °C; $\boldsymbol{[\alpha]^{23}_D}$ = − 23.0 (*c* 0.5 in MeOH); **IR (Neat)** ν_{max} 3318 (w), 2957 (w), 1731 (m), 1682 (s), 1634 (s) and 1510 (s) cm^{-1}; **^{1}H NMR** (400 MHz, DMSO-d_6, 80 °C): δ = 7.81 (s, 1H, Aib-NH), 7.47-7.27 (m, 11H, 10×ArH, + Leu-NH), 7.21-7.10 (m, 2H, ArH), 6.93-6.86 (m, 2H, ArH), 6.38 (br, 1H, Tyr-NH), 5.12 (s, 2H, OCH_2Ph), 5.07 (s, 2H, OCH_2Ph), 4.41-4.29 (m, 3H, 3×NCH), 3.70-3.59 (m, 1H, CH_2N), 3.48-3.88 (m, 1H, CH_2N), 2.96-2.68 (m, 2H, Tyr-CH_2), 2.09-1.93 (m, 2H, CH_2CH_2CH_2N), 1.91-1.78 (m, 1H, CH_2CH_2N), 1.66-1.49 (m, 4H, 1×CH_2CH_2N + CH_2CHMe$_2$), 1.41 (s, 3H, C(CH_3)$_2$), 1.36 (s, 3H, C(CH_3)$_2$), 1.31 (s, 9H, OC(CH_3)$_3$), 0.85 (d *J* 5.9 Hz, 3H, CH(CH_3)$_2$), 0.83 (d *J* 5.9 Hz, 3H, CH(CH_3)$_2$); **^{13}C NMR** (100 MHz, DMSO-d_6, 80 °C): δ = 173.9 (C=O), 172.2 (C=O), 171.1 (C=O), 170.5 (C=O), 156.9 (NC=O), 155.2 (ArC), 137.2 (CAr), 135.9 (ArC), 130.4 (ArCH), 129.8 (ArC), 128.4 (ArCH), 128.0 (ArCH), 127.8 (ArCH), 127.7 (ArCH), 127.6 (ArCH), 127.5 (ArCH), 114.4 (ArCH), 78.1 (OCMe$_3$), 69.1 (OCH_2Ph), 65.8 (OCH_2Ph), 60.1 (NCH), 55.9 (NCH), 54.0 (NCH), 50.7 (NCMe$_2$), 49.9 (CH_2N), 39.6 (*C*H_2CH_2CH_2N), 35.5 (Tyr-CH_2), 28.7 (CH_2*C*HMe$_2$), 28.2 (*C*HMe$_2$), 28.1 (OC(*C*H_3)$_3$), 25.9 (C(*C*H_3)$_2$), 24.8 (CH_2*C*H_2CH_2N), 24.1 (OC(*C*H_3)$_2$), 22.5 (CH(*C*H_3)$_2$), 21.8 (CH(*C*H_3)$_2$); **HRMS (ESI)** *m*/*z* calculated for $C_{43}H_{56}N_4NaO_8$ 779.3996 $(M+Na)^+$, found 779.4010, − 2.4 ppm error.

Boc-Leu-Ala-Phe-OH 2.109

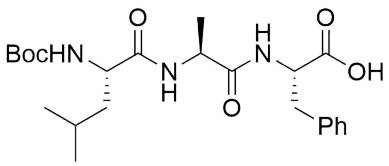

A solution of Boc-Leu-Ala-Phe-OBn **2.106a** (325 mg, 0.6 mmol, 1.0 eq) in methanol (5 mL) was added to a suspension of Pd/C (10% w/w) in methanol (5 mL)

under H_2 (1 bar). The resulting mixture was stirred at room temperature for 16 h. The reaction mixture was then filtered through a short plug of Celite® and concentrated in vacuo to give Boc-Leu-Ala-Phe-OH **2.109** as an off-white solid (258 mg, 96%).[251] **m.p.** 82-83 °C; **[α]$^{23}_{D}$** = − 13.5 (*c* 1.0 in MeOH); **IR (Neat)** ν_{max} 3300 (m), 2958 (m), 1644 (s) and 1514 (m) cm^{-1}; **^{1}H NMR** (400 MHz, CD_3OD): δ = 7.24-7.13 (m, 5H, ArH), 4.58 (dd *J* 7.6, 5.3 Hz, 1H, Leu-NCH), 4.33 (dt *J* 7.1, 6.8 Hz, 1H, Phe-NCH), 4.10-4.01 (m, 1H, Ala-NCH), 3.15 (dd *J* 13.9, 5.4 Hz, 1H, CH_2Ph), 2.97 (dd *J* 13.9, 5.4 Hz, 1H, CH_2Ph), 1.64 (sept *J* 6.7 Hz, 1H, C*H*Me$_2$), 1.45 (t *J* 7.2 Hz, 2H, C*H*$_2$CHMe$_2$), 1.40 (s, 9H, OC(CH$_3$)$_3$), 1.28 (d *J* 7.1 Hz, 3H, NCHC*H*$_3$), 0.90 (d, *J* 6.7 Hz, 3H, CH(C*H*$_3$)$_2$), 0.88 (d *J* 6.7 Hz, 3H, CH(C*H*$_3$)$_2$); **^{13}C NMR** (100 MHz, CD_3OD): δ = 175.3 (C=O), 174.5 (C=O), 174.4 (C=O), 157.9 (NC=O), 138.2 (ArC), 130.4 (ArCH), 129.4 (ArCH), 127.8 (ArCH), 80.6 (O*C*Me$_3$), 55.2 (Leu-NCH), 54.3 (Ala-NCH), 50.1 (Phe-NCH), 42.1 (*C*H$_2$CHMe$_2$), 38.4 (CH_2Ph), 28.7 (OC(*C*H$_3$)$_3$), 25.9 (CHMe$_2$), 23.5 (CH(*C*H$_3$)$_2$), 21.8 (CH(*C*H$_3$)$_2$), 18.4 (NCH*C*H$_3$); **HRMS (ESI)** *m*/*z* calculated for $C_{23}H_{35}N_3NaO_6$ 472.2424 (M+Na)$^+$, found 472.2413, 1.2 ppm error.

TFA·H-Leu-Ala-Phe-OH 2.110

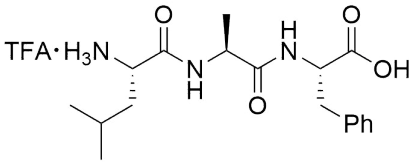

Acid **2.109** (90 mg, 0.2 mmol) was deprotected according to the general procedure for Boc deprotections to give TFA·H-Leu-Ala-Phe-OH **2.110** as a white solid (90 mg, 97%).[252] **m.p.** 189-191 °C; **IR (Neat)** ν_{max} 3265 (w), 3036 (w), 3967 (w), 2401 (w), 2344 (w), 1735 (m), 1646 (s), 1555 (w) and 1514 (w) cm^{-1}; **^{1}H NMR** (400 MHz, TFA-d): δ = 7.20-7.09 (m, 3H, ArH), 7.07-7.00 (m, 2H, ArH), 5.01-4.85 (m, 1H, Phe-NCH), 4.65-4.48 (m, 1H, Ala-NCH), 4.28-4.12 (m, 1H, Leu-NCH), 3.23 (dd *J* 14.3, 4.3 Hz, 1H, CH_2Ph), 3.01 (dd *J* 14.3, 8.5 Hz, 1H, CH_2Ph), 1.78-1.51 (m, 3H, Leu-CH$_2$CHMe$_2$), 1.32 (d *J* 6.3 Hz, 3H, NCHC*H*$_3$), 0.87 (d *J* 6.0 Hz, 3H, CH(C*H*$_3$)$_2$), 0.85 (d *J* 6.0 Hz, 3H, CH(C*H*$_3$)$_2$); **^{13}C NMR** (100 MHz, TFA-d): δ = 178.9 (C=O), 176.0 (C=O), 172.1 (C=O), 136.6 (ArC), 131.0 (ArCH), 131.0 (ArCH), 129.9 (ArCH), 56.2 (Phe-NCH), 55.8 (Leu-NCH), 52.5 (Ala-NCH), 42.4 (*C*H$_2$CHMe$_2$), 39.0 (CH_2Ph), 26.5 (CH$_2$*C*HMe$_2$), 23.2 (CH(*C*H$_3$)$_2$), 22.2 (CH(*C*H$_3$)$_2$), 18.8 (NCH*C*H$_3$); **HRMS (ESI)** *m*/*z* calculated for $C_{18}H_{28}N_3O_4$ 350.2080 (M+H)$^+$, found 350.2076, − 0.8 ppm error.

7.2.2 Solid-Phase Peptide Synthesis

7.2.2.1 General Procedure for Solid-Phase Peptide Synthesis in PC

The synthesis of peptides upon a solid-support was carried out in a 5 mL syringe fitted with a polypropylene frit. Preloaded ChemMatrix-HMPB resin (200 mg, 0.6 mmol g^{-1}) was first washed with PC (3 × 5 mL) and then swollen in PC (3.5 mL) for 1 h. In a separate vial, an Fmoc-amino acid (0.36 mmol, 3.0 eq.), HBTU (137 mg, 0.36 mmol, 3.0 eq.), HOBt (49 mg, 0.36 mmol, 3.0 eq.) and DIPEA (125 μL, 0.72 mmol, 6.0 eq.) were combined in PC (3.6 mL). After 3 min, this preactivated amino acid solution was added to the resin. Coupling reactions were performed for 1 h at ambient temperature and carried out in duplicate. Following each coupling reaction the resin was washed using PC (3 × 5 mL). Fmoc-deprotections were performed in duplicate (10 min followed by 20 min) using a freshly prepared solution of 20% (v/v) piperidine in PC (10-12 mL g^{-1}). Following deprotection the resin was washed using PC (3 × 5 mL). Once the full sequence was constructed and the final Fmoc-deprotection had been performed, the resin was washed using PC (3 × 5 mL) and 2-MeTHF (3 × 5 mL), and dried under reduced pressure. The peptide was then cleaved from the resin using TFA:TIPS:H_2O (95:2.5:2.5) (8-10 mL g^{-1}) for 2 h at ambient temperature. The resin was removed by filtration and the peptide precipitated into cold Et_2O, triturated and lyophilised.

7.2.2.2 Kaiser Test

Three reagent solutions were prepared according to the following protocol:
Reagent A: KCN (16.5 mg) was dissolved in 25 mL of deionised water. 1.0 mL of this solution was then diluted in 49 mL of pyridine.
Reagent B: Ninhydrin (1.0 g) was dissolved in 20 mL of *n*-butanol.
Reagent C: Phenol (40 g) was dissolved in 20 mL of *n*-butanol.
A sample of resin (10-15 beads) was then treated with 5 drops of each solution in a test tube. The mixture was heated at 110 °C for 5 min. A colour change from pale green/yellow to dark blue/purple signifies the presence of a free primary amine.

7.2.2.3 Chloranil Test

Two reagent solutions were prepared according to the following protocol:
Reagent A: Acetaldehyde (1 mL) was mixed with 49 mL of DMF
Reagent B: Chloranil (1 g) was dissolved in 49 mL of DMF
A sample of resin (10-15 beads) was then treated with a drop of each solution in a test tube. The mixture was allowed to stand at room temperature for 5 min. A

colour change from yellow/orange to dark blue/purple indicates the presence of a free secondary amine.

7.2.2.4 Solid-Phase Synthesis of TFA·H-Leu-Ala-Phe-OH 2.110

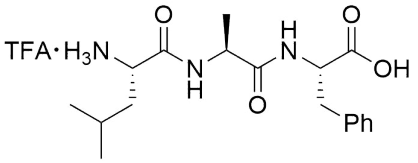

This tripeptide was prepared using the general method for solid-phase synthesis starting with ChemMatrix-HMPB-Phe-H resin and adding Fmoc-amino acids in the sequence Fmoc-Ala-OH then Fmoc-Leu-OH. TFA·H-Leu-Ala-Phe-OH **2.110** prepared in this way had identical analytical data to that prepared by solution phase synthesis.

7.2.2.5 Solid-Phase Synthesis of Bradykinin 2.112

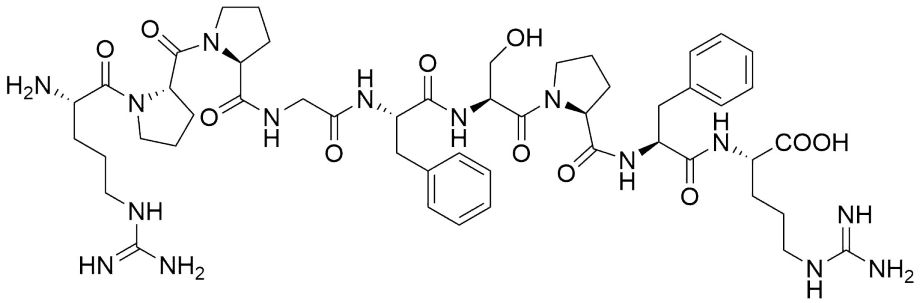

This nonapeptide was prepared using the general method for solid-phase synthesis using ChemMatrix-HMPB-Arg(Pbf)-H resin and adding Fmoc-amino acids in the sequence Fmoc-Phe-OH, Fmoc-Pro-OH, Fmoc-Ser(Bn)-OH, Fmoc-Phe-OH, Fmoc-Gly-OH, Fmoc-Pro-OH, Fmoc-Pro-OH and Fmoc-Arg(Pbf)-OH. After each step, successful coupling or deprotection was confirmed using either the chloranil or Kaiser colormetric tests. After cleavage from the resin, the peptide was precipitated into cold Et_2O, triturated (3 × 20 mL Et_2O) and lyophilized to give Bradykinin **2.112** as a white powder. Reverse phase HPLC retention time 11.8 min. **MS (ESI)** m/z 1060.6 $(M+H)^+$, 710.4, 642.3, 555.3, 530.8 $(M+2H)^{2+}$; **HRMS (ESI)** m/z calculated for $C_{50}H_{75}N_{15}O_{11}$ 530.787976 $(M+2H)^{2+}$, found 530.786911, − 2.0 ppm error.

7.3 Greener Solvents for Solid-Phase Synthesis

7.3.1 Determination of Resin Swelling

Resin (100 mg) was accurately weighed into a 2 mL syringe fitted with a polypropylene disc (void volume = 0.12 mL). Solvent (2 mL) was added and the syringe agitated for 1 h at room temperature. The solvent was removed by compressing the syringe piston. The resin was then allowed to return to its maximum volume by slowly withdrawing the piston. The volume was recorded and the degree of swelling calculated using the following formula:

$$\text{Degree of swelling (mL g}^{-1}) = 10 \times (\text{measured volume} - 0.12)$$

7.3.2 Synthesis of α-Amide 3.52

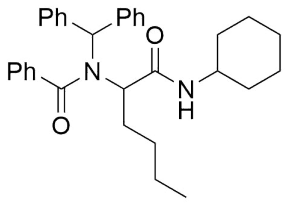

To MeOH or 2-MeTHF (1.5 mL) was added benzhydrylamine (207 μL, 1.2 mmol) and pentanal (128 μL, 1.2 mmol). The resulting solution was agitated at 28 °C for 10 min. To this solution was added benzoic acid (146.5 mg, 1.2 mmol) in anhydrous MeOH or 2-MeTHF (3 mL) followed by cyclohexyl isocyanide (149 μL, 1.2 mmol). The reaction was agitated for 1.5 h at 28 °C. The mixture was then evaporated *in vacuo* and the residue dissolved in EtOAc (20 mL). The organic solution was washed with 1 M HCl_{aq} (2 × 10 mL), saturated $NaHCO_3$ (2 × 10 mL) and brine (2 × 10 mL), dried (anhydrous $MgSO_4$) and filtered. The organic layer was concentrated *in vacuo* and the residue purified using flash column chromatography (20:80, EtOAc:PE) to give the α-amide **3.52** as a yellow oil (458 mg, 79% in MeOH; 434 mg, 75% in 2-MeTHF). $\boldsymbol{R_F}$ = 0.23, (20:80, EtOAc:PE); **IR (Neat)** ν_{max} 3302 (w), 2928 (s), 2856 (w), 1663 (s), 1617 (m) and 1525 (m) cm^{-1}; **^{1}H NMR** (400 MHz, $CDCl_3$): δ = 8.05 (br, 1H, N-H), 7.45-7.18 (m, 15H, ArH), 6.27 (s, 1H, $NCHPh_2$), 3.81-3.80 (m, 1H, NCHC=O), 3.66-3.57 (m, 1H, NHCH), 1.83-1.51 (m, 6H, $(CH_2)_3Me$), 1.40-0.99 (m, 10H, $(CH_2)_5$), 0.76 (t *J* 7.1 Hz, 3H, CH_3); **^{13}C NMR** (100 MHz, $CDCl_3$): δ = 174.3, 171.0, 137.2, 130.2, 129.3, 128.9, 128.7, 128.6, 128.2, 126.3, 77.4, 64.9, 47.6, 32.7, 32.6, 31.4, 29.1, 25.8, 24.6, 24.5, 22.5, 13.9; **HRMS (ESI)** *m/z* calculated for $C_{32}H_{38}N_2NaO_2$ 505.2820 $(M+Na)^+$, found 505.2825, − 1.5 ppm error.

7.3.3 Deprotection of α-Amino Amide 3.52

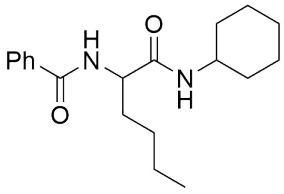

TFA (2 mL) was added to amide **3.52** (100 mg, 0.2 mmol) and the solution agitated for 4 h at room temperature. The reaction mixture was evaporated *in vacuo* and the residue purified using flash column chromatography (30:70, EtOAc:PE) to give compound **3.53** as a white solid (44 mg, 67%). $\boldsymbol{R_F}$ = 0.25, (30:70, EtOAc:PE); **m.p.** 163-164 °C; **IR (Neat)** ν_{max} 3264 (m), 3080 (w), 2934 (m), 2858 (w), 1659 (w) and 1551 (m) cm^{-1}; **^{1}H NMR** (400 MHz, $CDCl_3$): δ = 7.84-7.81 (m, 2H, ArH), 7.52-7.39 (m, 3H, ArH), 7.20 (d *J* 7.2 Hz, 1H, NH), 6.66 (d *J* 6.7 Hz, 1H, NH), 4.65 (dd *J* 14.7, 7.0 Hz, 1H, NCHCO), 3.80-3.71 (m, 1H, NCH), 1.93-1.56 (m, 6H, $(CH_2)_3Me$), 1.40-1.09 (m, 10H, $(CH_2)_5$), 0.85 (t *J* 7.0 Hz, 3H, CH_3); **^{13}C NMR** (100 MHz, $CDCl_3$): δ = 170.8, 167.1, 134.0, 131.6, 128.5, 127.1, 53.6, 48.3, 33.0, 32.8 (2 peaks), 32.7, 27.6, 25.4, 24.7, 22.5, 13.9; **HRMS (ESI)** *m/z* calculated for $C_{19}H_{28}N_2NaO_2$ 339.2040 $(M+Na)^+$, found 339.2043, 1.1 ppm error.

7.3.4 Solid-Supported Synthesis of α-Amino Amide 3.56

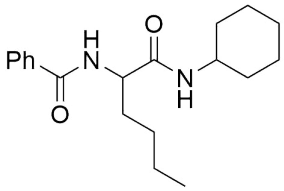

Resin with an Fmoc-protected Rink Linker (100 mg, Merrifield 1.0 mmol g^{-1}; ChemMatrix 0.49 mmol g^{-1}) was allowed to swell in DMF (2 mL) for 30 min. Then, a 20% (*v*/*v*) solution of piperidine in DMF (2 mL) was added and the resin agitated for 10 min. The resin was filtered and treated a second time with a 20% solution of piperidine in DMF (2 mL) for 10 min. The deprotected resin was then filtered, washed with DMF (2 mL), CH_2Cl_2 (2 mL), and dried under vacuum. A sample was subjected to the Kaiser test to confirm the presence of primary amines. The remaining resin was suspended in MeOH or 2-MeTHF (2 mL) for 30 min. Pentanal (10 eq. based on the resin loading) and cyclohexyl isocyanide (10 eq. based on resin loading) were added and the resin agitated for 18 h. The resin was then washed with DMF (5 × 5 mL), CH_2Cl_2 (5 × 5 mL), and dried under vacuum. The resin was treated with a 30% solution of TFA in CH_2Cl_2 (2 mL) for 3 h at room temperature.

Resin was removed by filtration and the filtrate was concentrated *in vacuo*. The residue was purified by flash column chromatography (30:70, EtOAc:PE) to give compound **3.56** as a white solid in the yields quoted in Table 3.5. Analytical and spectroscopic data were identical to those reported for compound **3.53** prepared by a solution-phase approach.

7.4 ROMP of an Amide Functionalised Oxanorbornene-Lactone

2-[(1*R*,5*S*,7*S*)-4-oxo-3,10-dioxatricyclo-[5.2.1.0^{1,5}]dec-8-en-5-yl]acetic acid 4.7

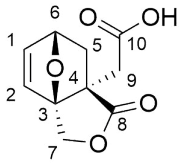

Acid **4.7** was prepared from itaconic anhydride and furfuryl alcohol using either of the procedures described below.

Solvent Free: Itaconic Anhydride (3.0 g, 26.7 mmol, 1.0 eq) was suspended in furfuryl alcohol (2.3 mL, 26.7 mmol, 1.0 eq), the slurry obtained was then allowed to stir at ambient temperature. After *circa* 5 h, the suspension has thickened to a paste and could no longer be stirred. The reaction mixture was left for a further 19 h until a tan solid had formed. The crude material was then purified by recrystallisation from acetone to give the target acid **4.7** as an off-white crystalline solid (3.81 g, 68%).

Reaction Solvent: Itaconic anhydride (25 g, 223 mmol, 1.0 eq) and furfuryl alcohol (19.4 mL, 223 mmol, 1.0 eq) were suspended in acetonitrile (12 mL) and the slurry allowed to stir at ambient temperature, after 24 h a white suspension had formed. The solid was removed by filtration and the filtrate was concentrated *in vacuo*. The concentrated filtrate was suspended in EtOAc (100 mL) and filtered. The solids obtained were combined and recrystallised from acetone, to give the target acid **4.7** as an off-white crystalline solid (19.95g, 43%).[181] **m.p.** 130-132 °C; **IR (Neat)** ν_{max} 3100 (m), 1776 (s) and 1733 (s) cm^{-1}; **^{1}H NMR** (400 MHz, CD_3OD): δ = 6.59 (dd *J* 5.9, 1.7 Hz, 1H, 1-H), 6.55 (d *J* 5.9 Hz, 1H, 2-H), 5.02 (dd *J* 4.7, 1.7 Hz, 1H, 6-H), 4.92 (d *J* 10.8 Hz, 1H, 7-H) 4.54 (d *J* 10.8 Hz, 1H, 7-H), 2.44-2.35 (m, 3H, 5/9-H), 1.55 (d *J* 12.3 Hz, 1H, 5-H); **^{13}C NMR** (100 MHz, CD_3OD): δ = 180.0 (8), 173.0 (10), 139.3 (1), 131.5 (2), 95.6 (3), 80.1 (6), 70.0 (7), 53.3 (4), 40.7 (9), 37.7 (5); **HRMS (ESI)** *m*/*z* calculated for $C_{10}H_{10}NaO_5$ 233.0420 $(M+Na)^+$, found 233.0417, 1.2 ppm error.

7.4.1 Synthesis of Trisubstituted Amides

7.4.1.1 General Procedure for the Synthesis of Trisubstituted Amides

Acid monomer **4.7** (2.0 g, 9.5 mmol) was suspended in anhydrous CH_2Cl_2 (5 mL) under an argon atmosphere. The suspension was cooled to 0 °C and oxalyl chloride

(12.0 mL of 2.0 M solution in CH_2Cl_2, 24.0 mmol) was added dropwise over 10 minutes, followed by DMF (4 drops). The suspension was stirred at ambient temperature until a solution was obtained. The obtained solution was concentrated *in vacuo*, to give a brown solid which was redissolved in anhydrous CH_2Cl_2 (10 mL) and cooled to 0 °C. A solution of disubstituted amine **4.38a-k** (14 mmol) and triethylamine (2.7 mL, 19.0 mmol) (or 5.4 mL, 38.0 mmol if using the TFA salt of amine **4.38a-k**) in CH_2Cl_2 (10 mL) was added dropwise over 10 minutes. The solution was allowed to stir at ambient temperature overnight, then additional CH_2Cl_2 (30 mL) and H_2O (50 mL) were added. The organic layer was separated and further washed with 1M HCl_{aq} (50 mL), 1M $NaHCO_3$ (50 mL), H_2O (50 mL) and brine (50 mL). The organic layer was dried ($MgSO_4$), filtered and concentrated *in vacuo*. The residue was then purified using flash column chromatography.

N,*N*-Dimethyl-2-[(5*S*,7*S*)-4-oxo-3,10-dioxatricyclo[5.2.1.$0^{1,5}$]dec-8-en-5-yl]acetamide 4.39a

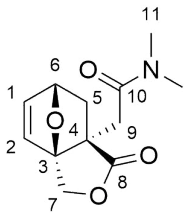

Acid monomer **4.7** (2 g, 9.52 mol) and dimethylamine hydrochloride **4.38a** (0.78 g, 9.52 mol) were coupled according to the general procedure for the synthesis of trisubstituted amides. The crude material was purified using flash column chromatography (0:100-10:90, MeOH:EtOAc) to give the target amide **4.39a** as a pale yellow crystalline solid (1.28 g, 57%). $\boldsymbol{R_F}$ = 0.23, (10:90, MeOH:EtOAc); **m.p.** 128-129 °C; **IR (Neat)** ν_{max} 3067 (w), 2959 (w), 1767 (s), 1633 (s) and 1504 (m) cm^{-1}; **^{1}H NMR** (400 MHz, $CDCl_3$): δ = 6.64 (d *J* 5.5 Hz, 1H, 2-H), 6.45 (dd *J* 5.5, 1.7 Hz, 1H, 1-H), 5.03 (d *J* 10.2 Hz, 1H, 9-H), 4.97 (dd *J* 4.9, 1.7 Hz, 1H, 6-H), 4.50 (d *J* 10.2 Hz, 1H, 9-H), 2.97 (m, 4H, 11-H & 7-H), 2.90 (s, 3H, 11-H), 2.50 (dd *J* 11.8, 4.9 Hz, 1H, 5-H), 2.07 (d *J* 14.4 Hz, 1H, 7-H), 1.30 (d *J* 11.8 Hz, 1H, 5-H); **^{13}C NMR** (100 MHz, $CDCl_3$): δ = 178.8 (8), 168.9 (10), 136.3 (1), 132.2 (2), 94.8 (3), 78.0 (6), 70.3 (9), 52.6 (4), 39.1 (7), 38.1 (11), 37.8 (5), 35.8 (11); **HRMS (ESI)** *m*/*z* calculated for $C_{12}H_{15}NNaO_4$ $(M+Na)^+$ 260.0893, found 260.0891, 1.3 ppm error.

_N_,_N_-diethyl-2-[(5_S_,7_S_)-4-oxo-3,10-dioxatricyclo[5.2.1.0^{1,5}]dec-8-en-5-yl]acetamide 4.39b

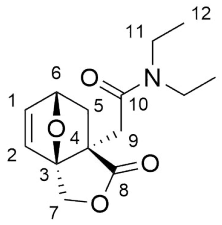

Acid monomer **4.7** (2 g, 9.52 mol) and diethylamine **4.38b** (0.98 mL, 9.52 mol) were coupled according to the general procedure for the synthesis of trisubstituted amides. The crude material was purified using flash column chromatography (90:10, EtOAc:PE) to give the target amide **4.39b** as a pale yellow crystalline solid (2.08 g, 82%). $\boldsymbol{R_F}$ = 0.32, (90:10, EtOAc:PE); **m.p.** 95-96 °C; **IR (Neat)** ν_{max} 2969 (w), 2937 (w), 1758 (s) and 1640 (s) cm^{-1}; **^{1}H NMR** (400 MHz, $CDCl_3$): δ = 6.70 (d *J* 5.9 Hz, 1H, 2-H), 6.45 (dd *J* 5.9, 1.5 Hz, 1H, 1-H), 5.05 (d *J* 9.9 Hz, 1H, 7-H), 4.98 (dd *J* 4.7, 1.4 Hz, 1H, 6-H), 4.50 (d *J* 9.9 Hz, 1H, 7-H), 3.56-3.37 (m, 2H, 11-H), 3.20-3.06 (m, 2H, 11-H), 2.96 (d *J* 14.5 Hz, 1H, 9-H), 2.52 (dd *J* 12.1, 4.7 Hz, 1H, 5-H), 2.01 (d *J* 14.3 Hz, 1H, 9-H), 1.28 (d *J* 12.1 Hz, 1H, 5-H), 1.12 (d *J* 7.0 Hz, 3H, 12-H), 1.09 (d *J* 7.0 Hz, 3H, 12-H); **^{13}C NMR** (100 MHz, $CDCl_3$): δ = 178.8 (8), 168.2 (10), 136.0 (1), 132.6 (2), 94.9 (3), 77.9 (6), 70.5 (7), 53.0 (4), 42.8 (11), 40.7 (11) 38.8 (9), 37.9 (5), 14.5 (12), 13.1 (12); **HRMS (ESI)** *m*/*z* calculated for $C_{16}H_{18}NO_4$ $(M+H)^+$ 288.1230, found 288.1219, 3.7 ppm error.

_N_,_N_-dipropyl-2-[(5_S_,7_S_)-4-oxo-3,10-dioxatricyclo[5.2.1.0^{1,5}]dec-8-en-5-yl]- acetamide 4.39c

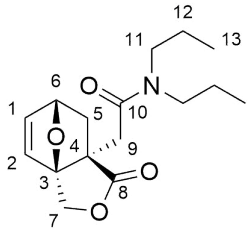

Acid monomer **4.7** (2 g, 9.52 mol) and dipropylamine **4.38c** (1.31 mL, 9.52 mol) were coupled according to the general procedure for the synthesis of trisubstituted amides. The crude material was purified using flash column chromatography (50:50, EtOAc:PE) to give the target amide **4.39c** as a yellow oil (1.59 g, 57%). $\boldsymbol{R_F}$ = 0.32, (70:30, EtOAc:PE); **IR (Neat)** ν_{max} 2965 (w), 2876 (w), 1765 (s) and 1631 (s) cm^{-1}; **^{1}H NMR** (400 MHz, $CDCl_3$): δ = 6.69 (d *J* 5.9 Hz, 1H, 2-H), 6.45 (dd *J* 5.9, 1.6 Hz, 1H, 1-H), 5.04 (d *J* 10.1 Hz, 1H, 7-H), 4.97 (dd *J* 4.7, 1.6 Hz, 1H, 6-H), 4.49

(d *J* 10.1 Hz, 1H, 7-H), 3.52-3.41 (m, 1H, 11-H), 3.38-3.29 (m, 1H, 11-H), 3.05-2.91 (m, 3H, 11-H, 9-H), 2.52 (dd *J* 11.8, 4.7 Hz, 1H, 5-H), 2.00 (d *J* 14.5 Hz, 1H, 9-H), 1.61-1.41 (m, 4H, 12-H), 1.27 (d *J* 11.8 Hz, 1H, 5-H), 0.87 (td *J* 7.6, 2.8 Hz, 6H, 13-H); **^{13}C NMR** (100 MHz, $CDCl_3$): δ = 178.8 (8), 168.6 (10), 135.9 (1), 132.7 (2), 94.9 (3), 77.9 (6), 70.5 (7), 53.0 (4), 50.3 (11), 48.1 (11), 38.9 (9), 37.9 (5), 22.4 (12), 21.0 (12), 11.4 (13), 11.3 (13); **HRMS (ESI)** *m/z* calculated for $C_{16}H_{24}NNaO_4$ $(M+Na)^+$ 316.1519, found 316.1523, −1.4 ppm error.

N,*N*-dibutyl-2-[(5*S*,7*S*)-4-oxo-3,10-dioxatricyclo[5.2.1.0^{1,5}]dec-8-en-5-yl]acetamide 4.39d

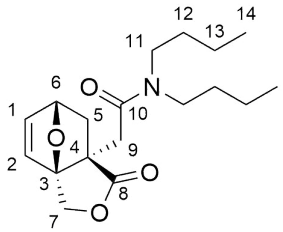

Acid monomer **4.7** (2 g, 9.52 mol) and dibutylamine **4.38d** (1.60 mL, 9.52 mol) were coupled according to the general procedure for the synthesis of trisubstituted amides. The crude material was purified using flash column chromatography (50:50, EtOAc:PE) to give the target amide **4.39d** as a colourless oil (2.33 g, 79%). $\boldsymbol{R_F}$ = 0.32, (50:50, EtOAc:PE); **IR (Neat)** ν_{max} 2958 (w), 2932 (w), 2873 (w), 1765 (s) and 1631 (s) cm^{-1}; **^{1}H NMR** (400 MHz, $CDCl_3$): δ = 6.70 (d *J* 5.6 Hz, 1H, 2-H), 6.45 (dd *J* 5.6, 1.4 Hz, 1H, 1-H), 5.04 (d *J* 10.4 Hz, 1H, 7-H), 4.98 (dd *J* 5.1, 1.7 Hz, 1H, 6-H), 4.50 (d *J* 10.4 Hz, 1H, 7-H), 3.53-3.43 (m, 1H, 11-H), 3.41-3.31 (m, 1H, 11-H), 3.06-2.97 (m, 2H, 11-H), 2.96 (d *J* 14.7 Hz, 1H, 9-H), 2.52 (dd *J* 11.6, 5.1 Hz, 1H, 5-H), 1.99 (d *J* 14.7 Hz, 1H, 9-H), 1.54-1.39 (m, 4H, 12-H), 1.34-1.22 (m, 5H, 13-H, 5-H), 0.91 (t *J* 7.1 Hz, 3H, 14-H), 0.91 (t *J* 7.1 Hz, 3H, 14-H); **^{13}C NMR** (100 MHz, $CDCl_3$): δ = 178.8 (8), 168.5 (10), 135.9 (1), 132.7 (2), 94.9 (3), 77.9 (6), 70.5 (7), 53.0 (4), 48.5 (11), 46.2 (11), 38.9 (5), 37.9 (9), 31.4 (12), 29.9 (12), 20.3 (13), 20.1 (13), 14.0 (14), 13.9 (14); **HRMS (ESI)** calculated for $C_{18}H_{27}NNaO_4$ $(M+Na)^+$ 344.1832, found 344.1818, 3.7 ppm error *m/z*.

N,*N*-Dioctyl-2-[(5*S*,7*S*)-4-oxo-3,10-dioxatricyclo[5.2.1.0^{1,5}]dec-8-en-5-yl]acetamide 4.39e

Acid monomer **4.7** (2 g, 9.52 mol) and dioctylamine **4.38e** (2.88 mL, 9.52 mol) were coupled according to the general procedure for the synthesis of trisubstituted amides. The crude material was purified by flash column chromatography (20:80, EtOAc:PE) to give the target amide **4.39e** as a colourless oil (1.28 g, 31%). $\boldsymbol{R_F}$

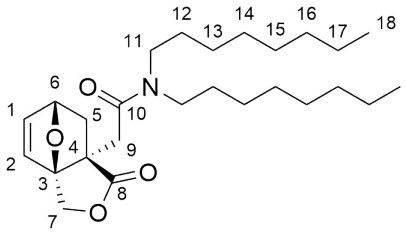

= 0.38, (40:60, EtOAc:PE); **IR (Neat)** ν_{max} 2954 (s), 2924 (s), 2854 (s), 1768 (s) and 1634 (s) cm^{-1}; **^{1}H NMR** (400 MHz, $CDCl_3$): δ = 6.70 (d *J* 5.9 Hz, 1H, 2-H), 6.45 (dd *J* 5.9, 1.8 Hz, 1H, 1-H), 5.03 (d *J* 9.7 Hz, 1H, 7-H), 4.98 (dd *J* 4.9, 1.8 Hz, 1H, 6-H), 4.49 (d *J* 9.7 Hz, 1H, 7-H), 3.54-3.29 (m, 2H, 11-H), 3.06-2.92 (m, 3H, 11-H/9-H), 2.51 (dd *J* 11.7, 4.7 Hz, 1H, 5-H), 1.99 (d *J* 14.4 Hz, 1H, 9-H), 1.57-1.38 (m, 4H, 12-H), 1.35-1.16 (m, 22H, 13-17-H/5-H), 0.88 (d *J* 5.6 Hz, 3H, 18-H), 0.86 (d *J* 6.3 Hz, 3H, 18-H); **^{13}C NMR** (100 MHz, $CDCl_3$): δ = 178.8 (8), 168.5 (10), 135.9 (1), 132.7 (2), 94.9 (3), 77.9 (6), 70.5 (7), 53.0 (4), 48.7 (11), 46.5 (11), 38.9 (9), 37.9 (5), 31.9, 31.9, 29.5, 29.4, 29.4, 29.3, 27.8, 27.1, 26.9, 22.8, 22.7, 14.2 (18), 14.2 (18); **HRMS (ESI)** *m/z* calculated for $C_{26}H_{44}NO_4$ $(M+H)^+$ 434.3265, found 434.3248, 4.8 ppm error.

N,*N*-Bis(2-ethylhexyl)-2-[(5S,7S)-4-oxo-3,10-dioxatricyclo[5.2.1.0^{1,5}]dec-8-en-5-yl] acetamide 4.39f

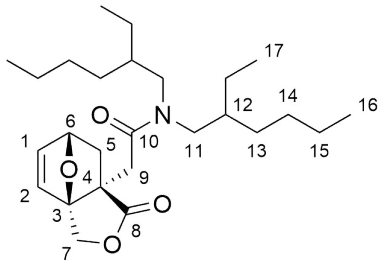

Acid monomer **4.7** (2 g, 9.52 mol) and bis(2-ethylhexyl)amine **4.38f** (2.86 mL, 9.52 mol) were coupled according to the general procedure for the synthesis of trisubstituted amides. The crude material was purified by flash column chromatography (30:70, EtOAc:PE) to give the target amide **4.39f** as a yellow oil, containing a mixture of diastereoisomers (2.87 g, 70%). $\boldsymbol{R_F}$ = 0.33, (30:70, EtOAc:PE); **IR (Neat)** ν_{max} 2957 (m), 2928 (m), 2873 (m), 1769 (s) and 1632 (s) cm^{-1}; **^{1}H NMR** (400 MHz, $CDCl_3$): δ = 6.71-6.65 (m, 1H, 1-H), 6.47-6.41 (m, 1H, 2-H), 5.06-5.00 (m, 1H, 7-H), 4.99-4.95 (m, 1H, 6-H), 4.53-4.44 (m, 1H, 7-H), 3.64-3.51 (m, 1H, 11-H), 3.35-3.20 (m, 1H, 11-H), 3.07-2.91 (m, 2H, 9-H/11-H), 2.88-2.78 (m, 1H, 11-H), 2.55-2.47 (m, 1H, 5-H), 2.04-1.95 (m, 1H, 9-H), 1.67-1.59 (m, 1H, 12-H), 1.54-1.43 (m, 1H, 12-H), 1.37-1.11 (m, 17H, 5-H/13-H/14-H/15-H/17-H), 0.92-0.82 (m, 12H, 16-H/18-H); **^{13}C NMR** (100 MHz, $CDCl_3$): δ = 178.7 (8),

169.4 (10), 135.9 (2), 132.7 (1), 94.9 (3), 77.9 (6), 70.4 (7), 53.1/53.0 (4), 52.6/52.1 (11), 49.7/49.1 (11), 39.5/39.3 (9), 39.0/38.9 (12), 38.0/38.0 (5), 37.4/37.1 (12), 30.6, 30.4, 28.9, 28.8, 23.9, 23.6, 23.4, 23.2, 14.3 (16), 14.2 (16), 11.1/11.0 (18), 10.6/10.5 (18); **HRMS (ESI)** m/z calculated for $C_{26}H_{44}NO_4$ $(M+H)^+$ 434.3265, found 434.3258, 0.5 ppm error.

N,*N*-Dibenzyl-2-[(5*S*,7*S*)-4-oxo-3,10-dioxatricyclo[5.2.1.0^{1,5}]dec-8-en-5-yl]acetamide 4.39g

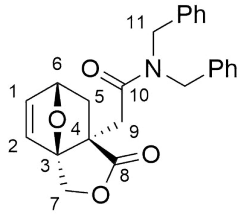

Acid monomer **4.7** (2 g, 9.52 mol) and dibenzylamine **4.38g** (1.83 mL, 9.52 mol) were coupled according to the general procedure for the synthesis of trisubstituted amides. The crude material was purified by flash column chromatography (2:98, MeOH:CH_2Cl_2) to give the target amide **4.39g** as a yellow crystalline solid (1.73 g, 47%). $\boldsymbol{R_F}$ = 0.18, (2:98, MeOH:CH_2Cl_2); **m.p.** 154-155 °C; **IR (Neat)** ν_{max} 3014 (w), 1778 (s), 1636 (s) and 1603 (m) cm^{-1}; **^{1}H NMR** (400 MHz, $CDCl_3$): δ = 7.39-7.24 (m, 6H, Ar-H), 7.24-7.19 (m, 2H, Ar-H), 7.11-7.05 (m, 2H, Ar-H), 6.66 (d *J* 5.8 Hz, 1H, 2-H), 6.43 (dd *J* 5.8, 1.7 Hz, 1H, 1-H), 5.05 (d *J* 10.1 Hz, 1H, 7-H), 5.02-4.96 (m, 2H, 6-H, 11-H), 4.66 (d *J* 17.8 Hz, 1H, 11-H), 4.54 (d *J* 10.1 Hz, 1H, 7-H), 4.29 (d *J* 17.8 Hz, 1H, 11-H), 4.18 (d *J* 14.8 Hz, 1H, 11-H), 3.02 (d *J* 14.8 Hz, 1H, 9-H), 2.52 (dd *J* 12.1, 4.3 Hz, 1H, 5-H), 2.17 (d *J* 14.8 Hz, 1H, 9-H), 1.26 (d *J* 12.1 Hz, 1H, 5-H); **^{13}C NMR** (100 MHz, $CDCl_3$): δ = 178.8 (8), 169.9 (10), 136.6 (ArC), 136.3 (1), 136.1 (ArC), 132.3 (2), 129.1 (ArCH), 128.9 (ArCH), 127.9 (ArCH), 127.9 (ArCH), 127.7 (ArCH), 126.3 (ArCH), 94.8 (3), 78.0 (6), 70.4 (7), 52.9 (3), 50.7 (4), 48.9 (11), 39.2 (9), 37.8 (5); **HRMS (ESI)** m/z calculated for $C_{24}H_{23}NNaO_4$ $(M+Na)^+$ 412.1519, found 412.1505, 4.2 ppm error.

Methyl-(2*S*)-1-[2-[(5*S*,7*S*)-4-oxo-3,10-dioxatricyclo[5.2.1.0^{1,5}]dec-8-en-5-yl]acetyl] pyrrolidine-2-carboxylate 4.39h

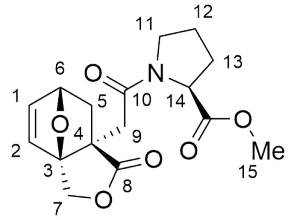

Acid monomer **4.7** (2 g, 9.52 mol) and proline methyl ester hydrochloride **4.38h** (2.30 g, 9.52 mol) were coupled according to the general procedure for the synthesis of trisubstituted amides. The crude material was purified by flash column chromatography (100:0, EtOAc:PE) to give the target amide **4.39h** as a white solid containing a mixture of diastereoisomers (2.47 g, 81%). $\boldsymbol{R_F}$ = 0.24, (100:0, EtOAc:PE); **m.p.** 102-103 °C; **IR (Neat)** ν_{max} 3003 (w), 2957 (w), 1759 (s), 1736 (s) and 1632 (s) cm^{-1}; **^{1}H NMR** (400 MHz, $CDCl_3$): δ = 6.70-6.63 (m, 1H, 2-H), 6.49-6.39 (m, 1H, 1-H), 5.11-4.92 (m, 2H, 6-H/7-H), 4.53-4.38 (m, 2H, 14-H/7-H), 3.74-3.57 (m, 4H, 15-H/11-H), 3.56-3.39 (m, 1H, 11-H), 3.03-2.73 (m, 1H, 9-H), 2.55-2.44 (m, 1H, 5-H), 2.24-1.87 (m, 5H, 9-H/12-H/13-H), 1.40-1.15 (m, 1H, 5-H); **^{13}C NMR** (100 MHz, $CDCl_3$): δ = 178.9/178.6 (8), 172.6/172.2 (15), 167.9/167.8 (10), 136.3/136.0 (1), 132.5/132.3 (2), 94.7/94.6 (3), 78.2/77.0 (6), 70.4/69.8 (7), 59.2/58.8 (14), 52.6/52.6 (4), 52.4/52.3 (16), 47.8 (11), 40.9/39.9 (9), 38.2/37.4 (5), 29.3 (13), 24.9/24.9 (12); **HRMS (ESI)** *m/z* calculated for $C_{16}H_{19}NNaO_6$ $(M+Na)^+$ 344.1105, found 344.1110, 2.0 ppm error.

Benzyl-2-[methyl-[2-[(5*S*,7*S*)-4-oxo-3,10-dioxatricyclo[5.2.1.0^{1,5}]dec-8-en-5-yl]acetyl]amino]acetate 4.39i

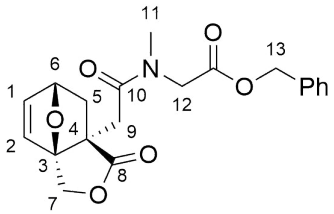

Acid monomer **4.7** (2 g, 9.52 mol) and *N*-methyl glycine benzyl ester hydrochloride **4.38i** (1.92 g, 9.52 mol) were coupled according to the general procedure for the synthesis of trisubstituted amides. The crude material was purified by flash column chromatography (80:20-100:0, EtOAc:PE) to give the target amide **4.39i** as a yellow crystalline solid (1.59 g, 45%). $\boldsymbol{R_F}$ = 0.4, (100:0, EtOAc:PE); **m.p.** 98-99 °C; **IR (Neat)** ν_{max} 2953 (w), 2983 (w), 1764 (s), 1739 (s) and 1641 (s) cm^{-1}; **^{1}H NMR** (400 MHz, $CDCl_3$, major rotamer): δ = 7.40-7.29 (m, 5H, ArH), 6.61 (d *J* 6.0 Hz, 1H, 2-H), 6.46 (dd *J* 6.0, 1.8 Hz, 1H, 1-H), 5.21-5.11 (m, 2H, 14-H), 5.02-4.91 (m, 2H, 6-H, 7-H), 4.47 (d *J* 10.4 Hz, 1H, 7-H), 4.32 (d *J* 17.3 Hz, 1H, 12-H), 3.88 (d *J* 17.3 Hz, 1H, 12-H), 3.06-2.78 (m, 4H, 11-H, 9-H), 2.51 (dd *J* 12.0, 4.6 Hz, 1H, 5-H), 2.17 (d *J* 14.8, 1H, 9-H), 1.31 (d *J* 12.0 Hz, 1H, 5-H); **^{13}C NMR** (100 MHz, $CDCl_3$, major rotamer): δ = 178.6 (8), 169.8 (10), 168.8 (13), 136.3 (1), 135.3 (ArC), 132.1 (2), 128.8 (ArCH), 128.7 (ArCH), 128.6 (ArCH), 128.5 (ArCH), 94.6 (3), 78.0 (6), 70.1 (7), 67.1 (14), 52.4 (4), 49.9 (12), 38.9 (5), 38.0 (9), 37.5 (11); **HRMS**

(ESI) m/z calculated for $C_{20}H_{21}NNaO_6$ $(M+Na)^+$ 394.1261, found 394.1247, 4.1 ppm error.

7.4.1.2 General Procedures for the Synthesis of Peptide Monomers 4.39j and 4.39k

7.4.1.3 General Coupling Procedure for the Synthesis of Peptide Monomers

To a suspension of *N*-Boc-Sar-OH (1 g, 5.29 mmol), an amino acid benzyl ester (1.0 eq.) and HOBt (0.77 g, 5.82 mmol) in DMF:CH_2Cl_2 (75:25, 0.2 M), at 0 °C, was added $NEtiPr_2$ (2.76 mL, 15.87 mmol). EDC (1.03 mL, 5.82 mmol) was added dropwise and the solution allowed to stir at room temperature for 16 h. The reaction mixture was then diluted using EtOAc (50 mL) and washed with 1 M HCl_{aq} (3 × 25 mL), saturated Na_2CO_3 (3 × 25 mL) and H_2O (3 × 25 mL). The organic layer was dried ($MgSO_4$), filtered and concentrated *in vacuo* and purified as detailed for each compound below.

7.4.1.4 General Procedure for the Boc Deprotection of Dipeptides

Dipeptide (500 mg) was dissolved in CH_2Cl_2 (5 mL). TFA (60 eq.) was added and the solution allowed to stir at room temperature for 3 h. The solution was then concentrated *in vacuo* to give the dipeptide TFA salt which could be used without further purification.

Boc-Sar-Gly-OBn

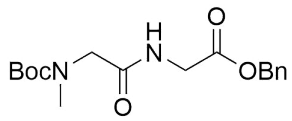

Boc-Sar-OH (1 g, 5.29 mmol, 1.0 eq.) and HCl·H-Gly-OBn (1.07 g, 5.29 mmol, 1.0 eq.) were coupled according to the general coupling procedure for the synthesis of dipeptides. The crude material was then purified using flash column chromatography (50:50, EtOAc:PE) to give the target Boc-Sar-Gly-OBn dipeptide as a yellow oil which crystallised upon standing (1.33 g, 75%). $\boldsymbol{R_F}$ = 0.3, (50:50, EtOAc:PE); **m.p.** 87-89 °C; **IR (Neat)** ν_{max} 3304 (w), 2972 (w), 1749 (m), 1692 (s), 1664 (s), 1558 (m) cm^{-1}; **^{1}H NMR** (400 MHz, $CDCl_3$): δ = 7.39-7.30 (m, 5H, ArH), 6.77-6.36 (br, 1H, NH), 5.17 (s, 2H, OCH_2Ph), 4.09 (d *J* 5.4 Hz, 2H, CH_2NH), 3.90 (s, 2H, CH_2NMe), 2.93 (s, 3H, NMe), 1.46 (s, 9H, $OC(CH_3)_3$); **^{13}C NMR** (100 MHz, $CDCl_3$): δ = 169.8 (C=O), 169.6 (C=O), 135.2 (ArC), 128.8 (ArCH), 128.7 (ArCH), 128.5 (ArCH), 80.9 ($C(CH_3)_3$), 67.3 (OCH_2Ph), 52.3 (CH_2NMe), 41.2 (CH_2NH),

35.8 (N*C*H$_3$), 28.4 (C(*C*H$_3$)$_3$); **HRMS (ESI)** *m/z* calculated for $C_{17}H_{24}N_2NaO_5$ $(M+Na)^+$ 359.1577, found 359.1584, 1.7 ppm error.

Boc-Sar-Sar-OBn

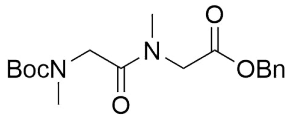

Boc-Sar-OH (1 g, 5.29 mmol, 1.0 eq.) and *para*-toluenesulfonate H-Sar-OBn (1.86 g, 5.29 mmol, 1.0 eq.) were coupled according to the general coupling procedure for the synthesis of dipeptides. The crude material was then purified using flash column chromatography (60:40, EtOAc:PE) to give the target Boc-Sar-Sar-OBn dipeptide as a yellow oil (1.74 g, 94%). $\boldsymbol{R_F}$ = 0.3, (60:40, EtOAc:PE); **m.p.** 78-79 °C; **IR (Neat)** ν_{max} 3007 (w), 2978 (w), 1741 (s), 1681 (s), 1659 (s) cm^{-1}; **^{1}H NMR** (400 MHz, $CDCl_3$, major rotamer): δ = 7.39-7.28 (m, 5H, ArH), 5.13 (s, 2H, OCH_2Ph), 4.20-3.88 (m, 4H, 2 × MeNC*H*$_2$), 3.03 (s, 3H, NMe), 2.90 (s, 3H, NMe), 1.45 (s, 9H, OC(CH$_3$)$_3$); **^{13}C NMR** (100 MHz, $CDCl_3$, major rotamer): δ = 169.4 (C=O), 169.1 (C=O), 156.3 (ArC), 128.7 (ArCH), 128.5 (ArCH), 128.4 (ArCH), 80.0 (O*C*(CH$_3$)$_3$), 67.0 (OCH_2Ph), 50.1 (MeN*C*H$_2$), 49.7 (MeN*C*H$_2$), 35.6 (NMe), 35.5 (NMe), 28.4 (OC(*C*H$_3$)$_3$); **HRMS (ESI)** *m/z* calculated for $C_{18}H_{26}N_2NaO_5$ $(M+Na)_+$ 373.1734, found 373.1740, − 2.4 ppm error.

TFA·H-Sar-Gly-OBn 4.38j

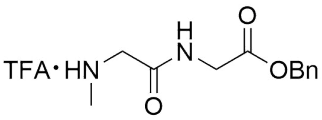

Boc-Sar-Gly-OBn (500 mg, 1.49 mmol, 1.0 eq.) was deprotected according to the general procedure for the deprotection of dipeptides to give TFA·H-Sar-Gly-OBn **4.38j** as a yellow oil (480 mg, 92%). **IR (Neat)** ν_{max} 3091 (w), 2828 (w), 1738 (m), 1667 (s) and 1563 (m) cm^{-1}; **^{1}H NMR** (400 MHz, $CDCl_3$): δ = 7.42-7.24 (m, 5H, ArH), 5.18 (s, 2H, CH_2OBn) 4.08 (s, 2H, CH_2NH), 3.85 (s, 2H, CH_2NHMe), 2.71 (s, 3H, NHMe); **^{13}C NMR** (100 MHz, $CDCl_3$): δ = 170.8 (COOBn), 167.1 (CONH), 160.9 (q *J* 37.4 Hz, 1C, CF_3COOH), 137.1 (ArC), 129.6 (ArCH), 129.4 (ArCH), 129.3 (ArCH), 117.0 (q *J* 287.3 Hz, 1C, CF_3COOH), 68.1 (CH_2OBn), 50.4 (CH_2NHMe), 42.0 (CH_2NH), 33.5 ($NHCH_3$); **HRMS (ESI)** *m/z* calculated for $C_{12}H_{17}N_2O_3$ $(M\text{-}CF_3COO^-)^+$ 237.1234, found 237.1236, − 0.8 ppm error.

TFA·H-Sar-Sar-OBn 4.38k

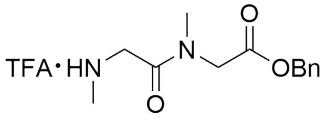

Boc-Sar-Sar-OBn (500 mg, 1.42 mmol, 1.0 eq.) was deprotected according to the general procedure for the deprotection of dipeptides to give TFA·H-Sar-Sar-OBn **4.38k** as a yellow oil (497 mg, 96%). **IR (Neat)** ν_{max} 3035 (w), 2821 (w), 1779 (w), 1744 (m) and 1659 (s) cm^{-1}; **^{1}H NMR** (400 MHz, $CDCl_3$, major rotamer): δ = 7.45-7.28 (m, 5H, ArH), 5.18 (s, 2H, CH_2COOBn), 4.25 (s, 2H, CH_2NMe), 4.13 (s, 2H, CH_2NHMe), 3.07 (s, 3H, NMe), 2.73 (s, 3H, NHMe); **^{13}C NMR** (100 MHz, $CDCl_3$, major rotamer): δ = 170.3 (COOBn), 167.4 (CONH), 160.9 (q *J* 38.6 Hz, 1C, CF_3COOH), 137.0 (ArC), 129.6 (ArC), 129.4 (ArCH), 129.3 (ArCH), 117.1 (q *J* 289.7 Hz, 1C, CF_3COOH), 68.1 (CH_2COOBn), 51.2 (CH_2NMe), 50.4 (CH_2NHMe), 35.8 (NMe), 33.5 (NHMe); **HRMS (ESI)** *m/z* calculated for $C_{13}H_{18}N_2NaO_3$ $(M+Na)^+$ 273.1210, found 273.1212, − 0.7 ppm error.

benzyl-2-[[2-[methyl-[2-[(5*S*,7*S*)-4-oxo-3,10-dioxatricyclo-[5.2.1.0^{1,5}]dec-8-en-5-yl]acetyl]amino]acetyl]amino]acetate 4.39j

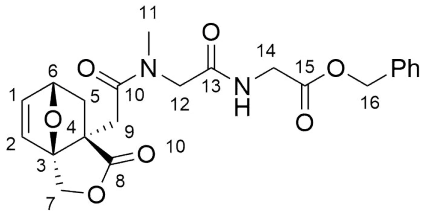

Acid monomer **4.7** (372 mg, 1.7 mmol, 1.0 eq.) and TFA·H-Sar-Gly-OBn **4.38kj** (620 mg, 1.77 mmol, 1.0 eq.) were coupled according to the general procedure for the synthesis of trisubstituted amides. The crude material was purified by flash column chromatography (80:20, EtOAc:Acetone) to give the target amide **4.39j** as a clear oil (493 mg, 65%). **IR (Neat)** ν_{max} 3348 (w), 2011 (w), 2951 (w), 1749 (s) and 1641 (s) cm^{-1}; **^{1}H NMR** (400 MHz, $CDCl_3$, major rotamer): δ = 7.39-7.29 (m, 5H, ArH), 6.92 (t *J* 5.7 Hz, 1H, N-H), 6.57 (d *J* 6.1 Hz, 1H, 2-H), 6.53 (dd *J* 6.1, 1.4 Hz, 1H, 1-H), 5.16 (s, 2H, 16-H), 5.02 (dd *J* 5.0, 1.4 Hz, 1H, 6-H), 4.95 (d *J* 10.6 Hz, 1H, 7-H), 4.56 (d *J* 10.6 Hz, 1H, 7-H), 4.31 (d *J* 16.0 Hz, 1H, 12-H), 4.12 (dd *J* 17.9, 5.7 Hz, 1H, 14-H), 4.01 (dd *J* 17.9, 5.7 Hz, 1H, 14-H), 3.80 (d *J* 16.0 Hz, 1H, 12-H), 3.03 (s, 3H, 11-H), 2.63 (d *J* 14.7 Hz, 1H, 9-H), 2.48 (dd *J* 12.6, 5.1 Hz, 1H, 5-H), 2.41 (d *J* 14.7 Hz, 1H, 9-H), 1.56 (d *J* 12.6 Hz, 1H, 5-H); **^{13}C NMR** (100 MHz, $CDCl_3$, major rotamer): δ = 178.9 (8), 169.9 (15), 169.5 (13), 168.7 (10),

137.6 (1), 135.3 (ArC), 131.2 (2), 128.8 (ArCH), 128.7 (ArCH), 128.6 (ArCH), 128.5 (ArCH), 94.4 (3), 78.5 (6), 69.8 (7), 67.2 (16), 52.8 (4), 51.9 (12), 41.2 (14), 37.8 (9), 37.6 (11), 37.0 (5); **HRMS (ESI)** m/z calculated for $C_{22}H_{24}N_2NaO_7$ $(M+Na)^+$ 451.1476, found 451.1475, − 0.1 ppm error.

benzyl-2-[methyl-[2-[methyl-[2-[(5*S*,7*S*)-4-oxo-3,10-dioxatricyclo-[5.2.1.0^{1,5}]dec-8-en-5-yl]acetyl]amino]acetyl]amino]acetate 4.39k

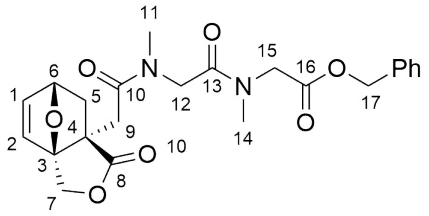

Acid monomer **4.7** (330 mg, 1.57 mmol, 1.0 eq.) and TFA·H-Sar-Sar-OBn **4.38k** (573 mg, 1.57 mmol, 1.0 eq.) were coupled according to the general procedure for the synthesis of trisubstituted amides. The crude material was purified by flash column chromatography (100:0-80:20, EtOAc:Acetone) to give the target amide **4.39k** as a yellow oil (398 mg, 57%). **IR (Neat)** ν_{max} cm^{-1}; **^{1}H NMR** (400 MHz, $CDCl_3$, major rotamer): δ = 7.40-7.29 (m, 5H, ArH), 6.67 (d *J* 5.6 Hz, 1H, 2-H), 6.45 (dd *J* 5.6, 1.8 Hz, 1H, 1-H), 5.21-5.11 (m, 2H, 17-H), 5.04-4.94 (m, 2H, 6-H/7-H), 4.61 (d *J* 16.4 Hz, 1H, 15-H), 4.48 (d *J* 9.8 Hz, 1H, 7-H), 4.33 (d *J* 17.5 Hz, 1H, 12-H), 3.98 (d *J* 17.5 Hz, 1H, 12-H), 3.81 (d *J* 16.4 Hz, 1H, 15-H), 3.08-2.94 (m, 6H, 11-H/14-H), 2.91-2.69 (m, 1H, 9-H), 2.53 (dd *J* 12.0, 4.8 Hz, 1H, 5-H), 2.22 (d *J* 15.2 Hz, 1H, 9-H), 1.33 (d *J* 12.0 Hz, 1H, 5-H); **^{13}C NMR** (100 MHz, $CDCl_3$, major rotamer): δ = 178.8 (8), 169.8 (10), 169.0 (13), 168.3 (16), 136.3 (1), 135.3 (ArC), 132.3 (2), 128.7 (ArCH), 128.6 (ArCH), 128.4 (ArCH), 128.3 (ArCH), 94.7 (3), 78.1 (6), 70.1 (7), 67.2 (17), 52.5 (4), 49.8 (12), 49.6 (15), 39.0 (9), 38.2 (5), 37.6 (14), 35.8 (11); **HRMS (ESI)** m/z calculated for $C_{23}H_{26}N_2NaO_7$ $(M+Na)^+$ 465.1632, found 465.1636, − 0.9 ppm error.

7.4.2 Ring-Opening Metathesis Polymerisation of Tertiary Amide Monomers

7.4.2.1 General Procedure for the ROMP of Amides 4.39a-k

The appropriate quantities of monomer(s) and catalyst G2 were separately dissolved in $(CH_2Cl)_2$. Each solution was degassed by three cycles of freeze-pump-thaw. The monomer solution was prewarmed to the desired temperature and the catalyst solution added. The reaction mixture was then stirred for 72 h. After this time, the polymerization was terminated by the addition of an excess of ethyl vinyl ether,

followed by stirring for a further 30 minutes. The solution was then filtered through a short plug of silica to remove catalyst residues. The solution was then precipitated into hexane. After settling, the hexane was carefully decanted and the polymer dried under reduced pressure.

7.4.2.2 Analytical Data and Spectra for Homopolymers 4.42a-k

Dimethyl Homopolymer 4.42a

^{1}H NMR Spectrum

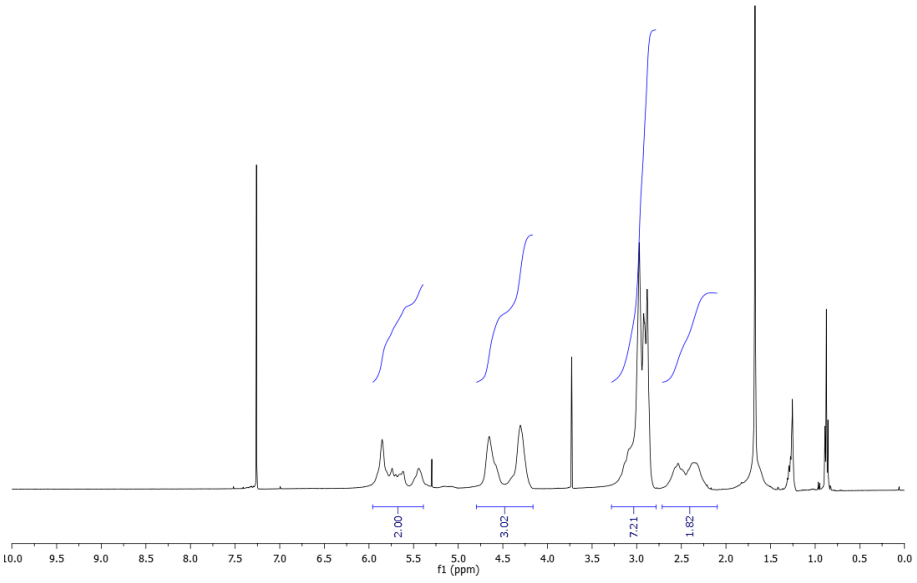

TGA Trace

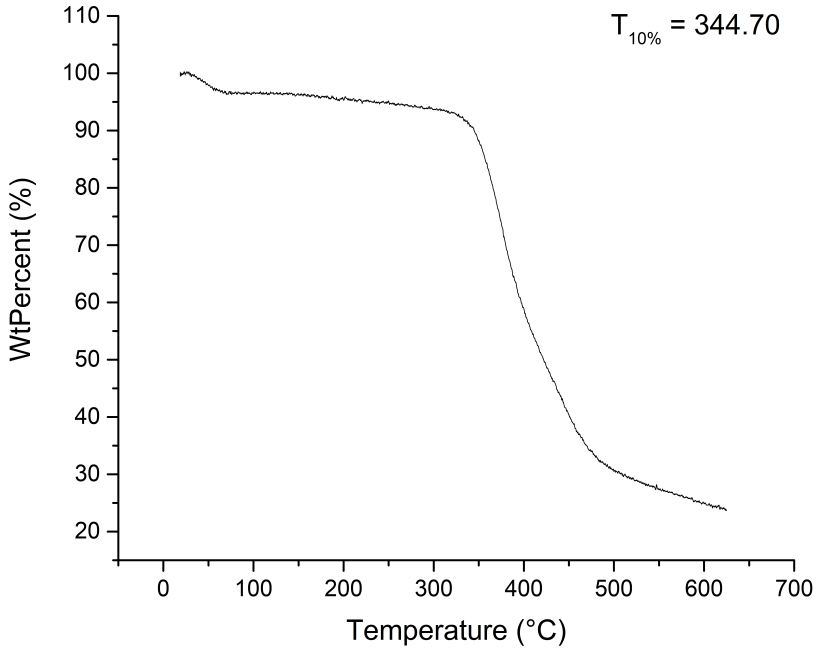

DSC Trace

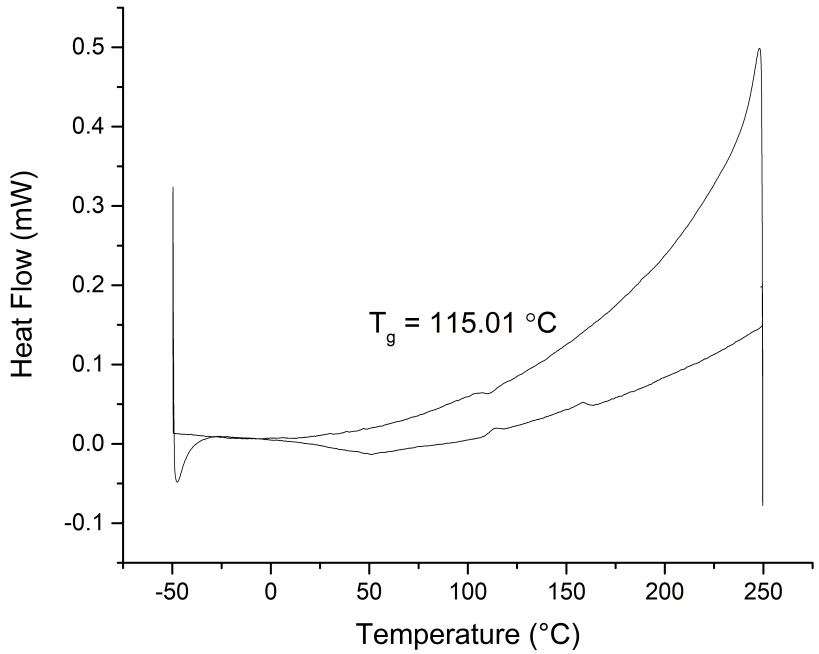

Infrared Spectrum

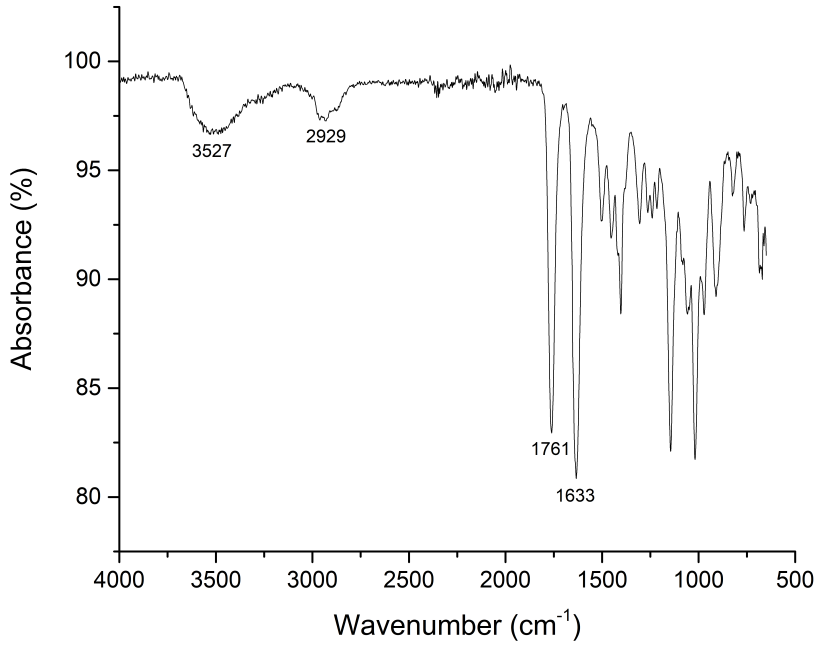

Diethyl Homopolymer 4.42b

^{1}H NMR Spectrum

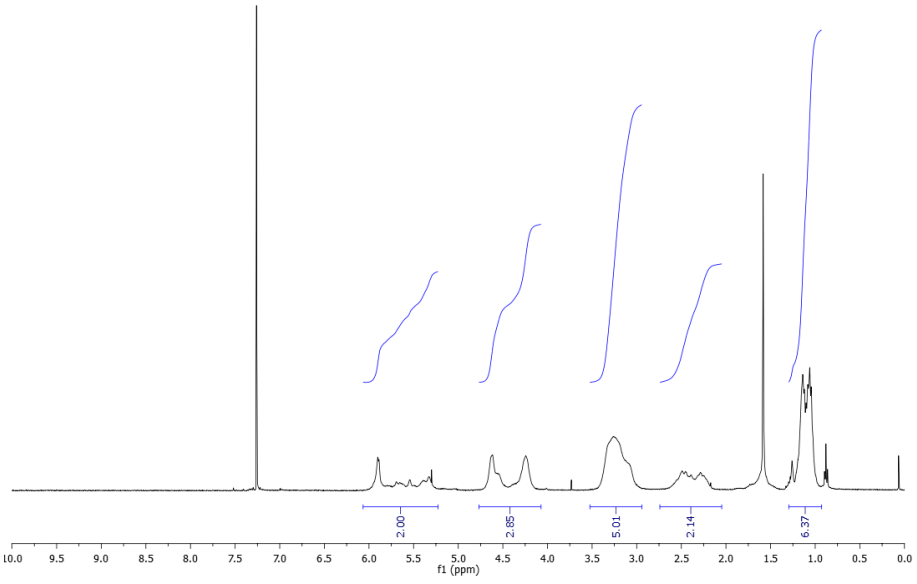

TGA Trace

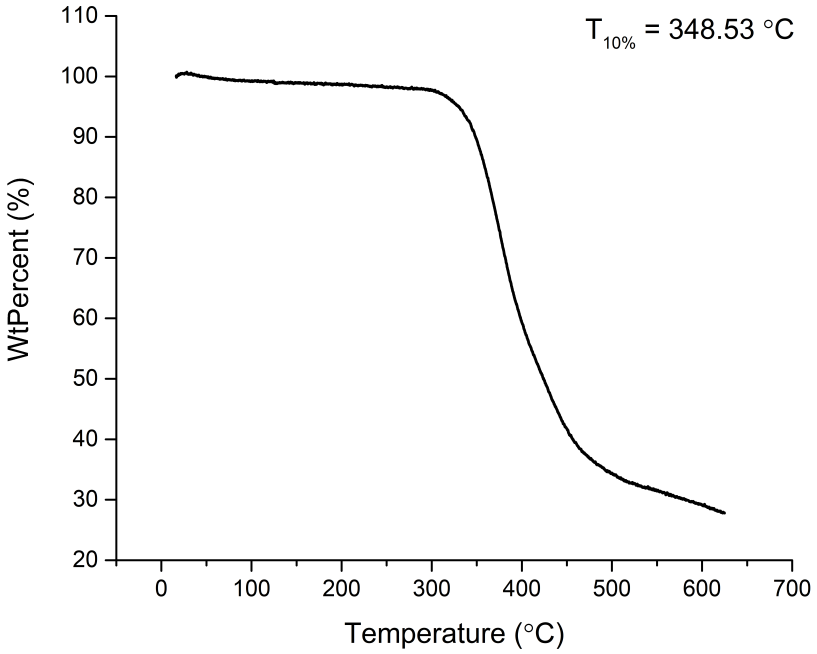

DSC Trace

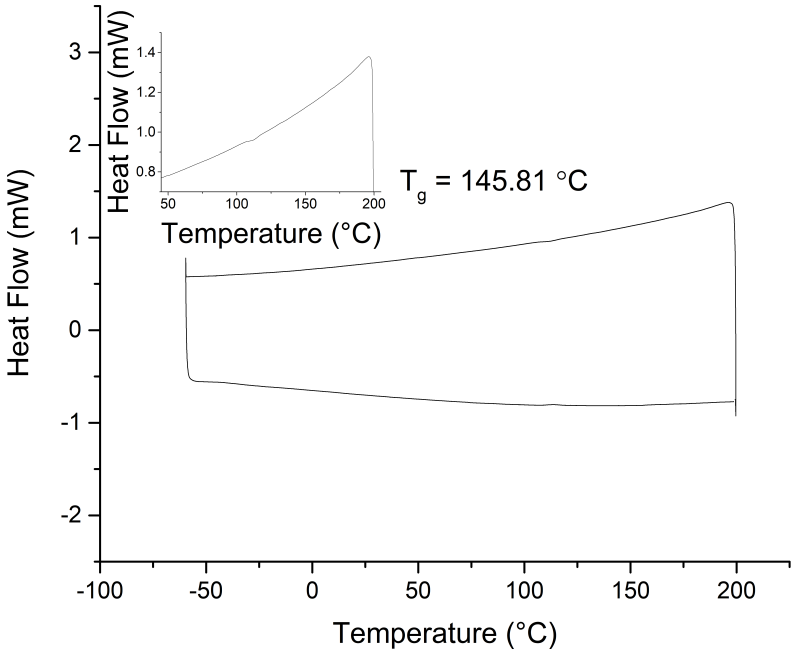

Infrared Spectrum

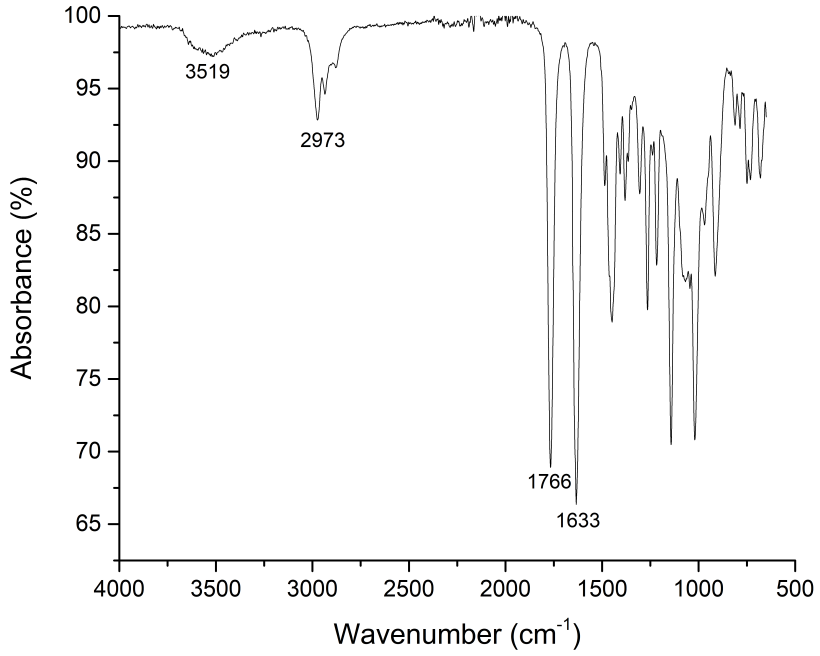

Dipropyl Homopolymer 4.42c

SEC Trace

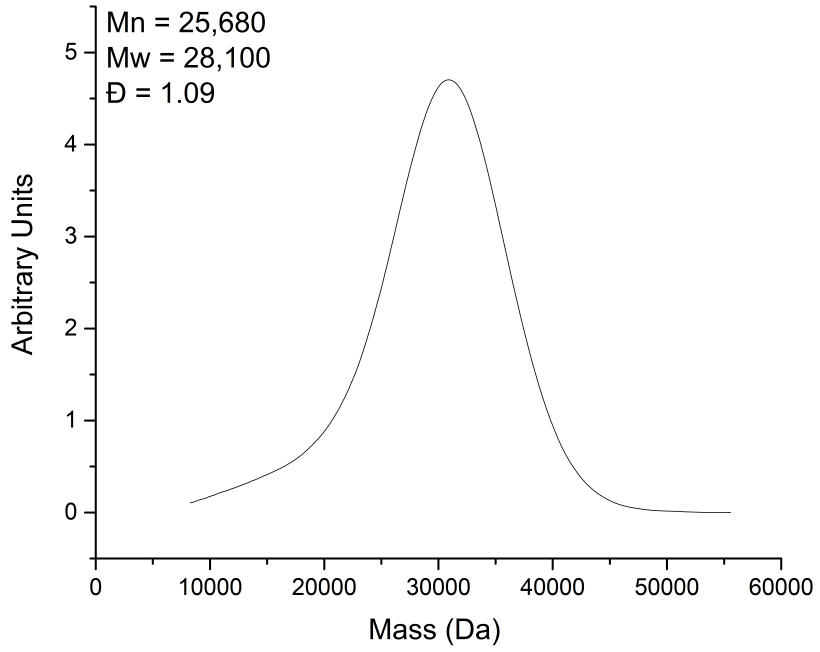

^{1}H NMR Spectrum

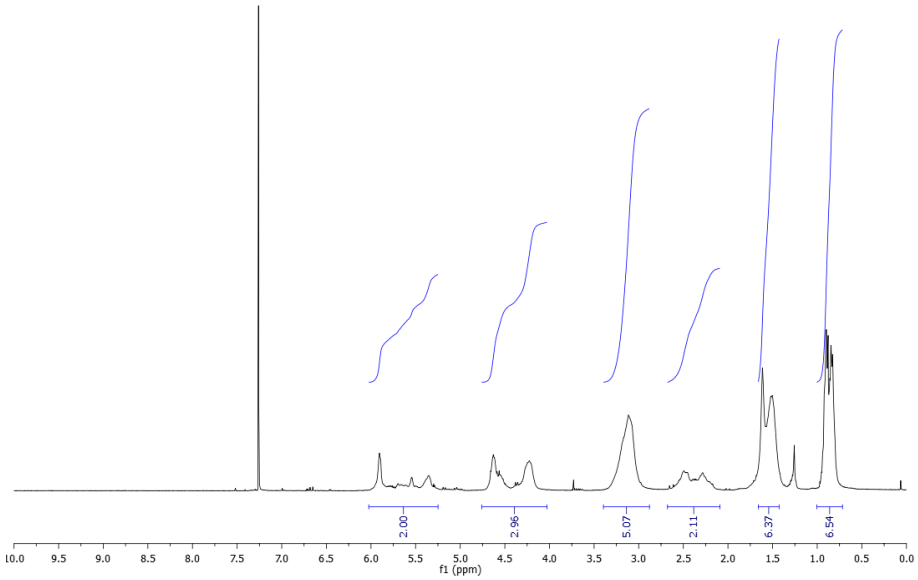

TGA Trace

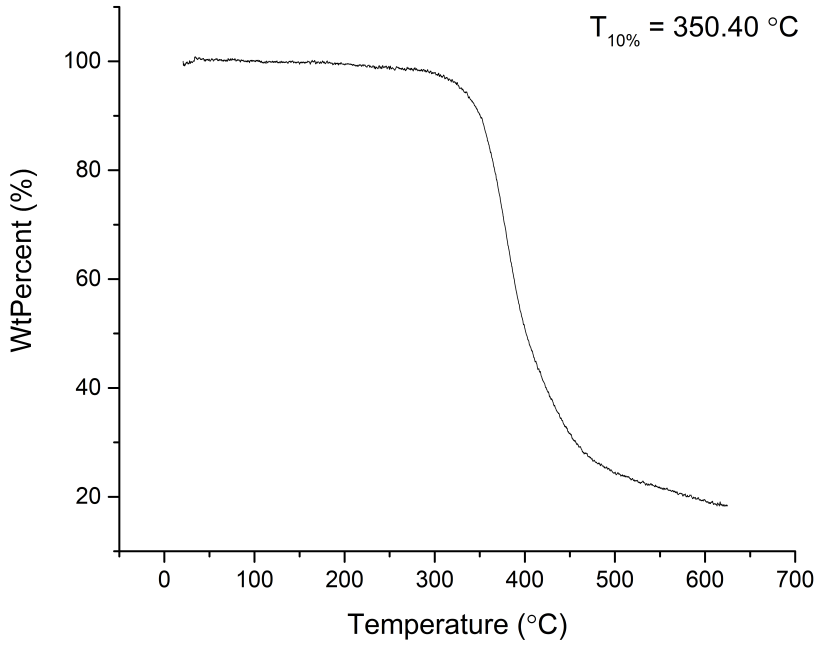

DSC Trace

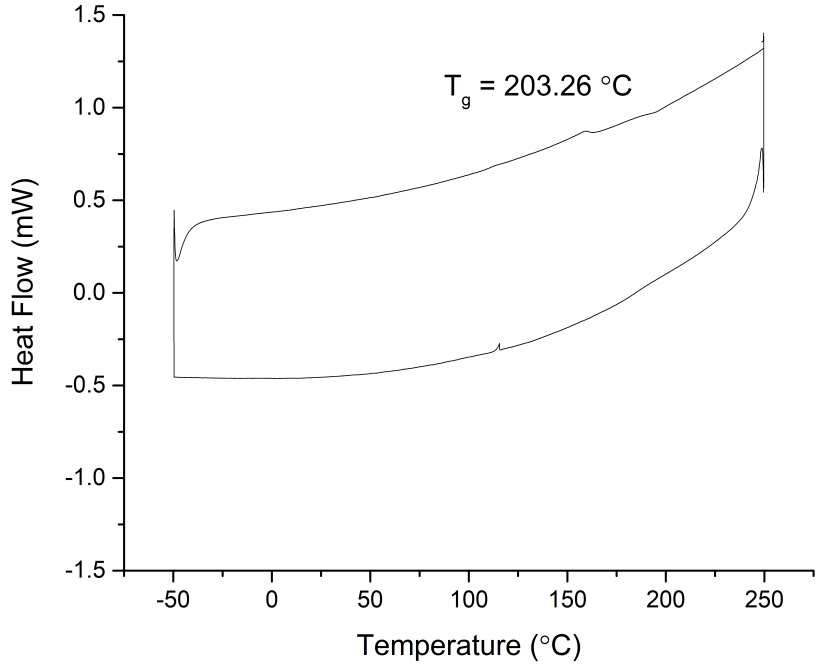

Infrared Spectrum

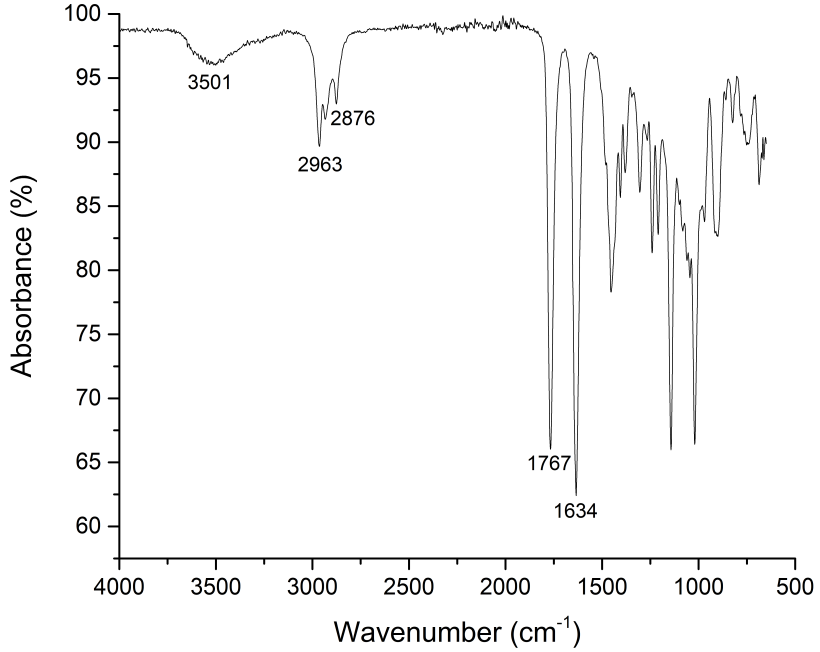

Dibutyl Homopolymer 4.42d

SEC Trace

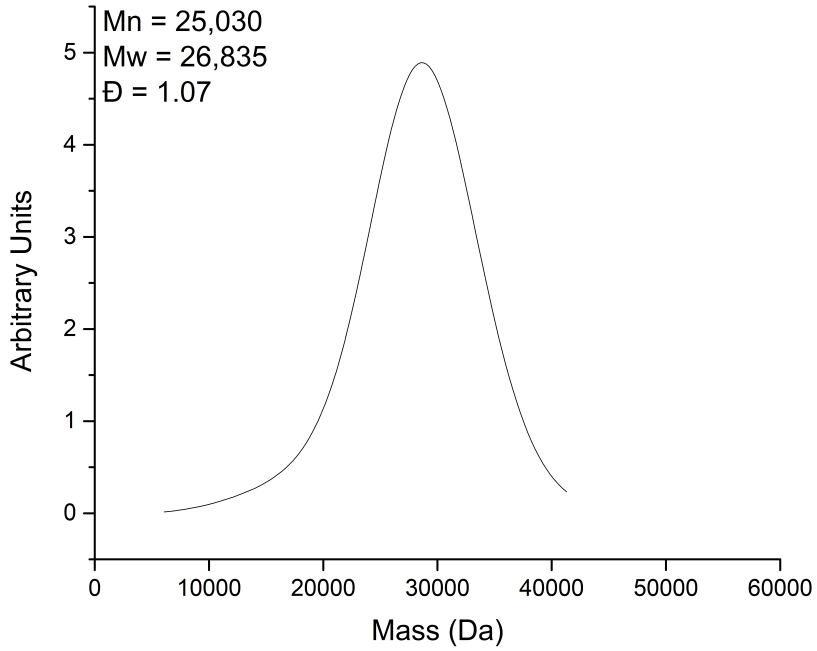

^{1}H NMR Spectrum

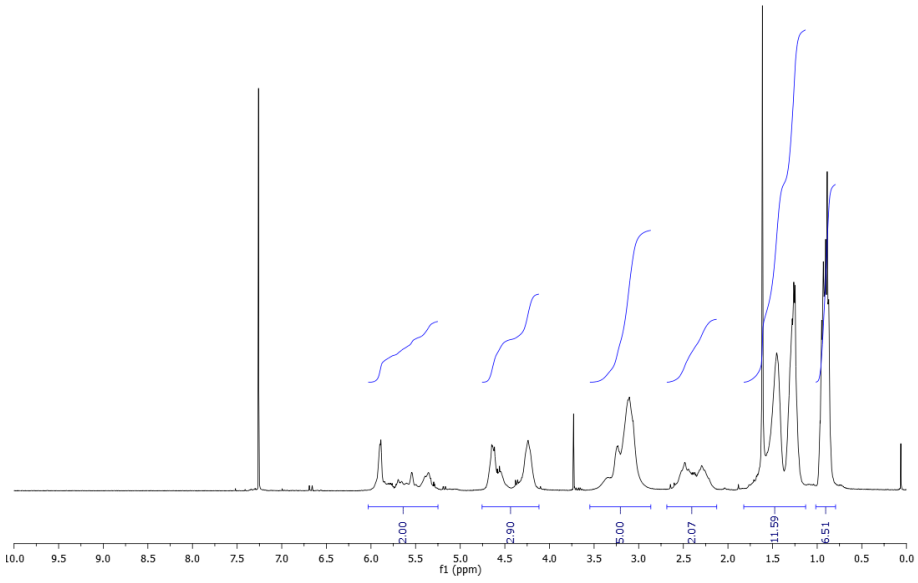

TGA Trace

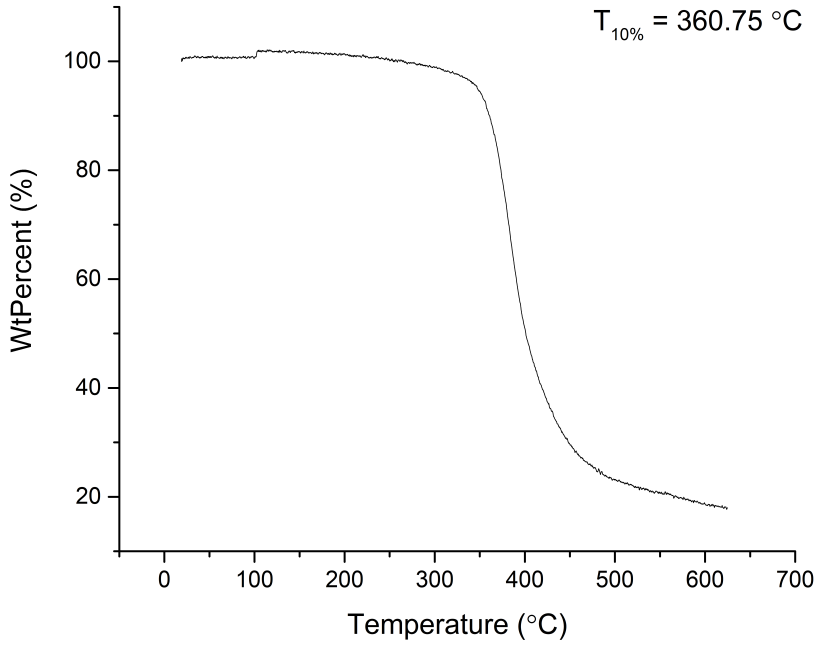

DSC Trace

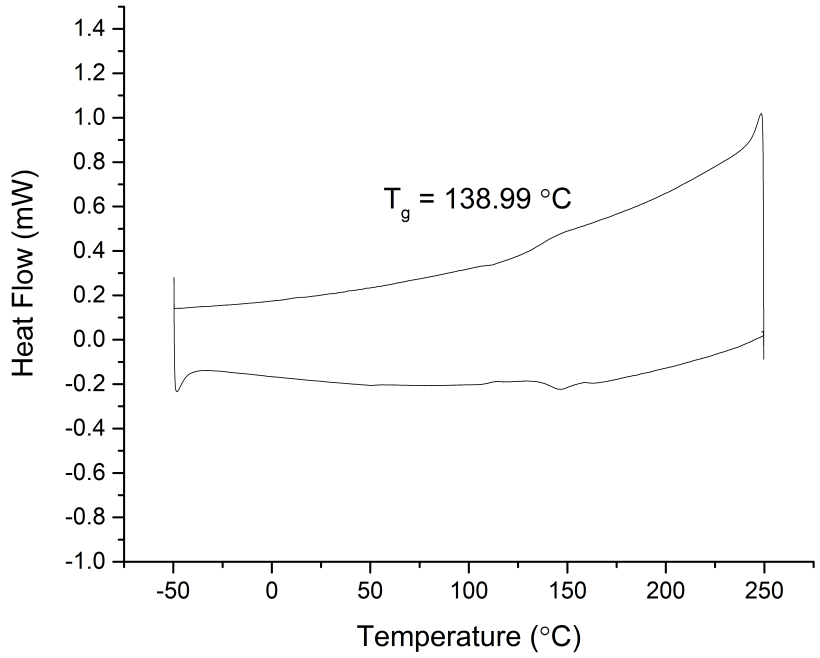

Infrared Spectrum

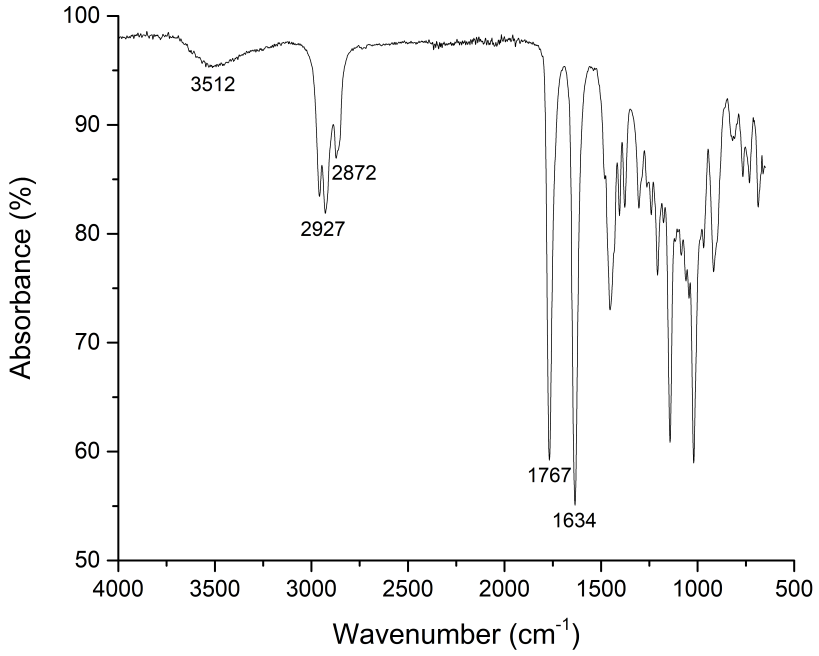

Dioctyl Homopolymer 4.42e

SEC Trace

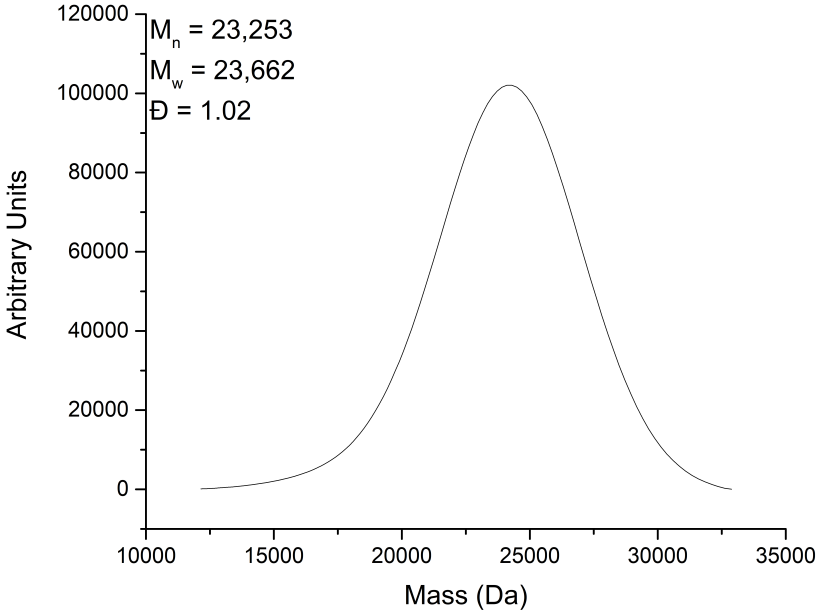

^{1}H NMR Spectrum

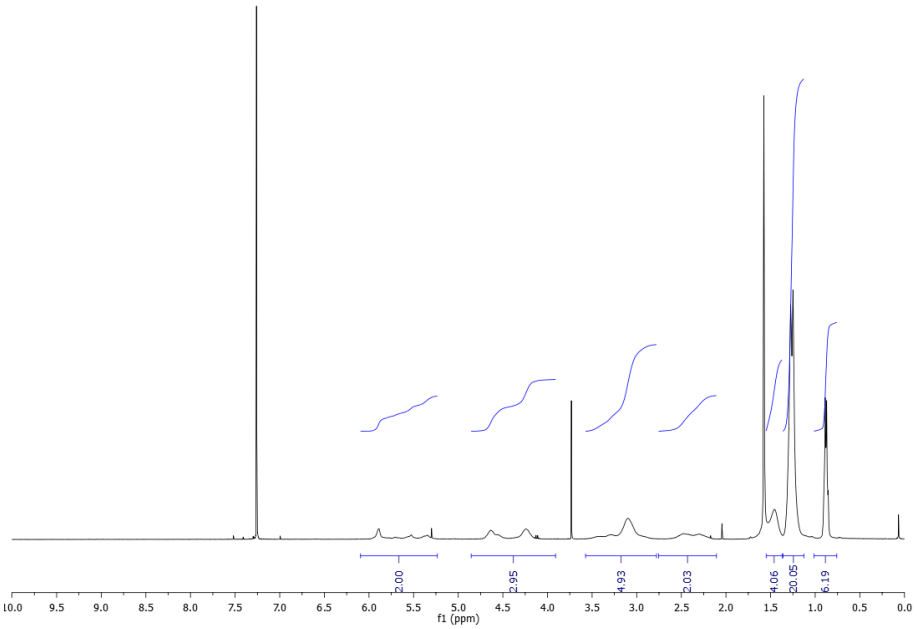

TGA Trace

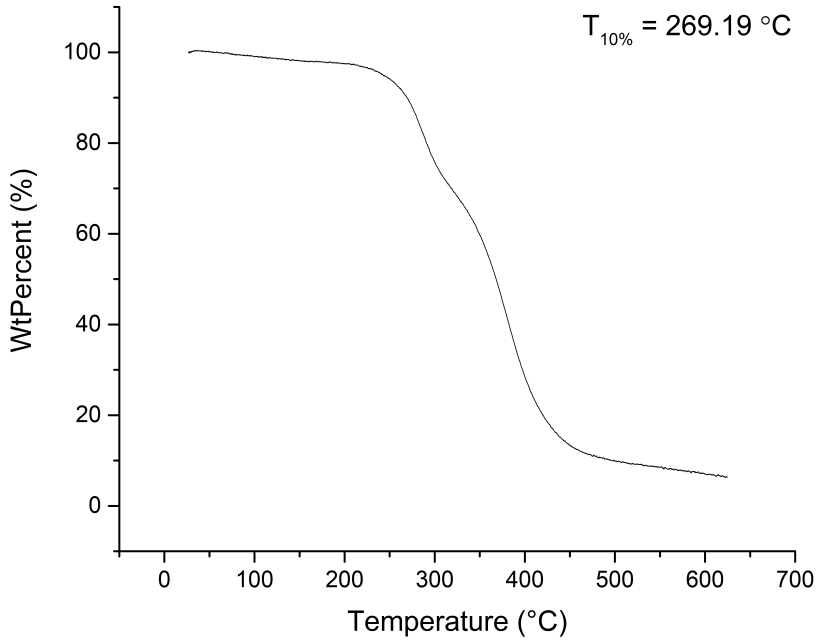

DSC Trace

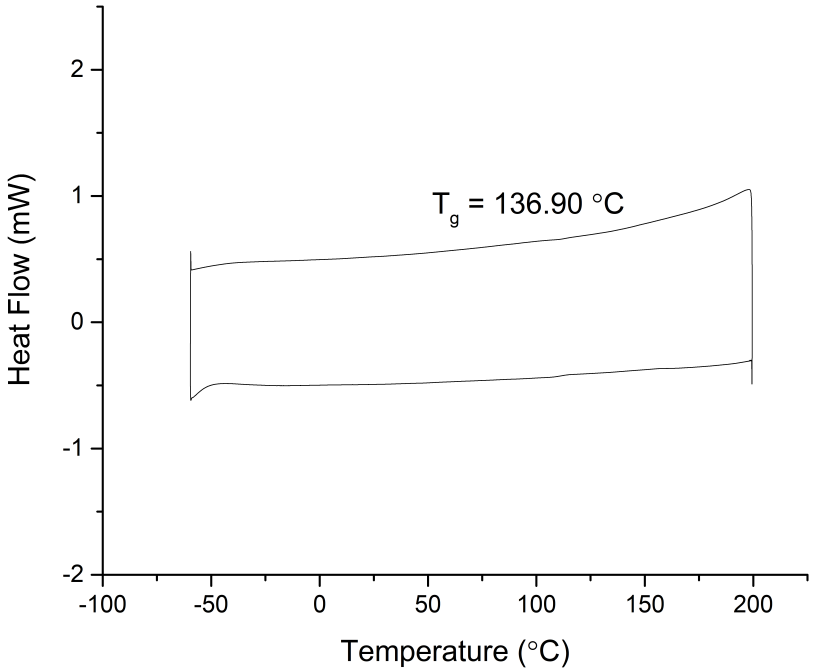

Infrared Spectrum

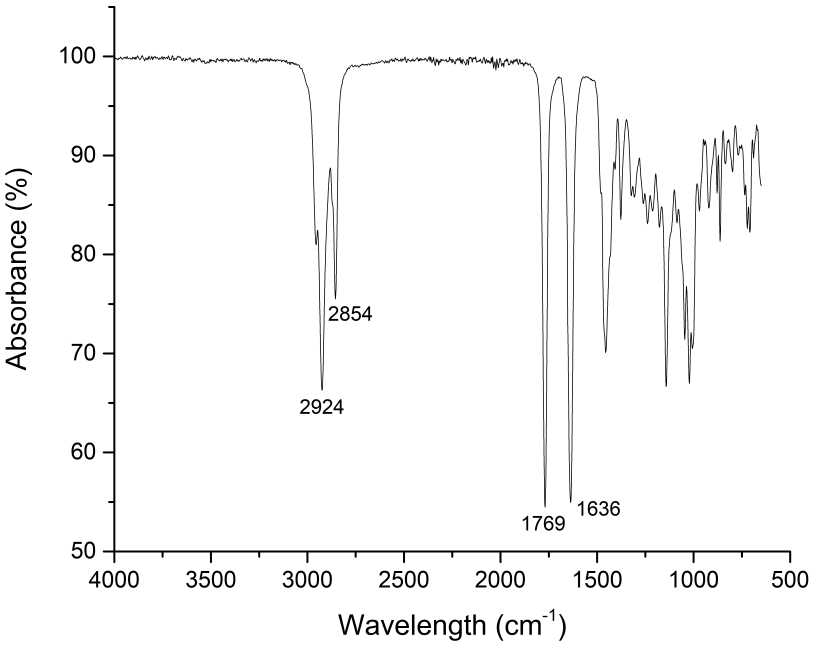

Bis-(2-ethylhexyl) Homopolymer 4.42f

SEC Trace

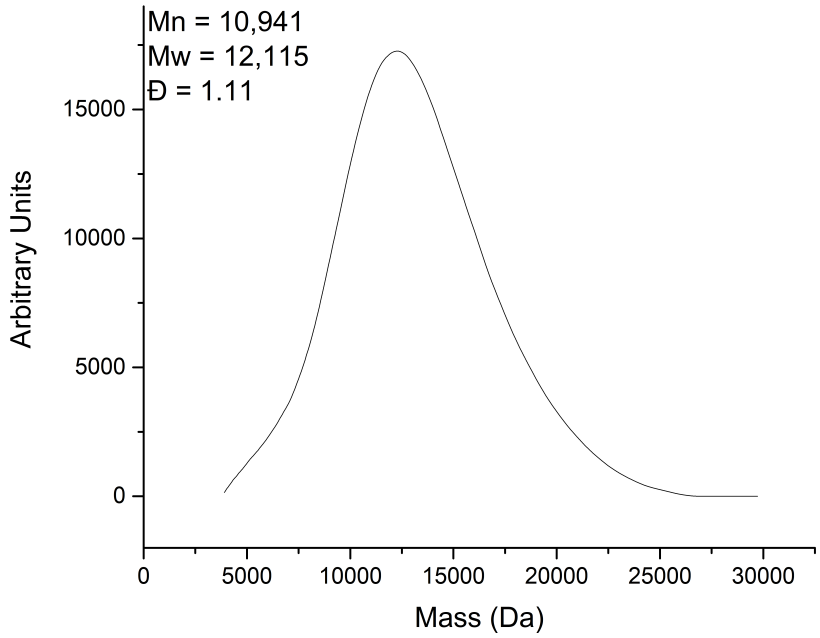

^{1}H NMR Spectrum

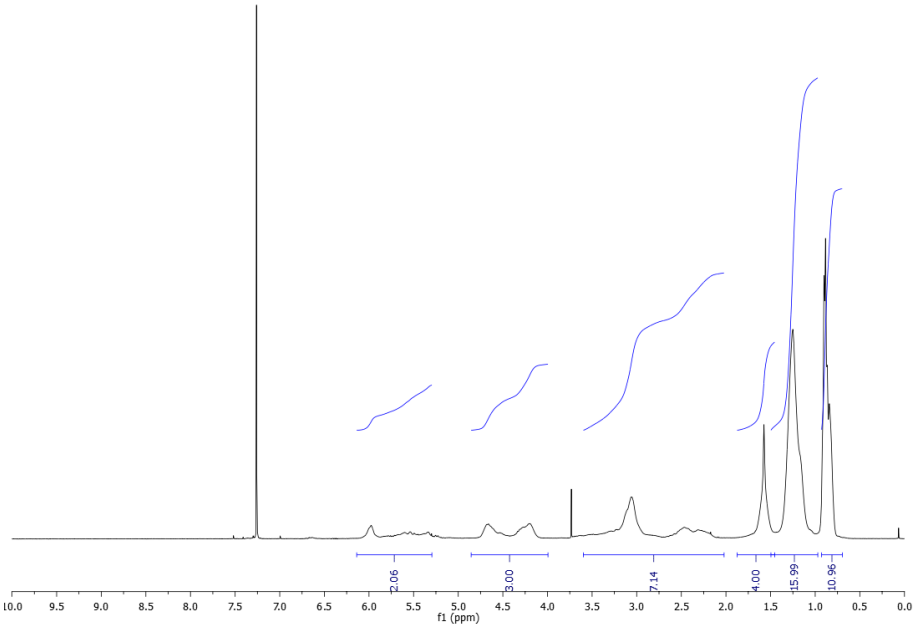

TGA Trace

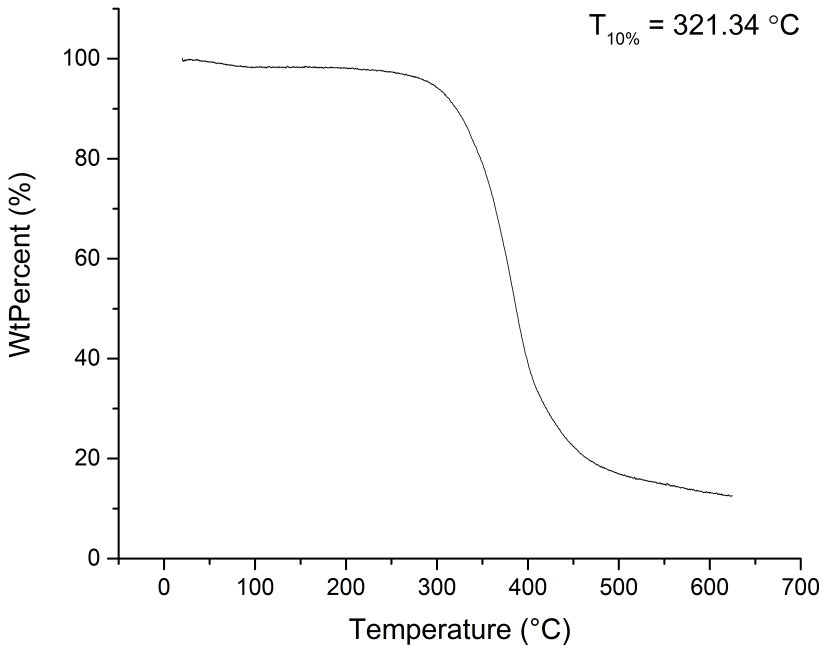

DSC Trace

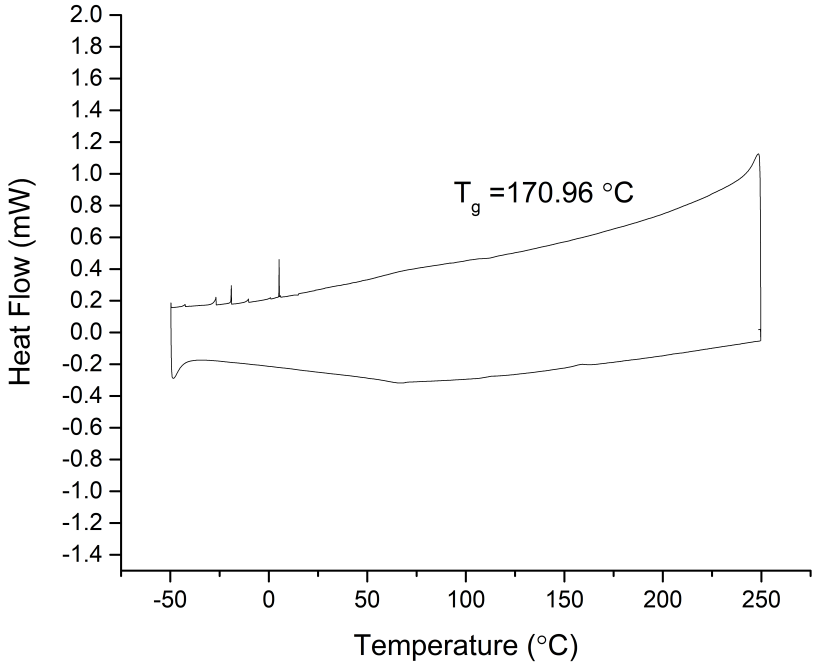

Infrared Spectrum

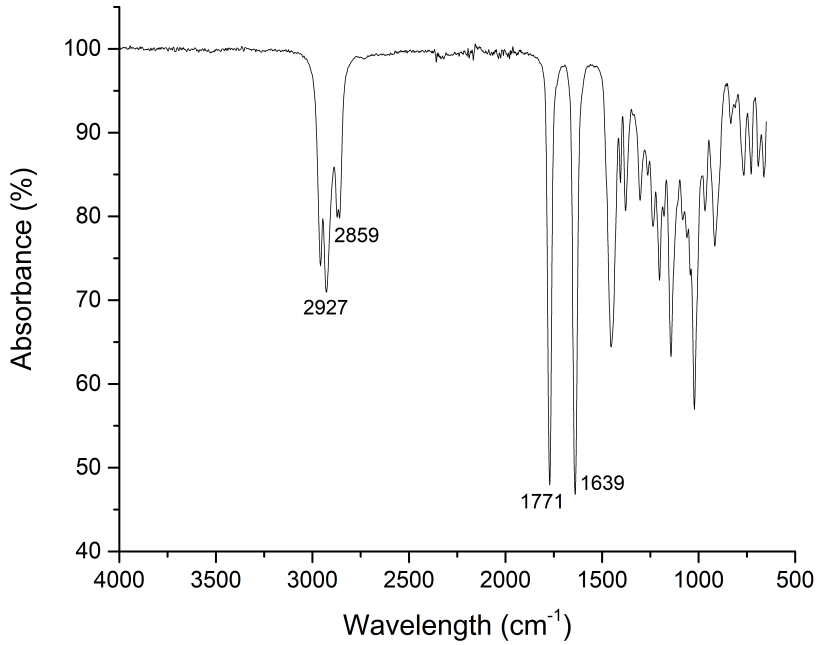

Dibenzyl Homopolymer 4.42g

SEC Trace

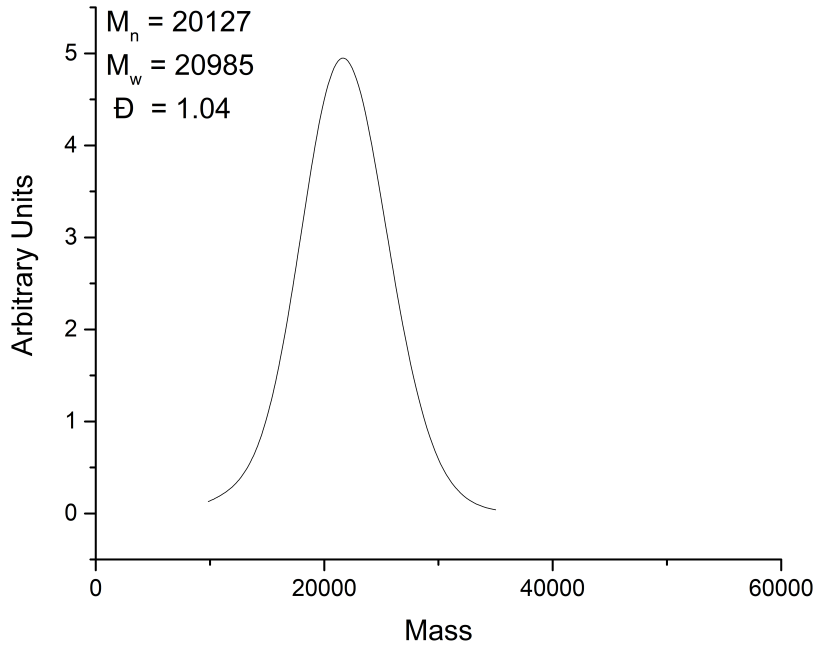

^{1}H NMR Spectrum

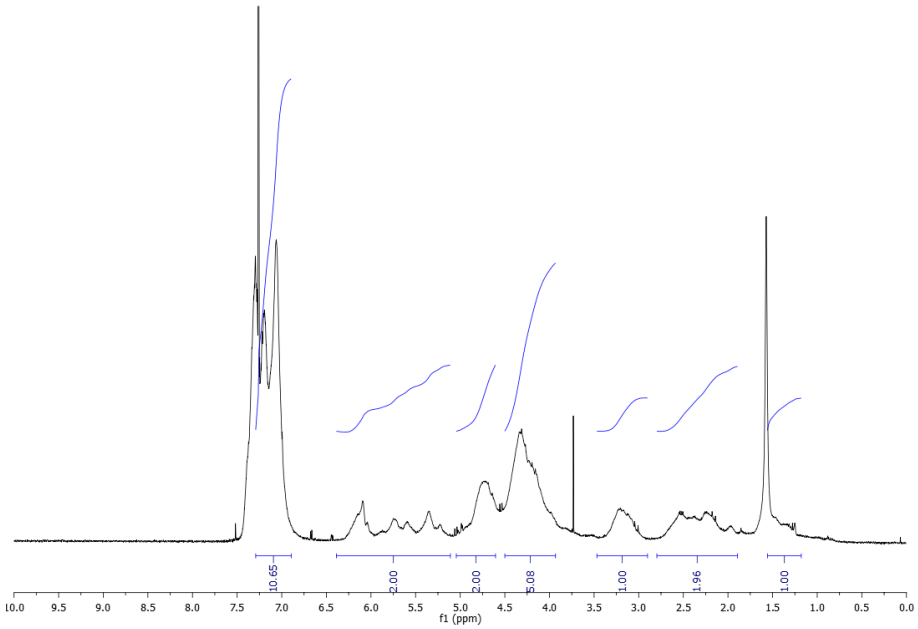

TGA Trace

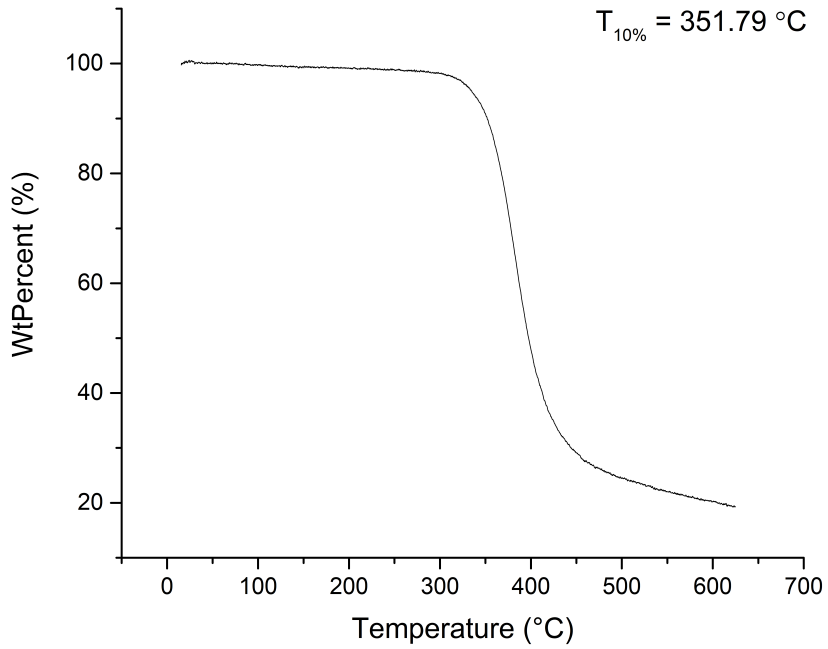

DSC Trace

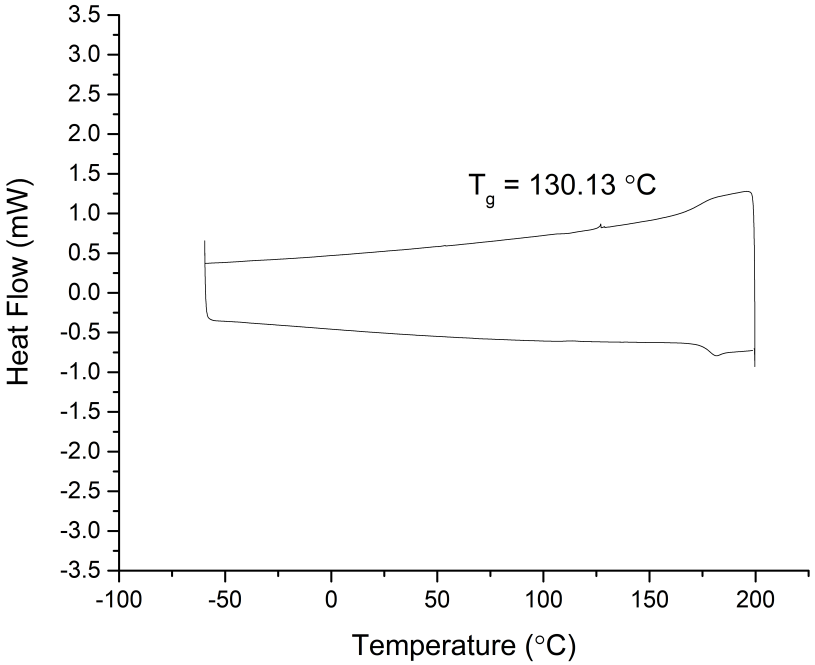

Infrared Spectrum

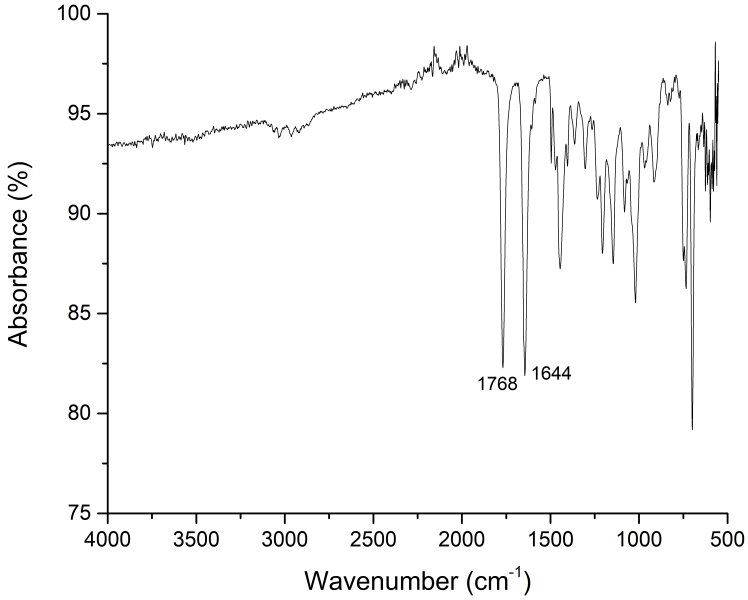

Proline Methyl Ester Homopolymer 4.42h

^{1}H NMR Spectrum

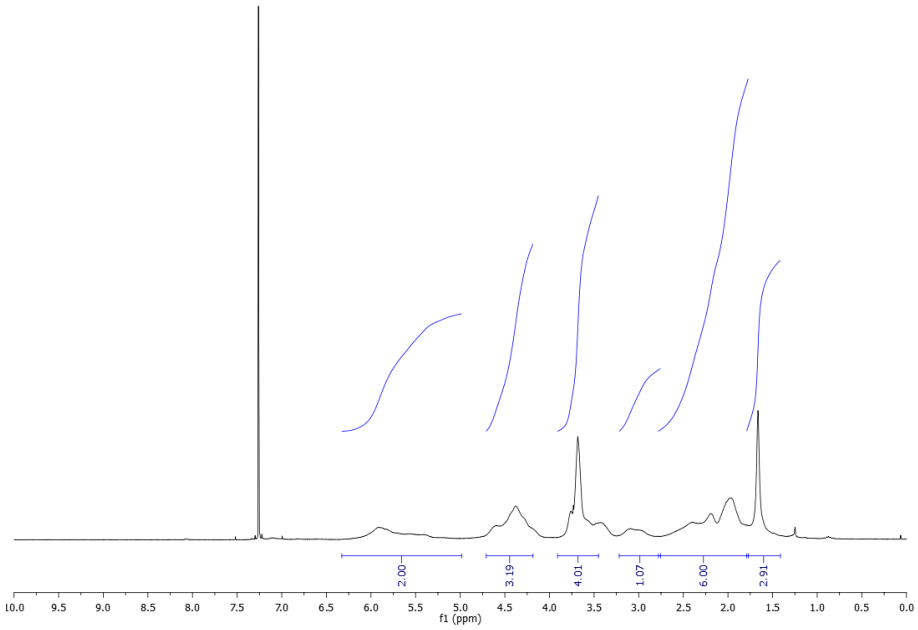

TGA Trace

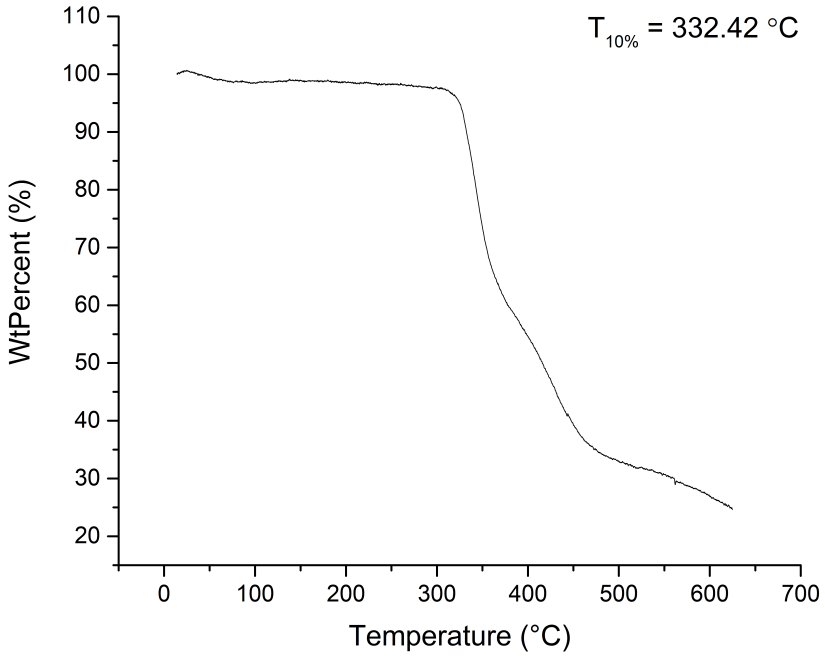

DSC Trace

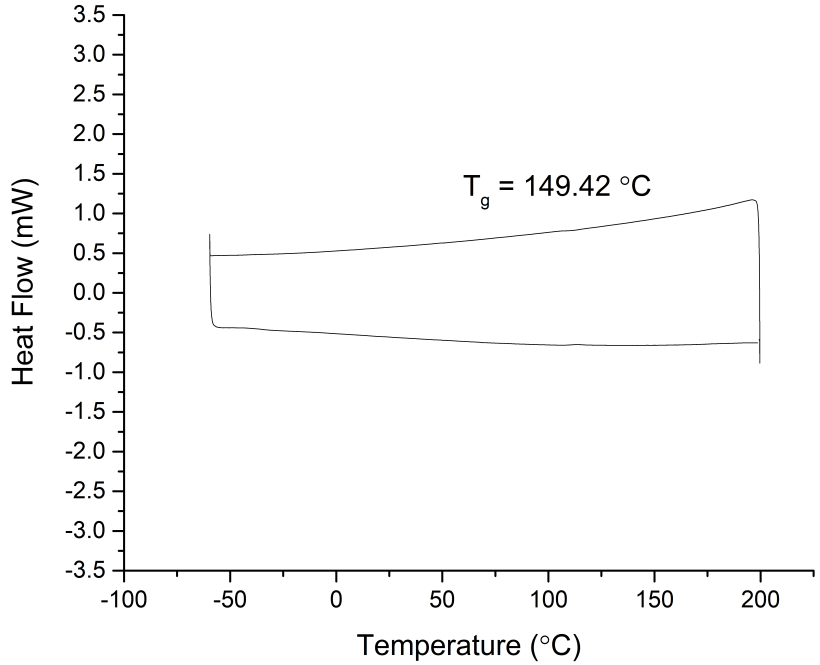

Infrared Spectrum

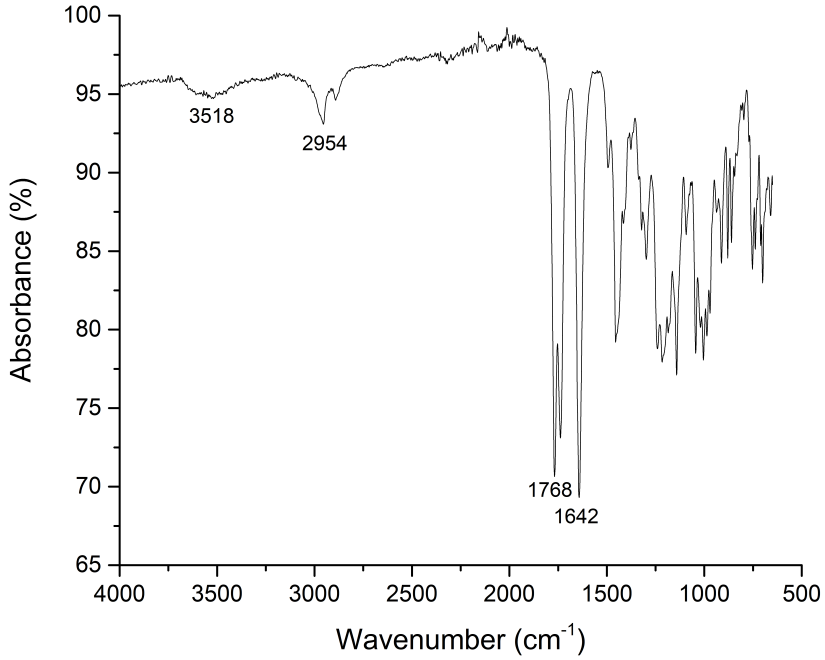

Sarcosine Benzyl Ester Homopolymer 4.42i

SEC Trace

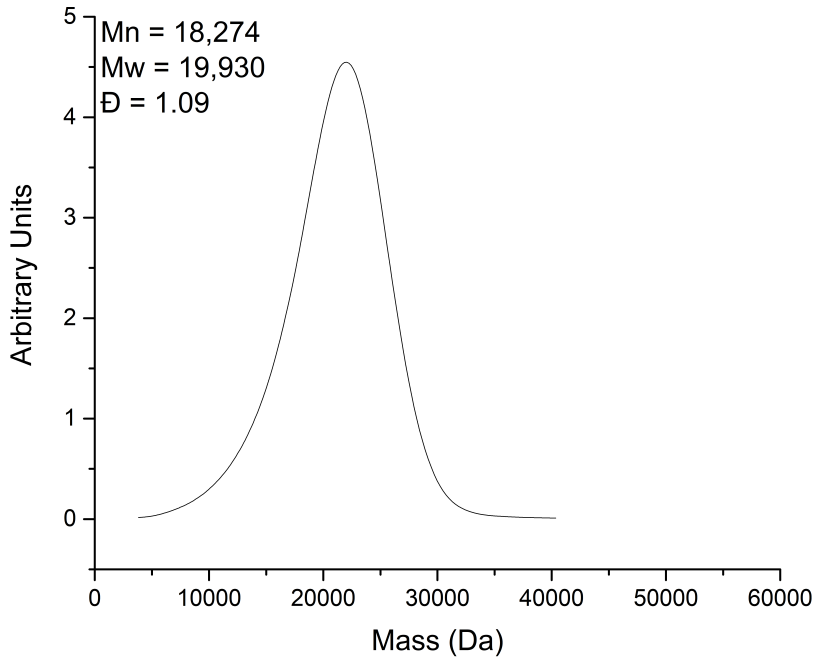

^{1}H NMR Spectrum

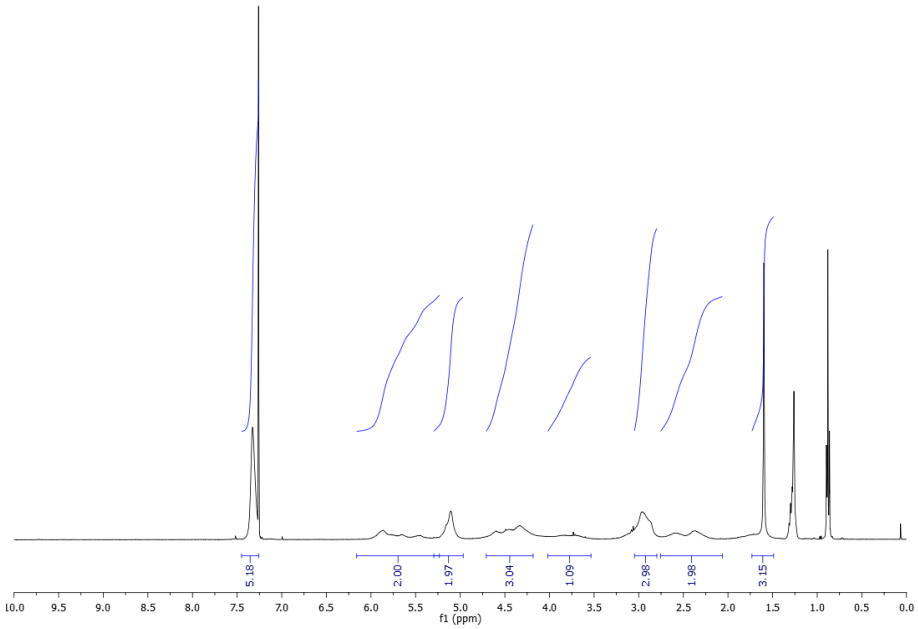

TGA Trace

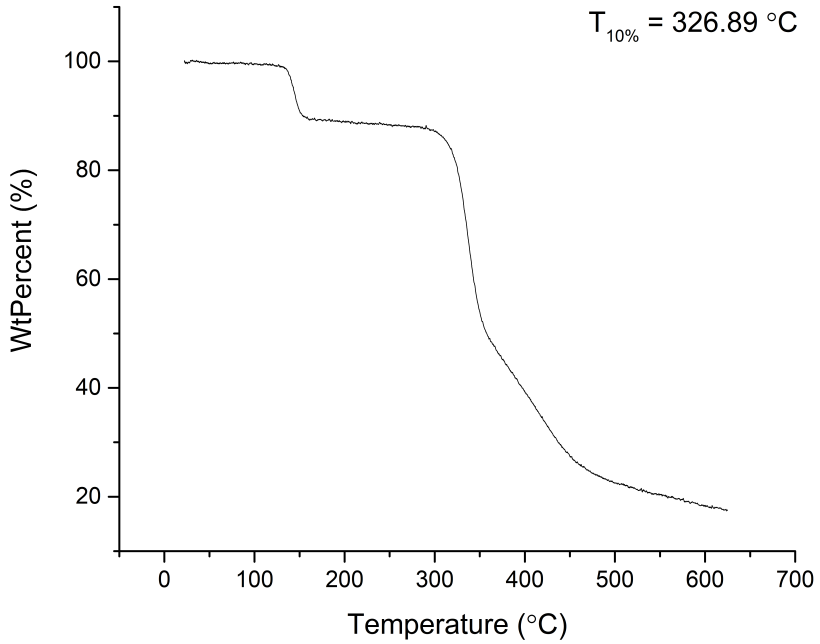

DSC Trace

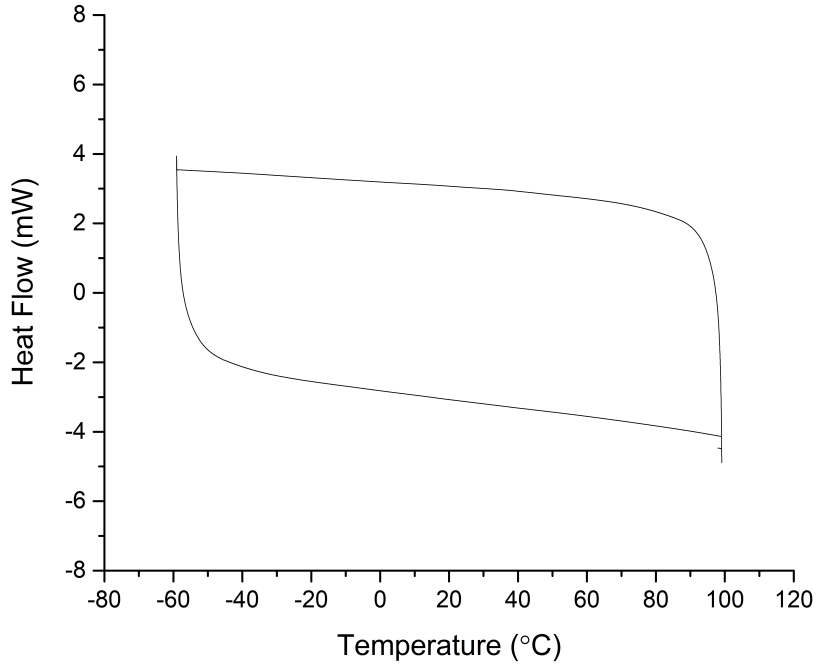

Infrared Spectrum

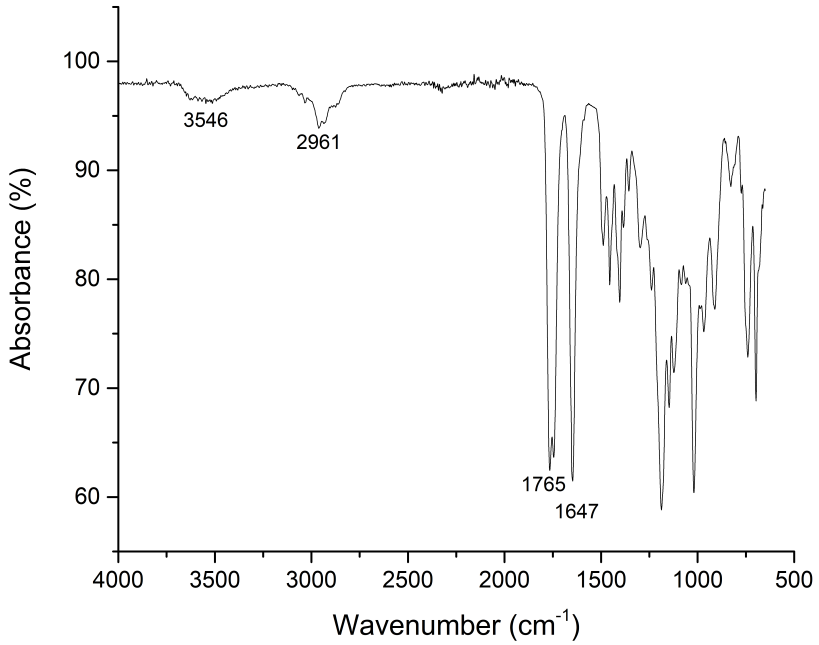

Sar-Gly Benzyl Ester Homopolymer 4.42j

^{1}H NMR Spectrum

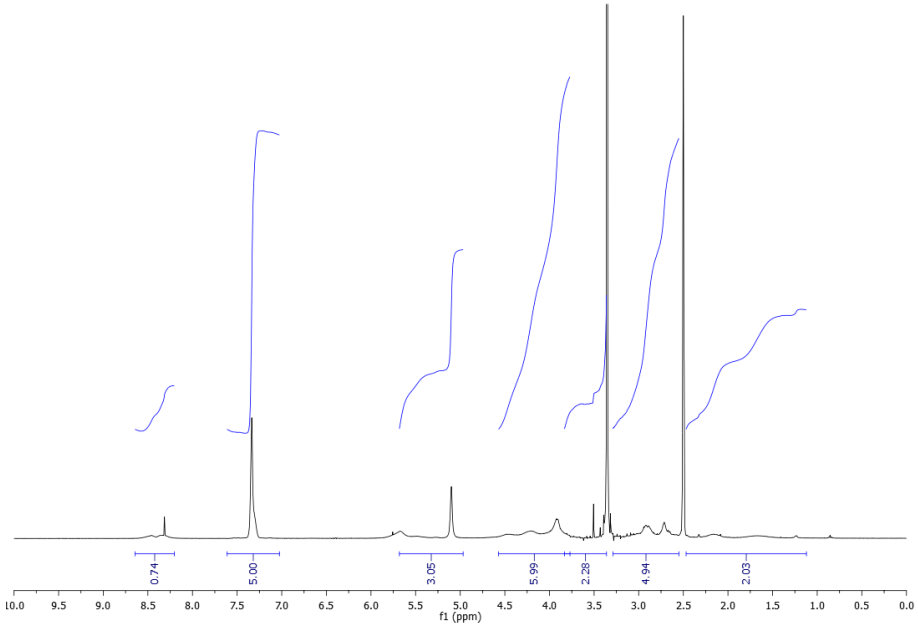

TGA Trace

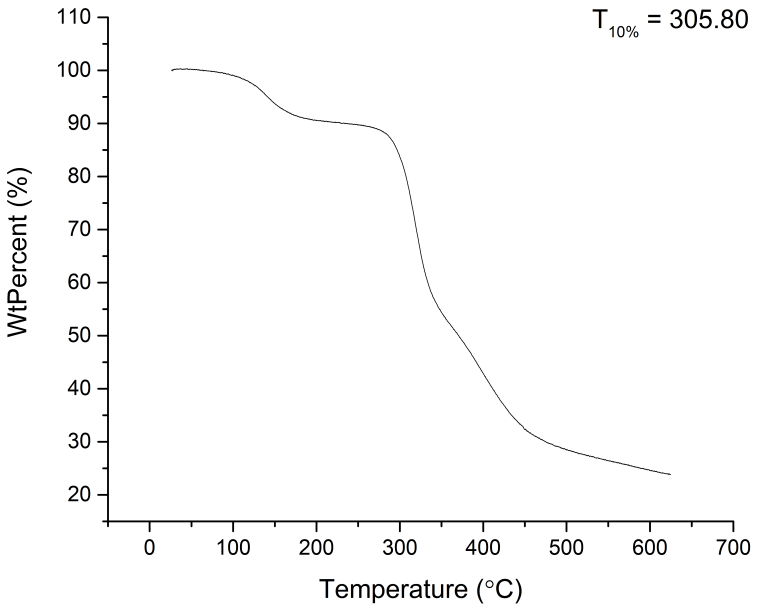

DSC Trace

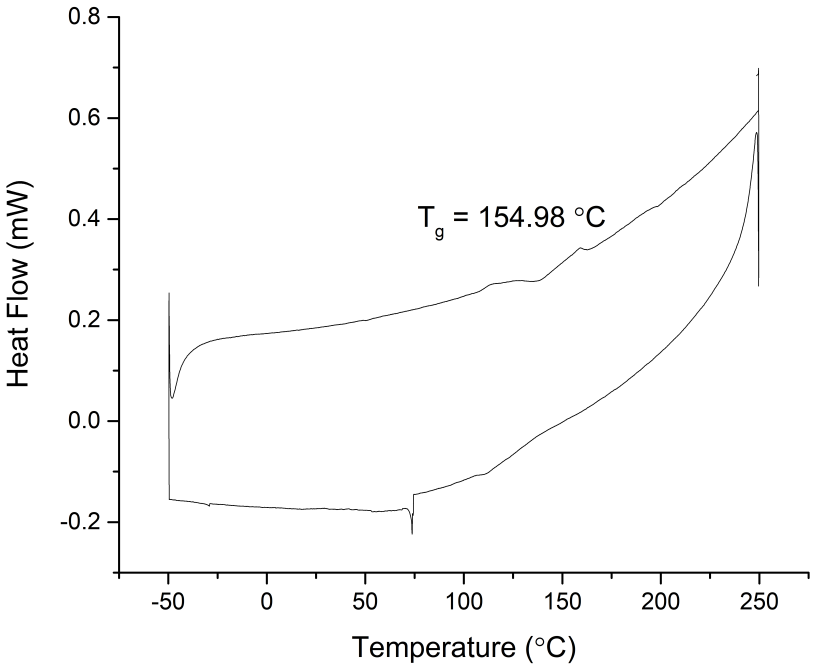

Infrared Spectrum

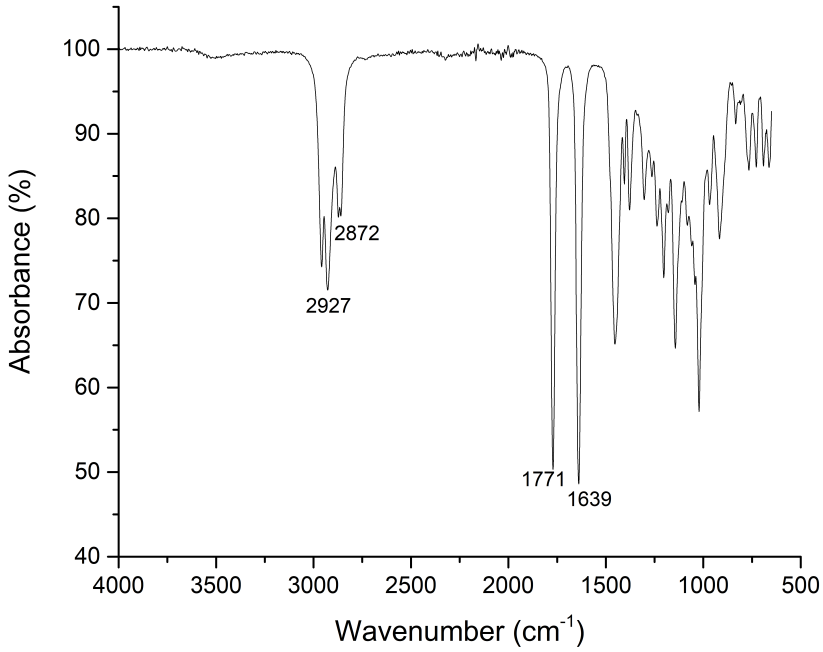

Sar-Sar Benzyl Ester Homopolymer 4.42k

^{1}H NMR Spectrum

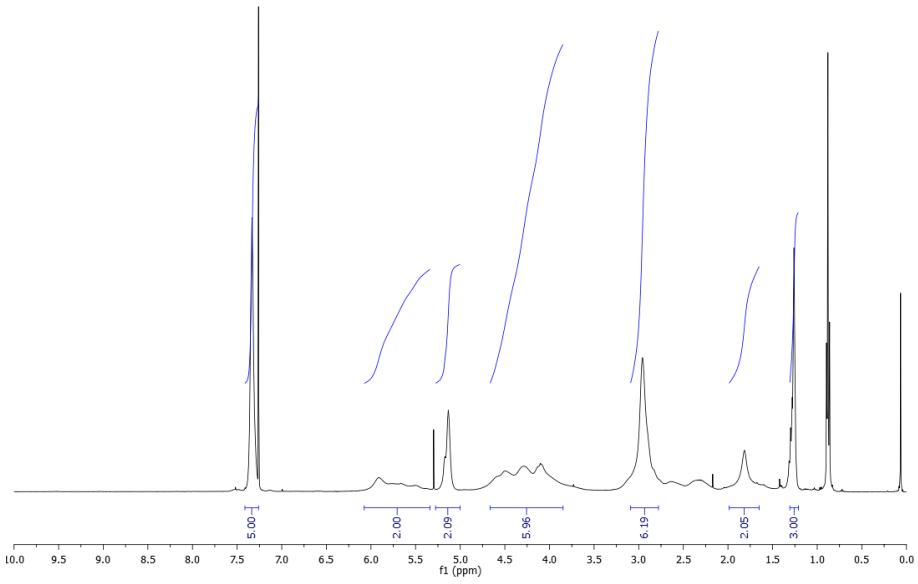

TGA Trace

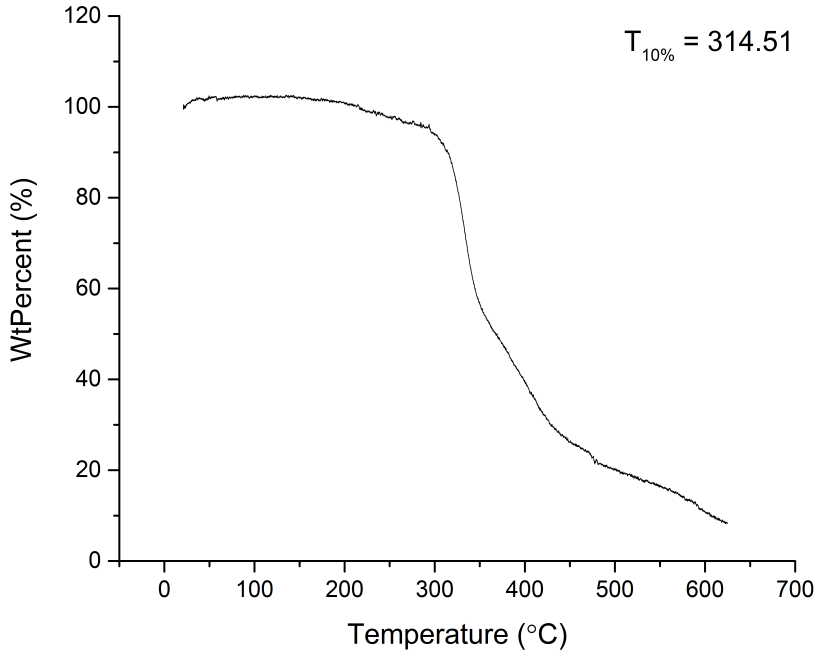

Infrared Spectrum

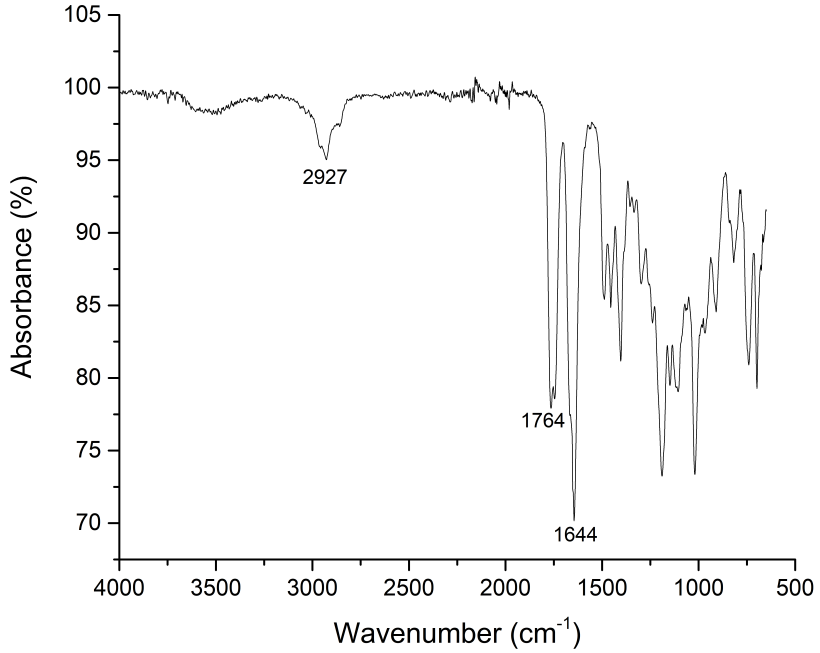

7.4.2.3 Analytical Data and Spectra for Random Co-polymers 4.43a-d

Propyl Sarcosine Benzyl Ester Copolymer 4.43a

SEC Trace

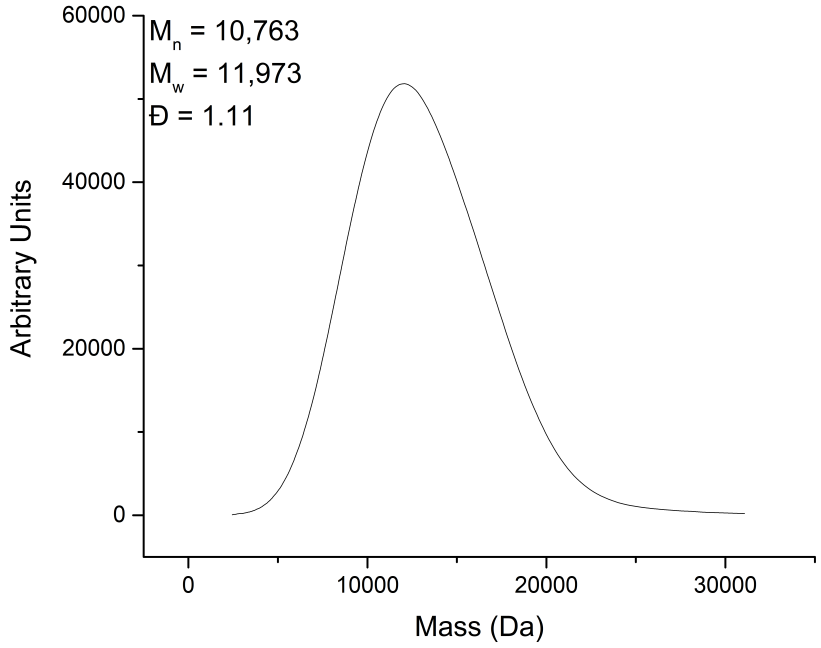

^{1}H NMR Spectrum

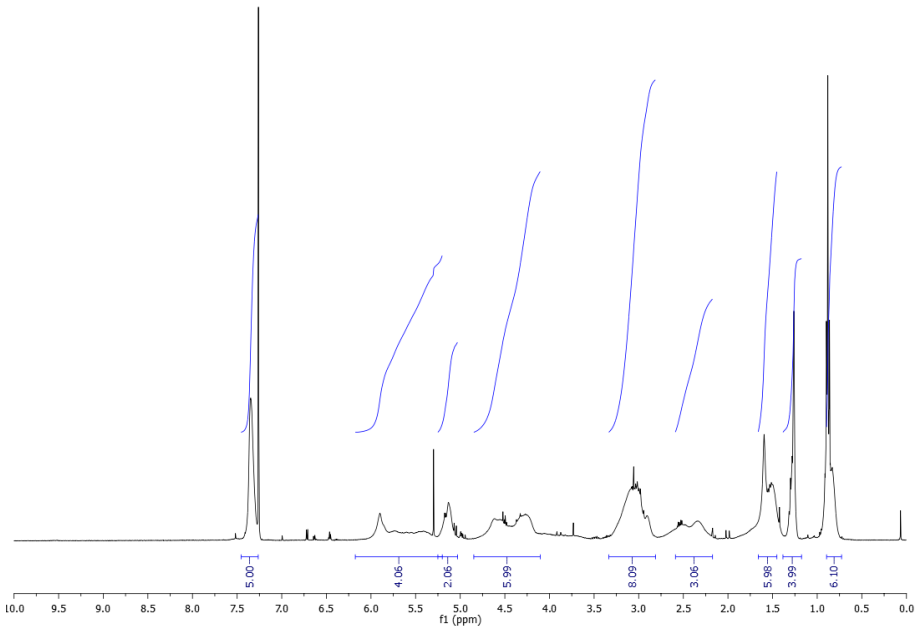

TGA Trace

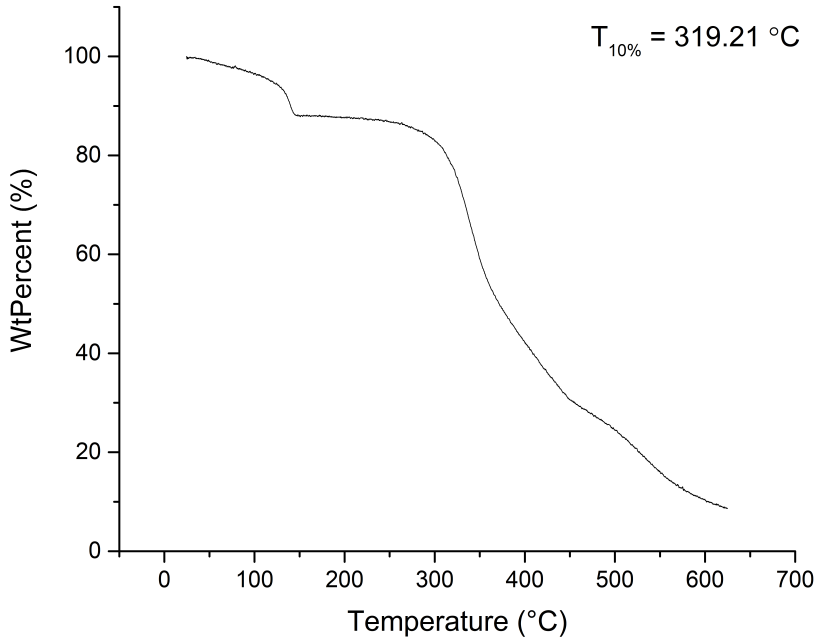

DSC Trace

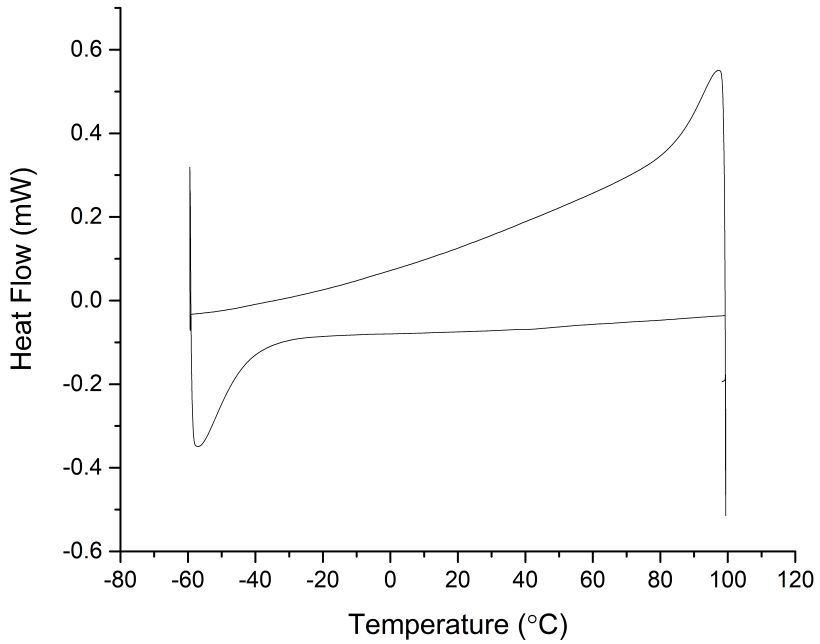

Infrared Spectrum

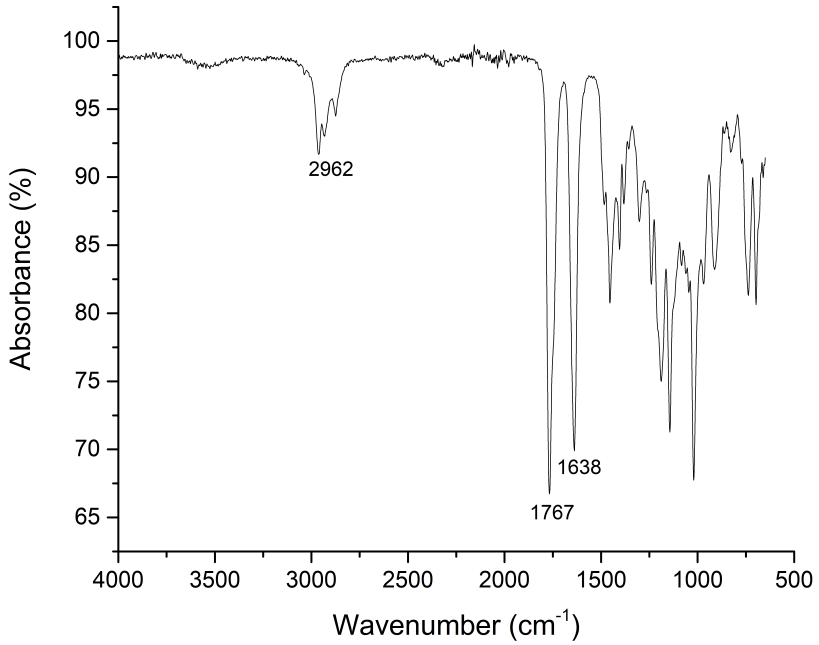

Ethyl Benzyl Copolymer 4.43b

SEC Trace

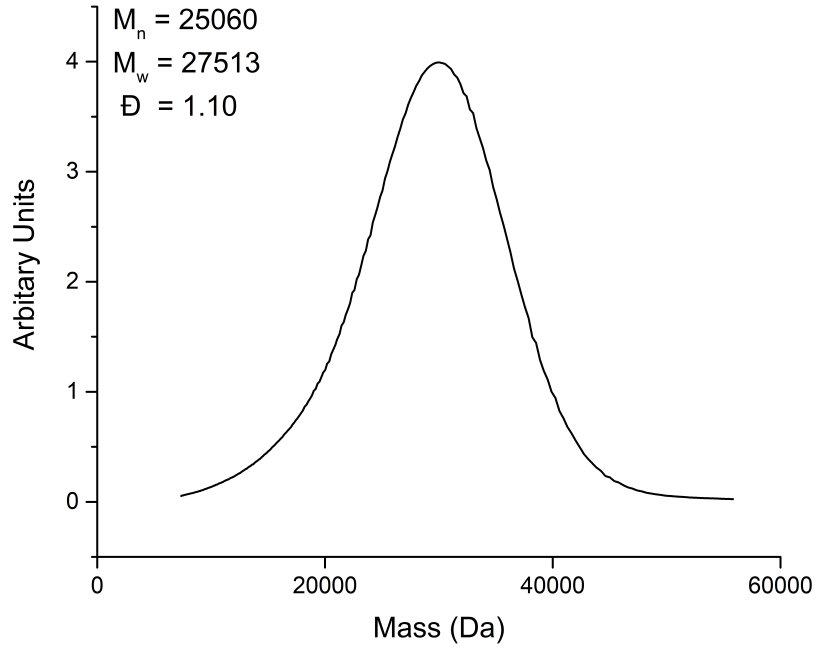

^{1}H NMR Spectrum

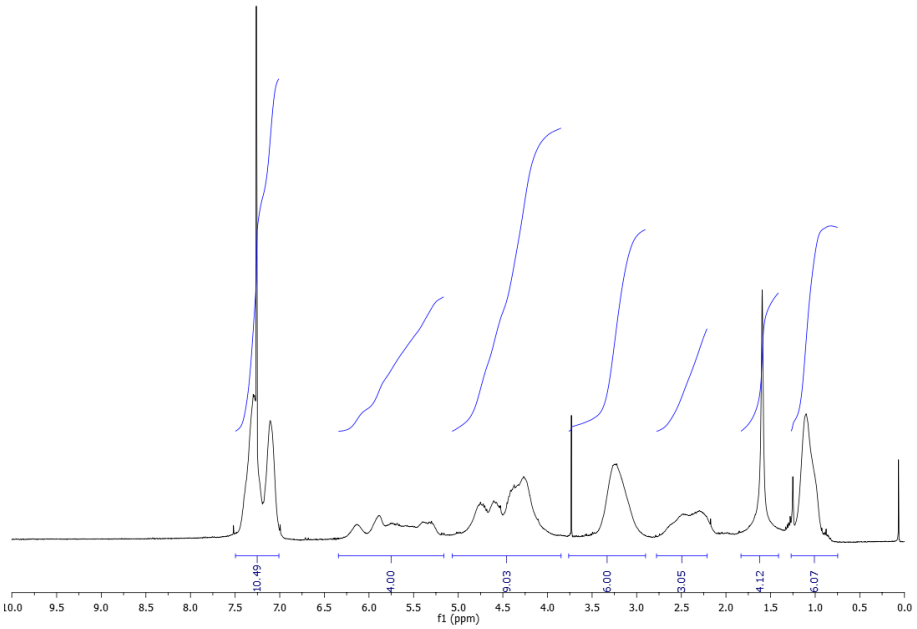

TGA Trace

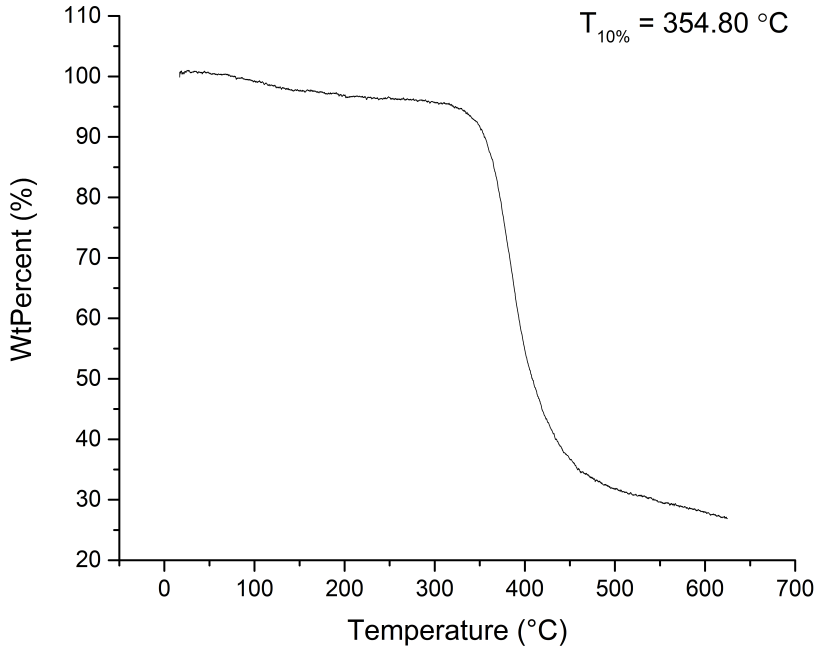

DSC Trace

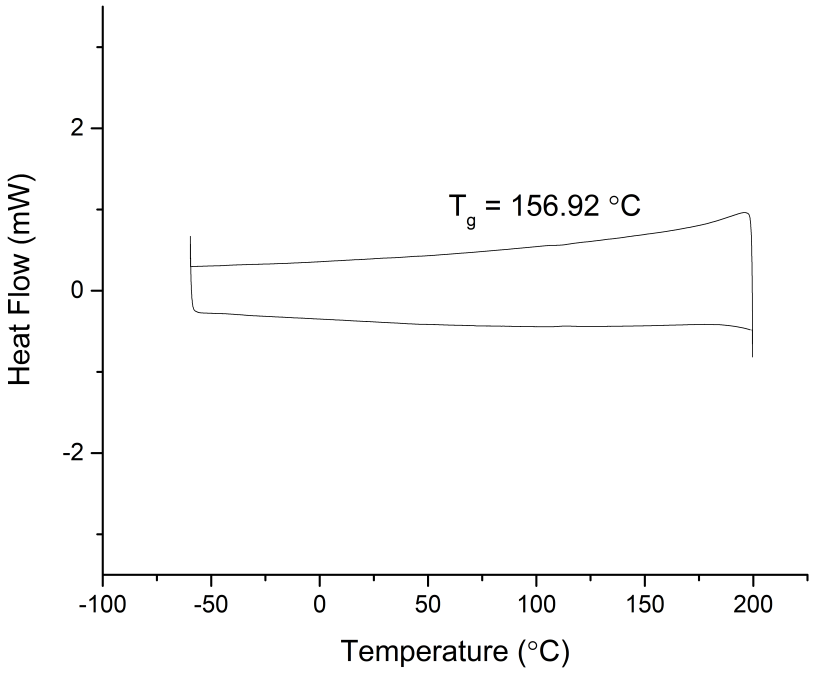

Infrared Spectrum

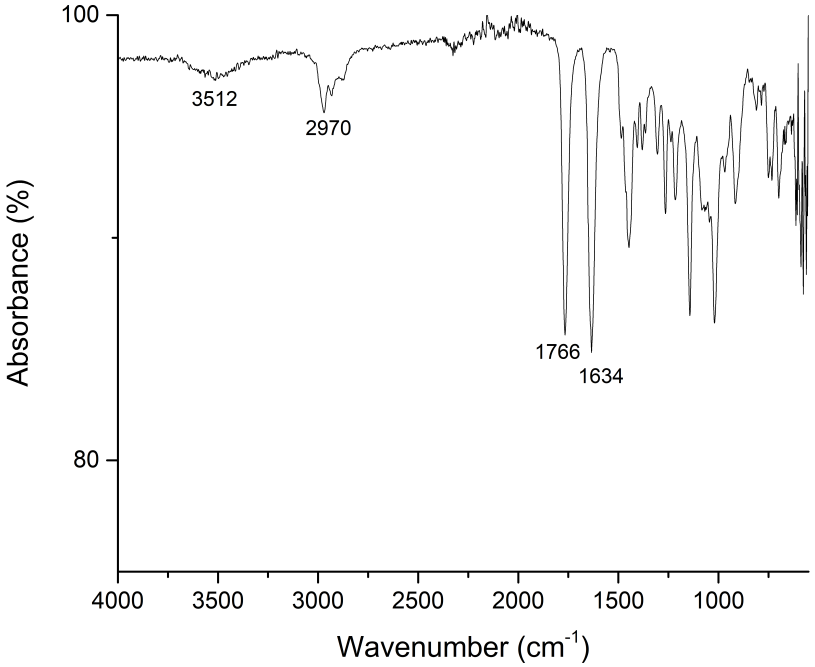

Butyl Proline Methyl Ester Copolymer 4.43c

SEC Trace

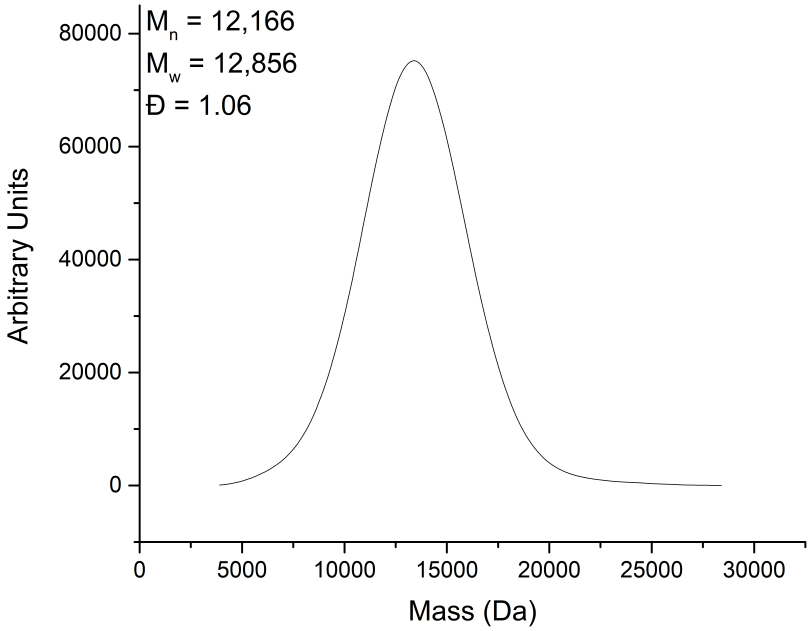

^{1}H NMR Spectrum

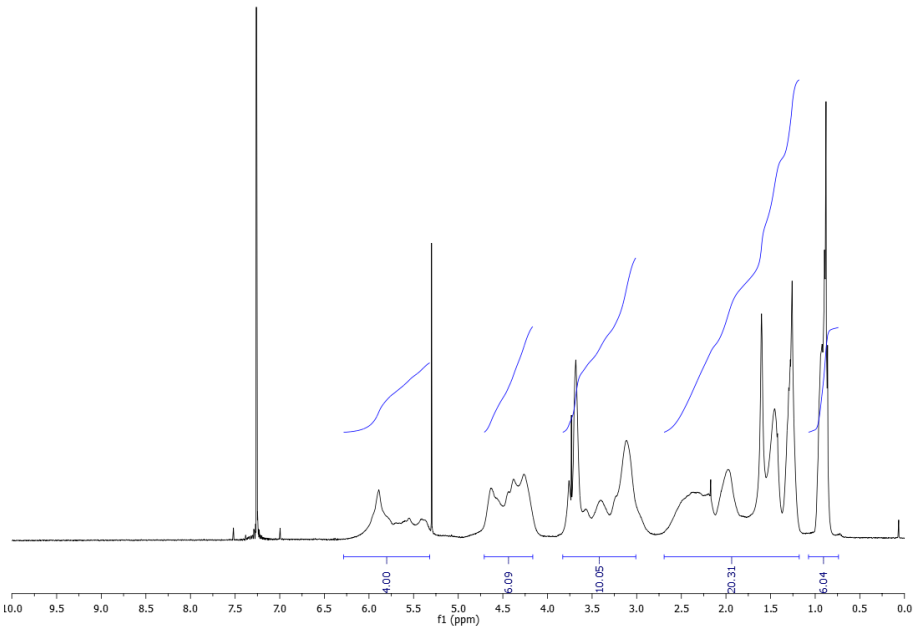

TGA Trace

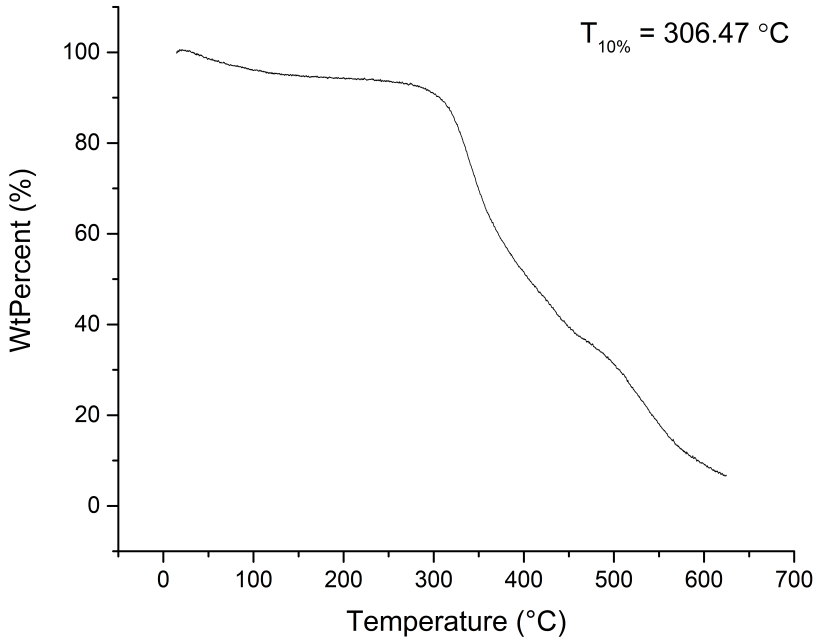

DSC Trace

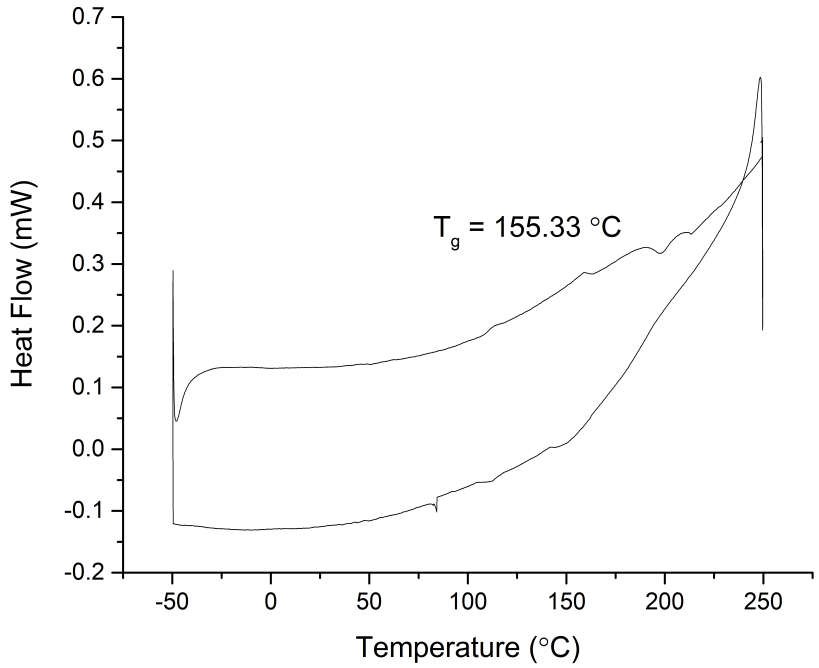

Infrared Spectrum

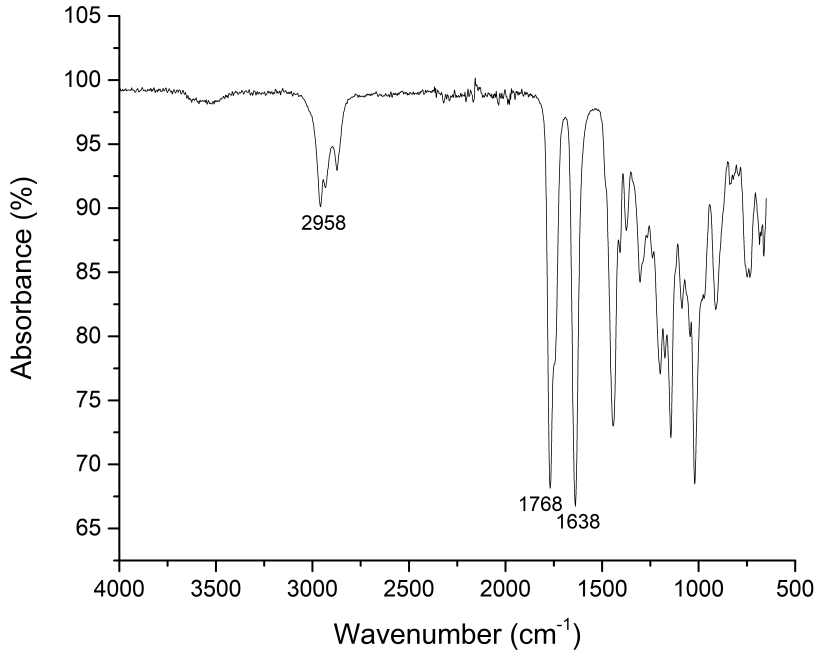

Methyl Sarcosine Benzyl Ester Copolymer 4.43d

^{1}H NMR Spectrum

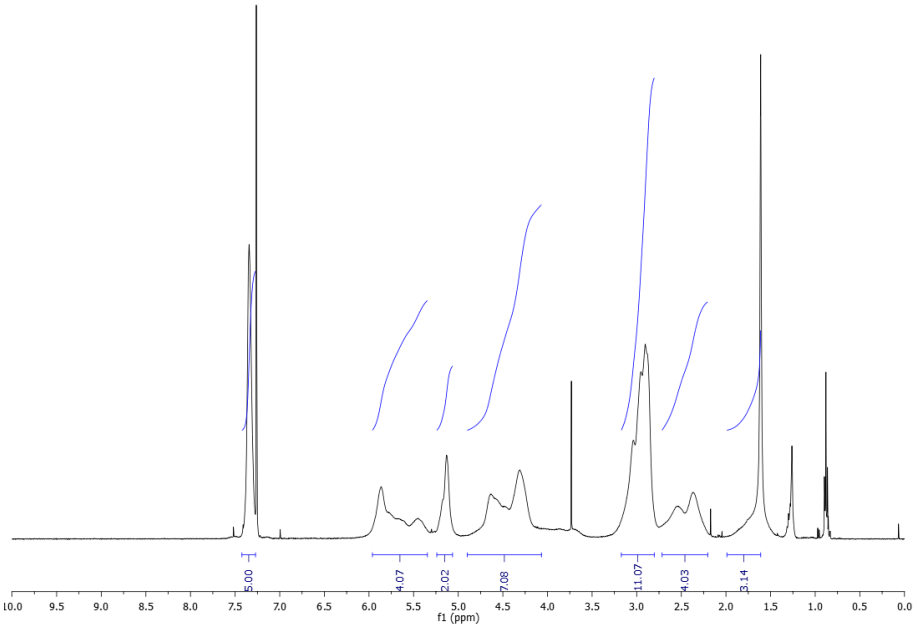

TGA Trace

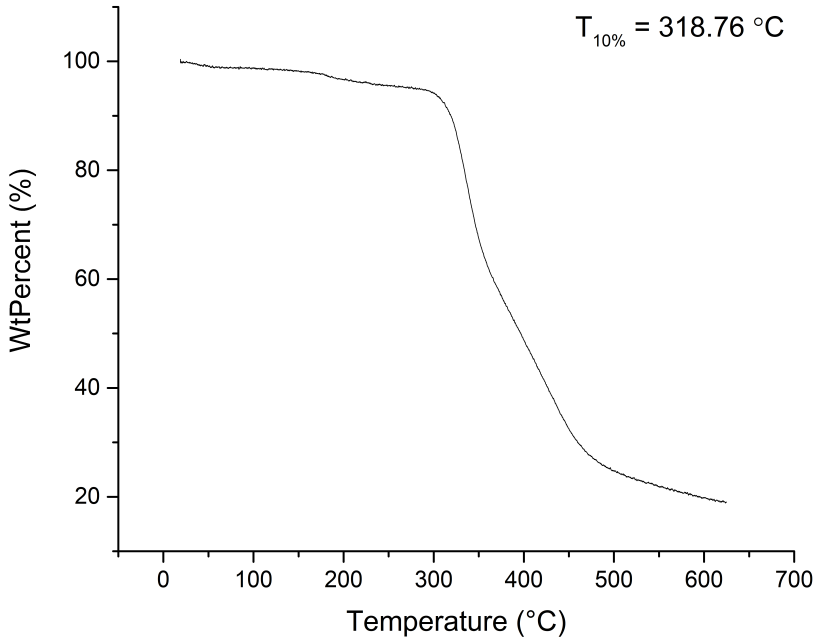

DSC Trace

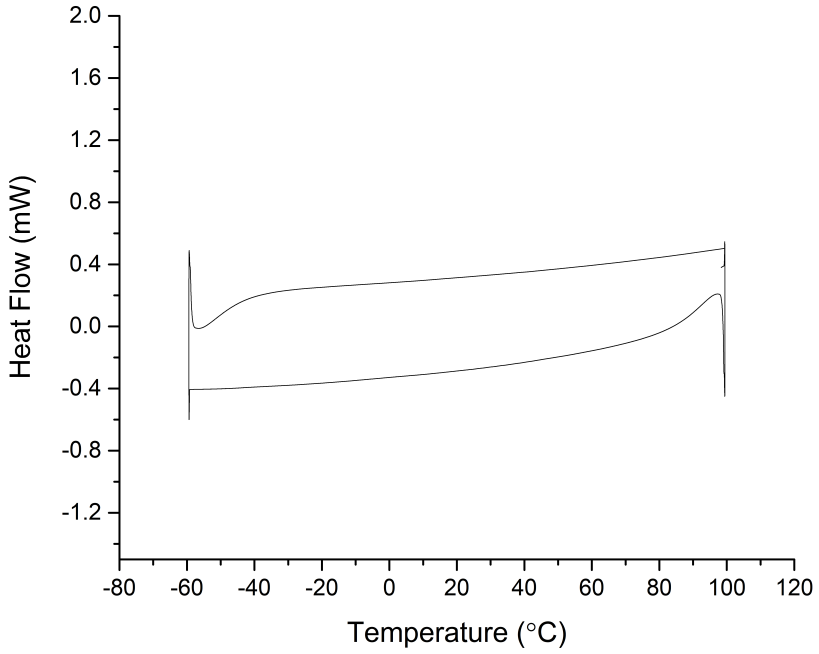

Infrared Spectrum

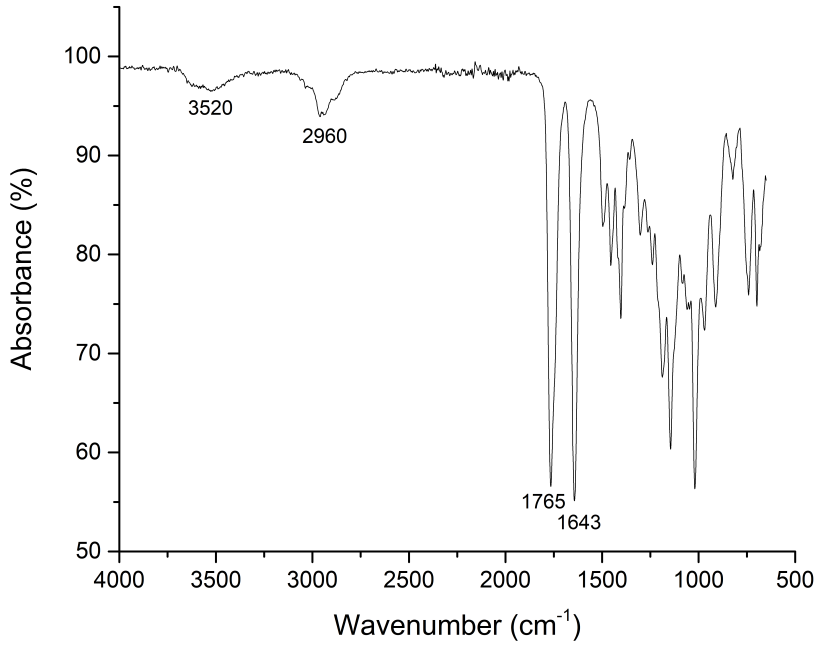

7.4.2.4 Procedure for the Synthesis of Dibenzyl/Diethyl Block Copolymer 4.45

Dibenzyl amide **4.39g** (39 mg, 0.1 mmol) and catalyst **G2** were combined in a Schlenk tube under argon. $(CH_2Cl)_2$ was degassed by three cycles of freeze-pump-thaw, then $(CH_2Cl)_2$ (1 mL) was added to the Schlenk tube containing the monomer/catalyst. The reaction mixture was then stirred at 40 °C for 13.6 h, which corresponds to 80% conversion, as determined by the kinetic plot obtained for monomer **4.39g**. After 13.6 h, a sample was taken and immediately analysed by ^{1}H NMR spectroscopy to determine the conversion. A second sample was then taken, end-capped by treatment with excess ethyl vinyl ether for 30 minutes, filtered through a silica plug and precipitated into hexane. The hexane was decanted and the sample dried under reduced pressure before being analysed by SEC. A solution of diethyl monomer **4.39b** (29 mg, 0.1 mmol) in $(CH_2Cl)_2$ (1 mL), which had been subjected to degassing by three cycles of freeze-pump-thaw, was then added to the reaction mixture. The reaction was monitored by SEC and ^{1}H NMR spectroscopy every 24 h for the next 48 h as the second block was incorporated according to the previously described procedure. After 48 h the polymer was end-capped by treatment with excess ethyl vinyl ether for 30 minutes. The polymer was then filtered through a plug of silica and precipitated into hexane. The hexane was decanted and the polymer dried under reduced pressure before being analysed by ^{1}H NMR spectroscopy and SEC.

7.4.2.5 General Procedure for Monitoring the Kinetics of Amide Homopolymerisation

The appropriate quantities of monomer and catalyst **G2** (1.7 mg, 1 mol%) were separately dissolved in $(CD_2Cl)_2$ (0.5 mL). Tetramethylsilane (1 drop) was then added to the monomer solution. Each solution was subjected to three cycles of degassing by freeze-pump-thaw. The monomer and catalyst solution were then combined. A sample of the reaction mixture was then transferred to an NMR tube equipped with a Young tap. The sample was sealed under argon and ^{1}H NMR spectra recorded at 40 °C every 30 mins for 24 h. Conversion was then determined by integrating monomer alkene peaks relative to the TMS peak.

7.5 Synthesis of Spirocyclic Oxanorbornene-Imides

7.5.1 General Procedure for the Synthesis of Disubstituted Amides

Acid **5.10** (2.0 g, 9.52 mmol, 1.0 eq) was suspended in anhydrous CH_2Cl_2 (5 mL) under an atmosphere of argon. The suspension was cooled to 0 °C and oxalyl chloride 2.0 M solution in CH_2Cl_2 (12 mL, 24 mmol, 2.5 eq) was added dropwise over 10 min, followed by DMF (4 drops). The suspension was stirred at ambient temperature until a solution was obtained. The obtained solution was concentrated *in vacuo*, to give the crude acid chloride as a brown solid. The crude material was redissolved in anhydrous CH_2Cl_2 (10 mL) and cooled to 0 °C. A solution of monosubstituted amine (9.52 mmol, 1.0 eq) and pyridine (0.77 mL, 9.52 mmol, 1.0 eq, 2.0 eq if using the amine salt) in CH_2CL_2 (10 mL) was added dropwise over 10 min. The solution was allowed to stir at ambient temperature overnight before diluting with CH_2Cl_2 (30 mL) and H_2O (50 mL). The organic layer was separated and further washed with 1 M HCl_{aq} (50 mL), H_2O (50 mL) and brine (50 mL). The organic layer was dried ($MgSO_4$), filtered and concentrated *in vacuo*.

_N_-Isopropyl-2-[(1_R_,5_S_,7_S_)-4-oxo-3,10-dioxatricyclo[5.2.1.0^{1,5}]dec-8-en-5-yl]acetamide 5.1a

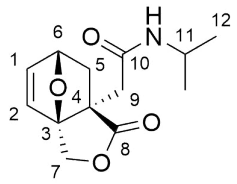

Acid **5.10** (2 g, 9.52 mmol) and isopropylamine (0.82 mL, 9.52 mol) were coupled according to the general procedure for the synthesis of disubstituted amides. The crude material was purified using flash column chromatography (80:20-100:0, EtOAc:PE) to give the target compound **5.1a** as a yellow oil (1.27 g, 53%) $\boldsymbol{R_F}$ = 0.19, (80:20, EtOAc:PE); **IR (Neat)** ν_{max} 3307 (w), 2971 (w), 1765 (s), 1643 (s) and 1536 (s) cm^{-1}; **^{1}H NMR** (400 MHz, $CDCl_3$): δ = 6.59 (d *J* 5.9 Hz, 1H, 2-H), 6.49 (dd *J* 5.9, 1.8 Hz, 1H, 1-H), 6.20-6.07 (br, 1H, N-H), 5.00 (dd *J* 4.8, 1.8 Hz, 1H, 6-H), 4.83 (d *J* 10.6 Hz, 1H, 7-H), 4.56 (d *J* 10.6 Hz, 1H, 7-H), 3.97 (dsep *J* 6.8, 5.6 Hz, 1H, 11-H), 2.48 (dd *J* 12.0, 4.8 Hz, 1H, 5-H), 2.30 (d *J* 14.3 Hz, 1H, 9-H), 2.19 (d *J* 14.3 Hz, 1H, 9-H), 1.29 (d *J* 12.0 Hz, 1H, 5-H), 1.11 (d *J* 6.6 Hz, 6H, 12-H); **^{13}C NMR** (100 MHz, $CDCl_3$): δ = 179.1 (8), 167.7 (10), 137.2 (1), 131.6 (2), 94.5 (3), 78.4 (6), 69.7 (7), 52.9 (4), 42.7 (9), 41.8 (11), 36.6 (5), 22.5 (12), 22.4 (12); **HRMS (ESI)** *m/z* calculated for $C_{13}H_{17}NNaO_4$ 274.1050 $(M+Na)^+$, found 274.1056, − 2.3 ppm error.

N-Butyl-2-[(1*R*,5*S*,7*S*)-4-oxo-3,10-dioxatricyclo[5.2.1.0^{1,5}]dec-8-en-5-yl]acetamide 5.1b

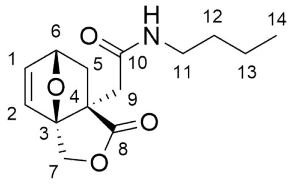

Acid **5.10** (2 g, 9.52 mmol) and butylamine (0.94 mL, 9.52 mol) were coupled according to the general procedure for the synthesis of disubstituted amides. The crude material was then purified using flash column chromatography (80:20, EtOAc:PE) to give the target compound **5.1b** as a white solid (1.71 g, 68%). $\boldsymbol{R_F}$ = 0.18, (80:20, EtOAc:PE); **m.p.** 83-84 °C; **IR (Neat)** ν_{max} 3240 (m), 3078 (w), 2961 (m), 2876 (w), 1768 (s), 1631 (s) and 1562 (m) cm^{-1}; **^{1}H NMR** (400 MHz, $CDCl_3$): δ = 6.60 (d *J* 5.9 Hz, 1H, 2-H), 6.51 (dd *J* 5.9, 1.7 Hz, 1H, 1-H), 6.30 (br, 1H, N-H), 5.02 (dd *J* 4.8, 1.7 Hz, 1H, 6-H), 4.84 (d *J* 10.7 Hz, 1H, 7-H), 4.59 (d *J* 10.7 Hz, 1H, 7-H), 3.20 (dt *J* 7.1, 2.5 Hz, 2H, 11-H), 2.50 (dd *J* 11.9, 4.8 Hz, 1H, 5-H), 2.33 (d *J* 14.3 Hz, 1H, 9-H), 2.26 (d *J* 14.3 Hz, 1H, 9-H), 1.51-1.42 (m, 2H, 12-H), 1.38-1.27 (m, 3H, 1×5-H + 2×13-H), 0.90 (t *J* 6.7 Hz, 3H, 14-H); **^{13}C NMR** (100 MHz, $CDCl_3$): δ = 179.3 (8), 168.5 (10), 137.4 (1), 131.5 (2), 94.6 (3), 78.5 (6), 69.7 (7), 52.8 (4), 42.7 (9), 39.7 (11), 36.6 (5), 31.4 (12), 20.1 (13), 13.8 (14); **HRMS (ESI)** *m/z* calculated for $C_{14}H_{19}NNaO_4$ 288.1202 $(M+Na)^+$, found 288.1206, 1.5 ppm error.

N-Hexyl-2-[(1*R*,5*S*,7*S*)-4-oxo-3,10-dioxatricyclo[5.2.1.0^{1,5}]dec-8-en-5-yl]acetamide 5.1c

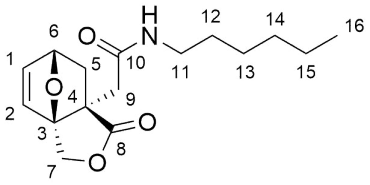

Acid **5.10** (2 g, 9.52 mmol) and hexylamine (1.26 mL, 9.52 mol) were coupled according to the general procedure for the synthesis of disubstituted amides. The crude material was then purified using flash column chromatography (70:30-100:0, EtOAc:PE) to give the target compound **5.1c** as a yellow crystalline solid (870 mg, 31%). $\boldsymbol{R_F}$ = 0.19, (70:30, EtOAc:PE); **m.p.** 62-62 °C; **IR (Neat)** ν_{max} 3303 (m), 2927 (m), 2855 (m), 1767 (s), 1669 (m), 1649 (s) and 1541 (s) cm^{-1}; **^{1}H NMR** (400 MHz, $CDCl_3$): δ = 6.60 (d *J* 5.7 Hz, 1H, 2-H), 5.67 (dd *J* 5.7, 1.6 Hz, 1H, 1-H), 6.39-6.32 (br, 1H, N-H), 5.01 (dd *J* 4.6, 1.6 Hz, 1H, 6-H), 4.84 (d *J* 10.5 Hz,

1H, 7-H), 4.57 (d *J* 10.5 Hz, 1H, 7-H), 3.18 (dt *J* 7.1, 6.8 Hz, 1H, 11-H), 2.49 (dd *J* 12.1, 4.6 Hz, 1H, 5-H), 2.32 (d *J* 14.6 Hz, 1H, 9-H), 2.25 (d *J* 14.6, 1H, 9-H), 1.52-1.41 (m, 2H, 12-H), 1.33-1.20 (m, 7H, 5-H, 13-H, 14-H, 15-H), 0.86 (t *J* 7.2 Hz, 3H, 16-H); **^{13}C NMR** (100 MHz, $CDCl_3$): δ = 179.3 (8), 168.5 (10), 137.3 (1), 131.5 (2), 94.5 (3), 78.5 (6), 69.7 (7), 52.8 (4), 42.7 (9), 39.9 (11), 36.6 (5), 31.5 (15), 29.3 (12), 26.6 (13), 22.6 (14), 14.1 (16); **HRMS (ESI)** *m/z* calculated for $C_{16}H_{23}NNaO_4$ 316.1519 $(M+Na)^+$, found 316.1525, − 1.9 ppm error.

N-Octyl-2-[(1*R*,5*S*,7*S*)-4-oxo-3,10-dioxatricyclo[5.2.1.0^{1,5}]dec-8-en-5-yl]acetamide 5.1d

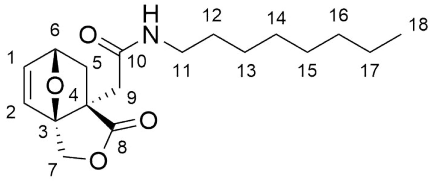

Acid **5.10** (2 g, 9.52 mmol) and octylamine (1.57 mL, 9.52 mol) were coupled according to the general procedure for the synthesis of disubstituted amides. The crude material was purified using flash column chromatography to give the target amide **5.1d** as a pale yellow crystalline solid (2.12 g, 69%). $\boldsymbol{R_F}$ = 0.3, (90:10, EtOAc:PE); **m.p.** 75-76 °C; **IR (Neat)** ν_{max} 3302 (m), 2918 (m), 2851 (m), 1767 (s), 1669 (m), 1649 (s) and 1543 (s) cm^{-1}; **^{1}H NMR** (400 MHz, $CDCl_3$): δ = 6.60 (d *J* 6.1 Hz, 1H, 2-H), 6.50 (dd *J* 6.1, 1.6 Hz, 1H, 1-H), 6.37-6.28 (br, 1H, N-H), 5.01 (dd *J* 4.8, 1.6 Hz, 1H, 6-H), 4.84 (d *J* 10.8 Hz, 1H, 7-H), 4.57 (d *J* 10.8 Hz, 1H, 7-H), 3.18 (dt *J* 12.3, 6.3 Hz, 2H, 11-H), 2.49 (dd *J* 12.3, 4.8 Hz, 1H, 5-H), 2.33 (d *J* 14.6 Hz, 1H, 9-H), 2.24 (d *J* 14.6 Hz, 1H, 9-H), 1.51-1.40 (m, 2H, 12-H), 1.34-1.17 (m, 11H, 5-H, 13-H, 14-H, 15-H, 16-H, 17-H), 0.86 (t *J* 7.1 Hz, 3H, 18-H); **^{13}C NMR** (100 MHz, $CDCl_3$): δ = 179.3 (8), 168.5 (10), 137.3 (1), 131.6 (2), 94.5 (3), 78.5 (6), 69.7 (7), 52.8 (4), 42.7 (9), 40.0 (11), 36.6 (5), 31.9 (12), 29.4 (13), 29.3 (14/15), 26.9 (16), 22.7 (17), 14.2 (18); **HRMS (ESI)** *m/z* calculated for $C_{18}H_{27}NNaO_4$ 344.1832 $(M+Na)^+$, found 344.1837, − 0.9 ppm error.

N-Benzyl-2-[(1*R*,5*S*,7*S*)-4-oxo-3,10-dioxatricyclo[5.2.1.0^{1,5}]dec-8-en-5-yl]acetamide 5.1e

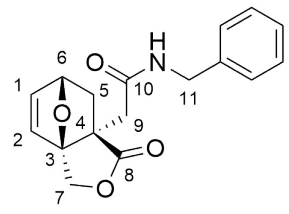

Acid **5.10** (2 g, 9.52 mmol) and benzylamine (1.04 mL, 9.52 mol) were coupled according to the general procedure for the synthesis of disubstituted amides. The crude material was purified using flash column chromatography (70:30-90:10, EtOAc:PE) to give the target material **5.1d** as a white crystalline solid (1.67 g, 58%). $\boldsymbol{R_F}$ = 0.30, (80:20, EtOAc:PE); **m.p.** 106-107 °C; **IR (Neat)** ν_{max} 3286 (m), 1765 (s), 1636 (s) and 1547 (s) cm^{-1}; **^{1}H NMR** (400 MHz, $CDCl_3$): δ = 7.31-7.25 (m, 2H, ArH), 7.24-7.18 (m, 3H, ArH), 6.75-6.66 (br, 1H, N-H), 6.54 (d *J* 5.8 Hz, 1H, 2-H), 6.45 (dd *J* 5.8, 1.6 Hz, 1H, 1-H), 4.95 (dd *J* 4.8, 1.6 Hz, 1H, 6-H), 4.75 (d *J* 10.6 Hz, 1H, 7-H), 4.51 (d *J* 10.6 Hz, 1H, 7-H), 4.37 (dd *J* 14.6, 5.8 Hz, 1H, 11-H), 4.30 (dd *J* 14.6, 5.8 Hz, 1H, 11-H), 2.41 (dd *J* 12.0, 4.9 Hz, 1H, 5-H), 2.32 (d *J* 14.8 Hz, 1H, 9-H), 2.23 (d *J* 14.8 Hz, 1H, 9-H), 1.25 (d *J* 12.0 Hz, 1H, 5-H); **^{13}C NMR** (100 MHz, $CDCl_3$): δ = 179.2 (8), 168.6 (10), 137.8 (1), 137.4 (ArC), 131.4 (2), 128.8 (ArCH), 127.8 (ArCH), 127.6 (ArCH), 94.5 (3), 78.5 (6), 69.6 (7), 52.8 (4), 43.9 (11), 42.5 (9), 36.6 (5); **HRMS (ESI)** *m/z* calculated for $C_{17}H_{17}NNaO_4$ 322.1050 $(M+Na)^+$, found 322.1049, 0.3 ppm error.

Benzyl-2-[[2-[(1*R*,5*S*,7*S*)-4-oxo-3,10-dioxatricyclo[5.2.1.0^{1,5}]-dec-8-en-5-yl]acetyl]amino]acetate 5.1f

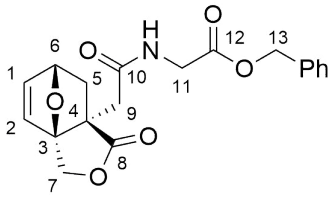

Acid **5.10** (2 g, 9.52 mmol) and glycine benzyl ester hydrochloride (1.92 g, 9.52 mol) were coupled according to the general procedure for the synthesis of disubstituted amides. The crude material was purified using flash column chromatography (80:20-100:0, EtOAc:PE) to give the target amide **5.1f** as a white crystalline solid (1.86 g, 55%). $\boldsymbol{R_F}$ = 0.38, (80:20, EtOAc:PE); **m.p.** 109-110 °C; **IR (Neat)** ν_{max} 3394 (m), 3300 (w), 1769 (s), 1742 (s), 1667 (m), 1647 (s) and 1547 (m) cm^{-1}; **^{1}H NMR** (400 MHz, $CDCl_3$): δ = 7.39 (m, 5H, ArH), 6.98-6.91 (br, 1H, N-H), 6.56 (d *J* 5.6 Hz, 1H, 2-H), 6.50 (dd *J* 5.6, 1.5 Hz, 1H, 1-H), 5.16 (s, 2H, 13-H), 4.99 (dd *J* 4.9, 1.7 Hz, 1H, 6-H), 4.82 (d *J* 10.4 Hz, 1H, 7-H), 4.57 (d *J* 10.4 Hz, 1H, 7-H), 4.13 (dd *J* 17.9, 5.9 Hz, 1H, 11-H), 3.91 (dd *J* 17.9, 5.9 Hz, 1H, 11-H), 2.50 (dd *J* 12.2, 4.9 Hz, 1H, 5-H), 2.41 (d *J* 14.9 Hz, 1H, 9-H), 2.34 (d *J* 14.9 Hz, 1H, 9-H), 1.36 (d *J* 12.2 Hz, 1H, 5-H); **^{13}C NMR** (100 MHz, $CDCl_3$): δ = 179.2 (8), 169.5 (12), 169.0 (10), 137.7 (1), 135.2 (ArC), 131.2 (2), 128.7 (ArCH), 128.6 (ArCH), 128.5 (ArCH), 94.4 (3), 78.6 (6), 69.4 (7), 67.3 (13), 52.4 (4), 41.9 (9), 41.6 (11), 36.7 (5); **HRMS (ESI)** *m/z* calculated for $C_{19}H_{19}NNaO_6$ 380.1105 $(M+Na)^+$, found 380.1103, − 0.1 ppm error.

(1*R*,4*S*,6*S*)-1'-Butyl-1-(hydroxymethyl)spiro[7-oxabicyclo[2.2.1]hept-2-ene-6,3'-pyrrolidine]-2',5'-dione 5.2

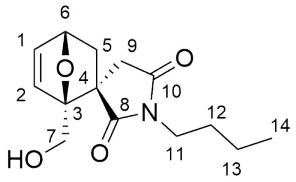

Acid **5.10** (2 g, 9.52 mmol, 1.0 eq) was suspended in CH_2Cl_2 (5 mL) under an atmosphere of argon. The suspension was cooled to 0 °C and oxalyl chloride 2.0 M in CH_2Cl_2 (12 mL, 24 mmol, 2.5 eq) was added dropwise over 10 min. The suspension was stirred for 2 h or until a solution was obtained. The solution was concentrated *in vacuo* and the crude material redissolved in CH_2Cl_2 (10 mL). The solution was cooled to 0 °C and a solution of butylamine (48 mmol, 5.0 eq) in CH_2Cl_2 (10 mL) was added dropwise. The solution was allowed to stir at room temperature overnight before diluting with CH_2Cl_2 (30 mL) and H_2O (50 mL). The organic layer was separated and further washed with 1 M HCl_{aq} (50 mL), H_2O (50 mL) and brine (50 mL). The organic phase was dried ($MgSO_4$), filtered and concentrated *in vacuo*. The crude material was purified using flash column chromatography (80:20, EtOAc:PE) to give the target imide **5.2** as a white crystalline solid (839 mg, 33%). $\boldsymbol{R_F}$ = 0.25, (80:20, EtOAc:PE); **m.p.** 69-70 °C; **IR (Neat)** ν_{max} 3396 (m), 3024 (w), 2946 (m), 2874 (m), 1767 (m), 1674 (s) and 1685 (s) cm^{-1}; **^{1}H NMR** (400 MHz, $CDCl_3$): δ = 6.65 (dd *J* 5.7, 1.7 Hz, 1H, 1-H), 6.48 (d *J* 5.7 Hz, 1H, 2-H), 5.13 (dd *J* 4.8, 1.7 Hz, 6-H), 4.02 (d *J* 11.6 Hz, 1H, 7-H), 3.90 (dd *J* 11.6, 4.1 Hz, 1H, 7-H), 3.50 (t *J* 7.4 Hz, 2H, 11-H), 2.72-2.61 (m, 2H, 5-H/9-H), 2.47-2.37 (m, 2H, OH/9-H), 1.59-1.48 (m, 3H, 12-H/5-H), 1.37-1.25 (m, 2H, 13-H), 0.91 (t *J* 7.3 Hz, 3H, 14-H); **^{13}C NMR** (100 MHz, $CDCl_3$): δ = 180.4 (8), 176.2 (10), 140.3 (1), 135.1 (2), 92.8 (3), 79.1 (6), 60.3 (7), 49.9 (4), 44.0 (5), 40.1 (9), 39.0 (11), 29.7 (12), 20.1 (13), 13.7 (14); **HRMS (ESI)** *m*/*z* calculated for $C_{14}H_{19}NNaO_4$ 288.1214 $(M+Na)^+$, found 288.1206, − 2.7 ppm error.

7.5.2 General Procedure for the Hydrogenation of Secondary Amides to Imides

Secondary amide (1.88 mmol, 1.0 eq) was dissolved in MeOH (1 mL) under argon, the addition of EtOAc may be necessary in some cases to obtain a solution. In a separate flask Pd/C (10% *w*/*w*) was suspended in MeOH (1 mL) under argon. H_2 was bubbled through the suspension of Pd/C for 10 min. The solution of secondary amide was then added to the catalyst suspension. The reaction mixture was allowed

to stir at room temperature for 16 h under H_2 (1 bar). The reaction mixture was then passed through a pad of Celite® and concentrated *in vacuo*.

(1*R*,2*S*,4*R*)-1'-Butyl-1-(hydroxymethyl)spiro[7-oxabicyclo[2.2.1]heptane-2,3'-pyrrolidine]-2',5'-dione 5.45b

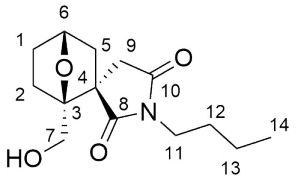

Butyl amide **5.1b** (100 mg) was hydrogenated according to the general procedure for the hydrogenation of alkyl/benzyl secondary amides. The crude material was purified using flash column chromatography (80:20-90:10, EtOAc:PE) to give the target compound **5.45b** as a clear oil (77 mg, 76%). $\boldsymbol{R_F}$ = 0.33, (90:10, EtOAc:PE); **IR (Neat)** ν_{max} 3460 (w), 2958 (w), 2874 (w), 1771 (w) and 1685 (s) cm^{-1}; **^{1}H NMR** (400 MHz, $CDCl_3$): δ = 4.72 (t *J* 5.3 Hz, 1H, 6-H), 3.93 (d *J* 5.3 Hz, 2H, 7-H), 3.49 (t *J* 7.3 Hz, 2H, 11-H), 2.97 (d *J* 17.9 Hz, 1H, 9-H), 2.71 (d *J* 17.9 Hz, 1H, 9-H), 2.52 (ddd *J* 12.1, 5.5, 2.6 Hz, 1H, 5-H), 2.02-1.91 (m, 2H, 1-H), 1.78-1.62 (m, 3H, 2-H, OH), 1.59-1.49 (m, 3H, 12-H/5-H), 1.37-1.23 (m, 2H, 13-H), 0.91 (t *J* 7.3 Hz, 3H, 14-H) ; **^{13}C NMR** (100 MHz, $CDCl_3$): δ = 180.5 (8), 175.7 (10), 90.4 (3), 77.4 (6), 62.7 (7), 52.6 (4), 45.3 (5), 39.2 (9), 38.8 (11), 31.3 (2), 29.7 (12/1), 20.1 (13), 13.7 (14); **HRMS (ESI)** *m/z* calculated for $C_{14}H_{21}NNaO_4$ 290.1363 $(M+Na)^+$, found 290.1368, − 2.5 ppm error.

(1*R*,2*S*,4*R*)-1'-Hexyl-1-(hydroxymethyl)spiro[7-oxabicyclo[2.2.1]heptane-2,3'-pyrrolidine]-2',5'-dione 5.45c

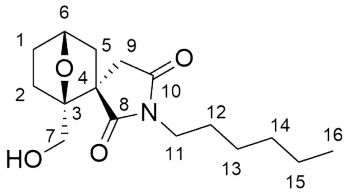

Hexyl amide **5.1c** (400 mg) was hydrogenated according to the general procedure for the hydrogenation of alkyl/benzyl secondary amides. The crude material was purified using flash column chromatography (80:20, EtOAc:PE) to give the target compound **5.45c** as a clear oil (378 mg, 94%). $\boldsymbol{R_F}$ = 0.32, (80:20, EtOAc:PE); **IR (Neat)** ν_{max} 3460 (w), 2931 (m), 2859 (w), 1771 (m) and 1686 (s) cm^{-1}; **^{1}H NMR** (400 MHz, $CDCl_3$): δ = 4.68 (t *J* 5.2 Hz, 1H, 6-H), 3.89 (s, 2H, 7-H), 3.44

(t J 7.5 Hz, 2H, 11-H), 2.96 (d J 18.4 Hz, 1H, 9-H), 2.68 (d J 18.4 Hz, 1H, 9-H), 2.48 (ddd J 11.9, 5.2, 2.5 Hz, 1H, 5-H), 2.34-2.18 (br, 1H, OH), 2.02-1.82 (m, 2H, 1-H/2-H), 1.75-1.60 (m, 2H, 1-H/2-H), 1.58-1.47 (m, 3H, 5-H/12-H), 1.30-1.19 (m, 6H, 15-H/14-H/13-H), 0.84 (t J 7.2 Hz, 3H, 16-H); **^{13}C NMR** (100 MHz, $CDCl_3$): δ = 180.5 (8), 175.8 (10), 90.4 (3), 77.1 (6), 62.6 (7), 52.6 (4), 45.2 (5), 39.2 (9), 39.0 (11), 31.4 (12), 31.2 (1), 29.6 (2), 27.5 (13), 26.5 (14), 22.6 (15), 14.1 (16); **HRMS (ESI)** m/z calculated for $C_{16}H_{25}NNaO_4$ 318.1676 $(M+Na)^+$, found 318.1676, 0.1 ppm error.

(1*R*,2*S*,4*R*)-1-(Hydroxymethyl)-1'-octyl-spiro[7-oxabicyclo[2.2.1]heptane-2,3'-pyrrolidine]-2',5'-dione 5.45d

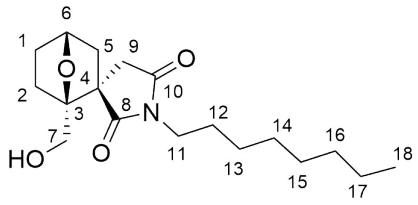

Octyl amide **5.1d** (100 mg) was hydrogenated according to the general procedure for the hydrogenation of alkyl/benzyl secondary amides. The crude material was purified using flash column chromatography (70:30) to give the target compound **5.45d** as a clear oil (98 mg, 98%) $\boldsymbol{R_F}$ = 0.26, (70:30, EtOAc:PE); **IR (Neat)** ν_{max} 3452 (w), 2926 (m), 2856 (m), 1771 (w) and 1688 (s) cm^{-1}; **^{1}H NMR** (400 MHz, $CDCl_3$): δ = 4.69 (t J 4.9 Hz, 1H, 6-H), 3.90 (s, 2H, 7-H), 3.45 (t J 7.3 Hz, 2H, 11-H), 2.97 (d J 18.3 Hz, 2H, 9-H), 2.69 (d J 18.3 Hz, 1H, 9-H), 2.52-2.45 (m, 1H, 5-H), 2.13-2.04 (br, 1H, OH), 2.01-1.88 (m, 2H, 1-H), 1.77-1.61 (m, 2H, 2-H), 1.58-1.47 (m, 3H, 5-H, 12-H), 1.30-1.18 (m, 10H, 13-H, 14-H, 15-H, 16-H, 17-H), 0.85 (t J 6.3 Hz, 3H, 18-H); **^{13}C NMR** (100 MHz, $CDCl_3$): δ = 180.5 (8), 175.8 (10), 90.4 (3), 77.4 (6), 62.7 (7), 52.6 (4), 45.3 (5), 39.2 (9), 39.1 (11), 31.9 (31.3), 29.6 (1), 29.3 (2), 29.2 (14), 27.6 (15), 26.9 (16), 22.7 (17), 14.2 (18); **HRMS (ESI)** m/z calculated for $C_{18}H_{29}NNaO_4$ 346.1989 $(M+Na)^+$, found 346.1992, − 0.5 ppm error.

(1*R*,2*S*,4*R*)-1'-Benzyl-1-(hydroxymethyl)spiro[7-oxabicyclo[2.2.1]heptane-2,3'-pyrrolidine]-2',5'-dione 5.45e

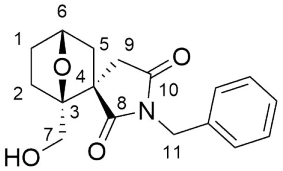

Benzyl amide **5.1e** (400 mg) was hydrogenated according to the general procedure for the hydrogenation of alkyl/benzyl secondary amides. The crude material was

purified using flash column chromatography (80:20-90:10, EtOAc:PE) to give the target compound **5.45e** as a clear oil (381 mg, 95%). $\boldsymbol{R_F} = 0.36$, (90:10, EtOAc:PE); **m.p.** 129-130 °C; **IR (Neat)** ν_{max} 3490 (m), 2978 (w), 1772 (m) and 1692 (s) cm^{-1}; **^{1}H NMR** (400 MHz, $CDCl_3$): δ = 7.40-7.35 (m, 2H, ArH), 7.31-7.23 (m, 3H, ArH), 4.67 (t, *J* 5.7 Hz, 1H, 6H), 4.65 (d *J* 14.1 Hz, 1H, 11-H), 4.60 (d *J* 14.1 Hz, 1H, 11-H), 3.80-3.67 (m, 2H, 7-H), 2.99 (d *J* 18.4 Hz, 1H, 9-H), 2.70 (d *J* 18.4 Hz, 1H, 9-H), 2.49 (ddd *J* 12.1, 5.7, 2.4 Hz, 1H, 5-H), 2.03-1.86 (m, 2H, 2-H, 1-H), 1.77-1.57 (m, 3H, 2-H, 1-H, OH), 1.53 (d *J* 12.1 Hz, 1H, 5-H); **^{13}C NMR** (100 MHz, $CDCl_3$): δ = 180.2 (8), 175.3 (10), 136.0 (ArC), 129.0 (ArCH), 128.7 (ArCH), 128.1 (ArCH), 90.3 (3), 77.2 (6), 62.9 (7), 52.9 (4), 44.9 (5), 42.6 (11), 39.3 (9), 31.3 (2), 29.9 (1); **HRMS (ESI)** m/z calculated for $C_{17}H_{19}NNaO_4$ 324.1206 $(M+Na)^+$, found 324.1206, 0.2 ppm error.

Appendix A

A.1 General

Amino Acid Abbreviations

Table A.1: Amino acid abbreviations.

Full Name	**Abbreviation 3-Letter**	**Abbreviation 1-Letter**
Alanine	Ala	A
Arginine	Arg	R
Asparagine	Asn	N
Aspartate	Asp	D
Cysteine	Cys	C
Glutamate	Glu	E
Glutamine	Gln	Q
Glycine	Gly	G
Histidine	His	H
Isoleucine	Ile	I
Leucine	Leu	L
Lysine	Lys	K
Methionine	Met	M
Phenylalanine	Phe	F
Proline	Pro	P
Serine	Ser	S
Threonine	Thr	T
Tryptophan	Trp	W
Tyrosine	Tyr	Y
Valine	Val	V

A.2 Cyclic Carbonates as Solvents for Peptide Synthesis

Chromatograms for Additional Racemisation Studies

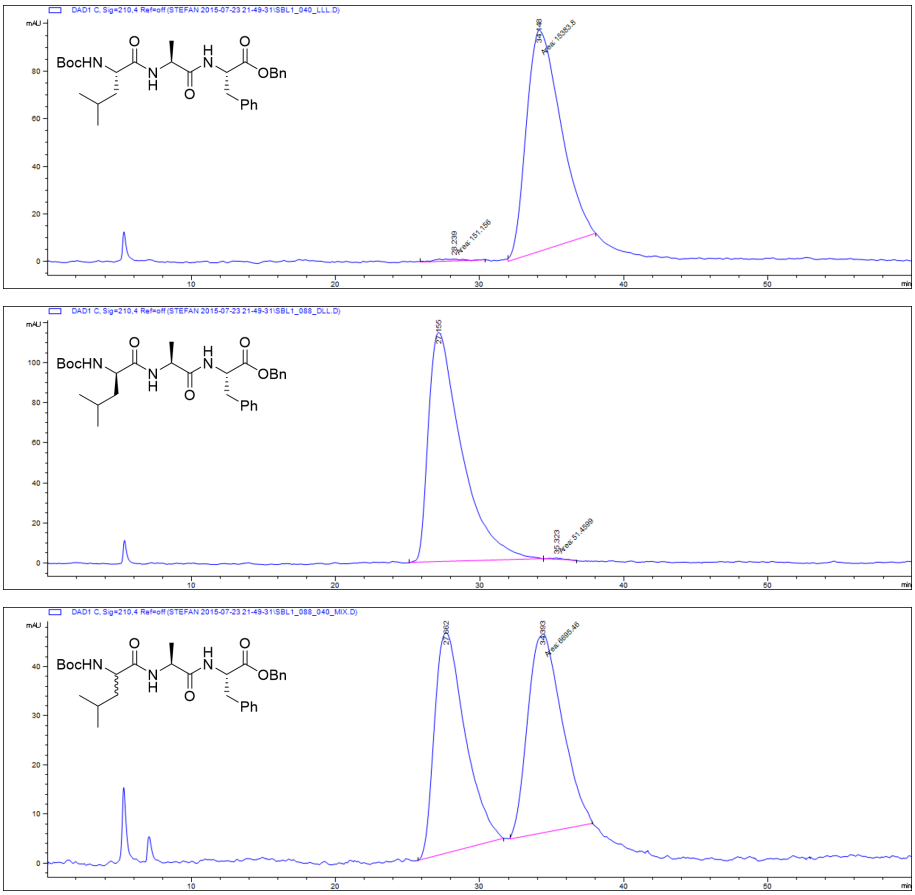

Figure A.1: Chiral HPLC chromatograms for Boc-Leu-Ala-Phe-OBn tripeptide, (*S*,*S*,*S*)-top **2.99**, (*R*,*S*,*S*)-middle **2.100** and racemic mixture-bottom.

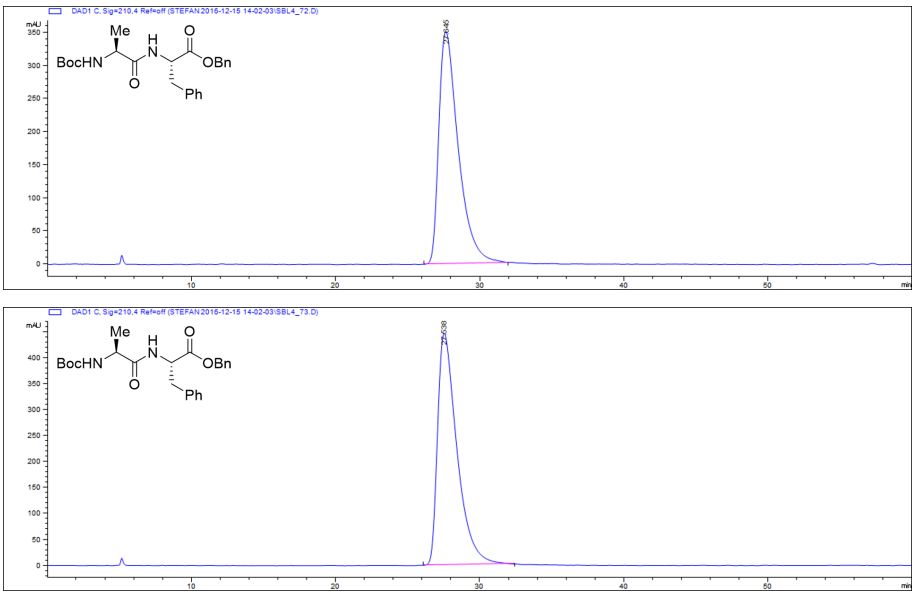

Figure A.2: Chiral HPLC chromatograms for the microwave assisted synthesis of Boc-Ala-Phe-OBn dipeptide **2.89** in CH_2Cl_2:DMF-top and PC-bottom.

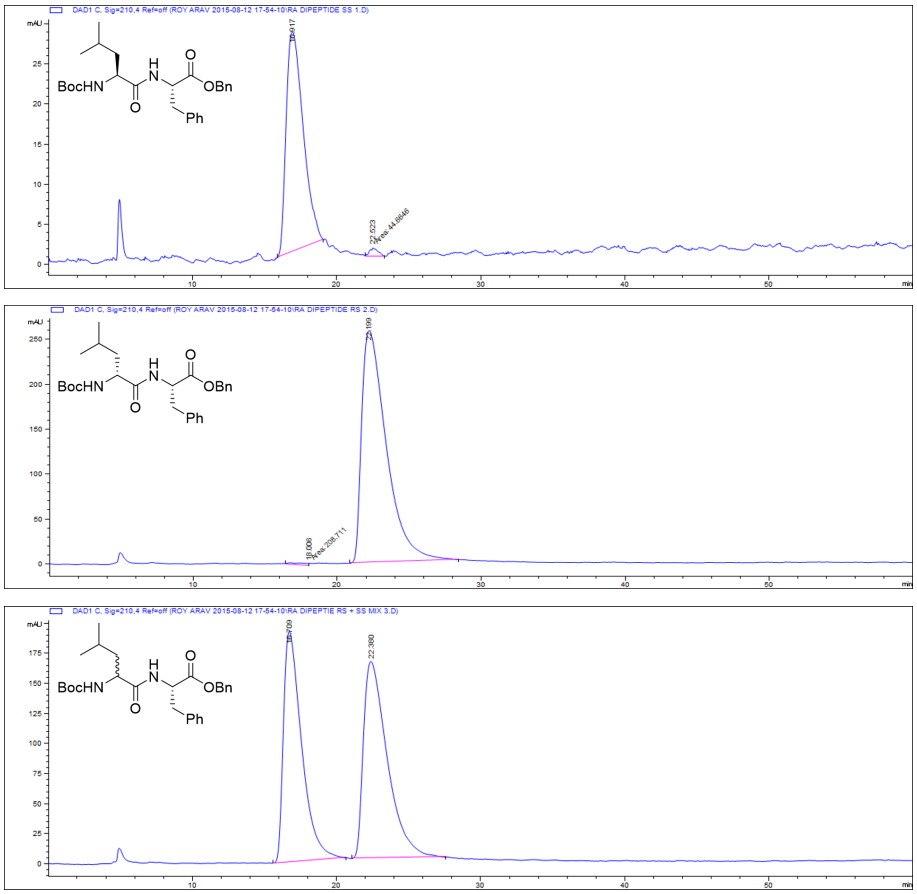

Figure A.3: Chiral HPLC chromatograms for Boc-Leu-Phe-OBn dipeptide, (*S*,*S*)-top **2.97**, (*R*,*S*)-middle **2.98** and racemic mixture-bottom, samples prepared by RA under the supervision of SL.

A.3 Greener Solvents for Solid-Phase Organic Synthesis

Allocation of Solvent Training Set to Groups

Merrifield Resin

Maximum swelling 6.3 mL g^{-1}; minimum swelling 1.8 mL g^{-1}

$n = 6$

Swelling Range (mL g^{-1})	Solvents	Rank
1.80 - 2.55	1, 2, 3, 4, 19, 20, 21, 22, 23	6
2.55 - 3.30	11, 17, 18	5
3.30 - 4.05	8	4
4.05 - 4.80		3
4.80 - 5.55	29	2
5.55 - 6.30	7, 12, 28, 30	1

$n = 5$

Swelling Range (mL g^{-1})	Solvents	Rank
1.80 - 2.70	1, 2, 3, 4, 19, 20, 21, 22, 23	5
2.70 - 3.60	11, 17, 18	4
3.60 - 4.50	8	3
4.50 - 5.40	29	2
5.40 - 6.30	7, 12, 28, 30	1

$n = 4$

Swelling Range (mL g^{-1})	Solvents	Rank
1.80 - 2.93	1, 2, 3, 4, 17, 19, 20, 21, 22, 23	4
2.93 - 4.05	8, 11, 18	3
4.05 - 5.18	29	2
5.18 - 6.30	7, 12, 28, 30	1

ParaMax Resin

Maximum swelling 7.8 mL g^{-1}; minimum swelling 1.8 mL g^{-1}

$n = 6$

Swelling Range (mL g^{-1})	Solvents	Rank
1.80 - 2.80	1, 2, 3, 19, 20, 21, 22, 23	6
2.80 - 3.80		5
3.80 - 4.80	17	4
4.80 - 5.80	4, 8, 11	3
5.80 - 6.80		2
6.80 - 7.80	7, 12, 28, 29, 30	1

$n = 5$

Swelling Range (mL g^{-1})	Solvents	Rank
1.80 - 3.00	1, 2, 3, 19, 20, 21, 22, 23	5
3.00 - 4.20		4
4.20 - 5.40	4, 8, 11, 17, 18	3
5.40 - 6.60		2
6.60 - 7.80	7, 12, 28, 29, 30	1

$n = 4$

Swelling Range (mL g^{-1})	Solvents	Rank
1.80 - 3.30	1, 2, 3, 19, 20, 21, 22, 23	4
3.30 - 4.80	16	3
4.80 - 6.30	4, 8, 11, 18	2
6.30 - 7.80	7, 12, 28, 29, 30	1

JandaJel Resin

Maximum swelling 8.8 mL g^{-1}; minimum swelling 1.8 mL g^{-1}

$n = 6$

Swelling Range (mL g^{-1})	Solvents	Rank
1.80 - 2.97	1, 2, 3, 4, 18, 21, 22, 23	6
2.97 - 4.13	17	5
4.13 - 5.30	19	4
5.30 - 6.47	8, 20, 29	3
6.47 - 7.63		2
7.63 - 8.80	7, 11, 12, 28, 30	1

$n = 5$

Swelling Range (mL g^{-1})	Solvents	Rank
1.80 - 3.20	1, 2, 3, 4, 18, 21, 22, 23	5
3.20 - 4.60	17	4
4.60 - 6.00	8, 19, 20	3
6.00 - 7.40	29	2
7.40 - 8.80	7, 11, 12, 28, 30	1

$n = 4$

Swelling Range (mL g^{-1})	Solvents	Rank
1.80 - 3.55	1, 2, 3, 4, 18, 21, 22, 23	4
3.55 - 5.30	17, 19	3
5.30 - 7.05	8, 19, 29	2
7.05 - 8.80	7, 11, 12, 28, 30	1

TentaGel Resin

Maximum swelling 5.5 mL g^{-1}; minimum swelling 1.8 mL g^{-1}

$n = 6$

Swelling Range (mL g^{-1})	Solvents	Rank
1.80 - 2.42	20, 22, 23	6
2.42 - 3.03	18, 19, 21	5
3.03 - 3.65	2, 4, 12	4
3.65 - 4.27	1, 3, 8, 11, 17, 28, 29	3
4.27 - 4.88	7	2
4.88 - 5.50	30	1

$n = 5$

Swelling Range (mL g^{-1})	Solvents	Rank
1.80 - 2.54	20, 22, 23	5
2.54 - 3.28	18, 19, 21	4
3.28 - 4.02	1, 2, 3, 4, 8, 11, 12, 17, 28, 29	3
4.02 - 4.76		2
4.76 - 5.50	7, 30	1

$n = 4$

Swelling Range (mL g^{-1})	Solvents	Rank
1.80 - 2.73	18, 19, 20, 22, 23	4
2.73 - 3.65	2, 4, 12, 21	3
3.65 - 4.58	1, 3, 8, 11, 17, 28, 29	2
4.58 - 5.50	7, 30	1

ArgoGel Resin

Maximum swelling 7.7 mL g^{-1}; minimum swelling 1.8 mL g^{-1}

$n = 6$

Swelling Range (mL g^{-1})	Solvents	Rank
1.80 - 2.78	20, 22, 23	6
2.78 - 3.77		5
3.77 - 4.75	1, 2, 4, 12, 18, 19, 21	4
4.75 - 5.73	3, 8, 11, 17, 28, 29	3
5.73 - 6.72	7	2
6.72 - 7.70	30	1

$n = 5$

Swelling Range (mL g^{-1})	Solvents	Rank
1.80 - 2.98	20, 22, 23	5
2.98 - 4.16	1, 4, 21	4
4.16 - 5.34	2, 3, 8, 11, 12, 17, 18, 19, 28, 29	3
5.34 - 6.52	7	2
6.52 - 7.70	30	1

$n = 4$

Swelling Range (mL g^{-1})	Solvents	Rank
1.80 - 3.28	20, 22, 23	4
3.28 - 4.75	1, 2, 4, 12, 18, 19, 21	3
4.75 - 6.23	3, 7, 8, 11, 17, 28, 29	2
6.23 - 7.70	30	1

HypoGel 200 Resin

Maximum swelling 4.8 mL g^{-1}; minimum swelling 1.8 mL g^{-1}

$n = 6$

Swelling Range (mL g^{-1})	Solvents	Rank
1.80 - 2.30	20, 21, 22, 23	6
2.30 - 2.80	2, 18, 19	5
2.80 - 3.30	1, 4, 8, 17	4
3.30 - 3.80	3, 11	3
3.80 - 4.30	12	2
4.30 - 4.80	7, 28, 29, 30	1

$n = 5$

Swelling Range (mL g^{-1})	Solvents	Rank
1.80 - 2.40	2, 19, 20, 21, 22, 23	5
2.40 - 3.00	1, 4, 8, 17, 18	4
3.00 - 3.60	3, 11	3
3.60 - 4.20	12	2
4.20 - 4.80	7, 28, 29, 30	1

$n = 4$

Swelling Range (mL g^{-1})	Solvents	Rank
1.80 - 2.55	2, 19, 20, 21, 22, 23	4
2.55 - 3.30	1, 4, 8, 17, 18	3
3.30 - 4.05	3, 11, 12	2
4.05 - 4.80	7, 28, 29, 30	1

NovaGel Resin

Maximum swelling 5.8 mL g^{-1}; minimum swelling 1.8 mL g^{-1}

$n = 6$

Swelling Range (mL g^{-1})	Solvents	Rank
1.80 - 2.47	19, 20, 21, 22, 23	6
2.47 - 3.13	1, 2, 18	5
3.13 - 3.80	4, 8, 11, 12, 17	4
3.80 - 4.47	3	3
4.47 - 5.13	7, 28, 29	2
5.13 - 5.80	30	1

$n = 5$

Swelling Range (mL g^{-1})	Solvents	Rank
1.80 - 2.60	19, 20, 21, 22, 23	5
2.60 - 3.40	1, 2, 8, 17, 18	4
3.40 - 4.20	4, 11, 12	3
4.20 - 5.00	3, 7, 28	2
5.00 - 5.80	29, 30	1

$n = 4$

Swelling Range (mL g^{-1})	Solvents	Rank
1.80 - 2.80	1, 2, 18, 19, 20, 21, 22, 23	4
2.80 - 3.80	4, 8, 11, 12, 17	3
3.80 - 4.80	3, 28	2
4.80 - 5.80	7, 29, 30	1

ChemMatrix Resin

Maximum swelling 9.8 mL g^{-1}; minimum swelling 1.8 mL g^{-1}

$n = 6$

Swelling Range (mL g^{-1})	Solvents	Rank
1.80 - 3.13	20, 23	6
3.13 - 4.47	4, 22	5
4.47 - 5.80	8, 12, 18, 20	4
5.80 - 7.13	1, 2, 7, 11, 17, 21	3
7.13 - 8.47	3, 28, 29	2
8.47 - 9.80	30	1

$n = 5$

Swelling Range (mL g^{-1})	Solvents	Rank
1.80 - 3.40	20, 23	5
3.40 - 5.00	4, 8, 19, 22	4
5.00 - 6.60	2, 11, 12, 17, 18	3
6.60 - 8.20	1, 7, 21, 28, 29	2
8.20 - 9.80	3, 30	1

$n = 4$

Swelling Range (mL g^{-1})	Solvents	Rank
1.80 - 3.80	20, 22, 23	4
3.80 - 5.80	4, 8, 18, 12, 19	3
5.80 - 7.80	1, 2, 7, 11, 17, 21, 28, 29	2
7.80 - 9.80	3, 30	1

SpheriTide Resin

Maximum swelling 5.3 mL g^{-1}; minimum swelling 1.8 mL g^{-1}

$n = 6$

Swelling Range (mL g^{-1})	Solvents	Rank
1.80 - 2.38	1, 2, 18, 19, 20	6
2.38 - 2.97	3, 4, 8, 12, 17, 23	5
2.97 - 3.55	11	4
3.55 - 4.13	7, 21, 22	3
4.13 - 4.72		2
4.72 - 5.30	28, 29, 30	1

$n = 5$

Swelling Range (mL g^{-1})	Solvents	Rank
1.80 - 2.50	1, 2, 18, 19, 20	5
2.50 - 3.20	3, 4, 8, 11, 12, 17, 23	4
3.20 - 3.90	7, 21, 22	3
3.90 - 4.60		2
4.60 - 5.30	28, 29, 30	1

$n = 4$

Swelling Range (mL g^{-1})	Solvents	Rank
1.80 - 2.68	1, 2, 8, 18, 19, 20	4
2.68 - 3.55	3, 4, 11, 12, 17, 23	3
3.55 - 4.43	7, 21, 22	2
4.43 - 5.30	28, 29, 30	1

3D Plots of HSPiP Predictions

Merrifield Resin

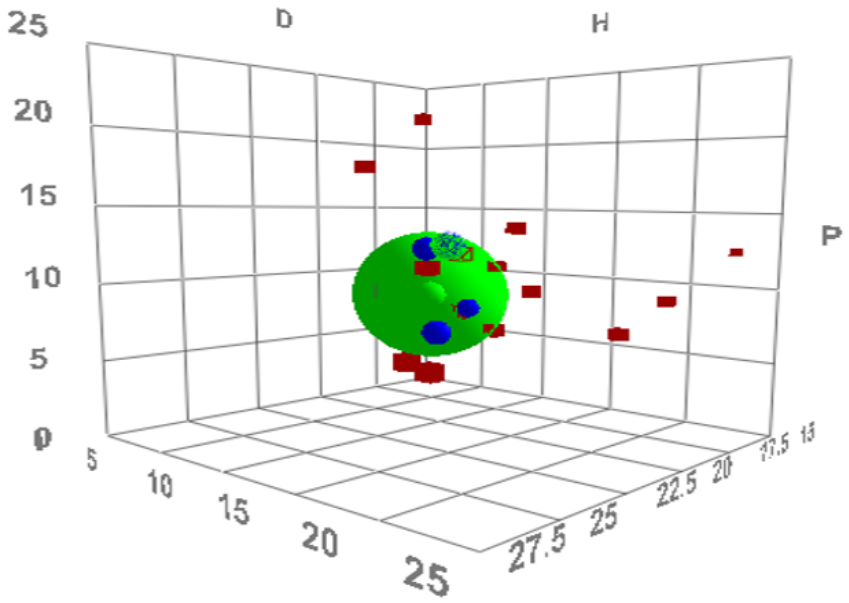

$n = 5$ groups

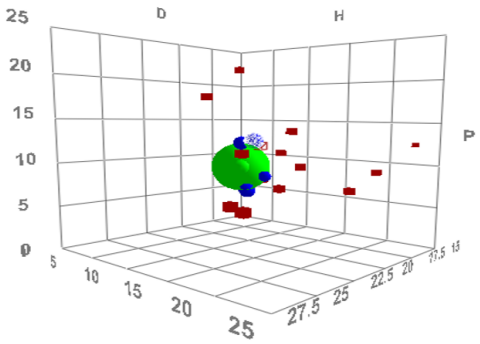

$n = 4$ groups

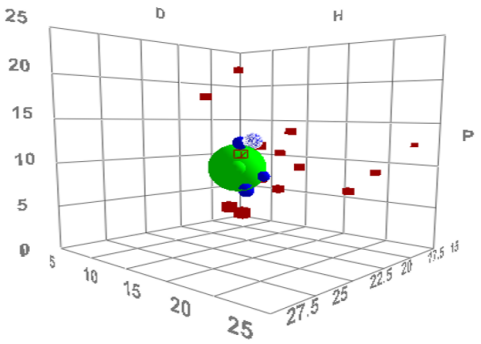

$n = 6$ groups

ParaMax Resin

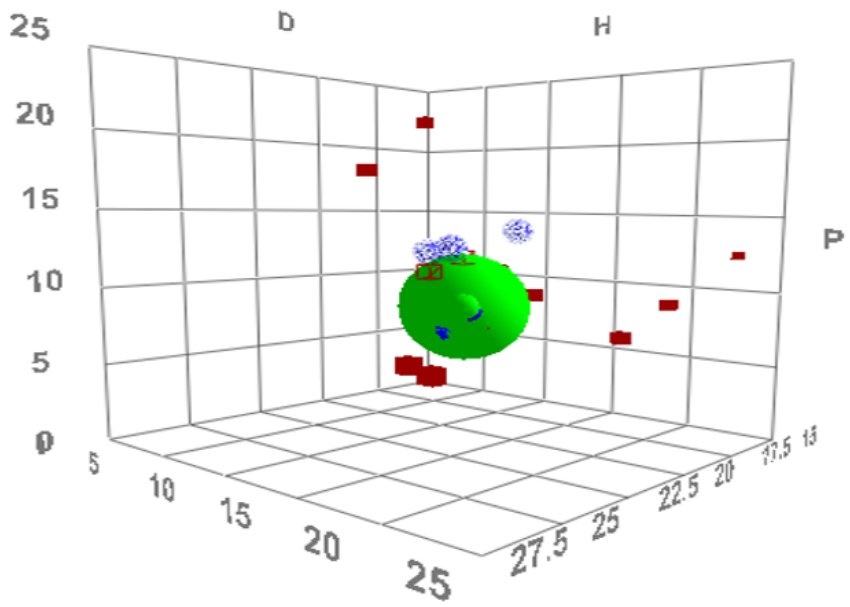

$n = 5$ groups

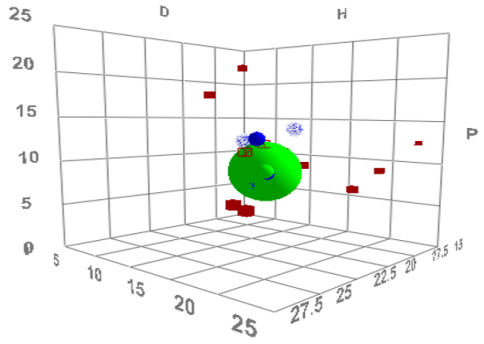

$n = 4$ groups

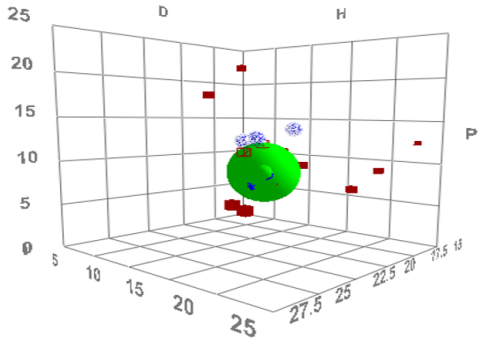

$n = 6$ groups

JandaJel Resin

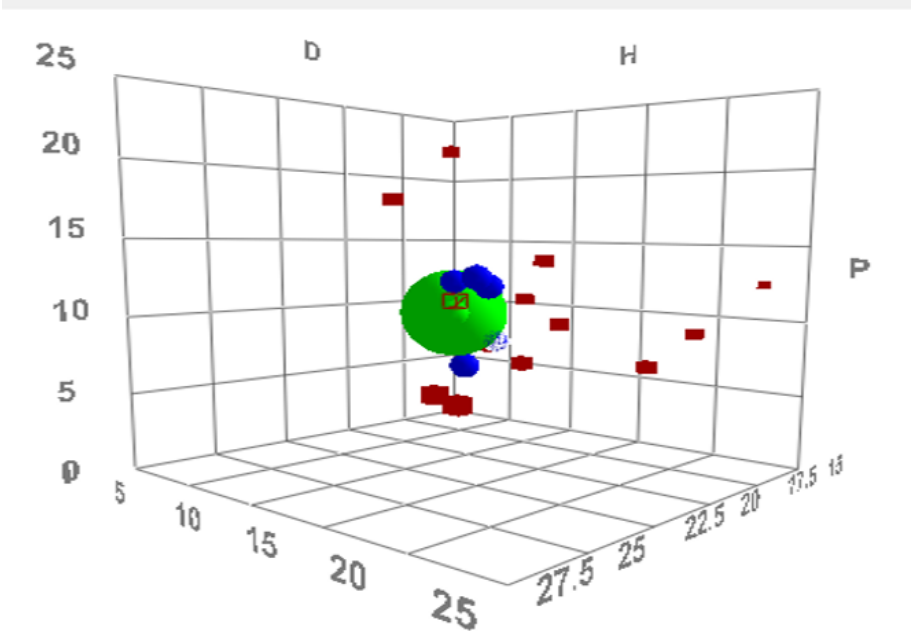

$n = 5$ groups

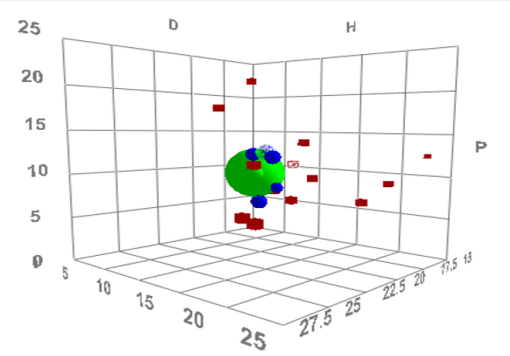

$n = 4$ groups

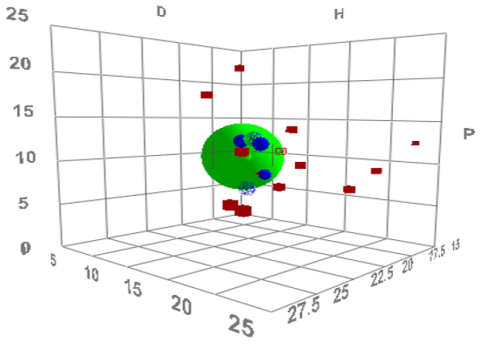

$n = 6$ groups

TentaGel Resin

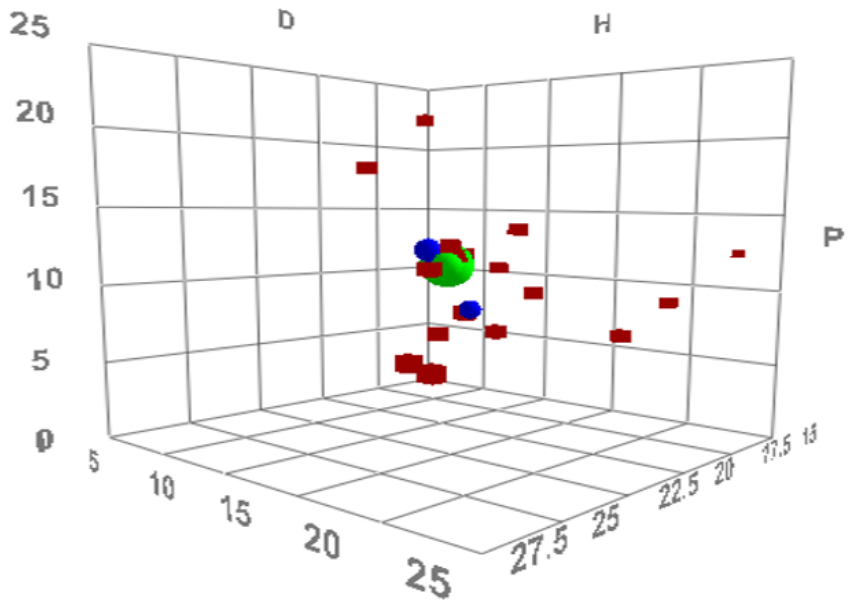

$n = 5$ groups

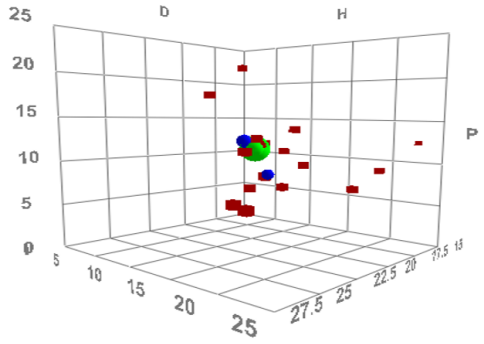

$n = 4$ groups

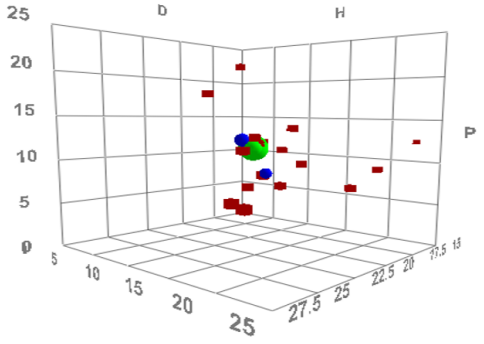

$n = 6$ groups

ArgoGel Resin

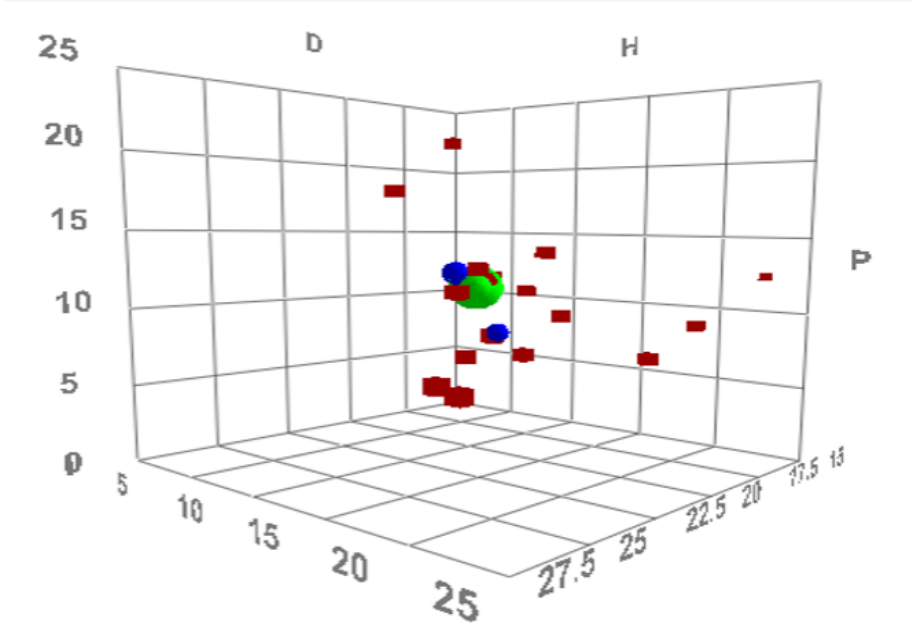

$n = 5$ groups

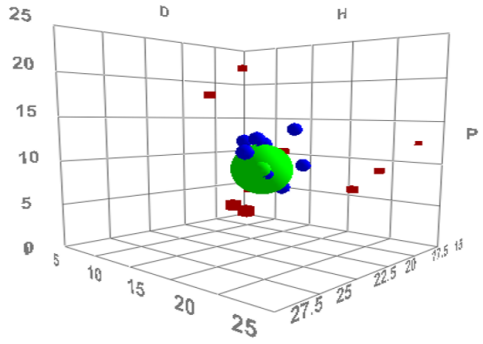

$n = 4$ groups

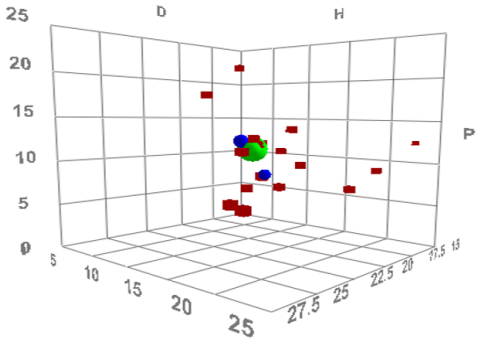

$n = 6$ groups

HypoGel 200 Resin

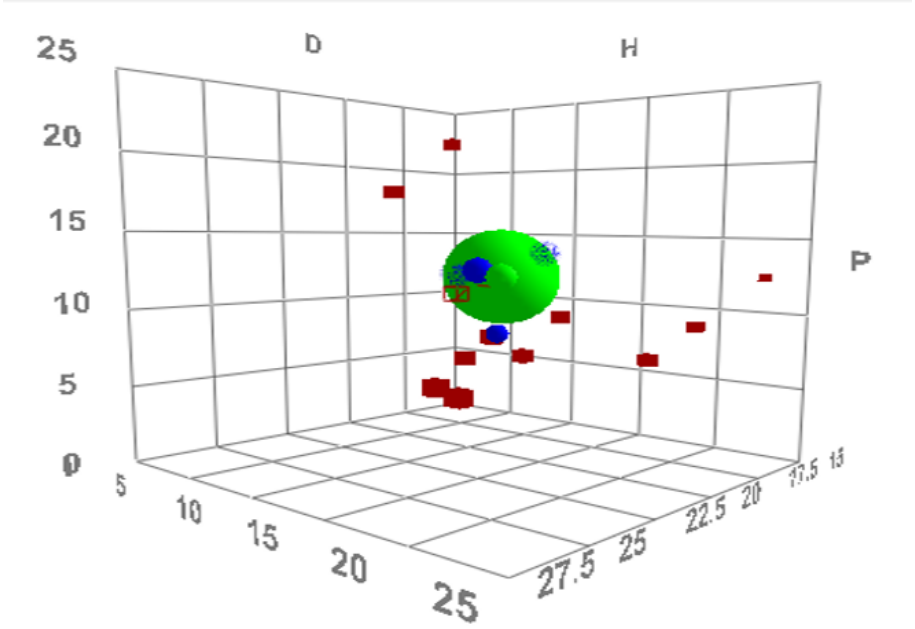

$n = 5$ groups

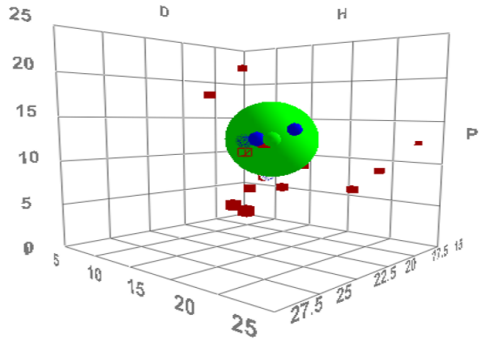

$n = 4$ groups

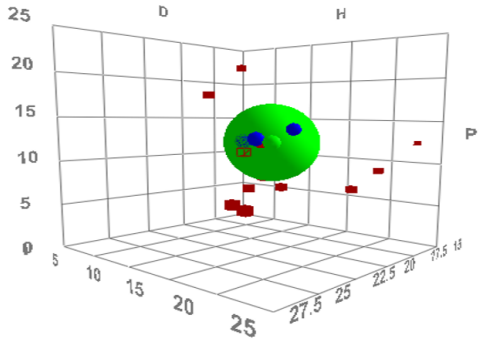

$n = 6$ groups

NovaGel Resin

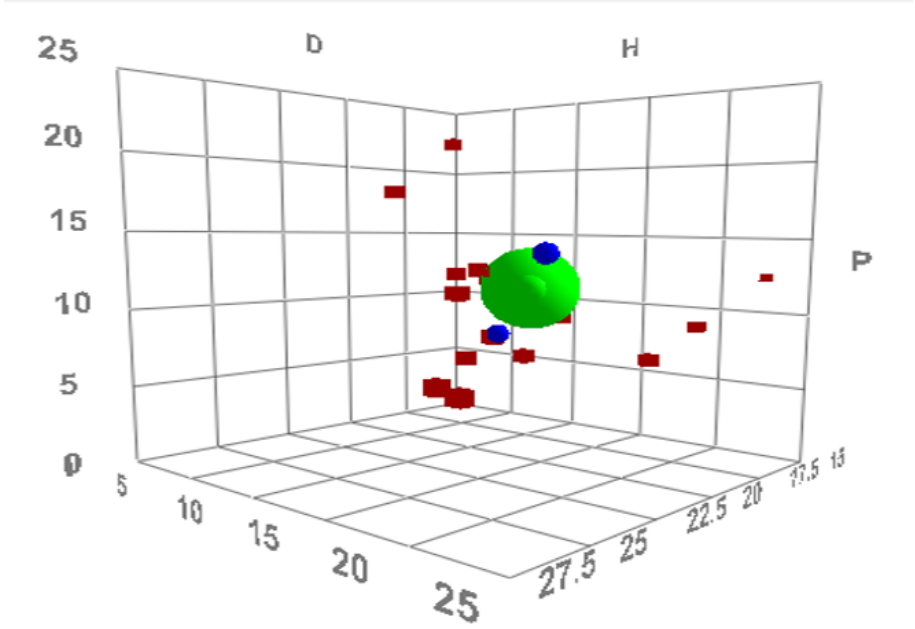

$n = 5$ groups

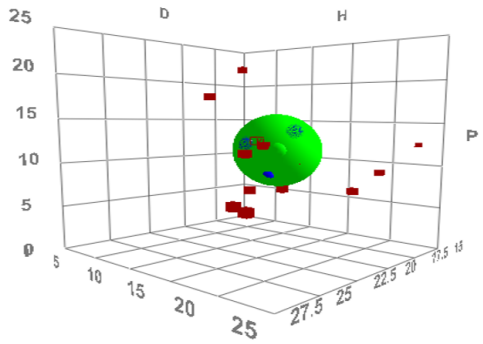

$n = 4$ groups

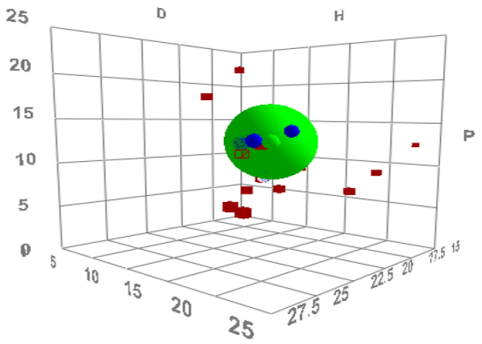

$n = 6$ groups

ChemMatrix Resin

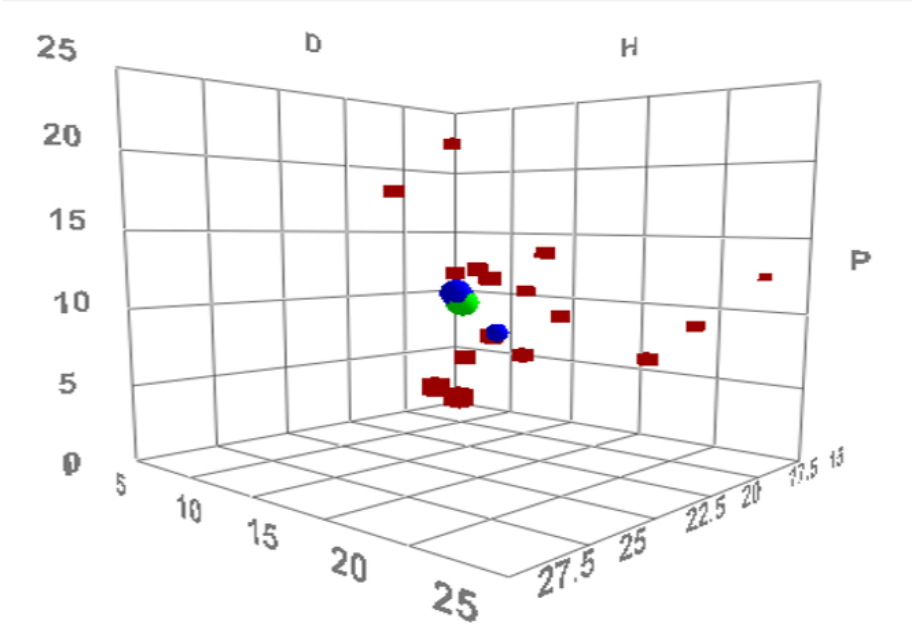

$n = 5$ groups

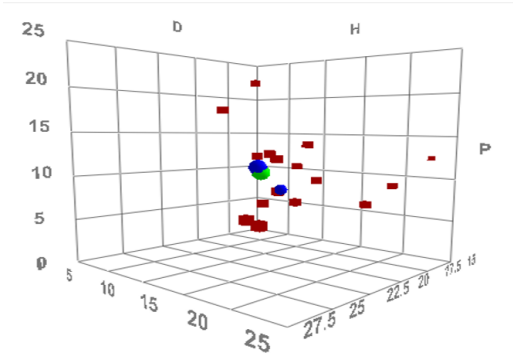

$n = 4$ groups

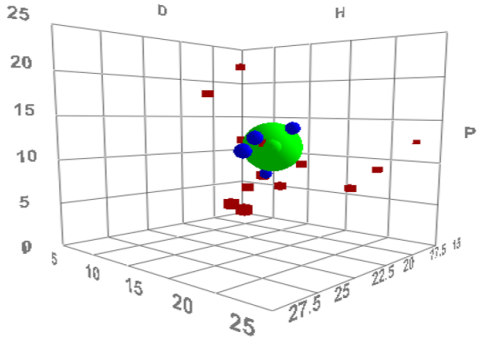

$n = 6$ groups

SpheriTide Resin

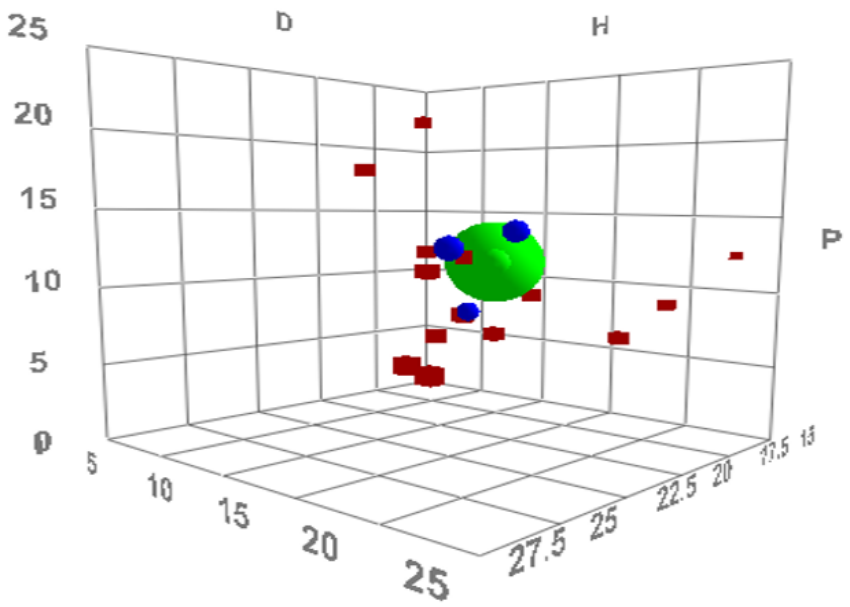

$n = 5$ groups

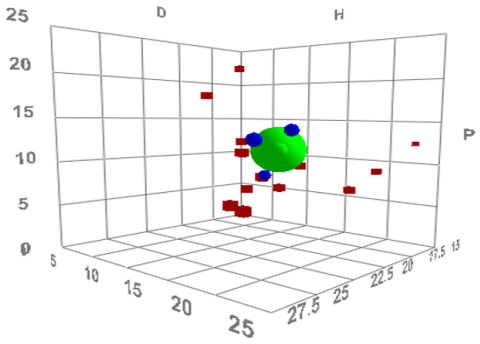

$n = 4$ groups

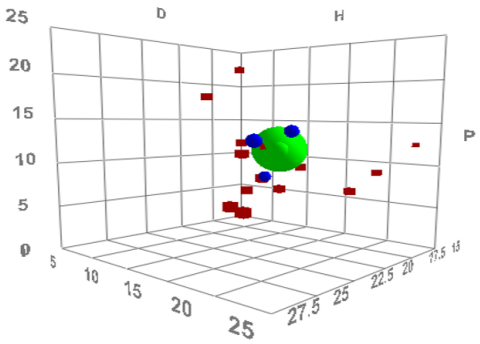

$n = 6$ groups

Resin Swelling for Predicted Solvents

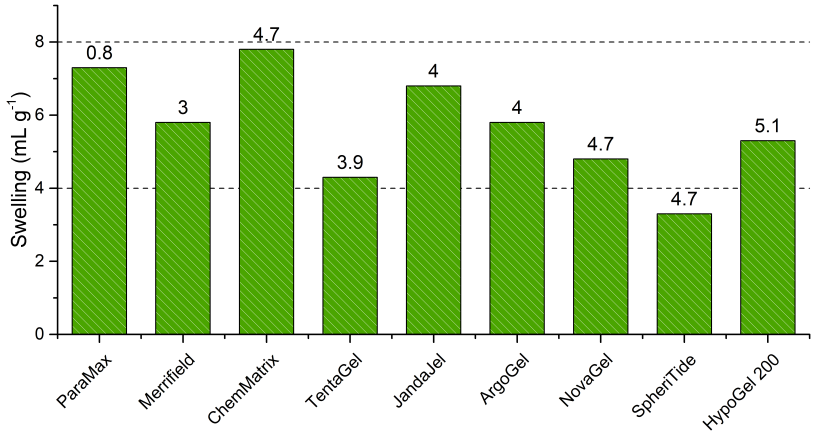

Figure A.4: The graph below is presented as a plot of amount of swelling rather than the % swelling shown in the main chapter. This is less appropriate for comparison between resins, but does indicate the amount of swelling relative to the 4.0 mL g^{-1} threshold for a good solvent (only SpheriTide did not meet this threshold). Resins are ranked from highest predicted swelling (left) to lowest (right) with the RMS deviation of the solvent parameters for dimethyl isosorbide **3.30** from those of an ideal solvent given as a number above each bar.

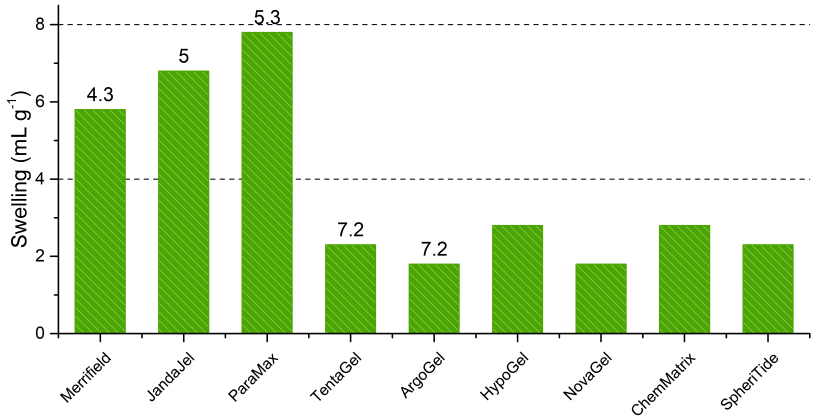

Figure A.5: The graph below is presented as a plot of amount of swelling rather than the % swelling shown in the main manuscript. This is less appropriate for comparison between resins, but does indicate the amount of swelling relative to the 4.0 mL g^{-1} threshold for a good solvent. Resins are ranked from highest predicted swelling (left) to lowest (right) with the RMS deviation of the solvent parameters for cyclopentyl methyl ether **3.31** from those of an ideal solvent given as a number above each bar. Where no number is given, the deviation is so large that the solvent is not in the "Predictions of solvents to swell each resin" table for that solvent.

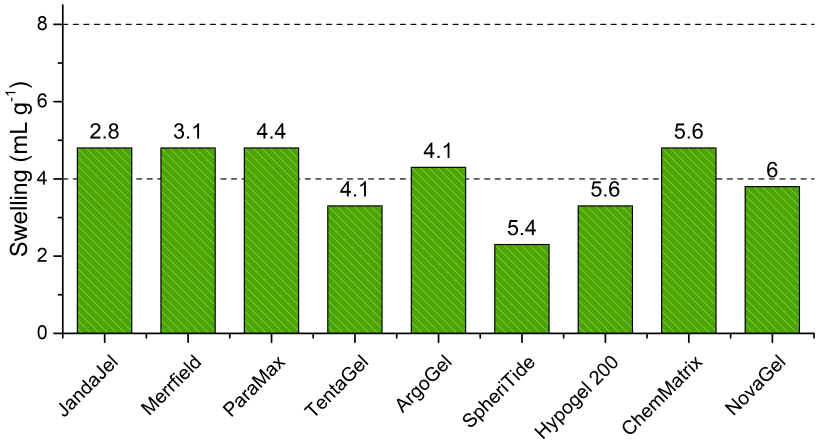

Figure A.6: The graph below is presented as a plot of amount of swelling rather than the % swelling shown in the main manuscript. This is less appropriate for comparison between resins, but does indicate the amount of swelling relative to the 4.0 mL g^{-1} threshold for a good solvent. Resins are ranked from highest predicted swelling (left) to lowest (right) with the RMS deviation of the solvent parameters for butan-2-one **3.20** from those of an ideal solvent given as a number above each bar.

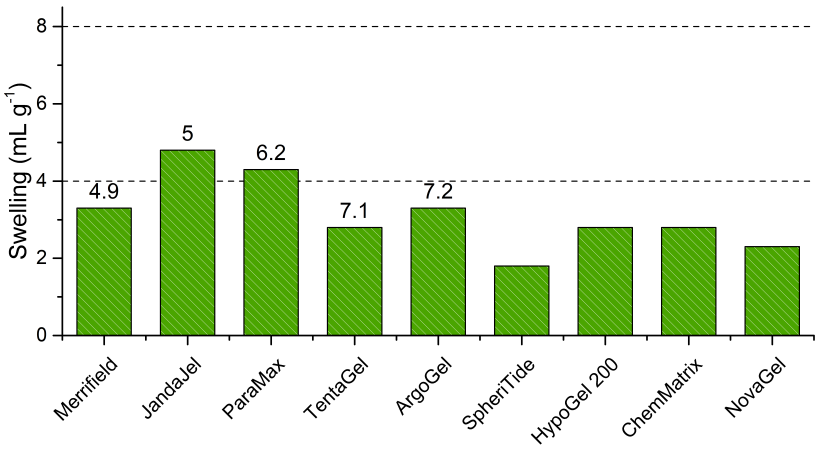

Figure A.7: The graph below is presented as a plot of amount of swelling rather than the % swelling shown in the main manuscript. This is less appropriate for comparison between resins, but does indicate the amount of swelling relative to the 4.0 mL g^{-1} threshold for a good solvent. Resins are ranked from highest predicted swelling (left) to lowest (right) with the RMS deviation of the solvent parameters for 4-methylpentan-2-one **3.21** from those of an ideal solvent given as a number above each bar. Where no number is given, the deviation is so large that the solvent is not in the "Predictions of solvents to swell each resin" table for that solvent.

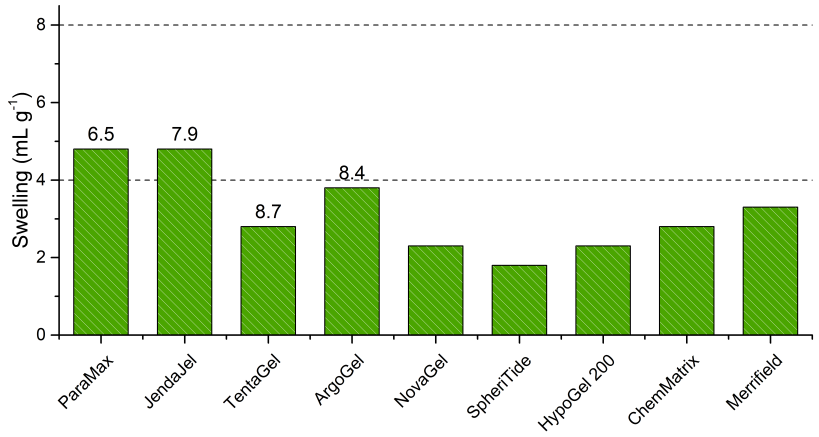

Figure A.8: The graph below is presented as a plot of amount of swelling rather than the % swelling shown in the main manuscript. This is less appropriate for comparison between resins, but does indicate the amount of swelling relative to the 4.0 mL g^{-1} threshold for a good solvent. Resins are ranked from highest predicted swelling (left) to lowest (right) with the RMS deviation of the solvent parameters for isopropyl acetate **3.24** from those of an ideal solvent given as a number above each bar. Where no number is given, the deviation is so large that the solvent is not in the "Predictions of solvents to swell each resin" table for that solvent.

Solvent List and Parameters Used for Mixed Solvent Study

Solvent	D	P	H	BPt	FPt	V@25	MPt
3.16	18	21.7	5.1	248	143	0.009	36
3.17	20	18	4.1	242	135	0.004	-48
3.18	18.8	10.6	6.9	-	-	-	-
3.19	15.5	10.4	7	56	-17	232	-95
3.20	16	9	5.1	80	-5	90.3	-87
3.21	15.3	6.1	4.1	116	16	19.8	-84
3.22	17.9	11.9	5.2	131	-	10.3	-51
3.23	15.8	5.3	7.2	77	-3	96.5	-84
3.24	14.9	4.5	8.2	89	-	60.4	-73
3.25	15.1	3.7	6.3	117	-	17.2	-99
3.26	16.9	11.5	6.3	186.5	72.4	0.549	-29.4
3.27	16.9	5	4.3	79	-	96.1	-137
3.29	17.8	4.4	6.9	154	-	3.4	-38
3.30	17.6	7.1	7.5	234	105	0.03	-50
3.31	16.7	4.3	4.3	106	0	35.5	-140
3.32	15.5	8.6	9.7	90	-	50	0
3.33	15.1	6.3	3.5	127	-	10	-43
3.34	17.2	1.8	4.3	177	43	1.61	-74
3.35	17.3	2.4	2.4	182.7	55.5	0.914	-45.1
3.36	14.7	12.3	22.3	65	12	128	-98
3.37	15.8	8.8	19.4	78	13	59.1	-114
3.38	15.8	6.1	16.4	82	14	43.4	-88
3.39	16	5.3	11.7	176	-	0.308	-34
3.40	15.5	16	42.3	100	-	21.8	0

A.4 Ring-Opening Metathesis Polymerisation of a Novel Bio-based Monomer Framework

Crystal Structure Data

_N_,_N_-Diethyl-2-[(5_S_,7_S_)-4-oxo-3,10-dioxatricyclo[5.2.1.0^{1,5}]dec-8-en-5-yl]acetamide 4.39b

Empirical formula	$C_{14}H_{19}NO_4$
Formula weight	265.30
Temperature/K	110.05(10)
Crystal system	monoclinic
Space group	Pc
a/Å	7.5433(6)
b/Å	7.1072(5)
c/Å	12.2710(7)
α/°	90
β/°	99.243(6)
γ/°	90
Volume/Å^3	649.33(8)
Z	2
ρ_{calc}g/cm^3	1.357
μ/mm^{-1}	0.819
F(000)	284.0
Crystal size/mm^3	0.215 × 0.119 × 0.108
Radiation	CuKα (λ = 1.54184)
2θ range for data collection/°	12.454 to 134.038
Index ranges	-5 ≤ h ≤ 9, -8 ≤ k ≤ 8, -14 ≤ l ≤ 13
Reflections collected	2127
Independent reflections	1339 [R_{int} = 0.0292, R_{sigma} = 0.0405]
Data/restraints/parameters	1339/2/174
Goodness-of-fit on F^2	1.028
Final R indexes [I>=2σ(I)]	R_1 = 0.0344, wR_2 = 0.0839
Final R indexes [all data]	R_1 = 0.0396, wR_2 = 0.0890
Largest diff. peak/hole / e Å^{-3}	0.19/-0.17
Flack parameter	-0.1(3)

N,*N*-Dibenzyl-2-[(5*S*,7*S*)-4-oxo-3,10-dioxatricyclo[5.2.1.$0^{1,5}$]dec-8-en-5-yl]acetamide 4.39g

Empirical formula	$C_{24}H_{23}NO_4$
Formula weight	389.43
Temperature/K	110.05(10)
Crystal system	orthorhombic
Space group	$Pna2_1$
a/Å	11.74335(11)
b/Å	9.93941(9)
c/Å	16.35387(18)
α/°	90
β/°	90
γ/°	90
Volume/Å^3	1908.85(3)
Z	4
ρ_{calc}g/cm^3	1.355
μ/mm^{-1}	0.746
F(000)	824.0
Crystal size/mm^3	0.184 × 0.13 × 0.061
Radiation	CuKα (λ = 1.54184)
2θ range for data collection/°	10.416 to 134.156
Index ranges	-14 ≤ h ≤ 14, -11 ≤ k ≤ 11, -16 ≤ l ≤ 19
Reflections collected	12874
Independent reflections	3108 [R_{int} = 0.0210, R_{sigma} = 0.0166]
Data/restraints/parameters	3108/1/263
Goodness-of-fit on F^2	1.078
Final R indexes [I>=2σ(I)]	R_1 = 0.0236, wR_2 = 0.0623
Final R indexes [all data]	R_1 = 0.0242, wR_2 = 0.0631
Largest diff. peak/hole / e Å^{-3}	0.15/-0.16
Flack parameter	-0.07(8)

Methyl-(2*S*)-1-[2-[(5*S*,7*S*)-4-oxo-3,10-dioxatricyclo[5.2.1.$0^{1,5}$]dec-8-en-5-yl]acetyl] pyrrolidine-2-carboxylate 4.39h

Empirical formula	$C_{16}H_{19}NO_6$
Formula weight	321.32
Temperature/K	110.05(10)
Crystal system	monoclinic
Space group	I2
a/Å	10.00340(10)
b/Å	7.17690(10)
c/Å	21.1803(2)
α/°	90
β/°	92.4690(10)
γ/°	90
Volume/Å^3	1519.19(3)
Z	4
ρ_{calc}g/cm^3	1.405
μ/mm^{-1}	0.908
F(000)	680.0
Crystal size/mm^3	0.282 × 0.081 × 0.061
Radiation	CuKα (λ = 1.54184)
2θ range for data collection/°	8.356 to 142.35
Index ranges	-10 ≤ h ≤ 12, -8 ≤ k ≤ 8, -25 ≤ l ≤ 25
Reflections collected	7598
Independent reflections	2748 [R_{int} = 0.0168, R_{sigma} = 0.0164]
Data/restraints/parameters	2748/1/226
Goodness-of-fit on F^2	1.076
Final R indexes [I>=2σ(I)]	R_1 = 0.0291, wR_2 = 0.0751
Final R indexes [all data]	R_1 = 0.0296, wR_2 = 0.0759
Largest diff. peak/hole / e Å^{-3}	0.14/-0.20
Flack parameter	0.01(5)

Homopolymerisation Kinetic Data

Polymerization of Monomer 4.39a

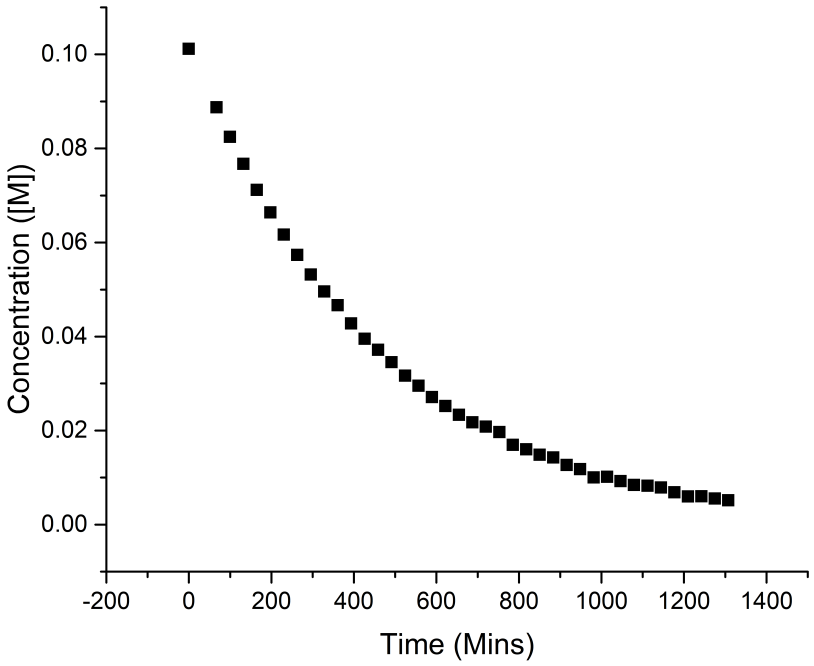

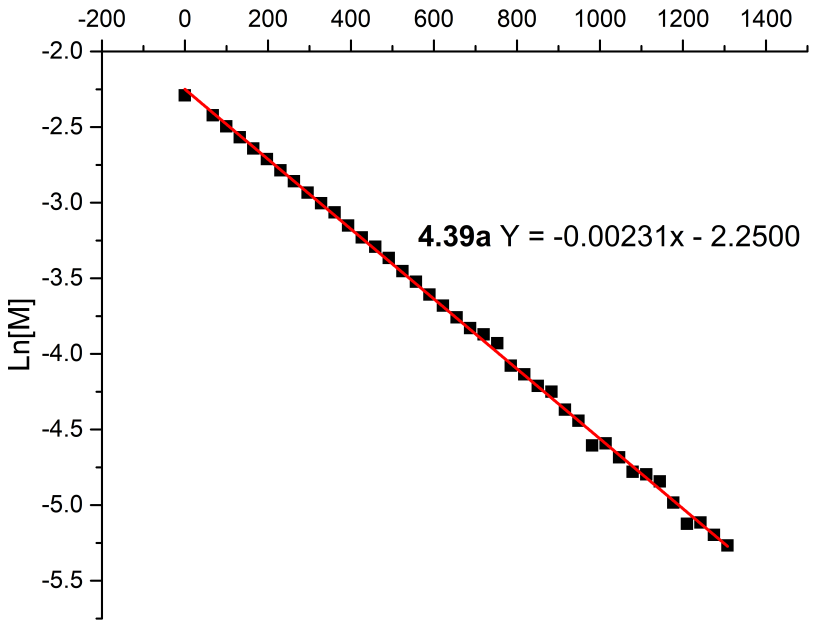

Polymerization of Monomer 4.39d

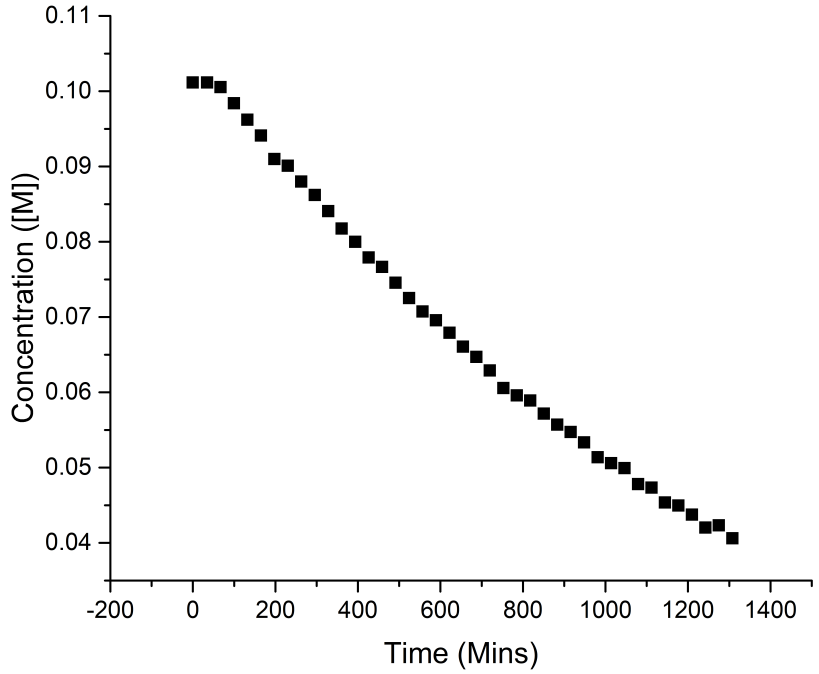

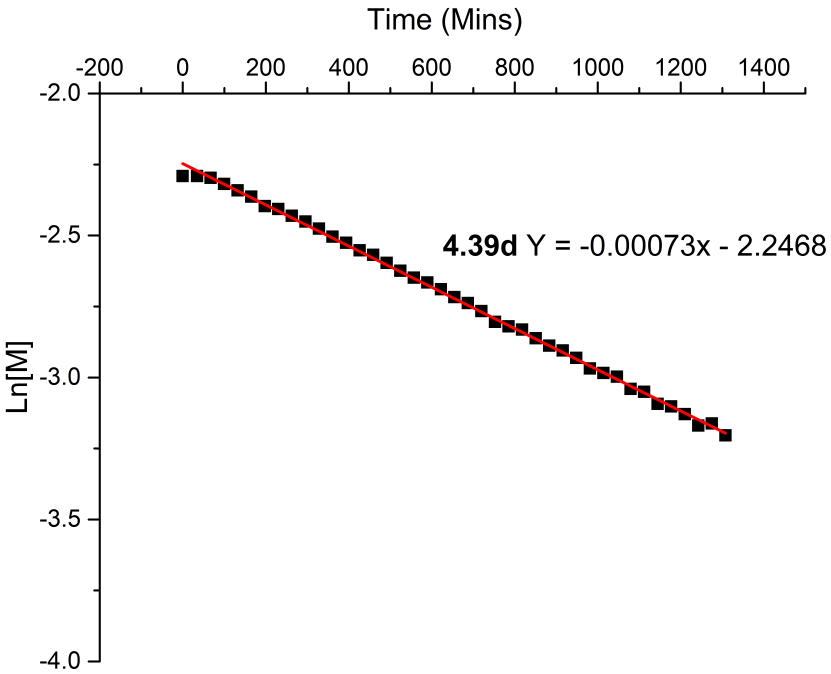

Polymerization of Monomer 4.39e

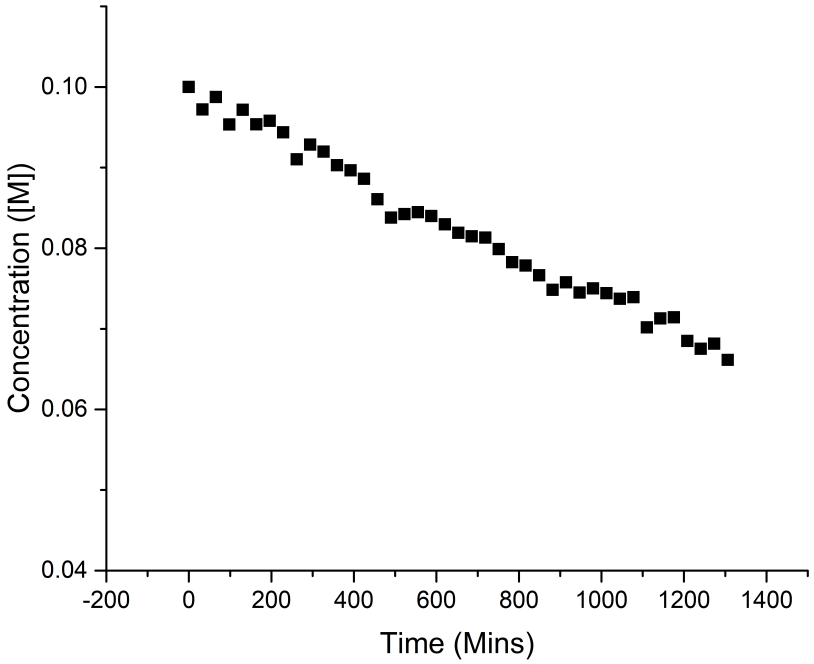

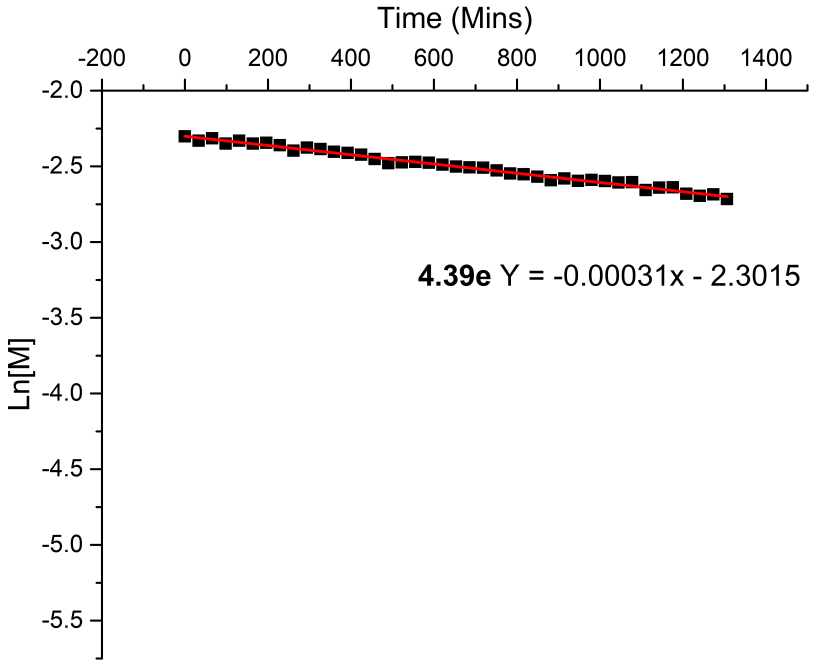

Polymerization of Monomer 4.39g

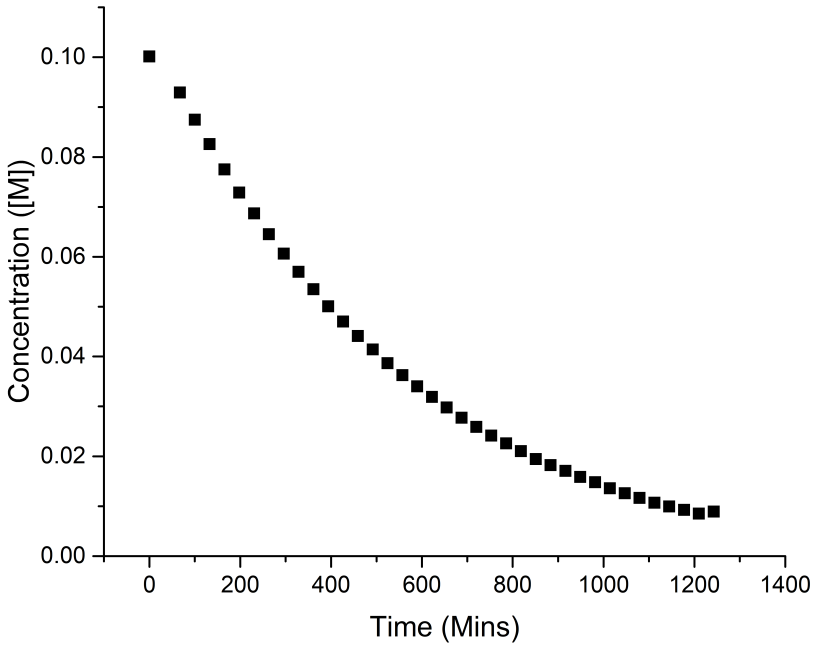

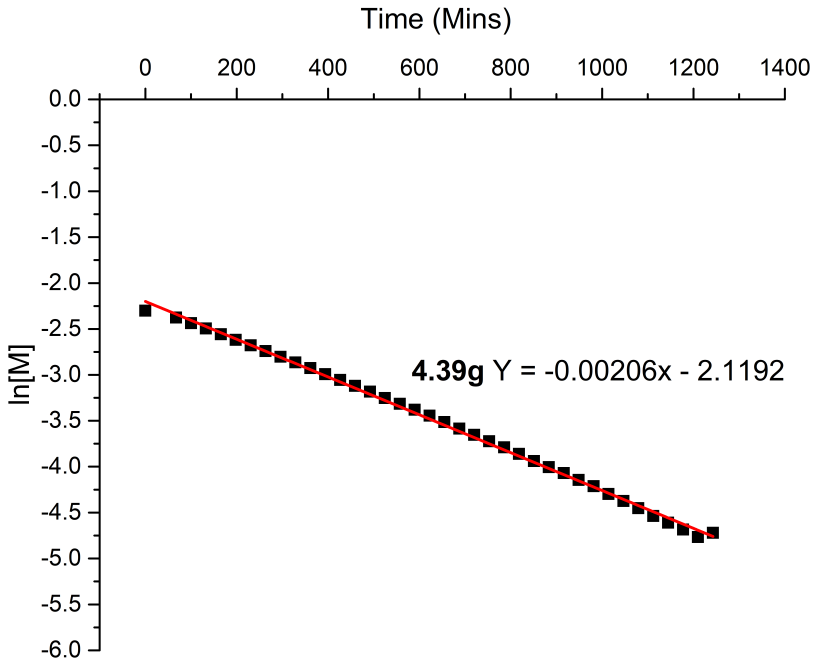

Polymerization of Monomer 4.39i

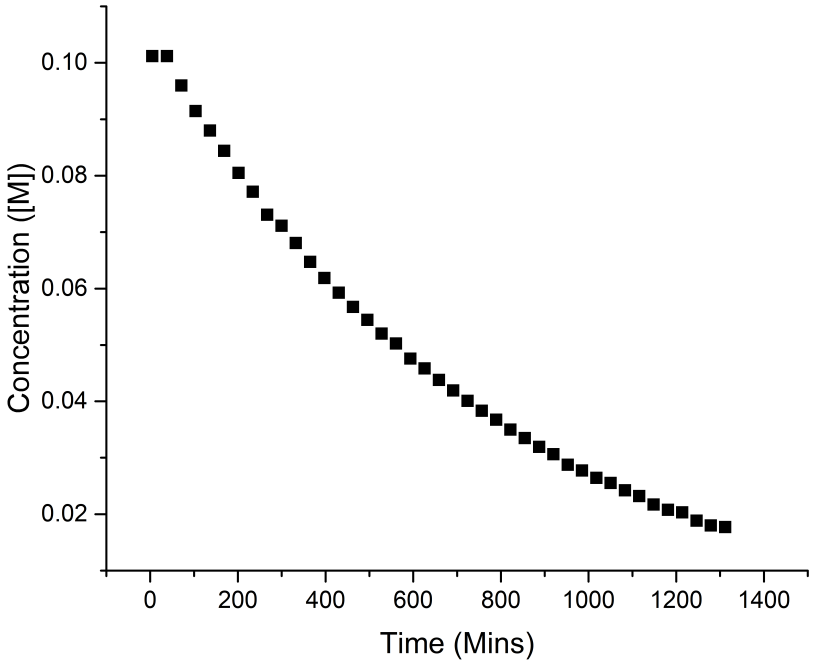

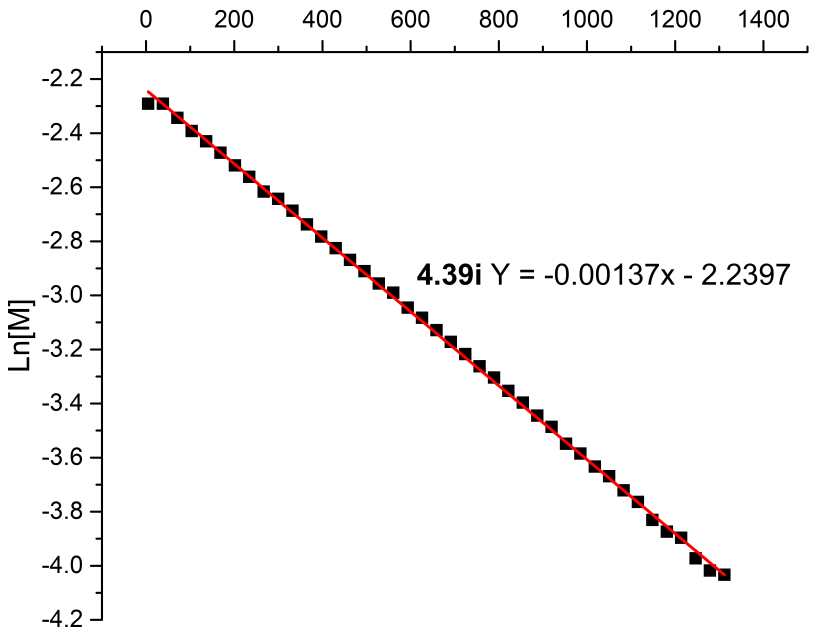

A.5 Investigation into the Synthesis and Application of an Unusual Spirocyclic Imide Species

Crystal Structure Data

_N_-Butyl-2-[(1_R_,5_S_,7_S_)-4-oxo-3,10-dioxatricyclo[5.2.1.0^{1,5}]dec-8-en-5-yl]acetamide 5.1b

Empirical formula	$C_{14}H_{19}NO_4$
Formula weight	265.30
Temperature/K	195.05(10)
Crystal system	monoclinic
Space group	$P2_{1/c}$
a/Å	10.289(2)
b/Å	15.4869(14)
c/Å	8.8304(13)
α/°	90
β/°	108.988(20)
γ/°	90
Volume/Å^3	1330.6(4)
Z	4
ρ_{calc}g/cm^3	1.324
μ/mm^{-1}	0.800
F(000)	568.0
Crystal size/mm^3	0.245 × 0.145 × 0.108
Radiation	CuKα (λ = 1.54184)
2θ range for data collection/°	9.09 to 142.204
Index ranges	$-12 \leq h \leq 11$, $-18 \leq k \leq 16$, $-10 \leq l \leq 10$
Reflections collected	8452
Independent reflections	2550 [R_{int} = 0.0820, R_{sigma} = 0.0673]
Data/restraints/parameters	2550/0/177
Goodness-of-fit on F^2	1.048
Final R indexes [I>=2σ(I)]	R_1 = 0.0633, wR_2 = 0.1656
Final R indexes [all data]	R_1 = 0.0990, wR_2 = 0.1982
Largest diff. peak/hole / e Å^{-3}	0.34/-0.27

(1*R*,4*S*,6*S*)-1'-Butyl-1-(hydroxymethyl)spiro[7-oxabicyclo[2.2.1]hept-2-ene-6,3'-pyrrolidine]-2',5'-dione 5.2

Empirical formula	$C_{14}H_{19}NO_4$
Formula weight	265.30
Temperature/K	110.00(10)
Crystal system	monoclinic
Space group	$P2_{1/n}$
a/Å	10.1424(3)
b/Å	6.9391(2)
c/Å	18.4871(6)
α/°	90
β/°	95.827(3)
γ/°	90
Volume/Å^3	1294.38(7)
Z	4
ρ_{calc}g/cm^3	1.361
μ/mm^{-1}	0.822
F(000)	568.0
Crystal size/mm^3	0.199 × 0.118 × 0.047
Radiation	CuKα (λ = 1.54184)
2θ range for data collection/°	9.56 to 134.09
Index ranges	$-12 \leq h \leq 11$, $-8 \leq k \leq 7$, $-21 \leq l \leq 22$
Reflections collected	4354
Independent reflections	2316 [R_{int} = 0.0139, R_{sigma} = 0.0205]
Data/restraints/parameters	2316/0/249
Goodness-of-fit on F^2	1.054
Final R indexes [I>=2σ(I)]	R_1 = 0.0306, wR_2 = 0.0756
Final R indexes [all data]	R_1 = 0.0345, wR_2 = 0.0783
Largest diff. peak/hole / e Å^{-3}	0.29/-0.18

(1*R*,2*S*,4*R*)-1'-Benzyl-1-(hydroxymethyl)spiro[7-oxabicyclo[2.2.1]heptane-2,3'-pyrrolidine]-2',5'-dione 5.45b

Empirical formula	$C_{17}H_{19}NO_4$
Formula weight	301.33
Temperature/K	110.05(10)
Crystal system	triclinic
Space group	P-1
a/Å	7.0699(3)
b/Å	8.8388(3)
c/Å	12.4503(4)
α/°	73.353(3)
β/°	77.663(3)
γ/°	82.866(3)
Volume/Å^3	726.54(5)
Z	2
ρ_{calc}g/cm^3	1.377
μ/mm^{-1}	0.806
F(000)	320.0
Crystal size/mm^3	0.482 × 0.234 × 0.135
Radiation	CuKα (λ = 1.54184)
2θ range for data collection/°	7.544 to 142.086
Index ranges	$-8 \leq h \leq 7$, $-10 \leq k \leq 10$, $-15 \leq l \leq 15$
Reflections collected	13157
Independent reflections	2775 [R_{int} = 0.0150, R_{sigma} = 0.0086]
Data/restraints/parameters	2775/0/203
Goodness-of-fit on F^2	1.043
Final R indexes [I>=2σ(I)]	R_1 = 0.0363, wR_2 = 0.0913
Final R indexes [all data]	R_1 = 0.0368, wR_2 = 0.0918
Largest diff. peak/hole / e Å^{-3}	0.25/-0.25

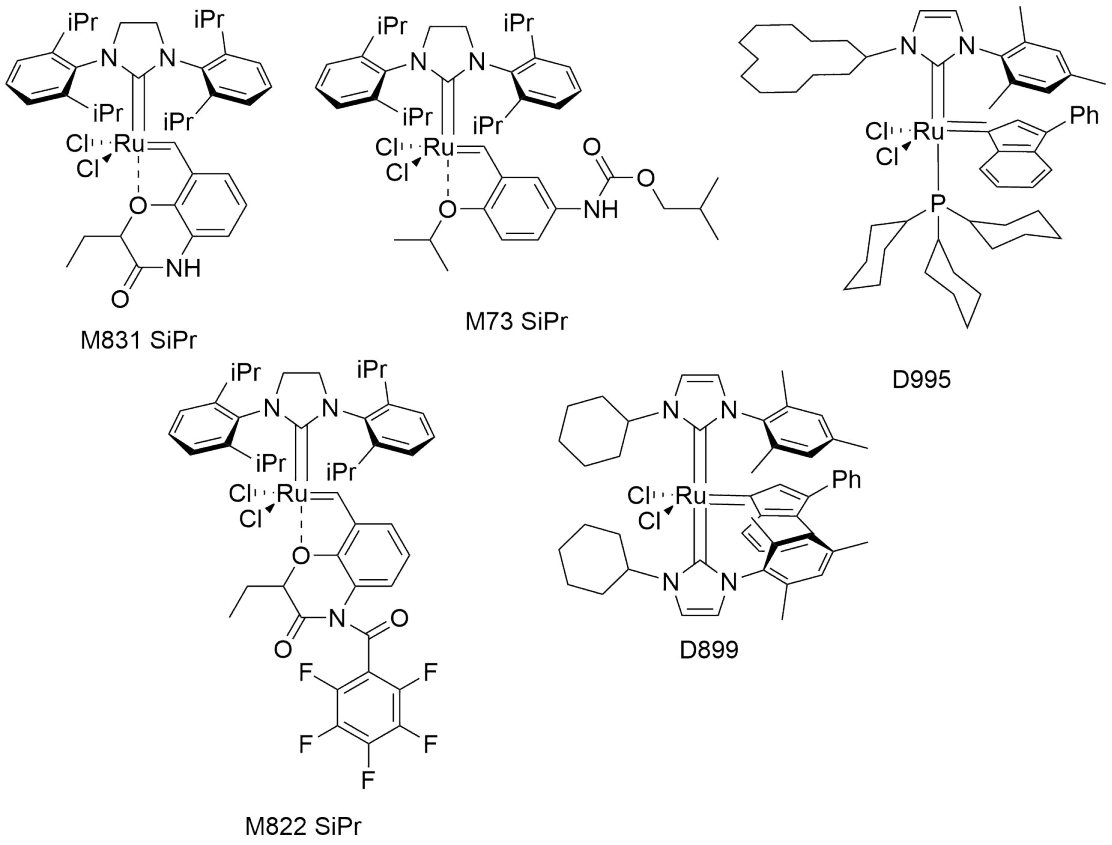

Figure A.9: Catalyst structures supplied by DEMETA S.A.S.

Table A.2: Demeta catalyst screening for the commercial diacid monomer.

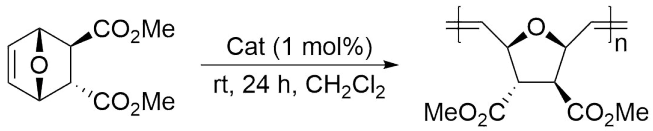

Entry	Catalyst	Temp (°C)	Conc. (M)	Time (h)	Conv. (%)[a]	Mn[b]	Mw[b]	Đ[c]
1	M73 SiPr	rt	0.1	24	100	25,514	32,791	1.29
2	M831 SiPr	rt	0.1	24	100	12,867	18,219	1.42
3	D899	rt	0.1	24	-	-	-	-
4	D995	rt	0.1	24	100	36,675	45,989	1.25
5	M833 SiPr	rt	0.1	24	100	21,008	23,260	1.11
6	G2	rt	0.1	24	100	41,264	54,817	1.33
7	M833 SiPr	rt	0.1	3	100	18,540	20,059	1.08
8	D996	rt	0.1	8	100	24,670	32,088	1.30

All polymerisations were carried out using a monomer:catalyst ratio of 100:1.[a] Conversion was determined by ^{1}H NMR spectroscopy.[b] Determined by SEC in THF at 23 °C and calibrated relative to polystyrene standards.[c] Đ= M_w/M_n.

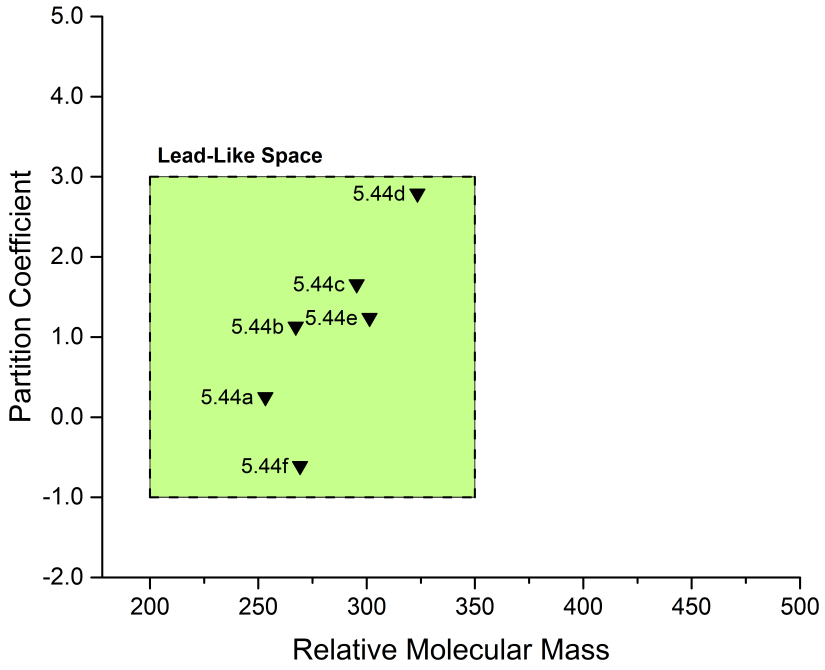

Figure A.10: Plot of relative molecular mass against lipophilicity for **5.44a-f** highlighting lead-like chemical space.

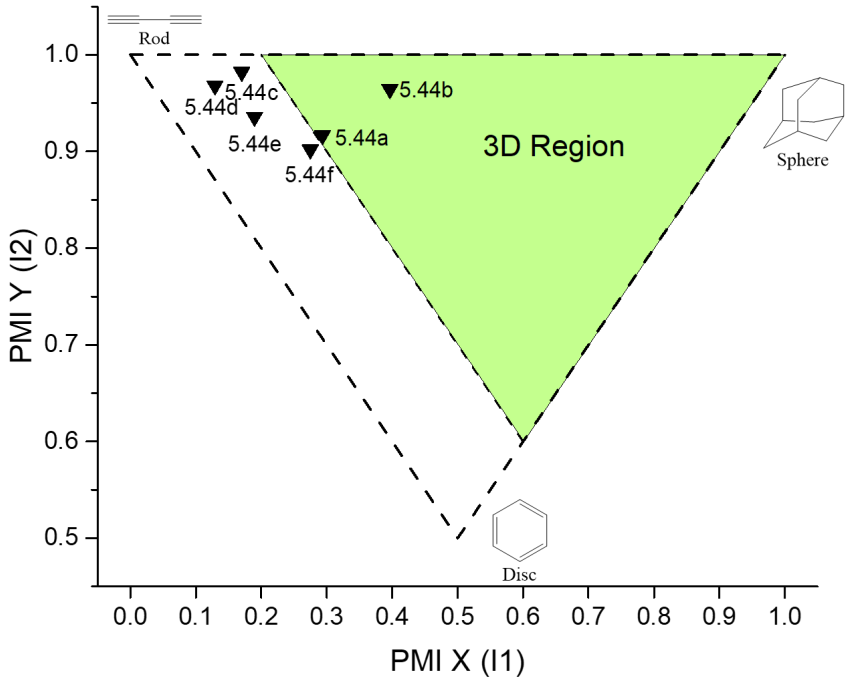

Figure A.11: PMI analysis of structures **5.44a-f**.

List of Abbreviations

°C	Degrees celsius
Đ	Dispersity
$(CH_2Cl)_2$	1,2-Dichloroethane
CH_2Cl_2	Dichloromethane
CO_2	Carbon dioxide
NEt_3	Triethylamine
α	Hydrogen bond donor
β	Hydrogen bond acceptor
δ	Hildebrand solubility parameter
ε	Dielectric constant
v*/*v	Volume to volume
w*/*w	Weight to weight
δ_c	Hydrogen bonding index
δ_d	Dispersion energy
δ_h	Hydrogen bonding energy
δ_p	Dipolar energy
δ_s	Hydrogen bonding solubility
π*	Dipolarity/polarizability
2-MeTHF	2-Methyltetrahydrofuran
ACS	American Chemical Society
AN	Acceptor number
API	Active pharmaceutical ingredient
Bn	benzyl
Boc	*tert*-butyloxycarbonyl
Cbz	Carboxybenzyl
CDI	1,1'-Carbonyldiimidazole
CEFIC	The European Chemical Industry Council
cLogP	Partition coefficient
COSY	Correlation spectroscopy
CPME	Cyclopentyl methyl ether

D	Dipole moment
d.e.	Diastereomeric excess
DAD	Diode array detector
DBU	1,8-Diazabicyclo[5.4.0]undec-7-ene
DEC	Diethyl carbonate
DEPT	Distortionless enhancement by polarization transfer
DFF	2,5-Furandicarboxaldehyde
DIC	*N*,*N*'-Diisopropylcarbodiimide
DIPEA	*N*,*N*-Diisopropylethylamine
DMA	*N*,*N*-Dimethylacetamide
DMC	Dimethyl carbonate
DMF	*N*,*N*-Dimethylformamide
DN	Donor number
DOE	Department of Energy
DSC	Differential scanning calorimetry
DVB	Divinylbenzene
EC	Ethylene carbonate
EDC	*N*-Ethyl-*N*-(3-dimethylaminopropyl)carbodiimide
EHS	Environmental health and safety
EPA	Environmental Protection Agency
ESI	Electrospray ionisation
EtOAc	Ethyl acetate
EtOH	Ethanol
FDCA	2,5-Furandicarboxylic acid
Fmoc	Fluorenylmethyloxycarbonyl
FT-IR	Fourier-transform infrared spectroscopy
GCIPR	Green Chemistry Pharmaceutical Round Table
GSK	GlaxoSmithKline
GVL	γ-Valerolactone
HBTU	*O*-(Benzotriazol-1-yl)-*N*,*N*,*N*',*N*'-tetramethyluronium hexafluorophosphate
HCl	Hydrochloric acid
HMBC	Heteronuclear multiple bond correlation
HMF	Hydroxymethylfurfural
HMPB	4-(4-Hydroxymethyl-3-methoxyphenoxy)butyric acid
HMQC	Heteronuclear multiple quantum coherence
HOAt	1-Hydroxy-7-azabenzotriazole
HOBt	1-Hydroxybenzotriazole
HPLC	High performance liquid chromatography

HRMS	High-resolution mass spectrometry
HSP	Hansen solubility paramteres
HSPiP	Hansen Solubility Paramteres in Practice
IMI	Innovative Medicines Initiative
IPA	Isopropyl alcohol
IR	Infra red
$\mathbf{K_{obs}}$	Observed rate constant
LC	Liquid chromatograph
LLAMA	Lead-likeness and molecular analysis
$\mathbf{M_w}$	Weight average molecular weight
$\mathbf{M_n}$	Number average molecular weight
MeCN	Acetonitrile
MEK	Methyl ethyl ketone
MeOH	Methanol
MIBK	Methyl isobutyl ketone
NBP	*N*-Butylpyrrolidinone
NMP	*N*-Methyl-2-pyrrolidone
NMR	Nuclear magnetic resonance
$\mathbf{NO_x}$	Nitrogen Oxide
OECD	Organisation for Economic Co-operation and Development
PA	Polyamide
Pbf	2,2,4,6,7-pentamethyldihydrobenzofuran-5-sulfonyl
PC	Propylene carbonate
PE	Petroleum ether
PEF	Polyethylene furanoate
PEG	Polyethylene glycol
PET	Polyethylene terephthalate
PMA	Phosphomolybdic acid
PMI	Principal moments of inertia
PS	Polystyrene
$\mathbf{R_F}$	Retardation factor
$\mathbf{R_0}$	Interaction radius
$\mathbf{R_a}$	Relative HSP distance
REACh	Registration, Evaluation, Authorisation & restriction of CHemicals
ROMP	Ring-opening metathesis polymerisation
$\mathbf{scCO_2}$	Supercritical carbon dioxide
SEC	Size-exclusion chromatography
$\mathbf{SO_x}$	Sulfur oxide
SPOS	Solid-phase organic synthesis

SPPS	Solid-phase peptide synthesis
SVHC	Substance of very high concern
T_g	Glass transition temperature
$T_{10\%}$	Thermal decomposition temperature
TFA	Trifluoroacetic acid
TGA	Thermogravimetric analysis
THF	Tetrahydrofuran
TLC	Thin layer chromatography
TMO	2,2,5,5-Tetramethyltetrahydrofuran
Trt	Trityl
UN	United Nations
UV	Ultra violet
VOC	Volatile organic compound
wt%	Weight percent

Bibliography

1. OECD, *Material Resources, Productivity and the Environment*; OECD Green Growth Studies; OECD Publishing: Paris, 2015.
2. Monastersky, R. *Nature* **2015**, *519*, 144–147.
3. Bloom, D. *Science* **2011**, *333*, 562–569.
4. United Nations in *Report of the United Nations Conference on the Human Environment,* (Stockholm) Sweden, June 5–6, 1972.
5. National Research Council Board on Sustainable Development, *Our Common Journey: A Transition Toward Sustainability*; National Academy Press: Washington, D.C., 1999.
6. United Nations Sustainable Development Goals. https://www.un.org/sustainabledevelopment/ (accessed Apr 12 2018).
7. OECD, *OECD Environmental Outlook to 2050*; OECD Publishing: Paris, 2012.
8. CEFIC How is the global chemicals industry doing?, http://www.cefic.org/Facts-and-Figures/Chemicals-Industry-Profile/ (accessed Apr 12 2018).
9. Warner, J. C.; Cannon, A. S.; Dye, K. M. *Environ. Impact Assess. Rev.* **2004**, *24*, 775–799.
10. Clark, J. H. *Green Chem.* **1999**, *1*, 1–8.
11. Clark, J. H. *Green Chem.* **2006**, *8*, 17–21.
12. Anastas, P. T.; Warner, J. C., *Green Chemistry: Theory and Practice*; Oxford University Press: Oxford, UK, 1998.
13. Anastas, P. T.; Kirchhoff, M. M. *Acc. Chem. Res.* **2002**, *35*, 686–694.
14. Anastas, P. T.; Eghbali, N. *Chem. Soc. Rev.* **2010**, *39*, 301–312.
15. Constable, D. J. C.; Jimenez-Gonzalez, C.; Henderson, R. K. *Org. Process Res. Dev.* **2007**, *11*, 133–137.

16. Alder, C. M.; Hayler, J. D.; Henderson, R.; Redman, A.; Shukla, L.; Shuster, L. E.; Sneddon, H. F. *Green Chem.* **2016**, *4*, 1166–1169.

17. Alfonsi, K.; Colberg, J.; Dunn, P. J.; Fevig, T.; Jennings, S.; Johnson, T. A.; Kleine, H. P.; Knight, C.; Nagy, M. A.; Perry, D. A.; Stefaniak, M. *Green Chem.* **2008**, *10*, 31–36.

18. Prat, D.; Pardigon, O.; Flemming, H. W.; Letestu, S.; Ducandas, V.; Isnard, P.; Guntrum, E.; Senac, T.; Ruisseau, S.; Cruciani, P.; Hosek, P. *Org. Proc. Res. Dev.* **2013**, *17*, 1517–1525.

19. Prat, D.; Hayler, J.; Wells, A. *Green Chem.* **2014**, *16*, 4546–4551.

20. Prat, D.; Wells, A.; Hayler, J.; Sneddon, H.; McElroy, C. R.; Abou-Shehada, S.; Dunn, P. J. *Green Chem.* **2016**, *18*, 288–296.

21. DeSimone, J. M. *Science* **2002**, *297*, 799–803.

22. Li, C.-J.; Chen, L. *Chem. Soc. Rev.* **2006**, *35*, 68–82.

23. Martinez, C. A.; Hu, S.; Dumond, Y.; Tao, J.; Kelleher, P.; Tully, L. *Org. Proc. Res. Dev.* **2008**, *12*, 392–398.

24. Jessop, P. G.; Mercer, S. M.; Heldebrant, D. J. *Energy Environ. Sci.* **2012**, *5*, 7240–7253.

25. Hart, R.; Pollet, P.; Hahne, D. J.; John, E.; Llopis-Mestre, V.; Blasucci, V.; Huttenhower, H.; Leitner, W.; Eckert, C. A.; Liotta, C. L. *Tetrahedron* **2010**, *66*, 1082–1090.

26. Clark, J. H.; Farmer, T. J.; Hunt, A. J.; Sherwood, J. *Int. J. Mol. Sci.* **2015**, *16*, 17101–17159.

27. Constable, D. J. C.; Dunn, P. J.; Hayler, J. D.; Humphrey, G. R.; Leazer, J. J. L.; Linderman, R. J.; Lorenz, K.; Manley, J.; Pearlman, B. A.; Wells, A.; Zaks, A.; Zhang, T. Y. *Green Chem.* **2007**, *9*, 411–420.

28. Shen, L.; Worrell, E.; Patel, M. *Biofuels, Bioprod. Biorefin.* **2010**, *4*, 25–40.

29. Lambert, S.; Wagner, M. *Chem. Soc. Rev.* **2017**, *46*, 6855–6871.

30. Geyer, R.; Jambeck, J. R.; Law, K. L. *Sci. Adv.* **2017**, *3*, 5.

31. Jambeck, J. R.; Geyer, R.; Wilcox, C.; Siegler, T. R.; Perryman, M.; Andrady, A.; Narayan, R.; Law, K. L. *Science* **2015**, *347*, 768–771.

32. Zhu, Y.; Romain, C.; Williams, C. K. *Nature* **2016**, *540*, 354–362.

33. Hernández, N.; Williams, R. C.; Cochran, E. W. *Org. Biomol. Chem.* **2014**, *12*, 2834–2849.

34. Llevot, A.; Dannecker, P. K.; von Czapiewski, M.; Over, L. C.; Söyler, Z.; Meier, M. A. *Chem. Eur. J.* **2016**, *22*, 11510–11521.

35. Gandini, A. *Green Chem.* **2011**, *13*, 1061–1083.

36. Bozell, J. J.; Petersen, G. R. *Green Chem.* **2010**, *12*, 539–554.

37. Eerhart, A. J. J. E.; Faaij, A. P. C.; Patel, M. K. *Energy Environ. Sci.* **2012**, *5*, 6407–6422.

38. Wilbon, P. A.; Chu, F.; Tang, C. *Macromol. Rapid Commun.* **2013**, *34*, 8–37.

39. Lligadas, G.; Ronda, J. C.; Galià, M.; Cádiz, V. *Mater. Today* **2013**, *16*, 337–343.

40. Alper, E.; Yuksel Orhan, O. *Petroleum* **2017**, *3*, 109–126.

41. Trott, G; Saini, P. K.; Williams, C. K. *Phil. Trans. R. Soc. A.* **2016**, *374*, 20150085.

42. Fosgerau, K.; Hoffmann, T. *Drug Discov. Today* **2015**, *20*, 122–128.

43. Lau, J. L.; Dunn, M. K. *Bioorganic Med. Chem.* **2018**, *26*, 2700–2707.

44. Andersson, L.; Blomberg, L.; Flegel, M.; Lepsa, L.; Nilsson, B.; Verlander, M. *Biopolymers* **2000**, *55*, 227–250.

45. Bray, B. L. *Nat. Rev. Drug Discov.* **2003**, *2*, 587–593.

46. Goodwin, D.; Simerska, P.; Toth, I. *Curr. Med. Chem.* **2012**, *19*, 4451–4461.

47. MacMillan, D. S.; Murray, J.; Sneddon, H. F.; Jamieson, C.; Watson, A. J. B. *Green Chem.* **2013**, *15*, 596–600.

48. Kim, T. H.; Kim, S. G. *Saf. Health Work* **2011**, *2*, 97–104.

49. Kennedy, G. L. *Crit. Rev. Toxicol.* **2012**, *42*, 793–826.

50. Candidate List of substances of very high concern for Authorisation. European Chemicals Agency (ECHA). https://echa.europa.eu/candidate-list-table (accessed Dec 4, 2017).

51. 2017 Greener Reaction Conditions Award. Environmental Protection Agency (EPA). https://www.epa.gov/greenchemistry/green-chemistry-challenge-2017-greener-reaction-conditions-award (accessed Dec 21, 2017).

52. Kunz, H. *Angew. Chem. Int. Ed.* **1978**, *17*, 67–68.

53. Tesser, G. I.; Balvert Geers, I. C. *Int. J. Pept. Protein Res.* **1975**, *7*, 295–305.

54. Sheehan, J. C.; Hlavka, J. J. *J. Org. Chem.* **1956**, *21*, 439–441.

55. Ho, G. J.; Emerson, K. M.; Mathre, D. J.; Shuman, R. F.; Grabowski, E. J. *J. Org. Chem.* **1995**, *60*, 3569–3570.

56. Anderson, G. W.; Zimmerman, J. E.; Callahan, F. M. *J. Am. Chem. Soc.* **1964**, *86*, 1839–1842.

57. Wang, Q.; Wang, Y.; Kurosu, M. *Org. Lett.* **2012**, *14*, 3372–3375.

58. Murakami, M.; Hayashi, M.; Tamura, N.; Hoshino, Y.; Ito, Y. *Tetrahedron Lett.* **1996**, *37*, 7541–7544.

59. Hojo, K.; Ichikawa, H.; Onishi, M.; Fukumori, Y.; Kawasaki, K. *J. Pept. Sci.* **2011**, *17*, 487–492.

60. Mahindra, A.; Nooney, K.; Uraon, S.; Sharma, K. K.; Jain, R. *RSC Advances* **2013**, *3*, 16810–16816.

61. Gabriel, C. M.; Keener, M.; Gallou, F.; Lipshutz, B. H. *Org. Lett.* **2015**, *17*, 3968–3971.

62. Cortes-Clerget, M.; Berthon, J.-Y.; Krolikiewicz-Renimel, I.; Chaisemartin, L.; Lipshutz, B. H. *Green Chem.* **2017**, 4263–4267.

63. Yazawa, K.; Numata, K. *Molecules* **2014**, *19*, 13755–13774.

64. Schellenberger, V.; Jakubke, H. D. *Angew. Chem. Int. Ed.* **1991**, *30*, 1437–1449.

65. Jakubke, H. D.; Kuhl, P.; Könnecke, A. *Angew. Chem. Int. Ed.* **1985**, *24*, 85–93.

66. Bordusa, F. *Chem. Rev.* **2002**, *102*, 4817–4867.

67. Noritomi, H.; Miyata, M.; Kato, S.; Nagahama, K. *Biotechnol. Lett.* **1995**, *17*, 1323–1328.

68. Erbeldinger, M.; Mesiano, A.; Russell, A. *Biotechnology Prog.* **2000**, *16*, 1129–1131.

69. Vallette, H. *Arkivoc* **2006**, *4*, 200–211.

70. Plaquevent, J.-C.; Levillain, J.; Guillen, F.; Malhiac, C.; Gaumont, A.-C. *Chem. Rev.* **2008**, *108*, 5035–5060.

71. Tietze, A. A.; Heimer, P.; Stark, A.; Imhof, D. *Molecules* **2012**, *17*, 4158–4185.

72. Declerck, V.; Nun, P.; Martinez, J.; Lamaty, F. *Angew. Chem. Int. Ed.* **2009**, *48*, 9318–9321.

73. Bonnamour, J.; Métro, T.-X.; Martinez, J.; Lamaty, F. *Green Chem.* **2013**, *15*, 1116–1120.

74. Maurin, O.; Verdié, P.; Subra, G.; Lamaty, F.; Martinez, J.; Métro, T. X. *Beilstein J. Org. Chem.* **2017**, *13*, 2087–2093.

75. Mahindra, A.; Patel, N.; Bagra, N.; Jain, R. *RSC Advances* **2014**, *4*, 3065–3069.

76. Hernandez, J. G.; Juaristi, E. *J. Org. Chem.* **2010**, *75*, 7107–7111.

77. Hojo, K.; Maeda, M.; Kawasaki, K. *J. Pept. Sci.* **2001**, *7*, 615–618.

78. Hojo, K.; Ichikawa, H.; Fukumori, Y.; Kawasaki, K. *Int. J. Pept. Protein Res.* **2008**, *14*, 373–380.

79. Wilson, M. E.; Paech, K; Zhou, W.-J.; Kurth, M. J. *J. Org. Chem.* **1998**, *63*, 5094–5099.

80. Hojo, K.; Maeda, M.; Kawasaki, K. *Tetrahedron* **2004**, *60*, 1875–1886.

81. Ojo, K. H.; Aeda, M. M.; Mith, T. J. S.; Ita, E. K.; Amaguchi, F. Y.; Amamoto, S. Y.; Awasaki, K. K. *Chem. Pharm. Bull.* **2004**, *52*, 422–427.

82. Hojo, K.; Maeda, M.; Kawasaki, K. *Tetrahedron Lett.* **2004**, *45*, 9293–9295.

83. Hojo, K.; Ichikawa, H.; Maeda, M.; Kida, S.; Fukumori, Y. *J. Pept. Sci.* **2007**, 493–497.

84. Hojo, K.; Hara, A.; Kitai, H.; Onishi, M.; Ichikawa, H.; Fukumori, Y.; Kawasaki, K. *Chem. Cent. J.* **2011**, *5*, 49–59.

85. Hojo, K.; Shinozaki, N.; Nozawa, Y.; Fukumori, Y.; Ichikawa, H. *Appli. Sci.* **2013**, *3*, 614–623.

86. Galanis, A. S.; Albericio, F.; Grøtli, M; Grotli, M. *Org. Lett.* **2009**, *11*, 4488–4491.

87. Ulijn, R.; Baragana, B.; Halling, P.; Flitsch, S. *J. Am. Chem. Soc.* **2002**, *124*, 10988–10989.

88. Haddoub, R.; Dauner, M.; Stefanowicz, F. A.; Barattini, V.; Laurent, N.; Flitsch, S. L. *Org. Biomol. Chem.* **2009**, *7*, 665–670.

89. De Marco, R.; Tolomelli, A.; Greco, A.; Gentilucci, L. *ACS Sustain. Chem. Eng.* **2013**, *1*, 566–569.

90. Blackmond, D. G.; Armstrong, A.; Coombe, V.; Wells, A. *Angew. Chem. Int. Ed.* **2007**, *46*, 3798–3800.

91. Acosta, G. A.; del Fresno, M.; Paradis-Bas, M.; Rigau-DeLlobet, M.; Côté, S.; Royo, M.; Albericio, F. *J. Peptide Sci.* **2009**, *15*, 629–633.

92. Zalipsky, S.; Chang, J. L.; Albericio, F.; Barany, G. *Reactive Polym.* **1994**, *22*, 243–258.

93. Jad, Y. E.; Acosta, G. A.; Khattab, S. N.; de la Torre, B. G.; Govender, T.; Kruger, H. G.; El-Faham, A.; Albericio, F. *Org. Biomol. Chem.* **2015**, *13*, 2393–2398.

94. Jad, Y. E.; Acosta, G. A.; Khattab, S. N.; de la Torre, B. G.; Govender, T.; Kruger, H. G.; El-Faham, A.; Albericio, F. *Amino Acids* **2015**, *48*, 419–426.

95. Jad, Y. E.; Acosta, G. A.; Govender, T.; Kruger, H. G.; El-Faham, A.; de la Torre, B. G.; Albericio, F. *ACS Sustain. Chem. Eng.* **2016**, *4*, 6809–6814.

96. Kumar, A.; Jad, Y. E.; El-Faham, A.; de la Torre, B. G.; Albericio, F. *Tetrahedron Lett.* **2017**, *58*, 2986–2988.

97. Schäffner, B.; Schäffner, F.; Verevkin, S. P.; Börner, A. *Chem. Rev.* **2010**, *110*, 4554–4581.

98. Jessop, P. G.; Jessop, D. A.; Fu, D.; Phan, L. *Green Chem.* **2012**, *14*, 1245–1259.

99. Peppel, W. J. *J. Ind. Eng. Chem.* **1958**, *50*, 767–770.

100. Comerford, J. W.; Ingram, I. D. V.; North, M.; Wu, X. *Green Chem.* **2015**, 1966–1987.

101. North, M *Chim. Oggi Chem. Today* **2012**, *30*, 3–6.

102. North, M.; Pasquale, R.; Young, C. *Green Chem.* **2010**, *12*, 1514–1539.

103. Büttner, H.; Longwitz, L.; Steinbauer, J.; Wulf, C.; Werner, T. *Top. Curr. Chem.* **2017**, *375*, 50–106.

104. Kohl, A; Buckinham, P. A. *Oil Gas J.* **1960**, 146.

105. Lewis, D. C.; Salazar, L. C.; Machac, J. R. Oil recovery employing alkylene carbonates, U. S. Patent, US 8403069 B2, Mar 26, 2013.

106. Machac, J. R.; Woodrum, S. A.; Klein, H. P.; Marquis, E. T. Propylene carbonate based cleaning compositions, U. S. Patent, US 6596677 B1, Jul 22, 2003.

107. Clements, J. H. *Ind. Eng. Chem. Res.* **2003**, *42*, 663–674.

108. Xu, K. *Chem. Rev.* **2004**, *104*, 4303–4417.

109. Behr, A.; Obst, D.; Schulte, C.; Schosser, T. *J. Mol. Cat. A: Chem.* **2003**, *206*, 179–184.

110. Bayardon, J.; Holz, J.; Schäffner, B.; Andrushko, V.; Verevkin, S.; Preetz, A.; Börner, A. *Angew. Chem. Int. Ed.* **2007**, *46*, 5971–5974.

111. Behr, A.; Roll, R. *J. Mol. Cat. A: Chem.* **2005**, *239*, 180–184.

112. Torborg, C.; Huang, J.; Schulz, T.; Schäffner, B.; Zapf, A.; Spannenberg, A.; Börner, A.; Beller, M. *Chem. Eur. J.* **2009**, *15*, 1329–1336.

113. Reetz, M. T.; Lohmer, G. *Chem. Commun.* **1996**, 1921–1922.

114. Parker, H. L.; Sherwood, J.; Hunt, A. J.; Clark, J. H. *ACS Sustain. Chem. Eng.* **2014**, *2*, 1739–1742.

115. Wang, J.-L.; He, L.-N.; Miao, C.-X.; Li, Y.-N. *Green Chem.* **2009**, *11*, 1317–1320.

116. Neubert, P.; Fuchs, S.; Behr, A. *Green Chem.* **2015**, *17*, 4045–4052.

117. Pieber, B.; Kappe, C. O. *Green Chem.* **2013**, *15*, 320–324.

118. Yu, B.; Diao, Z.-F.; Guo, C.-X.; Zhong, C.-L.; He, L.-N.; Zhao, Y.-N.; Song, Q.-W.; Liu, A.-H.; Wang, J.-Q. *Green Chem.* **2013**, *15*, 2401–2407.

119. Gautam, P.; Kathe, P.; Bhanage, B. M. *Green Chem.* **2017**, *19*, 823–830.

120. Gautam, P.; Gupta, R.; Bhanage, B. M. *Eur. J. Org. Chem.* **2017**, 3431–3437.

121. North, M; Pizzato, F; Villuendas, P *ChemSusChem.* **2009**, *2*, 862–865.

122. Clegg, W.; Harrington, R. W.; North, M.; Pizzato, F.; Villuendas, P. *Tetrahedron: Asymmetry* **2010**, *21*, 1262–1271.

123. Beattie, C.; North, M.; Villuendas, P. *Molecules* **2011**, *16*, 3420–3432.

124. Forero, J. S. B.; Carvalho, E. M. D.; Junior, J. J.; Silva, F. M. *Curr. Org. Synth.* **2015**, 102–107.

125. Nam, J.; Shin, D.; Rew, Y.; Boger, D. L. *J. Am. Chem. Soc.* **2007**, *129*, 8747–8755.

126. Pedersen, S. L.; Tofteng, A. P.; Malik, L.; Jensen, K. J. *Chem. Soc. Rev.* **2012**, *41*, 1826–1844.

127. Sopeña, S.; Laserna, V.; Guo, W.; Martin, E.; Escudero-Adán, E. C.; Kleij, A. W. *Adv. Synth. Catal.* **2016**, *358*, 2172–2178.

128. El-Faham, A.; Albericio, F. *Chem. Rev.* **2011**, *111*, 6557–6602.

129. Mazuela, J.; Verendel, J. J.; Coll, M.; Schäffner, B.; Börner, A.; Andersson, P. G.; Pàmies, O.; Diéguez, M. *J. Am. Chem. Soc.* **2009**, *131*, 12344–12353.

130. Vaino, A. R.; Janda, K. D. *J. Comb. Chem.* **2000**, *2*, 579–596.

131. Santini, R.; Griffith, M. C.; Qi, M. *Tetrahedron Lett.* **1998**, *39*, 8951–8954.

132. Garcia, F.; Albericio, F. *Chim. Oggi Chem. Today* **2008**, *26*, 29–34.

133. Ferreira, S. H.; Bartelt, D. C.; Greene, L. J. *Biochem.* **1970**, *9*, 2583–2593.

134. Prassas, I.; Eissa, A.; Poda, G.; Diamandis, E. P. *Nat. Rev. Drug Discov.* **2015**, *14*, 183–202.

135. Golias, C.; Charalabopoulos, A; Stagikas, D; Charalabopoulos, K; Batistatou, A *Hippokratia* **2007**, *11*, 124–128.

136. McCleary, R. J.; Kini, R. M. *Toxicon* **2013**, *62*, 56–74.

137. Merrifield, R. B. *J. Am. Chem. Soc.* **1964**, *86*, 304–305.

138. Merrifield, R. B. *Biochem.* **1964**, *3*, 1385–1390.

139. Cornille, A.; Blain, M.; Auvergne, R.; Andrioletti, B.; Boutevin, B.; Caillol, S. *Polym. Chem.* **2017**, *8*, 592–604.

140. Blain, M; Jean-Gerard, L; Auvergne, R; Benazet, D; Caillol, S; Andrioletti, B *Green Chem.* **2014**, *16*, 4286–4291.

141. Guo, W.; Gõnzalez-Fabra, J.; Bandeira, N. A.; Bo, C.; Kleij, A. W. *Angew. Chem. Int. Ed.* **2015**, *54*, 11686–11690.

142. Baizer, M.; Clark, J.; Smith, E. *J. Org. Chem.* **1957**, *22*, 1706–1707.

143. Najer, H; Chabrier, P; Giudicelli, R *Bull. Soc. Chim. Fr.* **1954**, *21*, 1142.

144. Ralhan, K.; KrishnaKumar, V. G.; Gupta, S. *RSC Adv.* **2015**, *5*, 104417–104425.

145. Olsén, P.; Oschmann, M.; Johnston, E. V.; Åkermark, B. *Green Chem.* **2018**, *20*, 469–475.

146. Merrifield, R. B. *J. Am. Chem. Soc.* **1963**, *85*, 2149–2154.

147. Hudson, D. *J. Comb. Chem.* **1999**, *1*, 403–457.

148. Gutte, B; Merrifield, R. B. *J. Biol. Chem.* **1971**, *246*, 1922–41.

149. Früchtel, J. S.; Jung, G. *Angew. Chem. Int. Ed.* **1996**, *35*, 17–42.

150. Coats, S. J.; Link, J. S.; Hlasta, D. J. *Org. Lett.* **2003**, 358–361.

151. Stobrawe, A.; Makarczyk, P.; Maillet, C.; Muller, J. L.; Leitner, W. *Angew. Chem. Int. Ed.* **2008**, *47*, 6674–6677.

152. Lawrenson, S. B. *Pure Appl. Chem.* **2018**, *90*, 157–165.

153. Li, W.; Yan, B. *J. Org. Chem.* **1998**, *63*, 4092–4097.

154. Hancock, W. S.; Prescott, D. J.; Vagelos, P. R.; Marshall, G. R. *J. Org. Chem.* **1973**, *38*, 774–781.

155. Sarin, V. K.; Kent, S. B.; Merrifield, R. B. *J. Am. Chem. Soc.* **1980**, *102*, 5463–5470.

156. Belmares, M.; Blanco, M.; Goddard, W. A.; Ross, R. B.; Caldwell, G.; Chou, S. H.; Pham, J.; Olofson, P. M.; Thomas, C. *J. Comput. Chem.* **2004**, *25*, 1814–1826.

157. Fields, G.; Fields, C. *J. Am. Chem. Soc.* **1991**, *113*, 4202–4207.

158. Suh, K. W.; Clarke, D. H. *J. Polym. Sci. A.* **1967**, *5*, 1671–1681.

159. Cilli, E. M.; Oliveira, E.; Marchetto, R.; Nakaie, C. R. *J. Org. Chem.* **1996**, *61*, 8992–9000.

160. Gutmann, V. *Electrochimica Acta* **1976**, *21*, 661–670.

161. Malavolta, L.; Oliveira, E.; Cilli, E. M.; Nakaie, C. R. *Tetrahedron* **2002**, *58*, 4383–4394.

162. Abbott, S., *Solubility Science Principles and Practice*, 1.0.1.2; Steven Abbott TCNF Ltd: Ipswitch, 2018, pp 60–90.

163. Braunshier, C.; Hametner, C. *QSAR Combi. Sci.* **2007**, *26*, 908–918.

164. Toy, P. H.; Janda, K. D. *Tetrahedron Lett.* **1999**, *40*, 6329–6332.

165. Li, W.; Yan, B. *J. Org. Chem.* **1998**, *63*, 4092–4097.

166. Gooding, O. W.; Baudart, S.; Deegan, T. L.; Heisler, K.; Labadie, J. W.; Newcomb, W. S.; Porco, J. A.; Eikeren, P. V. *J. Comb. Chem.* **1999**, *1*, 113–122.

167. Bagheri, M.; Beyermann, M.; Dathe, M. *Antimicrob. Agents Chemother.* **2009**, *53*, 1132–1141.

168. Adams, J. H.; Cook, R. M.; Hudson, D.; Jammalamadaka, V.; Lyttle, M. H.; Songster, M. F. *J. Org. Chem.* **1998**, *63*, 3706–3716.

169. García-Martín, F.; Quintanar-Audelo, M.; García-Ramos, Y.; Cruz, L. J.; Gravel, C.; Furic, R.; Côté, S.; Tulla-Puche, J.; Albericio, F. *J. Comb. Chem.* **2006**, *8*, 213–220.

170. SpheriTide - the sustainable support for peptide synthesis. CEM Corporation. http://www.cem.com/spheritide.html (accessed 9 June, 2016).

171. Sherwood, J.; De bruyn, M.; Constantinou, A.; Moity, L.; McElroy, C. R.; Farmer, T. J.; Duncan, T.; Raverty, W.; Hunt, A. J.; Clark, J. H. *Chem. Commun.* **2014**, *50*, 9650–9652.

172. Sherwood, J.; Parker, H. L.; Moonen, K.; Farmer, T. J.; Hunt, A. J. *Green Chem.* **2016**, *18*, 3990–3996.

173. Ismalaj, E.; Strappaveccia, G.; Ballerini, E.; Elisei, F.; Piermatti, O.; Gelman, D.; Vaccaro, L. *ACS Sustain. Chem. Eng.* **2014**, *2*, 2461–2464.

174. Aycock, D. F. *Org. Process Res. Dev.* **2007**, *11*, 156–159.

175. Tundo, P.; Selva, M. *Acc. Chem. Res.* **2002**, *35*, 706–716.

176. Byrne, F.; Forier, B.; Bossaert, G.; Hoebers, C.; Farmer, T. J.; Clark, J. H.; Hunt, A. J. *Green Chem.* **2017**, *19*, 3671–3678.

177. Clark, J. H.; Macquarrie, D. J.; Sherwood, J. *Green Chem.* **2012**, *14*, 90–93.

178. Lawrenson, S. B.; Arav, R.; North, M. *Green Chem.* **2017**, *19*, 1685–1691.

179. Cioc, R. C.; Ruijter, E.; Orru, R. V. A. *Green Chem.* **2014**, *16*, 2958–2975.

180. Marcaccini, S.; Torroba, T. *Nat. Protoc.* **2007**, *2*, 632–639.

181. Bai, Y.; De bruyn, M.; Clark, J. H.; Dodson, J. R.; Farmer, T. J.; Honoré, M.; Ingram, I. D. V.; Naguib, M.; Whitwood, A. C.; North, M. *Green Chem.* **2016**, *18*, 3945–3948.

182. Luterbacher, J. S.; Martin Alonso, D.; Dumesic, J. A. *Green Chem.* **2014**, *16*, 4816–4838.

183. Pehere, A. D.; Xu, S.; Thompson, S. K.; Hillmyer, M. A.; Hoye, T. R. *Org. Lett.* **2016**, *18*, 2584–2587.

184. Crowell, J. H. Production of Itaconic and Citraconic Anhydrides. US2258947 A. October 14, 1941.

185. Berovic, M.; Legisa, M. In *Biotechnol. Annu. Rev.* El-Gewely, M. R., Ed.; Elsevier: 2007; Vol. 13, pp 303–343.

186. Lange, J.-P.; van der Heide, E.; van Buijtenen, J.; Price, R. *ChemSusChem* **2012**, *5*, 150–166.

187. Leon, A.; Gargallo, L.; Horta, A.; Radić, D. *J. Polym. Sci. B* **1989**, *27*, 2337–2345.

188. León, A.; Gargallo, L.; Radić, D.; Horta, A. *Polymer* **1991**, *32*, 761–763.

189. Kassi, E.; Loizou, E.; Porcar, L.; Patrickios, C. S. *Eur. Polym. J.* **2011**, *47*, 816–822.

190. Mahmoud, E.; Watson, D. A.; Lobo, R. F. *Green Chem.* **2014**, *16*, 167–175.

191. Diels, O.; Alder, K. *Liebigs Ann.* **1928**, *460*, 98–122.

192. Diels, O.; Alder, K. *Ber. Dtsch. Chem. Ges.* **1929**, *62*, 554–562.

193. Skowerski, K.; Białecki, J.; Tracz, A.; Olszewski, T. K. *Green Chem.* **2014**, *16*, 1125–1130.

194. Bai, Y.; Clark, J. H.; Farmer, T. J.; Ingram, I. D. V.; North, M. *Polym. Chem.* **2017**, *8*, 3074–3081.

195. Froidevaux, V.; Negrell, C.; Caillol, S.; Pascault, J. P.; Boutevin, B. *Chem. Rev.* **2016**, *116*, 14181–14224.

196. Smith, D.; Pentzer, E. B.; Nguyen, S. T. *Polym. Rev.* **2007**, *47*, 419–459.

197. Sutthasupa, S.; Shiotsuki, M.; Sanda, F. *Polym. J.* **2010**, *42*, 905–915.

198. Coles, M. P.; Gibson, V. C.; Mazzariol, L.; North, M.; Teasdale, W. G.; Williams, C. M.; Zamuner, D. *J. Chem. Soc. Chem. Commun.* **1994**, 2505–2506.

199. Biagini, S. C. G.; Coles, M. P.; Gibson, V. C.; Giles, M. R.; Marshall, E. L.; North, M *Polymer* **1998**, *39*, 1007–1014.

200. Biagini, S. C. G.; Davies, R. G.; Gibson, V. C.; Giles, M. R.; Marshall, E. L.; North, M; Robson, D. A. *Chem. Comm.* **1999**, 235–236.

201. Biagini, S. C.; Gareth Davies, R.; Gibson, V. C.; Giles, M. R.; Marshall, E. L.; North, M. *Polymer* **2001**, *42*, 6669–6671.

202. Biagini, S. C. G.; Gibson, V. C.; Giles, M. R.; Marshall, E. L.; North, M. *J. Polym. Sci. A* **2008**, *46*, 7985–7995.

203. Sutthasupa, S.; Terada, K.; Sanda, F.; Masuda, T. *J. Polym. Sci. A* **2006**, *44*, 5337–5343.

204. Sutthasupa, S.; Sanda, F.; Masuda, T. *Macromol. Chem. Phys.* **2008**, *209*, 930–937.

205. Sutthasupa, S.; Sanda, F.; Masuda, T. *Polym. Prepr. (Am. Chem. Soc., Div. Polym. Chem.)* **2008**, *49*, 690–691.

206. Sutthasupa, S.; Terada, K.; Sanda, F.; Masuda, T. *Polymer* **2007**, *48*, 3026–3032.

207. Sutthasupa, S.; Sanda, F.; Masuda, T. *Macromolecules* **2009**, *42*, 1519–1525.

208. Sutthasupa, S.; Shiotsuki, M.; Masuda, T.; Sanda, F. *J. Am. Chem. Soc.* **2009**, *131*, 10546–10551.

209. Sutthasupa, S.; Shiotsuki, M.; Matsuoka, H.; Masuda, T.; Sanda, F. *Macromolecules* **2010**, *43*, 1815–1822.

210. Sutthasupa, S.; Sanda, F. *Eur. Polym. J.* **2016**, *85*, 211–224.

211. Maynard, H. D.; Okada, S. Y.; Grubbs, R. H. *Macromolecules* **2000**, *33*, 6239–6248.

212. Maynard, H. D.; Okada, S. Y.; Grubbs, R. H. *J. Am. Chem. Soc.* **2001**, *123*, 1275–1279.

213. Sanford, M. S.; Ulman, M.; Grubbs, R. H. *J. Am. Chem. Soc.* **2001**, *123*, 749–750.

214. Zheng, Y.; Tice, C. M.; Singh, S. B. *Bioorganic Med. Chem. Lett.* **2014**, *24*, 3673–3682.

215. Zhang, J.; Senthilkumar, M.; Ghosh, S. C.; Hong, S. H. *Angew. Chem. Int. Ed.* **2010**, *49*, 6391–6395.

216. Khosravi, E.; Feast, W. J.; Al-Hajaji, A. A.; Leejarkpai, T. *J. Mol. Catal. A: Chem.* **2000**, *160*, 1–11.

217. Slugovc, C. *Macromol. Rapid Commun.* **2004**, *25*, 1283–1297.

218. Zeng, Y.-B.; Liu, X.-L.; Zhang, Y.; Li, C.-J.; Zhang, D.-M.; Peng, Y.-Z.; Zhou, X.; Du, H.-F.; Tan, C.-B.; Zhang, Y.-Y.; Yang, D.-J. *J. Nat. Prod.* **2016**, *79*, 2032–2038.

219. Puerto Galvis, C. E.; Vargas Méndez, L. Y.; Kouznetsov, V. V. *Chem. Biol. Drug Des.* **2013**, *82*, 477–499.

220. Kok, S. H. L.; Chui, C. H.; Lam, W. S.; Chen, J.; Lau, F. Y.; Wong, R. S. M.; Cheng, G. Y. M.; Lai, P. B. S.; Leung, T. W. T.; Yu, M. W. Y.; Tang, J. C. O.; Chan, A. S. C. *Bioorg. Med. Chem. Lett.* **2007**, *17*, 1155–1159.

221. McCluskey, A.; Ackland, S. P.; Gardiner, E.; Walkom, C. C.; Sakoff, J. A. *Anti-Cancer Drug Des.* **2001**, *16*, 291–303.

222. McCluskey, A.; Walkom, C.; Bowyer, M. C.; Ackland, S. P.; Gardiner, E.; Sakoff, J. A. *Bioorg. Med. Chem. Lett.* **2001**, *11*, 2941–2946.

223. Hart, M. E.; Chamberlin, A. R.; Walkom, C.; Sakoff, J. A.; McCluskey, A. *Bioorg. Med. Chem. Lett.* **2004**, *14*, 1969–1973.

224. Hill, T. A.; Stewart, S. G.; Ackland, S. P.; Gilbert, J.; Sauer, B.; Sakoff, J. A.; McCluskey, A. *Bioorg. Med. Chem.* **2007**, *15*, 6126–6134.

225. Robertson, M. J.; Gordon, C. P.; Gilbert, J.; McCluskey, A.; Sakoff, J. A. *Bioorg. Med. Chem.* **2011**, *19*, 5734–5741.

226. Spare, L. K.; Falsetta, P.; Gilbert, J.; Harman, D. G.; Baker, M. A.; Li, F.; McCluskey, A.; Clegg, J. K.; Sakoff, J. A.; Aldrich-Wright, J. R.; Gordon, C. P. *ChemMedChem* **2017**, *12*, 130–145.

227. Thaqi, A.; Scott, J. L.; Gilbert, J.; Sakoff, J. A.; McCluskey, A. *Eur. J. Med. Chem.* **2010**, *45*, 1717–1723.

228. Sauer, B.; Gilbert, J.; Sakoff, J.; McCluskey, A. *Lett. Drug Des. Discov.* **2009**, *6*, 1–7.

229. Galkin, K.; Kucherov, F.; Markov, O.; Egorova, K.; Posvyatenko, A.; Ananikov, V. *Molecules* **2017**, *22*, 2210–2220.

230. De Mouilpied, A. T.; Rule, A. *J. Chem. Soc., Trans.* **1907**, *91*, 176–183.

231. Roberts, K. S.; Sampson, N. S. *J. Org. Chem.* **2003**, *68*, 2020–2023.

232. Nelson, D. J.; Queval, P.; Rouen, M.; Magrez, M.; Toupet, L.; Caijo, F.; Borré, E.; Laurent, I.; Crévisy, C.; Baslé, O.; Mauduit, M.; Percy, J. M. *ACS Catal.* **2013**, *3*, 259–264.

233. Clavier, H.; Caijo, F.; Borré, E.; Rix, D.; Boeda, F.; Nolan, S. P.; Mauduit, M. *Eur. J. Org. Chem.* **2009**, 4254–4265.

234. Colomer, I.; Empson, C. J.; Craven, P.; Owen, Z.; Doveston, R. G.; Churcher, I.; Marsden, S. P.; Nelson, A. *Chem. Commun.* **2016**, *52*, 7209–7212.

235. Nadin, A.; Hattotuwagama, C.; Churcher, I. *Angew. Chem. Int. Ed.* **2012**, *51*, 1114–1122.

236. Chambers, S. J.; Coulthard, G.; Unsworth, W. P.; O'Brien, P.; Taylor, R. J. *Chem. Eur. J.* **2016**, *22*, 6496–6500.

237. Bemis, G. W.; Murcko, M. A. *J. Med. Chem.* **1996**, *39*, 2887–2893.

238. Irwin, J. J.; Sterling, T.; Mysinger, M. M.; Bolstad, E. S.; Coleman, R. G. *J. Chem. Inf. Model.* **2012**, *52*, 1757–1768.

239. Henderson, R. K.; Hill, A. P.; Redman, A. M.; Sneddon, H. F. *Green Chem.* **2015**, *17*, 945–949.

240. Adams, J. P.; Alder, C. M.; Andrews, I.; Bullion, A. M.; Campbell-Crawford, M.; Darcy, M. G.; Hayler, J. D.; Henderson, R. K.; Oare, C. a.; Pendrak, I.; Redman, A. M.; Shuster, L. E.; Sneddon, H. F.; Walker, M. D. *Green Chem.* **2013**, *15*, 1542–1549.

241. Wang, Q.; Wang, Y.; Kurosu, M. *Org. Lett.* **2012**, *14*, 3372–3375.

242. Rehwinkel, H.; Steglich, W. EN *Synthesis* **1982**, 826–827.

243. Hagiwara, D.; Miyake, H.; Morimoto, H.; Murai, M.; Fujii, T.; Matsuo, M. *J. Med. Chem.* **1992**, *35*, 2015–2025.

244. Hewawasam, P.; Lopez, O. D.; Tu, Y.; Wang, X.; Xu, N.; Kadow, J. F.; Meanwell, N. A; Gupta, S. V. S. A. K.; Kumar, I. J. K.; Ponugupati, S. K.; Belema, M. Hepatitis C Virus Inhibitors, U.S. Patent, US2015/0023913, Jan 22, 2015.

245. Zhao, M.; Liu, J.; Zhang, X.; Peng, L.; Li, C.; Peng, S. *Bioorg. Med. Chem.* **2009**, *17*, 3680–3689.

246. Wu, F.-C.; Da, C.-S.; Du, Z.-X.; Guo, Q.-P.; Li, W.-P.; Yi, L.; Jia, Y.-N.; Ma, X. *J. Org. Chem.* **2009**, *74*, 4812–4818.

247. Kiso, Y.; Miyazaki, T.; Satomi, M.; Hiraiwa, H.; Akita, T. *J. Chem. Soc., Chem. Comm.* **1980**, 1029–1030.

248. Smyth, M; Laidig, G; Borchardt, R; Bunin, B; Crews, C; Musser, J; Schneekloth, J; Chabala, J Compounds for enzyme inhibition, U.S. Patent, US2005/0245435, Nov 3, 2005.

249. Carpino, L. A.; Xia, J.; El-Faham, A. *J. Org. Chem.* **2004**, *69*, 54–61.

250. Houghten, R. A.; Yu, Y. *J. Am. Chem. Soc.* **2005**, *127*, 8582–8583.

251. Haldar, D.; Drew, M. G. B.; Banerjee, A. *Tetrahedron* **2006**, *62*, 6370–6378.

252. Hamuro, Y.; Scialdone, M. A.; DeGrado, W. F. *J. Am. Chem. Soc.* **1999**, *121*, 1636–1644.